Investigating the role of IGF-1R in radio-sensitivity

Matthew Ellis

Exeter College, Oxford

Submission for the degree of Doctor of Philosophy

(DPhil)



Department of Oncology

University of Oxford

Trinity 2020

List of Contributors

I declare that the work presented below describes my own research work, except for the following experiments, which were performed with the help of others:

Dr Iolanda Vendrell - ***MRC Oxford Institute for Radiation Oncology, University of Oxford***

Liquid chromatography-mass spectrometry (LC-MS/MS) and initial analysis (outlined in chapter V).

Jack Mills - ***Macaulay laboratory***

Chromatin extraction experiments were performed jointly (Fig. 6.9). IP was performed by Jack (Fig. 6.11).

Acknowledgements

First and foremost, I would like to thank Val for numerous things, some of which are listed here. Your unwavering support and words of wisdom have been so instrumental and have shaped the trajectory of my career, crafting the idea of becoming a clinician scientist into an attainable goal. From nodding and smiling encouragingly during my interview all those years ago, to the never-ending references and advice you continue to provide, I appreciate it all. You have taught me the importance of solid experimental design, the merits of a tireless work ethic and how to juggle important responsibilities with kindness, compassion, and humility. Thank you for everything big and obvious, and for all the small things which to you are second nature, but to most other people, are not. Thank you for the supervision, the advice and the friendship.

To the Macaulay lab members, past and present: I am so grateful for your guidance and comradery - I had the most wonderful time with you all and can't wait to see where we all end up. I look forward to many reunions in the future! To John and Kristie, I am so appreciative of our friendship, and for filling my first year with so much laughter. I would like to thank all my previous supervisors over the years and my transfer, confirmation and DPhil examiners, from whom I have learned so much, and whose impact I am sure will be felt throughout this thesis and my future career.

To my Oxford friends: I look back so fondly on this time in my life, and I am so happy to have shared such a unique experience with such lovely people, making friends for life along the way. Thank you for helping me to unwind, and also work harder at times too! Non-Oxford friends: thank you for continuing your friendship with a perpetual student - it is much appreciated. Perhaps one day I'll be able to buy the pints.

A big thank you to my South African family - your endless support and often greater willingness to celebrate my lab victories than me meant so much, and I am extremely grateful. I am eternally grateful to Britt, for all the advice, laughter, and most of all, the companionship. Witnessing your passion for science and ceaseless hard work continues to inspire me every day. To leave Oxford with my thesis, and you by my side is a wonderful feeling.

I am grateful to my grandparents, who always stressed the importance of education (although as I write this in the second year of my fourth degree, I imagine they didn't expect me to take their advice quite so literally). To Ella and Basil, thank you for the love, the walks and the slobbery licks, and to Dad, Kate and Anna, for putting up with my never-ending lab talk, and for providing much needed relaxation and support. I thank you all.

Last but by no means least, thank you to Mum, for your endless sacrifice and encouragement to allow me to pursue my interests. Your positivity and work ethic are contagious, and this thesis is as much your achievement as it is mine.

Table of Contents

List of Contributors *1*

Acknowledgements *2*

List of Figures *9*

Chapter I: **9**

Chapter III: **9**

Chapter IV: **10**

Chapter V: **10**

Chapter VI: **11**

List of Tables *13*

Chapter V: **13**

List of Abbreviations *14*

Abstract *20*

Chapter I: Introduction *22*

1.1 The hallmarks of cancer **22**

1.1.1 Cell signalling in cancer 22

1.1.2 The tumour microenvironment 24

1.1.3 The IGF axis 25

1.1.4 The insulin receptor 28

1.1.5 PI3K/AKT/mTOR pathway 30

1.1.6 MAPK/ERK pathway 34

1.1.7 The IGF axis in cancer 35

1.1.8 IGFs and upstream growth factor signalling 40

1.2 Prostate cancer **40**

1.2.1 Role of androgens 41
1.2.2 PSA testing 42
1.2.3 Treatment 42
1.2.4 Endocrine resistance 43
1.3 Response to ionising radiation 44
1.3.1 Double strand breaks 46
1.3.2 DNA damage sensors 47
1.3.3 DSB repair pathways 50
1.3.4 Cell signalling and the DNA damage response 52
1.4 Gene editing 58
1.4.1 Gene knockout 58
1.4.2 Nucleotide substitutions 63
1.5 Hypothesis and aims 72
Chapter II: Materials & Methods 74
2.1 Cell culture 74
2.2 siRNA knockdown 75
2.3 Western blotting 75
2.4 Antibodies 77
2.5 2D clonogenic survival assay 79
2.6 CRISPR/Cas9 gene editing 80
2.6.1 Oligonucleotide list 80
2.6.2 Plasmid list 83
2.6.3 Annealing single-stranded oligonucleotides 83
2.6.4 Restriction enzyme digestion 83
2.6.5 Ligation of gRNAs into digested vectors 84
2.6.6 Bacterial transformations 84
2.6.7 Plasmid DNA purification 85

2.6.8 Plasmid transfections 85

2.6.9 Genomic DNA extraction and polymerase chain reaction 86

2.6.10 PCR product purification 87

2.6.11 Sanger sequencing 87

2.6.12 Alt-R genome editing detection 88

2.6.13 Golden Gate assembly 89

2.6.14 Data analysis tool for gene editing 90

2.7 Flow Cytometry 90

2.8 Cell-based ELISA 91

2.9 Membrane Localisation 92

2.10 Nuclear Localisation 92

2.11 Immunofluorescence 93

2.12 3D spheroid assay 94

2.13 CellTiter-Glo 3D cell viability assay 95

2.14 Proteomics and phosphoproteomics sample preparation 95

2.15 End Joining Assay 96

2.16 Chromatin Fractionation 97

2.17 TOPO TA cloning 98

2.18 Statistical analysis 98

CHAPTER III: Generation of IGF-1R compromised cells using CRISPR/Cas9 gene editing techniques 99

3.1 Testing effects of IGF-1R depletion in prostate cancer cells 99

3.2 Creation of IGF-1R null clones 102

3.3 Creation of IGF-1R mutant clone 111

3.3.1 HDR-mediated gene editing strategy to create IGF-1R kinase-dead clones 112

3.3.2 DSB-independent methods of nucleotide substitution 124

3.4 Discussion 134

CHAPTER IV: Testing the phenotype of IGF-1R compromised cells 137

4.1 Testing radio-sensitivity of IGF-1R null clones 137

4.2 Characterisation of IGF-1R$^{+/-}$ clone 140

4.2.1 Testing receptor kinase activity of the hypomorphic mutant clone 141

4.2.2 Subcellular localisation of the hypomorphic mutant clone 146

4.3 Exploring the effect of *IGF1R* gene dosage and kinase activity in radio-sensitisation 150

4.3.1 Clonogenic survival assays 150

4.4 Testing proliferation and radio-sensitivity in 3D 153

4.5 Investigating the cellular response to IR 159

4.5.1 DNA damage markers 159

4.5.2 Apoptosis 161

4.5.3 DNA damage foci 161

4.6 Discussion 165

CHAPTER V: Investigating the role of IGF-1R signalling in response to IR 173

5.1 Introduction 173

5.2 Sample preparation 174

5.3 Analysis of proteomic & phosphoproteomic data in WT and IGF-1R null clones 178

5.3.1 Proteomic Data 178

5.3.2 Phospho-proteomic Data 183

5.4 Discussion 203

5.4.1 Proteome 203

5.4.2 Phospho-proteome 204

CHAPTER VI: Investigation of the requirement for IGF-1R in non-homologous end joining *207*

6.1 Introduction **207**

6.2 Exploring the role of IGF-1R in non-homologous end joining **209**

6.3 Examining the effect of IGF-1R on DNA-PK$_{cs}$ phosphorylation **217**

6.4 Investigating DNA-PK$_{cs}$ recruitment to chromatin **227**

6.5 Discussion **230**

CHAPTER VII: Conclusion and future directions *241*

Reference list *249*

List of Figures

Chapter I:

Figure 1.1: IGF-1R structure.....26

Figure 1.2: The IGF axis.....29

Figure 1.3: The cellular response to DNA double strand breaks.....45

Figure 1.4: CRISPR mediated gene editing.....62

Figure 1.5: HDR-mediated nucleotide substitution.....65

Figure 1.6: The use of prime editing to generate nucleotide substitutions.....69

Figure 1.7: Optimised prime editing strategy to facilitate edited strand inclusion.....71

Chapter III:

Figure 3.1: IGF-1R depletion radio-sensitises DU145 and 22Rv1 cells. 102

Figure 3.2: Testing the efficiency of candidate gRNAs for successfully targeting IGF1R exon 2.....104

Figure 3.3: Generation and characterisation of IGF-1R null clones.....106

Figure 3.4: Summary of IGF-1R ELISA to identify IGF-1R null 22Rv1 clones. 107

Figure 3.5: Characterisation of IGF-1R null clones by Western blot.....108

Figure 3.6: Characterisation of IGF-1R null clones by Sanger sequencing. 110

Figure 3.7: Generation and selection of an apparently novel IGF-1R kinase-dead clone. 113

Figure 3.8: Summary of IGF-1R ELISA to identify candidate IGF-1R kinase-dead clones.116

Figure 3.9: Analysis of candidate IGF-1R kinase-dead clones by Western blotting.....117

Figure 3.10: Analysis of candidate IGF-1R kinase-dead clones by Sanger sequencing. 121

Figure 3.11: Sequencing of candidate kinase-dead clone alleles.....122

Figure 3.12: Summary of base editing attempts to generate the IGF-1R K1003R mutant....126

Figure 3.13: The design of prime editing constructs. 128

Figure 3.14: Results of prime editing. 131

Figure 3.15: Summary of IGF-1R ELISA to identify IGF-1R kinase-dead clones by prime editing. 134

Chapter IV:

Figure 4.1: IGF-1R null clones exhibit increased radio-sensitivity. 140

Figure 4.2: Western blot analysis of IGF-1R null and hypomorphic mutant clones in basal conditions. 145

Figure 4.3: Western blot analysis of IGF-1R null and hypomorphic mutant clones after IGF-1 stimulation. 145

Figure 4.4: Characterisation of the kinase activity of the hypomorphic mutant. 146

Figure 4.5: Immunofluorescence to investigate subcellular localisation of IGF-1R. 147

Figure 4.6: Subcellular fractionation to investigate localisation of the hypomorphic mutant clone. 149

Figure 4.7: The hypomorphic mutant clone mimics the radio-sensitization phenotype of IGF-1R null clones. 153

Figure 4.8: Examining radio-sensitivity of IGF-1R depleted cells in a 3D spheroid model. 155

Figure 4.9: Examining radio-sensitivity of IGF-1R null cells in a 3D spheroid model. 157

Figure 4.10: Examining radio-sensitivity of the hypomorphic mutant clone in a 3D spheroid model. 158

Figure 4.11: Examination of classical markers of DNA damage and apoptosis after irradiation. 160

Figure 4.12: Loss of IGF-1R results in increased γH2AX foci after 2 Gy irradiation. 164

Chapter V:

Figure 5.1: Overview of proteomics and phosphoproteomics screen method. 174

Figure 5.2: Analysis of samples for proteomic and phosphoproteomic screens.....177

Figure 5.3: Quality control assessment of proteomic samples. 180

Figure 5.4: Comparison of normalised protein abundance between proteomic samples. 180

Figure 5.5: Examination of the effect of IGF-1R status and irradiation on the proteome. 182

Figure 5.6: Heat map depicting differentially detected phospho-peptides. 184

Figure 5.7: Principal component analysis comparing phospho-proteins between samples...185

Figure 5.8: Examination of significantly altered phospho-proteins in IGF-1R WT clones upon irradiation using pathway analysis software. 187

Figure 5.9: Examination of significantly altered phospho-proteins in IGF-1R null clones upon irradiation using pathway analysis software. 189

Figure 5.10: Examination of significantly altered phospho-proteins in IGF-1R WT and null clones pre-irradiation using pathway analysis software. 191

Figure 5.11: Examination of significantly altered phospho-proteins in IGF-1R WT and null clones post-irradiation using pathway analysis software. 192

Figure 5.12: Examination of the effect of IGF-1R status and irradiation on the phospho-proteome. 193

Figure 5.13: Examination of the effect of IGF-1R status and irradiation on the mismatch repair pathway.....199

Figure 5.14: Examination of individual phosphorylation sites altered between samples.....203

Chapter VI:

Figure 6.1: Loss of IGF-1R increased relative levels of MMEJ. 212

Figure 6.2: Loss of IGF-1R decreased 53BP1 foci formation after IR.....214

Figure 6.3: Investigation of the effect of DNA-PK_{cs} inhibition on γH2AX foci in IGF-1R WT and null cells. 216

Figure 6.4: Quantification of γH2AX foci after DNA-PK$_{cs}$ inhibitor treatment in IGF-1R WT and null cells. 216

Figure 6.5: Analysis of response to increasing radiation dose in IGF-1R WT and null clones. 219

Figure 6.6: Analysis of phosphorylation of ATM and DNA-PK$_{cs}$ in the response to IR in IGF-1R WT and null clones. 222

Figure 6.7: Investigation of DNA-PK$_{cs}$ threonine 2609 phosphorylation after IR in IGF-1R WT and null cells. 224

Figure 6.8: Investigation of inhibition of major IGF-1R signalling pathways. 226

Figure 6.9: Examination of proteins bound to chromatin after IR. 230

Figure 6.10: Schematic of the organisation of DNA-PK$_{cs}$ domains and key phosphorylation sites. 233

Figure 6.11: Validation of nuclear IGF-1R interaction with DNA-PK$_{cs}$. 239

List of Tables

Chapter V:

Table 5.1: Differentially expressed proteins in proteomic analyses. 183

Table 5.2: Comparison of differentially altered phospho-proteins between unirradiated IGF-1R WT and null clones in phospho-proteomic analyses.....195

Table 5.3: Comparison of differentially altered phospho-proteins between IGF-1R WT and null clones post-irradiation in phospho-proteomic analyses.....197

List of Abbreviations

53BP1	P53-binding protein 1
ABCB6	ATP-binding cassette subfamily B member 6
ABE	Adenine base editor
ADT	Androgen deprivation therapy
AFF4	AF4/FMR2 family member 4
AGTRAP	Angiotensin I receptor-associated protein
APAF-1	Apoptotic protease-activating factor 1
APBA2	Amyloid beta precursor protein binding family A member 2
APOBEC1	Apolipoprotein B-editing enzyme, catalytic polypeptide-1
AR	Androgen receptor
ARE	Androgen responsive element
ARS	Aminoacyl-tRNA synthetase
ASF1B	Anti-silencing function 1B histone chaperone
ATAD2B	ATPase family AAA domain-containing protein 2B
ATM	Ataxia telangiectasia mutated
ATP	Adenosine triphosphate
ATR	ATM-Rad3-related
ATRIP	ATR-interacting protein
BAD	BCL-2 associated agonist of cell death
BAG3	BCL-2-associated athanogene 3
BAK	BCL-2 antagonist/killer 1
BAX	BCL-2 associated X
BAZ1A	Bromodomain adjacent to zinc finger domain 1A
BAZ1B	Bromodomain adjacent to zinc finger domain 1B
BAZ2A	Bromodomain adjacent to zinc finger domain 2A
BCL-2	B-cell lymphoma 2
BCL11A	B-cell lymphoma/leukaemia 11A
BCL_{XL}	B-cell lymphoma-extra large
BH3	Bcl-2 homology domain 3
BHLHA15	Basic helix-loop-helix family member A15
BIM	BCL-2-like protein 11
BNIP3	BCL-2 interacting protein 3
Bp	Base-pair
BRAF	Serine/threonine-protein kinase B-raf
BRCA1	Breast cancer susceptibility protein 1
BRCA2	Breast cancer susceptibility protein 2
BrdU	Bromodeoxyuridine
CA9	Carbonic anhydrase 9
Cas	CRISPR-associated
CASZ1	Castor zinc finger 1
CBE	Cytosine base editor
CDA1	Cytidine deaminase 1

CDK	Cyclin-dependent kinase
cDNA	complementary DNA
CHD1	Chromodomain helicase DNA binding protein 1
CHK2	Checkpoint kinase 2
CK2	Casein Kinase 2
CLDN3	Claudin 3
CLSPN	Claspin
cNHEJ	Classical non-homologous end joining
COPS3	COP9 signalosome subunit 3
CRISPR	Clustered regularly interspaced short palindromic repeat
CRPC	Castrate-resistant prostate cancer
CtIP	C-terminal binding protein interacting protein
CUL4B	Cullin 4B
DBC1	Deleted in breast cancer 1
dCas9	Dead-Cas9
DDR	DNA damage response
DDX1	DEAD-box helicase 1
DER	Dose enhancement ratio
DGAT1	Diacylglycerol O-acyltranferase 1
DHCR7	7-dehydrocholesterol reductase
DHT	Dihydrotestosterone
DNA	Deoxyribonucleic acid
DNA-PK	DNA-dependent protein kinase
DNA-PKcs	DNA-dependent protein kinase catalytic subunit
DNMT1	DNA methyltransferase 1
dNTP	deoxynucleoside triphosphate
DNTTIP2	Deoxynucleotidyltransferase terminal-interacting protein 2
DSB	Double-strand break
dsDNA	Double stranded DNA
EFHD2	EF-head domain family member D2
EGF	Epidermal growth factor
EGFR	Epidermal growth factor receptor
ELISA	Enzyme-linked immunosorbent assay
EMT	Epithelial-mesenchymal transition
ER	Endoplasmic reticulum
FACS	Fluorescence-activated cell sorting
FAK	Focal adhesion kinase
FAM21	Family with sequence similarity 21
FAS	Fas cell surface death receptor
FE	Relative fold enrichment
FGF	Fibroblast growth factor
FOXO	Class O of forkhead box
GAPDH	Glyceraldehyde 3-phosphate dehydrogenase
GBM	Glioblastoma
GC	Guanine-cytosine

GEMIN5	Gem nuclear organelle-associated protein 5
GFP	Green fluorescent protein
GFPT1	Glutamine-fructose-6-phosphate transaminase 1
GH	Growth hormone
GO	Gene Ontology
GRB2	Growth factor receptor-bound protein 2
gRNA	Guide RNA
GSK3	Glycogen synthase kinase 3
GTP	Guanosine triphosphate
Gy	Gray
HBB	Haemoglobin subunit β
HDAC	Histone deacetylase
HDR	Homology directed repair
HGG	High-grade glioma
HIF	Hypoxia-inducible factor
HIF-1α	Hypoxia-inducible factor 1 subunit α
HMGN5	High mobility group nucleosome binding domain 5
HNRNPC	Heterogeneous nuclear ribonucleoprotein C
HNRNPD	Heterogeneous nuclear ribonucleoprotein D0
HNRNPM	Heterogeneous nuclear ribonucleoprotein M
HNRNPU	Heterogeneous nuclear ribonucleoprotein U
HP1-β	Heterochromatin protein 1β
HR	Homologous recombination
HSPB6	Heatshock protein family B (small) member 6
HUWE1	HECT, UBA and WWE-containing E3 ubiquitin ligase 1
IF	Immunofluorescence
IP	Immunoprecipitation
IGF	Insulin-like growth factor
IGF-1R	Insulin-like growth factor 1 receptor
IGFBP	IGF binding protein
IHC	Immunohistochemistry
INSR	Insulin receptor
IR	Ionising radiation/irradiation
IRF2BP1	Interferon regulatory factor 2 binding protein 1
IRS	Insulin receptor substrate
JNK	JUN N-terminal kinase
KAP1	KRAB-associated protein 1
KAT	Lysine acetyltransferase
KD	Kinase-dead
LAP2A	Lamina-associated polypeptide 2, isoform alpha
LAP2B	Lamina-associated polypeptide 2, isoform beta
LC-MS/MS	Liquid chromatography-mass spectrometry
LH	Luteinising hormone
LHRH	Luteinising hormone-releasing hormone
LMNA	Lamin A/C

mAb	Monoclonal antibody
MAP2K	MAPK kinase
MAP4	Non-neuronal microtubule-associated protein
MAP4K	MAPK kinase kinase kinase
MAPK	Mitogen-activated protein kinase
MARS	Methionyl-tRNA synthetase
MCL-1	Myeloid leukaemia 1
MCM2	Minichromosome maintenance complex component 2
MDC1	Mediator of DNA damage checkpoint 1
miRNA	Micro RNA
MKK6	MAPK/ERK kinase 6
MMEJ	Microhomology-mediated end joining
MMP	Matrix metallopeptidase
MMR	Mismatch repair
MRE11	Meiotic recombination 11
mRNA	Messenger RNA
MSH6	MutS homolog 6
mTOR	Mechanistic target of rapamycin
mTORC1	Mechanistic target of rapamycin 1
mTORC2	Mechanistic target of rapamycin 2
MYO1C	Myosin 1C
NBS1	Nijmegen breakage syndrome 1
NHEJ	Non-homologous end joining
NOP9	NOP9 nucleolar protein
NuMA	Nuclear mitotic apparatus protein 1
P53	Tumour protein P53
PAICS	Phosphoribosylaminoimidazole carboxylase
PAK1	p21-activated kinase 1
PAM	Protospacer-adjacent motif
PAP	Prostate-specific acid phosphatase
PARP	Poly (ADP-ribose) polymerase
PBRM1	Polybromo 1
PBS	Primer binding site
PCa	Prostate cancer
PCNA	Proliferating cell nuclear antigen
PCR	Polymerase chain reaction
PDK1	Pyruvate dehydrogenase kinase 1
pegRNA	Prime editing guide RNA
PI3K	Phosphoinositide 3-kinase
PIKK	PI3K-like
PIP2	Phosphatidylinositol 4,5-bisphosphate
PIP3	Phosphatidylinositol 3,4,5-triphosphate
PKM2	Pyruvate kinase M2
PLK1	Polo-like kinase 1
PP2A	Protein phosphatase 2A

PPP6C	Protein phosphatase 6 catalytic subunit
PRAS40	Protein-rich AKT substrate 1
PSA	Prostate-specific antigen
PTEN	Phosphatase and tensin homologue deleted on chromosome 10
PTIP	Pax transactivation domain-interacting protein
RAC1	Rac family small GTPase 1
RANBP1	Ran-specific GTPase-activating protein 1
RB	RB transcriptional corepressor 1
RBMX	RNA-binding motif protein X-linked
RECQ4	ATP-dependent DNA helicase Q4
RFU	Relative fluorescence unit
RHEB	Ras homolog enriched in brain
RIF-1	RAP1-interacting factor 1
RNA	Ribonucleic acid
RNAPOL2	RNA polymerase 2
ROS	Reactive oxygen species
RPA32	Replication protein A
RRM2	Ribonucleotide reductase regulatory subunit M2
RT	Reverse transcriptase
SAFB	Scaffold attachment factor B
SAFB2	Scaffold attachment factor B2
SAGA	SPT-ADA-GCN5 acetyltransferase
SCAI	Suppressor of cancer cell invasion
SHC	Src homology 2 domain containing-transforming protein 1
siRNA	Small interfering RNA
SLC12A9	Solute carrier family 12 member 9
SLC9A1	Solute carrier family 9 member A1
SNRNP200	Small nuclear riboprotein U5 subunit 200
SNX2	Sorting nexin 2
SOAT1	Sterol O-acyltransferase 1
SOS	Son of sevenless
SPEN	Msx2-interacting protein
SPTY2D1	SPT2 chromatin protein domain containing 1
SRRM2	Serine/arginine repetitive matrix 2
SSB	Single-strand break
ssDNA	Single stranded DNA
ssODN	Single-stranded oligodeoxynucleotide
T7E1	T7 endonuclease I
TALE	Transcription activator-like effector
TALEN	Transcription activator-like effector nuclease
TF3C1	General transcription factor 3C polypeptide 1
TFDP1	Transcription factor Dp-1
TGF	Transforming growth factor
TKI	Tyrosine kinase inhibitor
TME	Tumour microenvironment

TMZ	Temozolomide
TOP2	DNA topoisomerase II
TOP2A	DNA topoisomerase IIα
TOP2B	DNA topoisomerase IIβ
TOR1AIP1	Torsin 1A-interacting protein
TRIP12	Thyroid hormone receptor interactor 12
TSC2	TSC complex subunit 2
TSP	Thrombospondin
U-G	Uracil-guanine
UBP36	Ubiquitin-specific peptidase 36
UIMC1	Ubiquitin interaction motif containing 1
USP	Ubiquitin-specific protease
UV	Ultraviolet light
VEGF	Vascular endothelial growth factor
VHL	Von Hippel-Lindau tumour suppressor
WIP1	Wild-type p53-induced phosphatase 1
WT	Wild-type
WT1	Wilms tumour 1
XLF	XRCC4-like factor
XRCC1	X-ray repair cross complementing 1
XRCC4	X-ray repair cross complementing 4
YBX2	Y-box binding protein 2
ZBTB21	Zinc finger and BTB domain containing 21
ZEB	Zinc finger E-box binding homeobox
ZFN	Zinc finger nuclease

Abstract

The insulin-like growth factor (IGF) axis is an important regulator of cancer cell proliferation, growth, invasion, and can also mediate therapy resistance. Inhibition or depletion of the type 1 IGF receptor (IGF-1R) has been shown by our laboratory and others to enhance sensitivity to ionising radiation (IR) and chemotherapy, and to impair repair of DNA double-strand breaks (DSBs). Our group also reported association of high *IGF1R* expression with radio-resistance and biochemical recurrence after IR for prostate cancer (PCa). The overall aim of this project was to investigate the molecular basis for IGF-1R-mediated radio-resistance using an androgen receptor-positive (AR+) PCa model. The first aim was to recapitulate in AR+ 22Rv1 PCa cells the radio-sensitisation phenotype observed previously. First, *IGF1R* gene silencing was shown to radio-sensitise AR- DU145 PCa cells as shown previously in our laboratory, with similar radio-sensitisation in 22Rv1 cells. Secondly, to test whether radio-resistance requires the kinase activity or structural functions of the receptor, CRISPR/Cas9 genome editing was used to generate $IGF1R^{-/-}$ 22Rv1 clones. Attempts were also made to generate cells expressing kinase-dead (KD) IGF-1R; although these efforts were unsuccessful, a hypomorphic $IGF1R^{+/-}$ clone was produced. In 2D clonogenic survival assays, $IGF1R^{+/-}$ and $IGF1R^{-/-}$ displayed enhanced radio-sensitivity, with dose enhancement ratios (DERs) of $\geq$ 1.46 at 2 Gy, comparable to effects of IGF-1R knockdown. IR-induced DNA damage was quantified using γH2AX foci, and $IGF1R^{+/-}$ and $IGF1R^{-/-}$ clones showed significantly increased DNA damage 10-60 minutes post-IR, suggesting increased damage induction. The third aim of this project was to perform unbiased proteomic and phosphoproteomic screens on IGF-1R proficient and deficient 22Rv1 cells before and after IR, to generate information on the role of IGF-1R signalling in the response to IR. Examination of the phosphoproteomic dataset suggested IGF-1R-dependent differences in IR-induced serine 3205 phosphorylation of the major DNA damage response (DDR) protein DNA-dependent protein kinase catalytic subunit (DNA-PK_{cs}),

required for classical non-homologous end joining (cNHEJ). This finding prompted exploration of a possible role for IGF-1R in cNHEJ. Indeed, experiments suggested that DNA repair dynamics were altered in *IGF1R*$^{-/-}$ clones, with increase in repair by microhomology-mediated end joining (MMEJ) and significantly reduced p53-binding protein 1 (53BP1) foci after IR compared to IGF-1R WT cells. Both findings suggested that cNHEJ was compromised. There was further evidence of a role for IGF-1R in cNHEJ, with significantly reduced IR-induced autophosphorylation of DNA-PK$_{cs}$ at serine 2056, and apparent absence of DNA-PK$_{cs}$ recruitment to chromatin in *IGF1R*$^{-/-}$ clones. These data are consistent with the reported need for DNA-PK$_{cs}$ chromatin recruitment to trigger autophosphorylation. In summary, data presented here support a role for IGF-1R in mediating radio-resistance; a KD clone would be needed to clarify whether this property requires the presence of IGF-1R protein and/or its kinase activity. Finally, a novel role was identified for IGF-1R in radio-resistance and cNHEJ by promoting DNA-PK$_{cs}$ recruitment to chromatin and autophosphorylation. These results have significance both for basic biology and clinical practice. The data shed light on the contribution of IGFs to the DNA damage response, with potential to inform treatment options, selection of patients for radiotherapy, and development of novel approaches to radio-sensitisation.

Chapter I: Introduction

1.1 The hallmarks of cancer

For normal cells to progress towards a neoplastic state, they must acquire certain novel characteristics, which ultimately result in uncontrollable proliferation, evasion of tumour suppressors, replicative immortality, increased angiogenesis and resistance to cell death (Carmeliet and Jain, 2000; Hanahan and Weinberg, 2011; Igney and Krammer, 2002; Kelland, 2007).

1.1.1 Cell signalling in cancer

Cancer cells often exhibit hyperactive signalling pathways, most functioning to sustain proliferative signalling. This can occur in different ways, culminating in effects on cell cycle control and changes to tissue architecture. The strategies that cells employ to maintain proliferative signalling include self-production of growth factors, stimulation of neighbouring cells to secrete required growth factor ligands and altering receptor expression/structure at the cell surface (Feitelson et al., 2015). Furthermore, to bypass ligand-mediated stimulation, cancer cells are able to constitutively activate signalling pathways downstream of the receptor, thus negating mitogenic signalling altogether (Davies and Samuels, 2010). Mutations that cause constitutive activation of signalling pathways have become clearer as genomic sequencing techniques have become more comprehensive and robust (Bailey et al., 2018). There is now a greater appreciation for the large variety of mutations that cancer cells accrue, and how these mutations provide tumour cells with a selective advantage over normal cells.

Proto-oncogenes, usually involved in cell growth and differentiation, are frequently mutated in tumours, and these mutations or altered expression patterns lead to activation of oncogenes, named for their ability to promote cancer-causing cellular characteristics. Classic examples of oncogenes include *SRC* (Czernilofsky et al., 1980; Martin, 2001), RAS (Pylayeva-Gupta et al., 2011; Reddy et al., 1982), *BCR-ABL* (Groffen et al., 1984; Salesse and Verfaillie, 2002; Shtivelman et al., 1985) and *MYC* (Meyer and Penn, 2008), all of which are either mutated, translocated or upregulated in the majority of cancers (Croce, 2008).

In addition to oncogenic mutations that directly activate signalling cascades, there are also mutations which deactivate inhibitory signals, leading to a similar pro-proliferative result. Tumour suppressors are proteins which function primarily to inhibit cell proliferation and tumour development, providing a mechanism for cells to arrest the cell cycle and undergo DNA repair or apoptosis (Sherr, 2004). Cancer cells are able to evade tumour suppressors, overriding cell cycle checkpoints, accumulating more mutations and increasing genomic instability (Negrini et al., 2010). Loss of tumour suppressor tumour protein P53 (*TP53*) and RB transcriptional corepressor 1 (*RB*) expression, and manipulation of the balance of apoptotic factors by tumour cells allows for cancer cells to resist apoptosis (Lowe and Lin, 2000; Mantovani et al., 2019; Niederst et al., 2015; Sherr and McCormick, 2002).

Normally, apoptosis or senescence occurs after a certain number of cell cycles (Campisi and d'Adda di Fagagna, 2007). This is predominantly due to the shortening of telomeres which protect the ends of chromosomes (Blasco et al., 1997). In cancer cells, telomerase, the enzyme tasked with extending telomeric DNA, is present at higher levels than in normal cells (Harley, 2008). Increased telomerase levels results in stabilisation of telomeres and continuous cell

divisions (Shay, 2016). This acquired ability to resist senescence and cell death allows oncogenic cells to become immortal.

1.1.2 The tumour microenvironment

Uncontrollable proliferation and evasion of inhibitory signals increases the demand for nutrients in the neoplasm. To counter this threat to tumour survival, cancer cells induce angiogenesis, providing new vessels to deliver nutrients and oxygen, and to remove carbon dioxide and metabolic by-products (Tonini et al., 2003). Activation of this angiogenic switch occurs upon manipulation of pro- and anti-angiogenic factors such as vascular endothelial growth factor (VEGF)-A and thrombospondins (TSPs), respectively (Bergers and Benjamin, 2003). The extent of neovascularisation varies between tumours, governed by the oncogenic cells themselves and the surrounding tumour microenvironment (TME).

The TME plays a critical role in cancer progression by providing specific signals and interactions to promote proliferation, invasion and finally metastasis. The initiation of metastasis involves the epithelial-mesenchymal transition (EMT), where amongst other adaptations, epithelial cells decrease expression of E-cadherin, a protein which functions to maintain adhesion between neighbouring cells (Lamouille et al., 2014). This change in plasticity allows epithelial cells to acquire the migratory and invasive properties of mesenchymal cells, resulting in local invasion, transport in the bloodstream, deposition at a distant site, and eventually the establishment of metastases (Kalluri and Weinberg, 2009).

In primary and metastatic tumours, cancer cells must avoid detection by the comprehensive immunosurveillance system evolved to prevent oncogenesis. The actions of immune cells to target and destroy cancer cells by recognition of tumour antigens is broadly successful. However, it provides an effective selection tool for tumour cells with specific mutations that facilitate the evasion of the immune system (Vinay et al., 2015). Selection of immune effector-resistant cells combined with the formation of an immune-suppressive environment within the TME promotes cancer progression, and significant research focus into immunotherapeutics has begun to yield promising results (Dougan et al., 2019; Waldman et al., 2020).

Many signalling pathways mutated in cancer influence core metabolic processes and as a result, cancer is increasingly regarded as a metabolic disease (Seyfried et al., 2014). Cancer-associated metabolic changes can maximise tumour cell survival in the nutrient-deprived TME (Sullivan et al., 2016) by promoting nutrient acquisition and assignment to pro-tumourigenic pathways (Anastasiou, 2016; Cairns et al., 2011). This is achieved by mutating key metabolic enzymes, and manipulating gene expression and the nutrient composition of the extracellular milieu (Pavlova and Thompson, 2016).

1.1.3 The IGF axis

The type 1 insulin-like growth factor receptor (IGF-1R) is a transmembrane receptor tyrosine kinase expressed in almost all normal tissues (Moschos and Mantzoros, 2002). It consists of two extra-cellular α-subunits comprising a binding site for a single molecule of ligand, and two β-subunits spanning the membrane which include the intracellular tyrosine kinase domains (Adams et al., 2000; De Meyts and Whittaker, 2002a; Ullrich et al., 1986) (Fig. 1.1).

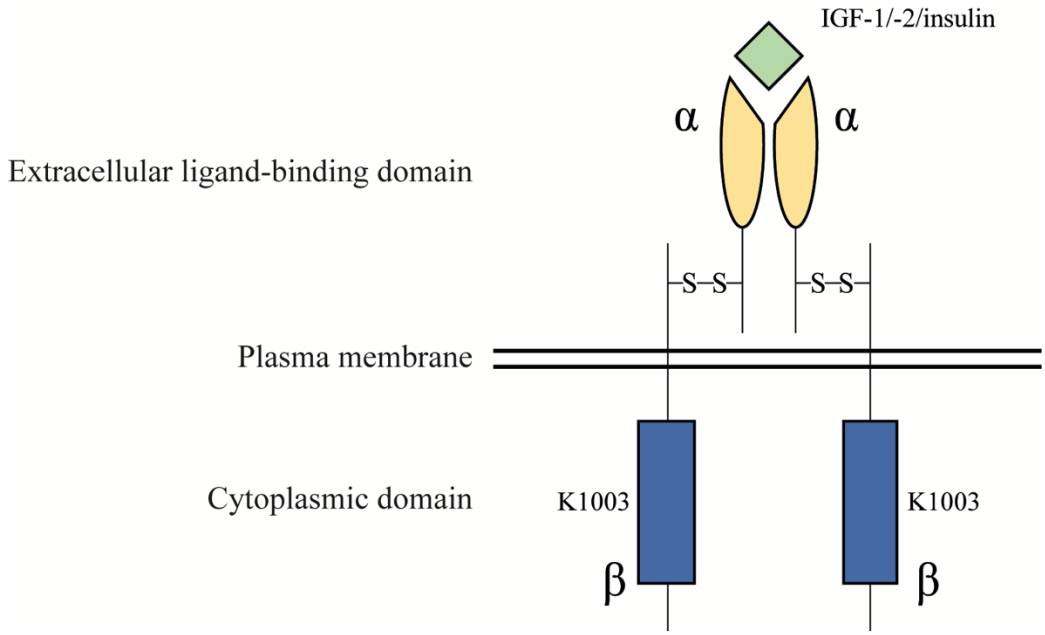

Figure 1.1: IGF-1R structure.
Schematic displaying the simplified structure of IGF-1R with the ligand (green), α subunit (yellow), and β subunit (blue) including K1003 at the ATP-binding site of the IGF-1R kinase domain (Kato et al., 1993).

Activation of the receptor is facilitated by binding of IGF-1, IGF-2 or insulin to the ligand-binding cleft of the α-subunits, with IGF-1 exhibiting much greater binding affinity (Baker et al., 1993; De Meyts et al., 1994). Serum IGFs mainly come from the liver, and IGF-1 in response to growth hormone (GH) (Ohlsson et al., 2009; Scarth, 2006). IGFs are important for mediating the effects of GH on normal development (Rosenfeld, 2005). In the unstimulated state, key residues tyrosine 1131, 1135 and 1136 in the activation loop act as a pseudo-substrate, blocking the active site (Jiang et al., 1996). Ligand-binding disrupts the auto-inhibited IGF-1R dimer, initiating a conformational rearrangement and the formation of an asymmetric active dimer (J. Li et al., 2019). Phosphorylation of tyrosine 1131 and 1135 in the activation loop destabilise the auto-inhibitory conformation, and tyrosine 1136 phosphorylation serves to stabilise the catalytically optimised conformation to allow substrate and adenosine triphosphate (ATP) access (Kato et al., 1994). IGF-1R activation predominantly leads to recruitment and phosphorylation of insulin receptor substrates (IRS) 1 and 2, and Src

homology 2 domain containing-transforming protein 1 (SHC), resulting in activation of multiple signalling pathways as discussed below.

Upon activation, internalised IGF-1R can translocate to the nucleus, be recycled to the plasma membrane or be degraded (Aleksic et al., 2018, 2010; Crudden et al., 2019; Sehat et al., 2007). Studies by the Macaulay group and others indicate that the receptor directly binds DNA, that nuclear translocation requires SUMOylation of the receptor, and that nuclear translocation is mediated by clathrin (Aleksic et al., 2010; Salani et al., 2010; Sehat et al., 2010). Once inside the nucleus, IGF-1R interacts with RNA polymerase 2 (RNAPOL2), increasing the expression of *JUN* and *FAM21* promoters, functioning as a transcriptional cofactor (Aleksic et al., 2018; Warsito et al., 2012). *JUN* has been shown to be upregulated in various carcinomas, enhancing proliferation and survival, and *FAM21* has a role in cell migration (Zech et al., 2011). A study has recently shown an interaction between nuclear IGF-1R and nuclear mitotic apparatus protein (NuMA) in IGF1R-overexpressing colorectal cancer cells, suggesting a regulatory role of nuclear IGF1R in the localisation of NuMA-p53-binding protein 1 (53BP1) after irradiation (IR) (Yang et al., 2021). Further, nuclear IGF-1R-mediated phosphorylation of proliferating cell nuclear antigen (PCNA) following IR has been reported, leading to PCNA ubiquitination, and subsequent regulation of replication fork stalling (Waraky et al., 2017). While interactions between DNA or nuclear proteins and nuclear IGF-IR have been described, the mechanisms involved in the observed radio-resistance have not been characterised.

1.1.4 The insulin receptor

The insulin receptor (INSR) exists as one of two isoforms arising through alternative splicing, INSR-A and INSR-B, which are usually expressed in foetal and adult tissue, respectively (Denley et al., 2004; Savkur et al., 2004). The INSR and IGF-1R evolved from one ancestral receptor and have developed distinct functions (Chitnis et al., 2008). INSR signalling predominantly has metabolic effects on the cell, whereas IGF-1R is principally involved in mitogenic and anti-apoptotic pathways (De Meyts et al., 1994; Kido et al., 2001). Relative affinity of IGF-1 for INSR-A and INSR-B is reported to vary between 9-41 nM and >30-390 nM, respectively (Benyoucef et al., 2007; Frasca et al., 1999; Yamaguchi et al., 1993), whereas IGF-1 is reported to have a sub-nM affinity (0.2-0.8 nM) for IGF-1R (Belfiore et al., 2009; Denley et al., 2004; Pandini et al., 2002) using ligand competition assays or bioluminescence resonance energy transfer (BRET). Further, affinity of insulin for IGF-1R has been shown to be between >30->1,000 nM, compared to 0.2-0.9 nM and 0.5-1.6 nM for INSR-A and INSR-B, respectively (Belfiore et al., 2009; Benyoucef et al., 2007; Denley et al., 2004; Frasca et al., 1999; Pandini et al., 2002; Yamaguchi et al., 1993).

The IGF-1R and INSR share a high degree of sequence similarity, with greater than 50% homology overall, and 84% homology in the tyrosine kinase domain (Adams et al., 2000; Pandini et al., 2002; Ullrich et al., 1986). This likeness enables the formation of hybrid receptors immediately upon translation of the pro-receptor. An uncleaved molecule of IGF-1R can undergo disulphide bonding with one molecule of uncleaved INSR. This occurs randomly in proportion to the amount each receptor is expressed (Chen et al., 2018). After the disulphide bonds have formed, normal cleavage can ensue by furins (Jaaks et al., 2016). In most tissues where both receptors are expressed, these hybrid receptors are the most represented receptor subtype (Bailyes et al., 1997). Studies suggest that IGF-1R/INSR hybrids have a greater affinity

for IGF-1 than insulin, resulting in activation, and thus behave more like IGF-1R (Soos et al., 1993). Further work using artificially generated hybrids containing the intracellular INSR domain indicate that these modified receptors exhibit greater effects on genes involved in metabolic pathways, whereas hybrids containing the IGF-1R intracellular domain are involved in cell proliferation (Cai et al., 2017). Additionally, Cai *et al.* demonstrated that performing the mutation L973F in INSR, to mimic F973 in IGF-1R, allows the mutated INSR to behave like IGF-1R (Cai et al., 2017). The amino acid substitution in the juxtamembrane region is able to differentiate between INSR and IGF-1R signalling and effect substrate specificity. Both INSR and IGF-1R signal via multiple pathways, primarily RAS-RAF-Mitogen-activated protein kinase (MAPK) and phosphoinositide 3-kinase (PI3K)-AKT (Baserga et al., 1997; Larsson et al., 2005) (Fig. 1.2).

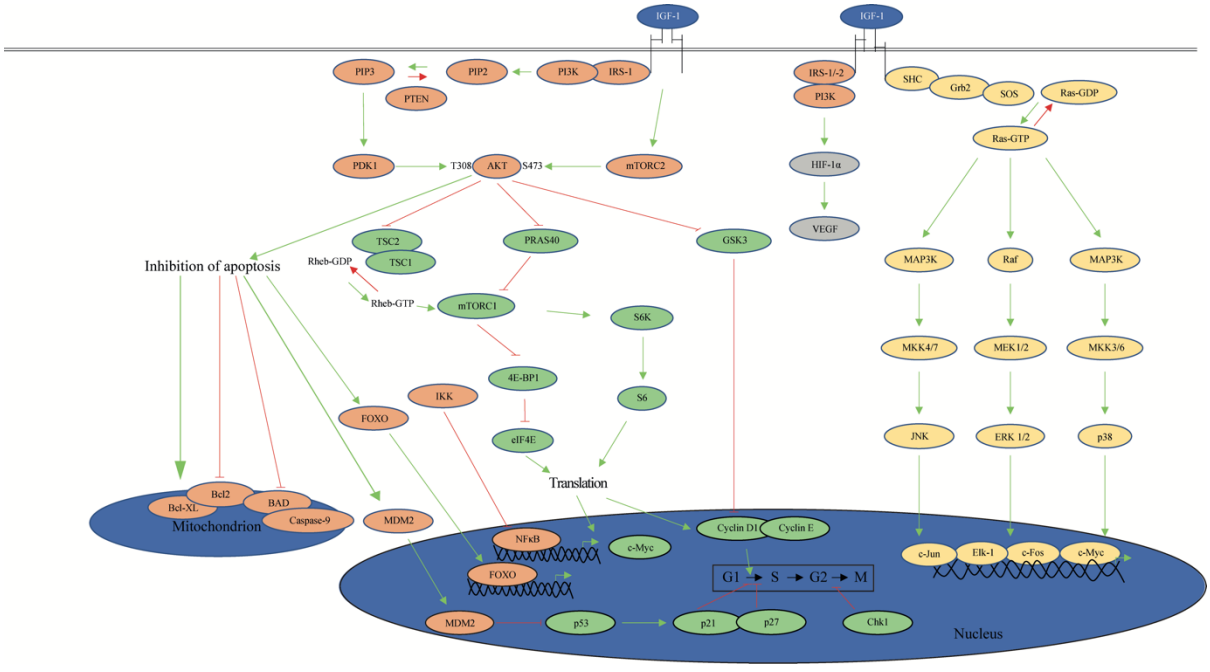

Figure 1.2: The IGF axis.
A schematic displaying the major signalling pathways downstream of IGF-1R. Activation (green arrows) and inhibition (red lines/arrows) of proteins are displayed. Proteins are highlighted according to broad effects on the cell (Orange = cell survival; green = cell growth and proliferation; yellow = invasion). This figure was adapted from Chitnis *et al.* 2008. Processes are described in more detail in text.

1.1.5 PI3K/AKT/mTOR pathway

The PI3K/AKT/mechanistic target of rapamycin (mTOR) pathway is involved primarily in metabolic, pro-growth and pro-survival mechanisms (Franke, 2008), thus playing an important role in tumour biogenesis and as a prognostic indicator for cancers from several distinct origins (K. Chen et al., 2014; Hennessy et al., 2005; Liu et al., 2009; Sobhani et al., 2018). When activated, PI3K localises to the intracellular side of the plasma membrane, converting phosphatidylinositol 4,5-bisphosphate (PIP2) to phosphatidylinositol 3,4,5-triphosphate (PIP3). The main function of PIP3 is to interact with PH domain-containing proteins, such as AKT and pyruvate dehydrogenase kinase 1 (PDK1), bringing them to the plasma membrane (Ebner et al., 2017; Franke et al., 1997; Stokoe, 1997). Once recruited, the two key phosphorylation sites on AKT, threonine 308 and serine 473, can be phosphorylated. PDK1 targets threonine 308 in the activating T-loop of AKT (Alessi et al., 1997), whereas mammalian target of rapamycin 2 (mTORC2) is the principal kinase involved in serine 473 phosphorylation (Sarbassov et al., 2005). The major suppressor of the PI3K-AKT axis is phosphatase and tensin homologue deleted on chromosome 10 (PTEN), which acts to catalyse the dephosphorylation of PIP3 back to PIP2, thus inhibiting AKT activity (Maehama and Dixon, 1998; Stambolic et al., 1998). *PTEN* mutations are common in most cancers and are a critical reason why the PI3K-AKT axis is one of the most frequently dysregulated oncogenic pathways (Chalhoub and Baker, 2009).

1.1.5.1 Cell survival

To promote cell survival, AKT activates pro-survival and inhibits pro-apoptotic proteins, both directly and indirectly. B-cell lymphoma 2 (BCL-2) family proteins are integral to the function of the intrinsic apoptotic pathway. The family consists of three different protein subtypes with vastly different roles, and disruption of this equilibrium dictates the fate of the cell. Some BCL-

2 family members, such as BCL-2, B-cell lymphoma-extra large (BCL-X_L) and myeloid leukaemia 1 (MCL-1), act as anti-apoptotic factors, binding to and neutralising pro-apoptotic BCL-2 family members; BCL-2 homology domain 3 (BH3)-only proteins (Leavy, 2008; Segal et al., 2007; Zhang et al., 2013), and BCL-2 associated X (BAX) and BCL-2 antagonist/killer 1 (BAK); mediators of mitochondrial outer membrane permeabilization (Baig et al., 2016). BH3-only proteins are tasked with binding and oligomerising BAX and BAK, and neutralising anti-apoptotic family members in response to stress signals. When the delicate balance between pro- and anti-apoptotic BCL-2 family members shifts towards cell death, BH3-only proteins stimulate BAX and BAK to oligomerise, and then permeabilise the mitochondrial membrane (Westphal et al., 2014). This leads to cytochrome c mobilisation into the cytoplasm, binding with apoptotic protease-activating factor 1 (APAF-1) and procaspase-9 (Beere and Green, 2017). This stimulates the activation of caspase-9 and ultimately caspase-3 and -7, which cleave the majority of proteins during apoptosis (Brentnall et al., 2013; Porter and Jänicke, 1999). The major pro-apoptotic proteins AKT interacts with are BH3-only proteins such as BCL-2 associated agonist of cell death (BAD), which target BCL-2 family members for degradation (Happo et al., 2012). Interestingly, pro-survival factors instigate AKT and MAPK pathway-mediated phosphorylation of BAD at separate sites (Datta et al., 1997; Fang et al., 1999; Peso et al., 1997), which, through 14-3-3 binding site formation, leads to abrogation of BAD interactions with its target proteins (Datta et al., 2000). AKT can phosphorylate procaspase-9, leading to decreased protease activity *in vitro* (Cardone et al., 1998).

At a transcriptional level, AKT is able to affect BH3-only proteins indirectly via pro-apoptotic members of the class O of forkhead box (FOXO) transcription factors (Tran et al., 2003). Nuclear phosphorylation of several of these transcription factors results in their removal into the cytoplasm by 14-3-3 proteins. This, in turn, attenuates FOXO-mediated transcription of

anti-survival genes such as BCL-2-like protein 11 (BIM), BCL-2 interacting protein 3 (BNIP3) and Fas cell surface death receptor (FAS) ligand (Brunet et al., 1999; Herold et al., 2013; Tran et al., 2003).

At the protein level, AKT phosphorylates both MDM2 and glycogen synthase kinase (GSK3) α/β, initiating and inhibiting, respectively, their roles in cell survival. MDM2 phosphorylation commences its nuclear translocation where it is able to block p53-mediated apoptosis (Mayo and Donner, 2001; Zhou et al., 2001b). One function of GSK3α/β is to inhibit the pro-survival BCL-2 family member MCL-1 (Maurer et al., 2006) – an action inhibited by AKT phosphorylation (Cross et al., 1995).

1.1.5.2 Cell growth

Many of the pro-growth effects of AKT are channelled through mechanistic target of rapamycin 1 (mTORC1) – a key component of the mTOR pathway. This pathway has separate branches that together coordinate growth factor signalling, energy status, oxygen availability and amino acid levels; providing a direct way for cancerous cells to respond to environmental changes exhibited within the TME (Pópulo et al., 2012; Saxton and Sabatini, 2017). Ultimately, mTOR pathway output results in translation initiation and ribosome biogenesis. In growth signalling, AKT functions primarily to inhibit the mTORC1 inhibitors TSC2 and protein-rich AKT substrate 1 (PRAS40) (Haar et al., 2007; Kovacina et al., 2003; Manning et al., 2002; Sancak et al., 2007; Tapon et al., 2001). Metabolic adaptations frequently result from mutations to the mTOR pathway (Guertin and Sabatini, 2007), causing increased fatty acid synthesis, glycolytic flux and decreased demand for ATP (DeBerardinis and Chandel, 2016; Shanware et al., 2014; Vincent et al., 2015; Wong, 2013). Members of the PI3K/AKT/mTOR pathway are

commonly dysregulated in cancer (Asati et al., 2016; Yang et al., 2019), and as a consequence, mTOR pathway inhibitors are an attractive treatment option for anti-cancer therapy (Yuan and Cantley, 2008).

1.1.5.3 Cell proliferation

AKT regulation of cell proliferation is mainly achieved through inhibition of cell cycle checkpoints. AKT can phosphorylate the cyclin-dependent kinase (CDK) inhibitors $p21^{Cip21/WAF1}$ and $p27^{Kip1}$, blocking nuclear localisation and therefore attenuating inhibition of cell cycle progression (Liang et al., 2002; Zhou et al., 2001a). As mentioned above, one role of GSK3α/β is to inhibit pro-survival proteins. As well as these, it also targets G1/S phase cell cycle transition proteins, marking them for proteasomal degradation (Diehl et al., 1998; Welcker et al., 2003). Phosphorylation of GSK3α/β by AKT, therefore, indirectly stabilises cyclin D/E and certain transcription factors such as *c-MYC* and *c-JUN* (Yeh et al., 2004).

1.1.5.4 AKT and the cell cycle

AKT has been reported to affect a plethora of cell cycle proteins directly and indirectly upon activation by growth factors, ultimately acting to promote cell cycle progression. Studies have shown both AKT-dependent activation of key cell cycle promoters *c-MYC* (Ahmed et al., 1997) and CDK2 (Maddika et al., 2008), and inhibition of multiple tumour suppressors such as RB (Brennan et al., 1997), p53 (Ogawara et al., 2002) and WEE1 (Katayama et al., 2005). Further, studies have indicated that AKT can inhibit $p27^{Kip1}$, which functions to arrest cells in G1 (Toyoshima and Hunter, 1994). These actions lead to both G_1/S and G_2/M transition. Cell cycle checkpoints provide damaged cells with the opportunity to enter cell cycle arrest, preventing the cell from accumulating additional mutations (Kastan and Bartek, 2004). Activated AKT

has been shown to override the G2 cell cycle checkpoint in a p53-independent fashion (Henry et al., 2001; Kandel et al., 2002) and suppress the recruitment and activation of checkpoint kinase 2 (CHK2) at DNA damage locations (Hirose et al., 2005).

1.1.6 MAPK/ERK pathway

The MAPK signalling cascades, consisting of MAPKs (ERK1-6, 7-8, JUN N-terminal kinase (JNK), p38), MAPK kinases (MAP2Ks) (MEK1-7), MAPK kinase kinases (MAP3Ks) (including RAF, MEKK, MLK) and MAPK kinase kinase kinases (MAP4Ks) (RAS, RAC, RHO, CDC42), function in response to stress and extracellular signals regulating cell proliferation and differentiation (Dhillon et al., 2007; Keshet and Seger, 2010; Plotnikov et al., 2011; Sabio and Davis, 2014). There are four distinct pathways: ERK and ERK5 which function to control cell growth and division (Mebratu and Tesfaigzi, 2009), while JNK and p38 pathways are responsible for stress and apoptosis (B. Cai et al., 2006; Ki et al., 2013; Xia et al., 1995). In the ERK pathway, ligand binding to receptor tyrosine kinases initiates the recruitment of SHC and growth factor receptor-bound protein 2 (GRB2) to the activated receptor. In turn, GRB2 recruits son of sevenless (SOS) to the plasma membrane where it activates guanosine triphosphate (GTP) loading of the RAS GTPase. Once RAS is activated, the MAP4K interacts with RAF, inducing sequential activation of the cascade. This results in activation of MEK1/2 and subsequently the MAPKs ERK1/2 in the cytoplasm. Stimulated ERK1/2 then translocates to the nucleus where it phosphorylates multiple transcription factors involved in proliferation, survival and mobility (Dhillon et al., 2007; Papa et al., 2019).

Both JNK and p38 branches of the MAPK pathway are activated by a range of cellular stresses such as ultraviolet light (UV), IR, reactive oxygen species (ROS) and DNA-damaging agents.

Stress is signalled to GTPases, including CDC42 and rac family small GTPase 1 (RAC1), initiating the signalling cascade, which ultimately culminates in gene regulation of cellular senescence and apoptosis pathways among others (Dhanasekaran and Reddy, 2008; Johnson and Nakamura, 2007; Zeke et al., 2016).

1.1.7 The IGF axis in cancer

1.1.7.1 IGF-1R overexpression

Upregulation of IGF-1R occurs frequently in the majority of common solid tumours, usually secondary to driver mutations in tumour suppressor genes such as breast cancer susceptibility protein 1 (*BRCA1)*, *TP53*, Wilms tumour 1 (*WT1*) or Von Hippel-Lindau tumour suppressor (*VHL*) (Maor et al., 2000; Werner et al., 1996, 1993; Yuen et al., 2007), conferring a negative prognosis (Donohoe et al., 2012; Kim et al., 2013; Matsubara et al., 2008; Parker et al., 2002; Spentzos et al., 2007; Takahari et al., 2009; Valsecchi et al., 2012; Yamamoto et al., 2012). Certain tumours have amplified *IGF1R*, such as in some breast cancers, thymic carcinomas, small-cell lung carcinomas and adrenocortical adenocarcinomas (Badzio et al., 2010; Mimae et al., 2012; Ribeiro et al., 2014; Spears et al., 2009). Germline *IGF1R* mutations are inactivating, causing pre- and post-natal growth retardation (Abuzzahab et al., 2003; Pfaeffle et al., 2011). Further, IGF-1R overexpression is transforming, however no activating or transforming mutations have been found in *IGF1R* (Kaleko et al., 1990), contrasting to epidermal growth factor receptor (*EGFR*) (Bethune et al., 2010). To further highlight the involvement of IGF-1R in cancer development, high levels of circulating IGF-1 have been correlated to risk of developing specific cancers (Chan et al., 1998; Hankinson et al., 1998; Renehan et al., 2004). Further, sufferers and mouse models of Laron syndrome, a congenital disorder associated with high levels of GH and low levels of IGF-1, have been shown to exhibit

near complete protection from cancer due to GH insensitivity resulting in low serum IGF-1 (Guevara-Aguirre et al., 2011; Janecka et al., 2016; Steuerman et al., 2011).

1.1.7.2 Aberrant IGF axis activation

Mutations in regulatory regions of *IGF1* and *IGF2* affect the levels of IGFs in circulation (Bonapace et al., 2003; Kasprzak and Adamek, 2019). Various cancers have shown loss of imprinting of IGF genes (Hartmann et al., 2005; Murphy et al., 2006; Zhao et al., 2009), resulting in activation of the normally maternal, silent allele (Cui et al., 2003; Leick et al., 2011). Additionally, overexpression of *IGF2* has been reported in mesenchymal tumours (Steigen et al., 2009) and *IGF1* and *IGF2* in gastric cancer cell lines (Yi et al., 2001).

IGF binding proteins (IGFBPs) regulate serum concentrations of IGF-1 and -2 and are principally produced in the liver, however breast, lung and ovarian cancers are documented to also express IGFBPs (Jaques et al., 1997; Schedlich et al., 1998; Wang et al., 2006). There are six IGFBPs, sharing ~50% protein sequence homology, with IGFBP-3 displaying the highest affinity for both IGFs (Kim et al., 1997; Shimasaki and Ling, 1991). Binding of IGFs to IGFBPs almost triples the IGF half-life in circulation (Lewitt et al., 1994) and one of the major functions of IGFBPs is to inhibit the interaction of IGFs with the INSR (Daughaday and Rotwein, 1989; Ding and Wu, 2018). In cancer, it has been reported that tumours secrete IGFBP proteases (such as prostate-specific antigen (PSA) in PCa) to manipulate free IGF levels (Cohen et al., 1994, 1992; Fielder et al., 1993; Maeda et al., 2009), cytoplasmic IGFBP-5 promotes cell proliferation and tumour progression (Akkiprik et al., 2009) in breast cancer, and IGFBP-3 is associated with shorter survival in glioblastoma patients (Santosh et al., 2010). As mentioned above, mutations to other IGF axis components in the PI3K/AKT/mTOR pathway

resulting in *PTEN* loss, or MAPK/AKT branch activation can also lead to IGF-1R pathway activation (Mulholland et al., 2012; Plas and Thompson, 2005; Stiles et al., 2004; Wang et al., 2012).

1.1.7.3 The IGF axis and the hallmarks of cancer

Data indicate that IGF-mediated signalling can impact multiple hallmarks of cancer through the plethora of signalling molecules downstream of the IGF axis. As mentioned in section 1.1.5 and 1.1.6, activation of MAPK/ERK and PI3K/AKT/mTOR pathways downstream of IGF-1R leads to increased proliferation, survival and differentiation. In addition to these well-characterised links between the IGF axis and these hallmarks, further evidence exists implicating IGF signalling in enhancing the cancer-promoting capabilities of cells.

1.1.7.3.1 Cell cycle

Cell cycle progression is orchestrated by a combination of cyclins and CDKs (Vermeulen et al., 2003). These proteins are activated and inactivated as a consequence of multiple signalling pathways including PI3K/AKT/mTOR and MAPK/ERK (Gao et al., 2004; Modi et al., 2012; Peponi et al., 2006; Ryu et al., 2010; Terada et al., 1999; Zhang and Liu, 2002). To advance through the G1/S checkpoint, D-type cyclins form complexes with CDK4/6, which in turn, phosphorylates RB (Topacio et al., 2019). Phosphorylation of RB abrogates the inhibitory interaction of RB with E2F, releasing the transcription factor which is able to promote specific genes to increase cell proliferation. E2F-responsive genes include cyclin E, which helps to activate CDK2, resulting in G1/S progression (Harbour and Dean, 2000; Young et al., 2003).

It has been demonstrated that IGF-1 can stimulate cell cycle transition by increasing cyclin D1 expression and RB phosphorylation (Dufourny et al., 1997; Rosenthal and Cheng, 1995). There are reports that IGF-mediated G1/S progression is induced through the PI3K/NF-κB pathway and also the MAPK/ERK pathway (Mawson et al., 2005; Ren et al., 2009). Further, in a study by Sell *et al.* in mouse embryonic fibroblasts, IGF-1R knockout cells were shown to arrest at the G1/S checkpoint (Sell et al., 1994). Work by Guillaume Rieunier in our group has documented that IGF blockade delays the passage through S phase due to ribonucleotide reductase regulatory subunit M2 (RRM2) downregulation, reduced deoxynucleoside triphosphate (dNTP) supply and slow replication fork progression (Rieunier et al., 2021). Additionally, studies of IGF-1 null cells indicated that IGF-1 was required for G2/M transition (Adesanya et al., 1999; Carrasco-Garcia et al., 2018; Min et al., 2012).

INK and CIP family members are able to inhibit CDKs and arrest the cell cycle, by binding monomeric CDK4/6 and cyclin-CDK complexes, respectively. There is substantial evidence of CIP family member $p21^{Waf1/Cip1}$ increasing upon IGF-1 stimulation (Dufourny et al., 1997; Dupont et al., 2000; Dupont and Le Roith, 2001) which is thought to inhibit cyclin E-CDK2 complexes. Conversely, $p21^{Waf1/Cip1}$ functions to activate cyclin D-CDK4/6 complexes, resulting in G1/S progression (Sherr and Roberts, 1999).

1.1.7.3.2 Epithelial-to-mesenchymal transition

EMT can stimulate IGF-1 production, resulting in increased IGF-1R activity and Slug expression, a transcription factor associated with promoting EMT (Sivakumar et al., 2009; Sterneck et al., 2020). Further, IGF-1R overexpression has been shown to activate the focal

adhesion kinase (FAK) signalling pathway, enhancing the invasive, migratory characteristics of triple-negative breast cancer cells (Taliaferro-Smith et al., 2015).

While autocrine ligand production and receptor overexpression can encourage EMT, activation of IGF-1R via ligand binding and further crosstalk between signalling pathways have been shown to enhance the migration and invasion of cancer cells. MAPK/ERK signalling after IGF-1 stimulation has been reported to increase zinc finger E-box binding homeobox (ZEB)-1 expression in prostate cancer cells, promoting EMT progression (Dupont et al., 2001; Graham et al., 2008). Additionally, inhibition or depletion of either the MAPK/ERK or PI3K/AKT/mTOR pathway leads to upregulation of the ZEB-2-targeting micro RNA (miRNA)-200c, and this subsequently results in less E-cadherin repression (H. Li et al., 2014). Inactivation of GSK-3β through MAPK/ERK- and PI3K/AKT/mTOR-mediated serine 9 phosphorylation, as a result of IGF-1R activation, serves to promote EMT by protecting Snail and Slug from degradation (Kim et al., 2007; H. Li et al., 2015; Zhou et al., 2004).

1.1.7.3.3 Angiogenesis

There is evidence that IGF-1, and subsequent IGF-1R activation, functions to promote angiogenesis. In rat aorta explants, addition of IGF-1 has been shown to stimulate angiogenesis, promoting formation of explants predominantly consisting of fibroblast-like cells (Nicosia et al., 1994). Activation of the PI3K/AKT pathway post-IGF-1 stimulation enhances the expression of pro-angiogenesis-related growth factors such as VEGF-A, transforming growth factor (TGF)-β, fibroblast growth factor (FGF)-1, matrix metallopeptidase (MMP)-2 and -9 (Lin et al., 2017). In fact, inhibition of IGF-1R signalling by blocking of ligand-receptor binding is able to abrogate VEGF-mediated angiogenesis (Bid et al., 2012). Further, a study

has demonstrated that an endogenous miRNA (miR-126), silenced in multiple cancers, targets IGFBP-2 leading to suppression of metastatic angiogenesis Functional IGFBP-2 is able to activate IGF-1R signalling and subsequently enhance endothelial cell recruitment (Png et al., 2012).

1.1.8 IGFs and upstream growth factor signalling

In addition to IGFs, other growth factors such as EGF, PDGF and FGF can stimulate signalling cascades within the cell. Upon binding, these growth factors initiate the dimerization and transphosphorylation of their specific receptors, and subsequent recruitment of signalling proteins/adaptor molecules akin to IGFs binding to IGF-1R (Heldin, 2013; Ornitz and Itoh, 2015; Wee and Wang, 2017). Recruitment of GRB2, SHC and SOS to EGFR, PDGFR and FGFR stimulate RAS signalling, leading to activation of MEK/ERK and PI3K/AKT signalling pathways (Forbes and Westwood, 2010). Similarly to IGFs therefore, these growth factors are able to promote cell proliferation and differentiation, cell motility, adhesion and metastasis, and inhibit apoptosis (Hakuno and Takahashi, 2018).

1.2 Prostate cancer

Prostate cancer (PCa) is responsible for 26% of all newly diagnosed cancers and accounts for 14% of cancer deaths in males in the UK ("Prostate cancer statistics | Cancer Research UK," n.d.). It is the second highest cause of mortality and morbidity among men worldwide, behind lung cancer ("Prostate cancer statistics | World Cancer Research Fund," n.d.).

1.2.1 Role of androgens

Androgens are key drivers of PCa (Gao et al., 2016; Green et al., 2012; Huggins et al., 1941; La Vignera et al., 2016; Takayama and Estrada, 2018). Luteinising hormone (LH) stimulates Leydig cells in the testes to produce testosterone and 5α reductases convert testosterone to dihydrotestosterone (DHT) (Heemers and Tindall, 2007).

The androgen receptor (AR) is a nuclear hormone receptor able to bind to DNA (Lubahn et al., 1988; Narayanan et al., 2010). Unstimulated AR resides in the cytoplasm, tethered to heat-shock proteins (Matsumoto et al., 2013). Both testosterone and DHT interact with the AR, causing a conformational change, subsequent dissociation of the AR from its chaperones and translocation to the nucleus. Here, the hormone receptor is able to bind androgen responsive elements (AREs) in the promoter region of AR target genes, altering the rate of transcription (Shang et al., 2002). Additionally, the AR interacts with nuclear coregulators such as histone-modifying enzymes and ubiquitin ligases, which serve to enhance or diminish AR transcriptional activity (Coffey et al., 2013; Heemers and Tindall, 2007; B. Li et al., 2014; Jianwei Zhang et al., 2016).

The AR is expressed ubiquitously within the body, predominantly involved in male development and fertility, but also sexual behaviour and bone formation (Arnold and Gorski, 1984; Bancroft, 1980; Kawano et al., 2003). Androgen signalling is critical to prostate development, as well as to cell proliferation and survival within the gland (Cunha et al., 2018; Schaeffer et al., 2008). PCa tumours rely on androgen signalling for growth and survival, and initial treatment for PCa focusses on androgen deprivation (Lupien et al., 2008). While initially productive, ultimately the establishment of androgen-independent tumours with acquired

androgen resistance due to genetic alterations, leads to PCa progression and death. As PCa progresses, frequency of *AR* mutations increases, and due to its presence on the X chromosome, *AR* mutations result in direct phenotypic consequences in males. *AR* amplification, mutation and AR coregulator changes all serve to allow PCa cells to circumvent the lack of androgen signalling, permitting survival and proliferation (Jernberg et al., 2017).

1.2.2 PSA testing

Initially to monitor PCa, prostate-specific acid phosphatase (PAP) activity was shown to be elevated in a significant number of patients (Huggins and Hodges, 1941), however in 1979, PSA was purified (Wang et al., 2002) and a more reliable correlation was demonstrated between PSA level and advancing PCa stage (Stamey et al., 1987). PCa incidence has increased since the introduction of PSA testing (Cook et al., 2015), with high-income countries displaying doubled PCa incidence, explained in part by earlier detection. However, nations with more gradual uptake of PSA testing have still exhibited increased occurrence (Hamoen et al., 2013), pointing towards an increased prevalence of risk factors. Along with race and family history, age seems to be the most reliable risk factor. In contrast to 0.1% of all PCa diagnosed in the under 50s, 75% of all cases are in men over the age of 65 (Patel and Klein, 2009), and in an ageing population, this disparity will continue to grow.

1.2.3 Treatment

Patients with localised disease confined to the prostate can be managed by active surveillance, with PSA monitoring every 3-6 months, radical surgery or radical radiotherapy, often combined with androgen deprivation therapy (ADT) (Hamdy et al., 2016). Patients with metastatic disease are managed by ADT, serving to deplete levels of circulating testosterone to

under 50ng/ml (Parmar et al., 1987). The addition of upfront docetaxel extends overall survival by 10-12 months (Clarke et al., 2019), and in oligometastatic disease, radiotherapy was demonstrated to be beneficial (Parker et al., 2018).

1.2.4 Endocrine resistance

Almost a third of patients undergoing radical prostatectomy or radiotherapy will develop recurrent disease, either biochemical recurrence (rising PSA without scan evidence of recurrence) or local or distant recurrence identified on scans. Recurrence occurring in patients already on luteinizing hormone-releasing hormone (LHRH) analogue therapy is termed castrate-resistant prostate cancer (CRPC) (Djavan et al., 2003; Khan et al., 2003). Once resistance develops, androgen biosynthesis inhibitors or AR blockers are implemented (abiraterone and enzalutamide, respectively) (de Bono et al., 2011; Ryan et al., 2015).

In PCa specifically, the Macaulay lab has shown that IGF-1R is overexpressed in primary cancers and also detectable in bone metastases (Hellawell et al., 2002), a correlation between upregulation of IGF-1R with progression to metastatic disease and castrate-resistant PCa (Turney et al., 2011) and association of nuclear IGF-1R with advanced tumour stage (Aleksic et al., 2018). Examination of PCa cells and clinical PCa specimens indicated upregulation of the PI3K-AKT axis in association with phosphorylated AR during CRPC development (Lin et al., 2001; McCall et al., 2008).

1.3 Response to ionising radiation

A variety of DNA lesions are induced by IR, serving to kill tumour cells, but this can also lead to the generation of oncogenic mutations in normal cells (Lomax et al., 2013). Irradiation is able to produce approximately 450 purine lesions, 850 pyrimidine lesions, 1000 single-strand breaks (SSBs) and 20-40 double-strand breaks (DSBs) per Gray (Gy) (Cadet et al., 2008) – markedly less than the ~50,000 lesions created by ROS in normal cells per day (Lomax et al., 2013). Although cells are exposed to more damage daily through normal processes, it is the spatial distribution of IR-induced DNA lesions which enhances the sensitivity of cancer cells to irradiation (Jenner et al., 1993; Riballo et al., 2004). DNA damage sites produced by IR are complex due to the number of different lesions present, and their clustered nature impacts the accessibility of DNA repair proteins to the damage site (Eccles et al., 2011; Lomax et al., 2002; Weinfeld et al., 2001). After irradiation, unrepaired DSBs are the most toxic (Khanna and Jackson, 2001), and thus the focus of this work concentrated on these lesions.

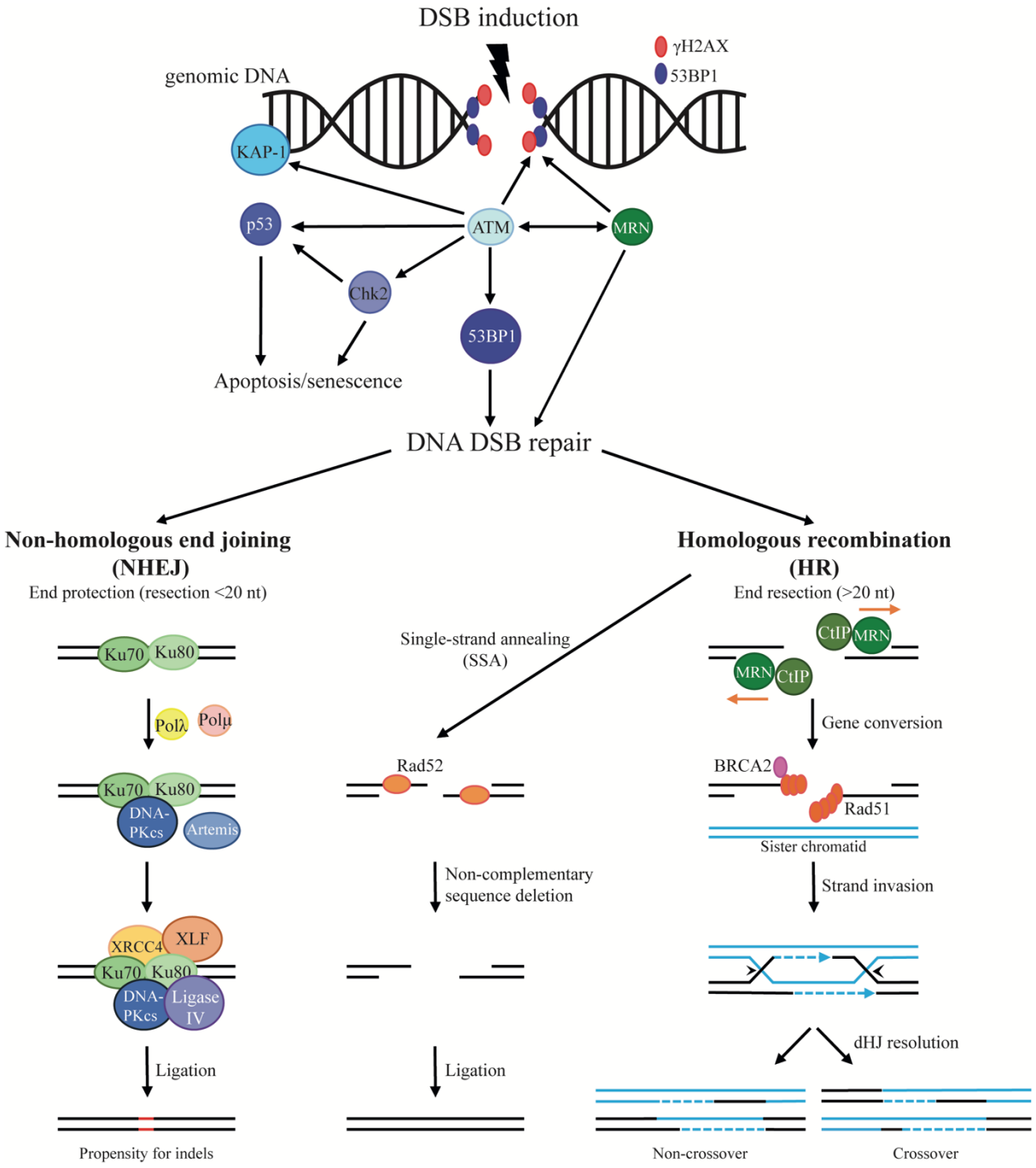

Figure 1.3: The cellular response to DNA double strand breaks.
Simplified schematic of the DNA damage response. DNA DSB repair occurs via two main pathways: homologous recombination (HR) or non-homologous end joining (cNHEJ). More detailed explanations are found in text. Figure was adapted from Chang *et al.*, 2017, Featherstone and Jackson, 1999.

1.3.1 Double strand breaks

When both DNA strands are broken simultaneously in close proximity, the chromatin structure is disrupted in such a way that specific repair mechanisms must be employed (Jackson, 2002; Khanna and Jackson, 2001; Lieber, 2010) (Fig. 1.3). DSBs are induced endogenously by factors such as chromosomal stress and polymerase-related errors, or by exogenous actions like UV light or IR (Jackson and Bartek, 2009). There is a causal link between DSB formation and induction of chromosomal translocations with tumourigenic potential (Lengauer et al., 1998; Richardson and Jasin, 2000). In fact, most losses or amplifications of chromosomal material are explained by inappropriate DSB repair events, and high incidences of DDR defects have been reported in human cancers (Iliakis et al., 2015; Janssen and Medema, 2013).

In response to DSBs, cells assess the damage, and utilise cell cycle checkpoints to allow for sufficient DNA repair to take place before re-entry into the cell cycle. If the damage is too catastrophic for the cell, it can result in cell death. If the damage is repairable however, DDR proteins orchestrate the activation of specific DNA repair pathways to faithfully correct the DNA lesion (Ciccia and Elledge, 2010).

Both error-prone and error-free DNA repair pathways modify chromatin structure to facilitate DSB repair, particularly in homologous recombination (HR), which requires extensive remodelling of the DNA surrounding the DSB (Kinner et al., 2008). The histone protein H2A variant, H2AX, has been shown to become phosphorylated at the carboxy terminus at serine 139 (γH2AX) in response to DSBs (Lowndes and Toh, 2005). The discrete nuclear foci formed are adjacent to the DSB, and correlate with the number of DSBs formed (Sedelnikova et al., 2002). The SQ phosphorylation motif on H2AX is recognised by the major DDR proteins

ataxia telangiectasia mutated (ATM), ATM-Rad3-related (ATR), and DNA-dependent protein kinase catalytic subunit (DNA-PK_{cs}) (Kuo and Yang, 2008), and this modification to the histone tail seems to facilitate the recruitment of a multitude of proteins involved in initiating specific pathways of the DDR (Kobayashi, 2004; Kobayashi et al., 2002; Kusch et al., 2004; Ward et al., 2003). The availability of antibodies specific to γH2AX allows for quantification of the accumulation of DSBs, and subsequent DSB repair (Rothkamm et al., 2003), as dephosphorylation of γH2AX occurs after DNA repair, reported to be carried out by protein phosphatase 2A (PP2A) and wild-type p53-induced phosphatase 1 (WIP1) (Cha et al., 2010; Chowdhury et al., 2005).

Ongoing DNA damage formation as a consequence of aberrant cell proliferation and replication stress promotes the selection of cancer cells with inactivated DDR components to allow malignant evolution (Halazonetis et al., 2008). In normal cells, DNA damage sensors have evolved to alert the cell of nascent DNA lesions and function as the primary responders in the DDR (Durocher and Jackson, 2001).

1.3.2 DNA damage sensors

The first stage in the cellular response to a DSB is to sense the damage and initiate signalling cascades aimed at controlling checkpoint mechanisms and promoting DNA repair. The major DDR sensors, ATM, ATR and DNA-PK_{cs} are large proteins tasked with maintaining the integrity of the genome (Blackford and Jackson, 2017). All are serine/threonine kinases, containing a PI3K-like (PIKK) protein kinase-family active site, each exhibiting distinct kinase activity (Maréchal and Zou, 2013). The PI3K signature in the active site of these kinases is critical to their cellular function as key responders to DNA damage – converting extracellular

signals into collective intracellular resolutions. ATM, ATR and DNA-PK_{cs} are recruited to the damage site by co-factors, which are specific for each kinase, and all three are able to autophosphorylate in response to DSBs (Blackford and Jackson, 2017). Together, these DDR sensors directly or indirectly affect more than one thousand DNA damage responders, co-ordinating the repair of genotoxic onslaughts (Ciccia and Elledge, 2010).

1.3.2.1 ATM

ATM is 350kDa in size and primarily responds to DSBs (Paull, 2015). It was discovered to be mutated in ataxia telangiectasia (Savitsky et al., 1995), an autosomal recessive neurodegenerative disorder characterised by progressive ataxia, a compromised immune system and higher risk of developing lymphoid cancers (McKinnon, 2012). Cells from these patients exhibit markedly higher radio-sensitivity (Taylor et al., 1975) – an effect that is mimicked in ATM-defective cancer cell lines (Ayars et al., 2017; Weber et al., 2016).

It was shown that ATM exists as homodimers, and upon DNA damage, ATM monomers dissociate, and through phosphorylation of four main sites, the kinase is activated (Bakkenist and Kastan, 2003). The protein kinase moves to the site of DNA damage and directly or indirectly orchestrates the DDR with meiotic recombination 11 (MRE11), RAD50 and Nijmegen breakage syndrome 1 (NBS1) as part of the MRN complex. NBS1 specifically recruits ATM to the DSB and is responsible for maintaining its proximity to the damaged DNA (Difilippantonio et al., 2007). Phosphorylation of MRN complex members by ATM, results in activation of specific components of the DDR (Di Virgilio et al., 2009; Gatei et al., 2011; Lim et al., 2000).

1.3.2.2 ATR

ATR is activated in response to a wider range of genotoxic stresses than ATM, principally single stranded DNA (ssDNA) intermediates during the resection of DSBs and stalled replication forks (Cimprich and Cortez, 2008; Shiotani and Zou, 2009). ATR is bound to ATR-interacting protein (ATRIP) in a complex, which is vital for maintaining the stability and actions of the protein kinase. After DNA damage, exposed nascent ssDNA is coated with replication protein A (RPA32) and ATRIP directly binds to the RPA32-coated ssDNA, recruiting the ATR-ATRIP complex to the damage (Zou and Elledge, 2003). In Seckel syndrome, low levels of ATR due to a pre-messenger RNA (mRNA) splicing mutation cause a hereditary form of microcephalic dwarfism, and an impaired response to DNA damage *in vitro* (O'Driscoll et al., 2003).

1.3.2.3 DNA-PK

DNA-PK is a very large complex made up of DNA-PK_{cs} and the Ku70/80 heterodimer (Dvir et al., 1993, 1992; Gottlieb and Jackson, 1993). Ku70/80 interacts with double stranded DNA by forming a basket-shaped structure encompassing the DNA ends in both a sequence- and ATP-independent manner (Blier et al., 1993; Mimori et al., 1990; Mimori and Hardin, 1986). In the absence of Ku70/80, DNA-PK_{cs} interacts transiently with DNA and exhibits minimal kinase activity. When bound to Ku70/80 however, kinase activity is significantly increased (Chan et al., 1996) and further, Ku70/80- or DNA-PK_{cs}-deficient cells exhibit increased radio-sensitivity (Lees-Miller et al., 1995; Taccioli et al., 1994), highlighting the importance of both members of the complex in the DDR.

1.3.3 DSB repair pathways

1.3.3.1 Non-homologous end joining

cNHEJ is initiated by Ku70/80 binding to double-stranded DNA (dsDNA) ends created by the DSB, encompassing the DNA, and rapidly recruiting DNA-PK$_{cs}$ (Mari et al., 2006; Uematsu et al., 2007). The barrel-shaped structure of the Ku70/80 heterodimer allows efficient sliding over the DSB and dynamic interaction between the DNA and Ku70/80 (Mari et al., 2006). The DNA-Ku70/80 scaffold permits the interaction with DNA-PK$_{cs}$, and there is persuasive evidence that around the DSB, there are two Ku70/80 and two DNA-PK$_{cs}$ molecules to undertake the repair (Weterings and Chen, 2008).

In the first instance, the Ku70/80-DNA-PK$_{cs}$ complex functions to capture and tether the damaged DNA ends. Activation of DNA-PK$_{cs}$ requires the association with Ku70/80, and autophosphorylation of the serine/threonine kinase is necessary for recruitment of processing enzymes as unphosphorylated DNA-PK$_{cs}$ protects the DNA ends from degradation or ligation (W. D. Block et al., 2004; Cui et al., 2005a; Akihiro Kurimasa et al., 1999; Reddy et al., 2004). DNA-PK$_{cs}$ then recruits X-ray repair cross complementing 4 (XRCC4), DNA ligase IV, XRCC4-like factor (XLF) and Artemis, which process and ligate the DNA strands (Lieber, 2010). This involves modification of non-complementary strands by addition or removal of nucleotides on ssDNA overhangs. This stage of cNHEJ is the most error-prone, sometimes resulting in the incorporation of insertions or deletions around the DSB. The DNA ligase IV/XRCC4 complex ligates the processed DNA ends, repairing the DSB (Budman et al., 2007; S. A. Nick McElhinny et al., 2000) (Fig. 1.3).

53BP1 interacts with damaged chromatin to aid recruitment of DDR proteins, promote progression through cell cycle checkpoints and contribute to DNA repair pathway choice (Panier and Boulton, 2014). 53BP1 and BRCA1 have roles in deciding whether DSBs are repaired by cNHEJ or HR (Chapman et al., 2013; Muñoz and Rouse, 2009; Zimmermann et al., 2013). The antagonistic relationship between these two proteins is centred around phosphorylation of 53BP1 and its localisation at the DSB (Symington and Gautier, 2011). 53BP1 is able to protect DNA ends from resection (and therefore HR) by recruiting RAP1-interacting factor 1 (RIF1) and pax transactivation domain-interacting protein (PTIP). To recruit these DNA end protectors, 53BP1 must be phosphorylated by ATM, but BRCA1 is able to inhibit the translocation of RIF1 to the DSB (Feng et al., 2015) and promote dephosphorylation of 53BP1 (Isono et al., 2017). As well as negatively impacting cNHEJ, BRCA1 is also able to promote HR. C-terminal binding protein interacting protein (CtIP) binds to the MRN complex, stimulating 5' DNA end resection – a process greatly enhanced by BRCA1 (Cruz-García et al., 2014). Further, formation of RAD51 filaments – essential for accurate HR – are regulated by BRCA1 (Cousineau et al., 2005; Sullivan and Bernstein, 2018).

When cNHEJ is compromised, cells can use alternative NHEJ/microhomology-mediated end joining (MMEJ) which is more error-prone. This repair process involves 5'-3' DNA end resection, creating small internal regions of homology which anneal together, before binding of polymerases to proximal single-stranded regions to synthesise complementary DNA, repairing the DSB (Chang et al., 2017; Sallmyr and Tomkinson, 2018; Sfeir and Symington, 2015).

1.3.3.2 Homologous recombination

HR repair is less error-prone but is a slower process that is usually restricted to S and G2 phases of the cell cycle due to the use of sister-chromatids as DNA templates for the repair process (Arnoult et al., 2017). dsDNA ends are resected in the 5' to 3' direction by specific nucleases, producing 3' ssDNA overhangs. The DNA overhangs are coated with RPA32 to protect the ssDNA and help to recruit the MRN complex. This complex recruits ATM and CtIP, and with the help of BRCA1 and breast cancer susceptibility 2 (BRCA2), RAD51 is able to invade the undamaged template strand and resolve the DSB (Dudáš and Chovanec, 2004; Johnson and Jasin, 2001) (Fig. 1.3).

1.3.4 Cell signalling and the DNA damage response

1.3.4.1 IGF-1R

Previous work by the Macaulay group has shown an association between high total IGF-1R expression and high primary Gleason grade and risk of metastasis in PCa biopsies. Additionally, high cytoplasmic and internalised receptor levels were associated with radio-resistance and biochemical recurrence after IR (Aleksic et al., 2017).

Inhibition or depletion of IGF-1R has been shown by our lab and others to enhance sensitivity to DNA damaging agents such as IR and cytotoxic drugs in prostate cancer, DNA-PK-proficient glioblastoma (GBM) and paediatric/young adult high-grade glioma (HGG) cells (Chitnis et al., 2014; Rochester et al., 2005; Simpson et al., 2020; Turney et al., 2012; Zhao and Gu, 2014a). Further, work in our group has suggested that IGF-1R inhibition impairs repair of DSBs by cNHEJ and HR (Chitnis et al., 2014; Turney et al., 2012). Upon further

investigation, using γH2AX foci as a readout for DNA damage, the Macaulay group observed a delay in γH2AX foci resolution rather than increased induction of DNA damage after IR (Chitnis et al., 2014; Turney et al., 2012). Although our group and others reported that IGF-1R can translocate to the nucleus (Aleksic et al., 2018, 2010; Sehat et al., 2010), IGF-1R does not appear to co-localise with γH2AX (Aleksic and Macaulay, unpublished). This suggests that a direct role for nuclear IGF-1R in DSB repair is unlikely, and implicates canonical signalling pathways downstream of IGF-1R. There is also evidence that the increased radio-sensitivity observed in IGF-1R compromised cells is not simply due to increased apoptosis, as after 3 Gy irradiation, no enhanced caspase 3/7 activity was seen in IGF-1R inhibited cells compared to control DU145 cells (Chitnis et al., 2014; Tezuka et al., 2001). The IGF axis is an important regulator of AKT-mTOR function (K. Chen et al., 2014) and studies indicate a role in DSB repair. Overexpression of IGF-1R significantly reduces UV-induced damage via the p38-MAPK pathway (Héron-Milhavet et al., 2001) and phosphorylates IRS-1, reported to release RAD51 to translocate to the nucleus for HR (Trojanek et al., 2003).

How IGF-1R is coupled to DSB repair pathways remains unclear, although there is evidence showing that metabolic reprogramming can dysregulate the DDR, and this can lead to increasing mutation rates, genomic instability and intra-tumour heterogeneity, contributing to cancer progression (Burrell et al., 2013; Chae et al., 2016). Metabolic intermediates can exert general effects on nucleotide supply, chromatin remodelling and accessibility, and can also influence the choice of specific DNA repair pathway (Turgeon et al., 2018). Reported links between metabolic processes and the DDR (Aird et al., 2015; Cosentino et al., 2011; Jeong et al., 2013; Sulkowski et al., 2018) include a requirement for pyruvate kinase M2 (PKM2) in repair of DSBs by HR (Sizemore et al., 2018), and the identification of Krebs cycle products fumarate and succinate as inhibiting α-ketoglutarate-dependent lysine demethylases KDM4A

and KDM4B, also shown to be required for HR (Sulkowski et al., 2018). Thus, through its involvement in metabolic reprogramming, the AKT-mTOR axis is implicated in regulating the DDR. However, there are conflicting data regarding the consequences of AKT and mTOR activity, with reports of compromised DSB repair when mTOR is inhibited (Mo et al., 2016), and conversely that the activity of the mTOR pathway impairs DNA repair via phosphorylation of E3 ubiquitin ligases (Schmid et al., 2018; Xie et al., 2018). Similarly, there are contradictory studies describing the influence of AKT on the DDR, with evidence of increased AKT activity inhibiting HR (Ma et al., 2018), while others find that AKT is activated by DSBs, promoting repair by cNHEJ (Xu et al., 2012). These observations are likely due to altered roles for AKT in differing models or molecular contexts.

1.3.4.2 PI3K/AKT/mTOR

The central DDR sensors DNA-PK$_{cs}$, ATM and ATR are all upstream of AKT in the DDR pathway (Blackford and Jackson, 2017; Boehme et al., 2008a; Bozulic et al., 2008; Caporali et al., 2008; Fraser et al., 2011). These three related kinases are able to activate AKT in response to DNA damage, each helping to orchestrate the cellular response to DNA damage.

Data suggest synergy between DNA-PK$_{cs}$ and AKT. Formation of an AKT-DNA-PK$_{cs}$ complex promotes DNA-PK$_{cs}$ binding to Ku70/80 and DNA-PK$_{cs}$ directly stimulates AKT kinase activity (Stronach et al., 2011; Toulany et al., 2017). Additionally, AKT-induced autophosphorylation of DNA-PK$_{cs}$ enables the release of DNA-PK$_{cs}$ from the damage site to allow ligation and termination of repair to occur (Toulany et al., 2012). Phosphorylated AKT (serine 473) also co-localises with phosphorylated ATM (serine 1981) and γH2AX at IR-induced DSB sites, and it has been reported that full activation of AKT in response to insulin

and IR is ATM-dependent (Fraser et al., 2011). AKT knockout mice mimic the radio-sensitivity phenotype of both ATM-deficient and DNA-PK_{cs}-deficient mice (Boehme et al., 2008b; Bozulic et al., 2008; Viniegra et al., 2005). In response to temozolomide (TMZ) treatment, cells phosphorylate AKT (serine 473), requiring the presence of ATR (Caporali et al., 2008). It is unknown whether ATR phosphorylates AKT directly however, or whether it is similar to indirect phosphorylation of AKT by ATM (Viniegra et al., 2005).

AKT phosphorylation of BRCA1 indirectly leads to cytoplasmic retention and subsequent suppression of RAD51 filament formation (Plo et al., 2008; Tonic et al., 2010). In breast cancer cell lines with high AKT levels, formation of BRCA1 and RAD51 foci post-IR are significantly reduced compared to cells with low AKT levels – an observation which is strengthened by the strong correlation of cytoplasmic BRCA1 and RAD51 with AKT activation in breast cancer biopsies (Plo et al., 2008). Indeed, constitutively active AKT expression in HCT116 cells strongly impairs RAD51, RPA32 and CtIP foci formation in response to DNA damage, an effect that is rescued by inhibition of AKT (Xu et al., 2010). These studies highlight an AKT effect in suppression of HR.

There are several studies suggesting that AKT promotes cNHEJ-mediated resolution of DSBs (Golding et al., 2009; Kao et al., 2007; Pedram et al., 2009; Toulany et al., 2010, 2008, 2006), and a report using a cell-free reporter assay indicating that AKT inhibition directly leads to cNHEJ pathway blockade (Fraser et al., 2011). Further, there is evidence that through retention of BRCA1 and RAD51, AKT is able to inhibit HR both *in vitro* and in breast cancer biopsies (Plo et al., 2008). Conversely however, there is a report of AKT functioning to impair cNHEJ through phosphorylation of XLF and subsequent cytoplasmic retention (Liu et al., 2015), AKT

stimulating HR in a RAD51-dependent manner (Mueck et al., 2017), and AKT inhibition abrogating radiation-induced DSB repair via HR (Mohammadian Gol et al., 2019). The contrasting accounts of AKT activity on DNA repair highlight the complexity of AKT signalling and the interest in developing AKT inhibitors for therapeutic benefit (Xu et al., 2012).

Irrespective of their roles in the DDR, inhibition of PI3K, AKT or mTOR has been shown to increase radio-sensitivity in multiple cancer types. AKT inhibition in p53-deficient oesophageal tumours, rapamycin treatment in pancreatic carcinoma cells and PI3K/AKT/mTOR pathway inhibition in radio-resistant prostate cancer cells exhibit increased radio-sensitivity (Chang et al., 2014; Dai et al., 2013; Leszczynska et al., 2015). Additionally, studies have indicated that AKT promotes cell survival post-IR and resistance to IR and chemotherapy *in vitro* (Brognard et al., 2001; Bussink et al., 2008; Gottschalk et al., 2005; Li et al., 2009; McKenna et al., 2003a; Toulany et al., 2008, 2012), and furthermore, that high expression of mTOR is associated with radio-resistance in cervical cancer (Kim et al., 2010). Indeed, hyperactivation of AKT has been shown to confer resistance to chemotherapy, tyrosine kinase inhibitors and radiotherapy by promoting anti-apoptotic signals (Liu et al., 2009).

1.3.4.3 MAPK/ERK

After irradiation, activated ERKs are able to enhance the activity of ATM, ATR and DNA-PK_{cs}, which have all been shown to stimulate ERK activity (Golding et al., 2007; Wei et al., 2011, 2010; Yan et al., 2007). This positive feedback loop functions to maintain DNA repair and promote survival in cancer cells (Ciccarelli et al., 2018; Golding et al., 2009; Marampon et al., 2011; Toulany et al., 2016; Yacoub et al., 2003; Yu et al., 2013). The MAPK/ERK

pathway primarily functions to regulate the cell cycle and respond to cellular stress. In response to IR, ERK activation helps cells to override the G2/M checkpoint (Abbott and Holt, 1999; Chambard et al., 2007), a crucial mechanism exploited by IR to increase therapeutic efficacy (Bernhard et al., 1995; Pawlik and Keyomarsi, 2004; Strasser-Wozak et al., 1998). In this way, MAPK/ERK signalling has been implicated in radio-resistance.

This evidence suggests that the radio-sensitivity displayed by IGF-1R depleted or inhibited cells previously in the Macaulay group could be due to disruption of PI3K/AKT/mTOR or MAPK/ERK signalling. Specific cell survival/apoptosis defects however, based on previous lab results, seem unlikely. IGF-1R could influence radio-sensitivity more broadly, via changes to cell cycle phase distribution or through modulation of chromatin accessibility. Indeed, IGFs have been linked to cell cycle progression (Girnita et al., 2007; Mairet-Coello et al., 2009; Ren et al., 2009) and to chromatin remodellers (Warsito et al., 2016), however no definitive mechanism involving IGF-1R and radio-resistance has been noted.

It had been assumed that all functions of the IGF axis require the kinase activity of IGF-1R, mediating signalling via the pathways described above. However there is evidence to suggest that there are roles of IGF-1R independent of its catalytic activity. The INSR and the IGF-1R double knockout cells were found to be resistant to apoptosis, sensitivity being rescued upon addition of either receptor in absence of ligand (Boucher et al., 2010a). Further, Boucher *et. al* discovered that unoccupied INSR and IGF-1R control expression of miRNAs and imprinted genes in mouse embryonic fibroblasts (Boucher et al., 2014). A kinase-deficient version of the closely related INSR has also been shown to mediate the activation of pyruvate dehydrogenase by insulin (Gottschalk, 1991). These examples offer the possibility of a similar structural

function of the receptor in DNA repair. Previous studies used overexpression of mutant receptors to investigate kinase-independent receptor functions, but genome editing techniques offer the possibility of modifying the endogenous receptor.

1.4 Gene editing

1.4.1 Gene knockout

1.4.1.1 Gene editing techniques to knockout genes before CRISPR/Cas9 technology

The precise gene editing techniques used today are a culmination of numerous advancements spanning decades of biomedical research, beginning with the discovery of the basic principles of genetics by Gregor Mendel in 19th century. The ability to manipulate the genome offers significant benefits both in uncovering natural biological mechanisms and also in the development of effective therapeutics, and significant effort was made to advance our understanding of how this could be achieved.

The first major breakthrough was that through homology-directed repair (HDR), mammalian cells were shown to integrate globin gene sequences into the human chromosomal β-globin locus. Homologous chromosomal sequences within the exogenous plasmid allowed for recombination and integration (Smithies et al., 1985), however it was inefficient, cell type-dependent, cell state-dependent and could result in random integration. To harness the promise of exogenous DNA incorporation, researchers began exploiting cellular DNA repair machinery by inducing targeted DSB formation. This was achieved by utilising meganucleases which recognise specific DNA sequences and cut both DNA strands (Rouet et al., 1994; Rudin et al., 1989). The use of targeted meganucleases increased editing efficiency however as DSB

formation is predominantly repaired by cNHEJ and the low probability that unique recognition sequences are close enough to desired target sites meant that this strategy for gene editing was deemed inadequate (Khan, 2019). It should be noted here that DSB creation by meganucleases are still used today in DNA repair pathway assays. Reporter assays use the nuclease I-SceI to create DSBs in specially designed constructs where once the DSB is repaired by a certain repair pathway, reconstitution of a green fluorescent protein (GFP) reporter allows for quantification of repair pathway efficiency (Gunn and Stark, 2012).

Work to uncover nucleases that could more specifically target areas of the genome led to the discovery of zinc fingers. The crucial ability of zinc finger motifs to recognise and bind to specific 3 nucleotide DNA sequences (Klug and Rhodes, 1987) allowed for the assembly of multiple zinc finger modules; facilitating selective targeting to specific gene loci. Selected zinc finger modules were therefore able to target any 18-21 nucleotide sequence in the human genome (Urnov et al., 2005). These modules were fused to the DNA cleavage domain of the FOK1 endonuclease (Kim et al., 1996) allowing for DNA cleavage at specific, pre-determined sites and for the first time, major focus could be directed towards gene editing using zinc finger nucleases (ZFNs). This was closely followed by the discovery of transcription activator-like effector (TALE) modules which could target one nucleotide (Boch et al., 2009; Moscou and Bogdanove, 2009) and, like the zinc finger modules, could be fused to the FOK1 cleavage domain (Christian et al., 2010; Li et al., 2011; Miller et al., 2011; F. Zhang et al., 2011). Transcription activator-like effector nucleases (TALENs) therefore offered the same level of endonuclease activity but could target with much more precision than ZFNs.

ZFNs and TALENs displayed enhanced editing efficiencies (Bibikova et al., 2001; Porteus and Baltimore, 2003) and therapeutic attempts were made (Hockemeyer et al., 2011; Sebastiano et al., 2011; Zou et al., 2011). However the expertise required to construct these chimeric nucleases meant that gene editing was not broadly accessible. In 2012, clustered regularly interspaced short palindromic repeat (CRISPR)/CRISPR-associated (Cas)9 genome editing was introduced as a system that was at least as efficient as ZFNs and TALENs, but importantly was much easier to construct and therefore more available to the wider research community (Cong et al., 2013a; Jinek et al., 2013; Mali et al., 2013).

1.4.1.2 Creation of knockout cell lines using CRISPR/Cas9 technology

The CRISPR system was discovered in *Escherichia coli* (Ishino et al., 1987) as part of an acquired bacterial immune system. Briefly, CRISPR repeat clusters were shown to be separated by non-repeating DNA sequences found to originate in viruses or other mobile genetic elements (Bolotin et al., 2005; Mojica et al., 2005; Pourcel et al., 2005), and each CRISPR element was confirmed to partner with well-conserved genes named *Cas* genes.

Later, invading phage sequences were shown to be incorporated as non-repeated DNA sequences (spacers) into the bacterial genome (Brouns et al., 2008) and Cas9 was revealed to have DNA catalytic activity (Garneau et al., 2010). The examination of CRISPR systems showed that the spacer sequence always had a very similar 3 nucleotide protospacer-adjacent motif (PAM) sequence downstream of the spacer, which was essential for its function (Deveau et al., 2008), and further work demonstrated that the CRISPR locus from one bacterium could be functional in another (Sapranauskas et al., 2011).

The classical CRISPR/Cas9 gene editing system harnesses all of these characteristics. Instead of parts of a viral genome, a short guide RNA (gRNA) that targets a region of interest can easily be cloned into the cloning backbone of a Cas9-containing vector (additional Cas variants exist for specific purposes (Makarova et al., 2020)). Other proteins have been used to produce overhanging DSBs at targeted sites (Fonfara et al., 2016), or which are smaller and more advantageous for therapeutic delivery (Edraki et al., 2019). Ideally, the gRNA should be ~20 nucleotides in length and have 40-60% guanine-cytosine (GC) content. The target site must include a PAM sequence; typically -NGG (however presently there are multiple PAM site variants allowing targeting of almost every part of the genome (Kleinstiver et al., 2015)) which occurs on average every 8 bases. The gRNA is transcribed from the spacer sequence, targeting the Cas9 endonuclease to the site of interest, and 3 nucleotides upstream of the PAM site; a DSB is created (Fig. 1.4).

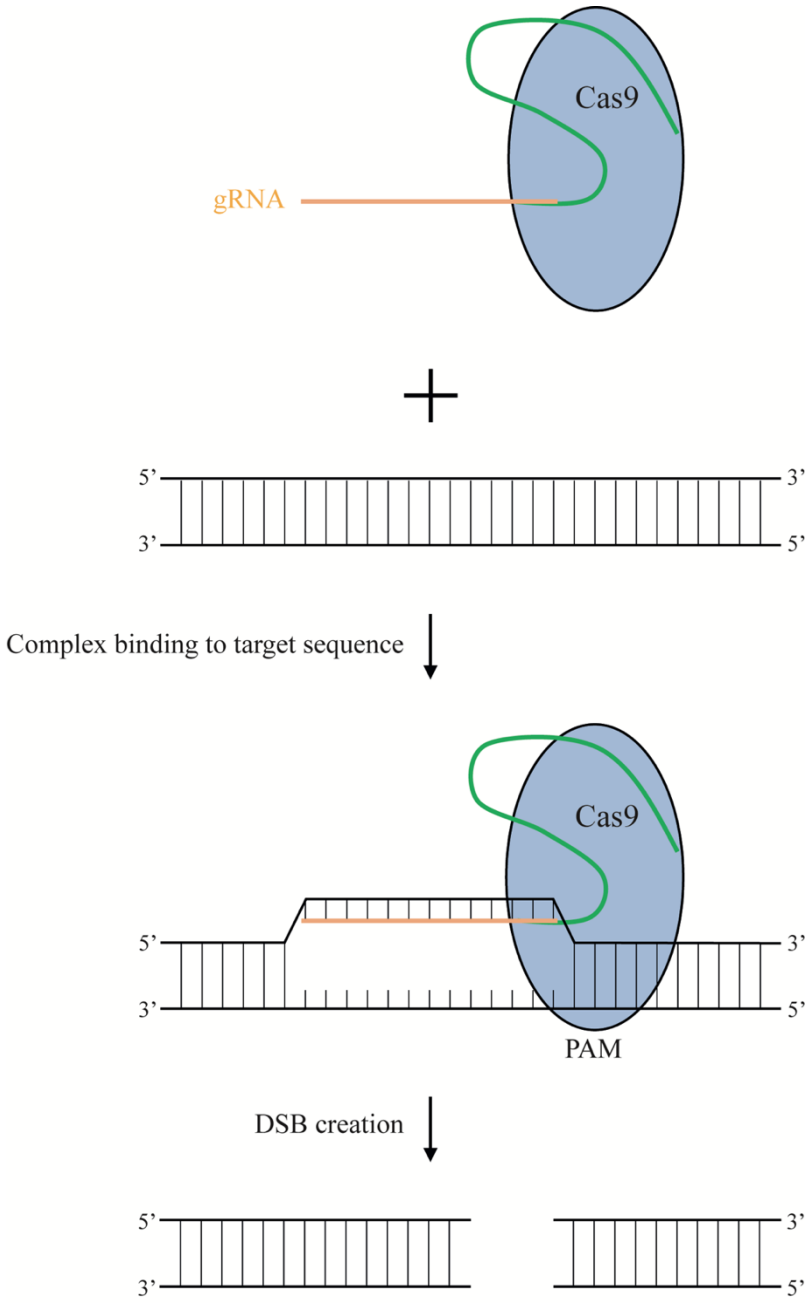

Figure 1.4: CRISPR mediated gene editing.
Diagram depicting the simplified mechanism of double-strand break creation using CRISPR/Cas9-mediated gene editing. The CRISPR/Cas9 complex identifies and binds with high selectivity to a target region of DNA using the guideRNA (orange), designed to be upstream of a protospacer adjacent motif (PAM). This facilitates double-stranded DNA cleavage by the Cas9 endonuclease. More information on the mechanism in text.

1.4.2 Nucleotide substitutions

1.4.2.1 DSB-dependent gene editing strategies to create amino acid substitutions

In the past, CRISPR/Cas9 gene editing has been used mainly as a method of genetic disruption utilising a nuclease to generate DSBs at target sites followed by exploitation of DSB repair machinery to incorporate the desired edit (Cong et al., 2013b; Jinek et al., 2012; Mali et al., 2013). The error-prone cNHEJ and MMEJ pathways help in inaccurate indel formation at the newly-formed DSB (Jeggo, 1998; Lukacsovich et al., 1994), and consequently knockout cell lines are generated with relative ease (Fu et al., 2013; Kim et al., 2019; Kosicki et al., 2018; Tsai et al., 2015). While an effective tool *in vitro*, the potential incorporation of undesirable mutations and the prevalence of pathogenic alleles requiring more accurate manipulation to correct (Landrum et al., 2015), has led to genetic engineering techniques becoming more precise and accessible in recent years (Adli, 2018). Harnessing CRISPR/Cas9 technology has increased the specificity of gene editing considerably, however performing targeted nucleotide substitutions is more nuanced than creating knockout clones.

1.4.2.2 HDR-mediated editing background

DSB-dependent nucleotide substitution strategies exploit the less error-prone HR repair pathway in cells to incorporate desired genetic changes (Okamoto et al., 2019). This method can be used for faithfully producing required insertions, deletions or substitutions of genetic material (Hsu et al., 2014). Co-transfection of a single-stranded oligodeoxynucleotide (ssODN) incorporating the edit between two homologous regions acts as a template to encode the required base change (Gallagher and Haber, 2018). HDR offers a more accurate and targeted method of DNA modification compared to cNHEJ but a markedly less efficient one (Jasin and Haber, 2016). It is hindered by HR restriction to G2 and S phase of the cell cycle, and the

increased efficacy of cNHEJ which usually prevails; further decreasing HDR-mediated nucleotide substitution efficiency. To improve HDR-mediated editing, both cell cycle-arresting compounds (such as nocodazole) and cNHEJ-inhibiting/HR-promoting small molecules have been successfully used (Lin et al., 2014).

Briefly, for HDR-mediated amino acid substitutions, a gRNA navigates an active Cas9 endonuclease to the target site, creating a DSB. Transfected in tandem is a ssODN complimentary to the region surrounding the cute site, except for the inclusion of the specific nucleotides required to produce the desired amino acid substitution (Nambiar et al., 2019). This small region of non-complementarity does not significantly alter the binding specificity of the ssODN to the DNA template, and facilitates the incorporation of the favoured nucleotides to generate the substitution (Fig. 1.5) (Okamoto et al., 2019).

It has been reported that the size of ssODN used can affect HDR-mediated gene editing efficiency (Elliott et al., 1998; Thomas et al., 1986) and so an array of ssODN lengths were designed. Based on the literature, asymmetric ssDNA donor templates can have significant advantages over symmetrical ssODNs (Richardson et al., 2016). ssODN asymmetry allows the Cas9 to remain bound to the targeted strand, limits excessive DNA-end resection and allows the 5’ DNA of the non-targeted strand to be displaced from the Cas9 with a suitable ssDNA donor. This asymmetry allows for infiltration into the DNA flap released by Cas9 cutting, and inclusion of the desired base substitution within the 24-36nt open bulge created. Additionally, incorporation of a silent mutation into the ssODN to disrupt the PAM site disables unwanted gRNA binding and subsequent DSB cutting of already-edited DNA (Okamoto et al., 2019).

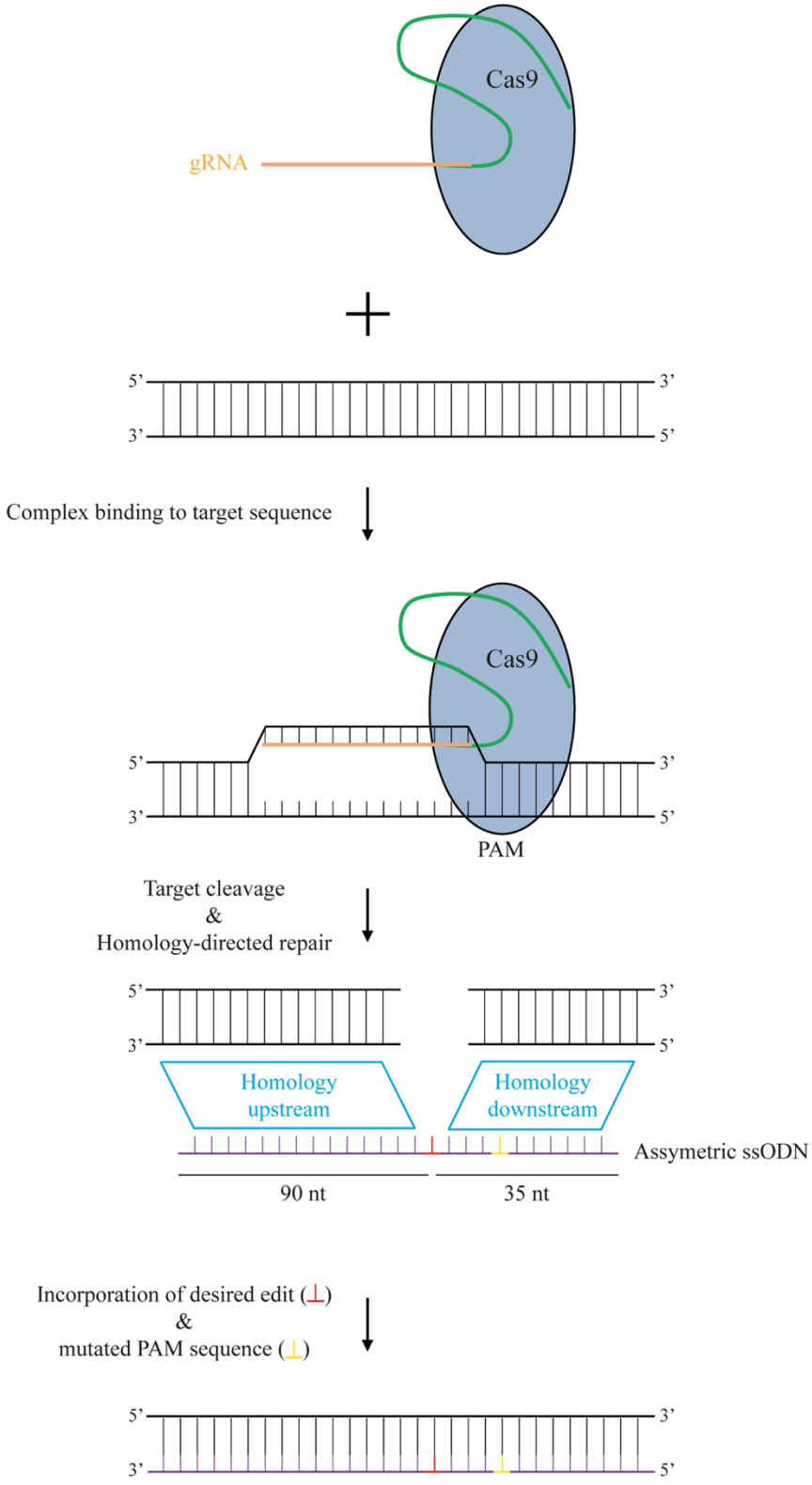

Figure 1.5: HDR-mediated nucleotide substitution.
Diagram displaying the simplified mechanism of HDR-mediated nucleotide substitution using CRISPR/Cas9 gene editing. Briefly, the double strand break is produced as described in figure 1.4, and co-transfection of an asymmetric single-stranded oligonucleotide (ssODN) encourages repair by homology-directed repair (HDR). The ssODN contains the desired edit, and a mutation of the PAM site so as to inhibit repeated DSB generation of the same DNA strand. A more detailed explanation of the mechanism can be found in the main text.

1.4.2.3 DSB-independent methods of nucleotide substitution

While the HDR-mediated method can be exploited to create gene disruption, rearrangement and base substitutions, the relative inefficiency and introduction of a DSB presents an immediate danger for exploiting this strategy for therapeutic benefit, due to the potential for generation of harmful mutations/irreparable DNA lesions at the target site (Cox et al., 2015). Of late, this has resulted in the development of editing techniques that do not sever both DNA strands, consequently avoiding major disruption to the DNA, incorporation of unwanted mutations and activation of DDR and pro-apoptotic pathways.

1.4.2.3.1 Base editing

The base editor comprises a base modification enzyme fused to a catalytically inactive Cas nuclease which is still able to be recruited to a specific part of the genome via a gRNA (Anzalone et al., 2020). The Cas9 is made inactive by D10A and H840A mutations (Rees and Liu, 2018). Binding of the gRNA to the dsDNA target liberates a section of ssDNA, allowing the base modification enzyme access to perform the desired substitution (Fig. 3.9A) (Komor et al., 2016).

Cytosine base editors (CBEs) utilise a cytidine deaminase (apolipoprotein B-editing enzyme, catalytic polypeptide-1 (APOBEC1) or cytidine deaminase 1 (CDA1)) to deaminate the exocyclic amine of a cytosine nucleotide into uracil. Removal of the H840A mutation and persistence of the D10A mutation on Cas9 facilitates the targeting of the strand that does not contain the PAM sequence (termed dead-Cas9 (dCas9)) (Rees and Liu, 2018). The selective nicking of the unedited strand forces preferential cellular repair of the uracil-guanine (U-G)

base pair to uracil-adenine (U-A), substantially increasing efficiency of the nucleotide substitution (Komor et al., 2016).

Adenine also contains an exocyclic amine capable of being deaminated, in this case into inosine which favours pairing to guanine. Gaudelli *et al.* constructed a mutant deoxyadenosine deaminase in *E. coli* able to convert adenine to inosine, fused to a wild-type deoxyadenosine deaminase for sufficient binding to dsDNA, lastly joined to a dCas9 (Gaudelli et al., 2017).

Adenine base editors (ABEs) serve to convert adenine to guanine with similar efficiencies to the conversion of cytosine by CBEs (Gaudelli et al., 2017). Both CBEs and ABEs can only perform their function on ssDNA sequences, meaning displacement of ssDNA upon base pairing between gRNA and the target dsDNA is vital to their function (Rees and Liu, 2018). The ABE 7.10 construct is able to convert A•T to G•C most efficiently when the target base is incorporated into position 4-7 of the gRNA. Thus, the dCas9 serves to open the desired ssDNA bubble, the segment of ssDNA generated is termed the 'R-loop', and the nature of the ssDNA bubble created is both unique to the base editor used and dictates the efficiency of editing for each nucleotide position within the target region (Gaudelli et al., 2020). The adenine deaminase is then able to facilitate the base conversion.

1.4.2.3.2 Prime editing

While base editing is a robust approach for making amino acid substitutions, as with HDR-mediated nucleotide substitutions, there are limitations. The constraints, such as bystander editing and a limited editing window have led to the creation of modified base editors with varying editing window lengths and non-NGG PAMs (Huang et al., 2019). These advances

have refined base editor usage under specific circumstances, such as swapping of purine or pyrimidine bases with ABEs or CBEs, respectively (Gaudelli et al., 2017; Komor et al., 2016; Yeh et al., 2019). The Liu group has been at the forefront of many of these novel methods, creating base editing and more recently, prime editing.

Prime editing and base editing have similar features in that the Cas9 endonuclease does not produce DSBs, requires the opening of the DNA R-loop and that the inactive Cas9 is also fused to an enzyme which serves to create the desired edit. Additionally, both methods benefit from single-stranded nicking close to the target site, to favour the repair of the unedited strand. The main differences between these two novel CRISPR/Cas9 techniques are that prime editing requires a nickase for initiation of editing and the catalytically impaired Cas9 is also tethered to a specifically engineered reverse transcriptase rather than a deaminase (Rees and Liu, 2018).

Although efficient, the major limitation of base editing is its inability to perform transversion mutations (Yan et al., 2020). Prime editing offers the opportunity to generate all possible nucleotide substitutions without creating a DSB or needing an exogenous ssDNA template. It is at least as efficient as HDR-mediated gene editing – Anzalone *et al.* demonstrate that the ratio of editing:indels for correction of the most common cause of sickle cell disease (haemoglobin subunit β (*HBB*) E6V mutation) using prime editing was 270-fold higher than when using HDR-mediated CRISPR/Cas9 methods in HEK293T cells (Anzalone et al., 2019). Further, prime editing has markedly fewer off-target effects.

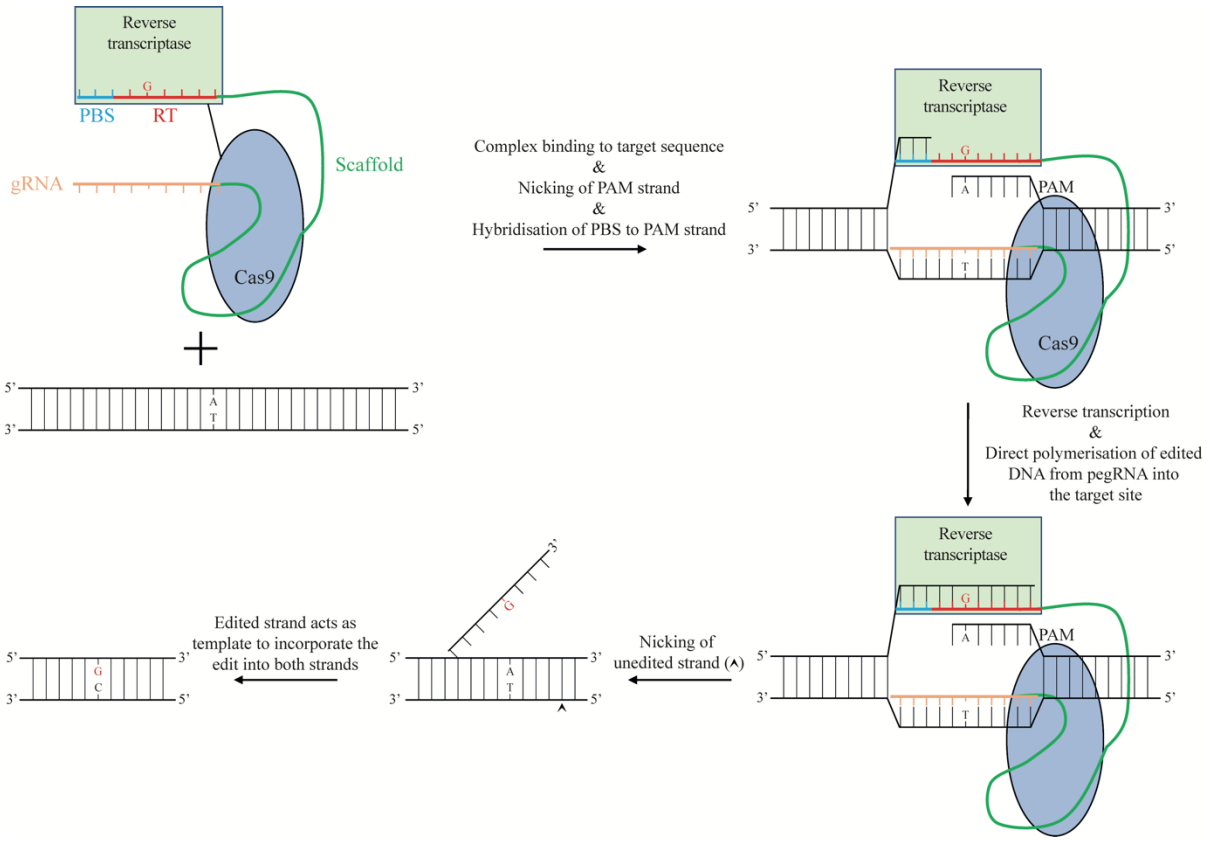

Figure 1.6: The use of prime editing to generate nucleotide substitutions.
Diagram displaying the simplified mechanism of harnessing prime editing to create nucleotide substitutions. Explanation of the mechanism in more detail in main text. Figure adapted from Anzalone *et al.*, 2019.

1.4.2.3.3 Prime editing mechanism

Classical CRISPR/Cas9 gene editing techniques use a gRNA whose specific function is to target the Cas9 complex to the target site (Ran et al., 2013). Prime editing exploits the flexible single-stranded DNA R-loop formed when the Cas9 complex binds to double stranded DNA (Jiang et al., 2016; Jinek et al., 2014) and a specifically designed gRNA construct, to both target the complex to the desired DNA region and also contain all the required information to act as a template to incorporate the edit (Anzalone et al., 2019) (Fig. 1.6). Upon cleavage of the PAM-containing strand, the 3' end of the nicked DNA R-loop is exposed and importantly, sufficiently accessible to prime DNA polymerisation.

A critical feature of gRNAs is that 5' or 3' extension does not affect Cas9 activity (Qi et al., 2013; Shechner et al., 2015; Tang et al., 2017). Therefore Anzalone *et al.* designed a construct that included a gRNA, the canonical gRNA scaffold and a prime editing extended gRNA (pegRNA) in an acceptor plasmid (Anzalone et al., 2019). The pegRNA sequence requires significant modification based on the individual edit site desired. The pegRNA contains a primer binding site (PBS) sequence and a DNA synthesis template (reverse transcriptase (RT)) sequence containing the desired edit. The former serves to target the 3' end of the exposed DNA R-loop nicked by the Cas9 nickase and acts as a primer for reverse transcription.

Successful targeting and priming produces an intermediate with a 5' unedited flap and a 3' edited flap containing the DNA sequence derived from the pegRNA (Fig. 1.7A). Incorporation of the 5' unedited flap is more thermodynamically favourable, however structure-specific endonucleases target 5' flaps for excision (Huggins et al., 2002; Liu et al., 2004). This usually results in a DNA heteroduplex with one edited strand and one unedited. To force the DNA repair machinery into using the edited strand as the template, a strategy employed by base editor-mediated editing is used to nick the unedited strand to stably incorporate the nucleotide substitution (Gaudelli et al., 2017; Komor et al., 2016; Nishida et al., 2016) (Fig. 1.7). Extensive experiments by Anzalone *et al.* demonstrated that nicking 14-116 bases from the pegRNA-induced nick site increases editing efficiency in the vast majority of cases, however the extent to which varies based on loci-specific factors. Further, as the PAM site sequence is present within the RT 3' extension, alteration of the PAM site to incorporate a silent mutation while disrupting further gRNA binding abrogates re-editing of successfully modified DNA, increasing editing efficiency (Anzalone et al., 2019).

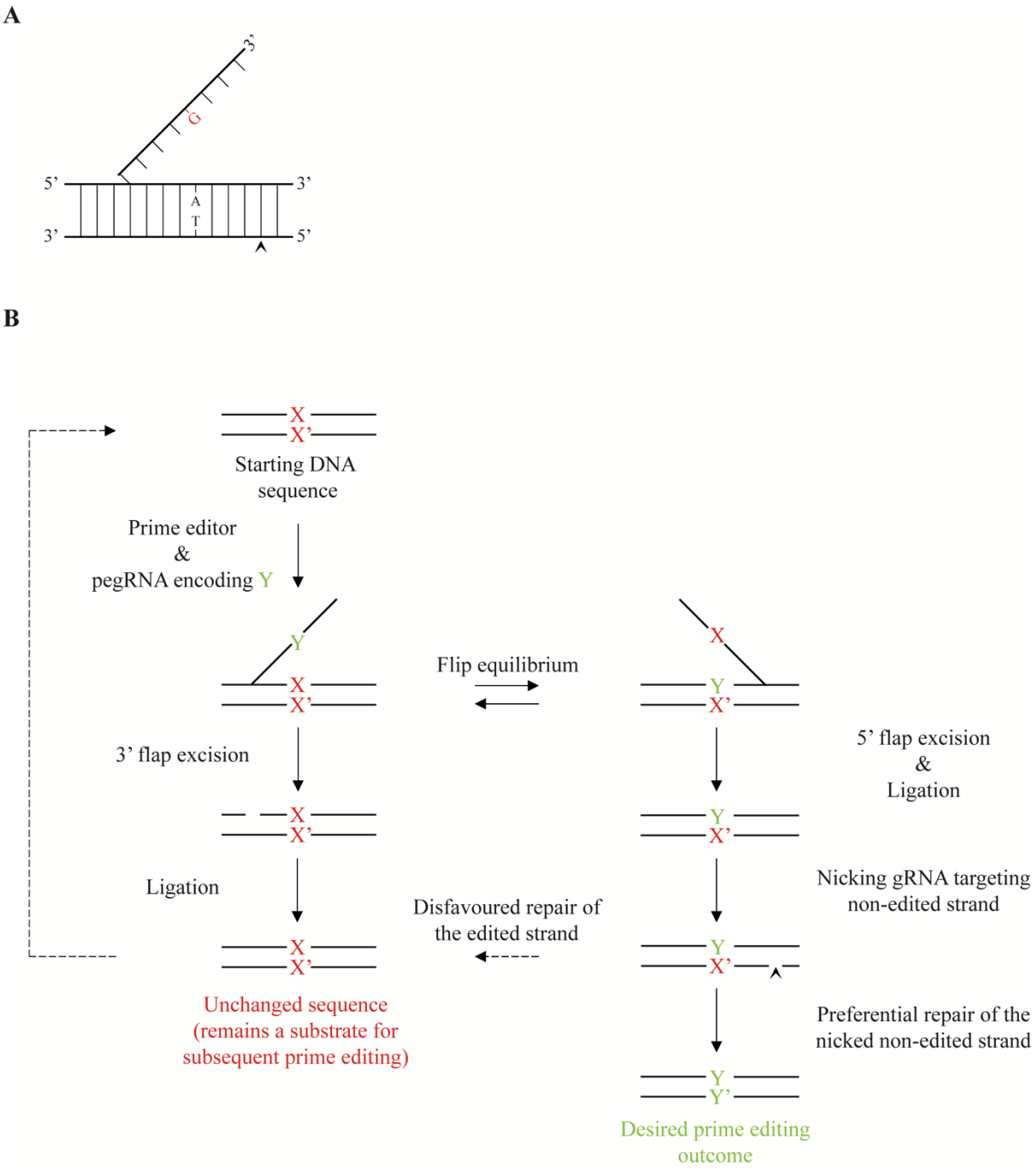

Figure 1.7: Optimised prime editing strategy to facilitate edited strand inclusion.
(A) A simplified diagram indicating the location of the intermediate 3' edited flap and the more thermodynamically stable 5' unedited flap. (B) A simplified diagram displaying the effect of nicking the unedited strand to force DNA repair machinery to use the edited strand as a template, to stably incorporate the nucleotide substitution. This process is described in more detail in main text. Figure adapted from Anzalone *et al.*, 2019.

1.5 Hypothesis and aims

The IGF-axis is an important regulator of cancer cell proliferation and invasion, and can also mediate therapy resistance (Aleksic et al., 2017; Codony-Servat et al., 2017; Hua et al., 2020; Kucab and Dunn, 2003; Simpson et al., 2020; Wang et al., 2019). Inhibition or depletion of IGF-1R has been shown by our lab and others to enhance sensitivity to IR and chemotherapy (Chitnis et al., 2014; Rochester et al., 2005; Simpson et al., 2020; Turney et al., 2012; Zhao and Gu, 2014b). Further, IGF-1R inhibition impairs repair of DSBs and there is evidence of association of high *IGF1R* expression with radio-resistance and biochemical recurrence after IR (Aleksic et al., 2017). All functions of IGF-1R were assumed to require the kinase activity of the receptor. However, evidence suggests that loss of unliganded IGF-1R can influence gene transcription, and that kinase-dead IGF-1R affects the response to apoptotic stimuli (Boucher et al., 2010a, 2014).

Therefore, it is unclear whether increased radio-sensitivity in IGF-1R depleted or inhibited cells is due to decreased receptor kinase activity or a consequential inability to provide a structural scaffold for protein interactions. Furthermore, it is not clear which pathway(s) downstream of IGF-1R are responsible for mediating radio-resistance. The ultimate objectives of this work are to assess whether IGF-1R kinase activity is essential for producing the increased radio-sensitive phenotype, and identify the proteins and processes that mediate effects of IGF-1R on the DNA damage response. We hypothesise that there is an uncharacterised link between IGF-1R and DNA repair, leading to increased radio-sensitisation when the IGF-axis is blocked.

Aims:

1. Test whether the radio-sensitisation phenotype induced by IGF-1R downregulation or inhibition (as reported in the Macaulay group in AR-negative DU145 prostate cancer cells (Chitnis et al., 2014)) is recapitulated by *IGF1R* gene silencing in the 22Rv1 prostate cancer cell line, which is AR-positive and therefore more clinically relevant.
2. To create and characterise IGF-1R null clones and cells expressing a kinase-dead IGF-1R using CRISPR/Cas9 genome editing, to assess whether effects of IGFs on the DDR require IGF-1R kinase activity or structural properties of the receptor.
3. To test whether clones expressing kinase-dead receptor or clones lacking IGF-1R exhibit enhanced radio-sensitivity.
4. To perform unbiased proteomic and phospho-proteomic screens on IGF-1R proficient and deficient prostate cancer cells to gain a better understanding of the role of IGF-1R signalling in the cellular response to irradiation.

Altogether, this work aims to further understand the metabolic regulation of the DDR with the hope of providing novel therapeutic targets for cancer treatment using hypothesis-led and unbiased approaches.

Chapter II: Materials & Methods

2.1 Cell culture

The AR-negative DU145 prostate cancer cell line was obtained from Cancer Research UK Laboratories, Clare Hall, Hertfordshire, UK. DU145 cells are derived from a brain metastasis in a 69 year old Caucasian male (Stone et al., 1978). The cells harbour P223L/V274F mutations in *TP53* producing non-functional p53 (Chappell et al., 2012), and *PTEN* +/- resulting in normal *PTEN* expression (Fraser et al., 2012). In nude mice, the cells form grade II adenocarcinoma consistent with primary prostatic cells. The 22Rv1 cell line were kindly provided by the Bodmer laboratory (Weatherall Institute of Molecular Medicine, University of Oxford, UK), derived from serial propagation in mice of AR-dependent CWR22 prostate cancer xenograft (Sramkoski et al., 1999). The cells are able to form tumours in mice and are *PTEN* wild-type and *TP53* WT/Q331R (Chappell et al., 2012; Fraser et al., 2012).

To test for mycoplasma infection, the MycoAlert detection kit (Lonza, UK|) was used according to manufacturer's instructions. Cells were cultured in Roswell Park Memorial Institute (RPMI) 1640 medium at 37 °C in 5% CO2, supplemented with 10% Fetal Bovine Serum (FBS) (Gibco, 10500064) and 100 units/ml of penicillin and 0.1 mg/ml streptomycin (ThermoFisher, 15140122). For routine passage, cells were washed in PBS (Sigma Aldrich, P4417) and dissociated with trypsin (Lonza, LZBE02-007E). After cells had been dissociated with trypsin and resuspended in normal culture media, cell suspension and trypan blue (Thermo Fisher, T10282) were mixed in 1:1 volume and the suspension was added to a disposable Countess chamber slide. The slide was counted using the Countess II Automated Cell Counter (Thermo Fisher, AMQAX1000).

2.2 siRNA knockdown

Cells were seeded at 750,000 cells/10 cm dish and the following day transfected with 50 nM of AllStars negative control (Qiagen, 1027280) (siControl) or IGF-1R small interfering RNA (siRNA) (Qiagen, Hs_IGF1R_1) (siIGF-1R). 6.8 µl of 20 µM siRNA stock was mixed with 1,523.5 µl Opti-MEM (ThermoFisher, 31985070) and incubated at room temperature for 10 mins. In parallel, 12.3 µl of Oligofectamine (ThermoFisher, 12252011) was mixed and incubated with 410 µl Opti-MEM. Both mixes were then added together and incubated at room temperature for 25 mins. Meanwhile, cells were washed twice with 7 ml room temperature Opti-MEM, before the addition of 780 µl Opti-MEM. After incubation, the siRNA-Oligofectamine complexes (volume totalling 1952 µl) were added drop by drop to the cells. Cells were incubated at 37 °C for 4 hours before addition of 11 ml RPMI-1640 and 273 µl FBS (final concentration 10%). After 48 hours, cell lysates were obtained for Western blot analysis or cells were reseeded for 2D clonogenic survival assays or 3D spheroid assays.

2.3 Western blotting

Cells were washed once with PBS (Sigma Aldrich, P4417) and lysed using RIPA buffer (Sigma Aldrich, R0278) supplemented with phosphatase inhibitor cocktail 2 and 3 (Sigma, P5726, P0044) and protease inhibitor (Roche, 11873580001). Cells were placed on ice for 30 mins, followed by centrifugation at (13,000 xg) for 10 mins at 4 °C. Supernatant was collected and soluble protein content measured using the Pierce™ BCA Protein assay (ThermoFisher, 23225) as per manufacturer's instructions.

Analysis was performed using a POLARstar Omega plate reader (BMG LabTech). Lysates were prepared with equal amounts of protein, and NuPAGE™ LDS Sample Buffer (4X) (Invitrogen, NP0007), supplemented with dithiothreitol (DTT) (Thermo Scientific, R0861) and water to 25 µl. Once prepared, samples were boiled at 95 °C for 5 mins and separated on either 4-15%, 7.5% or 10% Mini-PROTEAN TGX™ Precast Protein gels (BioRad, 4561081, 4561021, 4561031) depending on size of protein to be detected.

Protein transfer was carried out using the TurboTransfer Unit (BioRad, 1704150) onto a nitrocellulose membrane (BioRad, 1620116) at 125 mA for ~90 mins. Membranes were blocked for 1 hour at room temperature in 5% BSA (Sera care, 1900-0004) in PBS (Sigma Aldrich, P4417) supplemented with 0.01% Tween (Fisher Scientific, 10113103) (PBS-T) and primary antibody, diluted in 5% BSA in PBS-T, was incubated overnight shaking at 4 °C. Membranes were washed three times for 5 mins in PBS-T, before addition of secondary antibody, either HRP-conjugated goat anti-mouse or goat anti-rabbit (Cell Signalling Technologies, #7076, #7074) for 1 hour shaking at room temperature. After three additional 5 min PBS-T washes, proteins were detected by Clarity Western ECL Substrate (Biorad, 1705061) using the ChemiDoc XRS+ system (Biorad, 1708265).

2.4 Antibodies

Protein	Source	Company	Serial No.
53BP1	Rabbit	Novus Biologicals	NB100-304
AKT	Rabbit	Cell Signalling Technologies	9272
ATM	Rabbit	Abcam	Ab32420
Cleaved Caspase-3	Rabbit	Cell Signalling Technologies	9664
CHD1	Rabbit	Cell Signalling Technologies	4351
CHK2	Rabbit	Cell Signalling Technologies	2662
DNA-PK_{cs}	Mouse	Sigma	MABC1236
E-Cadherin	Rabbit	Cell Signalling Technologies	3195
ERK1/2	Mouse	Cell Signalling Technologies	4696
FK2	Mouse	Enzo	BML-PW0150-0025
H2AX	Rabbit	Cell Signalling Technologies	2595S
IGF-1R β	Rabbit	Cell Signalling Technologies	3027
IGF-1R β	Rabbit	Cell Signalling Technologies	9750
IGF-1R β	Mouse	Santa Cruz Biotechnology	sc-81167
KAP1	Rabbit	Cell Signalling Technologies	4123
Ku70	Rabbit	Abcam	Ab83501
Ku80	Mouse	Neomarkers	MS-285-P1
Lamin A/C	Rabbit	Abcam	Ab224816
p53	Rabbit	Abcam	Ab131442
PRAS40	Rabbit	Cell Signalling Technologies	2610
RAD51	Rabbit	Cell Signalling Technologies	8875
RB	Mouse	Cell Signalling Technologies	9309
RPA32	Rat	Cell Signalling Technologies	2208
S6	Rabbit	Cell Signalling Technologies	2217
TSC2	Mouse	Cell Signalling Technologies	3612
β-tubulin	Rabbit	Sigma Aldrich	T6074

Protein	Source	Company	Serial No.
Acetyl-Histone H3K9	Rabbit	Cell Signalling Technologies	9649
Acetyl-Histone H3K14	Rabbit	Cell Signalling Technologies	4318
Acetyl-(K120)-p53	Mouse	Abcam	Ab78316
Phospho-(T37/46)-4E-BP1	Rabbit	Cell Signalling Technologies	2855
Phospho-(T308)-AKT	Rabbit	Cell Signalling Technologies	9275
Phospho-(S473)-AKT	Rabbit	Cell Signalling Technologies	4060
Phospho-(S1981)-ATM	Rabbit	Abcam	Ab81292
Phospho-(T68)-CHK2	Rabbit	Cell Signalling Technologies	2661
Phospho-(S2056)-DNA-PK_{cs}	Rabbit	ThermoFisher	PA5-78130
Phospho-(S3205)-DNA-PK_{cs}	Goat	Lees-Miller Laboratory	N/A
Phospho-(T2609)-DNA-PK_{cs}	Mouse	Abcam	Ab18356
Phospho-(T202/Y204)-ERK1/2	Rabbit	Cell Signalling Technologies	4370
Phospho-(Y1316)-IGF-1R β	Rabbit	Abcam	Ab226871
Phospho-(Y1135/1136)-IGF-1R β/-(Y1150/1151)-INSR β	Rabbit	Cell Signalling Technologies	3024
Phospho-(S824)-KAP1	Rabbit	Abcam	Ab70369
Phospho-(T246)-PRAS40	Rabbit	Cell Signalling Technologies	2997
Phospho-(S807/811)-RB	Rabbit	Cell Signalling Technologies	9308
Phospho-(S4/8)-RPA32	Rabbit	Abcam	Ab243866
Phospho-(S240/244)-S6	Rabbit	Cell Signalling Technologies	5364
Phospho-(T1462)-Tuberin/TSC2	Rabbit	Cell Signalling Technologies	3611
Phospho-(S139)-Histone H2A.X	Mouse	Millipore	05-636
Alexa Fluor 488-conjugated goat anti-mouse	Mouse	Thermo Fisher	A20181
Alexa Fluor 594-conjugated goat anti-rabbit	Rabbit	Thermo Fisher	A11012

2.5 2D clonogenic survival assay

For examination of siRNA knockdown radio-sensitivity, transfections were carried out as described (section 2.2) and 48 hours later, cells were disaggregated and seeded at 3000 cells/10 cm dish in triplicate per condition. Clonogenic survival was then measured as described below.

For non-transfected cells, cells were seeded at a density of 3000 cells/10 cm dish in triplicate per condition. The following day, cells were irradiated at indicated doses using a Caesium-137 Irradiator (ORCRB, University of Oxford) and incubated at 37 °C in 5% CO_2 for 10-14 days until colonies of approximately 50 cells had developed. Cells were then washed in PBS (Sigma Aldrich, P4417) and fixed and stained in methanol:acetic acid 3:1, supplemented with 0.1% Brilliant Blue R (Sigma Aldrich, B0149) for 30 mins at room temperature. Dishes were washed in water and clonogenic survival was measured using the GELCount automated colony counter machine (Oxford Optronix).

2.6 CRISPR/Cas9 gene editing

2.6.1 Oligonucleotide list

Name	Sequence	Function
IGF1R_Exon2_1F	CACCGGCATCGACATCCGCAACGA	gRNAs to target exon 2 of *IGF1R* for IGF-1R null clone creation
IGF1R_Exon2_1R	AAACTCGTTGCGGATGTCGATGCC	
IGF1R_Exon2_2F	CACCACCTCACGGTCATCCGCGGC	
IGF1R_Exon2_2R	AAACGCCGCGGATGACCGTGAGGT	
IGF1R_Exon2_3F	CACCACCTGAGGAACATTACTCGG	
IGF1R_Exon2_3R	AAACCCGAGTAATGTTCCTCAGGT	
IGF1R_Exon2_4F	CACCGGATGCGGTGTCCAATAACT	
IGF1R_Exon2_4R	AAACAGTTATTGGACACCGCATCC	
IGF1R_Exon2_T7_F	CTGGAGAACTGCACGGTGAT	Primers to amplify region surrounding *IGF1R* exon 2 target site to examine CRISPR cutting efficiency
IGF1R_Exon2_T7_R	TGGTCTTCTCACACATCGGC	
IGF1R_Exon16_1F	TAGAGTTCCCCCAAAGCAC	Primers to amplify region surrounding K1003 of *IGF1R* exon 16
IGF1R_Exon16_1R	AGCCAAGAACATACTGGGAG	
IGF1R_Exon16_T7_F	GCCCTGACACCTCTTTTGGA	Primers to amplify region surrounding *IGF1R* exon 16 target site to examine CRISPR cutting efficiency
IGF1R_Exon16_T7_R	CAATCGCACCTGGGAGGAAT	

Name	Sequence	Function
IGF1R_Exon2_1F	CACCGGCATCGACATCCGCAACGA	gRNAs to target exon 2 of *IGF1R* for IGF-1R null clone creation
IGF1R_Exon2_1R	AAACTCGTTGCGGATGTCGATGCC	
IGF1R_Exon2_2F	CACCACCTCACGGTCATCCGCGGC	
IGF1R_Exon2_2R	AAACGCCGCGGATGACCGTGAGGT	
IGF1R_Exon2_3F	CACCACCTGAGGAACATTACTCGG	
IGF1R_Exon2_3R	AAACCCGAGTAATGTTCCTCAGGT	
IGF1R_Exon2_4F	CACCGGATGCGGTGTCCAATAACT	
IGF1R_Exon2_4R	AAACAGTTATTGGACACCGCATCC	
IGF1R_Exon2_T7_F	CTGGAGAACTGCACGGTGAT	Primers to amplify region surrounding *IGF1R* exon 2 target site to examine CRISPR cutting efficiency
IGF1R_Exon2_T7_R	TGGTCTTCTCACACATCGGC	
IGF1R_Exon16_1F	TAGAGTTCCCCCAAAGCAC	Primers to amplify region surrounding K1003 of *IGF1R* exon 16
IGF1R_Exon16_1R	AGCCAAGAACATACTGGGAG	
IGF1R_Exon16_T7_F	GCCCTGACACCTCTTTTGGA	Primers to amplify region surrounding *IGF1R* exon 16 target site to examine CRISPR cutting efficiency
IGF1R_Exon16_T7_R	CAATCGCACCTGGGAGGAAT	
IGF1R_K1003R_gRNA1_F	CACCGGCCATTAAAACAGTGAACG	gRNA K1 to target exon 16 of *IGF1R*
IGF1R_K1003R_gRNA1_R	AAACCCTCGTTCACTGTTTTAATG	
IGF1R_K1003R_gRNA2_F	CACCGGCCTCGTTCACTGTTTTAA	gRNA K2 to target exon 16 of *IGF1R*
IGF1R_K1003R_gRNA2_R	AAACTTAAAACAGTGAACGAGGCC	
IGF1R_K1003R_gRNA3_F	CACCGCTCGTTCACTGTTTTAATGG	gRNA K3 to target exon 16 of *IGF1R*
IGF1R_K1003R_gRNA3_R	AAACCCATTAAAACAGTGAACGAGC	
IGF1R_K1003R_ssODN	G*GTGAAAGATGAACCTGAAACCA GAGTGGCCATTAGAACAGTGAACG AAGCCGCAAGCATGCGTGAGAG*G	ssODN to incorporate K1003R using HDR-mediated editing. (*=phosphorothioate)
IGF1R_K1003R_ABE_1F	CACCGGTTAAAACAGTGAACGAGGCCGC	Variants of gRNA for attempts to create K1003R using adenine base editing
IGF1R_K1003R_ABE_1R	AAACGCGGCCTCGTTCACTGTTTTAACC	
IGF1R_K1003R_ABE_2F	CACCGATTAAAACAGTGAACGAGGCCGC	
IGF1R_K1003R_ABE_2R	AAACGCGGCCTCGTTCACTGTTTTAATC	
IGF1R_K1003R_ABE_3F	CACCGCCATTAAAACAGTGAACGAGGC	
IGF1R_K1003R_ABE_3R	AAACGCCTCGTTCACTGTTTTAATGGC	
IGF1R_K1003R_ABE_4F	CACCGTTTGGTCTCAGGCCATTAAAACAGTGAACGAGG	
IGF1R_K1003R_ABE_4R	AAACCCTCGTTCACTGTTTTAATGGCCTGAGACCAAAC	

Name	Sequence	Function
IGF1R_PE_gRNA_F	CACCAGATGAACCTGAAACCAGAGGTTTT	gRNA to target *IGF1R* exon 16 for prime editing
IGF1R_PE_gRNA_R	CTCTAAAACCTCTGGTTTCAGGTTCATCT	
PX458_Scaffold_F	AGAGCTAGAAATAGCAAGTTAAAATAAGGCTAGTCCGTTATC AACTTGAAAAAGTGGCACCGAGTCG	Scaffold sequence for prime editing
PX458_Scaffold_R	GCACCGACTCGGTGCCACTTTTTCAAGTTGATAACGGACTAG CCTTATTTTAACTTGCTATTTCTAG	
IGF1R_pegRNA_3ntRT_PBS_F	GTGCGTTCTAATGGCGACTCTGGTTTCAGGTT	pegRNA with constant PBS sequence, differing RT sequence (3nt, 6nt, 9nt, as described in main text)
IGF1R_pegRNA_3ntRT_PBS_R	AAAAAACCTGAAACCAGAGTCGCCATTAGAAC	
IGF1R_pegRNA_6ntRT_PBS_F	GTGCACTGTTCTAATGGCGACTCTGGTTTCAGGTT	
IGF1R_pegRNA_6ntRT_PBS_R	AAAAAACCTGAAACCAGAGTCGCCATTAGAACAGT	
IGF1R_pegRNA_9ntRT_PBS_F	GTGCTTCACTGTTCTAATGGCGACTCTGGTTTCAGGTT	
IGF1R_pegRNA_9ntRT_PBS_R	AAAAAACCTGAAACCAGAGTCGCCATTAGAACAGTGAA	
IGF1R_nickgRNA_-81_F	CACCCTGCCCAAGTTCCCGGCTCA	Nicking gRNA sequences to nick DNA at indicated positions surrounding K1003 to facilitate more efficient prime editing
IGF1R_nickgRNA_-81_R	AAACTGAGCCGGGAACTTGGGCAG	
IGF1R_nickgRNA_-54_F	CACCTGGGCAGGGGTCGTTTGGGA	
IGF1R_nickgRNA_-54_R	AAACTCCCAAACGACCCCTGCCCA	
IGF1R_nickgRNA_-27_F	CACCTGAAGGAGTTGCCAAGGGTG	
IGF1R_nickgRNA_-27_R	AAACCACCCTTGGCAACTCCTTCA	
IGF1R_nickgRNA_+21_F	CACCGGCCATTAAAACAGTGAACG	
IGF1R_nickgRNA_+21_R	AAACCGTTCACTGTTTTAATGGCC	
IGF1R_nickgRNA_+21AGA_F	CACCGGCCATTAGAACAGTGAACG	
IGF1R_nickgRNA_+21AGA_R	AAACCGTTCACTGTTCTAATGGCC	
IGF1R_nickgRNA_+41_F	CACCAGGCCGCAAGCATGCGTGAG	
IGF1R_nickgRNA_+41_R	AAACCTCACGCATGCTTGCGGCCT	
IGF1R_nickgRNA_+75_F	CACCCAACGAAGCTTCTGTGATGA	
IGF1R_nickgRNA_+75_R	AAACTCATCACAGAAGCTTCGTTG	
IGF1R_Ex2_Seq_F	ACCGAGTACTTGCTGCTGTT	Sequencing primer for *IGF1R* exon 2
IGF1R_Ex16_Seq_F	GATCACCATGAGCCGGGAAC	Sequencing primer for *IGF1R* exon 16

2.6.2 Plasmid list

Plasmid	Source
pSpCas9(BB)-2A-GFP (PX458)	Addgene #48138
XCAS9(3.7)-ABE(7.10)	Addgene #108382 (a kind gift from Dr Philip Hublitz (WIMM, University of Oxford))
pBS_hU6-sgRNA_EF1a_eGFP	A kind gift from Dr Philip Hublitz (WIMM, University of Oxford)
pCMV-PE2	Addgene #132775
pU6-Neo	A kind gift from Dr Thomas Roberts (DPAG, University of Oxford)
pcDNA3-EGFP	Addgene #13031
pDVG94	A kind gift from Dr Dik van Gent (Department of Molecular Genetics, Erasmus University of Rotterdam)

2.6.3 Annealing single-stranded oligonucleotides

ssODNs were designed using Ensembl (Hunt et al., 2018), UCSC Genome Browser (Kent et al., 2002), SnapGene Viewer (SnapGene software (from Insightful Science; available at snapgene.com)) and PrimerBLAST (Ye et al., 2012). All ssODNs were ordered from IDT and resuspended to a final concentration of 100 µM in ddH_2O. ssODNs were annealed by combining 1 µl of sense and anti-sense ssODN with 1 µl 10x T4 ligation buffer (NEB), 1 µl T4 PNK (NEB) and ddH_2O to a total volume of 10 µl. The ssODNs were phosphorylated and annealed in a thermocycler at 37 °C for 30 mins, 95 °C for 5 mins and ramp down to 25 °C at 5 °C/min.

2.6.4 Restriction enzyme digestion

1 µg of DNA was digested with desired restriction enzyme (listed below) for 60 mins at 37 °C (or 15 mins if a NEB Fast Digest enzyme). For cloning, product was run on 0.8-1% agarose gel (Sigma Aldrich, A9539) and gel purified as described in section 2.6.10.2.

2.6.5 Ligation of gRNAs into digested vectors

All vectors were digested according to conditions stated in section 2.6.4. Annealed ssODNs (gRNAs) (37.5 ng) were ligated into appropriate vector (50 ng) using 2x T7 DNA ligase buffer (NEB), T7 DNA ligase and ddH_2O to 20 µl. This was left at room temperature for 30 mins then used immediately for transformation (section 2.6.6) or stored at -20 °C.

2.6.6 Bacterial transformations

DH5α competent cells (NEB, C2987I) were thawed on ice for 10 mins and 2.5-5 µl of plasmid DNA was mixed with 50 µl DH5α competent cells and incubated on ice for 30 mins. Cells were heat-shocked at 42 °C for exactly 30 seconds and put back on ice for 5 mins. To these cells, 950 µl of room temperature S.O.C Outgrowth medium (NEB, B9020) was added, and the mixture was incubated at 37 °C for 1 hour shaking. After incubation, 50-150 µl of mixture was spread on Lysogeny Broth (LB) agar plates (Sigma, L3147) containing desired antibiotic (ampicillin (Sigma, A5354) or kanamycin (Sigma Aldrich, K1377)) at a final concentration of 100 µg/ml, and incubated overnight at 37 °C. The following day individual colonies were picked and incubated in LB (Miller) (Sigma Aldrich, L3522) and desired antibiotic shaking overnight at 37 °C, volume scaled for appropriate downstream plasmid DNA purification method. Glycerol stocks were made with 25% glycerol (Sigma Aldrich, G5516) and stored at -80 °C.

2.6.7 Plasmid DNA purification

2.6.7.1 Qiaprep spin miniprep kit

Overnight culture of *E. coli* in LB (Miller) (Sigma Aldrich, L3522) (5 ml) was pelleted at 6,800 xg for 3 mins at room temperature. DNA was prepared using the QIAprep Spin Miniprep Kit (Qiagen, 27106) according to manufacturer's instructions. DNA was eluted in 30 µl nuclease-free water (Invitrogen, AM9937) and the concentration of the eluted DNA was then measured using the NanoDrop One Microvolume UV-Vis Spectrophotometer (ThermoFisher, ND-ONE-W) according to manufacturer's instructions.

2.6.7.2 Midipreps

Overnight culture of *E. coli* in LB (Miller) (Sigma Aldrich, L3522) (50 ml) was pelleted at 6,000 xg for 15 mins at 4 °C. DNA was prepared using the HiSpeed Plasmid Midi Kit (Qiagen, 12643). The pellet was air-dried for 5-10 mins and redissolved in 1 ml of nuclease-free water (Invitrogen, AM9937). The concentration of the eluted DNA was then measured using the NanoDrop One Microvolume UV-Vis Spectrophotometer (ThermoFisher, ND-ONE-W) according to manufacturer's instructions.

2.6.8 Plasmid transfections

Cells were seeded in the appropriate sized plate/dish to be 60-80% confluent at time of transfection. Lipofectamine 3000 Reagent (Thermo Fisher, L3000008) was diluted in Opti-MEM medium and a master mix of DNA was prepared by diluting DNA in Opti-MEM and P3000 Reagent. Both solutions were mixed well and diluted DNA was added to diluted Lipofectamine 3000 Reagent in a 1:1 ratio. Mixture was incubated for 10-15 mins at room temperature before the DNA-lipid complex was added to cells in a drop-wise fashion. Transfection efficiency was

monitored using fluorescence where possible, by the ZOE Fluorescent Cell Imager (Biorad, 1450031EDU). For sequencing, genomic DNA was extracted 48 hours post-transfection. For downstream FACS or Alt-R genome editing detection, cells were isolated 72 hours after transfection.

2.6.9 Genomic DNA extraction and polymerase chain reaction

Genomic DNA was extracted using the GenELUTE™ Mammalian Genomic DNA Miniprep kit (Sigma Aldrich, G1N70) according to manufacturer's instructions. For gene-edited clonal analysis, genomic DNA was extracted using KAPA Express Extract kit (Roche, KK7100) according to manufacturer's instructions.

For polymerase chain reaction (PCR), primers were designed and checked using Primer-BLAST (Ye et al., 2012) (list below) and each reaction contained 1 µl (0.5 µM final concentration) of forward and reverse primers, 12.5 µl Phusion High-Fidelity PCR Master Mix with HF Buffer (ThermoFisher, F531S), 1 µl genomic DNA template and 9 µl nuclease-free water (Invitrogen, AM9937) to 25 µl. Reaction was performed as detailed below, with annealing temperatures indicated in primer table.

Temperature (°C)	Time	No. cycles
98	2 mins	
98	10 sec	30 cycles
Annealing Temp	30 sec	
72	45 sec	
72	5 mins	
4	∞	

When run on an agarose gel, 6x Loading Dye (NEB, B7021S) was added to PCR product, and sample was run on a 0.8-1% agarose (Sigma Aldrich, A9539) gel at 100 V for ~1 hour, using either a 100 base pair (bp) DNA ladder (NEB, N3231) or 1 kb DNA ladder (NEB, N3232). The gel was visualised using the ChemiDoc MP system (Biorad, 17001402).

2.6.10 PCR product purification

2.6.10.1 Column purification

PCR products were purified using the PCR Purification Kit (Qiagen, 28106) as per manufacturer's instructions. DNA concentrations were measured using the NanoDrop One Microvolume UV-Vis Spectrophotometer (ThermoFisher, ND-ONE-W) as per manufacturer's instructions.

2.6.10.2 Gel Extraction

PCR products were run on a 0.8-1% agarose gel (Sigma Aldrich, A9539) and visualised and excised under UV light. DNA in gel fragment was purified using the Qiaquick Gel Extraction Kit (Qiagen, 28706) according to manufacturer's instructions. DNA concentrations were measured using the NanoDrop One Microvolume UV-Vis Spectrophotometer (ThermoFisher, ND-ONE-W) according to manufacturer's instructions.

2.6.11 Sanger sequencing

PCR products and plasmid DNA were prepared according to Source Bioscience sequencing guidelines. 100 ng/µl plasmid DNA or 10 ng/µl purified PCR product in 5 µl H_2O, and 5 µl of 3.2 pmol sequencing primer in H_2O/reaction.

2.6.12 Alt-R genome editing detection

Genomic DNA of CRISPR/Cas9-treated cells was amplified using components of the Alt-R Genome Editing Detection Kit (IDT, 1075931) as follows (control B: same sequence as control A, but with 6 bp deletion):

Component	Sample (µl)	Alt-R Control A (µl)	Alt-R Control B (µl)
Forward Primer (10 µM)	1.25		
Reverse Primer (10 µM)	1.25		
Genomic DNA	1		
Alt-R Control A (Template/Primer mix)		2	
Alt-R Control B (Template/Primer mix)			2
Phusion HF MM	12.5	12.5	12.5
ddH_2O	9	10.5	10.5
Total	25	25	25

The PCR used the following conditions:

Step	Temperature (°C)	Time	Cycles
Denature	98	2 mins	1
Denature	98	10 secs	30
Anneal	Variable (primer specific) 67 for Control A and B	30 secs	
Extend	72	45 secs	
Extend	72	5 mins	1

To measure the extent of insertions/deletions formed, PCR products were then heated to 95 °C for 10 mins to separate double stranded DNA, and cooled slowly (95-85 °C at ramp rate -2 °C /sec, followed by 85-25 °C at ramp rate -0.3 °C /sec) to anneal single-stranded DNA together, forming heteroduplexes for T7 endonuclease 1 digestion (T7E1). Volumes as follows:

Component	Sample (µl)	Homoduplex Control (µl)	Heteroduplex Control (µl)
PCR Product	10	10 Control A	5 Control A 5 Control B
T7E1 Reaction Buffer (10x)	2	2	2
Nuclease-Free Water	6	6	6
Total	18	18	18

The difference in control A and B sequences highlighted above produces heteroduplexes. T7E1 was added to the hetero/homoduplexes formed in this reaction and the reaction was incubated at 37 °C for 1 hour. Products were run on a 1% agarose gel and band intensities calculated using ImageJ (NIH, USA). From this, specific gRNAs were selected for future null clone generation.

2.6.13 Golden Gate assembly

Golden Gate cloning is a method of assembling DNA fragments in a specific order using type IIS restriction enzymes, which cut at a region outside of the enzyme recognition sequence. This facilitates the creation of specific pre-designed overhangs, in this case in two annealed ssODNs, which are then able to be ligated together in a precise order, generating the required construct (Padgett and Sorge, 1996; Werner et al., 2012). Golden Gate assembly was carried out according to the manufacturer's instructions (NEB, E1601).

2.6.14 Data analysis tool for gene editing

After genomic DNA extraction using the KAPA Express Extract kit (Roche, KK7100) of cells transfected with prime editing constructs and an unedited clone, DNA was amplified by PCR and PCR products were purified using the PCR Purification Kit (Qiagen, 28106) according to the manufacturer's instructions. Purified PCR products were analysed by Sanger sequencing. The extent of editing within the sample was then measured using EditR software (Kluesner et al., 2018) which is designed to analyse Sanger sequencing traces by comparing to a control (unedited) sample. The user also inputs the gRNA sequence used to increase the accuracy of the editing efficiency calculation (www.baseeditr.com).

2.7 Flow Cytometry

After checking for satisfactory GFP signal at 48 hours post-transfection of GFP-tagged plasmids, cells were washed with PBS at 72 hours post-transfection. Cells were dissociated with trypsin and upon inactivation by addition of RPMI-1640, cells were transferred to the appropriately sized tube and centrifuged at 300 xg for 5 mins. The resulting cell pellet was resuspended in 0.5 ml flow media (2% FCS, 2 mM EDTA in PBS) and filtered through a 40 μm cell strainer (Falcon, 352340). The fluorescence-activated cell sorting (FACS) was carried out by Andrew Worth (Jenner Institute, University of Oxford, UK) where the top 20% GFP-positive cells were single cell-sorted into individual pre-warmed media-containing wells of five 96-well plates. The remaining top 50% GFP-positive cells were collected and grown as a bulk culture for sequencing analysis.

2.8 Cell-based ELISA

Cells were seeded into a 96-well plate with white walls and flat clear bottoms (Greiner, 655074) and incubated at 37 °C in 5% CO_2 in RPMI-1640 until 70-80% confluent. For dose-response experiments and phospho-ELISAs, cells were serum-starved overnight, and stimulated with IGF-1/insulin at indicated concentrations for 30 minutes. Medium was aspirated from wells and cells were immediately fixed with 100 µl 4% paraformaldehyde in TBS for 20 minutes shaking at room temperature. Cells were washed twice for 5 minutes in 0.5% Triton X-100 in TBS before being quenched by adding 1.2% H_2O_2, 0.5% Triton X-100 in TBS for 30 minutes at room temperature with agitation. Cells were washed once more with 0.5% Triton X-100 in TBS, before wells were blocked in 5% BSA in 0.5% Triton X-100 in TBS for 1 hour shaking at room temperature. After, blocking solution was aspirated and appropriate primary antibody was added (diluted in blocking buffer) and incubated overnight at 4 °C with agitation. Plate was covered in parafilm to minimise evaporation. The following day, cells were washed four times in 0.5% Triton X-100 in TBS for 5 minutes at room temperature, before addition of secondary antibody (1:2,000 anti-rabbit IgG, HRP-linked Antibody 7074) in blocking buffer) and incubation at room temperature for 1 hour with agitation. After three washes of 5 minutes with 0.5% Triton X-100 in TBS and one wash of 5 minutes with TBS at room temperature, 100 µl of tetramethylbenzidine solution (Sigma Aldrich, T0440) (equilibrated to room temperature) was added to each well. TMB was incubated with agitation in darkness for 25 minutes before being quenched by adding equal volume 2 M H_2SO_4. The absorbance of each well was measured using POLARstar OMEGA plate reader.

2.9 Membrane Localisation

Three dishes were plated at $1x10^6$ cells/15 cm dish and when 80% confluent, cells were harvested using a cell scraper and centrifuged at 300 xg for 5 mins. Membrane extraction was performed using the Mem-PER Plus Membrane Protein Extraction Kit (Thermofisher, 89842). Cell pellet was washed with 3 ml Cell Wash Solution and centrifuged for 5 mins at 300 xg. The supernatant was carefully removed, and the cell pellet was resuspended in 1.5 ml Cell Wash Solution, transferred to a centrifuge tube and centrifuged at 300 xg for 5 mins. The supernatant was then discarded, and 0.75 ml of Permeabilisation Buffer was added to the cell pellet, vortexed and incubated for 10 mins at 4 °C with constant mixing. Following centrifugation of permeabilised cells at 16,000 xg for 15 mins at 4 °C, the supernatant was removed containing the cytosolic proteins and transferred to a new tube. To the pellet, 0.5 ml of Solubilisation Buffer was added, and after resuspension, samples were incubated with constant mixing for 30 mins at 4 °C. Tubes were spun at 16,000 xg for 15 mins at 4 °C, before the supernatant containing solubilised membrane and membrane-associated proteins was collected. Protein concentrations were determined, and equal amounts of protein were run on a Western blot.

2.10 Nuclear Localisation

Cells were plated at a density of $1x10^6$ cells/15 cm dish in three dishes, and upon 80% confluency, cells were harvested with trypsin and centrifuged at 500 xg for 5 mins. Nuclear extraction was carried out using the NE-PER Nuclear and Cytoplasmic Extraction Kit (Thermo Fisher, 78833). Cells were washed by resuspending the cell pellet with PBS and transferred to a microcentrifuge tube. The cells were pelleted by centrifugation at 500 xg for 3 mins before the supernatant was carefully removed by pipette, and later syringe with needle, leaving the

pellet as dry as possible. The pellet was resuspended in 100 µl ice-cold Cytoplasmic Extraction Reagent 1 and vortexed on the highest setting for 15 seconds to fully suspend the cell pellet. The suspension was then incubated on ice for 10 mins, before addition of 11 µl ice-cold Cytoplasmic Extraction Reagent 2. The mixture was vortexed for 5 seconds on the highest setting, centrifuged for 5 mins at 16,000 xg and supernatant immediately transferred to a clean pre-chilled tube (cytoplasmic extract). The remaining insoluble fraction was resuspended in 100 µl ice-cold Nuclear Extraction Reagent and vortexed for 15 seconds on the highest setting. The samples were placed on ice and vortexed as before, every 10 mins for 40 mins. The suspensions were centrifuged at 16,000 xg for 10 mins at 4 °C and the nuclear fraction (supernatant) was immediately transferred to clean pre-chilled tubes. Protein concentrations were determined and equal amounts of protein were run on a Western blot.

2.11 Immunofluorescence

Coverslips were added to 6 well plate and washed once with ethanol (Sigma, 1590100500) and twice with PBS (Sigma Aldrich, P4417). Cells were seeded at 100,000 cells/well. For localisation experiments, cells were fixed the following day in 4% paraformaldehyde as described below. For irradiation experiments, plates were irradiated at 2 Gy the day after seeding and incubated at 37 °C for the required length of time. Cells were then fixed in 4% paraformaldehyde (ThermoFisher, 28906) in TBS for 12 minutes shaking at room temperature covered with foil. After washing carefully with TBS for 10 mins shaking at room temperature, 1 ml TBS was added to each well and plates were left at 4 °C until all cells were fixed. Cells were then permeabilised in 0.1% Triton X-100 (Sigma Aldrich, X100), 1% FCS in TBS at room temperature without shaking for 5 mins. Cells were then washed with TBS and blocked for 45 mins in 5% BSA in TBS shaking at room temperature. 60 µl of primary antibody (1:200

in 1% BSA in TBS) was applied to parafilm stretched over microscope slide, and coverslip was placed facedown onto parafilm, incubated at 4 °C overnight in the dark. The following morning, coverslips were washed in 6 well plates with TBS three times and 60 µl secondary antibody in 1% BSA in TBS was prepared and coverslips added as described above. Coverslips were incubated at room temperature in the dark for 1 hour, before a brief wash in TBS. Coverslips were then mounted using DAPI mounting media (Vectashield, H-1200) and allowed to dry at room temperature for 30 mins before being stored at 4 °C in the dark for future analysis. Foci were imaged using a Carl Zeiss 780 microscope (ORCRB, University of Oxford).

2.12 3D spheroid assay

Cells were seeded at a density of 5,000 cells/well in 160 µl RPMI-1640 in Ultra-Low Attachment 96 well plates (Corning, CLS7007). After 48 hours, plates were irradiated at indicated doses using a Caesium-137 Irradiator (ORCRB, University of Oxford). Individual wells were imaged each day using the GELCount automated colony counter machine (Oxford Optronix). Spheroid area was measured using ImageJ software and relative spheroid area was calculated relative to day 1 spheroid area. After final daily spheroid imaging, cells were subjected to a CellTiter-Glo 3D Viability Assay (Promega, G9681) described below (section 2.13).

2.13 CellTiter-Glo 3D cell viability assay

The CellTiter-Glo 3D reagent was equilibrated to room temperature gently rotating, to obtain a homogenous solution. After final spheroid imaging, 100 µl CellTiter-Glo 3D reagent equal to the volume of medium containing spheroids was added to each well. The plate was then mixed vigorously at 500 rpm in the POLARstar OMEGA plate reader for 5 mins to induce cell lysis. The plate was then incubated in darkness for 25 mins at room temperature before the luminescent signal was recorded using the POLARstar OMEGA plate reader.

2.14 Proteomics and phosphoproteomics sample preparation

22Rv1 cells, two wild-type clones, two IGF-1R-null clones and the hypomorphic mutant clone were plated in 10cm dishes (750,000 cells/plate, 3 plates/condition) and the following day, 22Rv1 cells were transfected with siControl or siIGF-1R (see section 2.2). After 48 hours, 2 Gy irradiation was given to the appropriate plates and 1 hour later, cell pellets were collected from all plates. Pellets were stored at -80 °C until phosphoproteomic preparation. After lysate collection, a small fraction of each lysate was used for an estimation of total protein per sample, and volumes were adjusted with RIPA buffer to normalise protein concentration. All proceeding steps were carried out in low-retention tubes (Fisher Scientific, 11313653), using low-retention pipette tips. Cell pellets were resuspended and washed in ice-cold PBS to remove proteins present in residual medium, and pelleted at 300 xg for 5 mins at 4 °C. PBS was removed and 700 µl RIPA buffer containing protease (Roche) and phosphatase inhibitor cocktail 2 and 3 (Sigma Aldrich) was used to lyse pellets. Lysis was carried out at 4 °C rotating for 15 mins, before being vortexed, then cell debris was pelleted at 17,900 xg for 10 mins at 4 °C. Supernatants were transferred to new tubes and protein concentration was measured using the BCA protein assay described in section 2.3. Protein amount in all samples was adjusted to

the lowest total amount possible (270 µg) in 700 µl with RIPA buffer. Samples were vortexed and 5 mM DTT was added to each sample, before an additional vortex. Samples were then incubated at room temperature for 30 mins covered with foil, and 20 mM iodoacetamide (IAA) (Sigma Aldrich) was added. Samples were incubated for 30 mins at room temperature in darkness. Samples were transferred to 15 ml Falcon tubes and 2256 µl of methanol was added to each. After this, 564 µl of chloroform was added and samples were vortexed. 1692 µl of LCMSMS water was added and samples were again vortexed, then centrifuged at room temperature for 6 mins at 3,000 xg. Precipitate formed in the middle of each sample and the upper aqueous phase was removed without disrupting precipitate at the interface. 1692 µl of methanol was added and samples were vortexed, before centrifugation at room temperature for 6 mins at 17,000 xg. Supernatant was removed and pellets were dried by Savant SpeedVac (Fisher Scientific, 15819206), before being denatured with 8 M urea in 20 mM HEPES buffer and digested with immobilised trypsin beads overnight. The following morning, samples were desalted using SOLA SPE cartridges, dried and reconstituted. Then 90% of each sample was enriched for phosphopeptides using the Agilent Bravo robot, and the remaining 10% was used to analyse the total proteome.

2.15 End Joining Assay

The pDVG94 plasmid was kindly provided by the van Gent laboratory. The plasmid was linearised using EcoRV (NEB, R0195S) and AfeI (NEB, R0652S), and purified using a plasmid miniprep kit (Qiagen, 27104). Cells were seeded in 6-well plates until ~50% confluency before transfection of 2 µg linearised pDVG94 using Lipofectamine 3000. After 2 days, plasmid DNA was recovered using a plasmid miniprep kit (Qiagen, 27104). To analyse the recovered plasmid, 1 µl of plasmid DNA was used for PCR amplification. Conditions used

were the same as in section 2.6.9, using DAR5 (5'-TGCTTCCGGCTCGTATGTTGGTTGGAAT -3') and FM30 (5'-CTCCATTTTAGCTTCCTTAGCTCCTG-3') primers, with annealing temperature of 55 °C. 5 µl of PCR reaction was digested in a total volume of 20 µl with BstXI (NEB, R0113S). Undigested and digested PCR product were run on a 4% agarose gel (Lonza, 50081) stained with SYBR Safe (ThermoFisher, S33102) and band intensities were quantified using ImageJ software, by the equation (120 bp product)/(180 bp product + 120 bp product).

2.16 Chromatin Fractionation

Cells were seeded in duplicate in 10 cm dishes (2 x 10^6 cells/dish) and the following day, if applicable, cells were pre-treated with inhibitor 4 hours prior to IR. Lysates from one plate from each condition were collected using RIPA buffer as detailed above in section 2.3. For remaining plate of each condition, media was removed, and plate was washed twice with ice-cold PBS. As much PBS as possible was removed, before addition of CSK (100 mM NaCl, 300 mM sucrose, 3 mM $MgCl_2$, 0.7% Triton X-100, 10 mM PIPES, pH 7.0, supplemented with 0.3 mg/ml RNase A) and incubation with agitation for 3 minutes. CSK was removed and re-added, before incubation with agitation for 3 minutes. Cells were washed three times with ice-cold PBS, before removal. SDS lysis buffer (2% SDS, 10% glycerol, 50 mM DTT, 62.5 mM Tris-HCl, pH 6.8) was added to plates, scraped and transferred to an Eppendorf. Samples were vortexed and boiled for 10 minutes, before being spun at 13,000 xg for 1 minute. Supernatants were transferred to new Eppendorfs and protein concentration was measured using the NanoDrop One machine. Samples were then prepared as in section 2.3 for Western blotting.

2.17 TOPO TA cloning

TOPO TA cloning was carried out according to manufacturer's instructions (Invitrogen, K4575-01). Briefly, PCR products were produced using a *Taq* polymerase, cloned into the pCR™2.1-TOPO® vector and transformed using One Shot™ TOP10 chemically competent *E. coli*. Colonies were picked, miniprepped and sent for sequencing to analyse allele sequences.

2.18 Statistical analysis

Statistical significance was determined using GraphPad Prism version 8.0.1 for Mac (GraphPad Software Inc, USA). Students t-test was used to assess differences between the means of two independent unrelated groups, and one-way ANOVA was used to assess differences between the means of more than two independent unrelated groups. Two-way ANOVA was used for trends between relative band intensities on Western blots and clonogenic survival curves. P-values for significance were calculated and stated in corresponding figure legends.

CHAPTER III: Generation of IGF-1R compromised cells using CRISPR/Cas9 gene editing techniques

3.1 Testing effects of IGF-1R depletion in prostate cancer cells

Previous work showed that IGF-1R knockdown or inhibition using the tyrosine kinase inhibitor AZ12253801 caused increased radio-sensitisation in the AR-negative DU145 prostate cancer cell line measured using 2D clonogenic survival assays (Chitnis et al., 2014; Turney et al., 2012). Initial experiments focussed on confirming this radio-sensitisation phenotype in DU145 cells upon compromisation of IGF-1R signalling. After confirmation of adequate siRNA-mediated IGF-1R knockdown by Western blot (Fig. 3.1A), clonogenic survival assays were performed on DU145 cells (Fig. 3.1B). Survival of siControl cells was comparable to that shown previously in the lab, and the increased radio-sensitisation of siIGF-1R cells was also similar to prior results (Chitnis et al., 2014).

The same experiment was performed using 22Rv1 cells. IGF-1R knockdown was confirmed (Fig. 3.1C) and IGF-1R depleted cells displayed greater radio-sensitivity at increasing radiation doses (Fig. 3.1D). These data were used to calculate dose enhancement ratios (DERs), (calculated as % survival of siControl/% survival of siIGF-1R). In DU145 cells, DER was ≥2.95 at 4 Gy, and in 22Rv1 cells, DER was ≥2.25 at the same dose (Fig. 3.1E). Across all doses, there was no major difference between the two cell lines. This indicated that IGF-1R depletion enhanced radio-sensitivity in 22Rv1 cells, and that radio-sensitisation by IGF-1R depletion was no less effective in 22Rv1 cells than in DU145 cells. Differential phosphorylation of AKT at serine 473 after IGF-1R knockdown in DU145 and 22Rv1 cells

suggested that AKT signalling may not be integral to the radiation response in DU145 cells (Fig. 3.1A, C). In selecting a cell line in which to create a stable model of compromised IGF-1R function, the 22Rv1 cell line was selected because while exhibiting a similar radio-sensitisation phenotype to DU145 cells, 22Rv1 cells express wild-type *TP53* and the AR, thus offering a more clinically relevant disease model (Chappell et al., 2012; Fraser et al., 2012; Sramkoski et al., 1999).

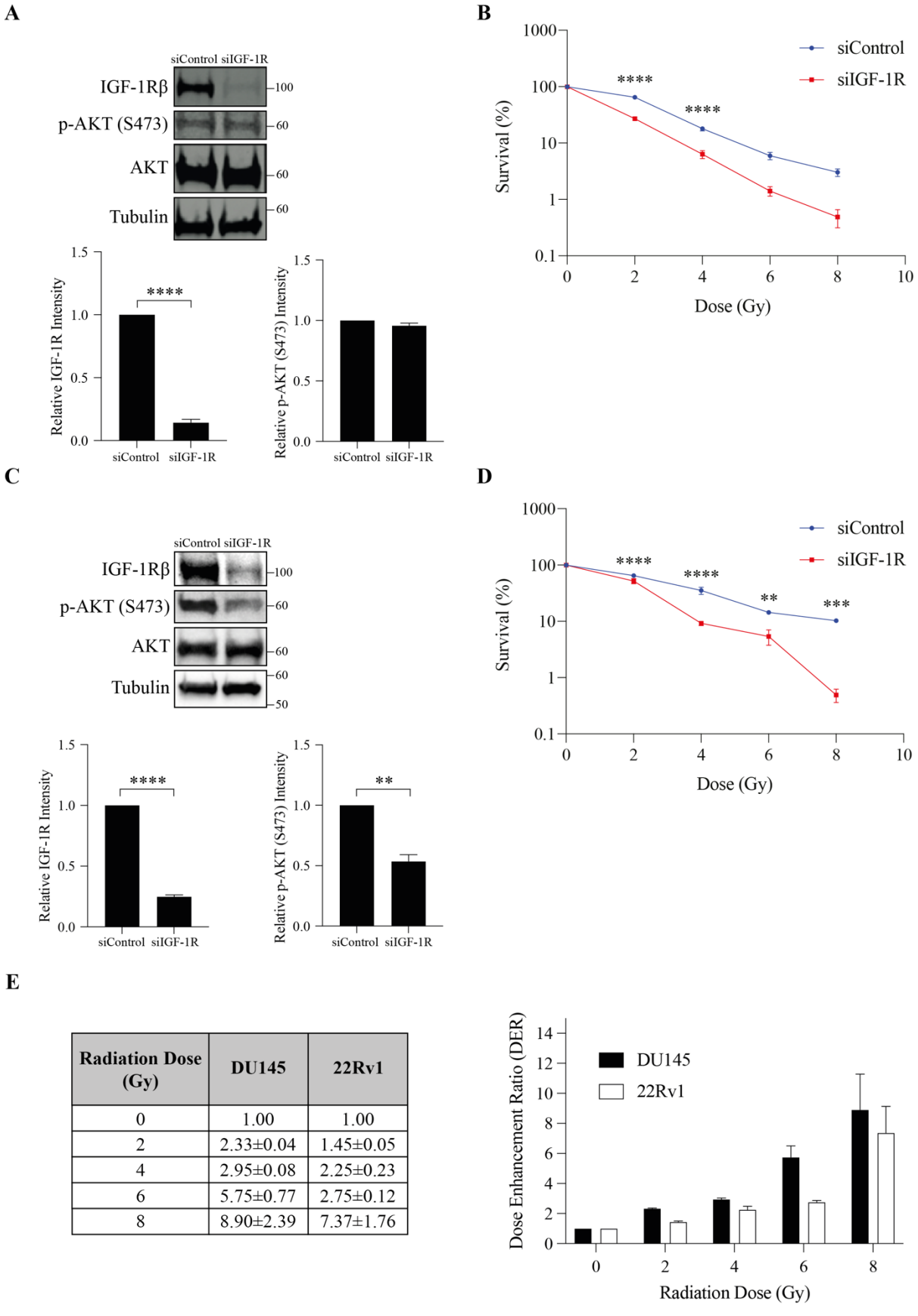

Radiation Dose (Gy)	DU145	22Rv1
0	1.00	1.00
2	2.33±0.04	1.45±0.05
4	2.95±0.08	2.25±0.23
6	5.75±0.77	2.75±0.12
8	8.90±2.39	7.37±1.76

Figure 3.1: IGF-1R depletion radio-sensitises DU145 and 22Rv1 cells.
DU145 cells were seeded in 10cm dishes (7.5 x 10^5 cells/dish), and the following day cells were transfected with 50nM siControl or siIGF-1R. (A) Whole cell lysates were collected 48 hours post-transfection and Western blot analysis was carried out to investigate the extent of IGF-1R knockdown, using β-tubulin as a loading control. IGF-1R knockdown was confirmed in three sets of independently prepared lysates. The data were analysed by unpaired student t-test, to determine statistical significance of band intensity differences (**p<0.0011; ****p<0.0001). (B) Parallel cultures were re-seeded in triplicate 48 hours after siRNA transfection (3.0 x 10^3 cells/10cm dish) and the next day, dishes were irradiated at indicated doses. After 11-14 days, visible colonies were stained with Coomassie Brilliant Blue and counted using GELCOUNT software. The graph displays colony survival as a percentage of survival in un-irradiated siControl-transfected cells. Each point represents the mean ± SEM of triplicate values of one experiment representative of three separate experiments. The data were analysed by 2 way ANOVA, to determine statistical significance of survival differences seen in IGF-1R depleted DU145 cells (****p<0.0001). (C) 22Rv1 cells were seeded in 10cm dishes (7.5 x 10^5 cells/dish), and 50nM transfections were performed with either siControl or siIGF-1R the next day. Whole cell lysates were collected 48 hours after transfection and levels of IGF-1R were assessed by Western blot to determine IGF-1R knockdown efficiency, using β-tubulin as a loading control. Adequate IGF-1R depletion was confirmed in three sets of independently prepared lysates. The data were analysed by unpaired student t-test (****p<0.0001). (D) Parallel cultures were re-seeded in 10cm dishes 48 hours post-transfection (3.0 x 10^3 cells/dish) and the following day cells were irradiated at indicated doses. After 11-14 days, visible colonies were stained with Coomassie Brilliant Blue and counted using GELCOUNT software. The graph displays colony survival as a percentage of survival in un-irradiated siControl-transfected cells. Each point represents the mean ± SEM of triplicate values of one experiment representative of three separate experiments. The data were analysed by 2 way ANOVA, to determine statistical significance of survival differences seen in IGF-1R knockdown 22Rv1 cells (**p<0.0011; ***p<0.0004; ****p<0.0001). (E) DERs for IGF-1R depleted DU145 and 22Rv1 cells were calculated as relative survival of siControl cells/relative survival of siIGF-1R cells at specific radiation doses. DERs for IGF-1R depleted 22Rv1 cells were calculated in triplicate for three independent experiments, pooled and the mean ± SEM was calculated.

3.2 Creation of IGF-1R null clones

To further examine the role of IGF-1R in radio-sensitivity, generation of IGF-1R null clones was attempted. While RNAi-based methods are time-effective methods to significantly reduce target protein levels, the transient nature, incomplete loss of function and high likelihood of off-target effects offer substantial disadvantages for full characterisation of a gene's function (Carthew and Sontheimer, 2009; Sigoillot and King, 2011). An advantage of techniques that create DSBs is that this leads to permanent disruption of the gene causing total loss of function. ZFNs and TALENs are able to create these stable changes to the genome, however designing and engineering the DNA binding domains is complicated and expensive (Boettcher and McManus, 2015; Gaj et al., 2013). CRISPR/Cas9 technology provides a more simple, inexpensive and highly specific method of generating stable loss-of-function mutants (Cho et

al., 2013; Gaj et al., 2013) and so this strategy was tested to create IGF-1R null clones in 22Rv1 cells.

Exon 1 of *IGF1R* encodes the signal peptide, which functions to transport the polypeptide chain into the endoplasmic reticulum (ER) membrane (Ullrich et al., 1986). This signal peptide is then cleaved by a signal peptidase and therefore was deemed unsuitable for targeting as would only target nascent IGF-1R. gRNAs specific for exon 2 of *IGF1R* were designed using Primer-BLAST, annealed and cloned into the BbsI site of the gRNA/Cas9 expression vector PX458 (Addgene #48138) (section 2.6) Successful cloning of the gRNAs into the plasmids was confirmed by Sanger sequencing.

To verify CRISPR/Cas9 targeting to exon 2 and to ascertain the efficiency of each candidate gRNA, genomic DNA was extracted 48 hours post-transfection and amplified by PCR for use in a T7E1 (T7 Endonuclease I) assay. T7E1 specifically cleaves heteroduplexes and therefore gRNA cutting efficiencies can be assessed by quantifying the band intensities of T7E1-digested fragments relative to the undigested fragments. T7E1 assay products were analysed by agarose gel electrophoresis, indicating that the most effective gRNA was gRNA 2 (Fig. 3.2). gRNA2 was chosen as the two bands generated at expected sizes (503 bp and 547 bp) were distinct and with few additional bands. gRNA1 did not show expected fragment sizes upon digestion (712 bp and 338 bp) and while gRNA3, and to a lesser extent gRNA4 showed expected digestion products (710 bp and 340 bp), presence of additional non-specific bands meant that these gRNAs could be cutting at other positions. The absence of a control without T7E1 digestion in genomic DNA would have been informative, however use of such a control in figure 3.3A

indicated that the fragments produced after T7E1 digestion by gRNA2-transfected genomic DNA were due to CRISPR/Cas9 cutting.

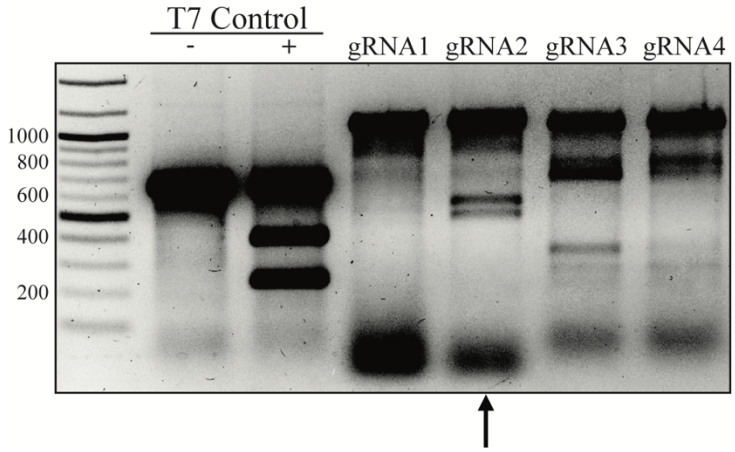

Figure 3.2: Testing the efficiency of candidate gRNAs for successfully targeting IGF1R exon 2.
Cloning of four different IGF1R exon 2-targeting gRNAs into pSpCas9(BB)-2A-GFP (PX458) was carried out. 22Rv1 cells were seeded in a 24 well plate to be 70-80% confluent the following day. Each gRNA was transfected into a separate well, and after 48 hours, genomic DNA was extracted and amplified by PCR. Digestion of PCR products was carried out using the T7E1-based Alt-R Genome Editing Detection Kit and the products were run on a 1% agarose gel. Lane 1: 100bp ladder; 2: negative control mix; 3: positive control mix; 4: gRNA1-PX458; 5: gRNA2-PX458; 6: gRNA3-PX458; 7: gRNA4-PX458. Arrow indicates gRNA selected for use to create IGF-1R null clones.

To generate IGF-1R null cells, the gRNA 2-containing PX458 vector was transfected into 22Rv1 wild-type (WT) cells using Lipofectamine 3000. After 48 hours, genomic DNA was extracted from a parallel transfected culture and a T7E1 assay indicated successful targeting of exon 2 of the receptor (Fig. 3.3A). The following day, cells from the primary transfected culture were single-cell sorted using FACS by their relative fluorescence, as the PX458 vector encodes constitutively expressed GFP. The top 20% of GFP-positive cells were sorted into separate wells of multiple 96 well plates, to increase the likelihood of isolating an IGF-1R null clone, as augmented GFP signal inside cells is indicative of higher transfection efficiency of the CRISPR/Cas9 plasmid (Fig. 3.3B).

Once the majority of single cell clones had expanded to form defined single colonies, after approximately three weeks, the 96 well plates were duplicated, one for continuing passage and one for analysis by an IGF-1R enzyme-linked immunosorbent assay (ELISA). The ELISA, created by Friedbichler *et al.* (Friedbichler et al., 2013) and modified for detection of total IGF-1R protein in DU145 prostate cancer cells by Dr E. Osher (Macaulay lab) was used to assess the presence of IGF-1R, or its absence due to disruption of the *IGF1R* gene (Fig. 3.3C).

22Rv1 cells expressing endogenous IGF-1R were used in the IGF-1R ELISA as a positive control, allowing measurement of receptor levels in candidate null clones to be relative to normal IGF-1R protein levels. To provide an indication of total IGF-1R signal at differing cell densities, cells were plated at increasing densities alongside the candidate IGF-1R null clones. A relative fluorescence unit (RFU) threshold of lower than ~0.15 was chosen as potentially indicative of low/absent IGF-1R (Fig. 3.3D). Of the several 96 well plates, the majority of single cell clones did not survive, and as a result, only clones reaching reasonable (≥65%) cell density were replated for analysis by ELISA (representative images of low and high cell densities are shown (Fig. 3.3E)). Of the 28 clones analysed, reduction in total IGF-1R levels was observed in 27 clones, with 17 clones showing RFU of 0.15 or less (Fig. 3.4).

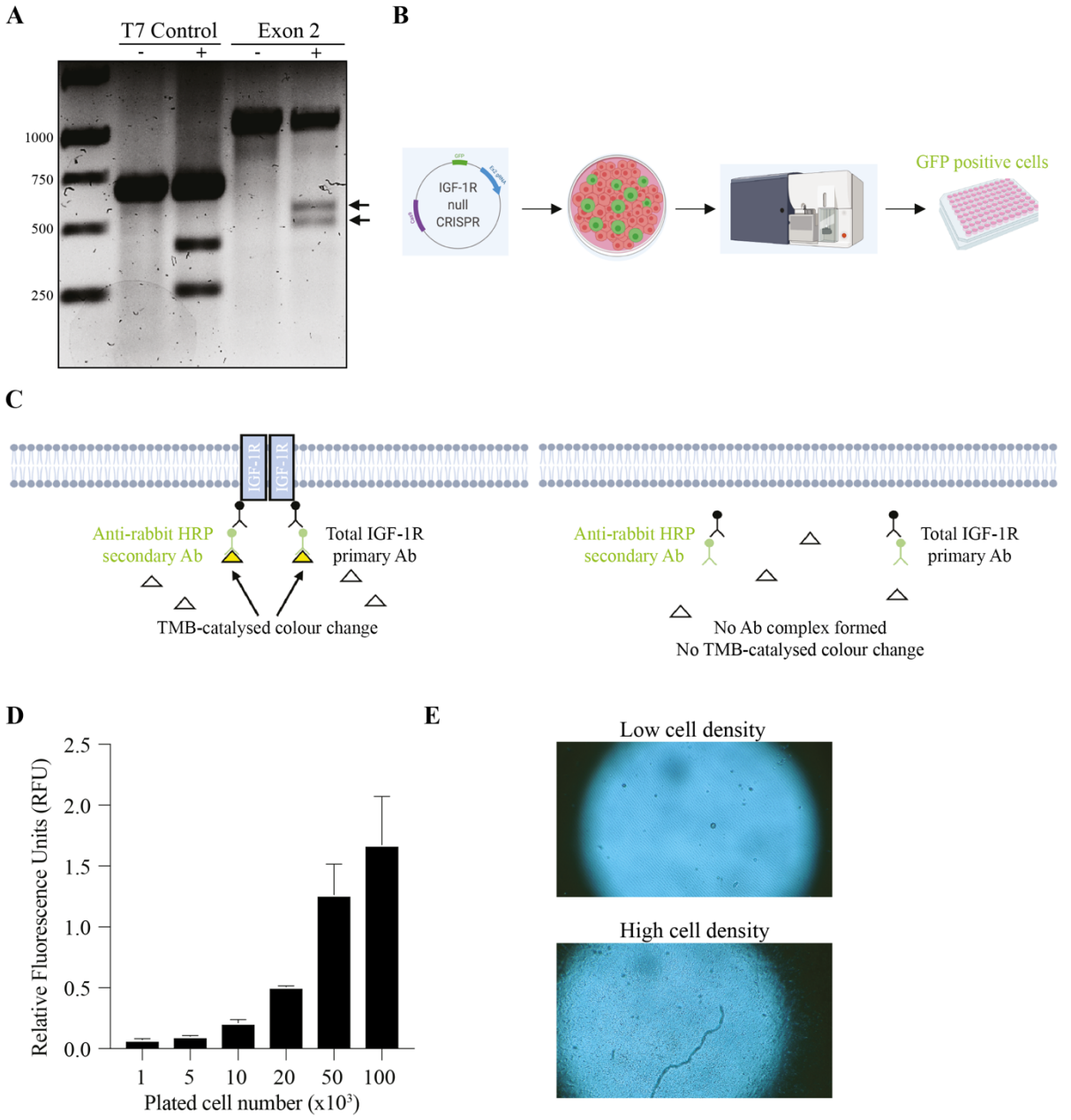

Figure 3.3: Generation and characterisation of IGF-1R null clones.
(A) 22Rv1 cells were seeded in 24 well plates (to be 70-80% confluent the following day) and the next day were transfected with gRNA2-PX458. After 48 hours, genomic DNA was extracted and CRISPR/Cas9 targeting efficiency was assessed using the ALT-R Genome Editing Detection Kit. Lane 1: 1kb DNA ladder; 2: negative control; 3: positive control; 4: gRNA2-PX458 transfected PCR products, without incubation with T7E1; 5: gRNA2-PX458 transfected PCR products with incubation with T7E1. Arrows indicate products at desired sizes, confirming efficient targeting of exon 2 of *IGF1R*. After confirmation of adequate targeting, parallel cultures were trypsinised and single-cell FACS sorted by their relative fluorescence into 96 well plates. (B) Schematic of IGF-1R null clone generation procedure. (C) Diagram illustrating the principle of the IGF-1R enzyme-linked immunosorbent assay (ELISA). Briefly, presence of IGF-1R allows total IGF-1R primary antibody to bind, and addition of anti-rabbit secondary antibody allows for a colour change upon TMB catalysis. Absence of IGF-1R produces no colour change. (D) Alongside the IGF-1R ELISA, 22Rv1 cells were seeded at increasing densities and relative fluorescence units (RFU) were measured using the POLARstar Omega plate reader to assess the sensitivity of the ELISA to detect changes in total IGF-1R signal. Each column represents the mean ± range of duplicate wells of one experiment. (E) Representative images of candidate IGF-1R null clones at low cell density (above) and high cell density (below).

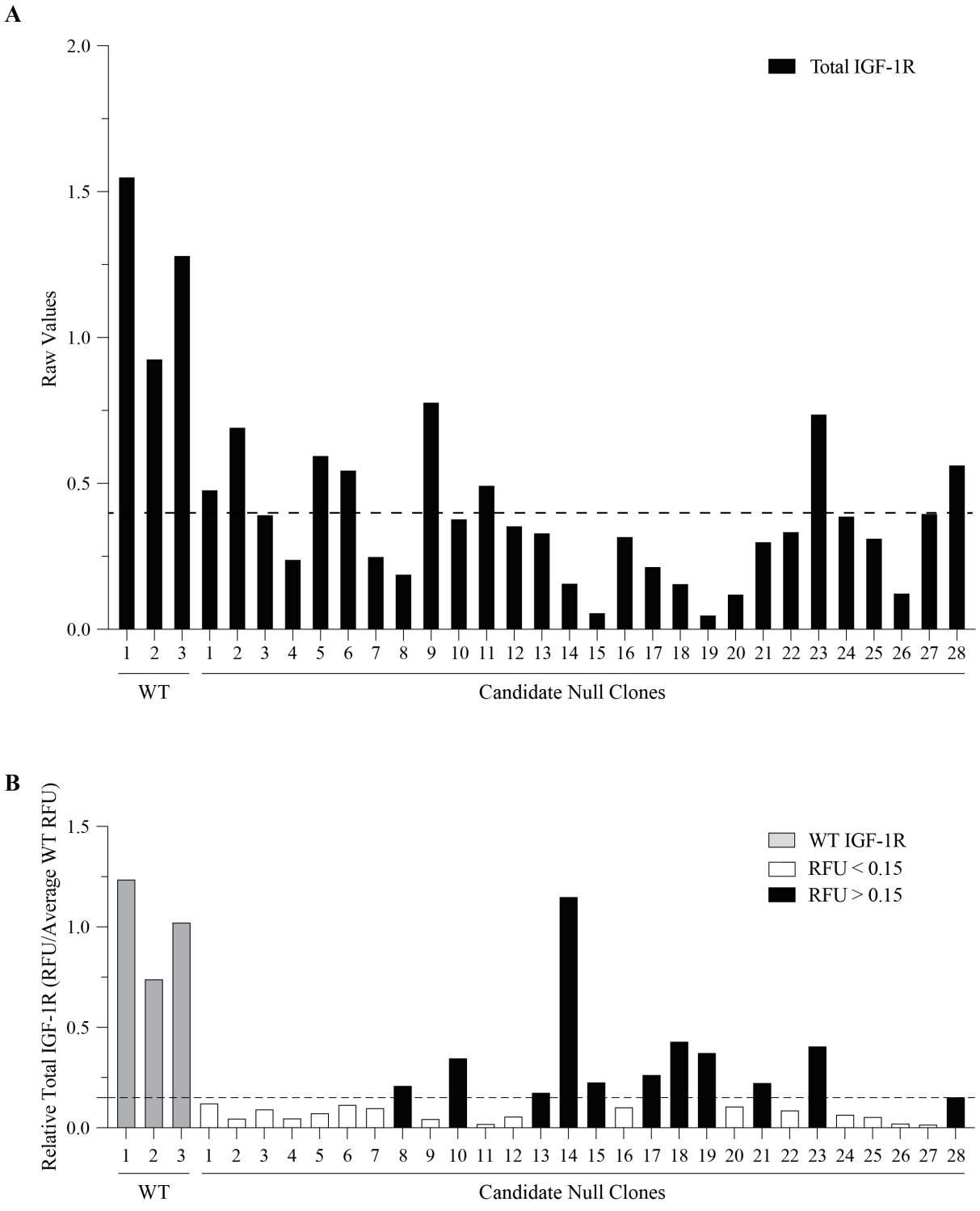

Figure 3.4: Summary of IGF-1R ELISA to identify IGF-1R null 22Rv1 clones.
(A) The IGF-1R ELISA was carried out with three wells of 22Rv1 cells (grey) as positive controls, and 28 candidate IGF-1R null clones (white). Graph shows the raw values obtained from the POLARstar Omega plate reader, with values under dashed line (0.4) considered to be low density clones. (B) Graph shows the relative values obtained from the POLARstar Omega plate reader. All clones exhibiting RFU<0.15 are highlighted in white, and clones where RFU>0.15 are highlighted in black. Black dashed line indicates RFU=0.15.

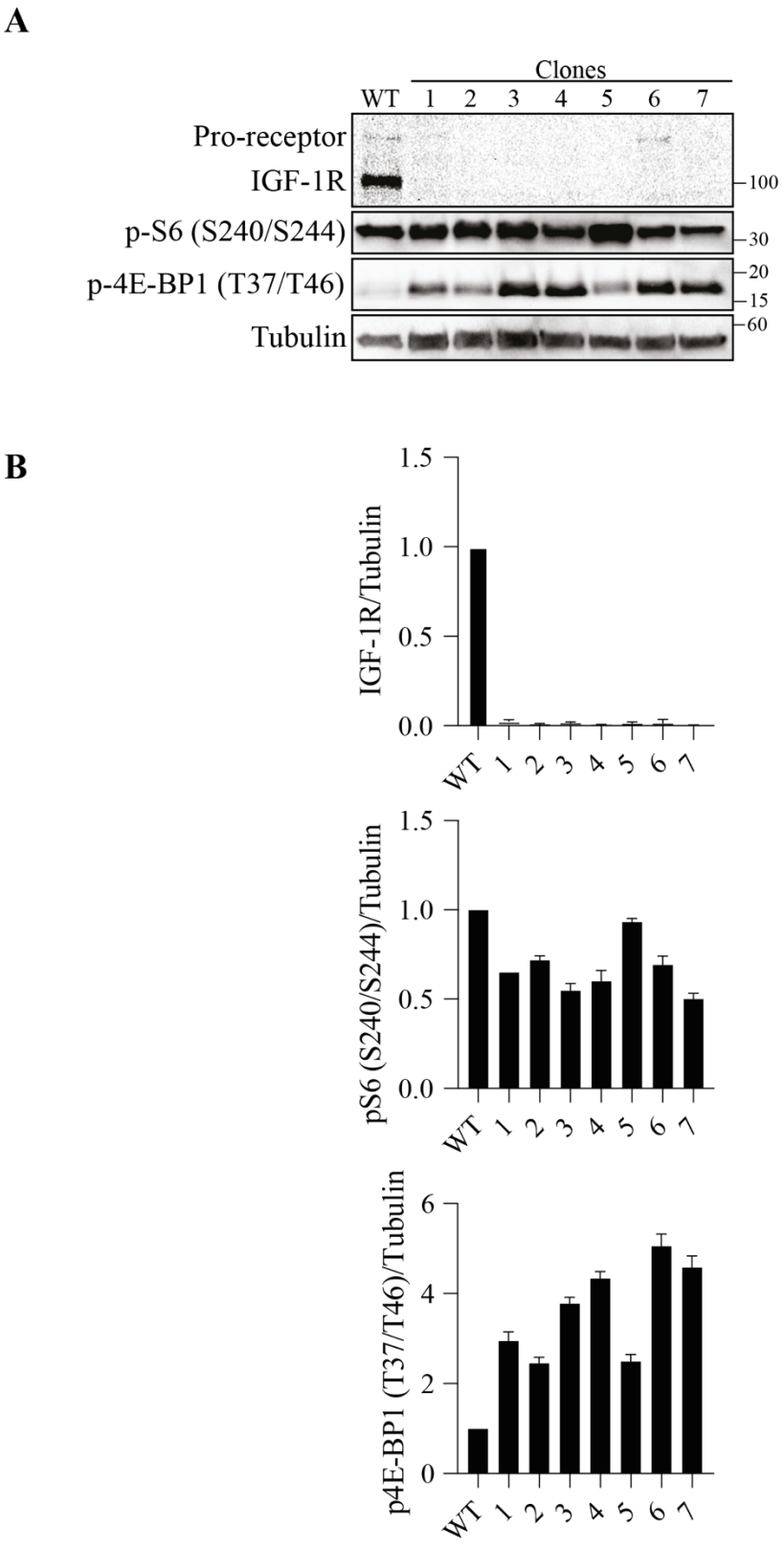

Figure 3.5: Characterisation of IGF-1R null clones by Western blot.
Whole cell lysates for 22Rv1 cells (WT) and 7 candidate IGF-1R null clones were analysed by Western blot for IGF-1R and downstream mTOR effectors with β-tubulin as a loading control. (B) Levels of indicated proteins expressed relative to WT 22Rv1 cells (n=3). The data were analysed by one-way ANOVA, to determine statistical significance of relative band intensity differences (IGF-1R: WT vs all clones ****$p<0.0001$; pS6: WT vs clones 1,2,3, 4, 6 and 7 ****$p<0.0001$; p4E-BP1: WT vs all clones ****$p<0.001$).

Due to the variable growth rates of the candidate null clones, the screening assay did not correct for cell number or protein content of each well. Therefore, cell density was examined in parallel wells of clones with RFU<0.15, as well as analysis of the raw values in the ELISA. Of these, 10 clones had few cells (correlating with Raw value <0.4 in figure 3.4A), accounting for the low RFU value in the ELISA (Fig. 3.4B). The remaining 7 promising candidate clones with raw value >0.4 in figure 3.4A and >50% well coverage by eye were replated from the corresponding duplicate plate, and expanded for further examination. Lysates were obtained and subsequent Western blot analysis indicated successful loss of IGF-1R protein expression, however 2 clones appeared to display the pro-receptor and were not used further (Fig. 3.5). Results suggested reduced S6 phosphorylation and increased 4E-BP1 phosphorylation in IGF-1R null clones compared to IGF-1R WT clones (Fig. 3.5), however phosphorylation signals of S6 and 4E-BP1 were variable between the clones, perhaps highlighting the high amount of crosstalk between upstream mTOR pathway components. Genomic DNA was extracted from encouraging candidate IGF-1R null clones, amplified and sequenced by Sanger sequencing. As is common after CRISPR-mediated editing, short insertions/deletions were shown in the clones (Fig. 3.6) (Allen et al., 2019). These changes altered the reading frame, and confirmed generation of IGF-1R null clones by targeting exon 2 of *IGF1R*. Cloning by limiting dilution was used to generate clones of untransfected 22Rv1 cells expressing WT IGF-1R for future analyses.

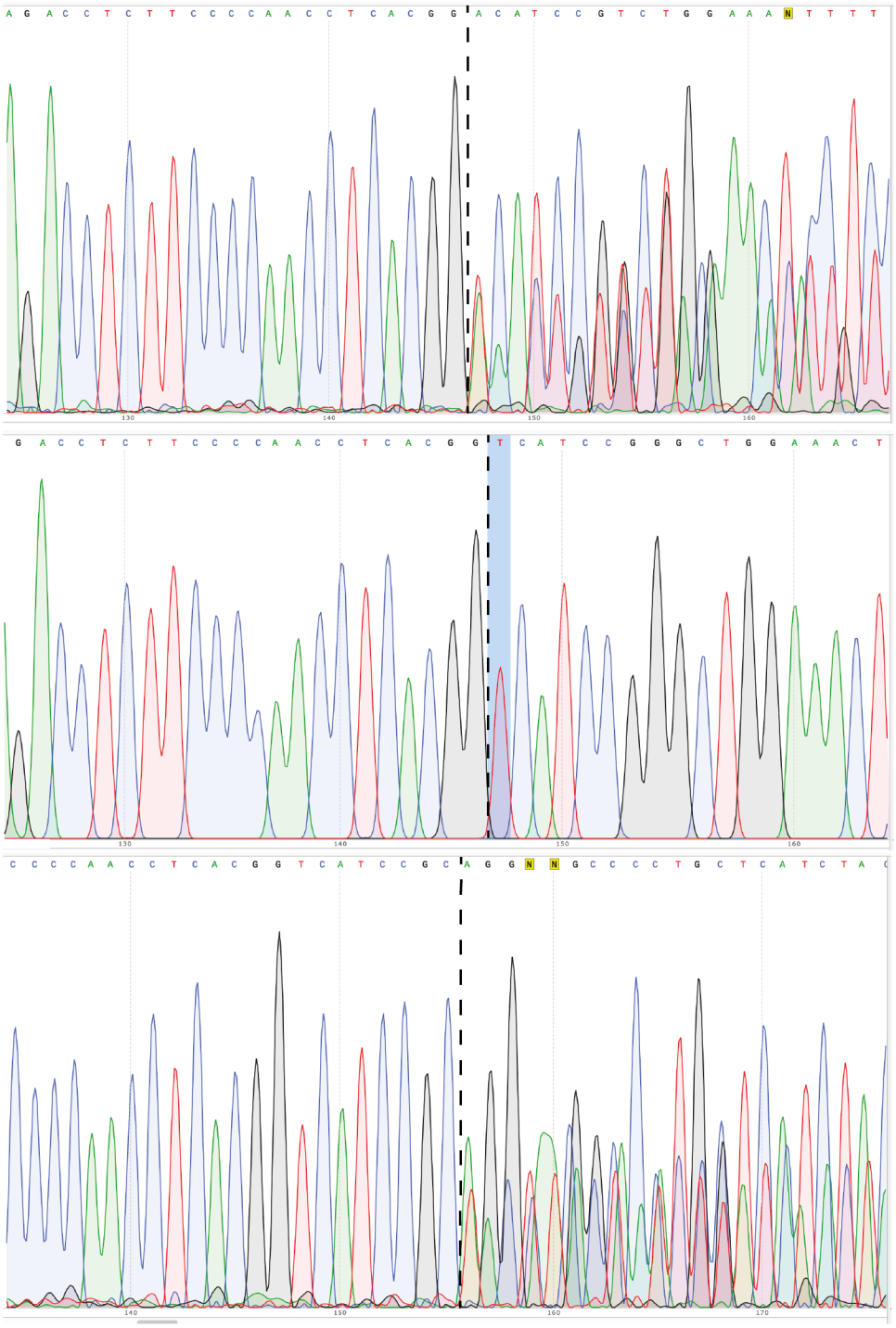

```
WT:      ...CCCCAACCTCACGGTCATCCGCGGCTGGAAACTCTTCTACAA...
Clone 2: ...CCCCAACCTCACGGACATCCG--TCTGGAAANTTTT...
Clone 3: ...CCCCAACCTCACGGTCATCCG-GGCTGGAAACT...
Clone 7: ...CCCCAACCTCACGGTCATCCGCAGGNNGCCCCTGCTCATCTA...
```

Figure 3.6: Characterisation of IGF-1R null clones by Sanger sequencing.
Genomic DNA analyses using Sanger sequencing illustrated the specific insertions (bold)/deletions (-) at the gRNA2-PX458 cut site (dashed line).

3.3 Creation of IGF-1R mutant clone

To explore the molecular basis for increased radio-sensitivity in IGF-1R-compromised cells, attempts were made to use CRISPR/Cas9-mediated gene editing to create a kinase-dead IGF-1R cell line, to examine whether a structural role of the receptor is sufficient in promoting radio-resistance. In the literature, Kato *et al.* characterised a K1003A/R mutation in exon 16 of the kinase domain, at the ATP-binding site rendering the IGF-1R kinase-inactive (Kato et al., 1993). This group and others have reported that the K1003A/R mutation abrogates all IGF-1-stimulated signalling and receptor ubiquitination (Kato et al., 1993; Kiely et al., 2002; Kruis et al., 2010; Sehat et al., 2007). The mutant K1003A/R complementary DNA (cDNA) is under the control of an exogenous promoter, resulting in overexpression of a dominant-negative form of IGF-1R which can bind ligands but has no kinase activity. Overexpression of a dominant-negative mutant receptor could impact regular cell signalling. Therefore, a clone exhibiting kinase-dead IGF-1R under the control of its endogenous promoter may be beneficial for comparison with clones expressing WT IGF-1R and IGF-1R null clones.

To differentiate structural and kinase functions of IGF-1R in promoting radio-resistance, efforts were made to generate a kinase-dead IGF-1R cell line. Amino acid codon sequences indicated that a lysine to arginine substitution would cause less disruption to the DNA sequence, altering one base from adenine to guanine, and so making this substitution was the next aim.

3.3.1 HDR-mediated gene editing strategy to create IGF-1R kinase-dead clones

Three gRNAs targeting exon 16 of *IGF1R* were designed, cloned and transfected to determine the most efficient for use in future editing. gRNA K2 was chosen due to comparable production of desired fragment sizes as gRNA K1, but with fewer off-target fragments, suggesting more specific cutting (Fig. 3.7A, B). Initially, 22Rv1 cells were co-transfected with the CRISPR/Cas9 plasmid containing gRNA K2 and a variety of ssODN designs. These included short sequences homologous to either side of the desired edit, akin to microhomology-mediated end joining gene editing techniques, and ssODNs with longer homology arms (Nakade et al., 2014). However, upon sequencing of genomic DNA extracted from transfected cells, no evidence of editing was observed. Treatment of cells with an HDR 'enhancer' molecule (Integrated DNA Technologies, 1081072) to enhance HDR by suppressing cNHEJ had no recognisable effect. Possible explanations for this stem from a relatively low (~36%) gRNA targeting efficiency coupled with inherently low HDR-mediated CRISPR/Cas9 editing.

A ssODN template was designed based on the model presented by Richardson *et al.*, with 24-36 nucleotides upstream and ~90 nucleotides downstream of the cut site (Fig. 1.5) (Richardson et al., 2016). If the gRNA is cutting at the desired location and the ssODNs are designed correctly, an HDR-mediated gene editing event should occur, however infrequently. Based on these principles, cells were transfected with the CRISPR/Cas9-gRNA K2 construct and the asymmetric ssODN.

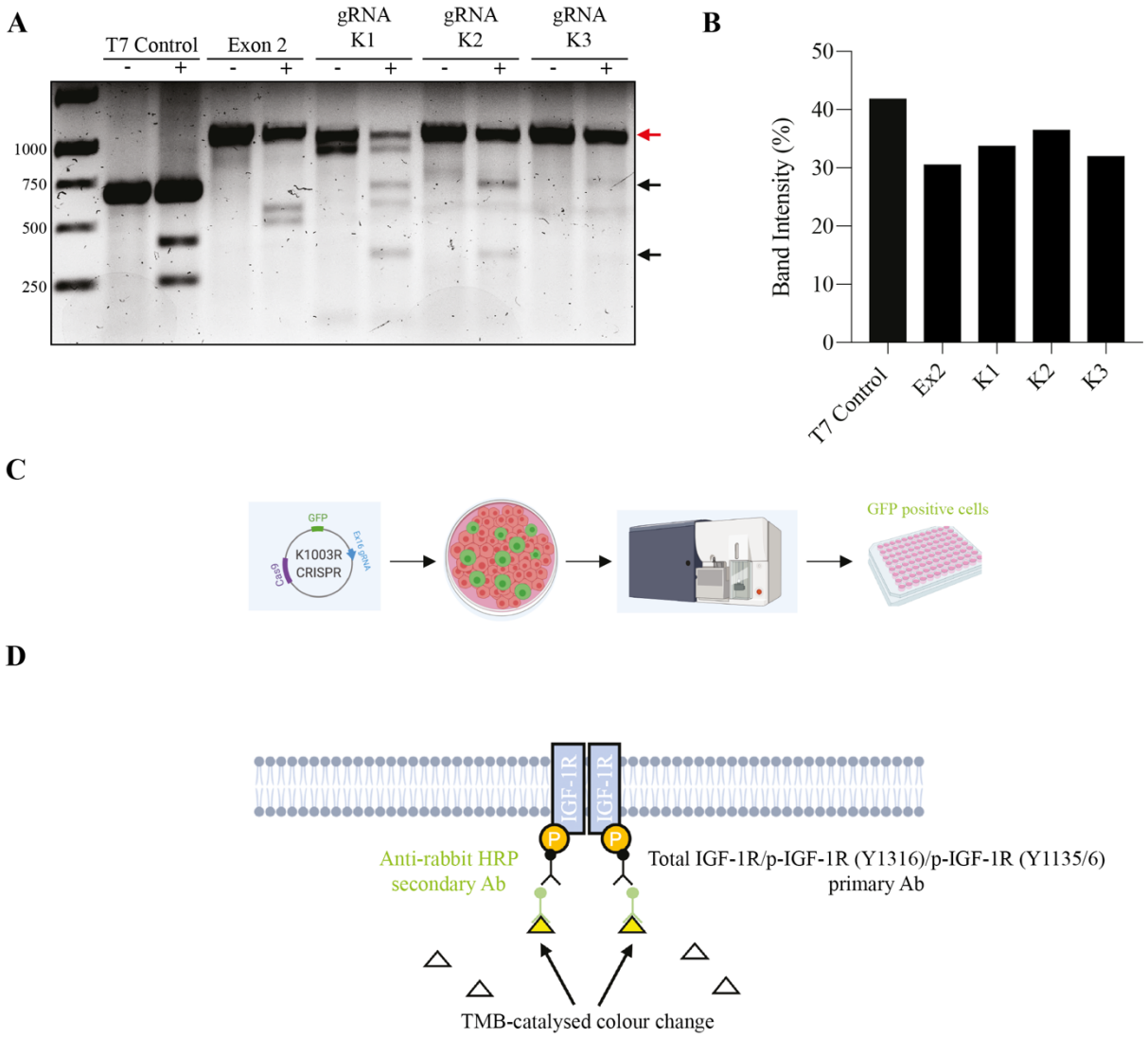

Figure 3.7: Generation and selection of an apparently novel IGF-1R kinase-dead clone.
(A) Cloning of three different IGF1R exon 16-targeting gRNAs into pSpCas9(BB)-2A-GFP (PX458) was carried out. 22Rv1 cells were seeded in a 24 well plate to be 70-80% confluent the following day. Each gRNA was transfected into a separate well, and after 48 hours, genomic DNA was extracted and amplified by PCR. Digestion of PCR products was carried out using the T7E1-based Alt-R Genome Editing Detection Kit and the products were run on a 1% agarose gel. Lane 1: 1 kb ladder; 2: negative control mix; 3: positive control mix; 4: gRNA2-PX458 transfected PCR products, without incubation with T7E1; 5: gRNA2-PX458 transfected PCR products, with incubation with T7E1; 6: gRNA K1-PX458 transfected PCR products, without incubation with T7E1; 7: gRNA K1-PX458 transfected PCR products, with incubation with T7E1; 8. gRNA K2-PX458 transfected PCR products, without incubation with T7E1; 9: gRNA K2-PX458 transfected PCR products, with incubation with T7E1; 10: gRNA K3-PX458 transfected PCR products, without incubation with T7E1; 11: gRNA K3-PX458 transfected PCR products, with incubation with T7E1. Arrows indicate predicted fragment sizes upon correct cutting of *IGF1R* exon 16. (B) Quantification of predicted band intensities using ImageJ. Band intensities were calculated by quantifying the intensity of predicted bands (black arrows, Fig. 3.7A) relative to the uncut PCR product band intensity (red arrow (Fig. 3.7A)). (C) Schematic of IGF-1R kinase-dead clone generation procedure. (D) Diagram illustrating the principle of the IGF-1R enzyme-linked immunosorbent assay (ELISA) adapted for detection of total IGF-1R, IGF-1R/INSR kinase activity (p-(Y1135/1136)-IGF-1R) and IGF-1R specific kinase activity (p-(Y1316)-IGF-1R). Briefly, presence of IGF-1R/phospho-(Y1135/1136)-IGF-1R/phospho-Y(1316)-IGF-1R allows the primary antibody to bind, and addition of anti-rabbit secondary antibody allows for a colour change upon TMB catalysis. Absence of signal produces no colour change. Colour change was measured using the POLARstar Omega plate reader.

Utilising the screening method used for generating IGF-1R null clones, cells were then single-cell FACS-sorted into 96 well plates, based on GFP expression from the PX458 vector, and when the majority of wells were confluent, colonies were triplicated into additional 96 well plates (Fig. 3.7C). Of the three replicate plates, one was left to expand, and when confluent, the remaining plates were used for a total IGF-1R ELISA (as used in Fig. 3.3, 3.4) and a phospho-IGF-1R ELISA as in Friebichler *et al*. 2013 (Fig. 3.7, 3.8) (Friedbichler et al., 2013). The purpose of performing two ELISAs was to cross-reference each clone, coupling the IGF-1R/INSR kinase activity (using phospho-(tyrosine 1135/1136)-IGF-1R levels as a read-out) with the total IGF-1R level (Fig. 3.8). The aim was to identify and discount clones where phospho-IGF-1R levels were low due to lack of receptor, or fully functioning kinase-active IGF-1R was present. To identify a threshold value to indicate possible creation of a kinase-dead clone, IGF-1R WT cells were assessed in the presence and absence of IGF-1 (25 nM) stimulation. As mentioned in section 1.1.4, IGF-1 has been reported to have a sub-nM affinity for IGF-1R, whereas 9-41 nM and >30-390 nM relative affinity to INSR-A and INSR-B, respectively (Benyoucef et al., 2007; Frasca et al., 1999; Yamaguchi et al., 1993). Furthermore, 22Rv1 cells have been shown to express INSR (Sarkar et al., 2019), and it has been noted that 10 nM IGF-1 is able to cross-react with INSR, meaning that 25 nM IGF-1 used here could activate INSR-A/-B (Boucher et al., 2010b). To differentiate IGF-1R activation, a phospho-tyrosine 1316-IGF-1R antibody was sourced and utilised in a later ELISA, and in future, using lower IGF-1 concentrations (such as 1-2 nM) would be unlikely to activate INSR-A/-B.

This experiment indicated that clones with ratios of phospho-IGF-1R signal to total IGF-1R signal <0.3 could be kinase-dead. Of the 22 wells assessed, 9 showed ratios suggestive of intact IGF-1R exhibiting little kinase activity (Fig. 3.8). Parallel wells of the 9 encouraging clones

were studied to confirm at least 50% well coverage, and of those clones, 5 seemed promising and all were expanded.

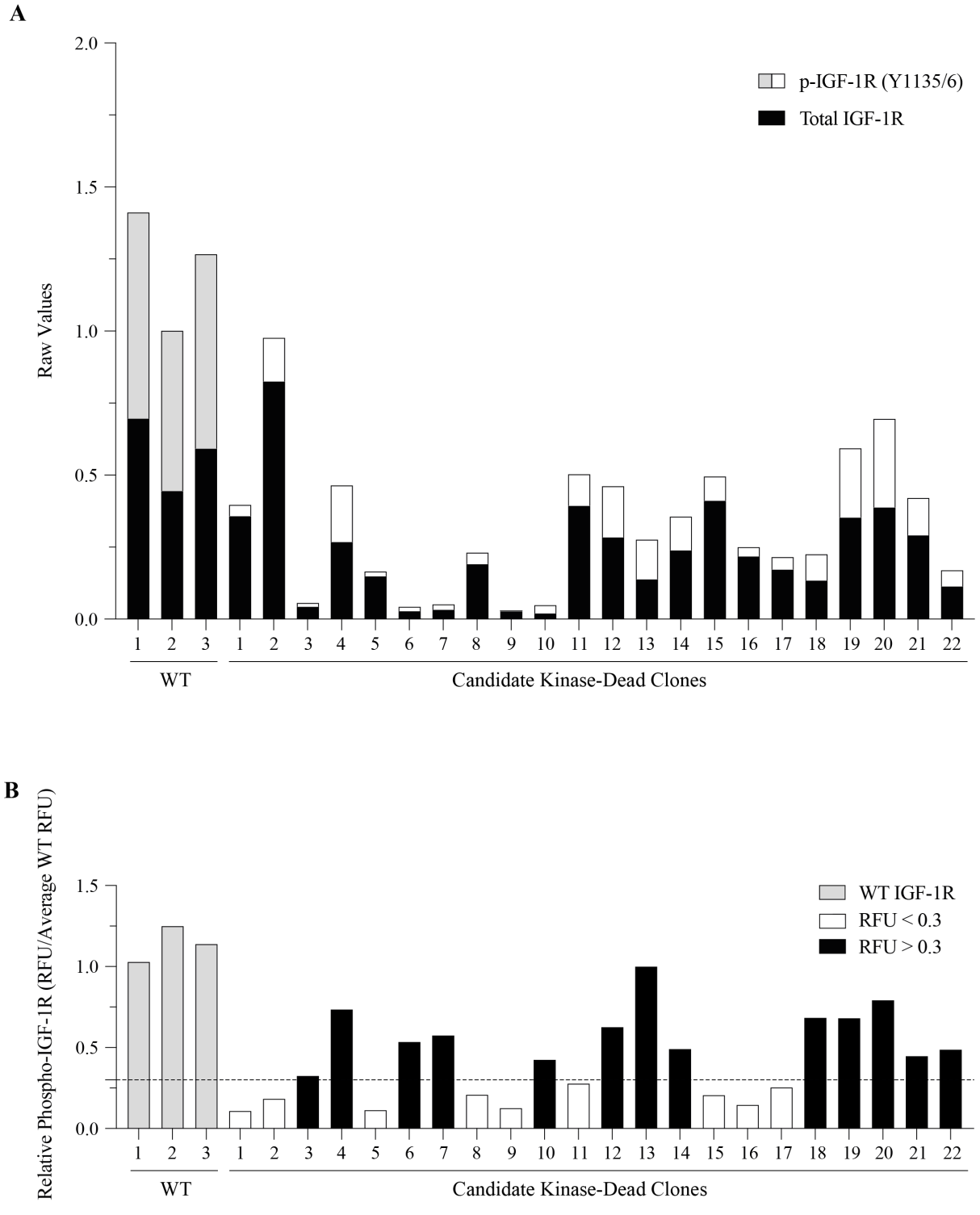

Figure 3.8: Summary of IGF-1R ELISA to identify candidate IGF-1R kinase-dead clones.
The phospho-Y1135/1136-IGF-1R ELISA was carried out with three wells of 22Rv1 cells (grey) as positive controls, and 22 candidate IGF-1R kinase-dead clones (white). Cells were serum-starved overnight, and stimulated with IGF-1 (25 nM) for 30 minutes before fixing. (A) Graph shows the raw values obtained from the POLARstar Omega plate reader. (B) RFU values of all candidate clones incubated with phospho-Y1135/1136-IGF-1R primary antibody were calculated relative to the RFU value from the same clone incubated with total IGF-1R primary antibody. Promising candidate kinase-dead clones (RFU ratio<0.3) are highlighted in white, and clones where RFU ratio>0.3 are highlighted in black. Black dashed line indicates RFU ratio=0.3.

Once all clones were confluent in parallel 6 well plates, cells were serum-starved overnight then stimulated with 25nM IGF-1 for 25 minutes before lysates were extracted. Western blot analysis was performed to test for presence of IGF-1R protein and absence of kinase activity (Fig. 3.9A). Primary antibodies towards phospho-tyrosine 1135/1136-IGF-1R/INSR and phospho-serine 473-AKT were used to monitor IGF-1R phosphorylation and phosphorylation of AKT at a residue associated with upstream IGF-1R kinase activity. Among the candidate kinase-dead clones were two (clones 2 and 3, Fig. 3.9A) exhibiting loss of IGF-1R but heightened tyrosine 1135/1136-IGF-1R/INSR phosphorylation and serine 473-AKT signal, and two clones with similar ratios of phospho-IGF-1R/INSR to IGF-1R and phospho-AKT to AKT as the WT clone (clones 4 and 5, Fig. 3.9A), these observations were likely due to INSR stimulation and stimulation of INSR and IGF-1R, respectively. The phospho-IGF-1R tyrosine 1135/1136 antibody is also able to detect INSR phosphorylation at a conserved motif (tyrosine 1150/1151). Therefore it is possible that the phospho-signal in the candidate clones with seemingly no IGF-1R could be explained by INSR phosphorylation. As discussed above, if time had permitted, testing of low IGF-1 concentrations (such as 1 or 5 nM) would have been useful, to examine whether IGF-1R null clones still showed a phospho-IGF-1R/INSR signal.

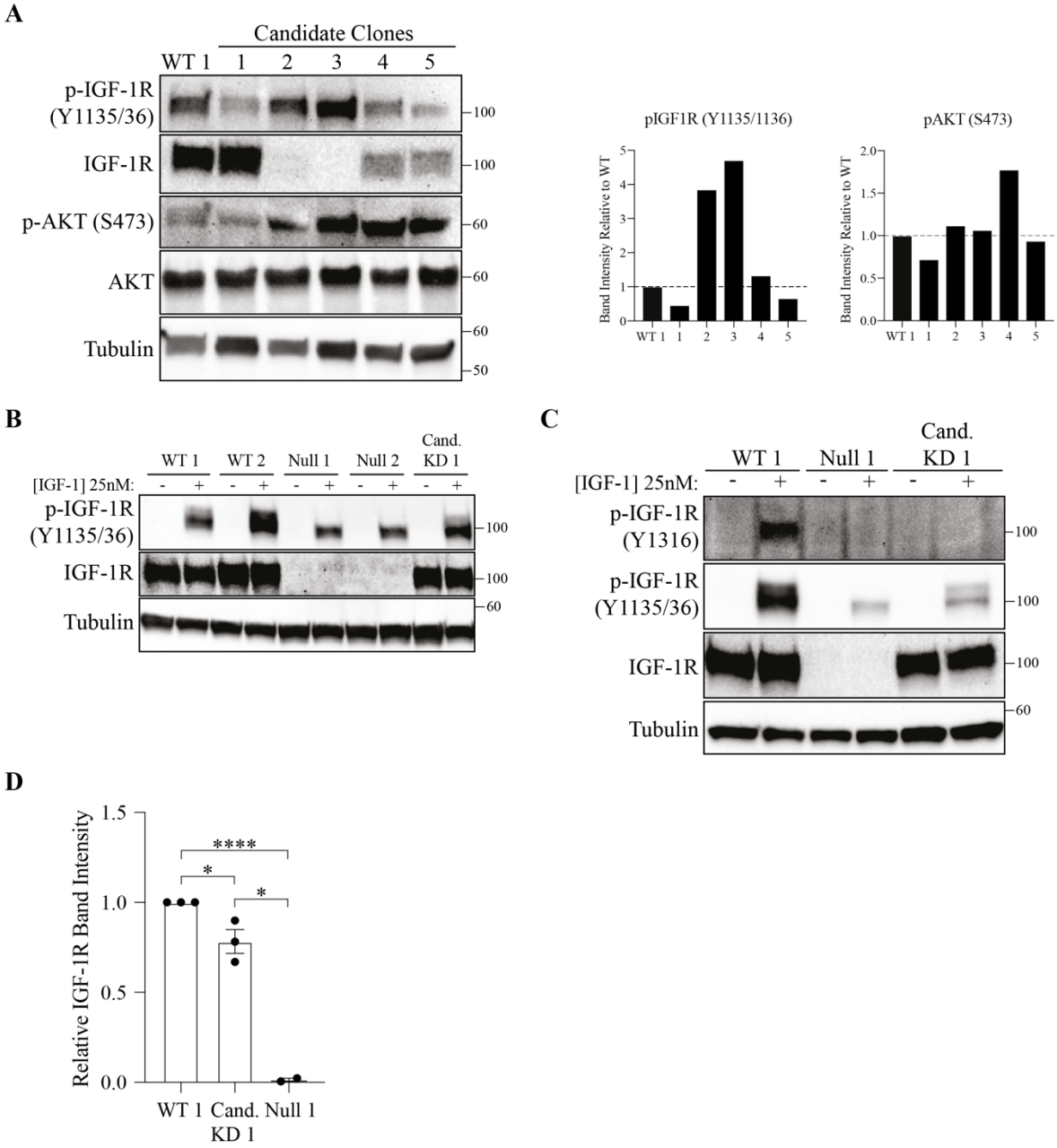

Figure 3.9: Analysis of candidate IGF-1R kinase-dead clones by Western blotting.
(A) Whole cell lysates for 22Rv1 cells (WT 1) and 5 candidate IGF-1R kinase-dead clones serum-starved and treated with IGF-1 (25 nM) were analysed by Western blot for IGF-1R expression, IGF-1R kinase activity, and downstream phospho-S473-AKT activity with β-tubulin as a loading control. Quantification of corresponding band intensities were calculated using ImageJ, and compared relative to WT 1 ratios as indicated by black dashed line. (B) 22Rv1 clones expressing WT IGF-1R, two validated 22Rv1 IGF-1R null clones and the candidate IGF-1R kinase-dead clone 1 were serum-starved overnight and stimulated with 25 nM IGF-1 for 20 minutes. Whole cell lysates were then extracted and used for Western blot analysis for kinase activity with β-tubulin as a loading control. (C) Clones expressing WT IGF-1R, IGF-1R kinase-dead clone 1 and IGF-1R null cells were serum-starved overnight and stimulated with 25 nM IGF-1 for 20 minutes. Whole cell lysates were then extracted and Western blot analysis was carried out for phospho-IGF-1R-specific signal, phospho-Y1135/1136-IGF-1R and total IGF-1R with β-tubulin as a loading control. (D) Band intensities for IGF-1R and tubulin from A-C of unstimulated WT 1, candidate KD clone 1 and Null 1 were quantified using ImageJ and compared relative to the WT 1 sample of each experiment (WT 1: n=3, Cand. KD: n=3, Null 1: n=2). The data were analysed by one-way ANOVA, to determine statistical significance of relative IGF-1R band intensity differences (*p<0.05; ***p<0.0005; ****p<0.0001).

Some of the candidate kinase-dead clones displayed similar or increased phospho-AKT signal to IGF-1R WT cells, or expressed no IGF-1R indicating that they were IGF-1R null (Fig. 3.9A). One candidate kinase-dead clone however (clone 1 in Fig 3.9A) exhibited less phospho-tyrosine 1135/1136-IGF-1R/INSR and phospho-S473-AKT signal upon IGF-1 stimulation compared to the WT clone, while expressing a comparable level of IGF-1R. To investigate this promising clone further, Western blot analysis was carried out on an additional WT clone, two previously characterised IGF-1R null clones and the candidate kinase-dead clone (Fig. 3.9B), all serum-starved and stimulated with IGF-1. The presence of IGF-1R was confirmed in the promising clone at levels similar to that of both WT clones. However, the appearance of a phospho-tyrosine 1135/1136-IGF-1R/INSR band not only in the candidate kinase-dead clone but also in the previously characterised IGF-1R null clones highlighted the need to use a more specific phospho-IGF-1R antibody to validate the loss of kinase activity.

A report by Rubini *et al.* suggested that phosphorylation of the tyrosine residue at position 1316 of the C-terminal of the receptor is unique to IGF-1R ligand activation (Rubini et al., 1999). While extensive homologies exist between IGF-1R and INSR in the juxtamembrane and kinase domains, the latter exhibiting 98% homology (Ullrich et al., 1986), the C-terminus has 44% homology, which provided an IGF-1R phosphorylation-specific antibody site. It was shown that INSR phosphorylation in cells expressing ~5 log above physiological INSR levels that phospho-INSR was not detected using the phospho-tyrosine 1316-IGF-1R antibody, and that this lack of detection was also displayed in a kinase-dead IGF-1R mutant (Rubini et al., 1999). Antibodies to this phosphorylation site have been used both for immunoblotting and IHC (Akiel et al., 2017; W.-J. Chen et al., 2014; Codony-Servat et al., 2019; Martinez-Quetglas et al., 2016; Maurel et al., 2016; Sundaresan et al., 2012; Wu et al., 2017; Yoneyama et al.,

2018), and after discovery and subsequent acquisition of this antibody, all relevant experiments in this thesis used it to check for IGF-1R-specific receptor phosphorylation.

Probing with an antibody for Y1316 phosphorylation on the same IGF-1-treated samples analysed previously indicated specific loss of IGF-1R phosphorylation in the candidate kinase-dead clone indistinguishable to that of the null clone, with clear phosphorylation of IGF-1R in the WT clone (Fig. 3.9C). Quantification of total receptor confirmed that IGF-1R was undetectable in null clone 1, while IGF-1R was clearly detectable at ~80% of mean levels in WT 22Rv1 cells (Fig. 3.9D). The presence of tyrosine 1135/1136 phosphorylation in null and candidate kinase-dead clones was thought to reflect the activation of functional INSR by 25 nM IGF-1.

Altogether, these results suggested the successful creation of a structurally intact, kinase-dead IGF-1R clone previously uncharacterised in the literature. Surprisingly, Sanger sequencing analysis showed that the desired HDR-mediated adenine to guanine substitution had not occurred. Upon further inspection, a nucleotide change three codons downstream of K1003 had been altered, exchanging an adenine for a guanine (Fig. 3.10A). This replaced an asparagine residue at position 1006 with an aspartic acid (N1006D) (Fig. 3.10B). To our knowledge, this mutation had not been described in the literature, nor had the contribution of N1006 to ATP binding. As the residue is very near to the ATP binding site at K1003 (Ullrich et al., 1986), it could be hypothesised that the aspartic acid may distort the ATP binding site.

However Western blot analyses indicated lower levels of IGF-1R detected in the candidate kinase-dead clone compared to in IGF-1R WT cells (Fig. 3.9). Further, work by the Macaulay

group and others (Aleksic et al., 2010; Sehat et al., 2010) showed that IGF-1R kinase activity was necessary for nuclear translocation, so detection of IGF-1R in nuclear extract shown here (Fig. 4.6B) was not consistent with the loss of kinase activity. To clarify genetic changes in this clone, TOPO TA cloning was carried out to sequence both alleles (Clark et al., 2019). Upon sequencing of 16 alleles, 9 displayed the N1006D mutation, however the remaining 7 alleles sequenced had incorporated an adenine base at the cut site causing a frameshift, a G>A mutation creating a stop codon at E1013, and the introduction of a stop codon at residue E1016 (Fig. 3.11). This suggested a single functioning allele and one containing a premature stop codon in this diploid cell line (Macaulay lab, unpublished).

A

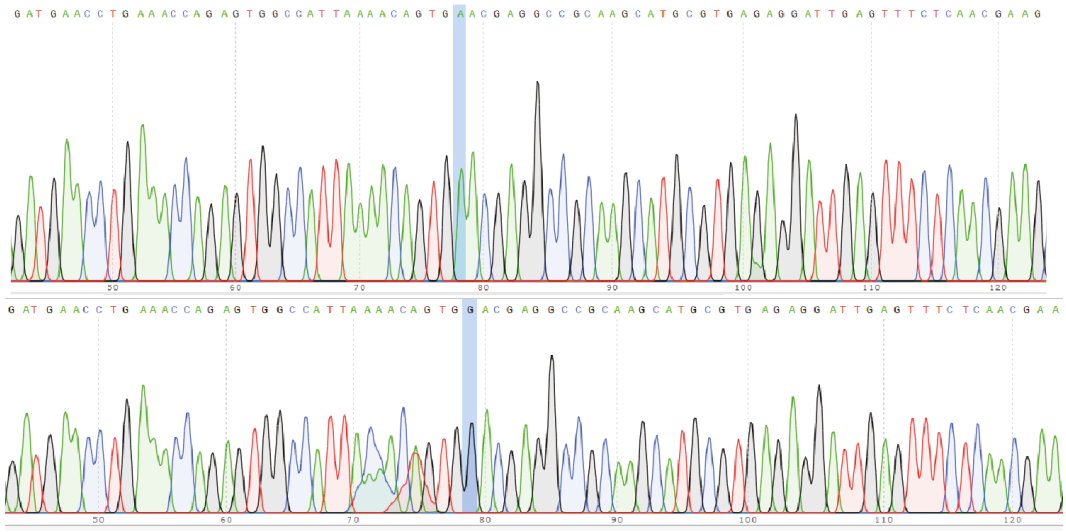

B

```
UCSC IGF1R: AGAGTGGCCATTAAAACAGTGAACGAGGCCGCAAGC
            R  V  A  I  K  T  V  N  E  A  A  S
22RV1 Parental: AGAGTGGCCATTAAAACAGTGAACGAGGCCGCAAGC
            R  V  A  I  K  T  V  N  E  A  A  S
KD Clone 1: AGAGTGGCCATTAAAACAGTGGACGAGGCCGCAAGC
            R  V  A  I  K  T  V  D  E  A  A  S
```

Figure 3.10: Analysis of candidate IGF-1R kinase-dead clones by Sanger sequencing.
(A) Genomic DNA was extracted from 22Rv1 parental cells and cells expressing the candidate IGF-1R kinase-dead clone 1. DNA was amplified by PCR and Sanger sequenced. Sequence analysis indicated an adenine to guanine substitution at the cut site of *IGF1R* in genomic DNA extracted from cells expressing IGF-1R kinase-dead clone 1. (B) More detailed analysis using the *IGF1R* sequence provided by the UCSC Genome Browser (https://genome.ucsc.edu/), indicated that the observed guanine substitution was within residue N1006, converting asparagine to aspartic acid.

A

IGF1R AAAACAGTGAACGAGGCCGCAAGCATGCGTGAGAGGATTGAGTTT
K T V N E A A S M R E R I E F

9/16: AAAACAGTGGACGAGGCCGCAAGCATGCGTGAGAGGATTGAGTTT
K T V D E A A S M R E R I E F

7/16: AAAACAGTGAAACGAGGCCGCAAGCATGCGTGAAAGGATTGAGTT
K T V K R G R K H A * K D * V

B

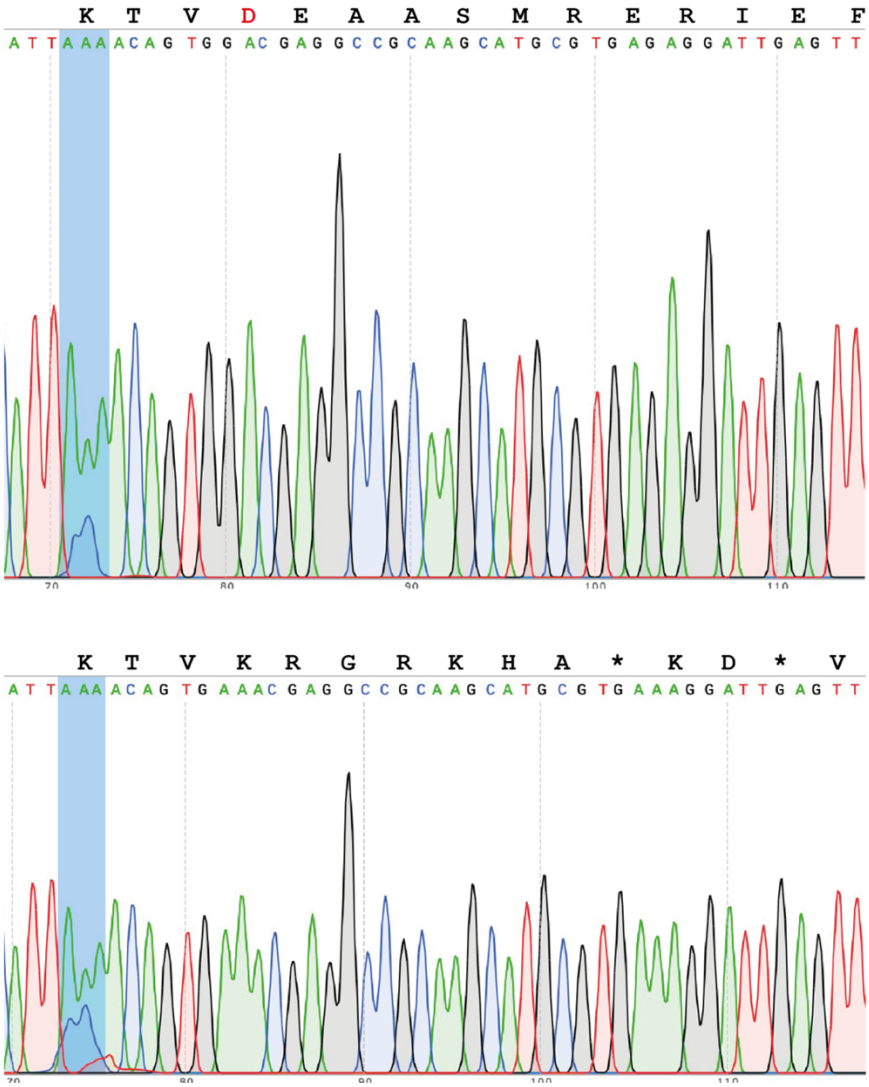

Figure 3.11: Sequencing of candidate kinase-dead clone alleles.
(A) Genomic and amino acid sequences of *IGF1R* provided by the UCSC Genome Browser (https://genome.ucsc.edu/) (top), alleles containing the N1006D substitution (middle), and alleles containing two stop codons (bottom). (B) Representative Sanger sequencing traces of an allele containing the N1006D substitution (top), and an allele containing two stop codons (bottom).

While a kinase-dead mutant had not been generated, loss of one *IGF1R* allele had been sufficient to abrogate phosphorylation of IGF-1R at tyrosine 1316 (Fig. 3.9C). Additionally, partial IGF-1R depletion was also sufficient to generate a radio-sensitive phenotype in this work (Fig. 3.1) and in previous results from the Macaulay group (Rochester et al., 2005; Turney et al., 2012). *IGF1R* gene dosage has been shown to have a phenotype in murine acute lymphoblastic leukaemia (ALL), and $IGF1R^{+/-}$ T-ALL cells showed severely compromised transplantability into syngeneic recipients (Gusscott et al., 2016; Medyouf et al., 2011). Furthermore, *IGF1R* haploinsufficiency has been reported to produce a major clinical phenotype resulting in microcephaly, growth retardation and mental retardation (Raile et al., 2006). Although these reports did not address potential effects on the DDR, growth retardation, microcephaly and other neurological defects are common phenotypes in inherited DDR syndromes including ataxia telangiectasia and Seckel syndrome, due to mutations in ATM and ATR respectively (O'Driscoll and Jeggo, 2008). Therefore, given these features in common between clinical *IGF1R* haploinsufficiency and congenital DDR defects, experimental work continued to characterise this hypomorphic $IGF1R^{+/-}$ mutant clone. In addition, this clone could be used to examine a gene dosage effect of *IGF1R* on glucose metabolism and growth.

3.3.2 DSB-independent methods of nucleotide substitution

3.3.2.1 Base editing

Generation of the published K1003R mutant would be beneficial in two respects. Firstly, it is confirmed to render IGF-1R kinase-inactive (Kato et al., 1993) and second, it would provide an additional IGF-1R kinase-dead mutant to strengthen subsequent functional assessment of the relative contributions of the kinase versus structural role of the receptor. Gene editing approaches which utilise DSBs to incorporate a desired edit always offer the possibility of genetic artefacts being introduced near the cut site (Zhang et al., 2015). Base editors function by nicking one strand of DNA near the desired edit (Fig. 3.11A), thus reducing the likelihood of incorporating any bystander edits (Rees and Liu, 2018).

The gRNA K2 sequence used to target exon 16 with an active Cas9 for HDR-mediated nucleotide substitution was used as it was previously shown to effectively navigate to K1003 (Fig. 3.7A, B) and crucially would allow the lysine residue to be within the target window of plasmid xCas9(3.7)-ABE(7.10). This gRNA would recruit the adenine deaminase to facilitate the conversion of the AAA (K) codon to AGA (R), rendering the kinase inactive. The gRNA was cloned into the pBS_hU6-sgRNA_EF1a_eGFP gRNA plasmid and transfected alongside the ABE 7.10 construct. Transfection efficiency was monitored by GFP level using fluorescence microscopy. (F. Wang et al., 2020)

Variation of gRNA length, position of the target adenine base within the gRNA sequence and transfection conditions were trialled however no evidence of base substitution at position 1003 was observed by Sanger sequencing (Fig. 3.11B, C). While successful targeting of the gRNA to the appropriate region of the genome by cloning into a catalytically active Cas9 (Fig. 3.7A,

B), and observation of high transfection efficiencies, one factor we were unable to discredit was the high proportion of adenine bases around the target (7 in 14 bases). Evidence from these initial experiments and from others suggest that an abundance of adenine bases adjacent to the target sequence can compromise effective adenine base editing (F. Wang et al., 2020). Some report creation of bystander edits *in addition* to the desired substitution (Rees and Liu, 2018), others suggest it hinders ABE activity (F. Wang et al., 2020). Because of these factors and the nature of the sequence at the desired site for editing, a different approach was attempted.

A

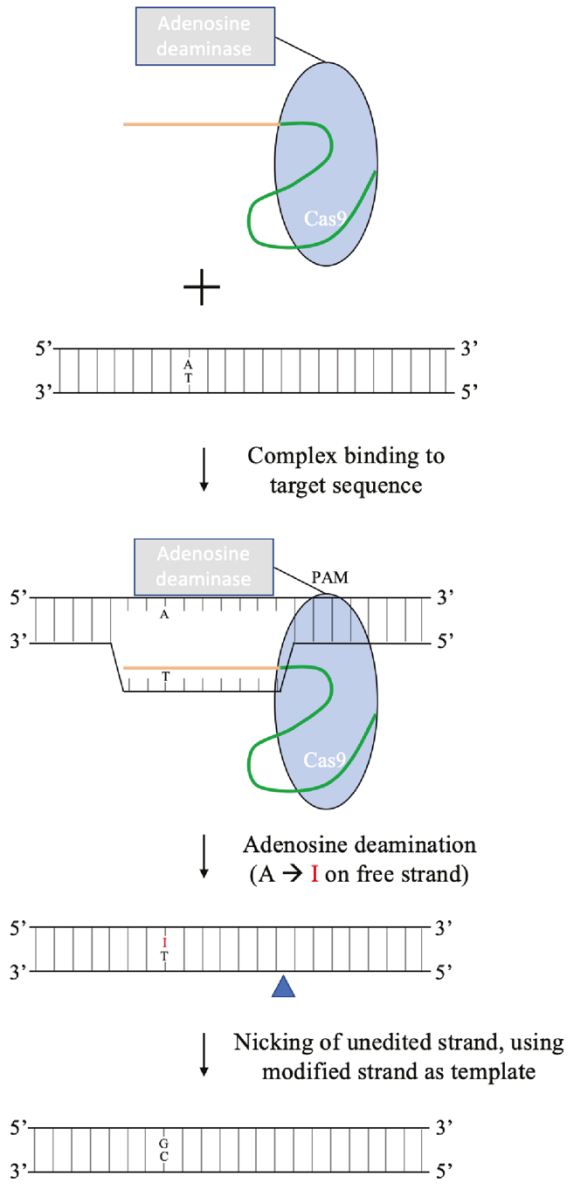

B

gRNA Name	Length	Adenines in Target Window
gRNA K2	20	3
ABE_1	19	2
ABE_2	20	3
ABE_3	23	1
ABE_4	30	N/A

C

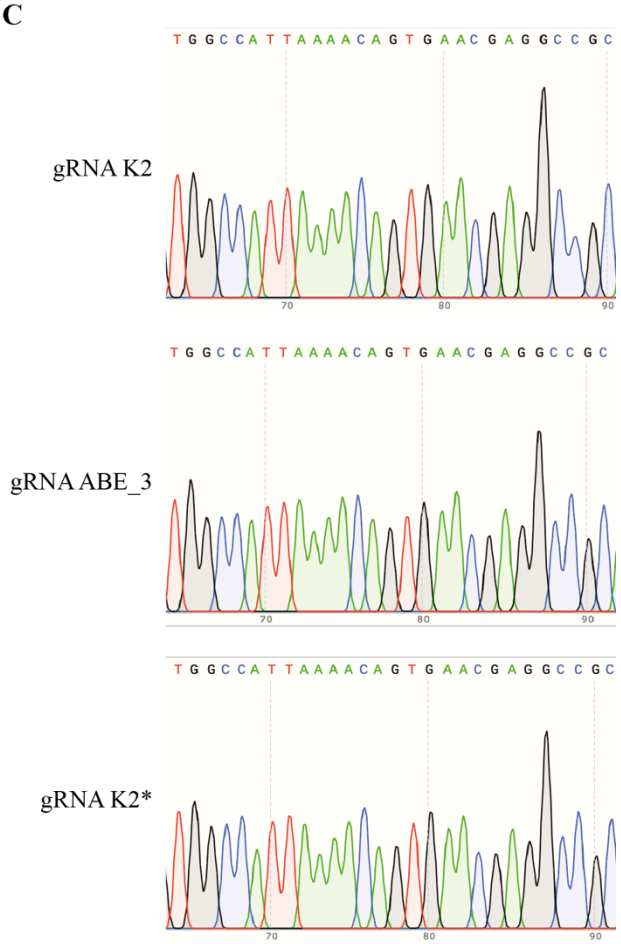

Figure 3.12: Summary of base editing attempts to generate the IGF-1R K1003R mutant.
(A) Simplified diagram depicting the mechanism of base editing. 22Rv1 cells were seeded in a 24 well plate to be 70-80% confluent the following day. Each gRNA variant was transfected into a separate well, and after 48 hours, genomic DNA was extracted, amplified by PCR and Sanger sequenced. (B) Table detailing variations in base editor gRNAs trialed, indicating length of gRNA and number of adenine bases within the 4-8 nt target window of the base editor. ABE_4 was designed based on Ryu *et al.* (2010) who reported that a 30 nt gRNA could improve efficiency in some cases (Ryu *et al.*, 2018). gRNA sequences detailed in methods (section 2.6.1). (C) Representative Sanger sequencing traces of exon 16 of *IGF1R* targeted by different gRNA sequences cloned into the pBS_hU6-sgRNA_EF1a_eGFP vector and transfection conditions (gRNA K2: used in Fig. 3.3 to effectively target exon 16 of *IGF1R*; gRNA K2+: gRNA ABE_3; gRNA K2*: double amount of Lipofectamine 3000 used in transfection of gRNA K2).

3.3.2.2 Prime editing

A separate strategy of DSB-independent nucleotide substitution involves the tethering of a specific pegRNA to prime 3' extension to incorporate the edit, to the gRNA scaffold and the spacer sequence. Prime editing works by targeting a RNA-programmable nickase to a RT, allowing for the priming, DNA synthesis and subsequent incorporation of the desired edit (Anzalone et al., 2019). This gene editing technique was a recent and timely development from the Liu lab, offering an alternative approach to base editing. Therefore, following identification of the N1006D mutant clone as hypomorphic, prime editing was attempted to introduce the desired mutation at K1003 of IGF-1R.

A gRNA was designed to target four amino acids upstream of K1003 to guide the prime editor complex to the correct location in the genome (Fig. 3.12A). Further, pegRNAs were devised containing a constant PBS sequence of 11 nucleotides, fused to three different RT lengths of 16, 19 and 22 nucleotides, each containing the desired edited nucleotide to create the K1003R substitution, and the altered PAM site (Fig. 3.12B, C). The three RT lengths that were trialled allowed for the position of the desired edit to be either 3, 6 or 9 nucleotides from the 5' end of the RT sequence, within the constraints advised by Anzalone *et al.*. It was decided to generate and transfect constructs with differing RT lengths because the Liu laboratory had been unable to find a consensus RT-PBS length for effective editing of all genes. They reported that individual lengths of the RT component resulted in major and unpredictable variation in editing efficiency of different genes (Anzalone et al., 2019). This prompted Anzalone *et al.* to advise initially altering one component of the pegRNA construct – either RT length or PBS length – in the first instance (Anzalone et al., 2019).

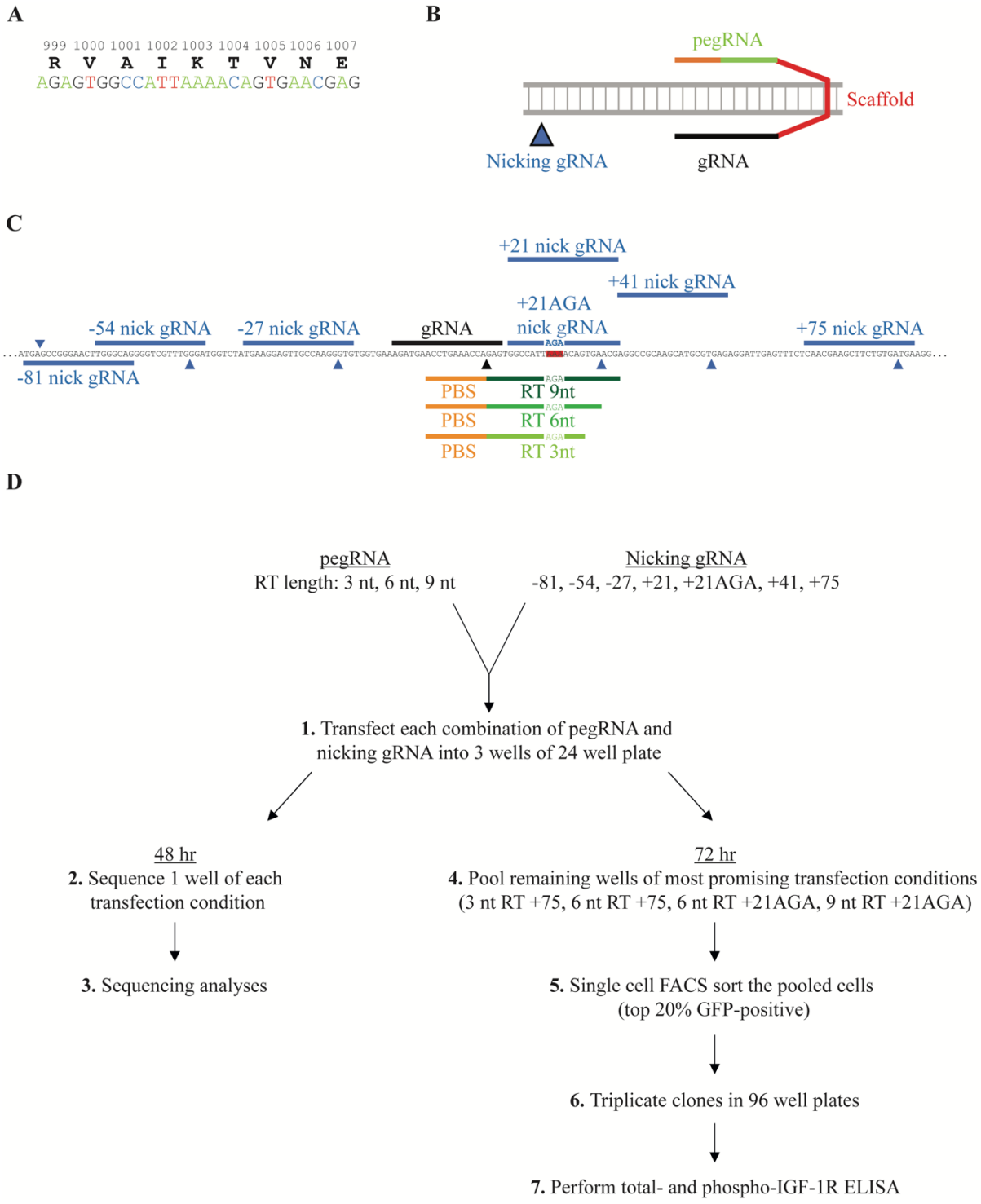

Figure 3.13: The design of prime editing constructs.
(A) Schematic of the *IGF1R* gene and amino acid sequence surrounding the desired edit site (highlighted in red). (B) Diagram of the components of the prime editor and an example target location for the nicking gRNA (blue); predicted nick site (blue arrowhead), gRNA (black); scaffold (red); pegRNA (green). (C) Schematic detailing the precise locations of each nicking gRNA and pegRNA trialed, as well as the gRNA used and nick sites (arrowheads). (D) Flow chart detailing the prime editing methodology.

Nicking gRNAs were also designed targeting a region spanning ~100 nucleotides either side of the cut site (Fig. 3.12C), as advised by Liu and colleagues (Anzalone et al., 2019). Two nicking gRNAs were devised which bound to the edit site (either pre- or post-edit), with the hope of further enhancing the shift in flap equilibrium to the favourable edit (Fig. 1.7). Successful cloning of each prime editing construct (gRNA-scaffold-RT (3/6/9nt)-PBS) into the pU6-Neo acceptor plasmid was achieved by Golden Gate assembly, as described in section 2.6.13. All nicking gRNAs were cloned into the pCMV-PE2 plasmid (Addgene, #132775).

Transfections of each of the three constructs with each of the seven nicking gRNAs and an eGFP plasmid (Addgene, #13031) were carried out in 24 well plates in triplicate (Fig. 3.12D, step 1). Transfection efficiency was monitored using fluorescence microscopy and after 48 hours the genomic DNA of one well per condition was extracted, amplified and sent for Sanger sequencing (Fig. 3.12D, step 2). As expected, analysis of sequencing data showed editing varied considerably between conditions, which appeared to vary more with the nicking gRNA location than RT length (Fig. 3.12D step 3, 3.13).

EditR software was used (as was advised at the Oxford Genome Engineering Forum, 2019) (Kluesner et al., 2018) to determine editing efficiencies of each transfection combination (section 2.6.14). It was likely that the editing efficiency was lower than stated by the software, which showed high editing percentages, as successful editing described by Anzalone *et al.* displayed much lower efficiencies (Anzalone et al., 2019). Therefore, the EditR software was only used as an indication of relative editing efficiencies of 22Rv1 cells using the corresponding prime editing and nicking gRNA transfection combinations (Fig. 3.13).

Absence of a nicking gRNA caused minimal editing across all RT-PBS lengths, indicative of incorporation of the 5' unedited flap (Fig. 3.13, row 1). Interestingly, using a nicking gRNA to focus 21 nucleotides downstream of the spacer target site, pegRNAs with RT lengths of 6 and 9 nt exhibited 31% and 25% guanine detection at the desired edit site, respectively, whereas the 3 nt RT length displayed wild-type sequence, 100% adenine (Fig. 3.13, row 2). These data provided hints of successful editing, albeit at low efficiencies. Upon examination of the desired edit site using a nicking gRNA targeting (+75, row 4) targeting 75 nt downstream of the spacer target site, 3nt and 6 nt RT lengths showed encouraging percentages of cells displaying guanine (90% and 89%, respectively). A similar editing efficiency was not seen in cells transfected with a pegRNA containing a 9 nt RT length (28%) (Fig. 3.13, row 4). To further enhance the base substitution, a nicking gRNA was used which specifically bound to the edited strand of DNA, 21 nt downstream of the spacer target site (i.e. contained the desired mutant AGA codon rather than AAA) (Fig. 3.12C). In theory, this would selectively nick the opposing strand of the already-edited DNA strand, increasing the likelihood of full incorporation of the nucleotide substitution. Analysis supported enhanced editing efficiency when utilising pegRNAs containing RT lengths of 6 nt and 9 nt, generating 94% and 95% guanine substitutions, respectively (Fig. 3.13, row 3). This test identified transfections performed using nicking gRNAs +21, +21AGA and +75 as the most promising (Fig. 3.13).

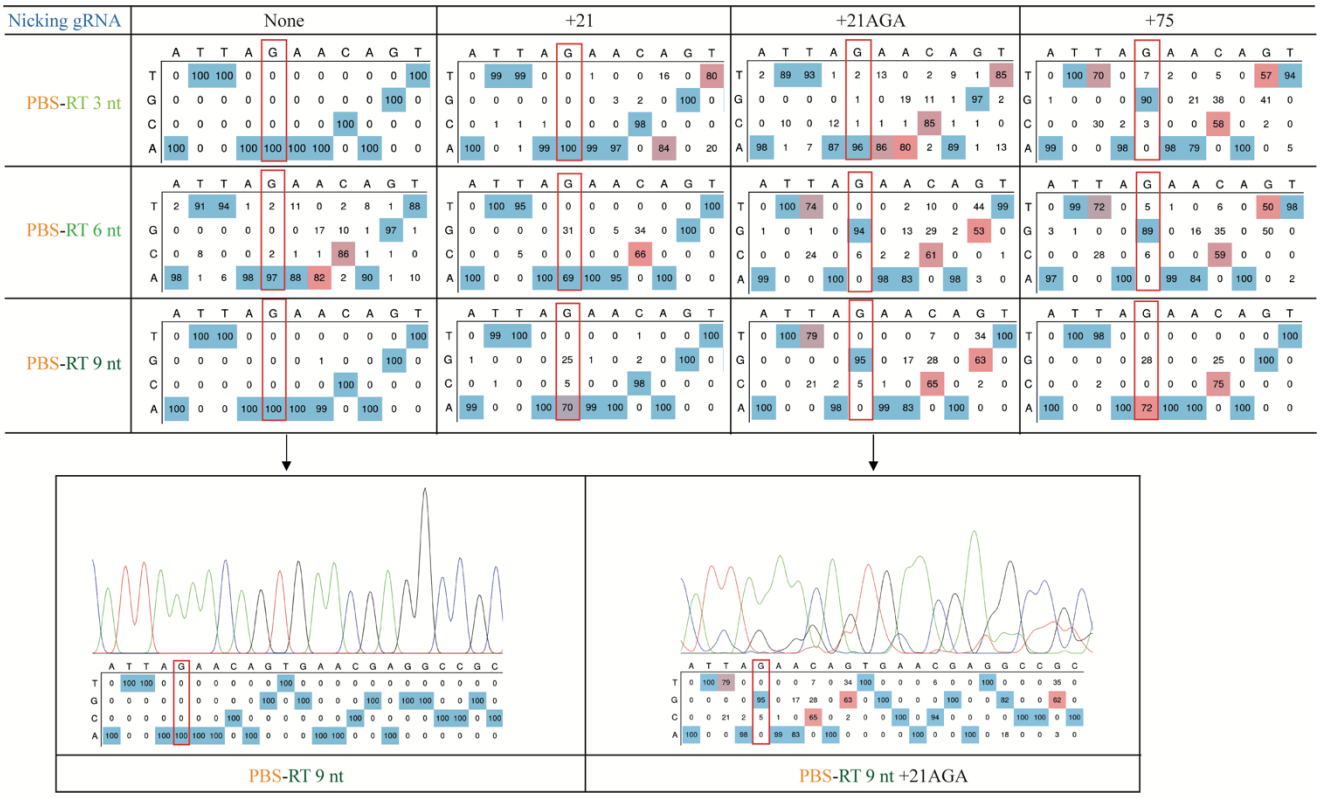

Figure 3.14: Results of prime editing.
22Rv1 cells were seeded in a 24 well plate to be 70-80% confluent the following day. Each prime editor construct and nicking gRNA combination was transfected into three parallel wells, and 48 hours post-transfection, genomic DNA was extracted and amplified by PCR from one well/condition. DNA was amplified by PCR, Sanger sequenced and subjected to analysis by EditR software (http://baseeditr.com/). The desired nucleotide for substitution is highlighted in red, and representative sequencing traces for unedited (below, left) and predicted edited DNA (below, right) are shown.

The two remaining replicate wells corresponding to each of these promising conditions were trypsinised at 72 hours post-transfection and pooled together (Fig. 3.12D, step 4). This cell population, containing cells transfected with pegRNA and nicking gRNA combinations indicating most efficient editing, were then single cell FACS-sorted. The top 20% GFP-positive cells were single cell sorted into five 96 well plates to maximise the likelihood of obtaining edited clones (Fig. 3.12D, step 4). The 96 well plates were grown, triplicated alongside three clones expressing WT IGF-1R to be analysed in parallel, and 63 candidate clones were expanded to the point where total and phospho-IGF-1R ELISAs could be carried

out (Fig. 3.12D, step 5). This step was done after the phospho-tyrosine 1316)-IGF-1R antibody became available, and so was used in this experiment. Of these 63 clones, 20 clones displayed encouraging signatures, individually exhibiting phospho-(tyrosine 1316)-IGF-1R:total IGF-1R ratios of under 0.3 (Fig. 3.12D step 7, 3.15).

At this point unfortunately, the laboratory was closed due to Covid-19, so 20 individual clones and the remaining unscreened 96 well plates were frozen down for later recovery and testing.

A

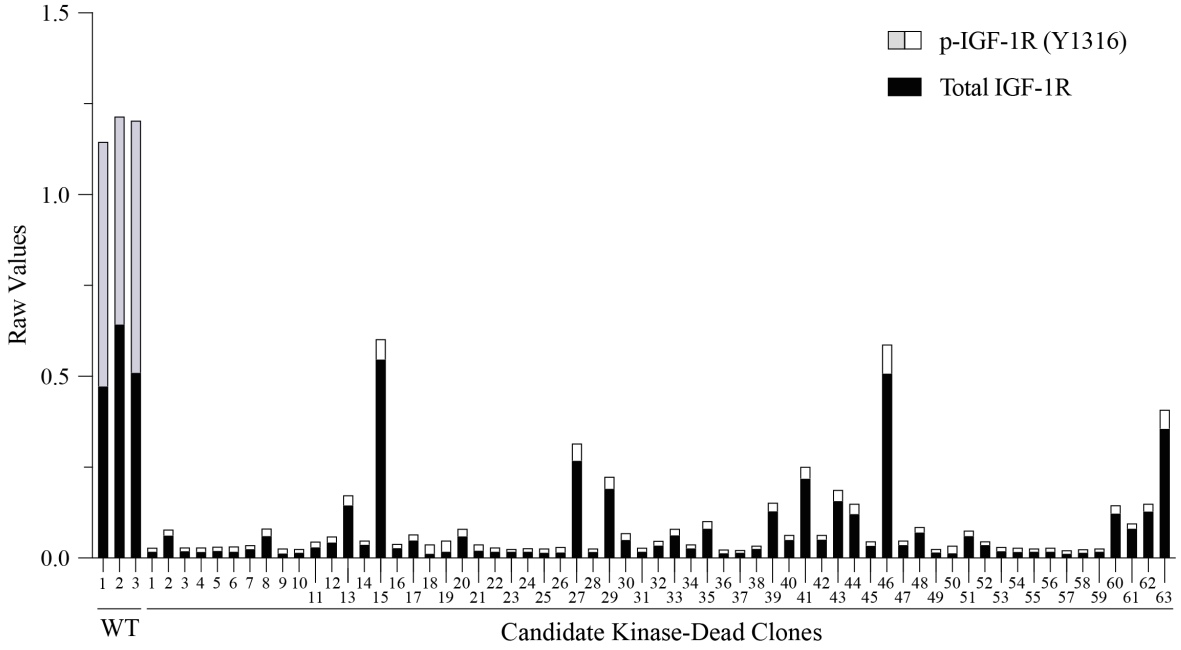
p-IGF-1R (Y1316)
Total IGF-1R
Raw Values
1.5
1.0
0.5
0.0
WT
Candidate Kinase-Dead Clones

B

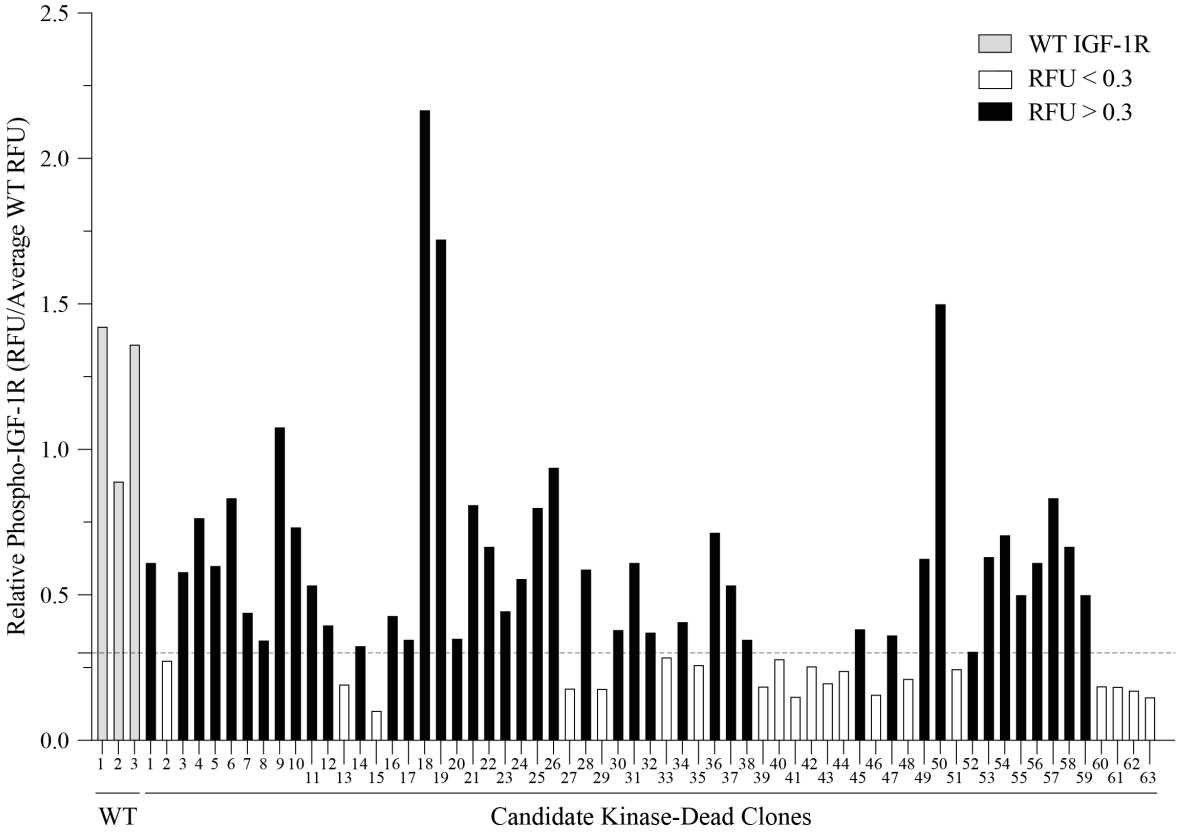
WT IGF-1R
RFU < 0.3
RFU > 0.3
Relative Phospho-IGF-1R (RFU/Average WT RFU)
2.5
2.0
1.5
1.0
0.5
0.0
WT
Candidate Kinase-Dead Clones

Figure 3.15: Summary of IGF-1R ELISA to identify IGF-1R kinase-dead clones by prime editing.
The phospho-Y1316-IGF-1R ELISA and total IGF-1R ELISA were carried out with three wells of 22Rv1 cells (grey) as positive controls and 63 candidate IGF-1R kinase-dead clones. Cells were serum-starved overnight, and stimulated with IGF-1 (25 nM) for 30 minutes before fixing. RFU values of all candidate clones incubated with phospho-Y1316-IGF-1R primary antibody were measured using the POLARstar Omega plate reader. (A) Graph shows the raw values obtained for each clone. (B) Graph shows phospho-Y1316-IGF-1R RFU values for all candidate clones calculated relative to the RFU value from the same clone incubated with total IGF-1R primary antibody. Promising candidate kinase-dead clones (RFU ratio<0.3) are highlighted in white, and clones where RFU ratio>0.3 are highlighted in black. Black dashed line indicates RFU ratio=0.3.

3.4 Discussion

Radio-sensitisation upon IGF-1R knockdown was confirmed in DU145 prostate cancer cells, reproducing the phenotype observed previously in our group (Fig. 3.1A-B). Further, the AR-positive 22Rv1 cell line was shown to display similar radio-sensitivity after receptor knockdown, correlating with IGF-1R knockdown and inhibition experiments by the Macaulay lab in other cell types (Fig. 3.1C-F) (Chitnis et al., 2014; Rochester et al., 2005; Simpson et al., 2020; Turney et al., 2012).

IGF-1R null clones were generated by targeting exon 2 of *IGF1R* and disruption of exon 2 resulted in complete loss of IGF-1R protein in multiple clones (Fig. 3.5). This is consistent with IGF-1R null clones engineered in DU145 cells in the lab (unpublished), as well as by others (Zhou et al., 2016). Sequencing analyses indicated that IGF-1R null clones exhibited unique indels as was anticipated by inducing a DSB using the CRISPR/Cas9 system (Fig. 3.6) (Allen et al., 2019). Western blot analysis highlighted two candidate null clones that exhibited absence of mature total IGF-1R, but expression of the pro-receptor (Fig. 3.5). The pro-receptor is cleaved by pro-protein convertases into the mature receptor, and this is dependent on cleavage at $RKRR^{740}$ (Khatib et al., 2001). A possible reason for the clones exhibiting the pro-receptor but lacking expression of the mature IGF-1R, is that the CRISPR-mediated modification of *IGF1R* may result in changes to the secondary structure of IGF-1R protein.

This could alter accessibility to the cleavage site, impacting pro-receptor cleavage by pro-protein convertases. Previous investigation in the lab indicated that alterations of upstream sequence can impact pro-receptor cleavage. The inclusion of a 15 amino acid insert into the α-subunit of IGF-1R, far upstream of $RKRR^{740}$, resulted in the absence of furin-mediated cleavage (Macaulay, unpublished). Treatment of IGF-1R WT cells with a pro-protein convertase inhibitor followed by Western blot analysis could be used to ascertain whether the pro-receptor signal persists, and therefore suggest a reason for the observed pro-receptor in these clones.

Several CRISPR strategies were attempted to create an IGF-1R kinase-inactive clone. HDR-mediated approaches using symmetric and asymmetric ssODNs, HDR enhancer molecules and altering transfection conditions exhibited no gene editing at the desired edit site. This method of amino acid substitution is inefficient (Mao et al., 2008; O'Brien et al., 2019), and is becoming less favourable as newer, more proficient techniques are being developed (Anzalone et al., 2019; Gaudelli et al., 2017; Komor et al., 2016; Rees and Liu, 2018; Yeh et al., 2018).

Evidence suggested the possible creation of an IGF-1R kinase-dead mutant through cNHEJ-mediated repair at the CRISPR cut site (Fig. 3.8-3.10). The absence of nearby editing and the location of the base substitution at the target site indicate error-prone repair, characteristic of cNHEJ (Bassing and Alt, 2004). The close proximity of N1006D to the ATP binding site offers the possibility that the exchange of guanine to adenine could distort the motif, leading to kinase inactivity. This mutation seemed to be so far uncharacterised in the literature.

Efforts to create the K1003R mutant using base editing were unsuccessful (Fig. 3.12). Observation of high transfection efficiencies and confirmation of gRNA binding efficiency were encouraging, however no evidence of editing was displayed. When detailing shortfalls of base editing, most reports point to insertion of additional edits rather than absence of editing (Rees and Liu, 2018; Rose et al., 2020). However, high frequency of adenine bases around the desired edit site and low cellular expression of ABE agents have been documented, both of which could have impacted these efforts (Jiang et al., 2020; F. Wang et al., 2020). Additional base editors created since the original discovery by Komor *et al.* offer slight alterations in design, which aim to improve editing efficiency in specific settings (Gaudelli et al., 2017; Komor et al., 2016; Rees and Liu, 2018). Further investigation of these novel base editor variants could uncover a more efficient method of generating the desired adenine to guanine base substitution.

Prime editing offered a timely alternative to base editing, and initial trials seemed promising (Fig. 3.14-15). Editing efficiencies at K1003 indicated correct targeting and further characterisation of the candidate K1003R clones will be carried out. If it does prove possible to create kinase-dead clones in addition to the IGF-1R null and hypomorphic clones generated here, these clones could provide a platform for further investigation of the effects of partial or complete loss of kinase activity or receptor expression on radio-sensitivity and the DDR. Additionally, the models could be used to examine the contribution of the receptor to other cancer hallmarks.

CHAPTER IV: Testing the phenotype of IGF-1R compromised cells

4.1 Testing radio-sensitivity of IGF-1R null clones

Creation of IGF-1R null clones enabled a comparison to be made of the effect of sustained loss of the receptor on radio-sensitisation compared to acute IGF-1R depletion by siRNA. This was important to further validate the increased radiation sensitivity when IGF-1R signalling is compromised, but also to investigate whether subsequent long-term compensatory mechanisms in IGF-1R null clones affected the phenotype. As shown previously (Fig. 3.5), IGF-1R null clones displayed varying levels of phospho-S6 (serine 240/S244) and phospho-4E-BP1 (threonine 37/46), both conventional readouts of mTOR signalling. Despite these apparent fluctuations in mTOR signalling, similar radio-sensitisation and basal survival at 0 Gy were observed (Fig. 4.1A, B), suggesting that signalling through mTOR may not be the driver of radio-sensitivity in IGF-1R compromised cells.

Due to time restrictions, two IGF-1R null clones were selected for further analysis. The selected IGF-1R null clones exhibited similar doubling times to the uncloned 22Rv1 parental cells and clones expressing WT IGF-1R (Fig. 4.1C). This supports data from Resnicoff *et al.* that IGF-1R is relatively unimportant for 2D growth (Resnicoff et al., 1994). Clonogenic survival assays were performed on the chosen IGF-1R null clones and clones expressing WT IGF-1R generated by serial-dilution. Results suggested a comparable level of sensitisation between IGF-1R WT cells and IGF-1R knockdown control (siControl) cells, and between cells depleted of IGF-1R and IGF-1R null clones with increasing radiation dose plated in parallel (Fig. 4.1D).

Specifically, DERs of ≥2.34 were calculated after 6 Gy irradiation in IGF-1R knockdown and null clones (Fig. 4.1E). IGF-1R knockdown was confirmed by Western blot analysis (Fig. 4.1F) and was similar to IGF-1R depletion in Fig. 3.1C, however produced lower DER values (Fig. 3.1D, E, 4.1D, E). This is likely due to precision of counting or small differences in extent of IGF-1R knockdown.

Overall, IGF-1R null cells displayed a radio-sensitisation phenotype analogous to that of IGF-1R knockdown cells, suggesting that there was no major compensation for loss of IGF-1R, in terms of ability to mediate radio-resistance. The next experiments investigated whether this function of IGF-1R related to its structural role in mediating radio-resistance in prostate cancer cells or its kinase activity.

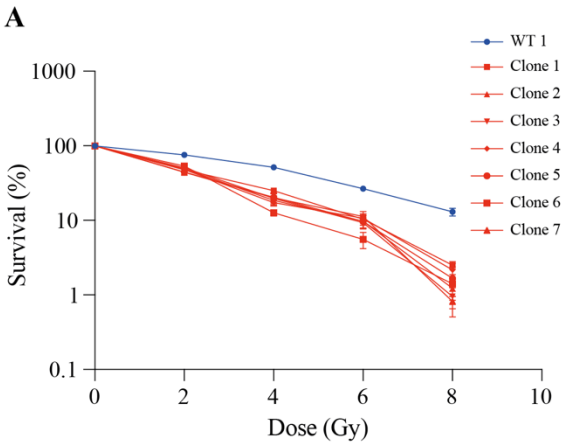

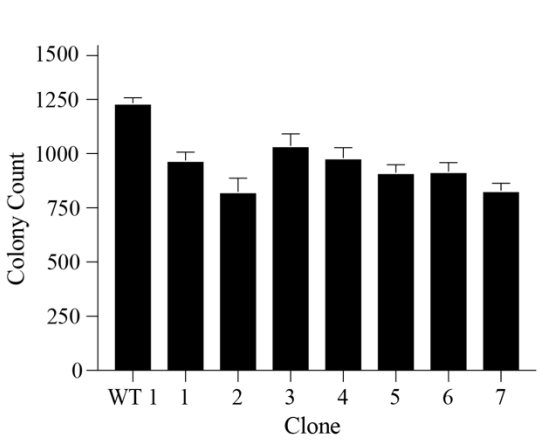

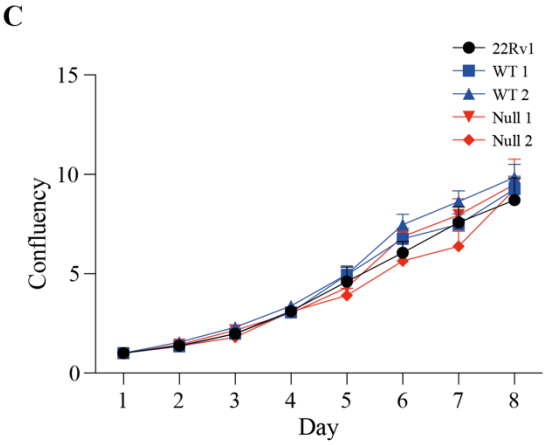

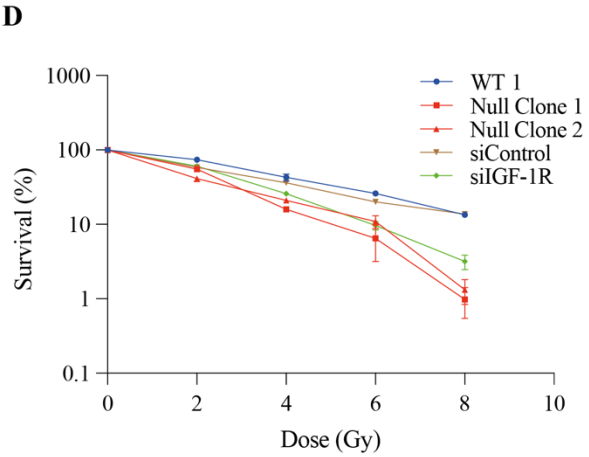

E

Radiation dose (Gy)	Null clone 1	Null clone 2	siIGF-1R
0	1.00	1.00	1.00
2	1.33±0.17	1.79±0.30	1.21±0.18
4	2.69±0.08	2.06±0.18	1.57±0.33
6	4.94±2.79	2.79±1.06	2.34±0.94
8	6.81±4.13	5.95±3.85	4.75±2.21

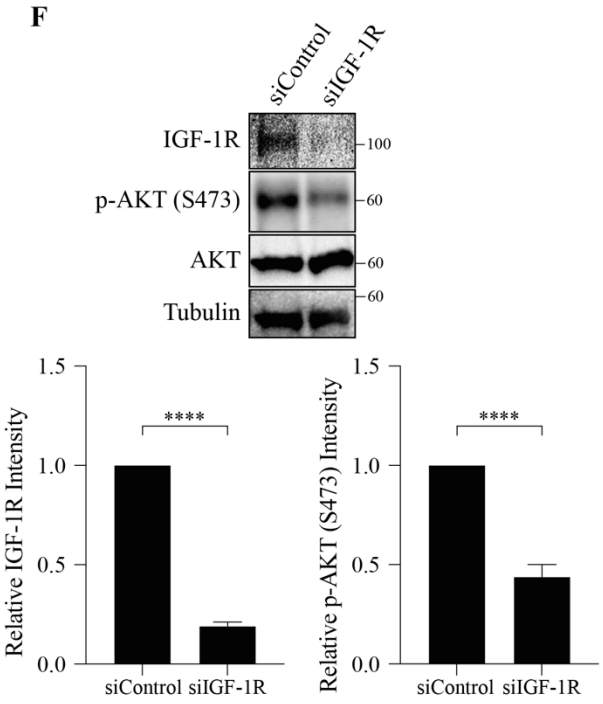

Figure 4.1: IGF-1R null clones exhibit increased radio-sensitivity.
(A) The 7 candidate IGF-1R null clones and a clone expressing WT IGF-1R were seeded in 10cm dishes (3.0 x 10^3 cells/dish) and the following day, dishes were irradiated at indicated doses. After 11-14 days, visible colonies were stained with Coomassie Brilliant Blue and counted using GELCOUNT software. The graph shows colony survival expressed as a percentage of survival of unirradiated controls. Points represent the mean ± SEM for triplicate values of one experiment. (B) The number of colonies on the unirradiated plates for each clone were examined to check for changes in basal survival. Each column represents the mean ± SEM of triplicate values in one experiment. The data were analysed by one-way ANOVA, and all candidate null clones exhibited significantly reduced basal survival when compared to IGF-1R WT clones (clone 4: *, clones 1, 5, 6: **, clones 2, 7: ***) (*p<0.0466; **p<0.01; ***p<0.001). (C) Parental 22Rv1 cells and clones expressing WT IGF-1R and IGF-1R null clones were plated in a 384 well plate in duplicate (1 x 10^3 cells/well) and confluency was monitored based on bright field image using the Incucyte Live-Cell Analysis System for 8 days. (D) Parental 22Rv1 cells were seeded in 10cm dishes (7.5 x 10^5 cells/dish), and the following day cells were transfected with 50nM siControl or siIGF-1R. 48 hours post-transfection, cultures were re-seeded in triplicate (3.0 x 10^3/dish) and a clone expressing WT IGF-1R and two IGF-1R null clones were also seeded (3.0 x 10^3/dish) in triplicate. The following day, dishes were irradiated at indicated doses. After 11-14 days, visible colonies were stained with Coomassie Brilliant Blue and counted using GELCOUNT software. The graph shows colony survival expressed as a percentage of survival of unirradiated controls. Points represent the mean ± SEM for triplicate values of one representative experiment of three independent experimental repeats. (E) DERs for relative survival of IGF-1R null clones were calculated as relative survival of WT cells/relative survival of IGF-1R null clones at specific radiation doses. IGF-1R depleted 22Rv1 cells were calculated as relative survival of siControl cells/relative survival of siIGF-1R cells at specific radiation doses. DERs were calculated from three independent experimental repeats. (F) 22Rv1 cells were seeded and transfected with siControl or siIGF-1R as in Fig. 3.1. Whole cell lysates were analysed by Western blot to confirm adequate IGF-1R depletion (n=3). The data were analysed by unpaired student t-test, to determine statistical significance of band intensity differences (****p<0.0001).

4.2 Characterisation of IGF-1R$^{+/-}$ clone

Data from previous lab members and results generated here implicate IGF-1R in the cellular response to irradiation. Inhibition, knockdown or knockout of the receptor increased radio-sensitivity, and further, previous data showed that IGF-1R inhibition delayed DSB resolution and reduced the activity of both major DNA repair pathways (Chitnis et al., 2014; Turney et al., 2012). Evidence of kinase-independent functions of IGF-1R (Boucher et al., 2014, 2010a; Vasilcanu et al., 2008) pose the question of whether prior results were due to loss of kinase activity or structural integrity of the receptor. The generation of a clone expressing a kinase-dead IGF-1R would allow for the investigation of functions of the kinase activity of the receptor that contribute to the radio-sensitisation phenotype.

Western blot analyses of the hypomorphic mutant clone showed the presence of IGF-1R (Fig. 3.9). Using an antibody specific for IGF-induced IGF-1R phosphorylation, phosphorylation of the hypomorphic mutant clone was clearly absent (Fig. 3.9C).

4.2.1 Testing receptor kinase activity of the hypomorphic mutant clone

Examination of basal signalling in IGF-1R compromised cells by Western blot analyses suggested a significant reduction in phospho-(threonine 202/tyrosine 204)-ERK1/2 levels compared to clones expressing WT IGF-1R, indicative of inhibition of downstream pathway signalling. No difference in phospho-(threonine 308)-AKT signal was observed between clones, and phosphorylation of AKT serine 473 was apparently increased in the hypomorphic mutant clone but not in other clones, however this result was influenced by difficulties of detecting phospho-serine 473 AKT by Western blot in this cell line (Fig. 4.2).

Western blot analyses of clones with different IGF-1R status after IGF-1 stimulation indicated that IGF-1R compromised cells displayed increased phospho-(serine 473)-AKT compared to clones expressing WT IGF-1R (Fig. 4.3). There are reports in the literature that activation of mTORC2 (mainly responsible for AKT serine 473 phosphorylation) requires inhibition of mTORC1 (Breuleux et al., 2009; Vadlakonda et al., 2013). It could be speculated that lack of IGF-1R kinase activity results in reduction of mTORC1, which could explain the increased AKT serine 473 signal in IGF-1R compromised cells upon IGF-1 stimulation. Phospho-(threonine 308)-AKT signal was similar between all clones after IGF-1 stimulation, possibly suggesting that INSR signalling is more responsible for PDK1 activation than IGF-1R (Fig. 4.3) (Hart and Vogt, 2011; Vadlakonda et al., 2013). Phosphorylation of TSC2 (threonine 1462) was significantly decreased in IGF-1R compromised cells compared to clones

expressing WT IGF-1R. This was indicative of pathway inhibition in IGF-1R null and hypomorphic clones as phosphorylation of TSC2 at threonine 1462 by AKT serves to disinhibit mTORC1 (S.-L. Cai et al., 2006). No major changes in phosphorylation of common AKT substrates were noted (Fig. 4.3), however due to Covid-19, time did not permit repetition of this experiment.

Both null 1 and 2 clones behaved very similarly in radio-sensitivity assays (Fig. 4.1D) and in assessment of downstream cell signalling responses to IGF-1 in both serum-starved and full medium conditions (Fig. 4.2, 4.3). Therefore, it was decided to perform further experiments using a single null clone and a single clone expressing WT IGF-1R was selected for comparison.

To further examine effects of the loss of kinase activity exhibited by the hypomorphic mutant clone, IGF-1 and insulin dose-response experiments were carried out by ELISA, using the phospho-(tyrosine 1135/1136)-IGF-1R/INSR antibody. This work was carried out prior to full characterisation of the candidate kinase dead clone as hypomorphic, and before the phospho-(tyrosine 1316)-IGF-1R antibody became available. These experiments were chosen to test the ligand responses via IGF-1R and INSR. As expected, stimulation with increasing concentrations of IGF-1 led to increased phosphorylation in a 22Rv1 clone expressing WT IGF-1R. Both the IGF-1R null clone and the hypomorphic mutant clone showed comparably low levels of phosphorylation, and therefore less kinase activity, increasing slightly in the presence of very high IGF-1 levels ([IGF-1] ≥125 nM, Fig. 4.4A). In response to insulin, phospho-IGF-1R/INSR tyrosine 1135/1136 signals were similar across all clones, representative of conserved INSR function. The marginally higher phosphorylation registered

in the IGF-1R WT clone is likely due to its kinase-active IGF-1R (Fig 4.4B). Although detecting phosphorylation of IGF-1R and INSR, these functional tests demonstrated that the hypomorphic mutant clone responded to ligand stimulation more akin to the IGF-1R null clone than the WT IGF-1R clone, suggesting reduction in IGF-1R kinase activity.

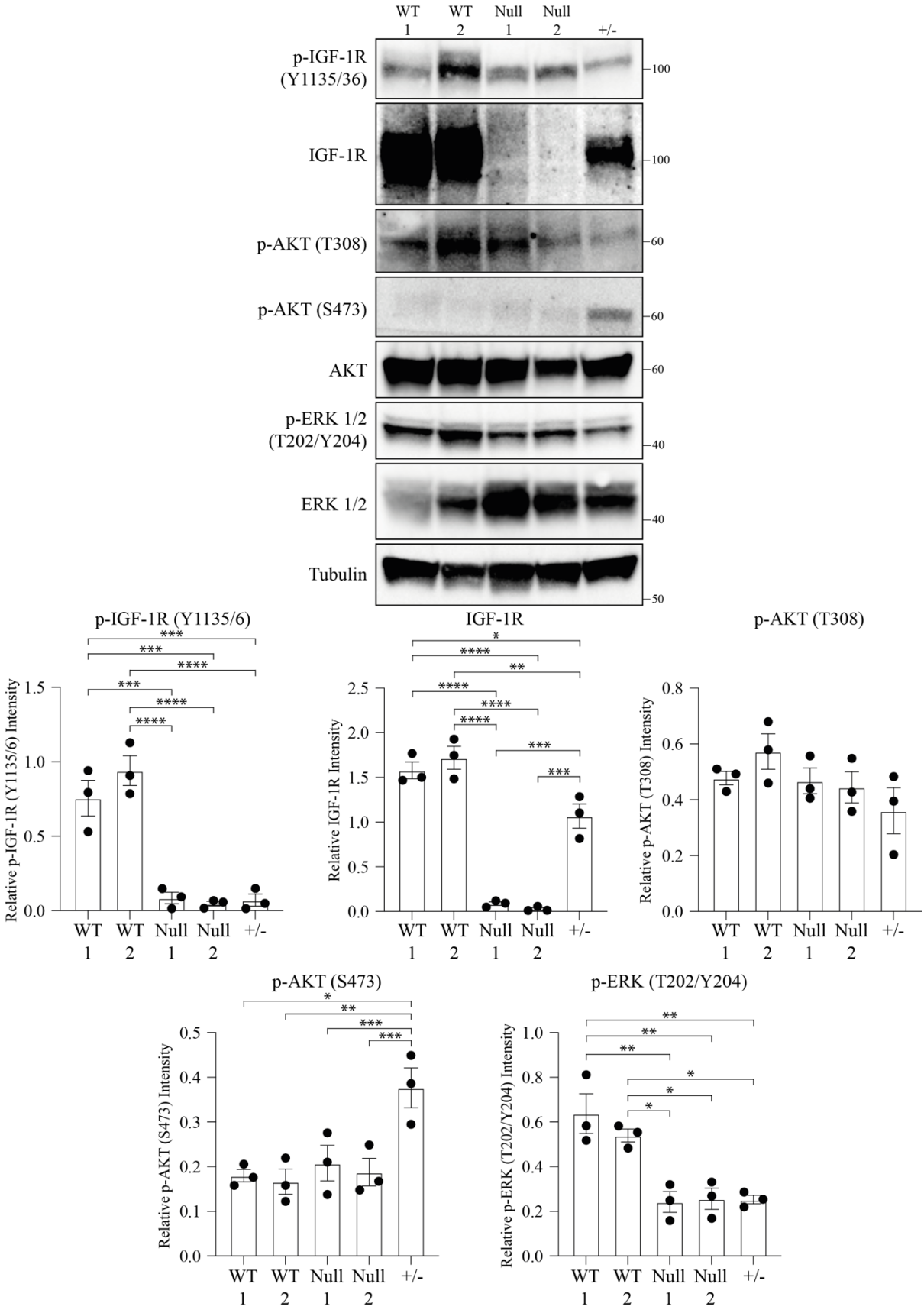
WT 1
WT 2
Null 1
Null 2
+/-
p-IGF-1R (Y1135/36)
IGF-1R
p-AKT (T308)
p-AKT (S473)
AKT
p-ERK 1/2 (T202/Y204)
ERK 1/2
Tubulin
100
100
60
60
60
40
40
50
p-IGF-1R (Y1135/6)
Relative p-IGF-1R (Y1135/6) Intensity
IGF-1R
Relative IGF-1R Intensity
p-AKT (T308)
Relative p-AKT (T308) Intensity
p-AKT (S473)
Relative p-AKT (S473) Intensity
p-ERK (T202/Y204)
Relative p-ERK (T202/Y204) Intensity

Figure 4.2: Western blot analysis of IGF-1R null and hypomorphic mutant clones in basal conditions.
One clone expressing WT IGF-1R, one IGF-1R null clone and the hypomorphic mutant clone were seeded into a 6 well plate and incubated until 70-80% confluent. Whole cell lysates were extracted of clones expressing WT IGF-1R, IGF-1R null clones and the hypomorphic mutant clone were analysed by Western blot for IGF-1R and downstream effectors with β-tubulin as a loading control. The blot shown is representative of three independent experiments. Quantification was performed using ImageJ software and a one-way ANOVA was used to determine the significance of differences between clones (*p<0.05, **p<0.01, ***p<0.001, ****p<0.0001).

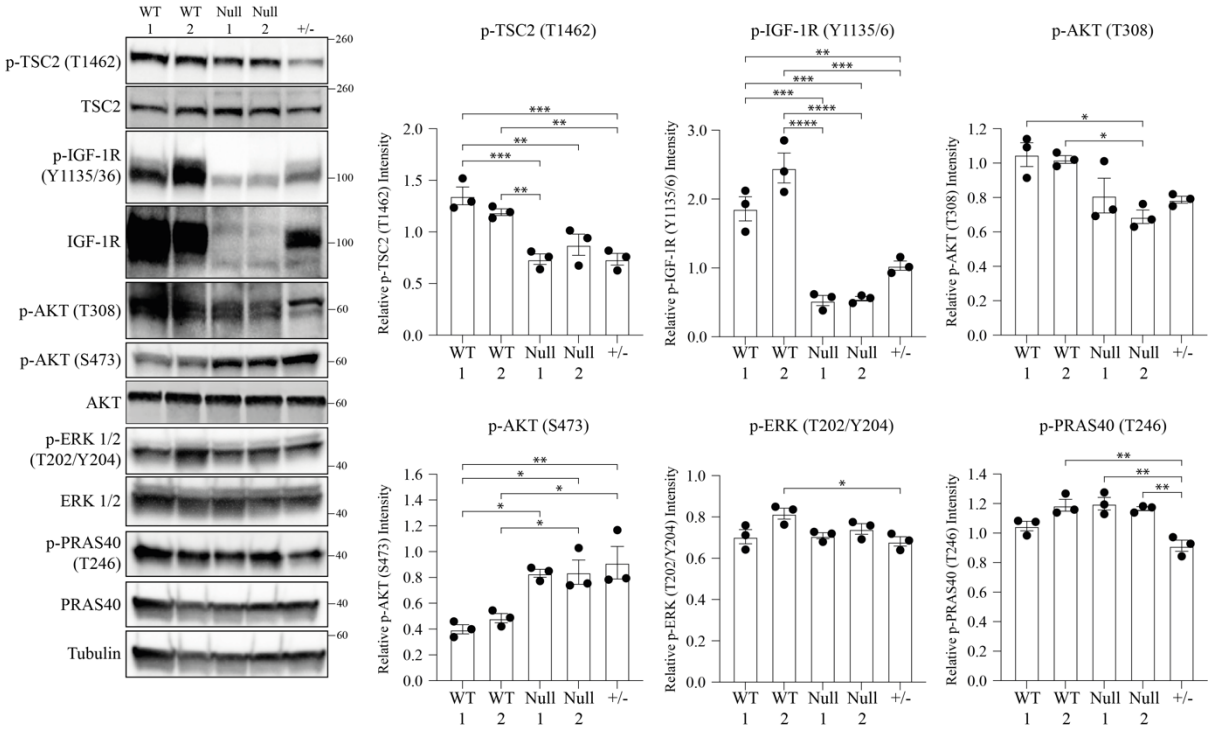

Figure 4.3: Western blot analysis of IGF-1R null and hypomorphic mutant clones after IGF-1 stimulation.
One clone expressing WT IGF-1R, one IGF-1R null clone and the hypomorphic mutant clone were seeded into a 6 well plate and incubated until 70-80% confluent. Cells were serum-starved overnight and stimulated with IGF-1 (25 nM) for 30 minutes, before lysates were extracted. Whole cell lysates of clones expressing WT IGF-1R, IGF-1R null clones and the hypomorphic mutant clone were analysed by Western blot for IGF-1R and downstream effectors with β-tubulin as a loading control. The blot shown is representative of three independent experiments. Quantification was performed using ImageJ software and a one-way ANOVA was used to determine the significance of differences between clones (*p<0.05, **p<0.01, ***p<0.001, ****p<0.0001).

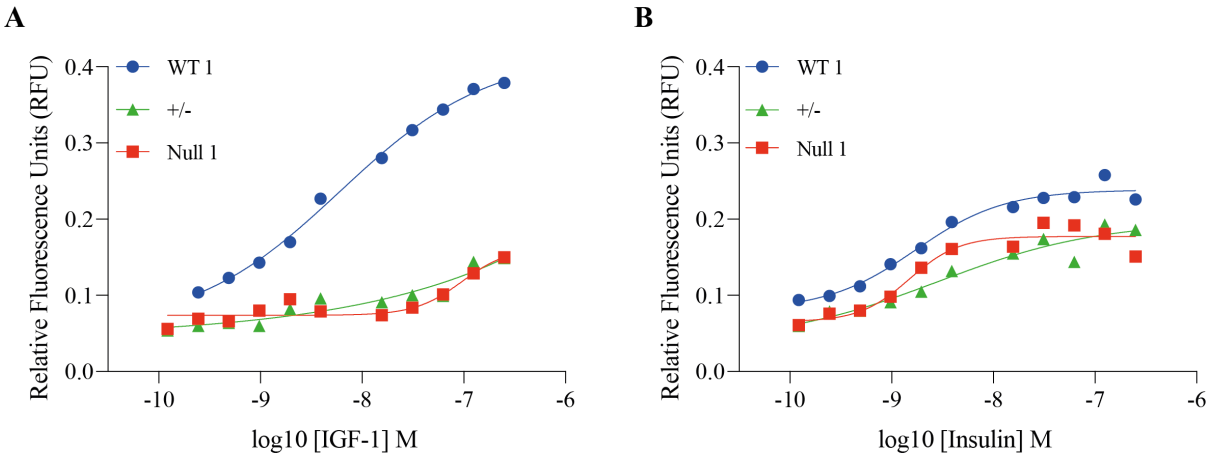

Figure 4.4: Characterisation of the kinase activity of the hypomorphic mutant.
(A) One clone expressing WT IGF-1R, one IGF-1R null clone and the hypomorphic mutant clone were seeded into a 96 well plate in duplicate and incubated until 70-80% confluent. Cells were serum-starved overnight and stimulated with increasing concentrations of IGF-1 for 30 minutes. Cells were fixed and incubated overnight with phospho-Y1135/1136-IGF-1R primary antibody, before incubation with anti-rabbit secondary antibody and addition of TMB. RFU values at increasing doses of IGF-1 were measured using the POLARstar Omega plate reader. (B) One clone expressing WT IGF-1R, one IGF-1R null clone and the hypomorphic mutant clone were seeded into a 96 well plate in duplicate and incubated until 70-80% confluent. Cells were serum-starved overnight and stimulated with increasing concentrations of insulin for 30 minutes. Cells were fixed and incubated overnight with phospho-Y1135/1136-IGF-1R primary antibody, before incubation with anti-rabbit secondary antibody and addition of TMB. RFU values at increasing doses of insulin were measured using the POLARstar Omega plate reader. Points represent the mean ± SEM (all SEM bars were smaller than the symbols showing the means) for triplicate values of one representative experiment of three independent experimental repeats, all with comparable results.

4.2.2 Subcellular localisation of the hypomorphic mutant clone

To further characterise the hypomorphic mutant clone, subcellular fractionation experiments were carried out to check that the receptor could still undergo insertion into the plasma membrane, as this could hinder any structure-specific role of the receptor at the membrane, within the cytoplasm or nucleus.

Work by Jack Mills (DPhil student, Macaulay Group) indicated that IGF-1R was difficult to detect by immunofluorescence (IF) in 22Rv1 cells (unpublished). Using clones expressing either WT IGF-1R, the hypomorphic mutant clone or an IGF-1R null clone, IGF-1R localisation was examined by IF using three IGF-1R-β-specific antibodies (CST #3027, CST

#9750, sc-81167). CST #3027 staining indicated very little staining in IGF-1R null cells, however in clones expressing WT IGF-1R there was more of a para-nuclear pattern, possibly of the ER or Golgi apparatus (Fig. 4.5, row 1), consistent with recently identified Golgi localisation reported by O'Connor's group (Rieger et al., 2020; Rieger and O'Connor, 2021). CST #9750 staining indicated a non-specific signal in IGF-1R null cells (Fig. 4.5, row 2), and sc-81167 displayed a non-specific nuclear signal in both clones with absence of extranuclear signal in IGF-1R null cells (Fig. 4.5, row 3). None of the antibodies tested detected interpretable signalling in clones expressing WT IGF-1R that was not present in IGF-1R null cells. Because of this issue, it was decided not to repeat the IF analysis in additional IGF-1R WT and null clones, and instead to seek alternative methods to examine localisation of the hypomorphic mutant clone.

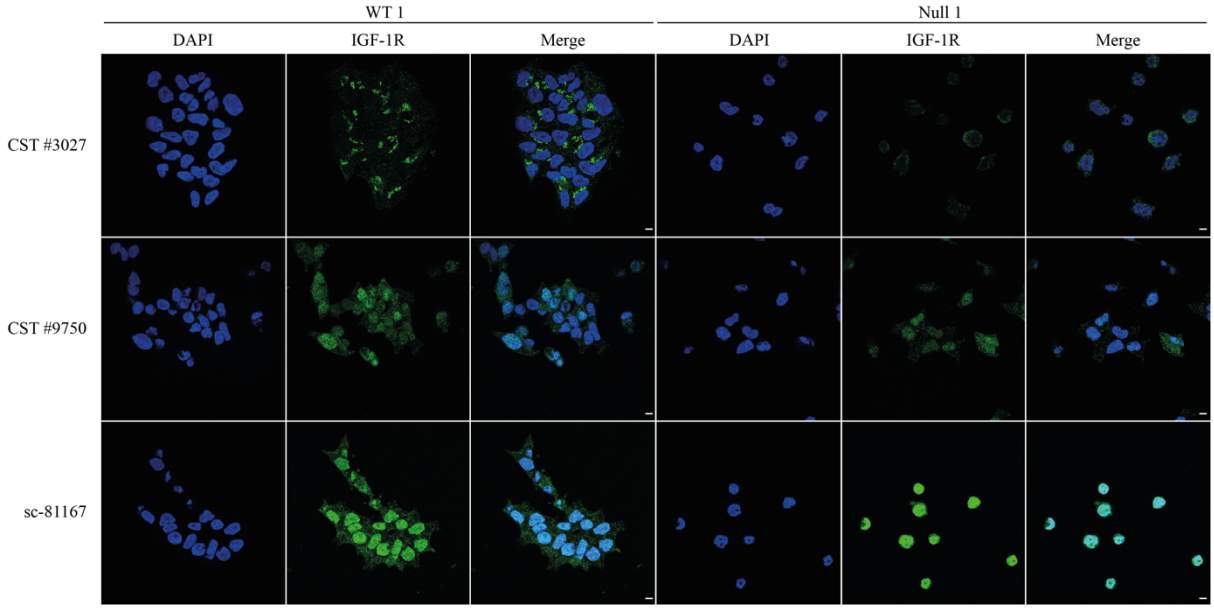

Figure 4.5: Immunofluorescence to investigate subcellular localisation of IGF-1R.
A clone expressing WT IGF-1R and an IGF-1R null clone were seeded on coverslips in 6 well plates in triplicate (1 x 10^5 cells/well). The following day, cells were fixed and incubated with either CST #3027, CST #9750 or sc-81167 IGF-1R antibodies overnight. After incubation with secondary antibody, cells were examined by IF. Images show nuclear DAPI (blue) and IGF-1R (green) and merged staining. Images were taken at 63x magnification, scale bar represents 10 µm.

As an alternative approach to investigate receptor localisation, membrane proteins were extracted from clones expressing either IGF-1R WT, null or the hypomorphic mutant clone using the MEM-PER Plus kit (ThermoFisher) as described in Chapter II (section 2.9). Cells were permeabilised with a mild detergent to isolate the soluble cytosolic fraction, and a second detergent was then used to collect the soluble membrane proteins. Using E-cadherin and tubulin as membrane and cytoplasmic markers, respectively, it was confirmed that unstimulated IGF-1R in both the WT and hypomorphic mutant clones, was present on the plasma membrane and not internalised into the cytoplasm (Fig. 4.6A).

Using the Nuclear and Cytoplasmic Extraction Kit (section 2.10) cell membranes were first disrupted, and cytoplasmic contents released. The intact nuclei were recovered from the cytoplasmic extract, and through centrifugation, nuclear proteins were collected. Isolation of nuclear protein fractions after stimulation with IGF-1 indicated translocation of the hypomorphic mutant clone to the nucleus, using lamin A/C as a nuclear membrane marker (Fig. 4.6B). Cells expressing WT IGF-1R were analysed in parallel, as a positive control for IGF-1R nuclear translocation. Because of the cost of the fractionation kits, these experiments used single IGF-1R$^{+/+}$, IGF-1R$^{+/-}$ and IGF-1R$^{-/-}$ clones. The intention was to repeat this assessment using one additional WT and null clone, but this was prevented by financial and time constraints.

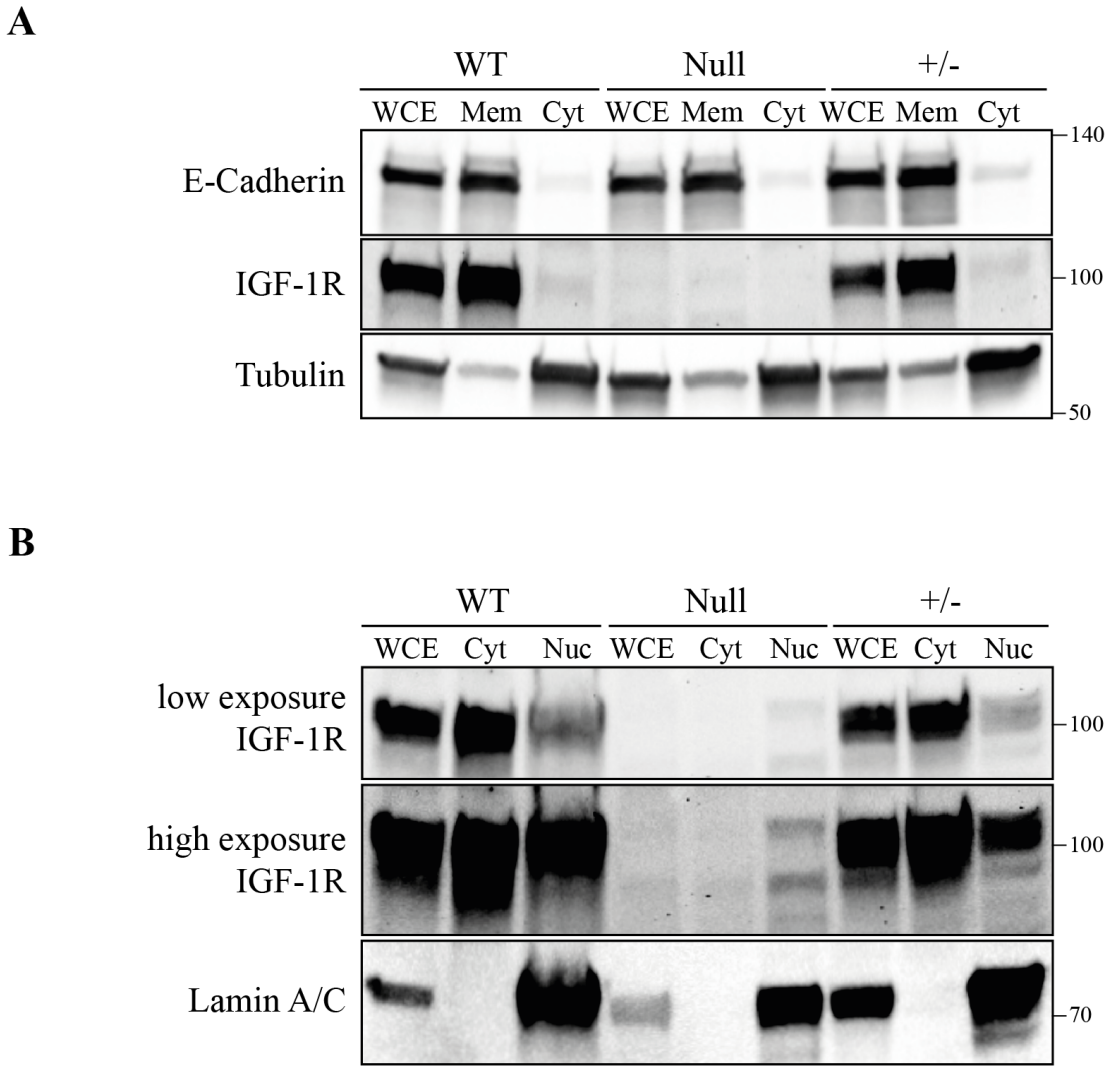

Figure 4.6: Subcellular fractionation to investigate localisation of the hypomorphic mutant clone.
(A) A clone expressing WT IGF-1R, an IGF-1R null clone and the hypomorphic mutant clone were plated in 15 cm dishes in triplicate (1 x 10^6/dish) and when 80% confluent, harvested and solubilised membrane and membrane-associated proteins were collected, as well as cytosolic proteins. Whole cell extracts, membrane fractions and cytosolic fractions were analysed by Western blot, using a membrane marker (E-cadherin) and β-tubulin as a loading control. (B) A clone expressing WT IGF-1R, an IGF-1R null clone and the hypomorphic mutant clone were plated in 15 cm dishes in triplicate (1 x 10^6/dish) and when 80% confluent, harvested and nuclear and cytoplasmic fractions were collected. Whole cell extracts, cytosolic and nuclear fractions were analysed by Western blot, using a nuclear membrane marker (lamin A/C). This blot is representative of three independent experimental repeats.

4.3 Exploring the effect of *IGF1R* gene dosage and kinase activity in radio-sensitisation

To investigate whether loss of endogenous IGF-1R kinase activity was a causal factor for the radio-sensitivity exhibited in IGF-1R-compromised prostate cancer cells, clonogenic survival assays were carried out comparing 22Rv1 clones expressing WT IGF-1R, a hypomorphic mutant clone and an IGF-1R null clone. The hypomorphic clone represents a state of stable IGF-1R downregulation, with greater relevance to clinical radiation responses of high vs low IGF-1R tumours (Aleksic et al., 2017), and less experimental variation than could be achieved using gene silencing.

4.3.1 Clonogenic survival assays

At increasing radiation doses, the sensitivity of the hypomorphic mutant clone was significantly greater than that of IGF-1R WT cells (Fig. 4.7A, B), mirroring the radio-sensitisation phenotype observed in the IGF-1R null clone. Further, the difference in DER values of the null and hypomorphic mutant clone was not statistically significant (Fig. 4.7C). As the hypermorphic mutant has both a lower level of IGF-1R expression than WT cells and also altered levels of phosphorylation (Fig. 3.9, 4.3, 4.4), this result could implicate IGF-1R expression and/or kinase activity in mediating radio-resistance. Additionally, radio-sensitivity could also be due to a threshold requirement for structural function(s) of the receptor. The influence of IGF-1R spans multiple signalling pathways (Larsson et al., 2005; Osher and Macaulay, 2019; Riedemann and Macaulay, 2006), and the radio-sensitisation phenotype displayed in 2D clonogenic assays could be due to various factors both singular or in combination. Repetition of this set of experiments using additional clones was intended, however incubator capacity limited the number of clonogenic assay plates that could be seeded

and cultured at once, and there was insufficient time to perform repeat assays on other clones. If time had permitted, WT 2 and null 2 clones would have been tested in clonogenic radiation assays.

A

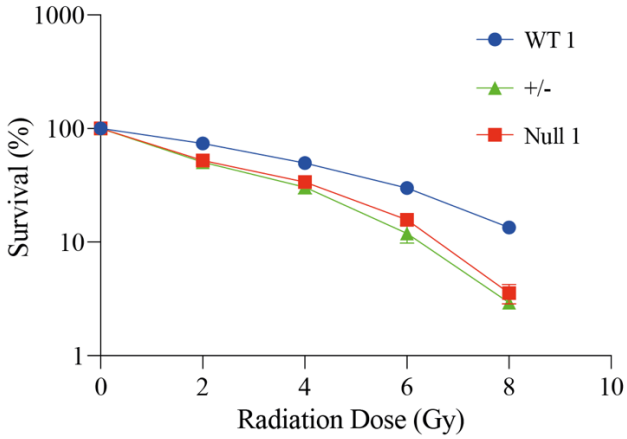

B

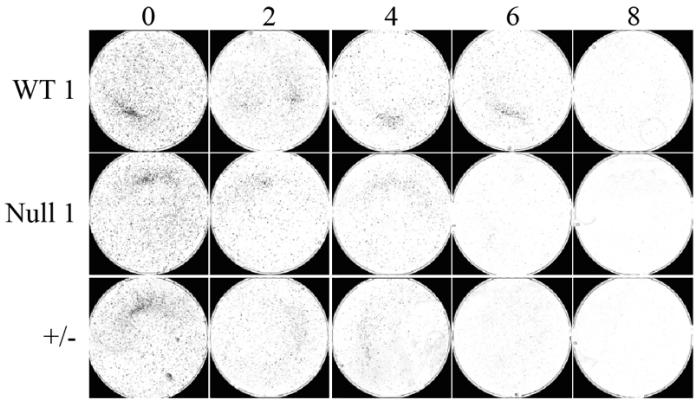

C

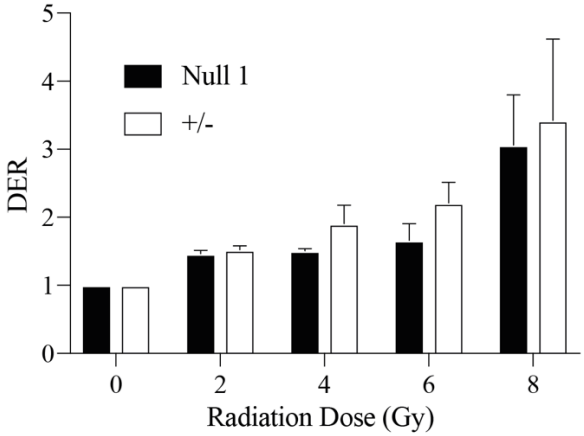

Radiation Dose (Gy)	Null 1	+/-
0	1.00	1.00
2	1.46±0.07	1.52±0.08
4	1.51±0.05	1.91±0.38
6	1.66±0.35	2.21±0.43
8	3.06±1.04	3.42±1.69

Figure 4.7: The hypomorphic mutant clone mimics the radio-sensitization phenotype of IGF-1R null clones.
(A) A clone expressing WT IGF-1R, an IGF-1R null clone and the hypomorphic mutant clone were seeded in 10 cm dishes (3.0×10^3 cells/dish) and the following day, dishes were irradiated at indicated doses. After 11-14 days, visible colonies were stained with Coomassie Brilliant Blue and counted using GELCOUNT software. (B) Images taken by GELCOUNT of clonogenic assay showing visible Coomassie Brilliant Blue colonies at each radiation dose (Gy). (C) A comparison of DERs for survival of an IGF-1R null clone and the hypomorphic mutant clone were calculated as relative survival of WT cells/relative survival of IGF-1R null clone or the hypomorphic mutant clone at specific radiation doses. Graph: mean ± SEM DER from 3 independent assays.

4.4 Testing proliferation and radio-sensitivity in 3D

As an additional measure of radio-sensitivity, 3D spheroid assays were attempted. The rationale for this was that IGF-1R has been shown to have a greater role in 3D growth than in 2D growth (Resnicoff et al., 1994). If spheroids exhibited a similar growth response at increasing radiation doses to their 2D counterparts, it could provide a readout for IGF-1R radio-sensitivity that is more relevant to *in vivo* tumour growth.

This assay was first tested in cells depleted of IGF-1R using siRNA, to see whether the radio-sensitisation effect of IGF-1R depletion at the time of irradiation seen in 2D clonogenic assays here (Fig. 3.1) and by others (Chitnis et al., 2014; Turney et al., 2012) could be replicated in 3D. Initially, 22Rv1 cells were plated and forward-transfected with siControl or siIGF-1R according to the usual protocol. The following morning, cells were trypsinised and 5,000 were transferred to each well of a low-adherence 96 well plate. After 48 hours, spheroids had formed and cells were irradiated at increasing doses. Using GELCOUNT software, spheroid area was monitored, and after 9 days, cell viability was measured by a CellTiter-Glo 3D assay.

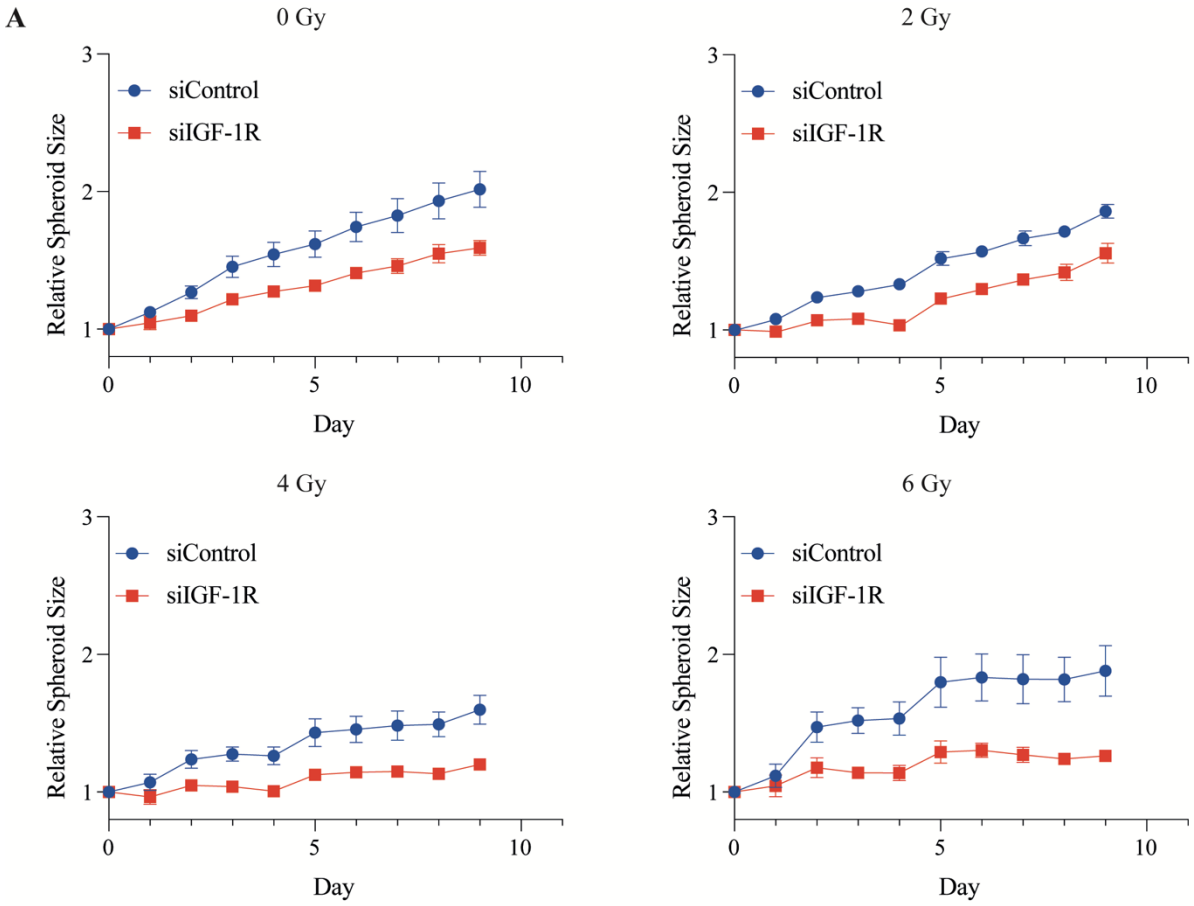
A
0 Gy
2 Gy
4 Gy
6 Gy
siControl
siIGF-1R
Relative Spheroid Size
Day
1
2
3
0
5
10

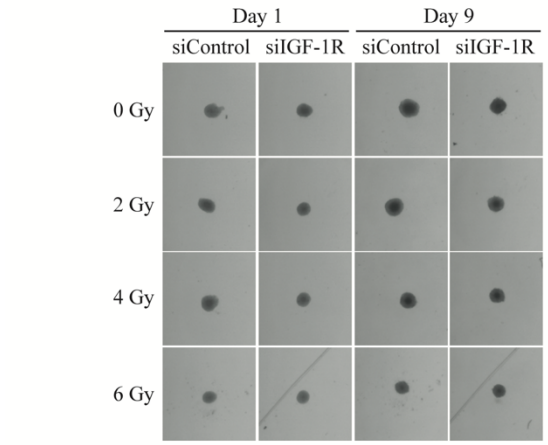
B
Day 1
Day 9
siControl
siIGF-1R
siControl
siIGF-1R
0 Gy
2 Gy
4 Gy
6 Gy

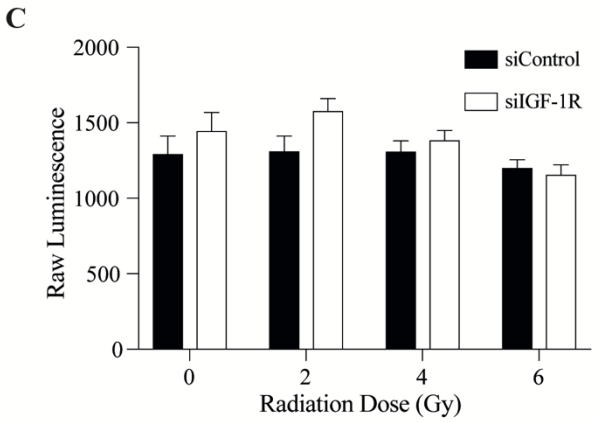
C
siControl
siIGF-1R
Raw Luminescence
2000
1500
1000
500
0
0
2
4
6
Radiation Dose (Gy)

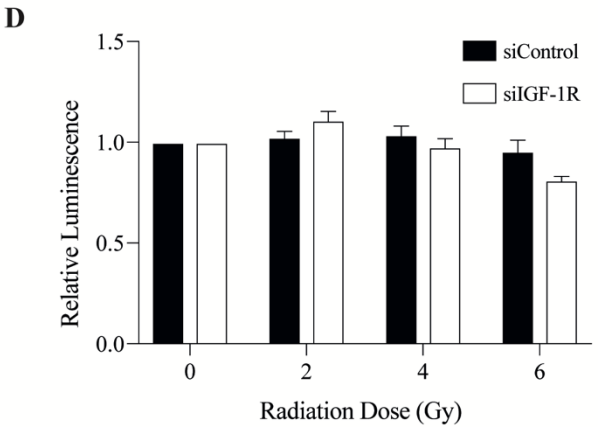
D
siControl
siIGF-1R
Relative Luminescence
1.5
1.0
0.5
0.0
0
2
4
6
Radiation Dose (Gy)

Figure 4.8: Examining radio-sensitivity of IGF-1R depleted cells in a 3D spheroid model.
22Rv1 cells were seeded in 10 cm dishes (7.5 x 10^5 cells/dish) and the following day transfected with siControl or siIGF-1R as per method used in Fig. 3.1. The next day cells were re-seeded in low-adherence 96 well plates (5 x 10^3 cells/well) and after 48 hr, cells were irradiated at indicated doses. (A) Individual wells were imaged for 9 days using GELCOUNT software and spheroid area measured using ImageJ. Relative spheroid area was calculated relative to spheroid area at day 1. Each point represents the mean ± SEM for sextuplicate values in one experiment representative of three separate experiments. (B) Representative GELCOUNT images of spheroids formed from 22Rv1 cells transfected with siControl or siIGF-1R at day 1 and day 9 post-IR at indicated doses. On day 9, 1 volume of CellTiter-Glo 3D reagent was added to 1 volume of medium containing spheroid in triplicate. After vigorous mixing for 5 minutes to induce cell lysis and incubation in the dark, the luminescent signal was measured using the POLARstar OMEGA plate reader. (C) Graph showing raw luminescence values of spheroids formed from 22Rv1 cells transfected with siControl or siIGF-1R at day 9. Each column represents the mean ± SEM in triplicate from one representative experiment of three separate experiments. (D) Graph showing raw luminescence values of spheroids formed from 22Rv1 cells transfected with siControl or siIGF-1R at day 9, relative to spheroid luminescence value at day 1. Each column represents the mean ± SEM in triplicate from one representative experiment of three separate experiments.

A decrease in spheroid area consistent with a reduction in IGF-1R signalling was indeed observed in spheroids depleted of IGF-1R compared to control spheroids transfected with non-silencing control siRNA (Fig. 4.8A, B) but there were no significant changes in cell viability in 3D (Fig. 4.8C, D). While increasing radiation doses caused progressive reduction in the rate of spheroid expansion, these effects were seen both in spheroids formed of cells transfected with control or IGF-1R siRNAs, indicated no that there was no increase in relative radio-sensitivity (Fig. 4.8). Consistent with these results, comparison of cells expressing WT IGF-1R with IGF-1R null cells suggested that loss of IGF-1R reduced 3D growth (Fig. 4.9A, B, 4.10A), had no major effect on cell viability (Fig. 4.9C, D, 4.10B, C), and did not enhance radio-sensitivity (Fig. 4.9A, 4.10A). While it would have been preferential to use two IGF-1R WT and null clones for these analyses, the CellTiter Glo 3D reagent was too expensive, and preference was given to obtain three repeats using singular clones.

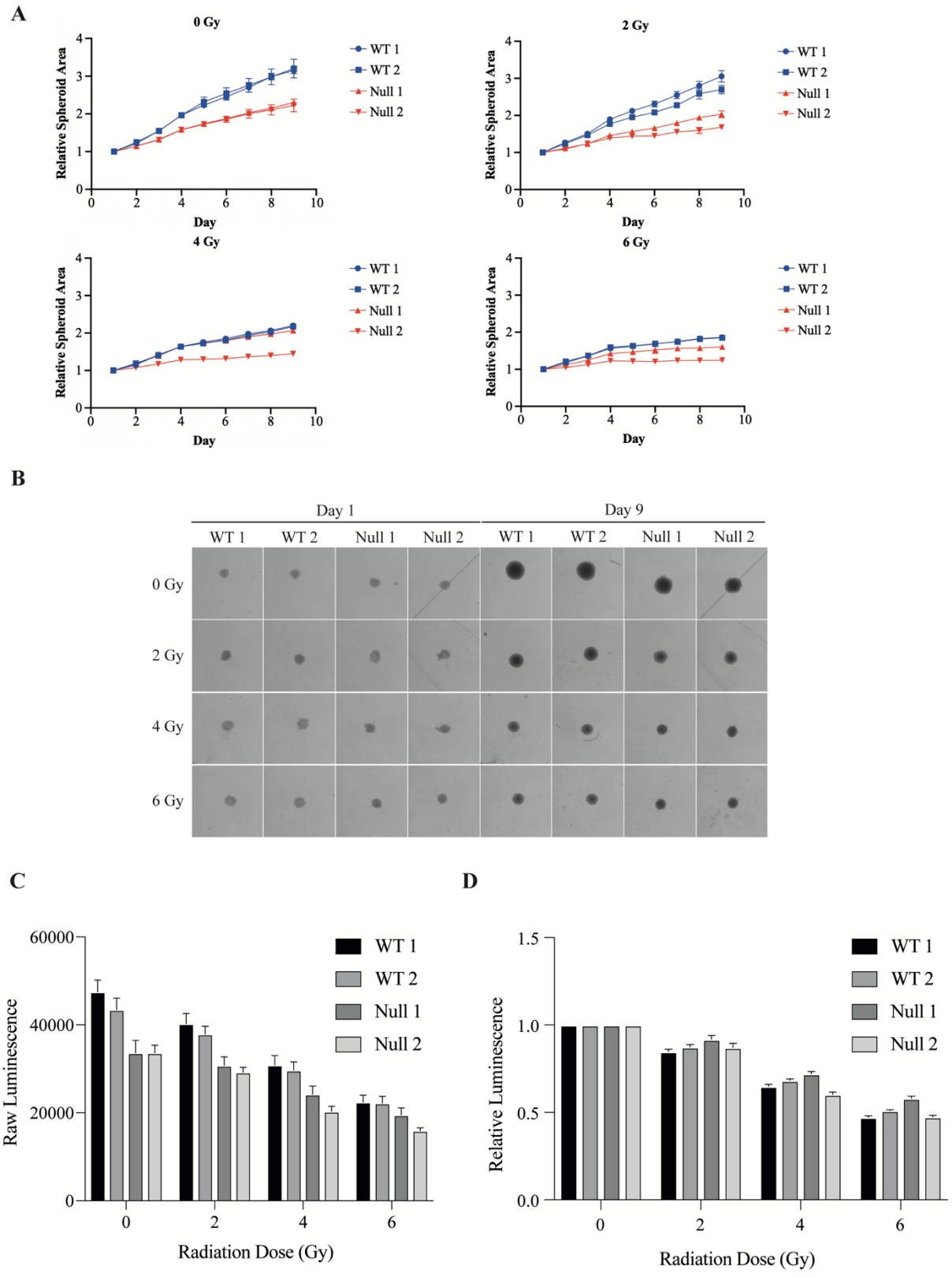
A
0 Gy
2 Gy
4 Gy
6 Gy
Relative Spheroid Area
Day
WT 1
WT 2
Null 1
Null 2
B
Day 1
Day 9
WT 1
WT 2
Null 1
Null 2
0 Gy
2 Gy
4 Gy
6 Gy
C
Raw Luminescence
Radiation Dose (Gy)
D
Relative Luminescence
Radiation Dose (Gy)

Figure 4.9: Examining radio-sensitivity of IGF-1R null cells in a 3D spheroid model.
22Rv1 clones expressing WT IGF-1R and IGF-1R null clones were seeded in low-adherence 96 well plates (5 x 10^3 cells/well) and after 48 hr, cells were irradiated at indicated doses. (A) Individual wells were imaged for 9 days using GELCOUNT software and spheroid area measured using ImageJ. Relative spheroid area was calculated relative to spheroid area at day 1. Each point represents the mean ± SEM for sextuplicate values in one experiment representative of three separate experiments. (B) Representative GELCOUNT images of spheroids formed from 22Rv1 clones expressing WT IGF-1R and IGF-1R null clones at day 1 and day 9 post-IR at indicated doses. On day 9, the CellTiter-Glo 3D viability assay was carried out as in Fig. 4.8. (C) Graph showing raw luminescence values of spheroids formed from 22Rv1 clones expressing WT IGF-1R and IGF-1R null clones at day 9. Each column represents the mean ± SEM in triplicate from one representative experiment of three separate experiments. (D) Graph showing raw luminescence values of spheroids formed from 22Rv1 clones expressing WT IGF-1R and IGF-1R null clones at day 9, relative to spheroid luminescence value at day 1. Each column represents the mean ± SEM in triplicate from one representative experiment of three separate experiments.

In summary, while loss of IGF-1R had enhanced radiation sensitivity in 2D assays in 22Rv1 cells, consistent with previous reports from our lab and others in other cell lines (Chitnis et al., 2014; Iwasa et al., 2009; Macaulay et al., 2001; Turney et al., 2012), there was no apparent increase in radio-sensitivity in 3D. The reasons for this discrepancy were unclear, potentially due to compensation by signalling pathways activated in 3D vs 2D. Since radio-sensitivity was detected in conventional 2D clonogenic survival assays, and other assays to examine the underpinning mechanism used cultures growing in 2D, the decision was made to continue investigating the role of IGF-1R in radio-sensitivity in 2D, and reasons for this decision are discussed below.

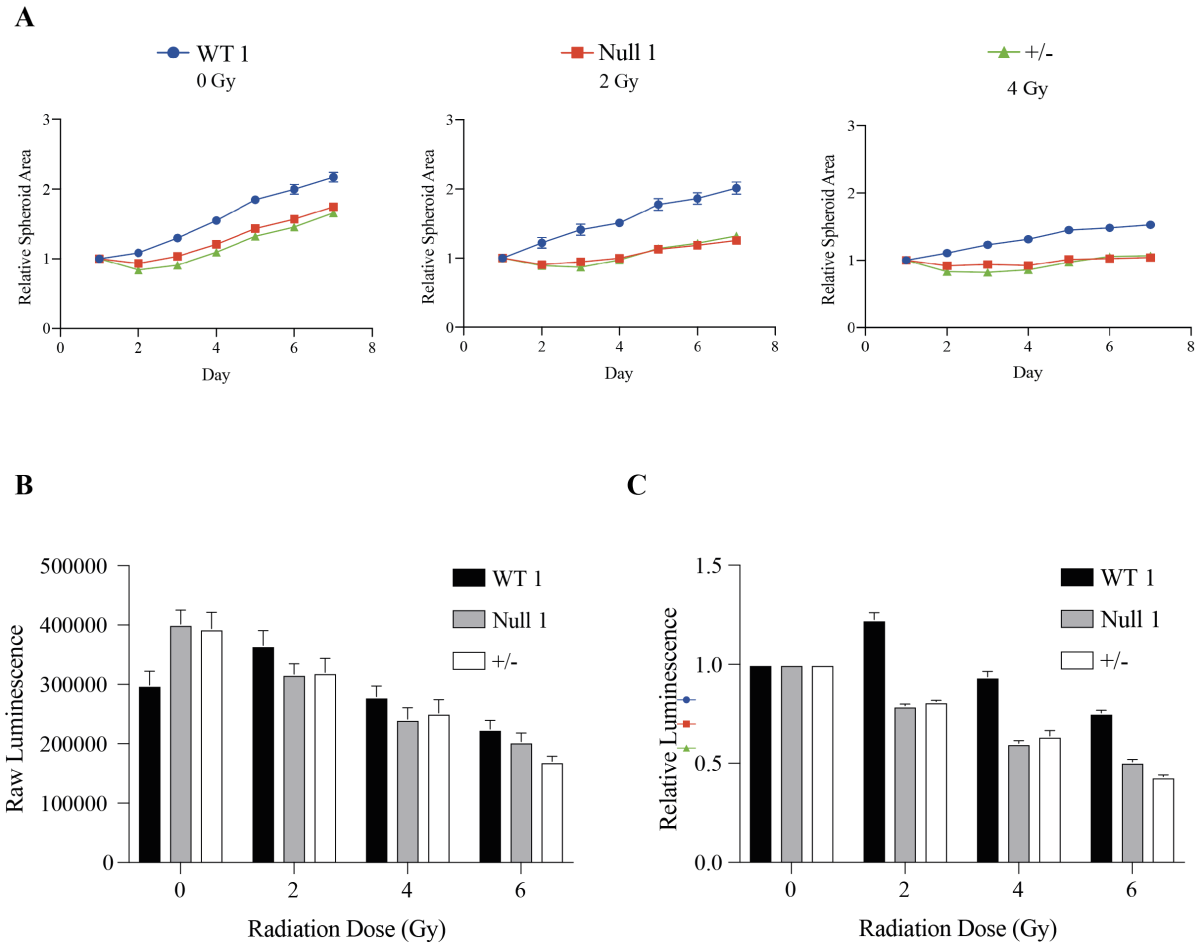

Figure 4.10: Examining radio-sensitivity of the hypomorphic mutant clone in a 3D spheroid model. A clone expressing WT IGF-1R, an IGF-1R null clone and the hypomorphic mutant clone were seeded in low-adherence 96 well plates (5 x 10^3 cells/well) and after 48 hr, cells were irradiated at indicated doses. (A) Individual wells were imaged for 7 days using GELCOUNT software and spheroid area measured using ImageJ. Relative spheroid area was calculated relative to spheroid area at day 1. Each point represents the mean ± SEM for sextuplicate values in one experiment representative of three separate experiments. On day 7, the CellTiter-Glo 3D viability assay was carried out as in Fig. 4.8 and 4.9. (B) Graph showing raw luminescence values of spheroids formed from a 22Rv1 clone expressing WT IGF-1R, an IGF-1R null clone and the hypomorphic mutant clone at day 7. Each column represents the mean ± SEM in triplicate from one representative experiment of three separate experiments. (C) Graph showing raw luminescence values of spheroids formed from a 22Rv1 clone expressing WT IGF-1R, an IGF-1R null clone and the hypomorphic mutant clone at day 7, relative to spheroid luminescence value at day 1. Each column represents the mean ± SEM in triplicate from one representative experiment of three separate experiments.

4.5 Investigating the cellular response to IR

To further investigate the role of IGF-1R kinase activity in radiation sensitivity, lysates were collected at time intervals after irradiation up to 8 hours. This allowed for the monitoring of the cellular response to irradiation, aiming to identify pathway(s) responsible for the radio-sensitive phenotype.

4.5.1 DNA damage markers

Phosphorylation of the DNA damage markers phospho-CHK2 (threonine 68) and KRAB-associated protein 1 (KAP1) (serine 824) were examined by Western blot analyses. CHK2 is a serine/threonine kinase phosphorylated at threonine 68 by ATM in response to DNA damage. This phosphorylation leads to dimerization and activation of CHK2, and subsequent induction of apoptosis, cell cycle checkpoints or DNA repair (Zannini et al., 2014). ATM also phosphorylates KAP1 at serine 824 in response to DNA damage, which improves DNA accessibility for repair proteins (Jang et al., 2018). Alterations in the phosphorylation patterns of these two key DDR proteins may suggest a defect in the DNA damage response. While there were no obvious changes in phosphorylation pattern over the 8 hour period for either protein, when normalised to the relative tubulin signal, phospho-CHK2 seemed higher in the hypomorphic mutant clone but investigation of phospho-KAP1 signal suggested possible heightened phosphorylation in the null clone, albeit over a shorter time frame (Fig. 4.11A, B). This single experiment did not show any substantial differences, and it would have been informative to both use multiple clones and assess timepoints earlier than 10 minutes. Unfortunately, radiator space, the time required to shut down the irradiator, ensure door was securely locked, and transfer the irradiated plates from the irradiator back to the bench meant this was not possible.

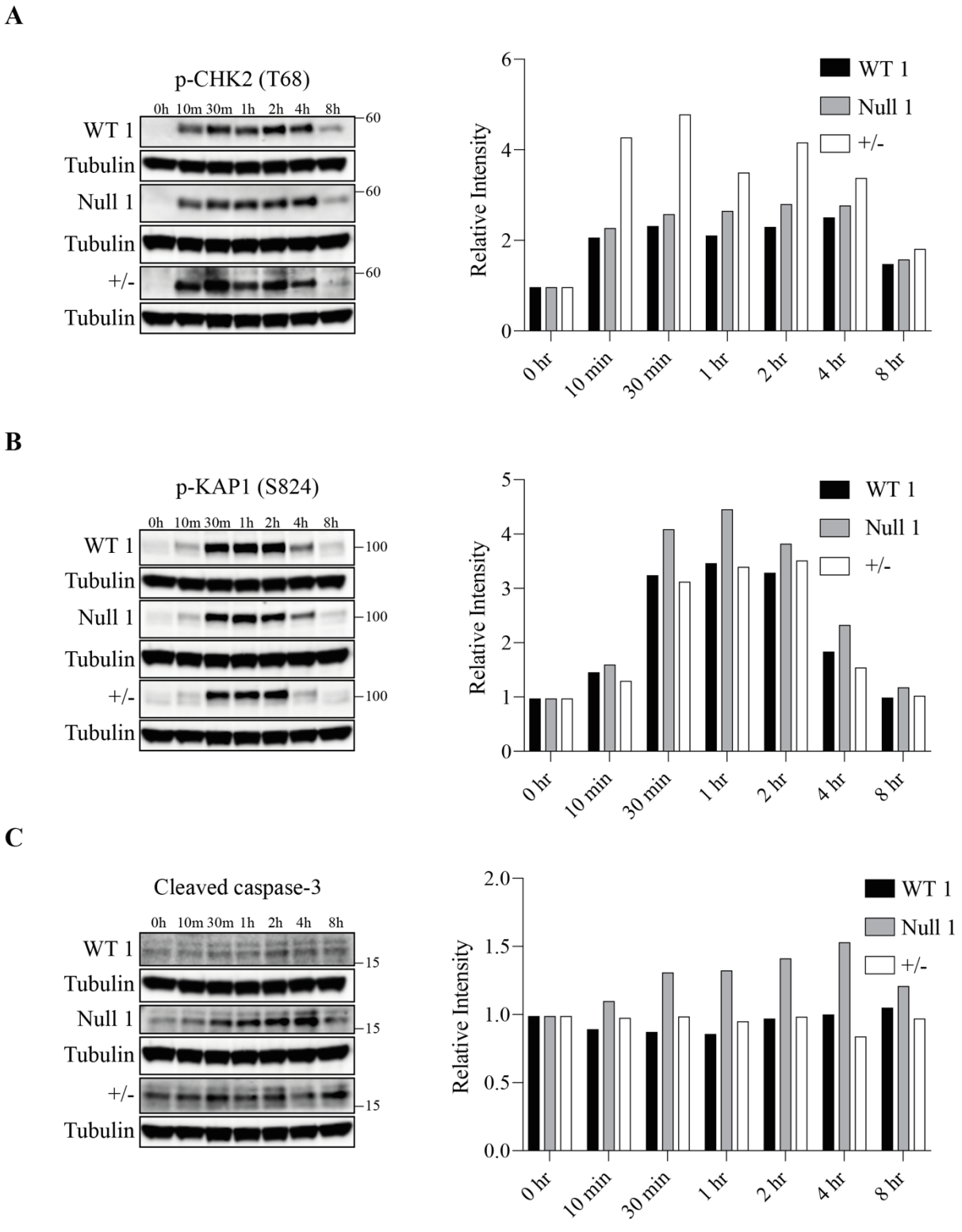

Figure 4.11: Examination of classical markers of DNA damage and apoptosis after irradiation.
A clone expressing WT IGF-1R, an IGF-1R null clone and the hypomorphic mutant clone were seeded in 6 well plates (3 x 10^5 cells/well) and the following day, subjected to 2 Gy irradiation. Whole cell lysates were analysed by Western blot for (A) phospho-T68-CHK2, (B) phospho-S824-KAP1 and (C) cleaved caspase-3, with β-tubulin as a loading control. Band intensities were quantified using ImageJ software and calculated for each clone relative to the intensity pre-IR.

4.5.2 Apoptosis

Another possibility for the observed radio-sensitisation is an anti-survival/pro-apoptotic response. In response to pro-apoptotic signals, caspase-3 is cleaved into its active state, where it is able to degrade a multitude of cellular proteins (Porter and Jänicke, 1999). Levels of the apoptosis indicator cleaved caspase-3 were examined and the results suggested that the IGF-1R null clone exhibited increased apoptotic activity in response to irradiation, while the hypomorphic mutant clone and the IGF-1R WT clone behaved similarly (Fig. 4.11C). It must be noted that sensitivity of the cleaved caspase-3 antibody, and Western blot quality are likely to affect band intensity comparisons, and if time had permitted, this experiment would have been repeated.

4.5.3 DNA damage foci

To examine if increased radio-sensitisation correlated with greater DNA damage, and whether a defective repair pathway might be causal, a clone expressing WT IGF-1R and an IGF-1R null clone were plated on coverslips and subjected to 2 Gy IR. Cells were fixed at specific intervals post-IR, and IF was performed, using a standard method for assessment of global DNA damage by monitoring both quantity and resolution of foci formed by γH2AX (Tanaka et al., 2007).

The time intervals chosen to compare γH2AX foci were pre-IR, 1 hour- and 24 hours-post IR. These time points were decided based on prior γH2AX experiments in DU145 cells in the lab (Chitnis et al., 2014), examination of p-CHK2 (threonine 68) and p-KAP1 (serine 824) signals from Western blot analyses in 22Rv1 cells (Fig. 4.11A, B), and investigation of the literature (Lehmann et al., 2007). These sources indicated that 22Rv1 cells exhibit maximal γH2AX foci between 30 minutes and 1 hour post-IR and so, to explore the extent of DNA damage induced

by IR and also repair pathway dynamics, this time point was selected. It has been reported that by 24 hours post-IR, γH2AX foci in 22Rv1 cells are typically resolved (Lehmann et al., 2007) and that if foci persist, it would suggest defective HR repair (Barbieri et al., 2019; Mariotti et al., 2013).

Examination of γH2AX foci at 0 hr (pre-IR) indicated minimal foci in both clones (Fig. 4.12A, column 1). Comparison of clones fixed 10 minutes after IR indicated a greater number of γH2AX foci in the IGF-1R null clone compared to the clone expressing WT IGF-1R (Fig. 4.12A, column 2). Foci numbers were greater in the IGF-1R null cells compared to cells expressing WT IGF-1R at 1 hour post-IR (Fig. 4.12A, column 3), and 24 hours after irradiation, γH2AX foci were largely resolved in all clones (Fig. 4.12A, column 4).

Quantification of foci numbers confirmed these visual differences. At 10 minutes and 1 hour after IR, IGF-1R null cells displayed significantly higher numbers of γH2AX foci compared to IGF-1R WT cells. By 24 hours, there was no significant difference in γH2AX foci number signifying a similar resolution of foci across both clones by this time point (Fig. 4.12B).

A

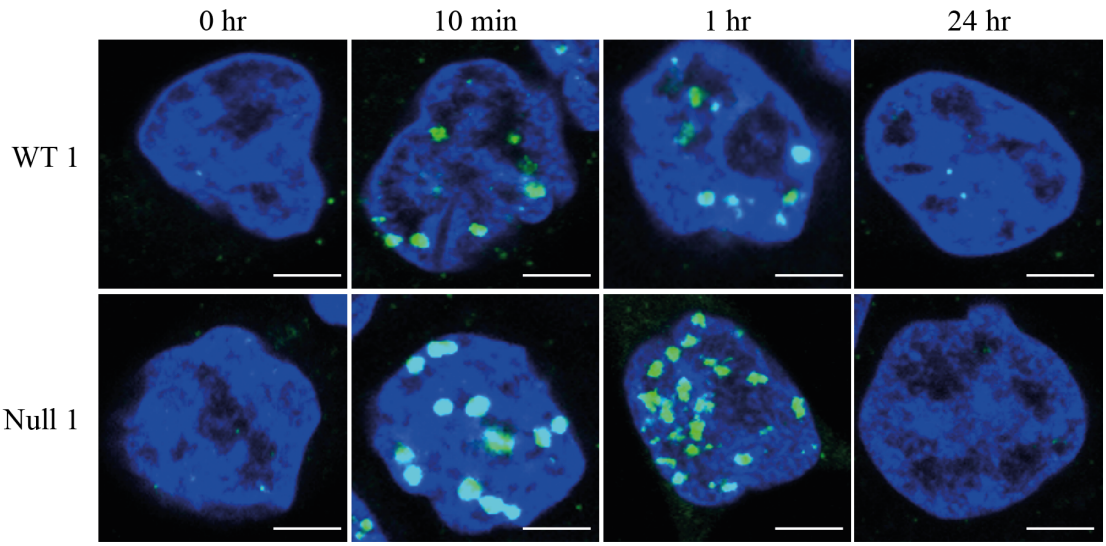
0 hr
10 min
1 hr
24 hr
WT 1
Null 1

B

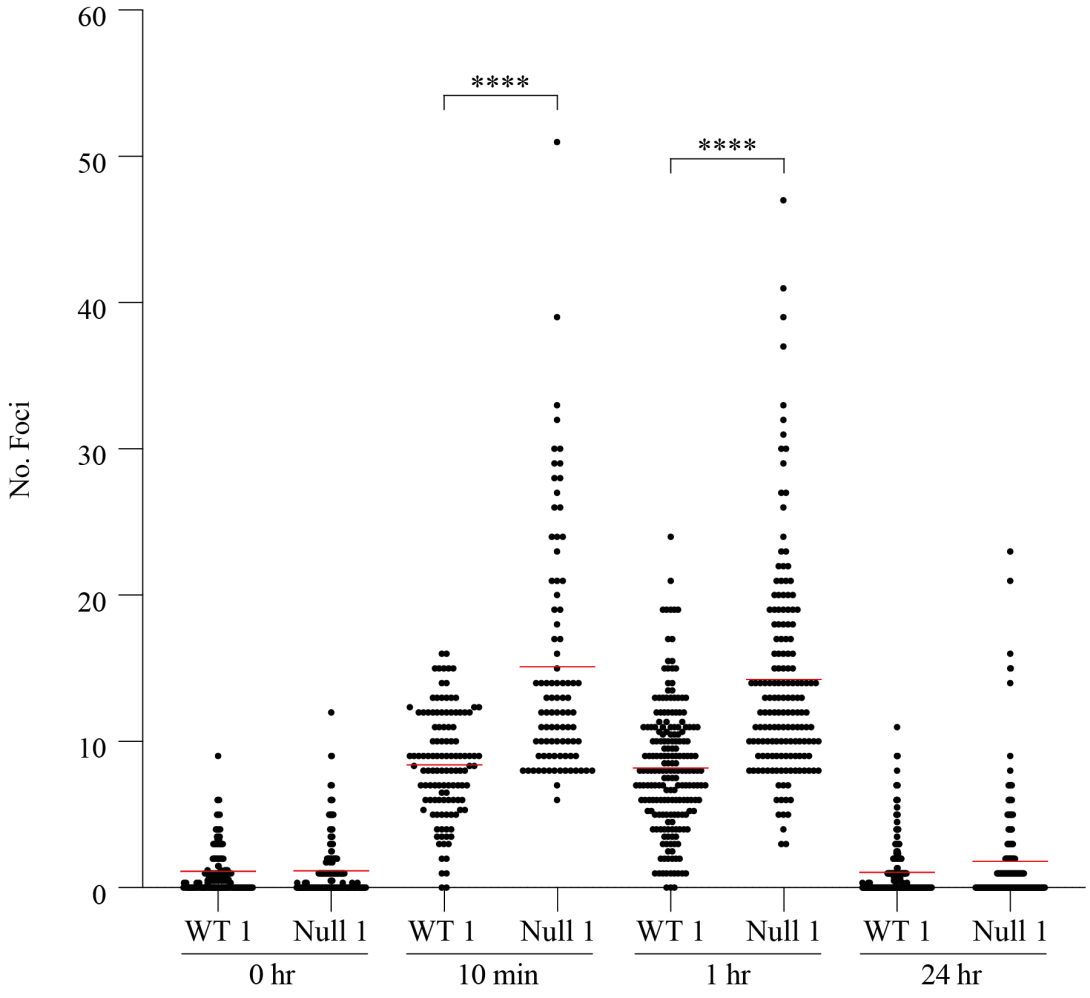
No. Foci
60
50
40
30
20
10
0
****
****
WT 1
Null 1
WT 1
Null 1
WT 1
Null 1
WT 1
Null 1
0 hr
10 min
1 hr
24 hr

Figure 4.12: Loss of IGF-1R results in increased γH2AX foci after 2 Gy irradiation.
A clone expressing WT IGF-1R and an IGF-1R null clone were seeded on coverslips in triplicate in 6 well plates (1 x 10^5 cells/well) and the following day required wells were subjected to 2 Gy irradiation. (A) At time points up to 24 hr, cells were fixed and stained for γH2AX. Images show merged nuclear DAPI (blue) and γH2AX (green) staining in unirradiated cells (0 hr) and cells at 10 mins, 1 hr and 24 hr post-IR. Images were taken at 63x magnification, scale bar represents 10 μm. (B) Quantification of γH2AX foci pooled from three independent experimental repeats. Foci were counted using ImageJ software in 9 separate fields and the graph shows the number of foci in each cell counted. Red line indicates mean number of γH2AX foci/cell. A one-way ANOVA was used to determine the significance of differences between clones at each timepoint (****$p<0.0001$).

Timing of γH2AX foci resolution serves as an indication of major DNA repair pathway defects with peak foci numbers observed at 30 mins post-IR, dependent on cell line (Mah et al., 2010; Marková et al., 2007). The majority of γH2AX foci resolution occurs by cNHEJ within 4 hours of DSB induction, while slower foci resolution (~24 hr) is indicative of repair by HR (Löbrich 2017). These data suggested an increased induction of DNA damage and a possible defect in cNHEJ in IGF-1R null cells compared to clones expressing WT IGF-1R, after 2 Gy irradiation.

4.6 Discussion

The newly generated IGF-1R null clones were subjected to increasing doses of IR in parallel with IGF-1R depleted cells, and examined using 2D clonogenic assays (Fig. 4.1). Radio-sensitisation of IGF-1R null clones was similar to cells transfected with IGF-1R siRNA (Fig. 4.1). Western blot analyses of IGF-1R null clones indicated variations in signalling downstream of IGF-1R in the IGF-1R/AKT/mTOR axis, specifically targets of mTOR (Fig. 4.2-3). This suggested that the increased radio-sensitivity of IGF-1R null clones might not be due to changes in mTOR signalling, in contrast to reports in other model systems (Choi et al., 2020; Ushijima et al., 2015; Wanigasooriya et al., 2020). Further, examination of ligand responses by phospho-receptor ELISA (Fig. 4.4A, B) suggested a similar reduction in IGF-induced receptor phosphorylation in the IGF-1R null clone and the hypomorphic mutant clone, akin to Western blot analysis using the phospho-tyrosine 1316-IGF-1R antibody (Fig. 3.9C). However the ligand response ELISAs were carried out prior to obtaining this antibody, and the phospho-tyrosine 1135/36 IGF-1R antibody that was used in this assay is also capable of detecting INSR phosphorylation. Therefore, ELISAs would need to be repeated with the phospho-tyrosine 1316-IGF-1R antibody to draw specific conclusions about IGF-1R vs INSR responses to IGF-1 and insulin in the IGF-1R hypomorphic and null clones.

Due to a lack of specificity of all IGF-1R antibodies tested in 22Rv1 cells here and by previous lab members in IF experiments (Fig. 4.5), localisation of IGF-1R expressed by the hypomorphic mutant clone had to be attempted using a different method. By selectively isolating membrane proteins and nuclear protein fractions from clones expressing WT IGF-1R and the hypomorphic mutant clone, as well as IGF-1R null cells, localisation of the receptor was investigated. IGF-1R was detected in the membrane in the hypomorphic mutant clone, and

further, localised to the nucleus upon IGF-1 stimulation (Fig. 4.6). While kinase activity seemed to be reduced in the hypomorphic mutant (Fig. 3.9), the nuclear translocation displayed in figure 4.6 was not consistent with previous work by the Macaulay group and others (Aleksic et al., 2010; Sehat et al., 2010), who reported that IGF-1R kinase activity is essential for receptor translocation to the nucleus. This result suggested kinase activity still remained in the hypomorphic mutant. It would be informative to perform further studies to quantify IGF-1R kinase activity in the hypomorphic mutant clone and compare with WT IGF-1R kinase activity. This could be achieved by utilising an ADP-Glo Kinase Assay (Promega, PRV9401) to measure the activity of the receptor in phosphorylating a peptide derived from human IRS-1 residues 891-902. This substrate contains the motif EYVNIE that when tyrosine phosphorylated creates a binding site for GRB2 (White, 2002).

The radio-sensitisation phenotype of the hypomorphic mutant clone was comparable to that of the IGF-1R null clone in 2D clonogenic assays (Fig. 4.7). This suggested that there was a change in this clone that was responsible for the increased radio-sensitivity. This correlated with previous work by the Macaulay group and others, showing cells depleted of IGF-1R and cells treated with IGF-1R inhibitors displayed increased radio-sensitisation (Aleksic et al., 2017; Chitnis et al., 2014; Turney et al., 2012; Zhao and Gu, 2014c).

Attempts to measure radio-sensitivity using a 3D method more representative of an *in vivo* setting did not show changes that paralleled results of 2D radiation survival assays. Reductions in spheroid area of cells depleted of IGF-1R, *IGF1R* +/- and -/- cells over time compared to clones expressing WT IGF-1R were shown, however these were independent of irradiation (Fig. 4.8-10). This suggested that in 3D, the presence of IGF-1R might lead to protection from

apoptosis, which is reported not to be a major influence on 2D radio-sensitivity (Tezuka et al., 2001). Indeed, previous work from our lab in prostate and GBM models reported that radio-sensitisation caused by IGF-1R inhibition was not accompanied by evidence of apoptosis induction (Chitnis et al., 2014; Simpson et al., 2020). Further, comparison of responses to xentuzumab in 2D vs 3D, while in a different cell type (colorectal cancer), showed increased phosphorylation of a product detected at ~95 kDa, below that of phopsho-IGF-1R signal, upon xentuzumab treatment in 3D, whereas this was absent in 2D (Xiaoning Wu et al., 2021). This finding suggested possible compensatory INSR signalling in 3D. Differential processing of IGF-1R has been reported in 2D vs 3D (Han et al., 2020) together with altered signalling via AKT-mTOR (Riedl et al., 2017) which may have impacted the response to IR in results displayed here. Additionally, due to specifics of the experimental methods, the duration of the 2D and 3D assays are dissimilar, which could also influence the difference in outcomes observed.

It has been well-established that cells display different characteristics in specific regions of the spheroid, which are in part due to gradients of oxygen and nutrient availability (Beaumont et al., 2013; Langan et al., 2016; Mehta et al., 2012; Riffle et al., 2017). Indeed, there are reports of heterogeneity in cell proliferation, metabolic activity and DDR signalling (Bloch et al., 2014; Favaro et al., 2012; Kunz-Schughart et al., 1996; LaRue et al., 2004; Pacheco-Marín et al., 2016). In particular, the oxygen gradient within a spheroid generates a hypoxic core, which has been shown to activate survival pathways and induce resistance to IR (Langan et al., 2016; Leek et al., 2005; Patiar and Harris, 2006; Riffle et al., 2017). Radio-resistance occurs because DNA damage requires oxygen to react with free radicals produced during IR (Gray et al., 1953; Hatfield et al., 2015). Of relevance to the current work, a study investigating post-IR survival in murine breast cancer cells showed that the DNA-PK_{cs} inhibitor NU7441 radio-sensitised

cells cultured in 2D at 4 Gy. In contrast, spheroids and cells treated as spheroids before being plated as monolayers displayed no increase in radio-sensitivity, although did show growth delay at 4 Gy (Yu et al., 2020). These findings are comparable to the differential response to radiation in 2D and 3D observed here in response to IGF-1R depletion or deletion (Fig. 4.8-4.10), and suggest the need for caution in extrapolating results of 2D radio-sensitivity assays to the clinic (Leek et al., 2016). After giving due consideration to these concerns, it was decided to continue with assays based on 2D cultures for the following reasons. From a practical standpoint, quantification of radiation-induced foci requires imaging of 2D adherent cultures. Furthermore, the amount of soluble protein that can be extracted from small spheroids is sufficient to perform only very limited analysis by Western blot, as was found in recent work from our lab (X Wu et al., 2021). Finally, 2D radiation survival assays remain the 'gold standard' approach to assess radio-sensitivity, and data from these studies, including quantification of DERs, have been found to be relevant in identifying potentially useful clinical radio-sensitisers (Harrington et al., 2011). Work shown here indicated DERs which could be indicative of useful effect (DER>1.2-1.5) in cells where IGF-1R kinase activity was depleted or absent (Fig. 4.1E, 4.7C), suggesting a role for IGF-1R in radio-resistance.

As discussed above, differences in the hypoxic fraction could contribute to differences in radio-sensitisation observed in 2D and 3D cultures (Fig. 4.1, 4.7, 4.8-10). Hypoxia-induced stabilisation of the transcription factor hypoxia-inducible factor (HIF) 1 subunit alpha (HIF-1α) drives upregulation of genes required for the cellular adaptation to hypoxia (Choudhry and Harris, 2018; Kallio et al., 1997; Ratcliffe, 2013). Hypoxia has been reported to downregulate the HR proteins BRCA1 (Bindra et al., 2005), RAD51 (Bindra et al., 2004; Bindra and Glazer, 2007) and the DNA mismatch repair proteins MLH1 and PMS2 (Collins et al., 2011). In contrast, hypoxia is reported to activate DNA damage-independent ATM and ATR signalling,

although this effect is principally relevant to protection from hypoxia-induced dNTP depletion replication stress (Bristow and Hill, 2008; Ng et al., 2018).

It has been demonstrated that hypoxia signalling and IGF signalling have a reciprocal relationship, with HIF-1α promoting the expression of genes encoding IGFBP-2, IGFBP-3 and IGF-2, and IGFs inducing HIF-1α expression (Feldser et al., 1999; Leek et al., 2005). Hypoxia has been reported to augment IGF-1 and IGF-1R expression in the heart and lungs of rats (Eliasz et al., 2010; Moromisato et al., 1996) and IGF-2 has been identified as an important HIF-1α target gene that promotes cell survival (Feldser et al., 1999). IGF-1 has been shown to induce HIF-1α expression in human colorectal cancer cells (Fukuda et al., 2002) and further, work has shown that IGF-1R signalling is able to protect cells from oxidative stress and hypoxia (Eliasz et al., 2010), and that IGFs can stabilise HIFs, and upregulate VEGF, thus increasing cell survival in response to low oxygen conditions (Treins et al., 2005).

A possible explanation for the absence of radio-sensitisation in IGF-1R null spheroids (Fig. 4.9) could be that there was a reduction in IGF-induced survival signalling, increasing the volume of the hypoxic core of the spheroids, thereby increasing radio-resistance. This theory could be tested by performing immunohistochemistry (IHC) to look at carbonic anhydrase 9 (CA9), HIF-1α or pimonidazole levels (Durand and Raleigh, 1998; Kang et al., 2015; Snell et al., 2014; Tailor et al., 2010; Talks et al., 2000), or monitoring the activity of CA9 using confocal microscopy to assess pH changes (Leek et al., 2016; Swietach et al., 2009). In addition, hypoxia-induced expression of IGF-2 would activate the variant INSR (INSR-A) (Sciacca et al., 2003, 1999), which could compensate for the lack of IGF-1R in the null

spheroids (Forest et al., 2015; Frasca et al., 1999). These factors could contribute to masking of the effect of IGF-1R loss on the response to IR.

Changes to the phosphorylation of the DNA damage markers CHK2 and KAP1 were not observed between clones, however comparison of the apoptotic response to IR of cells expressing WT IGF-1R, no IGF-1R or the hypomorphic mutant clone indicated increased apoptotic activity in cells lacking IGF-1R, which is a predictable effect of loss of IGF-1R signalling (Fig. 4.11) (Baserga et al., 1997; Larsson et al., 2005; Zhao et al., 2004). To confirm these findings it may be informative in future to assess the radiation response of other markers such as phosphorylation of H2AX, ATM or p53 (Huang and Zhou, 2020; Tichý et al., 2009; Yoshida et al., 2003). Further investigation by Western blot using additional time points up to 72 hours post-IR and probing for additional apoptotic markers such as cleaved caspase 7 or cleaved caspase 9 would be beneficial. Previous work in the Macaulay group indicated that the observed radio-sensitivity of IGF-1R depleted/inhibited DU145 cells was not accompanied by an increase in short-term (24-48 hours) apoptosis (Chitnis et al., 2014). This suggested that radio-sensitivity was not simply due to reduced cell survival. However, DU145 cells harbour non-functional *TP53* and 22Rv1 cells express WT *TP53* which could explain differences between cell lines (Chappell et al., 2012; Fraser et al., 2012). Additional assays to investigate apoptosis such as flow cytometry for annexin V/PI or a microplate assay to measure caspase activity could provide more insight as to whether the apoptotic response is impacted by loss of IGF-1R.

Examination of γH2AX foci indicated that there was a significant increase in foci by 10 minutes post-IR in IGF-1R null cells compared to cells expressing WT IGF-1R (Fig. 4.12). This

indicated a greater accumulation of damage initially after IR when IGF-1R was deleted. The disparity in γH2AX foci numbers between clones expressing functional and non-functional IGF-1R became larger at 1 hour post-IR, consistent with findings that foci numbers are highest at 30 minutes post-IR (Fig. 4.12) (Kühne et al., 2004; Mariotti et al., 2013). These findings are somewhat consistent with previous data generated in the lab, as defects in cNHEJ and HR were reported using DNA repair reporter assays in HEK293 reporter cells where IGF-1R was inhibited (Chitnis et al., 2014). Chitnis *et al.* did not detect differences in the amount of damage incurred within the first hour post-IR upon IGF-1R inhibition, however differences emerged within 4 hours, with an excess of unrepaired breaks at 24 hours in DU145 cells (Chitnis et al., 2014). In pHGG cells, IGF-1R treatment with BMS754807, the IGF-1R small molecule inhibitor, resulted in more γH2AX foci basally and at 2 hours post-IR (Simpson et al., 2020). These data suggest that the radio-sensitisation effect of IGF-1R compromised cells varies with cell line. This could be due to differences in genotype between cell lines, which affect cell cycle proteins or DNA repair proteins, such as DU145 cells expressing mutant *TP53*, which is likely to affect cell cycle distribution and access to sister chromatids to use in HR (Chappell et al., 2012; Fraser et al., 2012). Additionally, a report has shown that repair kinetics differ between prostate cancer cell lines, with 22Rv1 cells displaying almost complete resolution of γH2AX foci after 24 hours, similar to data presented here (Gilbreath et al., 2021). Further, approaches used by previous lab members used transient methods to manipulate IGF-1R by inhibitors and siRNA, whereas here IGF-1R was stably knocked out by gene editing. The outcomes of IGF axis blockade are likely to be affected by differences in potency, off-target effects and speed of onset/duration of inhibition, contributing to the discrepancy between data shown here and by previous lab members.

Additionally, γH2AX focus size was increased in IGF-1R null cells compared to cells expressing WT IGF-1R at 10 minutes and 1 hour post-IR (Fig. 4.12). Focus size is reported to be cell cycle phase-dependent, with smaller foci in G1 and larger foci in mitotic cells or cells treated with chromatin modifying agents post-IR (Löbrich et al., 2010; Reitsema et al., 2004)

Altogether, these data provide further evidence that IGF-1R kinase activity may be responsible for mediating radio-resistance (Fig. 4.1, 4.7). Additionally, work suggested that lack of IGF-1R may cause induction of more damage due to differences in γH2AX foci number at 10 minutes post-IR (Fig. 4.12), but not defects in repair. A greater effect of IGF-1R inhibition on cNHEJ than HR was reported by the Macaulay group previously using HEK293T DNA repair reporter assays (Chitnis et al., 2014). An increase in damage foci was not observed at 30 mins in IGF-1R compromised cells, however earlier timepoints were not tested (Chitnis et al., 2014). One could speculate that stable loss of kinase activity as opposed to the acute effect of IGF-1R depletion or inhibition may lead to an increased propensity for DNA damage or impact the cellular response to DNA damage.

Alterations to signalling pathways, as a direct result of IGF-1R inactivity or through compensatory mechanisms, could have major effects on factors that influence chromatin accessibility, as shown by Sassone-Corsi *et al.* in cells in which EGF signalling was disrupted, or expression/activation of DNA repair proteins, as demonstrated by Estrada-Bernal *et al.* by MEK1/2 inhibition (Estrada-Bernal et al., 2015; Sassone-Corsi et al., 1999). It was still unclear which signalling pathways and/or cellular processes mediate the radio-protective effect of functional IGF-1R. Work focussed on unbiased proteomic and phosphoproteomic screens to investigate candidate pathways that link IGF-1R to the DDR.

CHAPTER V: Investigating the role of IGF-1R signalling in response to IR

5.1 Introduction

Following irradiation, IGF-1R compromised 22Rv1 cells exhibited increased DNA damage and reduced survival in 2D assays (Fig. 4.1, 4.7). The enhanced radio-sensitivity was consistent with previous data in the lab in IGF-1R depleted AR-negative DU145 prostate cancer cells and HEK293T reporter cells (Fig. 3.1) (Chitnis et al., 2014; Turney et al., 2012), suggesting that IGF-1R may have a role in the cellular response to IR. The pattern of γH2AX foci after IR shown here was different to previous data, suggesting that more damage was induced in experiments using 22Rv1 cells (Fig. 4.12), rather than the delayed repair reported by a past lab member (Chitnis et al., 2014). Elucidating the causal mechanism for this increased DNA damage and reduced survival is challenging.

Direct inactivating mutations of DDR proteins, dysregulation of cell cycle checkpoints, altered thresholds for apoptosis and changes to chromatin conformation can all impact the cellular response to irradiation (Falk et al., 2008; Goi et al., 1997; Menoyo et al., 2001; Painter, 1982; Smith and Seo, 2002; Strasser-Wozak et al., 1998). Further, the complexity of downstream IGF-1R signalling coupled with the multitude of potential reasons for the observed radio-sensitisation phenotype, suggested that an unbiased strategy may have merit. Proteomic and phosphoproteomic approaches were pursued, aiming to uncover both clues to the role of IGF-1R in radio-sensitisation and additionally, to provide a dataset to investigate the influence of IGF-1R kinase activity on normal cellular function using the unirradiated samples.

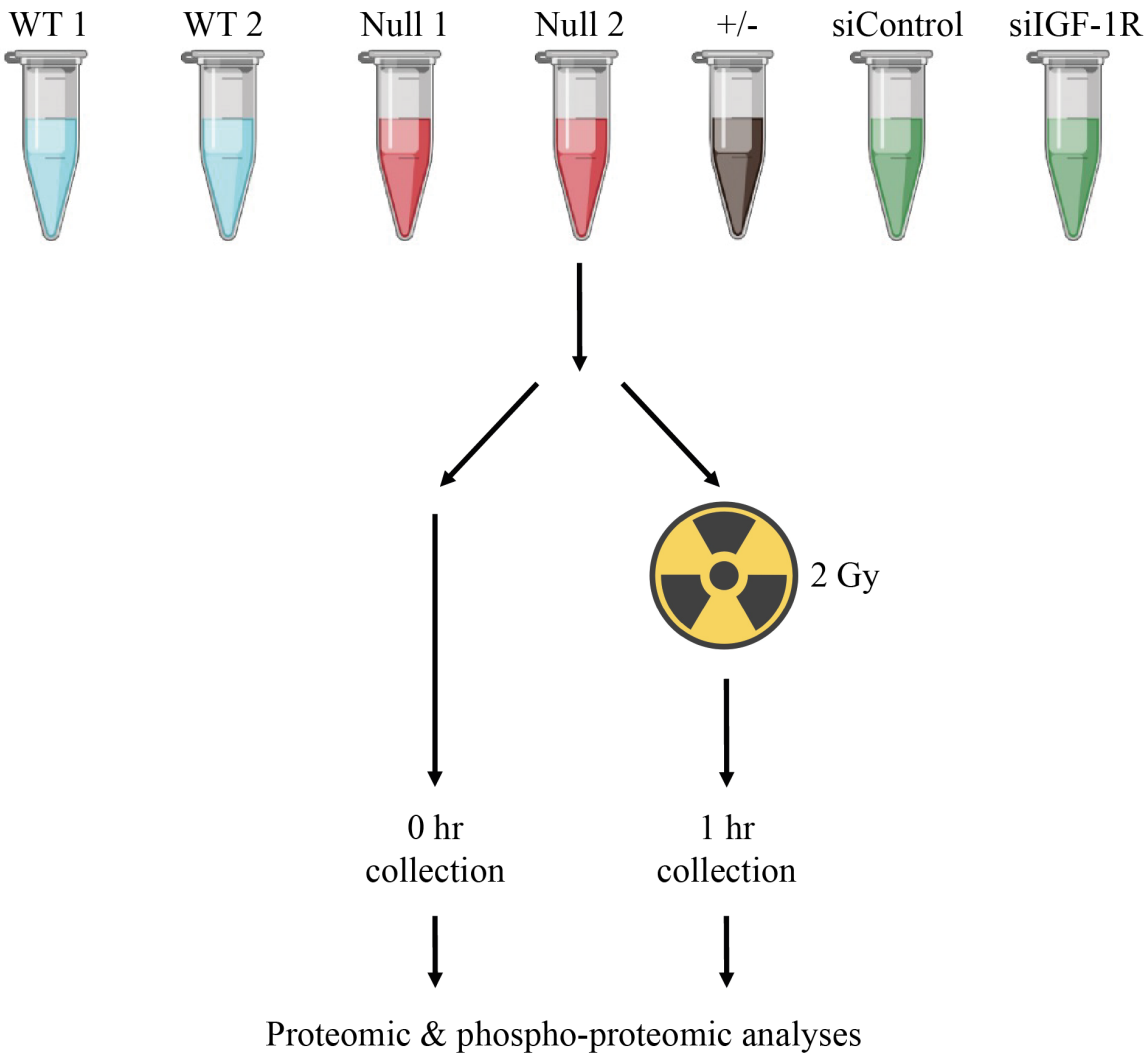

Figure 5.1: Overview of proteomics and phosphoproteomics screen method.
Diagram of the screening method used to assess the role of IGF-1R signalling in radio-resistance.

5.2 Sample preparation

The response to DNA damage begins immediately after insult (Jackson and Bartek, 2009) and because of the temporary nature of protein phosphorylation (Ubersax and Ferrell Jr, 2007), timepoint selection for sample collection was critical. The response of IGF-1R WT, null and hypomorphic mutant clones to IR, using Western blot analyses of phospho-CHK2 (T68) and phospho-KAP1 (S824) as indicators, suggested full induction of a DDR at 30 minutes post-IR (Fig. 4.11). In γH2AX foci experiments, data showed differences between IGF-1R WT clones

and IGF-1R compromised cells at 10 mins and 1 hour post-IR (Fig. 4.12). This suggested that IGF-1R function was important at these timepoints. Given that the response to IR is triggered immediately after damage induction, it may have been informative to collect additional samples within a few minutes of irradiation. The 1 hour timepoint post-IR was chosen in light of the time taken to move irradiated cells back to bench for lysis, and the finding that the excess of γH2AX foci in IGF-1R null cells was comparable at 10 minutes and 1 hour (Fig. 4.12). However it must be acknowledged that at 1 hour some very early phosphorylation events may have resolved and were missed in the analysis. Although γH2AX phosphorylation is well-known to be an important early event required for recruitment of key DDR factors, it has been reported that some events occur before H2AX phosphorylation in mammalian cells. DNA breaks have been shown to induce rapid phosphorylation of heterochromatin protein 1β (HP1-β) by casein kinase 2 (CK2), leading to release of HP1-β from chromatin. This process enables relaxation of heterochromatin to allow access of the repair machinery (Ayoub et al., 2008; Podhorecka et al., 2010). The time required for cell harvesting and lysis made collection at the 10 min time-point impractical, so a decision was made to examine responses pre-IR and 1 hour post-IR. These time-points also complemented previous lab data showing maximum increase in γH2AX foci at 1 hour post-IR in IGF-1R inhibited DU145 prostate cancer cells compared with controls (Chitnis et al., 2014).

To examine the effect of acute and long-term loss of IGF-1R kinase activity on cellular radio-sensitivity, IGF-1R depleted cells, IGF-1R null clones and the hypomorphic mutant clone were used. Transfection of 22Rv1 cells with siControl or siIGF-1R was carried out 48 hours before, while WT clones and IGF-1R compromised cells were plated 16 hours prior to 2 Gy irradiation. This dose was chosen as it was shown to elicit a substantial DDR without causing significant cell death (Fig. 4.11). Lysates were collected pre-IR and 1 hour post-IR using RIPA buffer

supplemented with protease and phosphatase inhibitors. The experimental design outlined in figure 5.1 allowed for study of effects of loss of IGF-1R signalling in basal culture conditions without ligand, and also specifically in response to DNA damage.

Western blot analyses were carried out on the cell lysates to check for extent of IGF-1R knockdown in siIGF-1R cells and for evidence of a predictable response to IR in all cells (Fig. 5.2A). siControl cells seemed to display less IGF-1R than WT or kinase-dead clones, which had often been seen in the lab following siRNA transfection, however this was partly due to uneven sample loading. Nonetheless, siIGF-1R cells showed 62.7% IGF-1R knockdown upon quantification, relative to siControl cells (Fig. 5.2B). Phosphorylation of KAP1 (serine 824) was raised by an average of ~3-fold in all samples post-IR (Fig. 5.2C) and CHK2 phosphorylation (threonine 68) was increased by ~1.4-fold on average (Fig. 5.2D), indicating proper induction of DNA damage, with no apparent differences in IGF-1R compromised cells. No significant difference in phosphorylation of AKT at serine 473 was observed post-IR in IGF-1R compromised cells (Fig. 5.2E).

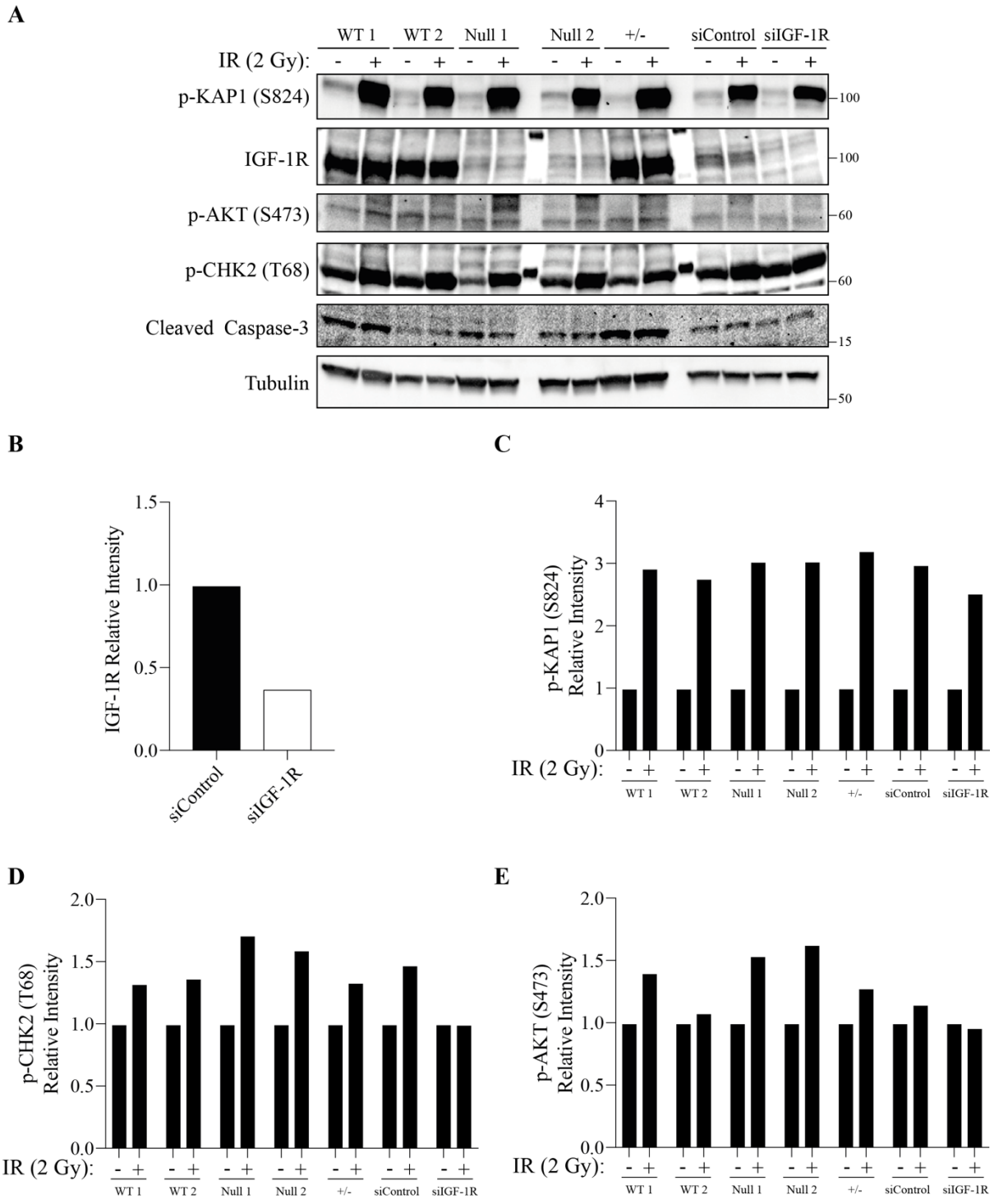

Figure 5.2: Analysis of samples for proteomic and phosphoproteomic screens.
Whole cell extracts of 22Rv1 cells including IGF-1R null clones, clones expressing WT IGF-1R, the hypomorphic mutant clone, and control or IGF-1R siRNA transfectants were irradiated (2 Gy, 1 hr) and prepared for proteomic and phospho-proteomic assessment as described in section 2.14. (A) Whole cell lysates were analysed by Western blot for (B) adequate IGF-1R knockdown, evidence of a predictable response to IR by (C) phospho-KAP1 (S824) and (D) phospho-CHK2 (T68) levels, and (E) AKT signalling by phospho-AKT (S473) levels, with β-tubulin as a loading control. Band intensities were quantified using ImageJ software and calculated for each clone relative to the intensity pre-IR.

5.3 Analysis of proteomic & phosphoproteomic data in WT and IGF-1R null clones

5.3.1 Proteomic Data

Proteomic analyses showed that the distribution of normalised protein abundance across IGF-1R WT and null clones was comparable (Fig. 5.3). In the planning stage of this experiment, there were sufficient funds for only one siControl and siIGF-1R replicate, and because of the complexity of the analysis, and that duplicate IGF-1R WT and null clones were included, it was decided to focus solely on comparison of IGF-1R WT and null clones. Hierarchical clustering indicating how the different experimental conditions cluster together based on normalised protein abundance showed broad similarity among all conditions (Pearson coefficient>0.8), with greater similarity between all unirradiated or all irradiated clones (Fig. 5.4A). Principal component analysis highlighted possible clustering of pre-IR samples and post-IR samples (Fig. 5.4B). From this point I interrogated the data by generating volcano plots, plotting statistical significance against fold change (Fig. 5.5), to study changes in total protein levels between clones. After examination of previous phosphoproteomic screens in the literature (An et al., 2019; Nasa et al., 2020; Zadora et al., 2019), thresholds for significance were set at protein abundance levels increased or reduced by 1.3 fold, with a $-\log_{10}$[p-value]>1.3 (representative of a p-value<0.05) for pathway analyses, and a $-\log_{10}$[p-value]>2 (p-value<0.01) for individual protein/phospho-sites.

Attempts were made to normalise each individual phospho-protein abundance value to the corresponding protein abundance value in the proteomic dataset. However, this was not possible, as not all phospho-proteins were detected in the proteomic samples. After taking advice from Professor Ian Mills and Dr Iolanda Vendrell, abundance values for each phospho-

protein were normalised to the average protein abundance value across all proteins in the same sample.

A

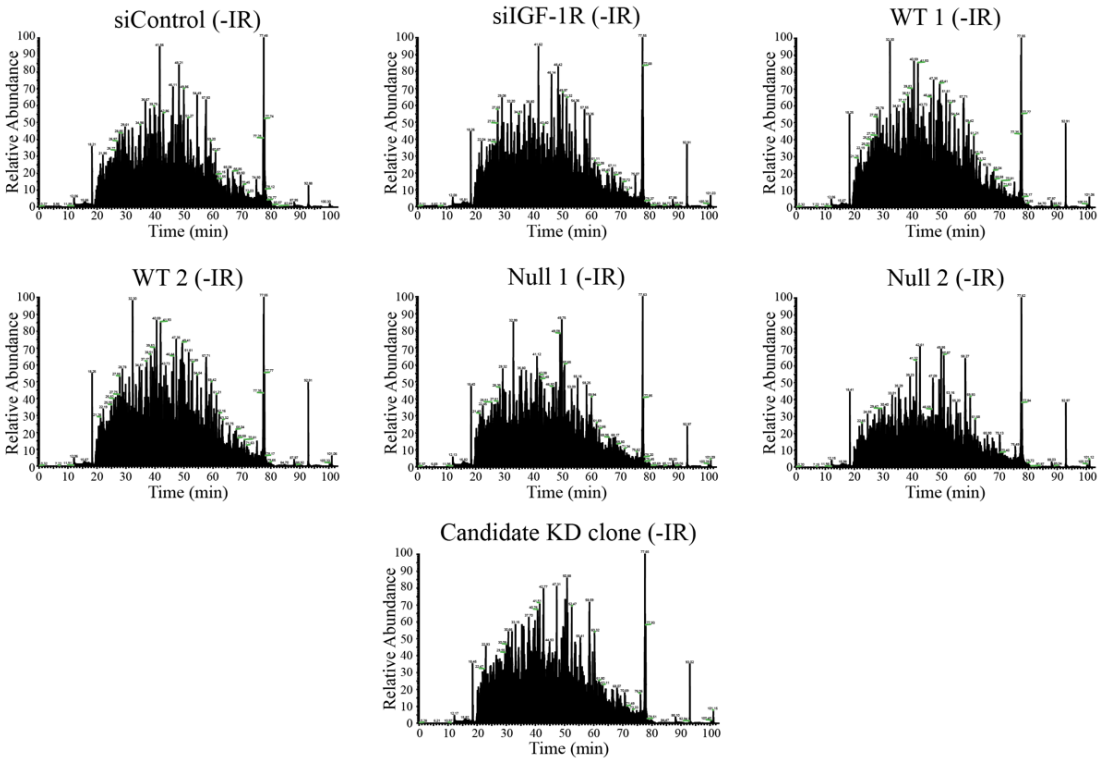

B

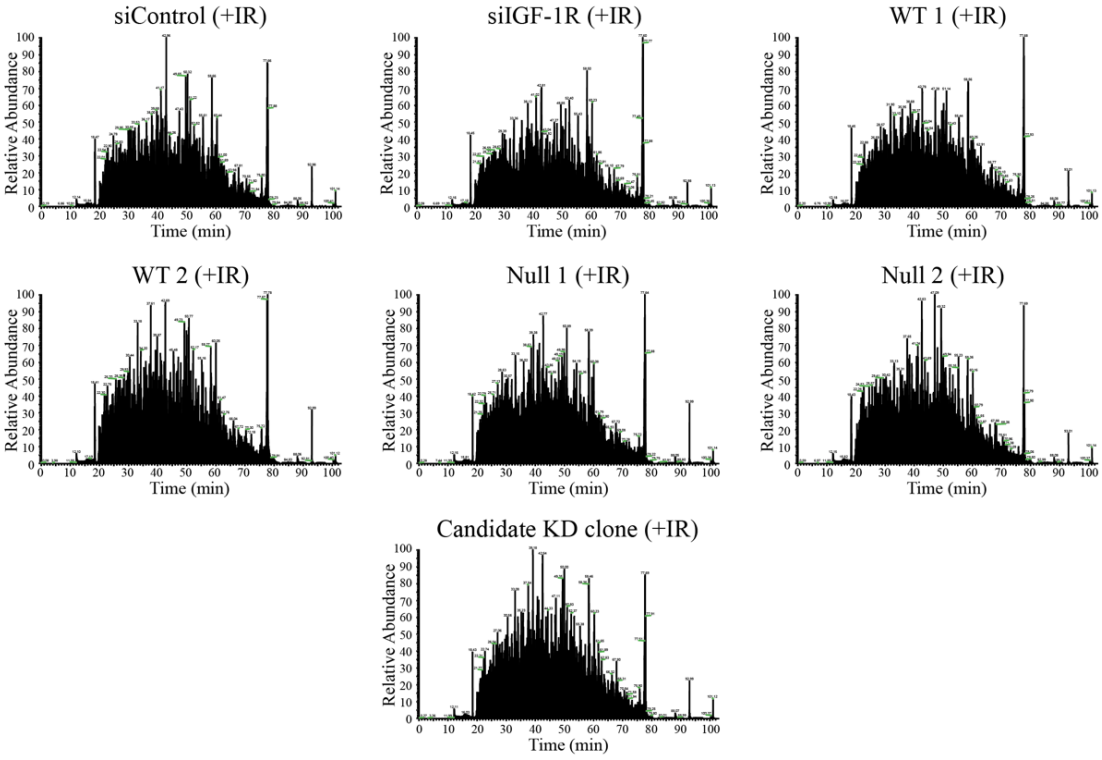

Figure 5.3: Quality control assessment of proteomic samples.
Data provided by Iolanda Vendrell detailing total ion chromatogram of 1 hour gradient LC_MSMS analysis of tryptic peptide mixtures of total cell lysates of clones expressing WT IGF-1R, IGF-1R null clones, a hypomorphic mutant clone, siControl and siIGF-1R transfected cells (A) pre-IR and (B) post-IR.

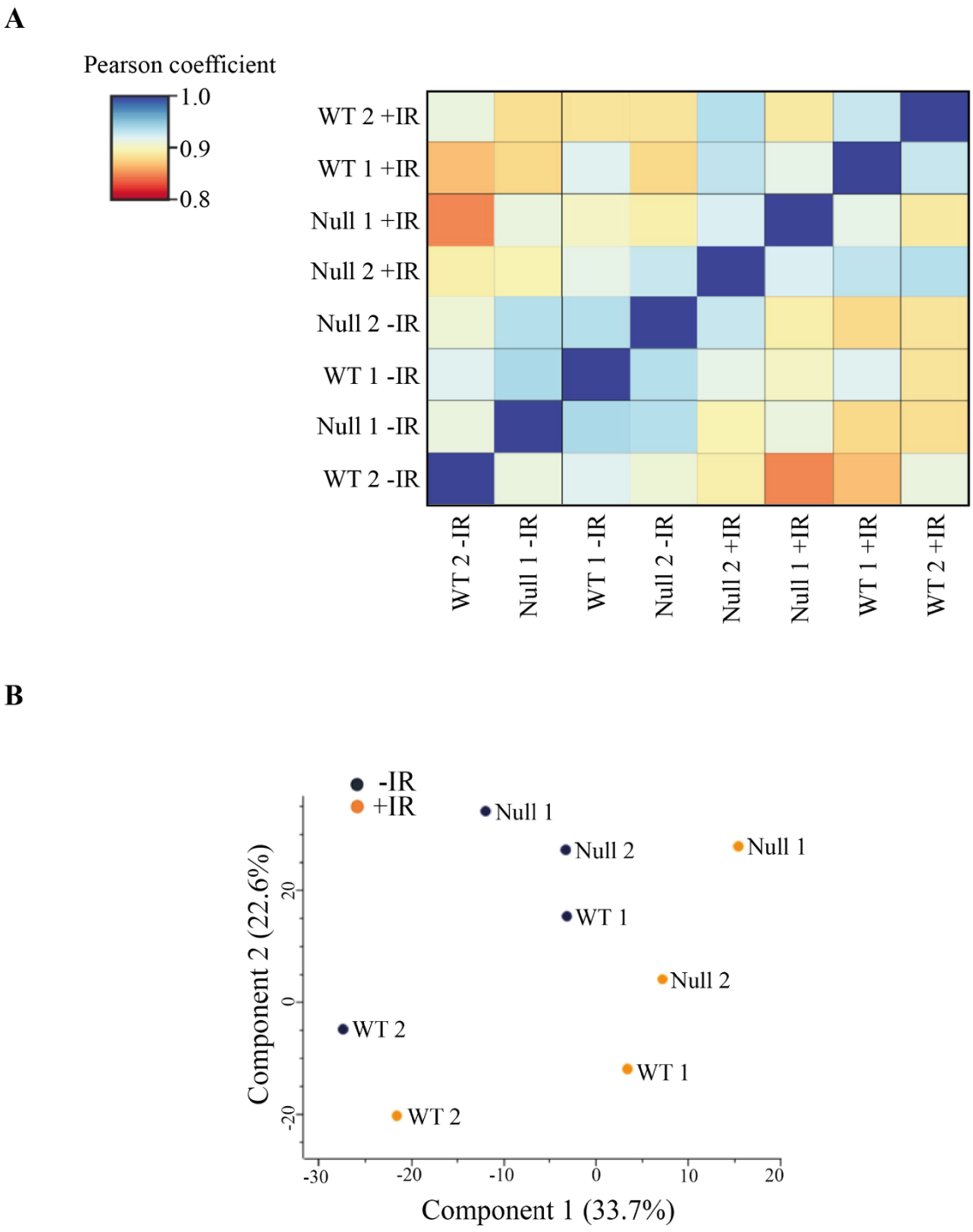

Figure 5.4: Comparison of normalised protein abundance between proteomic samples.
Data provided by Dr Iolanda Vendrell comparing the IGF-1R WT and null clone samples pre- and post- 2 Gy IR using (A) Pearson correlation coefficient, and (B) principal component analysis.

Analysis of IGF-1R WT cells pre- and 1 hr post- 2 Gy IR indicated that no proteins were significantly increased >1.3 fold post-IR (Fig. 5.5). However 6 proteins were significantly decreased >1.3 fold after IR, claudin 3 (CLDN3), diacylglycerol O-acyltransferase 1 (DGAT1), ATP binding cassette subfamily B member 6 (ABCB6), sterol O-acyltransferase 1 (SOAT1), angiotensin II receptor-associated protein (AGTRAP), solute carrier family 12 member 9 (SLC12A9) (Fig. 5.5A, Table 5.1). Broadly, these proteins are involved in metabolic processes, regulation of cell adhesion and nutrient transport (Boswell-Casteel et al., 2017; Maeda et al., 2013; Milatz et al., 2010; Oni et al., 2020; Song et al., 2021; Yen et al., 2005). DAVID software was used to investigate Gene Ontology biological processes associated with these differentially expressed proteins, suggesting the response to hypoxia (AGTRAP, CLDN3), transmembrane transport (ABCB6, SLC12A9) and very low-density lipoprotein particle assembly (DGAT1, SOAT1) pathways as significantly altered. Comparison of IGF-1R null cells pre- and post-IR also showed no significant increase in any proteins post-IR, with only 3 proteins significantly decreased post-IR: methionyl-tRNA synthetase (MARS), glutamine-fructose-6-phosphate transaminase 1 (GFPT1) and NOP9 nucleolar protein (NOP9) (Fig. 5.5B, Table 5.1). These proteins are associated with RNA synthesis, RNA binding and hexosamine synthesis (DeHaven et al., 2001; Ko et al., 2000; Thomson et al., 2007; Jun Zhang et al., 2016). Assessment of protein levels in unirradiated IGF-1R WT and null clones showed differential detection of 2 proteins: basic helix-loop-helix family member A15 (BHLHA15), a protein involved in the regulation of MyoD transcriptional activity (Lemercier et al., 1998), was significantly increased in null clones, and EF-hand domain family member D2 (EFHD2) was significantly increased in IGF-1R WT cells (Fig. 5.5C, Table 5.1). Examination of IGF-1R WT and null clones after IR showed IGF-1R null clones displayed significantly increased expression of myosin IC (MYO1C), involved in glucose transporter recycling (Bose et al., 2002) (Fig. 5.5D, Table 5.1). The lack of major differences in total proteome within clones pre-

and post-IR was expected and was consistent with the short time course. The analysis was carried out to assess basal differences in protein expression, which could have been informative in unpicking the radiation response of the clones. However, given the well-characterised role of the IGF-axis in regulating transcription and translation (Baserga, 1999; Foulstone et al., 2005; Solomon-Zemler et al., 2017), the very limited basal (i.e. pre-IR) differences in differentially expressed proteins was unanticipated.

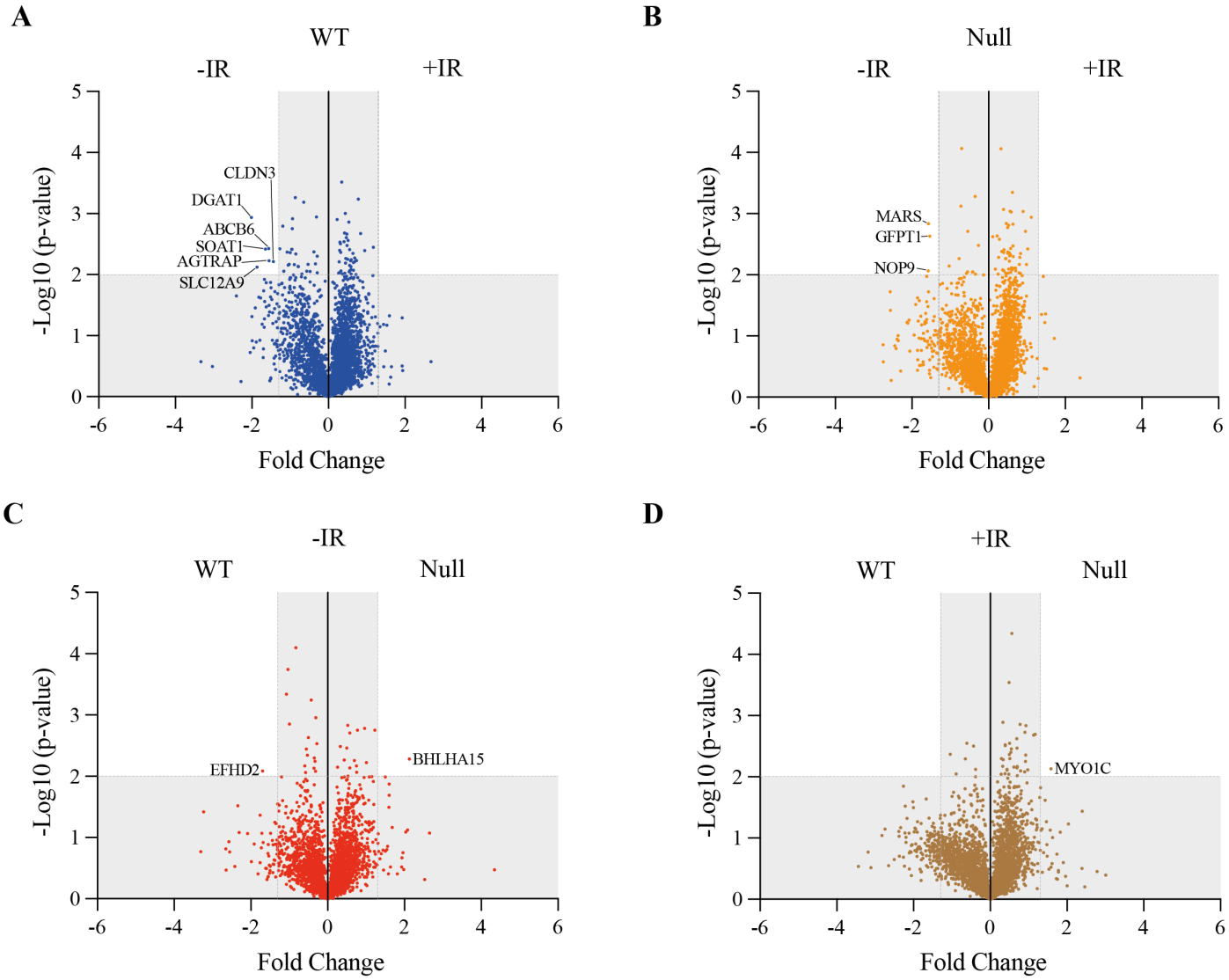

Figure 5.5: Examination of the effect of IGF-1R status and irradiation on the proteome.
Volcano plots (-Log_{10} (p-value) vs actual fold change for examination of effect of 2 Gy irradiation treatment or IGF-1R status on the proteome. Comparison of effect of irradiation on (A) IGF-1R WT clones, (B) IGF-1R null clones, (C) basal proteomic changes between IGF-1R WT and null clones, and (D) proteomic changes between IGF-1R WT and null clones 1 hr after 2 Gy IR. Proteins with actual fold changes >1.3 and statistically significant (p-value <0.01) are labelled. Grey shaded area indicates proteins with actual fold changes <1.3 and/or no statistically significant difference (p-value >0.01).

Proteins identified as differentially expressed by LC-MS/MS			
WT ± IR	**Null ± IR**	**WT vs Null -IR**	**WT vs Null +IR**
ABCB6 ↓	GFPT1 ↓	BHLHA15 ↑	MYO1C ↑
AGTRAP ↓	MARS ↓	EFHD2 ↓	
CLDN3 ↓	NOP9 ↓		
DGAT1 ↓			
SLC12A9 ↓			
SOAT1 ↓			

Table 5.1: Differentially expressed proteins in proteomic analyses.
Table detailing the proteins identified as differentially expressed by LC-MS/MS. Arrows show direction of change post-IR and in IGF-1R null cells (duplicate clones) vs WT cells (duplicate clones). Comparison of data were performed using two-way ANOVA with Tukey's multiple comparisons test. P-values <0.01 were considered statistically significant.

5.3.2 Phospho-proteomic Data

Analysis of normalised phosphoproteomic data by hierarchical clustering indicated that both IGF-1R null clones and one WT clone pre-IR exhibited similar phospho-proteomes, and that post-IR, both IGF-1R WT clones and one null clone also had comparable levels of phosphorylated proteins (Fig. 5.6). Using principal component analysis, all unirradiated samples clustered in a similar region, and after IR all samples exhibited separation from their corresponding unirradiated sample, suggesting changes to the phosphoproteome in all samples after IR (Fig. 5.7).

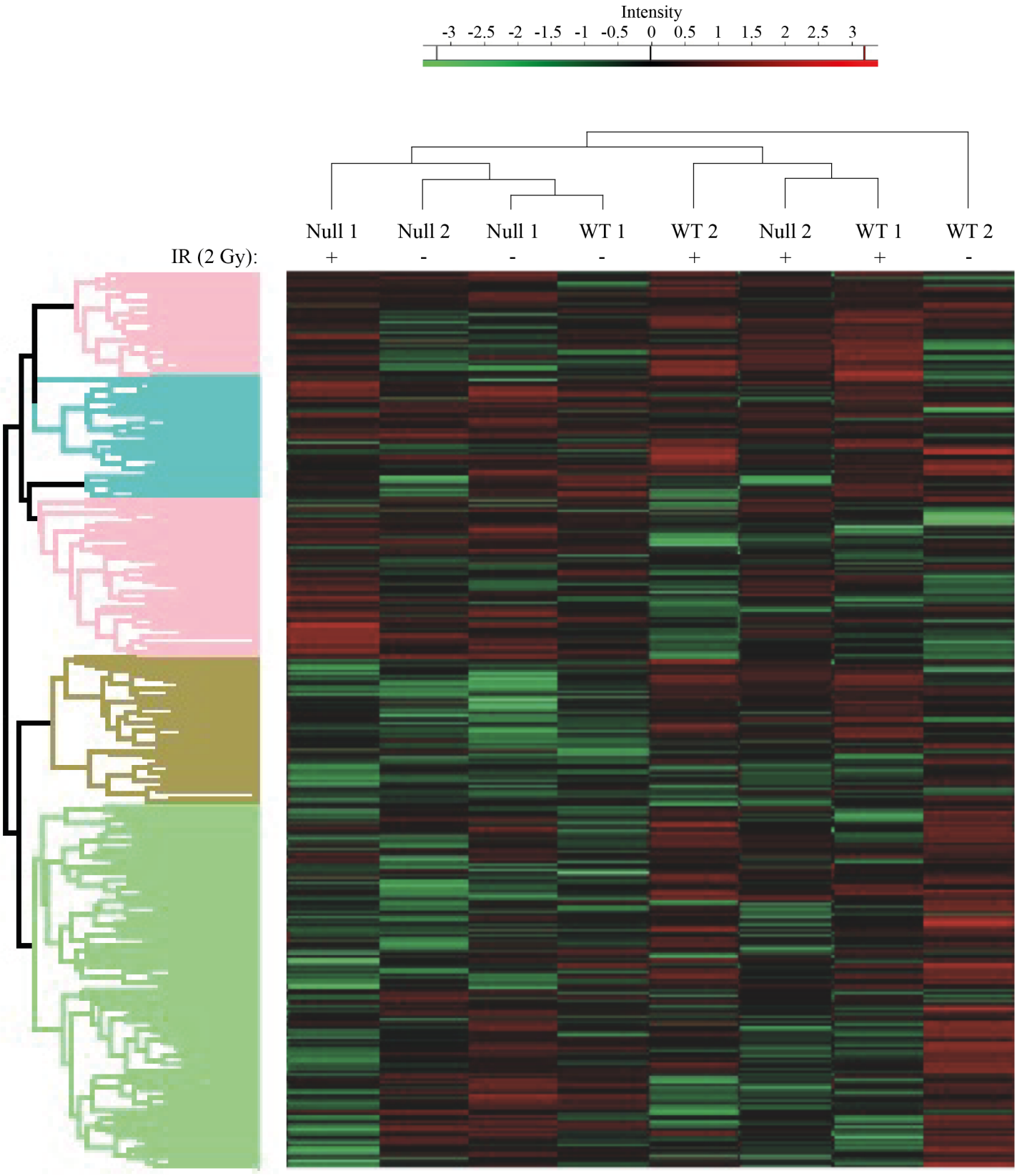

Figure 5.6: Heat map depicting differentially detected phospho-peptides.
Heat map indicating levels of phospho-proteins detected using LC-MS/MS in each condition. Z-scores were calculated by Dr Iolanda Vendrell to determine peptide abundance in relation to the mean (average) of all detected peptides, where Z-score 0 indicates that a value is equal to the mean score, and Z-score 1 indicates a value that is one SD from the mean score. Cluster analysis was performed after Z-score normalisation, and normalised Z-scores are displayed using a red-green scale.

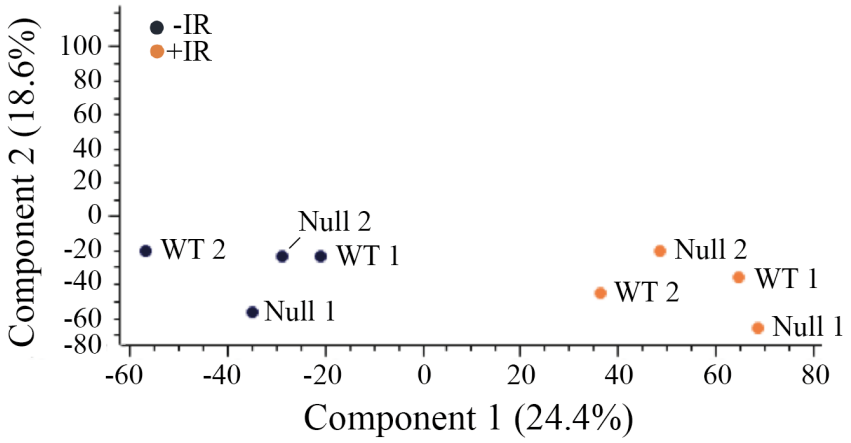

Figure 5.7: Principal component analysis comparing phospho-proteins between samples.
Principal component analysis of the samples plotting principal component 1 vs principal component 2.

Using DAVID software to investigate Gene Ontology biological processes, significantly increased phosphorylated proteins in IGF-1R WT cells pre-IR compared to post-IR were shown to be involved in protein SUMOylation (e.g. 53BP1 (also known as TP53BP), mediator of DNA damage checkpoint 1 (MDC1), DNA topoisomerase II alpha (TOP2A), DNA topoisomerase II beta (TOP2B)), DNA repair (e.g. 53BP1, CHK2, bromodomain adjacent to zinc finger domain 1B (BAZ1B), MDC1, RIF1), chromatin remodelling (e.g. ATPase family AAA domain-containing protein 2A (ATAD2A), ATPase family AAA domain-containing protein 2B (ATAD2B)) and mRNA splicing (e.g. gem nuclear organelle associated protein 5 (GEMIN5), heterogenous nuclear ribonucleoprotein M (HNRNPM), heterogenous nuclear ribonucleoprotein U (HNRNPU), small nuclear riboprotein U5 subunit 200 (SNRNP200), Msx2-interacting protein (SPEN), serine/arginine repetitive matrix 2 (SRRM2)) (Fig. 5.8A). Proteins exhibiting significantly increased phosphorylation post-IR in IGF-1R WT cells compared to pre-IR were associated with DNA methylation (e.g. DNMT1, KMT2A, KMT2D), DNA damage checkpoints (e.g. 53BP1, claspin (CLSPN)) and transcriptional regulation (e.g. 53BP1, DEAD-box helicase 1 (DDX1), DNMT1, deoxynucleotidyltransferase terminal-

interacting protein 2 (DNTTIP2), high mobility group nucleosome binding domain 5 (HMGN5), interferon regulatory factor 2 binding protein 1 (IRF2BP1), KMT2D, SPT2 chromatin protein domain containing 1 (SPTY2D1), Y-box binding protein 2 (YBX2), zinc finger and BTB domain containing 21 (ZBTB21)) (Fig. 5.8B).

A

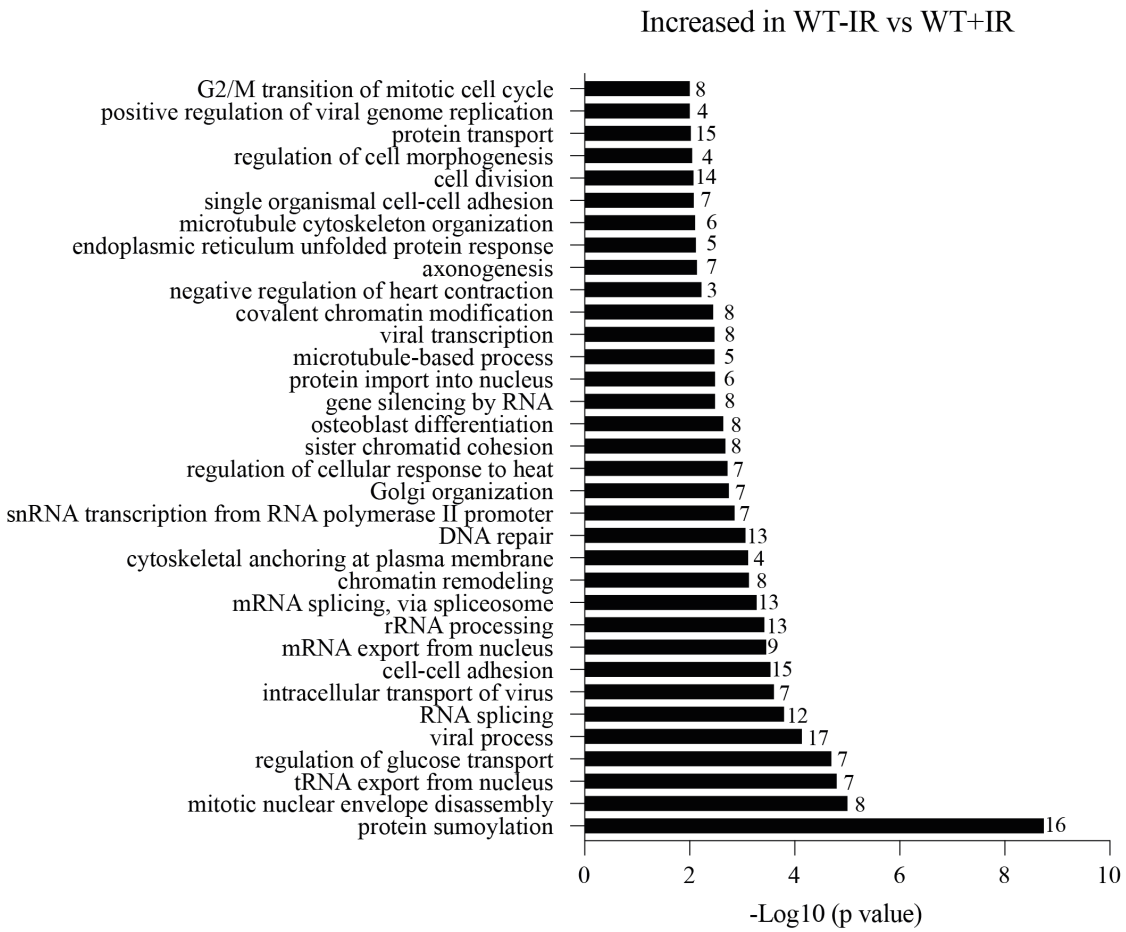

B

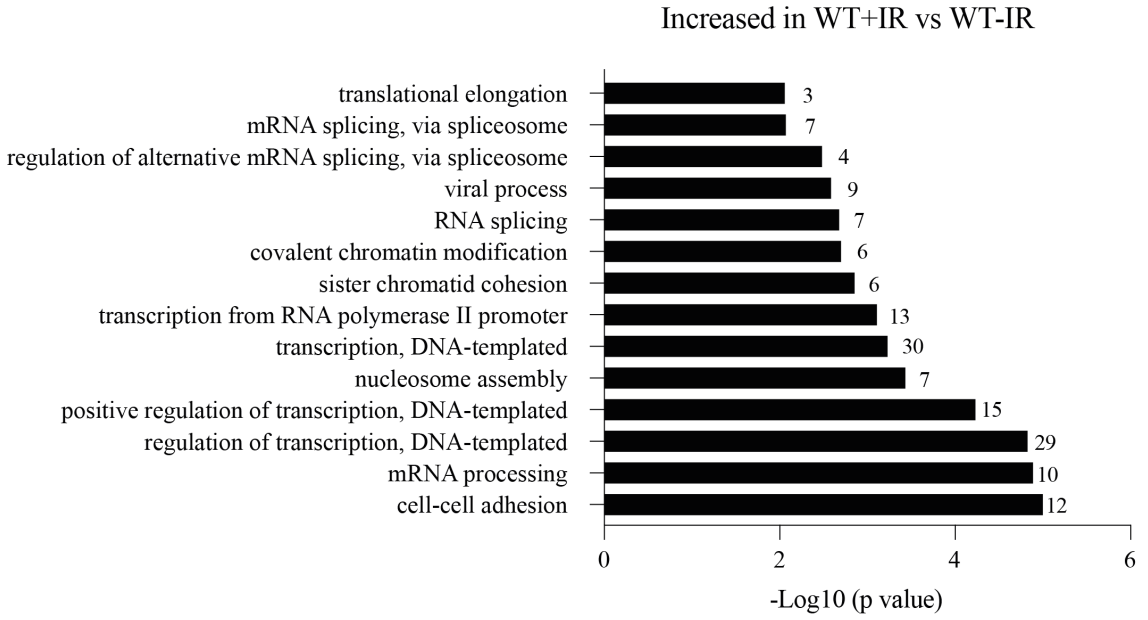

Figure 5.8: Examination of significantly altered phospho-proteins in IGF-1R WT clones upon irradiation using pathway analysis software.
Gene Ontology analysis of IGF-1R WT samples pre- and post-IR was performed using DAVID software. Phospho-proteins included were those increased/decreased >1.3 fold with a p-value<0.05 ((A) 491 phospho-proteins, (B) 191 phospho-proteins).

In IGF-1R null cells, analysis with DAVID software showed processes such as DNA repair (e.g. 53BP1, BRCA1, CHK2, MDC1, RIF1, RNF168), nucleotide excision repair (e.g. COP9 signalosome subunit 3 (COPS3), cullin 4B (CUL4B)) and chromatin remodelling (e.g. bromodomain adjacent to zinc finger domain protein 1A (BAZ1A), bromodomain adjacent to zinc finger domain protein 2A (BAZ2A), polybromo 1 (PBRM1), SWI/SNF related, matrix associated, actin dependent regulator of chromatin subfamily C member 2 (SMARCC2)) were significantly increased pre-IR compared to post-IR (Fig. 5.9A). After IR, processes such as transcription (e.g. 53BP1, anti-silencing function 1B histone chaperone (ASF1B), B-cell lymphoma/leukaemia 11A (BCL11A), castor zinc finger 1 (CASZ1), DDX1, scaffold attachment factor B (SAFB), scaffold attachment factor B2 (SAFB2)), protein SUMOylation (e.g. 53BP1, BCL11A, heterogenous nuclear ribonucleoprotein C (HNRNPC)) and regulation of mRNA processing (e.g. SAFB, SAFB2) were significantly increased compared to unirradiated IGF-1R null cells (Fig. 5.9B).

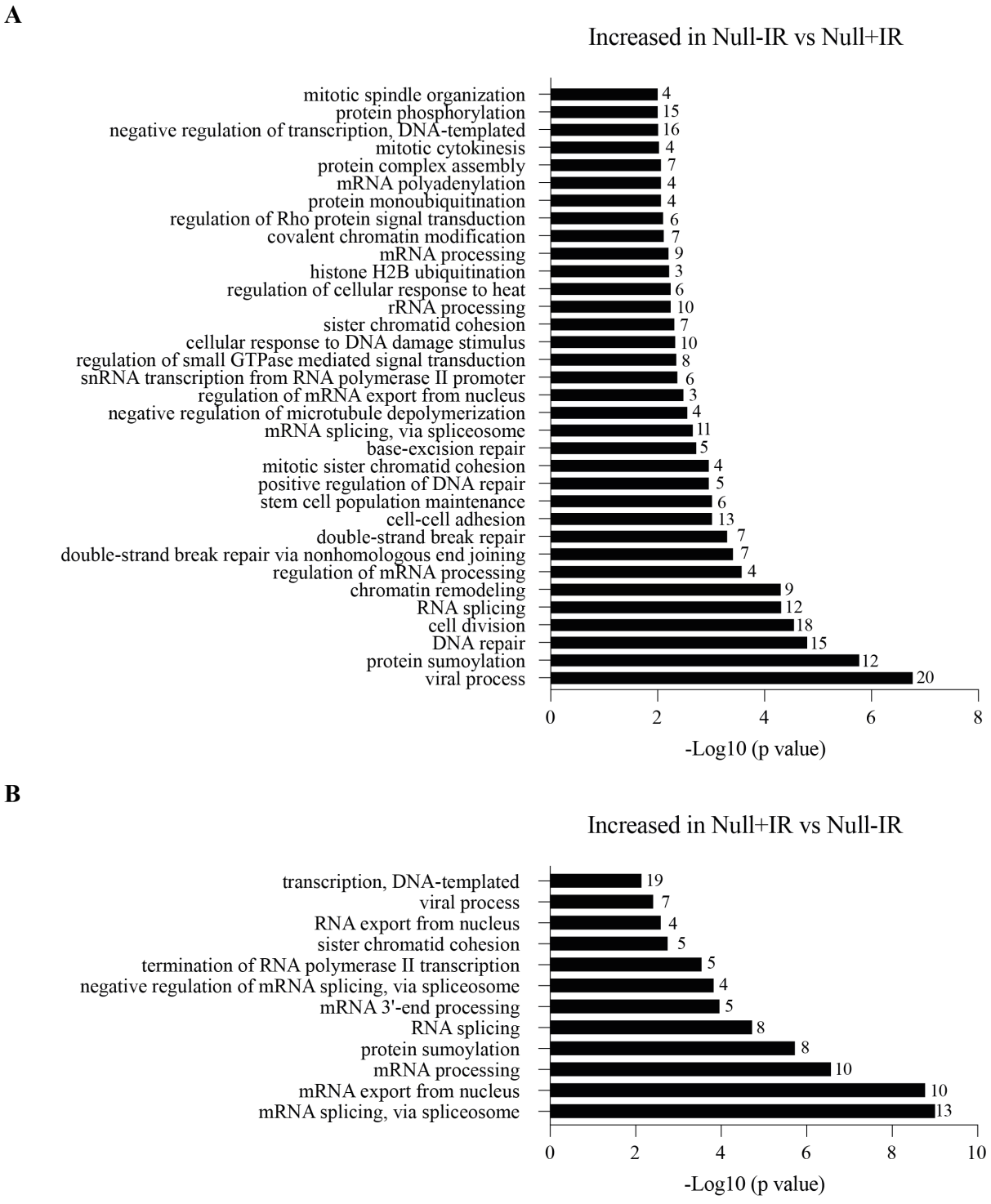

Figure 5.9: Examination of significantly altered phospho-proteins in IGF-1R null clones upon irradiation using pathway analysis software.
Gene Ontology analysis of IGF-1R null samples pre- and post-IR was performed using DAVID software. Phospho-proteins included were those increased/decreased >1.3 fold with a p-value<0.05 ((A) 387 phospho-proteins, (B) 123 phospho-proteins).

Comparison of unirradiated clones indicated that phosphorylation levels of proteins associated with DSB repair via cNHEJ, cell-cell adhesion and gene expression were significantly increased in IGF-1R WT cells (Fig. 5.10A). These included BRCA1, MDC1, RIF1, ubiquitin interaction motif containing 1 (UIMC1), Ran-specific GTPase-activating protein 1 (RANBP1) and RNA-binding motif protein X-linked (RBMX). Further, examination of phosphorylation sites significantly increased in IGF-1R null clones showed processes involved in chromatin modification (e.g. RB, SMARCC2, CHD2), transcriptional regulation (e.g. general transcription factor 3C polypeptide 1 (TF3C1), CHD2, transcriptional regulator ATRX (ATRX), AF4/FMR2 family member 4 (AFF4)) and DNA repair (e.g. RAD18, ATP-dependent DNA helicase Q4 (RECQ4), thyroid hormone receptor interactor 12 (TRIP12)) to be altered compared to IGF-1R WT clones (Fig. 5.10B).

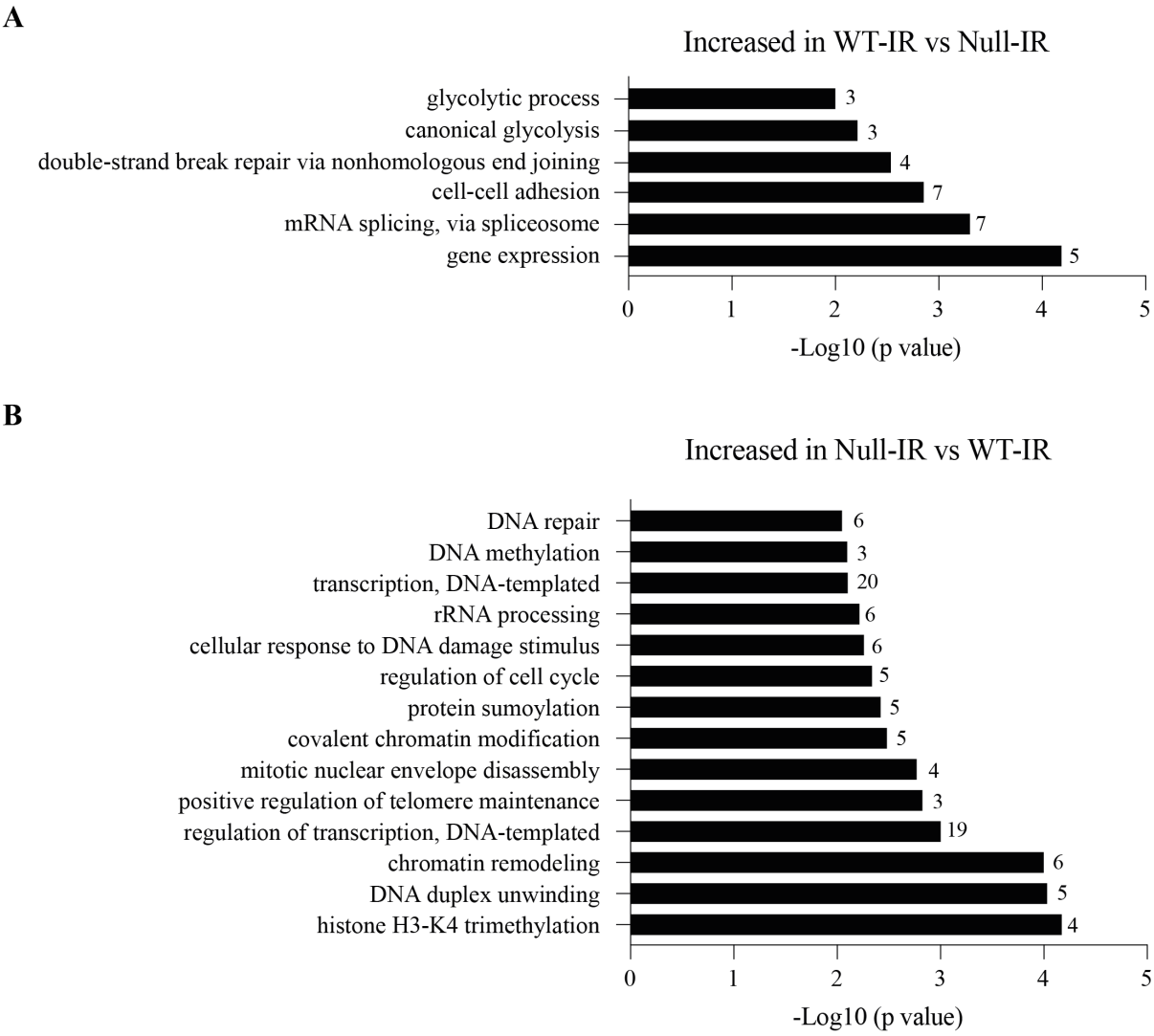

Figure 5.10: Examination of significantly altered phospho-proteins in IGF-1R WT and null clones pre-irradiation using pathway analysis software.
Gene Ontology analysis of IGF-1R WT and null samples pre-IR was performed using DAVID software. Phospho-proteins included were those increased/decreased >1.3 fold with a p-value<0.05 ((A) 95 phospho-proteins, (B) 113 phospho-proteins).

Comparison of IGF-1R WT and null clones post-IR identified biological processes associated with proteins that were significantly more highly phosphorylated in IGF-1R WT cells including cell-cell adhesion, positive regulation of intracellular estrogen receptor signalling and microtubule bundle formation (Fig. 5.11A). Significantly increased phosphorylated proteins in IGF-1R null clones post-IR indicated biological processes involved in protein SUMOylation, chromatin remodelling and mitotic nuclear envelope disassembly to be increased (Fig. 5.11B).

A

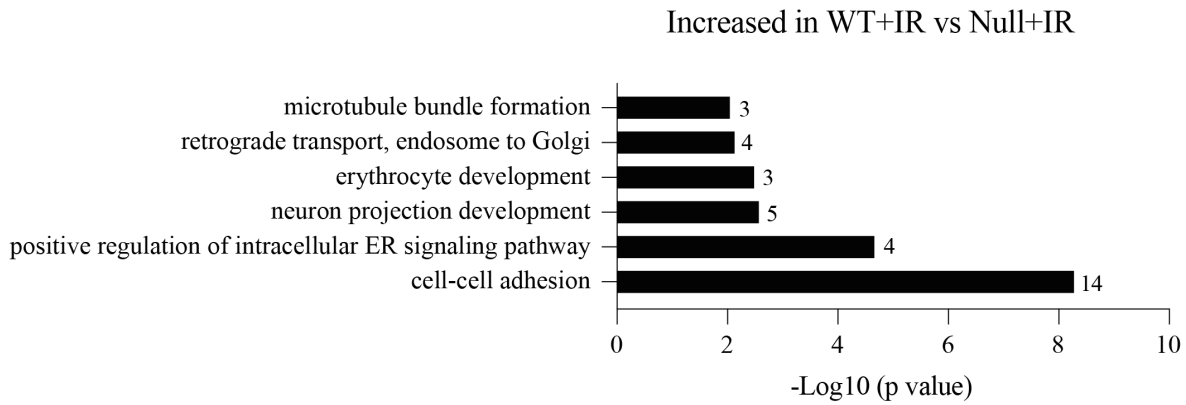

B

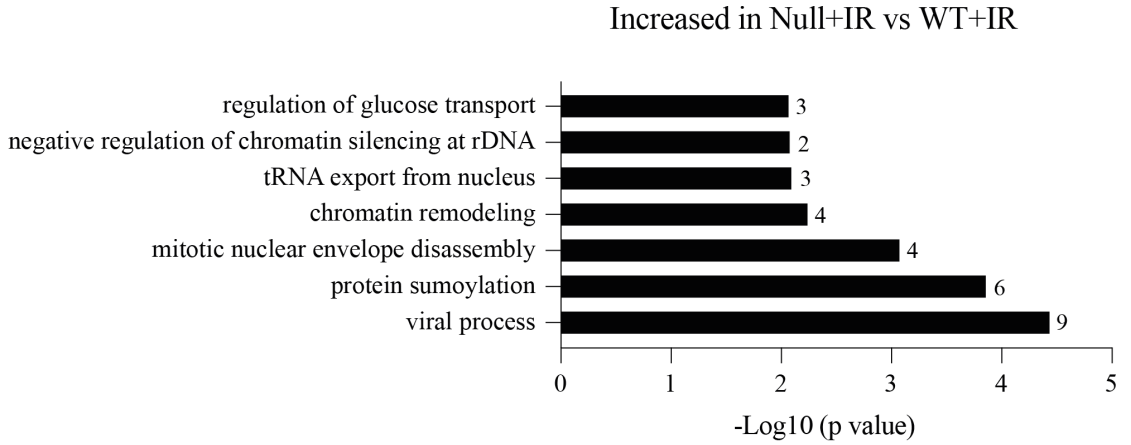

Figure 5.11: Examination of significantly altered phospho-proteins in IGF-1R WT and null clones post-irradiation using pathway analysis software.
Gene Ontology analysis of IGF-1R WT and null samples post-IR was performed using DAVID software. Phospho-proteins included were those increased/decreased >1.3 fold with a p-value<0.05 ((A) 133 phospho-proteins, (B) 105 phospho-proteins).

Volcano plots were produced to study phosphoproteomic changes between samples pre- and post-IR. The same thresholds were used as in the plots for the proteomic analyses, and proteins containing the significantly altered (p-value<0.01) phosphorylation site are labelled in the plots. Comparison between IGF-1R WT clones pre- and post-IR uncovered 129 phosphorylation sites in 94 proteins that were significantly increased pre-IR including 12 53BP1 sites, 4 MDC1 sites, phosphorylation of NUMA1, DNA topoisomerase 2 (TOP2), Chk2, serine/threonine-protein kinase B-raf (BRAF) and RIF1 (Fig. 5.12A). There were 45

phosphorylation sites in 41 proteins significantly increased in WT cells post-IR compared with pre-IR, including DNA methyltransferase 1 (DNMT1), 53BP1, MRE11, KMT2A and KMT2D (Fig. 5.12A). In IGF-1R null cells, the levels of 89 phosphorylation sites in 68 proteins were significantly increased pre-IR compared with post-IR, including MDC1, TSC complex subunit 2 (TSC2), and HECT, UBA and WWE domain containing E3 ubiquitin protein ligase 1 (HUWE1) (Fig. 5.12B).

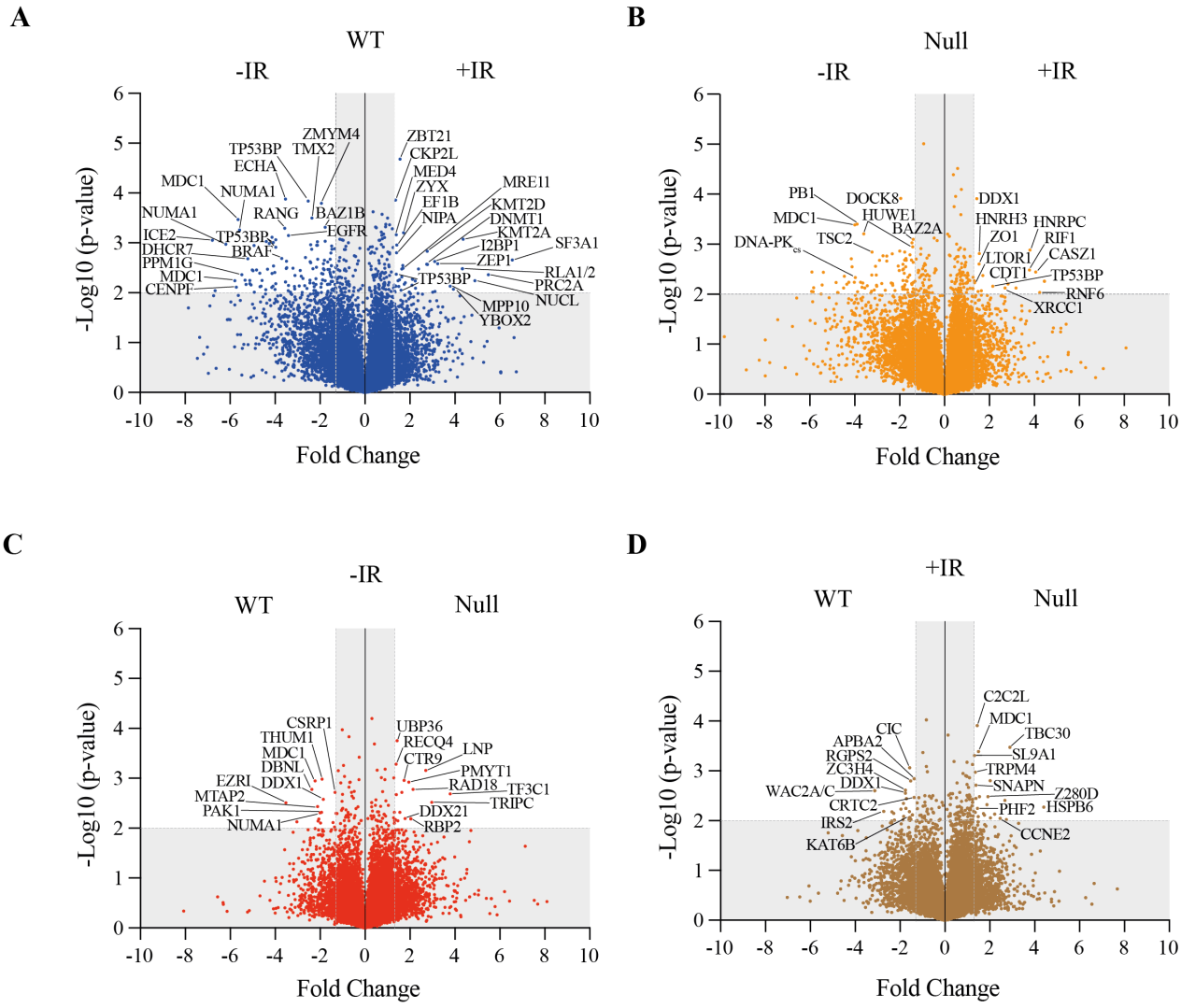

Figure 5.12: Examination of the effect of IGF-1R status and irradiation on the phospho-proteome. Volcano plots (-Log_{10} (p-value) vs actual fold change for examination of effect of 2 Gy irradiation treatment or IGF-1R status on the phospho-proteome. Comparison of effect of irradiation on (A) IGF-1R WT clones, (B) IGF-1R null clones, (C) basal phospho-proteomic changes between IGF-1R WT and null clones, and (D) phospho-proteomic changes between IGF-1R WT and null clones 1 hr after 2 Gy IR. Phospho-proteins with actual fold changes >1.3 and statistically significant (p-value <0.01) are labelled. Grey shaded area indicates phospho-proteins with actual fold changes <1.3 and/or no statistically significant difference (p-value >0.01).

Conversely, post-IR, detection of 18 phospho-sites in 18 proteins such as DDX1, RIF1, X-ray repair cross complementing 1 (XRCC1) and 53BP1 were significantly increased compared with pre-IR (Fig. 5.12B). These significantly altered phosphorylation signals were in proteins associated with the cellular response to DNA damage (Hyun et al., 2017; Mattarocci et al., 2017; Panier and Boulton, 2014; Salvador Moreno et al., 2019; Stewart et al., 2003; Stolz et al., 2011; Zha et al., 2009), which was expected.

Comparison of basal differences between the phosphoproteome of IGF-1R WT and null cells highlighted 14 phosphorylation sites in 13 proteins significantly increased in IGF-1R WT clones and 20 in 20 proteins in IGF-1R null clones (Table 5.2). Phosphorylation of proteins such as MDC1, NUMA1 and p21-activated kinase 1 (PAK1) were increased in IGF-1R WT clones, whereas RAD18, RECQ4 and ubiquitin-specific peptidase 36 (UBP36) were significantly increased in IGF-1R null cells pre-IR (Fig. 5.12C).

Proteins identified as differentially phosphorylated by LC-MS/MS pre-IR			
Increased in IGF-1R WT cells		**Increased in IGF-1R null cells**	
Protein	**Phospho-site**	**Protein**	**Phospho-site**
CSRP1	S192	BOP1	S126/S127
DBNL	S269	CCNB2	S92
EP15R	S255	CTR9	S1020/S1021
EZRI	S535	DDX21	S567
F122A	S37	FXRD1	S189
F122A	S143/S147	LAP2B	T154/S158
GOPC	S376	LMNA	S619
MDC1	S1086	LNP	T179
MPP8	S188	PMYT1	S473
MTAP2	S833	PLPL7	S355
NUMA1	S820	RAD18	S471
PAK1	T230	RBP2	S1993
SAFB2	S233	RECQ4	S323
THUM1	S86/S88	RGPD1	T1302
		RGPD8	Y11/T19/S21
		TF3C1	S1865
		TRIPC	T1377
		UBP36	S807
		ZBED4	S624
		ZC3H1	S1046

Table 5.2: Comparison of differentially altered phospho-proteins between unirradiated IGF-1R WT and null clones in phospho-proteomic analyses.
Table detailing the phospho-proteins and corresponding phosphorylation sites identified by LC-MS/MS as significantly differentially phosphorylated by two-way ANOVA with Tukey's multiple comparisons test. P-values <0.01 were considered statistically significant.

Investigation of IGF-1R WT and null clones post-IR generated 27 significantly increased phosphorylation sites in 26 proteins in IGF-1R WT cells and 21 significantly increased sites of phosphorylation in 22 proteins in IGF-1R null cells (Table 5.3). IRS-2 phosphorylation was increased in WT cells post-IR, which hinted at functioning IGF-axis regulation (Copps and White, 2012; Jiang and Steinle, 2010; Lingohr et al., 2002) (Fig. 5.12D). Further, pathway

analysis suggested pathways involved in cell-cell adhesion (BCL-2-associated athanogene 3 (BAG3), sorting nexin 2 (SNX2) and phosphoribosylaminoimidazole carboxylase (PAICS)), protein transport (amyloid beta precursor protein binding family A member 2 (APBA2), family with sequence similarity 21 member A (FAM21A), family with sequence similarity 21 member C (FAM21C)) and retrograde transport (SNX2, FAM21A, FAM21C) were increased in IGF-1R WT cells post-IR vs IGF-1R null cells (Fig. 5.12D). Several proteins involved broadly in protein localisation to the nucleus (lamin A/C (LMNA) and torsin 1A-interacting protein (TOR1AIP1)) and the cellular response to hypoxia (LMNA and solute carrier family 9 member A1 (SLC9A1)) were significantly increased post-IR in IGF-1R null cells compared to IGF-1R WT cells (Fig. 5.12D). Differential detection of phosphorylated DNA damage/repair proteins was not apparent in these comparisons.

Proteins identified as differentially phosphorylated by LC-MS/MS post-IR			
Increased in IGF-1R WT cells		**Increased in IGF-1R null cells**	
Protein	**Phospho-site**	**Protein**	**Phospho-site**
3BP1	S544	AREL1	S337
ANKZ1	S361	C2C2L	S613/T621/S623
APBA2	S480	CCNE2	S383
ASML	S239	EPIPL	T1543
BAG3	T489	HSPB6	S16
CARL1	S968	KI67	T1233
CIC	S142/S146	KI67	T1801
CLIP1	S348	LMNA	S619
CLIP2	S352	MDC1	S1086
CRTC2	S433	MYO1C	S408
EHBP1	S171	PHF2	S474/T479
I2BP2	S406	SL9A1	S602
IRS2	S560	SLTM	S170
IRS2	T1202	SNAPN	S126
K1671	S128	TBC30	S744
KAT6B	S889	TOIP1	S156
MAP1A	S2019	TRPM4	S728
MAP4	S696	TTC7A	S690/T693
NUFP2	S629	UTP11	S241
PRC2B	T225	Z280D	S806
PAICS	S107	ZO3	S369
RGPS2	T326/S329		
SNX2	T104		
FAM21A	S802		
FAM21C	S802		
ZC3H4	S1269/S1275		

Table 5.3: Comparison of differentially altered phospho-proteins between IGF-1R WT and null clones post-irradiation in phospho-proteomic analyses.
Table detailing the phospho-proteins and corresponding phosphorylation sites identified as differentially detected by LC-MS/MS. Comparison of data were performed using two-way ANOVA with Tukey's multiple comparisons test. P-values <0.01 were considered statistically significant.

Analysis of these datasets uncovered changes in DDR proteins including MDC1, 53BP1 and DNA-PK$_{cs}$. More specifically, patterns of differential phosphorylation were observed in proteins involved in DNA mismatch repair (MMR) as well as DSB repair and apoptosis regulation (MDC1 T652, T654, S1086, S1096, LMNA S619, lamina-associated polypeptide 2, isoform alpha (LAP2A) S424, lamina-associated polypeptide 2, isoform beta (LAP2B) T154, S159, T160, T208, and the core MMR protein mutS homolog 6 (MSH6) S227 (Frederiksen et al., 2021)), with significantly increased phosphorylation in IGF-1R null clones pre- and post-IR compared to the corresponding IGF-1R WT clones (Fig. 5.13). Examination of the MMR process in the literature indicated that the phospho-sites in this analysis were uncharacterised, apart from serine 652 of LMNA, which when phosphorylated, has been reported to promote intracellular localisation and activity, resulting in nuclear laminar reorganisation (Lee et al., 2008). Nonetheless, increased phosphorylation of multiple MMR proteins in IGF-1R null clones vs WT clones basally and upon irradiation indicated possible MMR pathway involvement in the radio-sensitisation phenotype observed (Fig. 4.1, 5.13).

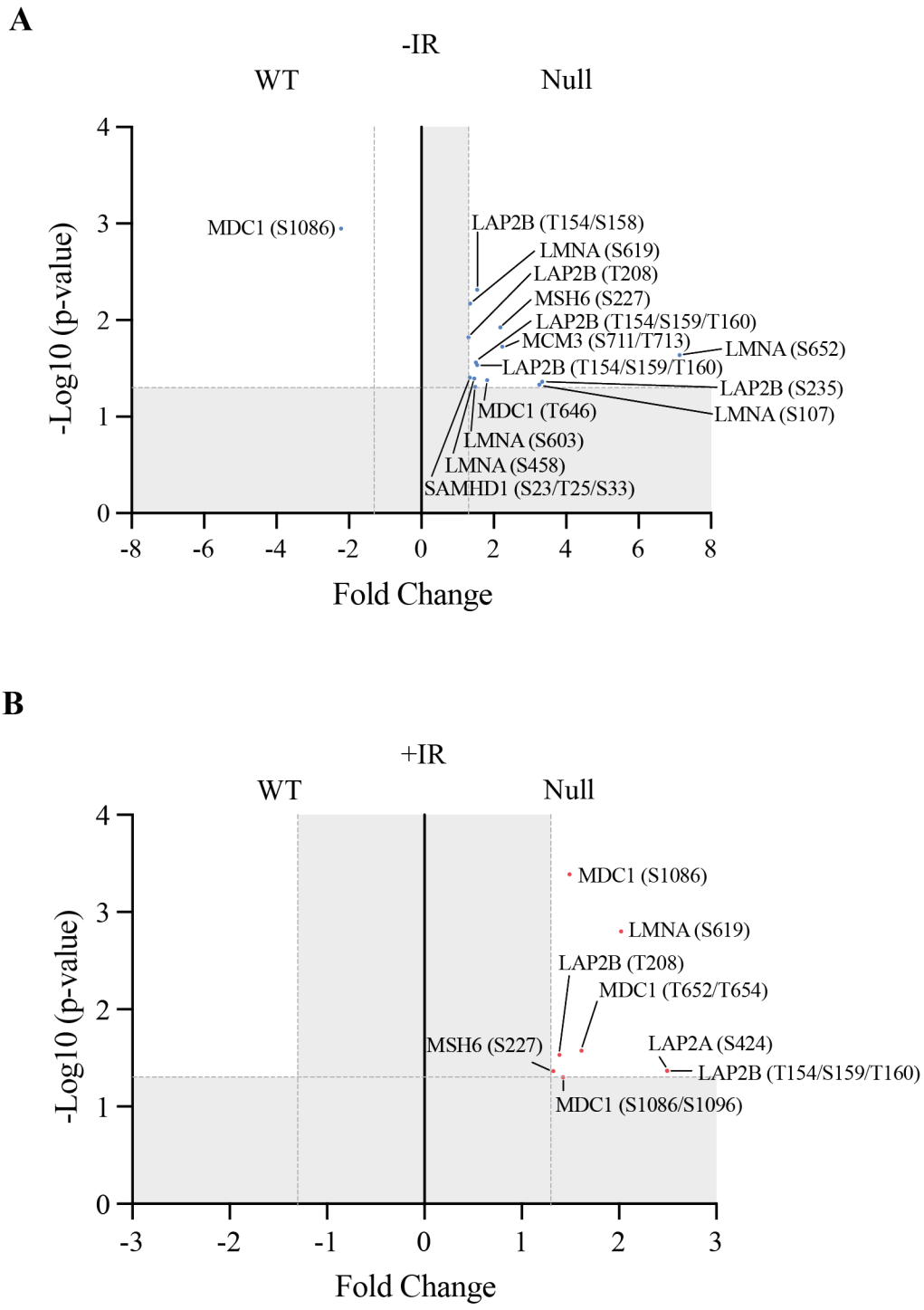

Figure 5.13: Examination of the effect of IGF-1R status and irradiation on the mismatch repair pathway. Volcano plots (-Log_{10} (p-value) vs actual fold change for examination of effect of 2 Gy irradiation and IGF-1R status on the phosphorylation of proteins that can contribute to mismatch repair. Comparison of effect of IGF-1R status (A) basally, and (B) 1 hr post- 2 Gy IR. Phospho-proteins with actual fold changes >1.3 and statistically significant (p-value <0.05) are labelled. Grey shaded area indicates phospho-proteins with actual fold changes <1.3 and/or no statistically significant difference (p-value >0.05).

Examination of individual phosphorylation sites detected by LC-MS/MS uncovered several proteins of interest which were significantly altered between conditions (Fig. 5.14). Non-neuronal microtubule-associated protein (MAP4) promotes microtubule assembly (Nguyen et al., 1999; Shigematsu et al., 2018) and displayed significantly increased phosphorylation at serine 696 in both IGF-1R null clones post-IR compared to IGF-1R WT clones (Fig. 5.14A). This phosphorylation site has been reported to be phosphorylated by CDK1, MAPK/ERK kinase 6 (MKK6) and P38A, leading to cytoskeletal reorganisation (Kitazawa et al., 2000; L. Li et al., 2015; Ookata et al., 1997). Phosphorylation of the heat shock protein family B (small) member 6 (HSPB6) on serine 16 has been associated with inhibition of apoptosis and inhibition of cell motility (Edwards et al., 2012; Matsushima-Nishiwaki et al., 2016; Nicolaou et al., 2008). IGF-1R WT clones exhibited significantly higher levels of serine 16 phosphorylation compared to IGF-1R null clones post-IR (Fig. 5.14B). Significantly increased levels of 7-dehydrocholesterol reductase (DHCR7) phosphorylation at serine 14 in IGF-1R WT cells after IR compared with IGF-1R null clones (Fig. 5.14C) suggested possible induction of DHCR7 enzymatic activity through IGF-1R (Prabhu et al., 2017). BRAF phosphorylation at serine 446 was significantly increased in irradiated IGF-1R null cells compared with IGF-1R WT cells (Fig. 5.14D). Phosphorylation at this site by ras homolog enriched in brain (RHEB), TSC2 and PAK1 has been reported to induce BRAF enzymatic activity and induce the interaction with HRAS (Karbowniczek et al., 2006; Tran et al., 2005). Detection of one 53BP1 phospho-site, serine 380, was significantly increased in unirradiated IGF-1R WT cells pre- vs post-IR, whereas phosphorylation at this residue was significantly increased upon IR in IGF-1R null cells compared to unirradiated IGF-1R null clones (Fig. 5.14E). Phosphorylation of 53BP1 at serine 380 has been reported to be essential for its binding to suppressor of cancer cell invasion (SCAI) before DNA damage. Subsequent phosphorylation of SCAI after DNA damage promotes HDR-mediated repair through inhibition of RIF1 (Isobe et al., 2017). Significantly

increased phosphorylation post-IR in IGF-1R null clones suggests a possible mechanism for IGF-1R in DDR pathway choice in response to IR.

In IGF-1R WT cells, irradiation induced a significant increase in DNA-PK$_{cs}$ phosphorylation at serine 3205 compared to unirradiated IGF-1R WT and IGF-1R null cells (Fig. 5.14F). Phosphorylation at serine 3205 has been shown to induce DNA repair and cell cycle regulation, and is phosphorylated by ATM, polo-like kinase 1 (PLK1) and by autophosphorylation, and dephosphorylated by protein phosphatase 6 catalytic subunit (PPP6C) (Douglas et al., 2014; Neal et al., 2020). Serine 3205 phosphorylation was induced by IR in IGF-1R null clones but the magnitude of induction was less than in WT cells and was not statistically significant ($p=0.12$). This absence of significant increase in serine 3205 phosphorylation of DNA-PK$_{cs}$ in IGF-1R null cells after IR vs unirradiated IGF-1R WT and null cells might be relevant to previous data indicating differential cNHEJ response depending on IGF-1R status (Chitnis et al., 2014), although it must be noted that there was no significant difference between serine 3205 phosphorylation in IGF-1R WT and null cells post-IR.

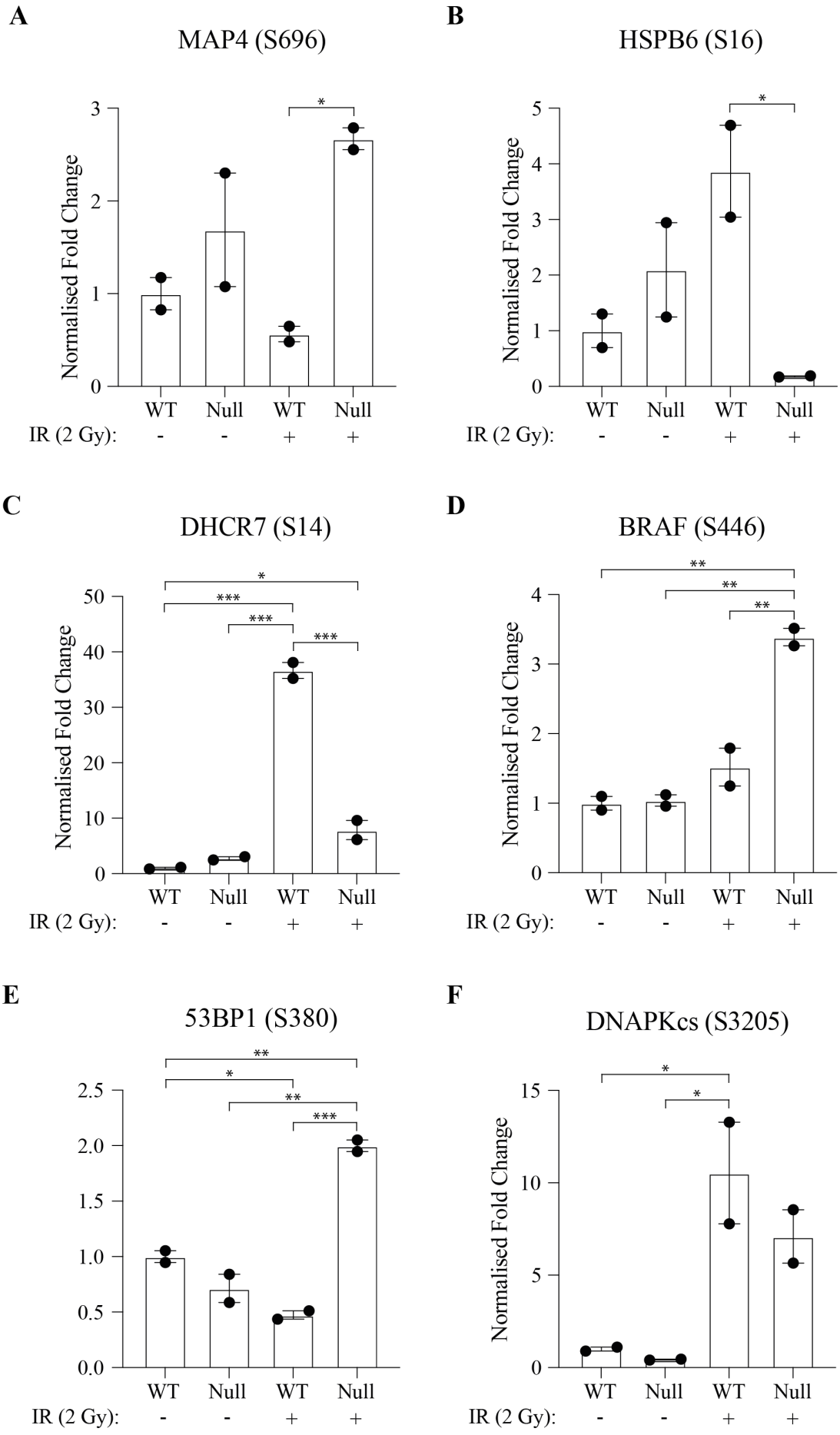
A
MAP4 (S696)
Normalised Fold Change
WT Null WT Null
IR (2 Gy): - - + +
B
HSPB6 (S16)
Normalised Fold Change
WT Null WT Null
IR (2 Gy): - - + +
C
DHCR7 (S14)
Normalised Fold Change
WT Null WT Null
IR (2 Gy): - - + +
D
BRAF (S446)
Normalised Fold Change
WT Null WT Null
IR (2 Gy): - - + +
E
53BP1 (S380)
WT Null WT Null
IR (2 Gy): - - + +
F
DNAPKcs (S3205)
Normalised Fold Change
WT Null WT Null
IR (2 Gy): - - + +

Figure 5.14: Examination of individual phosphorylation sites altered between samples.
Individual phospho-peptide abundance values were normalized to the mean abundance value of the individual phospho-peptide abundance of unirradiated IGF-1R WT clones. Graphs show means and individual data points from analysis of duplicate IGF-1R WT and null clones. A one-way ANOVA was used to determine the significance of differences between clones (*p<0.05, **p<0.01, ***p<0.001).

5.4 Discussion

5.4.1 Proteome

Analysis of the proteome suggested a lack of major differences within clones pre- and post-IR, which was consistent with the short interval between irradiation and cell lysis (Fig. 5.5, Table 5.1). Comparison between clones pre-IR indicated very limited basal differences in differentially detected proteins, which was unexpected given the well-characterised role of the IGF-axis in regulating transcription and translation (Hao et al., 2020; Poreba and Durzynska, 2020). Compensatory signalling via other receptors upstream of the mTOR pathway could help to explain this finding (Laplante and Sabatini, 2013; Showkat et al., 2014). Pathway analysis of proteomic changes suggested differences in hypoxia response, lipoprotein assembly and transmembrane transport pathways between IGF-1R WT clones pre- and post-IR, however, given the limited number of differentially expressed proteins in these comparisons, no conclusions can be drawn from the pathway analyses.

Inspection of individual proteins altered between samples suggested that MARS was downregulated after IR in IGF-1R null cells, perhaps to stop translation initiation during DNA damage repair (Fig. 5.5, Table 5.1) (Kwon et al., 2011). This was consistent with unpublished data in the Macaulay lab which indicated that aminoacyl-tRNA synthetase (*ARS*) genes were amongst the most upregulated genes in RNA-seq analyses upon IGF treatment. Differences in proteins involved in glucose metabolism (such as decreased expression of GFPT1 post-IR in

IGF-1R null cells) shown here (Fig. 5.5, Table 5.1) could have similar effects to published work indicating a role for metabolic proteins in DSB repair, such as PKM2 (Sizemore et al., 2018).

5.4.2 Phospho-proteome

While proteomic analysis detected very few changes between IGF-1R WT and null clones (Fig. 5.5, Table 5.1), there was more evidence of phospho-proteomic differences between IGF-1R WT and null clones, and within each clone pre/post-IR (Fig. 5.8-12, Table 5.2-3). Differential phosphorylation upon IR was expected as phosphorylation of proteins occurs in response to IR and is important in regulating the DDR, as are acetylation, ubiquitylation, methylation, PARylation and NEDDylation (Brown and Jackson, 2015; Polo and Jackson, 2011). To more comprehensively assess the role of the IGF-axis in the cellular response to IR, it would be informative to investigate these post-translational modifications, which can be detected by mass spectrometry (Afjehi-Sadat and Garcia, 2013; Ehrich et al., 2005; Jungmichel et al., 2013; Kori et al., 2017; Larsen et al., 2006)

Analysis of the phospho-proteomic data indicated the absence of many well-characterised IGF-responsive phosphorylations on IGF-1R itself and its downstream effectors (Fig. 5.12, Table 5.2-3). Given the consensus that IGF-1R only phosphorylates tyrosine residues (De Meyts and Whittaker, 2002a; Favelyukis et al., 2001; Pautsch et al., 2001), these findings could be explained in part by the limited detection of tyrosine phosphorylations in the dataset. Other techniques such as tyrosine phospho-proteomics (Bian et al., 2016) or anti-phospho-tyrosine IP followed by LC-MS (Zheng et al., 2005) using IGF-1R WT and kinase-dead cells could be employed to assess direct IGF-1R phosphorylations. Differential phosphorylation of IRS-2 was

observed in IGF-1R WT cells vs null cells after IR which was consistent with regulation of the IGF-axis by IGF-1R (Fig. 5.12, Table 5.3) (Copps and White, 2012; Jiang and Steinle, 2010; Lingohr et al., 2002). Additionally, no detection of phospho-AKT peptides was predictable given the inability to consistently detect AKT phosphorylation of serine 473 by Western blot in 22Rv1 cells.

Pathway analyses suggested differential phosphorylations of proteins involved in metabolism, cytoskeletal organisation and molecular chaperones (Fig. 5.8-11). While not directly associated with DNA damage induction or repair, these pathways have been reported to impact the DDR. Indeed, it was described that PKM2, a kinase involved in cancer cell metabolic reprogramming, is phosphorylated by ATM in response to IR, promoting HR (Sizemore et al., 2018). Further, chromatin accessibility can be impacted by cytoskeletal organisation, also affecting DNA repair dynamics (Spichal and Fabre, 2017), and numerous reports have suggested that molecular chaperones are involved in the regulation of DDR proteins (Dubrez et al., 2020; Pennisi et al., 2015; Sottile and Nadin, 2018; Wawrzynow et al., 2018; Wonkyoung et al., 2019). Altogether, differential activation of these pathways could contribute to the radio-sensitisation phenotype observed in IGF-1R null clones.

Several pathways associated with radiation response were shown to be altered using DAVID software. Specifically, phosphorylation of proteins in DNA repair and chromatin remodelling pathways were suggested to be increased in unirradiated IGF-1R null cells compared to post-IR (Fig. 5.9), which could indicate a lack of effective DDR both by improper activation of DDR proteins and alterations to the access of the damage site (De Schutter and Nuyts, 2009; Takata et al., 2013).

Examination of phosphorylation changes to DDR proteins indicated differences to MMR pathway proteins, with increased phosphorylation of sites on MDC1, LMNA, LAP2A, LAP2B and MSH6 in IGF-1R null clones compared to IGF-1R WT clones (Fig. 5.13). While MMR is not a component of the classical DSB response (Blackford and Jackson, 2017), reports have noted that MMR can contribute to DSB repair (Meyers et al., 2003; Zhang et al., 2009). Although the phospho-sites detected are uncharacterised in the literature, phosphorylation could act to disrupt MMR in IGF-1R null cells, and it would be worthwhile to investigate this by Western blot and by using a mismatch repair assay (Dunlop et al., 1997, p. 199; Matheson and Hall, 2003).

The increase in DNA-PK_{cs} phosphorylation at the DNA repair-inducing serine 3205 residue in IGF-1R WT cells post-IR vs unirradiated WT cells was expected (Fig. 5.14) (Neal et al., 2020). However, relative reduction in post-IR phosphorylation in IGF-1R null cells together with differential phosphorylation of 53BP1, indicated a possible defect in cNHEJ in IGF-1R null cells in response to IR (Fig. 5.14). These data were consistent with previous work in the Macaulay group suggesting an altered cNHEJ response based on IGF-1R status after IR (Chitnis et al., 2014). Differential phosphorylation of major DDR proteins at phospho-sites reported to be important for activation of DSB repair and pathway choice prompted further investigation (Isobe et al., 2017; Neal et al., 2020, 2011).

CHAPTER VI: Investigation of the requirement for IGF-1R in non-homologous end joining

6.1 Introduction

After induction of a DSB, Ku70/Ku80 binds to the broken DNA ends, facilitating the recruitment of DNA-PK$_{cs}$, forming the holoenzyme DNA-PK (Bekker-Jensen et al., 2006; Uematsu et al., 2007; Yoo and Dynan, 1999). Subsequently additional cNHEJ factors, including Artemis, DNA ligase IV, XRCC4 and XLF are recruited to carry out direct ligation of the DNA ends (Blackford and Jackson, 2017; Costantini et al., 2007; Mari et al., 2006; S. Nick McElhinny et al., 2000; Uematsu et al., 2007), and DNA-PK$_{cs}$ also phosphorylates Ku70 to aid its removal from the DSB, progressing the DNA repair process (Jette and Lees-Miller, 2015; Lee et al., 2016). Therefore DNA-PK$_{cs}$ functions to promote cNHEJ, but has also been implicated in HR, helping to increase efficiency of MRN cleavage by engaging with DNA ends (Deshpande et al., 2020). Further, DNA-PK$_{cs}$ can influence the choice of repair pathway by promoting or blocking end resection by autophosphorylation or phosphorylation by ATM and CtIP (Blackford and Jackson, 2017; Goodarzi et al., 2006; Jiang et al., 2015).

Previous data in the Macaulay group indicated that inhibition of IGF-1R resulted in increased radio-sensitivity, and that IGF-1R and DNA-PK$_{cs}$ may function in the same pathway in response to irradiation in DU145 cells and glioblastoma cells (Chitnis et al., 2014). Further, DNA repair pathway reporter assays in HEK293 cells suggested that treatment with AZ12253801, an IGF-1R tyrosine kinase inhibitor (TKI), resulted in suppression of both cNHEJ and HR (Chitnis et al., 2014). Additional work indicated a ligand-independent interaction between nuclear IGF-1R and Ku80 (Aleksic et al., 2018), and immunoprecipitation

(IP) interactome experiments and subsequent validatory IPs performed by Jack Mills (DPhil student) suggested an interaction between IGF-1R and DNA-PK$_{cs}$ in the nucleus (unpublished). Indeed, work recently published by the Larsson group also detected DNA-PK$_{cs}$ in the nuclear IGF-1R interactome of colorectal cancer cells. Although this specific interaction was not investigated, this study did reveal an important IGF-regulated interaction between 53BP1 and the nuclear mitotic apparatus protein NuMA (Yang et al., 2021).

Further investigation of links between IGF-1R and cNHEJ were prompted by the observed radio-sensitivity in DU145, PC3, 22Rv1 and GBM cells upon IGF-1R depletion, inhibition or knockout shown here (Fig. 3.1, 4.1) and previously (Chitnis et al., 2014; Simpson et al., 2020; Turney et al., 2012; Zhao and Gu, 2014a) Detection of increased γH2AX foci 10 minutes and 1 hour post-IR in IGF-1R null clones compared to IGF-1R WT clones (Fig. 4.12) was also consistent with a role of IGF-1R in the rapid response to DNA damage via cNHEJ. Data implicating DNA-PK$_{cs}$ included validated interaction between IGF-1R and DNA-PK$_{cs}$ by Jack Mills (DPhil student, Macaulay group) and the Larsson group (Yang et al., 2021), and the phosphoproteomic dataset (Chapter V) which suggested the absence of a significant increase in radiation-induced phosphorylation of serine 3205 of DNA-PK$_{cs}$ in IGF-1R null 22Rv1 cells, whereas this response was seen in IGF-1R WT cells (Fig. 5.14F).

Altogether, experiments carried out in this thesis, work done by Macaulay lab members and reports in the literature, suggested a hitherto uncharacterised role of IGF-1R in cNHEJ and DNA-PK$_{cs}$ activation. Therefore, efforts focused on investigating this relationship.

6.2 Exploring the role of IGF-1R in non-homologous end joining

Initial experiments investigated a possible cNHEJ defect in IGF-1R null 22Rv1 cells using two strategies. The first strategy involved the use of an end-joining assay developed by the van Gent laboratory (Verkaik et al., 2002) using the pDVG94 plasmid, to quantify the relative contributions of microhomology-mediated end joining MMEJ or cNHEJ. When cNHEJ is defective, the amount of MMEJ in cells increases (Chang et al., 2017; Sallmyr and Tomkinson, 2018; Sfeir and Symington, 2015). Other end-joining assays require stable integration of reporter plasmids, such as the EJ7 system (Bhargava et al., 2018), whereas the linearised pDVG94 plasmid can be transiently transfected, and end-joining is examined by PCR amplification and restriction enzyme digest of the joining site of the linear substrate (Verkaik et al., 2002).

Briefly, as described in the Methods (section 2.18), plasmid (pDVG94) was linearised, transfected into 22Rv1 cells, and plasmid DNA was isolated 48 hours post-transfection. The region around the break site was amplified by PCR, and if the plasmid was repaired by cNHEJ, no BstXI restriction site will be present. Conversely, if MMEJ occurred, a BstXI restriction site would be created, and digestion and gel electrophoresis of the PCR product was used to indicate the relative amounts of cNHEJ vs MMEJ repair. The pDVG94 vector was linearised, producing 7739, 603 and 304 bp fragments. As positive controls for compromised cNHEJ, IGF-1R WT and null cells were treated with the DNA-PK_{cs} inhibitor NU7441 for 4 hours prior to IR. Cells were then subjected to 2 Gy IR and immediately following this, the 7739 bp linearised fragment was transfected into the cells. After 48 hours, plasmid DNA was isolated from untreated IGF-1R WT and null cells or treated with NU7441 (1μM), and amplified by PCR. Digestion of the PCR product with BstXI was carried out, and fragments were separated

by gel electrophoresis. If the plasmid was repaired by cNHEJ, a 180 bp fragment would be observed, and if MMEJ, BstXI-digested fragments of sizes 120 bp and 60 bp would be detected (Fig. 6.1A).

Additional BstXI products were detected between the 180 bp and 120 bp fragments which were not reported in other published data (Fig. 6.1B), although a ~100 bp fragment in undigested samples has been reported previously (W. Li et al., 2019). Attempts to reduce non-specific products included increasing the number of PCR cycles and altering annealing temperatures. However these efforts did not alter the appearance of additional products, which could be due to BstXI digestion of genomic DNA present in the plasmid preparation. Both Hirt (to extract all extrachromosomal DNA) and plasmid miniprep kit (to extract plasmid DNA) are advised in the provided van Gent laboratory protocol and advice from Nicole Verkaik (van Gent laboratory) suggested both methods were effective. Initially both genomic and plasmid DNA were isolated using the Kapa Express Extract kit, which produced additional fragments. To attempt to reduce genomic DNA and additional products, Qiagen plasmid miniprep kit was used, however the same products were present. Use of radio-labelled PCR primers, as in Verkaik *et al.*, could help to eliminate detection of the observed additional products (Verkaik et al., 2002). The successful assessment of plasmid DNA quality by 260/280 ratio prior to transfection, and the presence of distinct fragments at the predicted uncut 180 bp PCR product and 120 bp product of digestion, supported the validity of the assay.

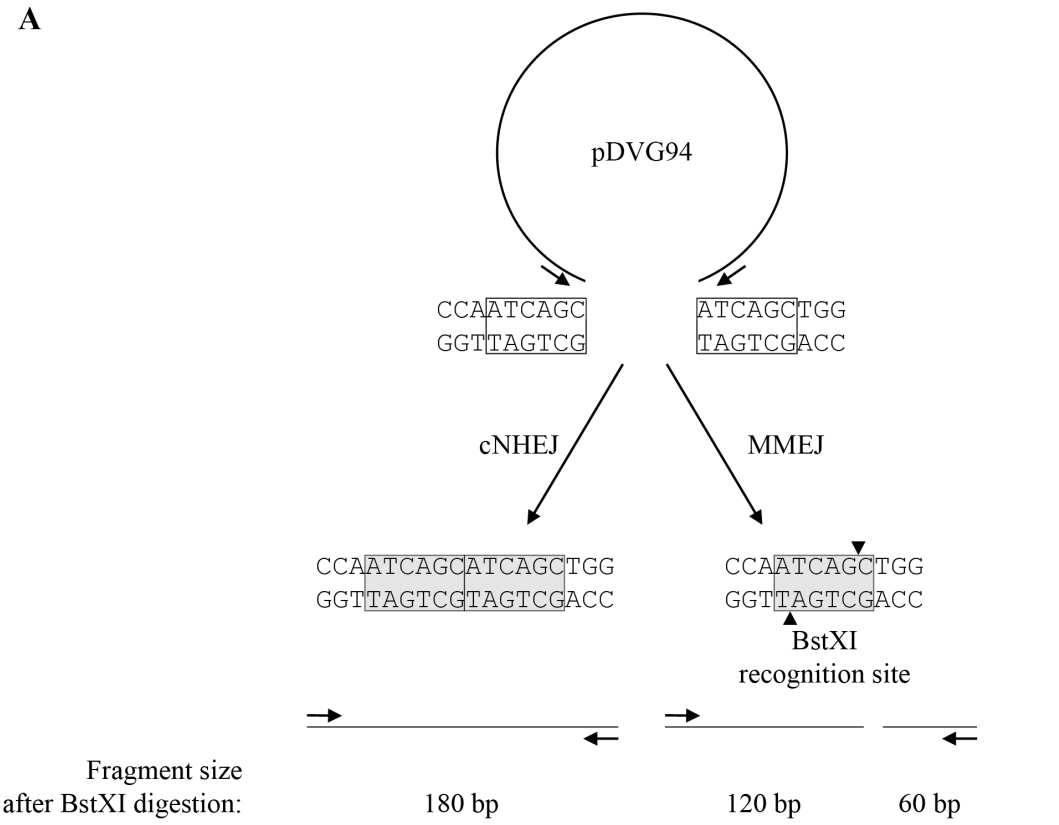
A
pDVG94
CCAATCAGC
GGTTAGTCG
ATCAGCTGG
TAGTCGACC
cNHEJ
MMEJ
CCAATCAGCATCAGCTGG
GGTTAGTCGTAGTCGACC
CCAATCAGCTGG
GGTTAGTCGACC
BstXI
recognition site
Fragment size
after BstXI digestion:
180 bp
120 bp
60 bp

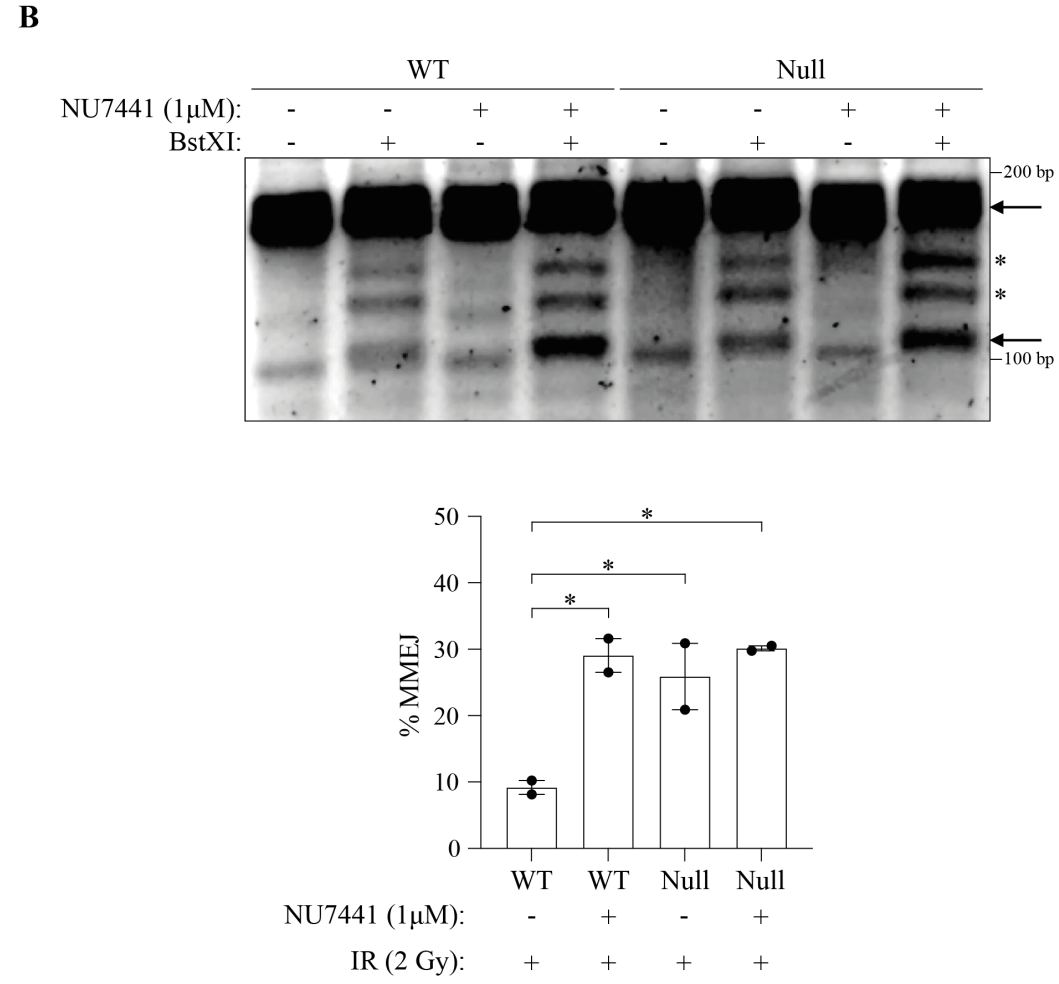
B
WT
Null
NU7441 (1μM): - - + + - - + +
BstXI: - + - + - + - +
200 bp
100 bp
*
*
% MMEJ
50
40
30
20
10
0
*
*
*
WT WT Null Null
NU7441 (1μM): - + - +
IR (2 Gy): + + + +

Figure 6.1: Loss of IGF-1R increased relative levels of MMEJ.
(A) Schematic adapted from Verkaik *et al*. depicting the end joining assay. Briefly, the pDVG94 plasmid was linearized by digestion with AfeI and EcoRV, producing blunt-ends, each with a 6 bp repeat sequence (ATCAGC). WT clone 1 and null clone 1 were transiently transfected with the linearized 7739 bp fragment of pDVG94, and after 48 hr, plasmid DNA was isolated by minipreparation. The 180 bp region flanking the plasmid break site was amplified by PCR (using primers indicated by arrows), and digested with BstXI. If cells have repaired the linearized plasmid using MMEJ, a BstXI recognition site was created, and the relative level of MMEJ was determined by quantification of the 120 bp product produced upon BstXI digestion and subsequent agarose gel electrophoresis. (B) Agarose gel electrophoresis of PCR products untreated or pre-treated for 4 hr with NU7441, and ±BstXI digestion as specified. Electrophoretic mobility of intact PCR product (180 bp) and BstXI-digested PCR product (120 bp) indicated by black arrows. Additional products detected only in BstXI digests indicated (*). Product intensities were quantified using ImageJ software and data were analysed by one-way ANOVA to determine the statistical significance of differences in relative MMEJ (*$p<0.05$).

IGF-1R WT cells pre-treated with NU7441 showed increased 120 bp product compared to untreated cells (Fig. 6.1B), which correlated with other published data using this assay where the function of key cNHEJ proteins was disrupted (Harvey et al., 2018; W. Li et al., 2019; Oh et al., 2014; Yuan et al., 2015). Further, there appeared to be more 120 bp product in IGF-1R null cells than in IGF-1R WT cells (Fig. 6.1B). Upon quantification, relative levels of MMEJ were determined. Treatment with NU7441 in IGF-1R WT and null cells led to significantly increased MMEJ compared to untreated IGF-1R WT cells. Untreated IGF-1R null cells exhibited significantly increased relative levels of MMEJ (20-30%) compared to IGF-1R WT cells (~10%) (Fig. 6.1B). However these data should be interpreted with caution as the assay was only performed twice. Additional repeats would have been completed if time had permitted. The results suggested possible defective cNHEJ, correlating with data presented here (Fig. 4.12) and by previous lab members (Chitnis et al., 2014).

The second strategy employed to examine cNHEJ activity was to check for 53BP1 foci pre- and post-IR. The p53-binding protein 53BP1 has been described to physically block end-resection, a key step in the initiation of HR, and to negatively regulate resection nucleases (Bothmer et al., 2010; Bunting et al., 2010; Ceccaldi et al., 2016; Chapman et al., 2013; Daley and Sung, 2014; Ochs et al., 2016). These actions serve to promote cNHEJ and inhibit HR, and

quantification of 53BP1 foci has been used to assess cNHEJ function (Popp et al., 2017; Zimmermann et al., 2013).

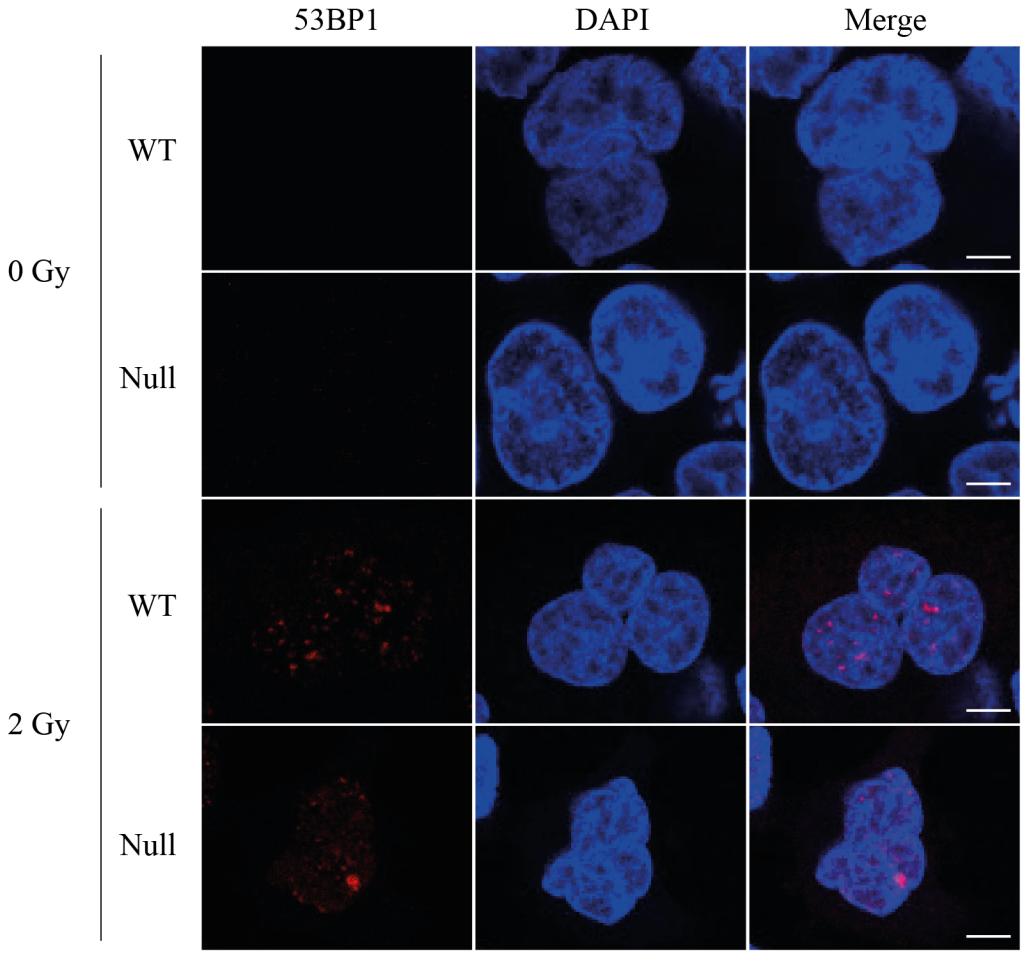

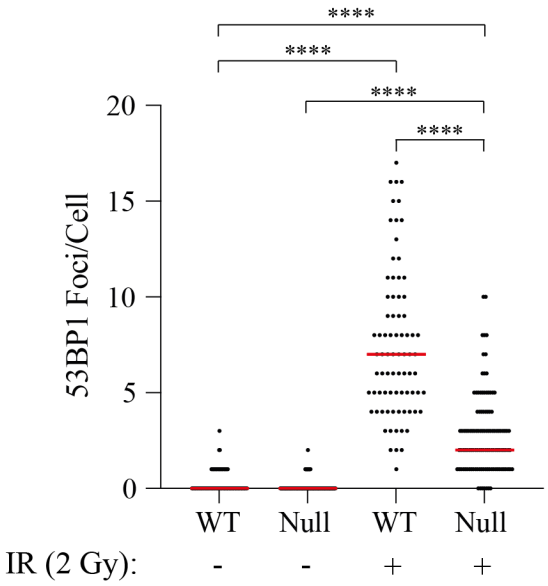

Figure 6.2: Loss of IGF-1R decreased 53BP1 foci formation after IR.
A clone expressing WT IGF-1R (WT clone 1) and an IGF-1R null (Null clone 1) clone were seeded on coverslips in triplicate in 6 well plates (1 x 10^5 cells/well) and the following day required wells were subjected to 2 Gy irradiation. Cells were fixed 10 minutes after IR and stained for 53BP1. Images show 53BP1 (red), nuclear DAPI (blue) and both merged in unirradiated cells and cells at 10 mins post-IR. Images were taken at 63x magnification, scale bar represents 10 μm. Quantification of 53BP1 foci pooled from three independent experimental repeats was carried out using ImageJ software in 9 separate fields and the graph shows the number of foci in each cell counted. Red line indicates mean number of 53BP1 foci/cell. A one-way ANOVA was used to determine the significance of differences between clones (****$p<0.0001$).

IGF-1R WT and null clones were plated on coverslips and the following day, subjected to 2 Gy IR. After 10 minutes, cells were stained with 53BP1 antibody and examined by IF. Upon quantification, significantly more 53BP1 foci were present in IGF-1R WT cells compared to null cells, indicating a possible defect in cNHEJ upon IGF-1R loss (Fig. 6.2). Duplicate IGF-1R WT and null clones were shown to exhibit similar within-genotype behaviour in previous assays relevant to DDR, for example in figures 4.1, 4.3 and 4.4. Given the time to image foci in each clone pre-/post-IR and the cost of confocal time being limiting, it was deemed preferable to perform independent experimental repeats on these individual clones rather than only single analysis of multiple clones. These considerations also applied to the analyses by IF (Fig. 6.3, 6.7) shown below.

The differences between IGF-1R WT and null cells observed using the pDVG94 end-joining assay (Fig. 6.1), variation in γH2AX foci at 10 minutes and 1 hour post-IR (Fig. 4.12), and quantification of 53BP1 foci (Fig. 6.2) suggested a role of IGF-1R in cNHEJ in DSB repair after IR. These data prompted further investigation, and given the findings of the phospho-proteomic study described in Chapter V, these investigations focussed on the role of the key cNHEJ protein DNA-PK_{cs}.

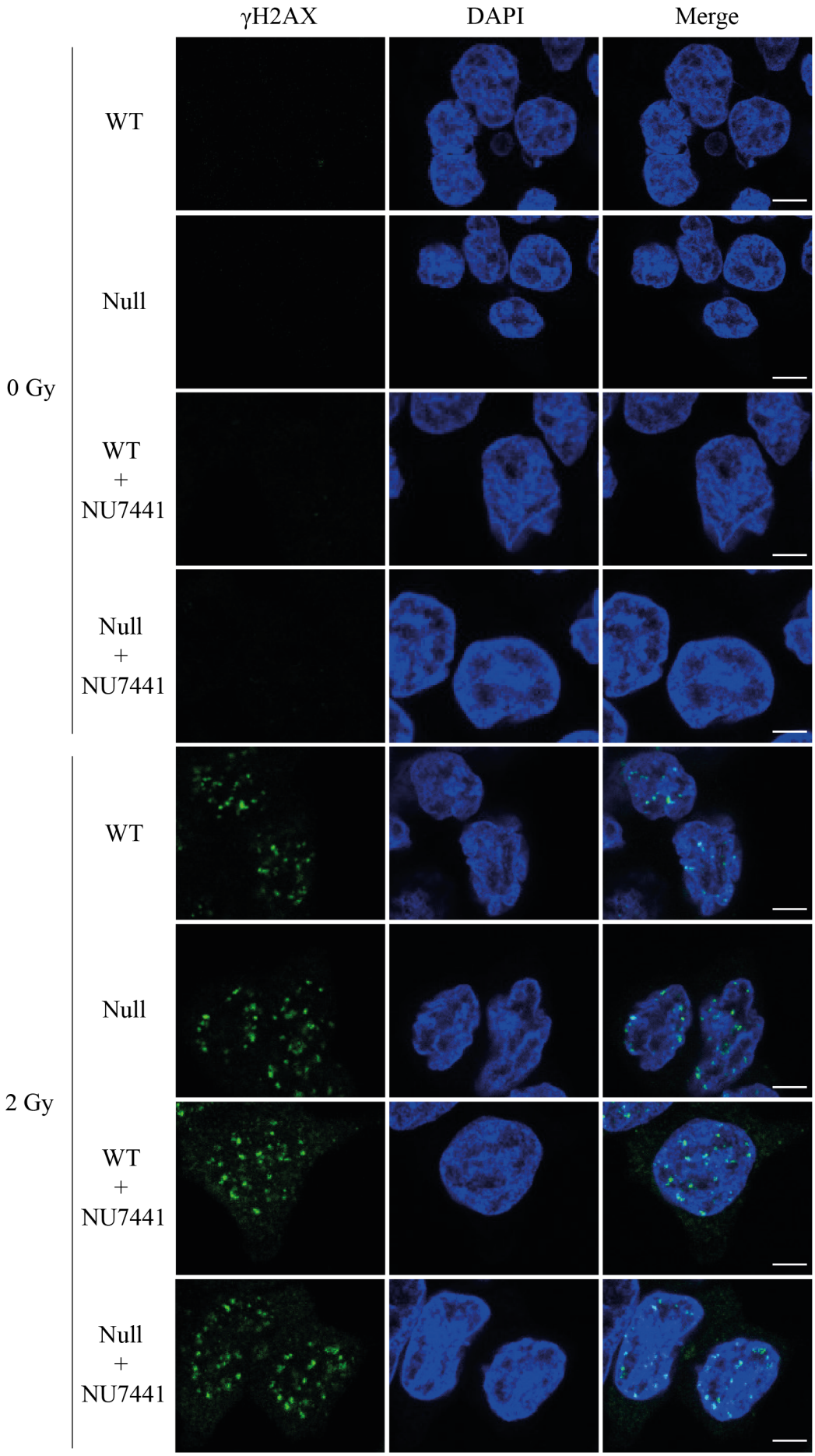
γH2AX
DAPI
Merge
0 Gy
WT
Null
WT + NU7441
Null + NU7441
2 Gy
WT
Null
WT + NU7441
Null + NU7441

Figure 6.3: Investigation of the effect of DNA-PK$_{cs}$ inhibition on γH2AX foci in IGF-1R WT and null cells.
A clone expressing WT IGF-1R (WT clone 1) and an IGF-1R null (Null clone 1) clone were seeded on coverslips in triplicate in 6 well plates (1 x 10^5 cells/well) and the following day required wells were subjected to 2 Gy irradiation. Cells were fixed 10 minutes after IR and stained for γH2AX. Images show γH2AX (green), nuclear DAPI (blue) and both merged in unirradiated cells and cells at 10 mins post-IR. Images were taken at 63x magnification, scale bar represents 10 μm, and are representative images from three independent experimental repeats.

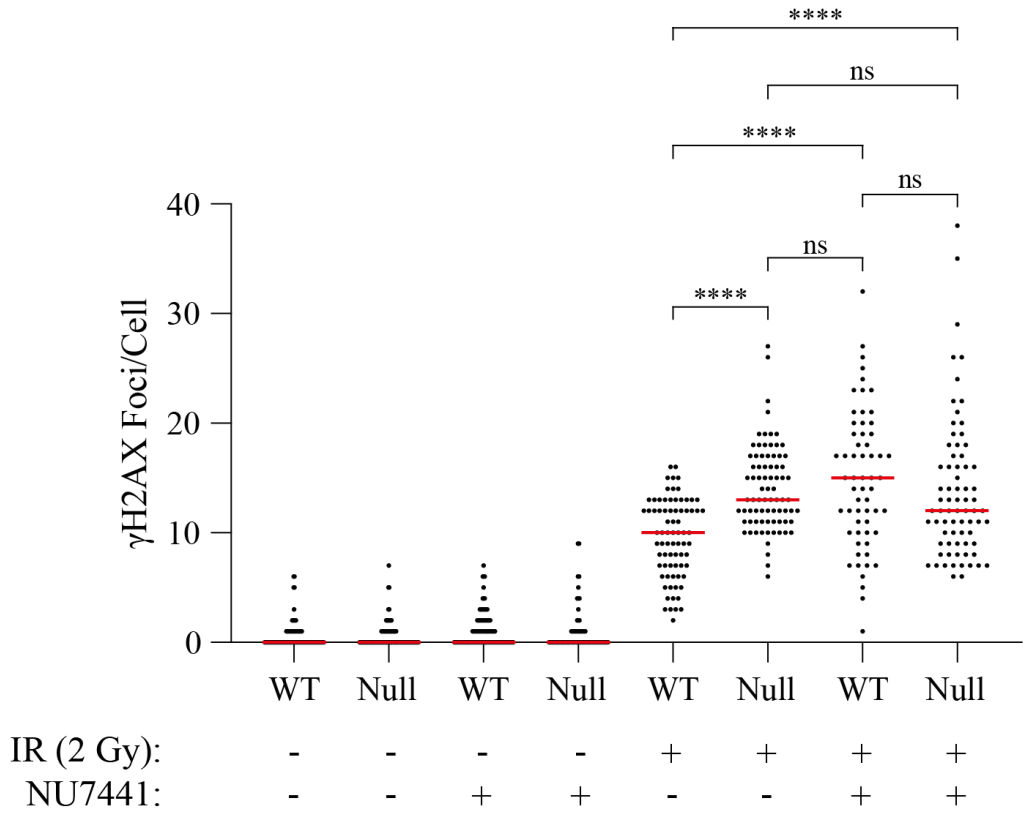

Figure 6.4: Quantification of γH2AX foci after DNA-PK$_{cs}$ inhibitor treatment in IGF-1R WT and null cells.
Quantification of γH2AX foci pooled from three independent experimental repeats was carried out using ImageJ software in 9 separate fields (>70 cells) and the graph shows the number of foci in each cell counted. Red line indicates mean number of γH2AX foci/cell. A one-way ANOVA was used to determine the significance of differences between clones (****$p<0.0001$).

To study whether the status of DNA-PK$_{cs}$ affected γH2AX focus formation in IGF-1R WT and null 22Rv1 clones, cells were subjected to 1μM NU7441 or solvent control 4 hours prior to IR. Cells were fixed 10 minutes after 2 Gy IR, and γH2AX foci were visualised as above (Fig. 6.3). Quantification showed significantly increased γH2AX foci in IGF-1R null cells post-IR compared to IGF-1R WT cells post-IR, confirming the previous result (Fig. 4.12, 6.3, 6.4). Further, there was no significant difference in IGF-1R null cells post-IR with or without

NU7441, suggesting that DNA-PK$_{cs}$ inhibition has no effect in cells that lack IGF-1R (Fig. 6.3, 6.4). Increased γH2AX foci post-IR in IGF-1R WT cells pre-treated with NU7441 compared to untreated WT cells post-IR highlighted the role of DNA-PK$_{cs}$ in DNA repair (Fig. 6.3, 6.4). Lastly, γH2AX foci numbers were not significantly different between IGF-1R WT cells pre-treated with NU7441 and IGF-1R null cells post-IR with or without NU7441, which suggested that with respect to DSB repair post-IR, IGF-1R operates in the same pathway as DNA-PK$_{cs}$ (Fig. 6.3, 6.4).

6.3 Examining the effect of IGF-1R on DNA-PK$_{cs}$ phosphorylation

In the phosphoproteomics data in chapter V, phosphorylation of DNA-PK$_{cs}$ at serine 3205 was significantly decreased by a greater extent post-IR in IGF-1R null cells compared to IGF-1R WT cells (Fig. 5.14F). Together with the observations detailed above, data from Jack Mills (Fig. 6.11) and the Larsson group suggesting interaction between nuclear IGF-1R and DNA-PK$_{cs}$ (Yang et al., 2021), we hypothesised that DNA-PK$_{cs}$ phosphorylation might be altered in IGF-1R null cells in response to IR, leading to alteration of cNHEJ dynamics. Phosphorylation of serine 3205 was identified by the Lees-Miller laboratory (Chen et al., 2005; Douglas et al., 2014; Jette and Lees-Miller, 2015), who developed an antibody for this phospho-site. After contacting Professor Lees-Miller, she kindly sent her last remaining aliquot of the antibody. IGF-1R WT and null cell lysates were collected pre- and post-IR and Western blot analysis was carried out. However, despite multiple efforts using different blotting conditions with advice from Professor Lees-Miller, no signal was detected using the DNA-PK$_{cs}$ serine 3205 antibody. Having detected but failed to validate this DNA-PK$_{cs}$ phosphorylation, efforts focused on other DNA-PK$_{cs}$ phosphorylation sites for which well-characterised phospho-antibodies were available.

Serine 2056 and threonine 2609 phosphorylation have been associated with radio-resistance (Deshpande et al., 2020; Jiang et al., 2015; Mohiuddin and Kang, 2019) and phosphorylation of threonine 2609 has been shown to be necessary for DSB repair (Block et al., 2004; Chan et al., 2002a; Crowe et al., 2020; Ding et al., 2003; Nagasawa et al., 2011, 2017). Cell lysates collected pre- and post-IR in IGF-1R WT cells and null cells were analysed by Western blot. As with the serine 3205 antibody, the threonine 2609 antibody detected no signal. Strikingly however, phosphorylation of serine 2056 was increased post-IR at all radiation doses in IGF-1R WT cells compared to IGF-1R null cells, with the greatest disparity in phosphorylation between clones exhibited at 8 Gy (Fig. 6.5). Further, phosphorylation of RPA32 at serine 4/serine 8 was also increased in IGF-1R WT cells, a site reported to be mainly phosphorylated by DNA-PK_{cs} (Ashley et al., 2014; Binz et al., 2004; Leimbacher et al., 2019; Liaw et al., 2011; Maréchal and Zou, 2013). Phosphorylation of KAP1 at serine 824 showed the expected increase post-IR. The reason for high basal phosphorylation of CHK2 at threonine 68 in IGF-1R WT cells was unclear and was different from the low basal level seen previously (Fig. 4.11A). However the post-IR responses of these phosphorylation events were not different between IGF-1R WT and IGF-1R null clones (Fig. 6.5), consistent with results shown previously (Fig. 5.2), suggesting no loss of ATM function in IGF-1R null cells (White et al., 2006; Zhou et al., 2000; Ziv et al., 2006).

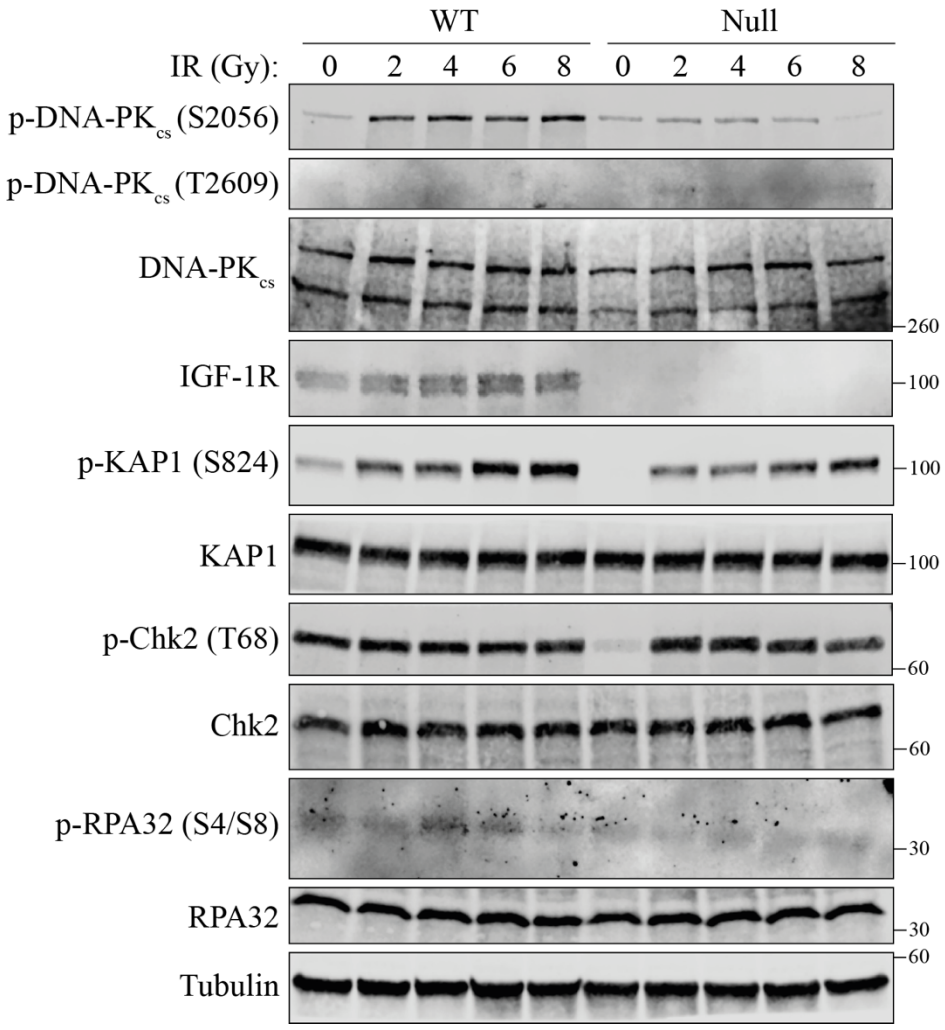

Figure 6.5: Analysis of response to increasing radiation dose in IGF-1R WT and null clones. IGF-1R WT (WT clone 1) and IGF-1R null (Null clone 1) clones were plated in 10 cm dishes (1 x 10^6 cells/dish), the following day were irradiated at indicated doses and whole cell lysates were extracted 10 minutes post-IR. Whole cell lysates were used for Western blot analysis using β-tubulin as a loading control, and the same result was obtained using a second set of independently prepared lysates (n=2).

The observed difference in serine 2056 phosphorylation implicated IGF-1R either directly or indirectly, in phosphorylation of DNA-PK_{cs} in response to IR. Due to the highly conserved nature of the PIKK domains of the major DDR kinases (Blackford and Jackson, 2017), cell lysates were obtained pre- and post-8 Gy IR, the dose at which there was the clearest difference between IGF-1R WT and null cells (Fig. 6.5). Western blotting was performed for phosphorylation of ATM at serine 1981, to examine whether a similar difference in phosphorylation was observed between IGF-1R WT and null cells post-IR. No significant

difference in phosphorylation of ATM serine 1981 was observed between IGF-1R WT and null clones after IR, consistent with the lack of difference in KAP1 and CHK2 phosphorylation (Fig. 5.2, 6.5). In contrast there was again greater phosphorylation of DNA-PK_{cs} at serine 2056 in IGF-1R WT cells, and repeat experiments confirmed that the difference was significant (Fig. 6.6), while there was no increase in IR-induced phospho-serine 2056 in IGF-1R null cells.

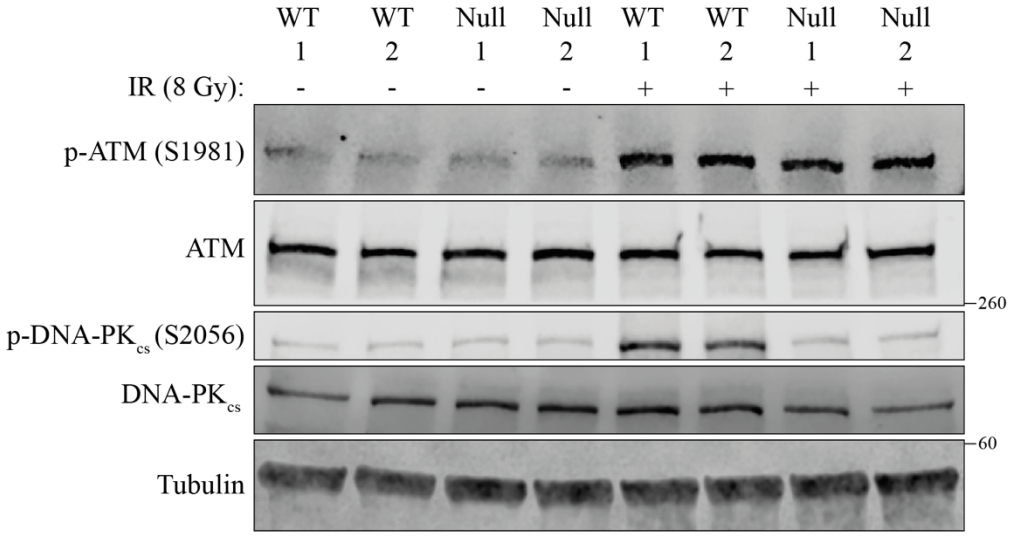
WT 1
WT 2
Null 1
Null 2
WT 1
WT 2
Null 1
Null 2
IR (8 Gy): - - - - + + + +
p-ATM (S1981)
ATM
p-DNA-PKcs (S2056)
DNA-PKcs
Tubulin
260
60

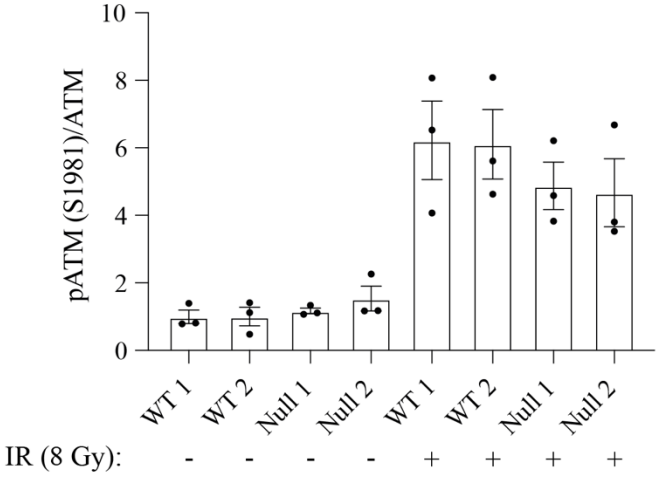
pATM (S1981)/ATM
0
2
4
6
8
10
WT 1
WT 2
Null 1
Null 2
WT 1
WT 2
Null 1
Null 2
IR (8 Gy): - - - - + + + +

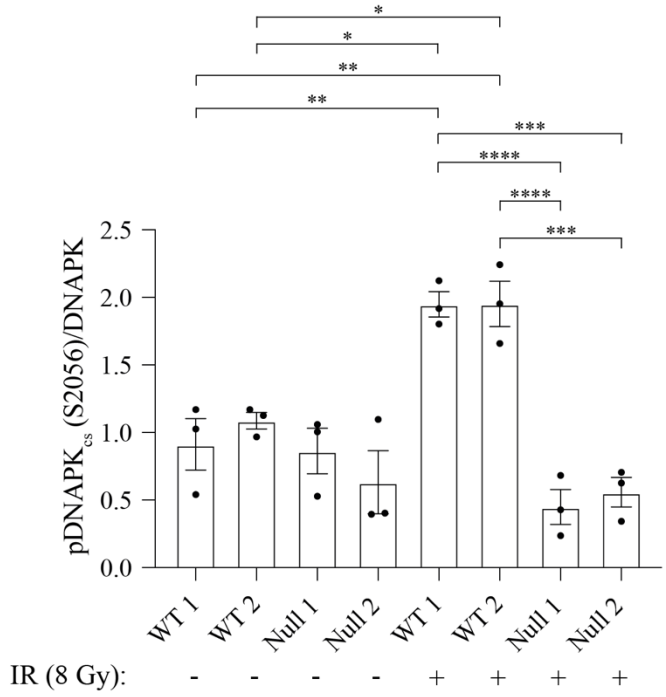
*
*
**
**
***
****
****
***
pDNAPKcs (S2056)/DNAPK
0.0
0.5
1.0
1.5
2.0
2.5
WT 1
WT 2
Null 1
Null 2
WT 1
WT 2
Null 1
Null 2
IR (8 Gy): - - - - + + + +

Figure 6.6: Analysis of phosphorylation of ATM and DNA-PK$_{cs}$ in the response to IR in IGF-1R WT and null clones.
Two IGF-1R WT and two IGF-1R null clones were plated in 10 cm dishes (1 x 10^6 cells/dish) and the following day dishes were subjected to 8 Gy irradiation. Whole cell lysates were extracted 10 minutes post-IR and used for Western blot analysis using β-tubulin as a loading control. The blot shown is representative of three independent experiments. Quantification was performed using ImageJ software and a one-way ANOVA was used to determine the significance of differences between clones (*p<0.05, **p<0.01, ***p<0.001, ****p<0.0001).

To further investigate the apparent effect of IGF-1R status on DNA-PK$_{cs}$ phosphorylation, IF was performed on IGF-1R WT and null cells pre- and post-IR, to detect foci formed by serine 2056 and threonine 2609 phosphorylated DNA-PK$_{cs}$. In contrast to detection in Western blot, serine 2056 phosphorylation could not be detected by IF (not shown), but these experiments did detect IR-induced phospho-threonine 2609 DNA-PK$_{cs}$ foci. Quantification showed significantly increased foci after IR in both IGF-1R WT and null cells. Additionally, there were significantly more phospho-threonine 2609 DNA-PK$_{cs}$ foci 10 min after IR in IGF-1R WT cells compared to IGF-1R null cells (Fig. 6.7).

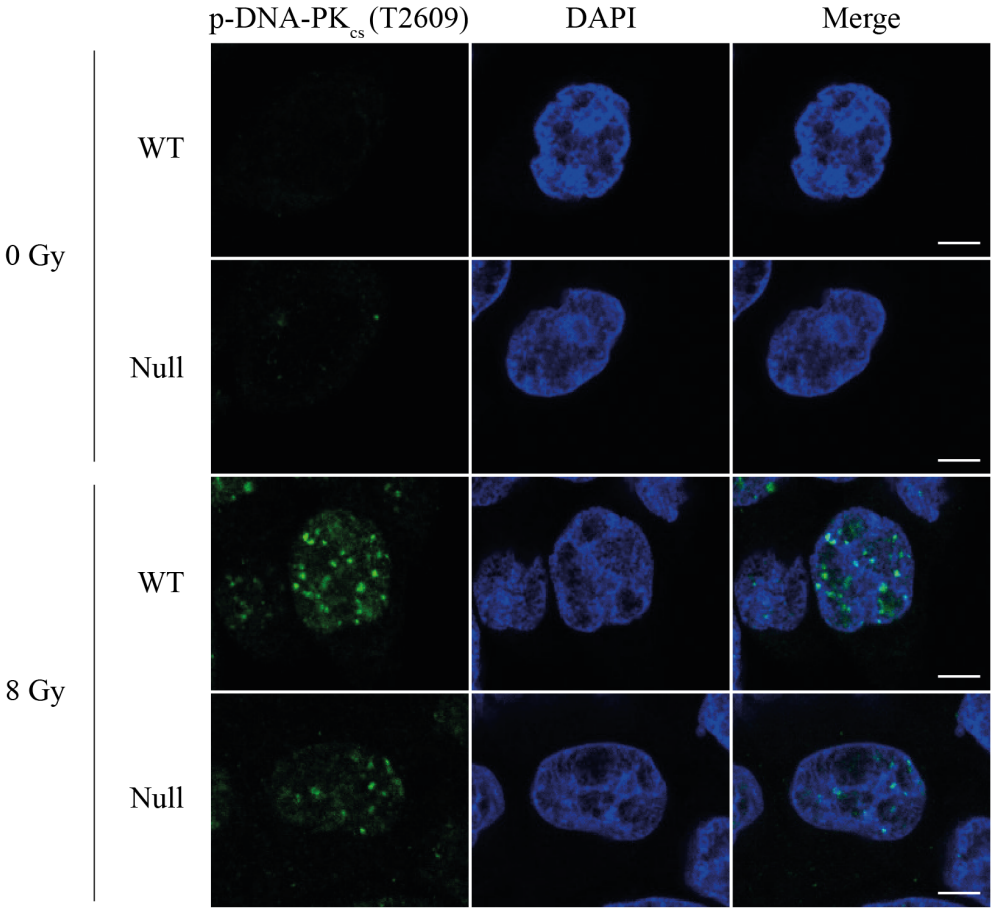
p-DNA-PKcs (T2609)
DAPI
Merge
0 Gy
8 Gy
WT
Null
WT
Null

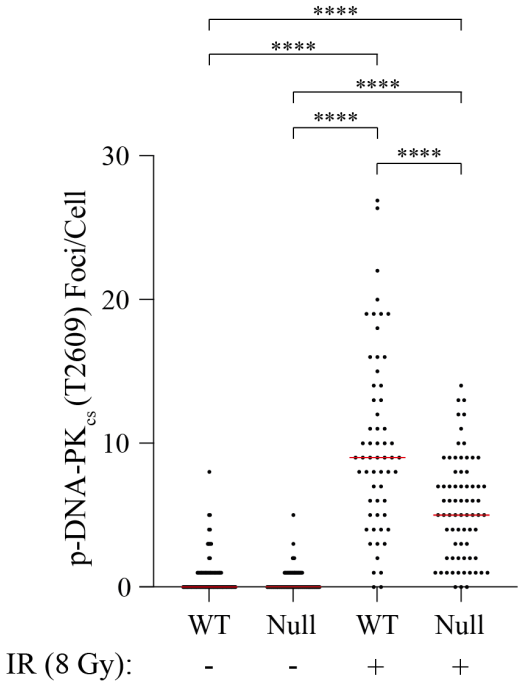
****
****
****
****
****
30
20
10
0
p-DNA-PKcs (T2609) Foci/Cell
WT
Null
WT
Null
IR (8 Gy):
-
-
+
+

Figure 6.7: Investigation of DNA-PK$_{cs}$ threonine 2609 phosphorylation after IR in IGF-1R WT and null cells.
A clone expressing WT IGF-1R (WT clone 1) and an IGF-1R null clone (Null clone 1) were seeded on coverslips in triplicate in 6 well plates (1 x 10^5 cells/well) and the following day required wells were subjected to 8 Gy irradiation. Cells were fixed 10 minutes after IR and stained for p-DNA-PK$_{cs}$ T2609. Images show p-DNA-PK$_{cs}$ T2609 (green), nuclear DAPI (blue) and both merged in unirradiated cells and cells at 10 mins post-IR. Images were taken at 63x magnification, scale bar represents 10 μm. Red line indicates mean number of γH2AX foci/cell. Quantification of p-DNA-PK$_{cs}$ T2609 foci pooled from three independent experimental repeats was performed using ImageJ software and a one-way ANOVA was used to determine the significance of differences between clones (****$p<0.0001$).

Given the apparent differences in DNA-PK$_{cs}$ phosphorylation of serine 2056 between IGF-1R WT and null cells, inhibition of the major IGF-1R signalling pathways was carried out, to see whether inhibition of these pathways in IGF-1R WT cells led to comparable reduction or loss of DNA-PK$_{cs}$ phosphorylation. IGF-1R WT cells were treated with BI885578 (IGF-1R TKI), Trametinib (MEK1/2 inhibitor), AZD5363 (AKT inhibitor) or NU7441 (DNA-PK inhibitor) for 4 hours prior to IR.

Western blot indicated inhibition of IGF-1R and MEK1/2 by absence of detectable phosphorylation of IGF-1R and ERK1/2 at tyrosine 1135/6, and threonine 202 and tyrosine 204, respectively (Fig. 6.8). The bioactivity of AZD5363 was confirmed by inhibition of phospho-S6 (serine 240/244), while AKT phosphorylation on serine 473 was strikingly increased, likely reflecting feedback attempts to activate AKT in response to allosteric inhibition by AZD5363 (Greenwood et al., 2011) (Fig. 6.8). AKT phosphorylation was not otherwise detectable in control-treated cells or in the other treatment conditions, consistent with previous attempts.

Although clearly inhibiting IGF-1R phosphorylation, BI885578 treatment did not appear to impact DNA-PK$_{cs}$ serine 2056 phosphorylation, contrasting with the difference observed

between IGF-1R WT and null clones (Fig. 6.8). Further, Trametinib treatment displayed no change in DNA-PKcs serine 2056 phosphorylation (Fig. 6.8). Upon AZD5363 treatment, Western blot displayed decreased DNA-PK_{cs} phosphorylation at serine 2056, with no apparent effect on ATM phosphorylation (Fig. 6.8). In the absence of detectable basal phospho-AKT it was unclear whether other pathways could have compensated for IGF-1R inhibition, although reduction in S6 phosphorylation was detected in BI885578-treated cells.

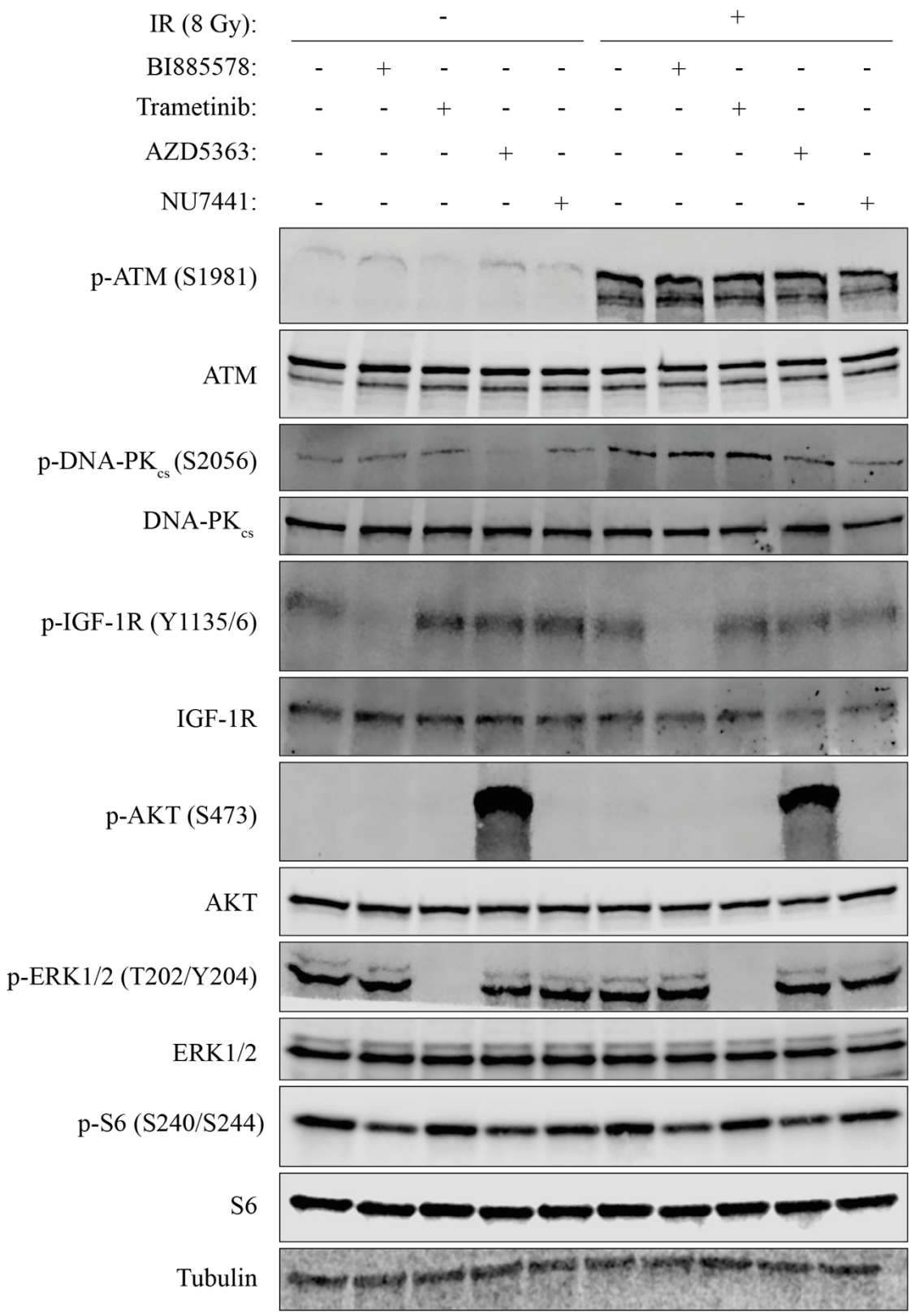

Figure 6.8: Investigation of inhibition of major IGF-1R signalling pathways.
IGF-1R WT cells were plated in 10 cm dishes (1 x 10^6 cells/dish) and the following day required dishes were treated with specified inhibitor 4 hours pre-IR (8 Gy). Whole cell lysates were extracted 10 minutes post-IR and used for Western blot analysis using β-tubulin as a loading control. Western blot is representative of three independent repeats.

6.4 Investigating DNA-PK$_{cs}$ recruitment to chromatin

Thus, Western blot and IF showed differences between IGF-1R WT and null cells in IR-induced DNA-PK$_{cs}$ serine 2056 and threonine 2609 phosphorylation and RPA32 phosphorylation at serine 4 and 8 (Fig. 6.5-6.7). These findings prompted the investigation of a direct functional effect of differential DNA-PK$_{cs}$ phosphorylation, which occurs upon recruitment to DNA (Gell and Jackson, 1999; Singleton et al., 1999). DNA-PK$_{cs}$ activity may be required for the dissociation of Ku70/80 from chromatin, to allow later stages of cNHEJ to proceed (Andrew Blackford, personal communication). Based on the apparent differences in DNA-PK$_{cs}$ phosphorylation and cNHEJ function observed in IGF-1R null cells post-IR compared to IGF-1R WT cells, we hypothesised that in IGF-1R null cells, Ku70/80 might show prolonged retention on chromatin post-IR.

Many repair factors are connected to chromatin via RNA, making it difficult to visualise these components at DSB sites using IF (Bekker-Jensen et al., 2006; Britton et al., 2013; Polo and Jackson, 2011). Development of an RNase- and detergent-based extraction method allows for assessment of chromatin-bound proteins via Western blot (Britton et al., 2013; Brown et al., 2015; Fantini et al., 2017; Ochi et al., 2015). This strategy was utilised to obtain chromatin fractions, and whole cell extracts were collected in parallel. IGF-1R WT and null cell lysates and chromatin were collected pre- and post-IR at the indicated time points, and subjected to Western blot analysis. In whole cell extracts, phosphorylation of ATM at serine 1981 was similar at each time point between IGF-1R WT and null cells. DNA-PK$_{cs}$ serine 2056 phosphorylation and RPA32 phosphorylation at serine 4/serine 8 were increased in IGF-1R WT cells compared to IGF-1R null cells, which was consistent with previous Western blot analyses implicating an effect on DNA-PK (Fig. 6.5-6.7, 6.9A). Upon inspection of proteins

associated with chromatin in irradiated IGF-1R null cells, both ATM and RAD51 appeared to be recruited to chromatin to a lesser extent than in IGF-1R WT cells, but this result must be repeated to confirm (Fig. 6.9B), as the careful preparation of chromatin was a lengthy procedure, and there was insufficient time to repeat this experiment.

Increase in chromatin-bound DNA-PK$_{cs}$ signal was detected in IGF-1R WT cells in response to IR (Fig. 6.9B). In contrast, DNA-PK$_{cs}$ was not detected on chromatin in IGF-1R null cells, which could explain or contribute to the differential radio-sensitivity observed here and in previous studies upon IGF-1R inhibition or depletion (Chitnis et al., 2014; Simpson et al., 2020; Turney et al., 2012; Zhao and Gu, 2014a) (Fig. 3.1, 4.1, 4.7). Chromatin-bound Ku was detected in IGF-1R WT cells and more faintly in IGF-1R null cells, although levels appeared unchanged pre- and post-IR (Fig. 6.9B). This differs from the reported damage-induced recruitment of Ku70/80 (Britton et al., 2013; Brown et al., 2015; Fantini et al., 2017; Ochi et al., 2015), however in the absence of damage-induced recruitment shown here, it is difficult to comment on Ku retention time.

A

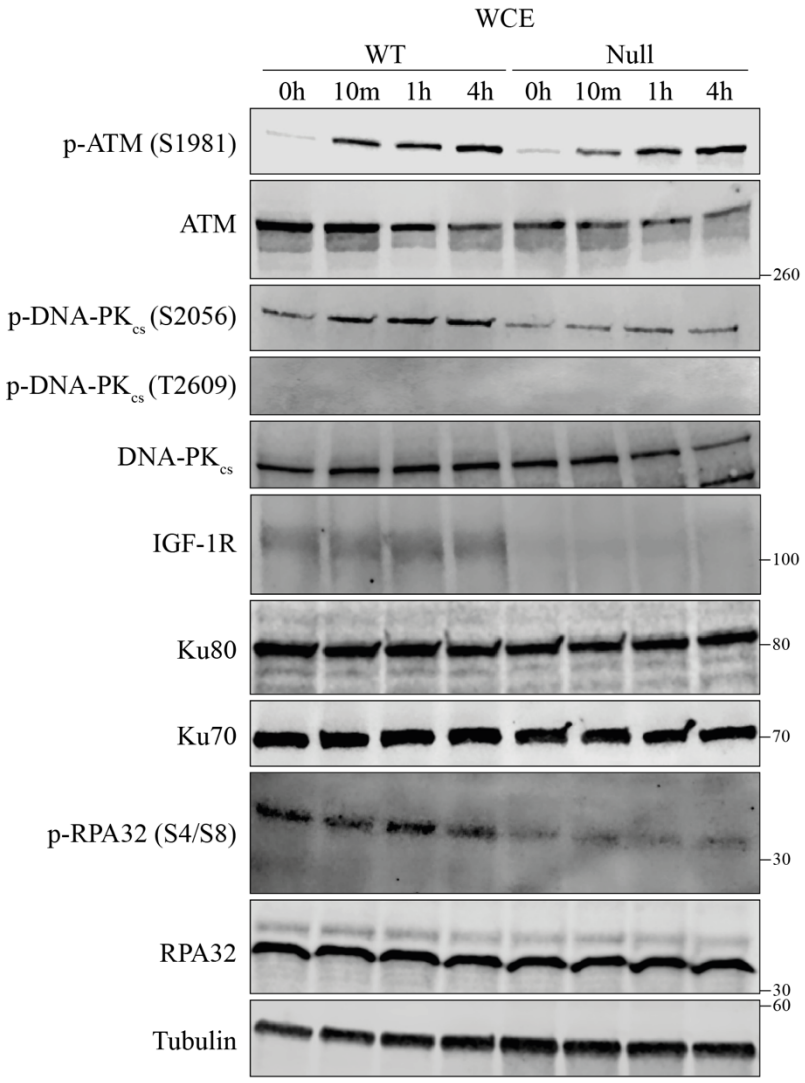
WCE
WT
Null
0h 10m 1h 4h 0h 10m 1h 4h
p-ATM (S1981)
ATM
p-DNA-PKcs (S2056)
p-DNA-PKcs (T2609)
DNA-PKcs
IGF-1R
Ku80
Ku70
p-RPA32 (S4/S8)
RPA32
Tubulin
260
100
80
70
30
30
60

B

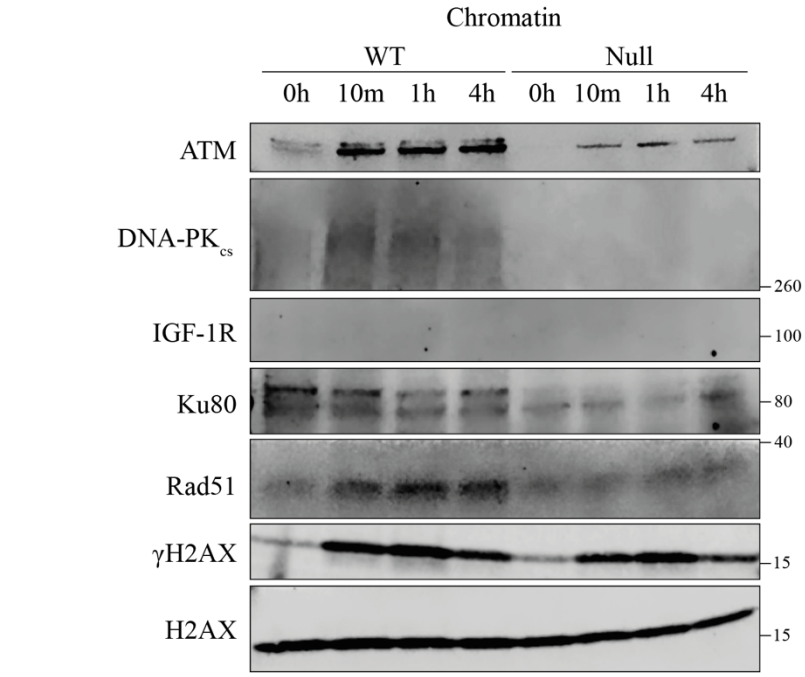
Chromatin
WT
Null
0h 10m 1h 4h 0h 10m 1h 4h
ATM
DNA-PKcs
IGF-1R
Ku80
Rad51
γH2AX
H2AX
260
100
80
40
15
15

Figure 6.9: Examination of proteins bound to chromatin after IR.
IGF-1R WT (WT clone 1) and null (Null clone 1) cells were plated in 10 cm dishes (1 x 10^6 cells/dish) in duplicate, and the following day required dishes were irradiated at 8 Gy. Whole cell lysates and chromatin fractions were collected in parallel at indicated time points post-IR and used for Western blot analysis using β-tubulin (for whole cell lysates) and H2AX (for chromatin fractionation) as loading controls.

6.5 Discussion

Work presented in this chapter suggested that the apparent radio-sensitisation phenotype of IGF-1R null cells could be because of cNHEJ defects due to loss of DNA-PK_{cs} recruitment and autophosphorylation. Results suggested that there was an increase in use of MMEJ to rejoin linearised plasmid in IGF-1R null cells (Fig. 6.1-2), and that DNA-PK_{cs} inhibition caused increased γH2AX foci in IGF-1R WT cells, but not in IGF-1R null cells (Fig. 6.3-4). Taken together, these data indicated that IGF-1R activity might affect DNA-PK_{cs} function in cNHEJ.

The relative proportion of cells employing MMEJ after IR was assessed by an end-joining assay, as cells use error-prone MMEJ when important cNHEJ components are not functioning (Guirouilh-Barbat et al., 2007; Sfeir and Symington, 2015; Sharma et al., 2015; Simsek and Jasin, 2010). Results suggested that pharmacological DNA-PK_{cs} inhibition may have caused an increase in use of MMEJ in IGF-1R WT cells (from ~10% in controls to ~30% after DNA-PK_{cs} inhibition, (Fig. 6.1)). This was consistent with other published data where DNA-PK_{cs} was inhibited (9-14% in controls vs 33-37% in DNA-PK_{cs} inhibitor-treated cells (Harvey et al., 2018; W. Li et al., 2019; Oh et al., 2014)). IGF-1R null cells exhibited similar relative levels of MMEJ (20-30%, (Fig. 6.1)) to DNA-PK_{cs} inhibitor-treated cells (~30%, (Fig. 6.1)). The detection of additional products as well as the 180 and 120 bp fragments upon BstXI digestion has been shown in other publications (Harvey et al., 2018; Oh et al., 2014), and were assumed to have been derived from digestion of genomic DNA present in the plasmid preparations. Additionally, the presence of a 100 bp product detected in some conditions without BstXI

treatment was consistent with other reports (Harvey et al., 2018; Oh et al., 2014). The initial publication detailing this assay used radio-labelled primers to only detect the 180 and 120 bp products, which could be used here to avoid visualising additional products (Verkaik et al., 2002).

Similarities between NU7441-treated WT cells and control-treated IGF-1R null cells were investigated further by quantification of γH2AX foci. IGF-1R null cells exhibited similar levels of γH2AX foci as IGF-1R WT cells treated with DNA-PK_{cs} inhibitor, and significantly more foci than untreated IGF-1R WT cells (Fig. 6.3-4). While novel, results from the end-joining assay and IF presented here (Fig. 6.1-4) were consistent with an epistatic relationship between IGF-1R and cNHEJ, as implicated previously in the Macaulay group in prostate cancer and glioblastoma cell lines (Chitnis et al., 2014). If time had permitted, clonogenic radiation survival assays would have been used to check for epistasis, by treating cells prior to irradiation with xentuzumab, NU7441 or in combination.

Given the role of 53BP1 in blocking end resection and therefore promoting cNHEJ (Bouwman et al., 2010; Cao et al., 2009; Daley and Sung, 2014), 53BP1 foci were quantified. IGF-1R WT cells exhibited significantly greater numbers of 53BP1 foci post-IR, further suggesting defective cNHEJ in cells lacking IGF-1R (Fig. 6.2). This specific effect is a novel finding and the functional implications are consistent with cNHEJ reporter assay results from the Macaulay lab (Chitnis et al., 2014).

Data shown here suggests that IGF-1R might be required for DNA-PK_{cs} to undergo serine 2056 phosphorylation (Fig 6.5-6, 6.9), and chromatin fractionation experiments indicated that

recruitment of DNA-PK$_{cs}$ to chromatin could be undetectable in IGF-1R null cells (Fig. 6.9). This apparent finding could be of major functional significance, so it will be important to repeat this experiment. Specifically, it has been reported that autophosphorylation is triggered by DNA-PK$_{cs}$ recruitment to chromatin (Blackford and Jackson, 2017; Gell and Jackson, 1999; Singleton et al., 1999), which may be consistent with data shown here (Fig. 6.5-6.6, 6.9). The presence of DNA-PK$_{cs}$ on chromatin has been shown to block nuclease-mediated degradation and premature ligation, but also interrupt efficient ligation (Block et al., 2004; Calsou et al., 1999; Cui et al., 2005b; Uematsu et al., 2007; Weterings et al., 2003; Weterings and van Gent, 2004). Further, remodelling associated with autophosphorylation of DNA-PK$_{cs}$ has been shown to release DNA ends, increasing accessibility for processing enzymes, resulting in more accurate repair (Block et al., 2004; Crowe et al., 2020; Cui et al., 2005b; Ding et al., 2003; Dynan and Yoo, 1998; Meek, 2020; Reddy et al., 2004; Weterings et al., 2003; S. Zhang et al., 2011). It has been proposed therefore, that DNA-PK$_{cs}$ serves to guard DNA ends until conditions are optimal, before autophosphorylation causes destabilisation of the DNA-PK complex and increased accessibility for ligases and other processing enzymes (Uematsu et al., 2007; Weterings et al., 2003; Weterings and van Gent, 2004).

The overall structure of DNA-PK$_{cs}$ consists of N-terminal Huntingtin, elongation factor 3, PP2A and TOR1 (N-HEAT), middle HEAT (M-HEAT), FRAP, ATM, TRRAP (FAT), kinase and FAT C-terminal (FATC) domains (Yin et al., 2017) (Fig. 6.10). The N-HEAT domain forming an open ring and the M-HEAT domain preserving the structural integrity of the DNA-PK complex provides a DNA-binding tunnel, where the inner surface contains many positively charged residues to promote DNA binding (Chen et al., 2021). Further, Ku70/80 interacts with the N-HEAT and M-HEAT domains and the catalytic pocket of the kinase domain is oriented externally for substrate phosphorylation (Chaplin et al., 2021; Chen et al., 2021). Two

autophosphorylation clusters located in the M-HEAT domain contain the major phosphorylation sites serine 2056 and threonine 2609 in the PQR and ABCDE clusters, respectively (Cui et al., 2005b; Imseng et al., 2018; Kurosawa, 2021; Meek, 2020) (Fig. 6.10).

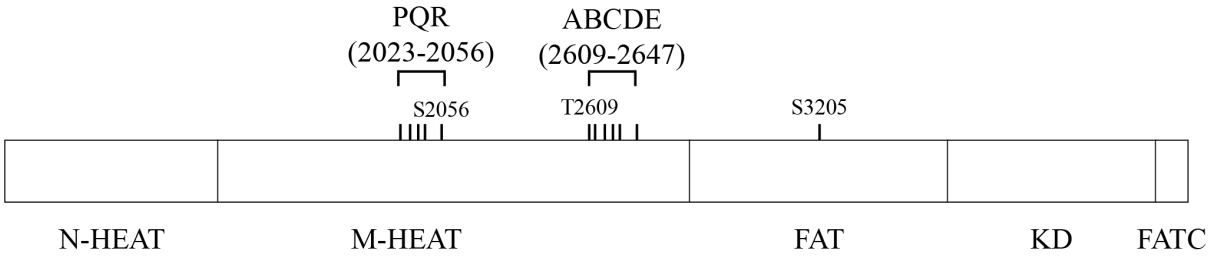

Figure 6.10: Schematic of the organisation of DNA-PK$_{cs}$ domains and key phosphorylation sites.
Diagram depicting the location of domains within DNA-PK$_{cs}$ and key phosphorylation sites, adapted from Kong *et al.* (2011).

Elucidating the role of DNA-PK$_{cs}$ autophosphorylation at the ABCDE and PQR clusters has proven difficult, and there are conflicting reports in the literature regarding requirement for recruitment to and dissociation from chromatin. Some reports provide evidence that inhibition or loss of the kinase domain, or non-phosphorylatable mutation of threonine 2609 prevents the release of DNA-PK$_{cs}$ from DNA ends, and that autophosphorylation correlates with abrogation of kinase activity and dissociation from DNA (Douglas et al., 2002; A Kurimasa et al., 1999; Uematsu et al., 2007; Zhao et al., 2006). Further, ABCDE cluster phosphorylation is reported to cause the removal of DNA-PK$_{cs}$ from chromatin (Block et al., 2004; Dobbs et al., 2010; Douglas et al., 2007, 2001; Hammel et al., 2010; Merkle et al., 2002), and the process occurs faster in DNA-PK$_{cs}$ WT cells compared to those with alanine substitutions at serine 2056 and threonine 2609 to prevent autophosphorylation (Hammel et al., 2010; Uematsu et al., 2007). The apparent requirement of threonine 2609 DNA-PK$_{cs}$ autophosphorylation for its removal from chromatin contrasts with data shown here in IGF-1R WT cells, where threonine 2609

phosphorylation of DNA-PK$_{cs}$ was potentially detected by IF (Fig. 6.7) together with DNA-PK$_{cs}$ recruitment to chromatin (Fig. 6.9). One possibility for this discrepancy was that the observed phospho-DNA-PK$_{cs}$ threonine 2609 foci in IF experiments could in fact have been detecting 53BP1 foci, rather than changes in phospho-DNA-PK$_{cs}$ (Fig. 6.2, 6.7). This is because the abundance of SQ motifs at the N-terminus of 53BP1 can be recognised by phospho-DNA-PK$_{cs}$ antibodies raised to related phospho-motifs (Anderson et al., 2001; Matsuoka Shuhei et al., 2007). Therefore, it is possible that the images shown in figure 6.7 were actually foci formed by 53BP1, not phospho-threonine 2609 DNA-PK$_{cs}$. Indeed, comparing figures 6.2 and 6.7, the detected differences between IGF-1R WT and null cells were very similar. Phosphorylation of DNA-PK$_{cs}$ at threonine 2609 was not detected by Western blot in figure 6.9. This could be due to a technical issue with the antibody, which could be addressed in the future by testing multiple antibodies to this phospho-epitope. Additionally, threonine 2609 phosphorylation could be below the limit of detection in 22Rv1 cells. This could be tested by analysing lysates in parallel from an alternative cell line where threonine 2609 DNA-PK$_{cs}$ phosphorylation was previously detected (eg. HeLa or H1299 cells (Chan et al., 2002b; Noh and Juhnn, 2020). Further Western blot analyses of cell lysates with a functional phospho-DNA-PK$_{cs}$ threonine 2609 antibody is required to make any conclusions on the role of IGF-1R in the autophosphorylation of this residue. The availability of a DNA-PK$_{cs}$ knockout or kinase-dead cell line would be beneficial to resolve this issue.

To further add to the complexity, evidence suggests that phosphorylation of serine 2056 and threonine 2609 are antagonistic, with serine 2056 responsible for inhibiting end processing, whereas threonine 2609 phosphorylation promotes it (Cui et al., 2005). Additionally, autophosphorylation of ABCDE sites allows for accessible DNA ends while DNA-PKcs is still present on DNA (Goodarzi et al., 2006; Reddy et al., 2004). This report is consistent with data

shown here that DNA-PK$_{cs}$ may persist on chromatin after autophosphorylation, although the observed reduction in phosphorylation of serine 2056 in IGF-1R null cells requires further investigation (Fig. 6.9). Further, prevention of autophosphorylation has been reported to be highly radio-sensitising and these cells exhibited defective DNA repair (Block et al., 2004; Ding et al., 2003). Additionally, HR was also suppressed, providing evidence that autophosphorylation might affect DDR pathway choice (Cui et al., 2005). This would correlate with the observation of reduced RAD51 presence on chromatin in IGF-1R null cells (Fig. 6.9), and the reduction in HR (albeit to a lesser degree than changes in cNHEJ) identified in IGF-1R inhibited repair reporter cells in previous work from our group (Chitnis et al., 2014).

The possible requirement of IGF-1R for DNA-PK$_{cs}$ serine 2056 phosphorylation identified here (Fig. 6.5-6), could be related to the apparent requirement for DNA-PK$_{cs}$ recruitment to chromatin (Fig. 6.9). Indeed, a report has detailed that autophosphorylation was required for a conformational modification of the DNA-PK complex bound to DNA ends before ligation, and a remodelling defect due to lack of DNA-PK$_{cs}$ autophosphorylation caused increased radio-sensitivity and defective repair of IR-induced DSBs (Ding et al., 2003). However, multiple groups have reported no correlation between DNA-PK$_{cs}$ autophosphorylation and dissociation from DNA (Cary et al., 1997; Ding et al., 2003; Weterings et al., 2003; Yoo and Dynan, 1999). In fact, a report noted that autophosphorylation was crucial for a conformational modification of the DNA-PK complex bound to DNA ends before ligation, and further that a remodelling defect due to a lack of DNA-PK$_{cs}$ autophosphorylation caused increased radio-sensitivity and defective repair of IR-induced DSBs (Ding et al., 2003). Increased phosphorylation of serine 2056-DNA-PK$_{cs}$ has been reported 1 hour after IR in patient derived prostate cancer explants, and the authors suggest that this is indicative of induction of NHEJ (Gilbreath et al., 2021), which correlates with conclusions presented here.

Data presented here could implicate IGF-1R in the recruitment of DNA-PK$_{cs}$ to chromatin (Fig. 6.9). Given the IGF-1R-dependent phosphorylation of serine 2056 of DNA-PK$_{cs}$ (Fig. 6.5-6) and the requirement of Ku for DNA-PK$_{cs}$ autophosphorylation, it is reasonable to suggest that Ku recruitment might be impacted by IGF-1R, as DNA-PK$_{cs}$ recruitment has been reported to occur after initial Ku binding to DNA ends (Gell and Jackson, 1999; Singleton et al., 1999). To test whether Ku recruitment is detectable in cells expressing WT IGF-1R and altered in IGF-1R null cells, it would be beneficial to use the radio-mimetic agent phleomycin (Mehta and Haber, 2014; Tounekti et al., 2001). This agent can be used for short-term (1 hr) exposure *in vitro* at concentrations that generate many more DSBs than 8 Gy IR (Andrew Blackford, personal communication), and it is this much greater damage induction that has been required to assess damage-induced Ku recruitment in previous reports (Brown et al., 2015; Ochi et al., 2015).

Recruitment of DNA-PK$_{cs}$, and Ku if also affected, may require signalling via IGF-1R. The novel IGF-1R-dependent DNA-PK$_{cs}$ autophosphorylation site shown here (Fig. 6.5-6) was likely not directly caused by IGF-1R, in contrast to ATM/ATR which can phosphorylate threonine 2609, as the consensus is that IGF-1R only phosphorylates tyrosine residues on itself and other proteins such as IRS-1 (De Meyts and Whittaker, 2002b). Therefore, it is probable that the phosphorylation of DNA-PK$_{cs}$ is indirect via downstream signalling from IGF-1R.

Consistent with this, inhibition of IGF-axis components suggested that defective signalling through AKT might be causing the decreased DNA-PK$_{cs}$ phosphorylation in IGF-1R null cells post-IR (Fig. 6.8). This correlated with previous reports that activated AKT can interact with DNA-PK$_{cs}$ and promote DNA-PK$_{cs}$ autophosphorylation and activation, and DSB repair (Choi

et al., 2010; Toulany et al., 2017, 2012, 2008, 2006). Further, an AKT/DNA-PK$_{cs}$ complex was shown to bind to DNA duplex ends bound by Ku, using an *in vitro* DNA-cellulose pull-down assay (Toulany et al., 2012), although this report did not assess this binding in the context of chromatin binding in live cells. It must be noted here that IGF-1R inhibition did not cause a comparable decrease post-IR in serine 2056 phosphorylation as seen in IGF-1R null clones (Fig. 6.8), although repeat experiments would be required to confirm these differences. This discrepancy between pathway blockade due to enzyme inhibition or loss has been shown by poly (ADP-ribose) polymerase (PARP) inhibition experiments. Inhibition of PARP was demonstrated to be more effective than loss of PARP in disrupting DNA repair in the context of BRCA1/2 loss, as inhibition caused PARP trapping as well as inhibition of PARP activity, further disturbing the DNA damage response (Ashworth and Lord, 2018; Helleday, 2011; Lord and Ashworth, 2017; Ström et al., 2011; Strumberg et al., 2000). In that case enzyme inhibition was more effective than PARP loss, whereas the opposite effect was seen here. Reduction in phospho-serine 2056 DNA-PK$_{cs}$ in IGF-1R null (Fig. 6.5-6) vs IGF-1R-inhibited (Fig. 6.8) 22Rv1 cells could reflect the different duration of IGF-axis disruption, acute using IGF-1R TKI vs chronic in IGF-1R-deleted cells, and/or presence of inactive receptor vs receptor loss. To resolve these differences, it would be beneficial to test DNA-PK$_{cs}$ serine 2056 phosphorylation using cells expressing a kinase-dead IGF-1R and perform clonogenic assays with signalling inhibitor pre-treatment prior to irradiation.

In parallel with this work, Jack Mills (DPhil student, Macaulay Group) has been investigating interactions of nuclear IGF-1R in 22Rv1 cells, following previous reports of nuclear IGF-1R by our group and others (Aleksic et al., 2018, 2010; Sehat et al., 2010). Jack's proteomic analysis of the nuclear IGF-1R interactome in the IGF-1R WT and null clones, that were generated here, returned DNA-PK$_{cs}$ as the most significantly enriched in cells expressing WT

IGF-1R (unpublished). DNA-PK_{cs} was also among the proteins identified in analysis of the nuclear IGF-1R interactome in HCT116 colorectal cancer cells by the Larsson group (Yang et al., 2021). The latter study did not validate the IGF-1R:DNA-PK_{cs} interaction or investigate its potential significance, but did report IGF-1R interaction with NuMA, that is required to regulate the function of 53BP1 in DNA repair (Yang et al., 2021).

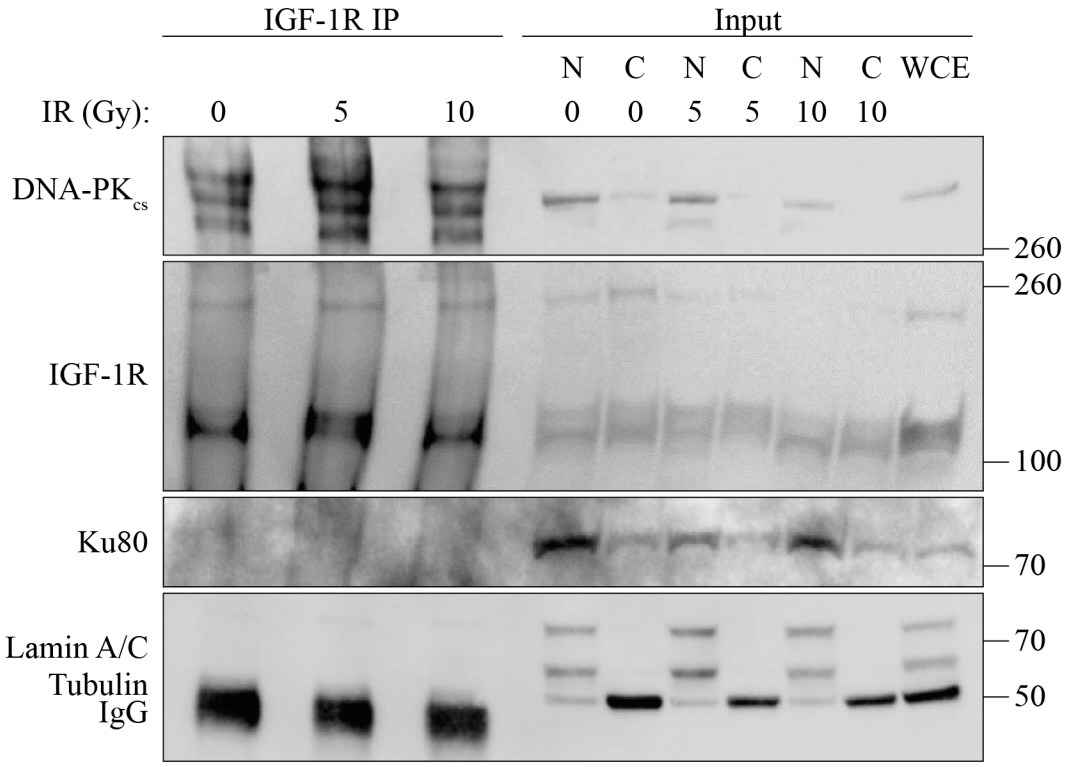

Figure 6.11: Validation of nuclear IGF-1R interaction with DNA-PK$_{cs}$.
Immunoprecipitation (IP) by Jack Mills using 22Rv1 cells. Cells were fractionated and nuclear lysates were immunoprecipitated with antibodies for IgG (as a control) or IGF-1Rβ. IPs were analysed by Western blot, as well as nuclear (N), cytoplasmic (C) and whole cell extract (WCE) input controls. Subcellular fractionation was checked by blotting for nuclear marker lamin A/C (~70 and 65 kDa, respectively) and cytosolic marker β-tubulin (55 kDa).

The interaction of IGF-1R with DNA-PK$_{cs}$ was validated in 22Rv1 cells by Jack Mills using IP experiments, on nuclear fractions isolated using a method that predominantly recovers soluble proteins from the nucleus, rather than proteins bound to chromatin or membrane proteins in the nuclear envelope (Fig. 6.11). This could explain the absence of IGF-1R on chromatin but presence of DNA-PK$_{cs}$ shown here in IGF-1R WT cells. Additionally, Jack found no evidence of interaction between IGF-1R and Ku80, suggesting IGF-1R does not interact with the DNA-PK complex, only DNA-PK$_{cs}$. These data correlate with previous data in the Macaulay group indicating that IGF-1R does not co-localise with γH2AX (Aleksic and Macaulay, unpublished).

In summary, work presented in this chapter has shown that IGF-1R loss may impact DNA repair pathway choice, autophosphorylation of DNA-PK_{cs} on serine 2056, and possibly DNA-PK_{cs} recruitment to chromatin post-IR. These data suggest a requirement of IGF-1R for proper DNA-PK_{cs} function in response to IR, which could implicate the use of IGF-axis inhibitors with radiotherapy to overcome radio-resistance by affecting cNHEJ.

CHAPTER VII: Conclusion and future directions

The main aim of this project was to investigate the molecular basis for IGF-1R-mediated radio-resistance using an AR-positive 22Rv1 prostate cancer model. Firstly, the radio-sensitisation effect exhibited upon IGF-1R depletion previously in the lab (Chitnis et al., 2014; Turney et al., 2012) was observed in AR positive 22Rv1 prostate cancer cells (Fig. 3.1). Therefore, this cell line was used as a model in which to attempt to generate IGF-1R null (Fig. 3.2-3.6) and kinase-dead clones using CRISPR/Cas9 gene editing techniques (Fig. 3.7-15). Efforts using HDR-mediated gene editing (Fig. 3.7-11) and base editing (Fig. 3.12) to generate the published IGF-1R K1003A/R kinase-dead mutant (Kato et al., 1993; Ullrich et al., 1986) proved unsuccessful, while prime editing showed promising preliminary results (Fig. 3.14-15). Creation of a hypomorphic mutant (Fig. 3.11) provided a useful tool to examine the gene dosage effect of IGF-1R in mediating radio-resistance, and in the future, it would be worth pursuing prime editing to generate clones expressing the IGF-1R K1003R mutant, after encouraging preliminary analyses detailed here (Fig. 3.14-15). Due to time constraints it was not possible to complete the expansion, sequencing and characterisation of prime-edited clones potentially harbouring K1003R IGF-1R.

Therefore, the hypomorphic clone and IGF-1R null clones were used in parallel with cloned parental 22Rv1 cells expressing endogenous WT IGF-1R to explore possible radio-sensitisation in IGF-1R compromised cells. IGF-1R null clones and the hypomorphic mutant were found to exhibit similar radio-sensitisation in 2D clonogenic survival assays as seen upon IGF-1R depletion (Fig. 3.1, 4.1, 4.7). A 3D model was developed to measure radio-sensitivity, revealing that spheroids formed from IGF-1R null cells or cells expressing hypomorphic IGF-1R grew more slowly, but were no more radio-sensitive than cells expressing WT IGF-1R (Fig.

4.9-10). This could potentially be due to the presence of hypoxic regions of spheroids (Patiar and Harris, 2006) and compensation by signalling pathways activated in 3D vs 2D (Riedl et al., 2017), and suggested that mechanisms through which IGFs regulate cell survival differ from those regulating radio-resistance. IGF-1R compromised cells also displayed increased γH2AX foci at 10 minutes and 1 hour post-IR compared to clones expressing WT IGF-1R (Fig. 4.12). This suggested increased damage induction in clones lacking IGF-1R.

Unbiased proteomic and phosphoproteomic screens were performed pre- and post-IR to investigate the molecular pathways underpinning the radio-sensitivity phenotype. Analysis of the proteomic and phosphoproteomic data focused only on clones expressing WT IGF-1R and IGF-1R null cells. Biological pathway analysis using DAVID software highlighted differential phosphorylation of metabolic pathway proteins, chromatin remodelling factors and DDR proteins (Fig. 5.8-11). Examination of individual phosphorylation sites uncovered multiple as yet uncharacterised sites in the literature, however some reported phosphorylation sites on proteins such as 53BP1 and DNA-PK_{cs} were detected (Fig. 5.12-14, Table 5.2-3). Subsequent investigation of DNA-PK_{cs} phosphorylation in IGF-1R WT and null clones suggested that IGF-1R might be involved in DNA-PK_{cs} phosphorylation after IR (Fig. 6.5-6). Further, cNHEJ may also be compromised in IGF-1R null cells (Fig. 6.1-2), and that IGF-1R may contribute to the recruitment of DNA-PK_{cs} to chromatin (Fig. 6.9).

These data presented here indicate the possibility of blocking IGF signalling to interfere with DNA repair pathways, with the aim of sensitising cancer cells to radiotherapy. Multiple strategies have been developed to impede IGF-1R signalling including molecular approaches, anti-IGF-1R agents and targeting of IGF ligands. Depletion of IGF-1R using antisense

oligonucleotides or siRNAs has been shown to inhibit prostate cancer xenograft growth (Furukawa et al., 2010) and enhance sensitivity to radiotherapy, chemotherapy, and targeted agents *in vitro* (Chitnis et al., 2014; Simpson et al., 2020; Turney et al., 2012; Zhao and Gu, 2014a). However, limitations of siRNAs including short half-life, instability and poor uptake into cells, have hindered their clinical use. Strategies to overcome these issues have focussed on delivery approaches and chemical modifications, and there are many clinical trials of siRNAs, including some in cancer (El Dika et al., 2019; Hattab et al., 2021; Kumthekar et al., 2021; Xiong et al., 2021).

Monoclonal antibodies (mAbs) targeting IGF-1R aim to selectively block IGF binding and instigate IGF-1R internalisation and degradation. They cause increased circulating growth hormone, IGF-1 and IGFBP3 due to compensatory activation of the hypothalamic-pituitary axis (Pollak, 2012, 2008). Early phase clinical trials for cancer patients have produced mostly negative results, although some patients have exhibited durable responses (Anderson et al., 2016; Tolcher et al., 2009), however no effective predictive biomarkers to identify these patients were found in advance. Encouraging data indicated that 10-14% of Ewing sarcoma patients responded to IGF-1R mAb treatment, and that there could be a benefit from treating in combination with an mTOR inhibitor (Amin et al., 2020). A common side effect of IGF-1R targeting antibodies is dose-limiting hyperglycaemia (Pandini et al., 2007; Sachdev et al., 2006). Inhibition of IGF-1R causes an endocrine response leading to glucose intolerance, and co-downregulation of INSR in IGF-1R:INSR hybrid receptors, leading to increased growth hormone and IGFBP3, which both impair glucose tolerance (Pollak et al., 2004). If dosing of IGF-1R inhibitor is interrupted or reduced due to hyperglycaemia, high ligand levels can potentially lead to rebound tumour growth.

Small molecule TKIs have been developed to block IGF-1R kinase activity and thus downstream signalling. The major difficulty associated with IGF-1R TKIs is the high sequence homology between IGF-1R and INSR-A/B kinase domains, and 100% identity between the ATP-binding clefts (Favelyukis et al., 2001; Tennagels and Werner, 2013). This poses a problem, as while blocking compensatory INSR-A signalling, IGF-1R TKIs also directly compromise metabolic insulin signalling via INSR-B. Further, due to the short half-like exhibited by small molecule TKIs, intermittent inhibition of IGF-1R can lead to increased signalling when TKI-mediated blockade is absent (Jones et al., 2015; Macaulay et al., 2016). The reported presence of an endocrine feedback system while IGF-1R signalling is inhibited (Yee, 2015), leads to high IGF and insulin levels, a phenomenon possibly implicated in rebound tumour growth upon receptor reactivation and hypoglycaemia (Jones et al., 2015; Macaulay et al., 2016). To counter this, multiple reports highlight the use of IGF-1R inhibitors with metformin (Cao et al., 2016, 2015; Xie et al., 2014; Xue et al., 2021). Metformin exhibits anti-proliferative effects in breast cancer cells, inhibits migration and invasion in pancreatic cancer cells, causes downregulation of IGF-1R signalling in uterine serous carcinoma cells, and lowers blood sugar levels in mice (Bao et al., 2012; Horakova et al., 2019; Sarfstein et al., 2013; Zakikhani et al., 2006).

Non-ATP competitive IGF-1R inhibitors such as INSM-18 and AXL1717 have been shown to inhibit IGF-1R but not INSR, however they also block additional targets including c-erbB2/HER2/neu receptor and CDK1 (Aiken et al., 2017; Waraky et al., 2014; Weroha and Haluska, 2008; Youngren et al., 2005). Due to the lack of single agent activity, many IGF-1R inhibitor trials have been discontinued. Given preclinical data that identify IGF-1R as a mediator of treatment resistance (Benito-Jardón et al., 2019; Heskamp et al., 2015; Isozaki et al., 2016; Strub et al., 2018; Zhang et al., 2018), focus has moved to exploring the effects of

IGF-1R inhibitors in combination (Di Cosimo et al., 2015; Guenther et al., 2019; R. Wang et al., 2020), such as with CDK4/6 inhibitor treatment, which demonstrated a synergistic effect *in vitro* and impaired tumour progression and prolonged survival in mouse models (Guenther et al., 2019).

Given these shortcomings of IGF-1R TKI and mAb treatments, IGF ligand-neutralising antibodies have been trialled to block IGF-1R and INSR-A activity without impacting INSR-B-mediated insulin signalling and glucose metabolism (Friedbichler et al., 2013; Haluska et al., 2014). Xentuzumab, an IGF-1 and IGF-2 inhibitor, has been reported to block both human and murine IGFs, facilitating preclinical monitoring. The IGF neutralising antibody has displayed anti-cancer activity in combination with mTOR inhibition in human tumour xenografts, and growth abrogation in rats (Friedbichler et al., 2013; Mireuta et al., 2014). Currently, xentuzumab is being tested in combination in several clinical trials for EGFR-mutant lung cancer, prostate cancer and hormone receptor positive breast cancer (NCT02191891, NCT02204072, NCT03659136). A Phase II clinical trial explored the use of xentuzumab in combination with everolimus and exemestane in patients with hormone receptor positive breast cancer. While there was no overall benefit from addition of xentuzumab, there was significant benefit in patients with non-visceral disease (Schmid et al., 2021). The results of this trial were sufficient to justify opening a new Phase II trial in patients with non-visceral disease (NCT03659136) and a new Phase II trial with the CDK4/6 inhibitor abemaciclib in breast cancer (NCT02123823). Xentuzumab has also been tested in a Phase II trial of xentuzumab in combination with enzalutamide after disease progression on docetaxel and abiraterone treatment (NCT02204072). Preliminary data suggest that progression-free survival was not altered compared to treatment with enzalutamide alone (Hussain et al., 2019); subgroup analysis is ongoing.

Amid the multitude of failed clinical trials, certain patients have been noted to respond extremely positively to IGF-1R signalling blockade (Aleksic et al., 2016; Olmos et al., 2010; Tolcher et al., 2009). These results hint at specific situations where inhibition of IGF-1R signalling could be exploited to produce desirable outcomes. Preclinical modelling and tissue analysis by the Macaulay lab and others is aiming to uncover predictive biomarkers to influence patient selection (Pitts et al., 2010; Rieunier et al., 2021; Simpson et al., 2017; Weyer-Czernilofsky et al., 2020; X Wu et al., 2021). In prostate cancer, preclinical data suggest that loss of PTEN renders tumours refractory to xentuzumab (Weyer-Czernilofsky et al., 2020).

Inhibition of IGF-1R has been trialled to decrease the chemo-resistance associated with IGF-1R. Groups have shown that treatment with IGF-1R inhibitor after administration of chemotherapy is significantly more effective at generating tumour growth delay, and that IGF-1R inhibition causes cell cycle arrest (de Bono et al., 2014; Ramcharan et al., 2015; Zeng et al., 2009). Similarly, IGF-1R-mediated radio-resistance has been reported by the Macaulay group and others in paediatric high-grade glioma, breast, prostate, head and neck cancers (Aleksic et al., 2017; Qureishi et al., 2019; Simpson et al., 2020; Turner et al., 1997). These data suggest that IGF-1R inhibition in combination with radiotherapy could be effective (de Bono et al., 2014; Flanigan et al., 2010).

Novel drug-radiotherapy combination strategies to enhance the biological effects of radiation focus on altering the tumour microenvironment, increasing the immune response, hindering resistance mechanisms or disrupting DNA repair mechanisms (Sharma et al., 2016). Mechanisms of reducing tumour hypoxia have been shown to be radio-sensitising, and signalling pathways that regulate radio-resistance have also been investigated, such as the

EGFR inhibitor cetuximab (Bonner et al., 2006; Nieder et al., 2012), PI3K inhibitor buparlisib (McGowan et al., 2019) and the mitochondrial metabolism inhibitor atovaquone (Skwarski et al., 2021).Targeting of downstream IGF-axis pathways have been shown to increase radio-sensitivity *in vitro* and *in vivo* (Kim et al., 2005; McKenna et al., 2003b), and pathway activation associates with poor clinical outcomes (Dergham et al., 1997; Gupta et al., 2004, 2002). In PCa, IGF-1R has been shown to associate with adverse outcomes after radical radiotherapy (Aleksic et al., 2017). Further, in multivariate analysis, cytoplasmic and total IGF-1R were independently associated with risk of overall recurrence, and cytoplasmic IGF-1R was an independent predictor of biochemical recurrence post-radiotherapy (Aleksic et al., 2017). These findings suggest that IGF-1R could be used as a predictive biomarker to inform treatment decisions, such as between radical surgery and radiotherapy for localised prostate cancer.

Work shown here may suggest that IGF-axis inhibitors could be useful in combination with radiotherapy to overcome radio-resistance by impacting cNHEJ. However, while potentially effective in the short-term, cNHEJ blockade offers the potential for long-term tissue toxicity due to the majority of normal cells residing in G1 where only cNHEJ-mediated repair occurs (Biehs et al., 2017; Delacôte and Lopez, 2008; Hahn et al., 2009). This reservation appears not to be insuperable, given that DNA-PK_{cs} inhibitors are being developed as therapeutic strategies (Willoughby et al., 2020), and are being tested clinically with radiotherapy in patients with advanced solid tumours (NCT02516813), or advanced head and neck (NCT04533750) or rectal cancer (NCT03770689). Similar to the rationale of McGowan et al., initial examination of the effect of IGF-1R pathway inhibition on radiation response in patients should combine an IGF inhibitory antibody dose escalation study with palliative radiotherapy in the first instance (McGowan et al., 2019). If well-tolerated, clinical trials of IGF ligand-neutralising antibodies

in combination with radical radiotherapy could be explored, with the aim of improving outcomes for patients with prostate cancer.

Reference list

Abbott, D.W., Holt, J.T., 1999. Mitogen-activated Protein Kinase Kinase 2 Activation Is Essential for Progression through the G2/M Checkpoint Arrest in Cells Exposed to Ionizing Radiation. Journal of Biological Chemistry 274, 2732–2742. https://doi.org/10.1074/jbc.274.5.2732

Abraham, R.T., 2001. Cell cycle checkpoint signaling through the ATM and ATR kinases. Genes & Development 15, 2177–2196. https://doi.org/10.1101/gad.914401

Abuzzahab, M.J., Schneider, A., Goddard, A., Grigorescu, F., Lautier, C., Keller, E., Kiess, W., Klammt, J., Kratzsch, J., Osgood, D., Pfäffle, R., Raile, K., Seidel, B., Smith, R.J., Chernausek, S.D., 2003. IGF-I Receptor Mutations Resulting in Intrauterine and Postnatal Growth Retardation. N Engl J Med 349, 2211–2222. https://doi.org/10.1056/NEJMoa010107

Adams, T.E., Epa, V.C., Garrett, T.P.J., Ward*, C.W., 2000. Structure and function of the type 1 insulin-like growth factor receptor. Cellular and Molecular Life Sciences CMLS 57, 1050–1093. https://doi.org/10.1007/PL00000744

Adesanya, O.O., Zhou, J., Samathanam, C., Powell-Braxton, L., Bondy, C.A., 1999. Insulin-like growth factor 1 is required for G2 progression in the estradiol-induced mitotic cycle. Proc Natl Acad Sci U S A 96, 3287–3291. https://doi.org/10.1073/pnas.96.6.3287

Adli, M., 2018. The CRISPR tool kit for genome editing and beyond. Nature Communications 9, 1911. https://doi.org/10.1038/s41467-018-04252-2

Afjehi-Sadat, L., Garcia, B.A., 2013. Comprehending dynamic protein methylation with mass spectrometry. Curr Opin Chem Biol 17, 12–19. https://doi.org/10.1016/j.cbpa.2012.12.023

Ahmed, N.N., Grimes, H.L., Bellacosa, A., Chan, T.O., Tsichlis, P.N., 1997. Transduction of interleukin-2 antiapoptotic and proliferative signals via Akt protein kinase. Proc Natl Acad Sci U S A 94, 3627–3632. https://doi.org/10.1073/pnas.94.8.3627

Aiken, R., Axelson, M., Harmenberg, J., Klockare, M., Larsson, O., Wassberg, C., 2017. Phase I clinical trial of AXL1717 for treatment of relapsed malignant astrocytomas: analysis of dose and response. Oncotarget 8, 81501–81510. https://doi.org/10.18632/oncotarget.20662

Aird, K.M., Worth, A.J., Snyder, N.W., Lee, J.V., Sivanand, S., Liu, Q., Blair, I.A., Wellen, K.E., Zhang, R., 2015. ATM couples replication stress and metabolic reprogramming during cellular senescence. Cell Rep 11, 893–901. https://doi.org/10.1016/j.celrep.2015.04.014

Akiel, M., Guo, C., Li, X., Rajasekaran, D., Mendoza, R.G., Robertson, C.L., Jariwala, N., Yuan, F., Subler, M.A., Windle, J., Garcia, D.K., Lai, Z., Chen, H.-I.H., Chen, Y., Giashuddin, S., Fisher, P.B., Wang, X.-Y., Sarkar, D., 2017. IGFBP7 Deletion Promotes Hepatocellular Carcinoma. Cancer Res 77, 4014. https://doi.org/10.1158/0008-5472.CAN-16-2885

Akkiprik, M., Hu, L., Sahin, A., Hao, X., Zhang, W., 2009. The subcellular localization of IGFBP5 affects its cell growth and migration functions in breast cancer. BMC Cancer 9, 103. https://doi.org/10.1186/1471-2407-9-103

Alcendor Ralph R., Gao Shumin, Zhai Peiyong, Zablocki Daniela, Holle Eric, Yu Xianzhong, Tian Bin, Wagner Thomas, Vatner Stephen F., Sadoshima Junichi, 2007. Sirt1 Regulates Aging and Resistance to Oxidative Stress in the Heart. Circulation Research 100, 1512–1521. https://doi.org/10.1161/01.RES.0000267723.65696.4a

Aleksic, T., Browning, L., Woodward, M., Phillips, R., Page, S., Henderson, S., Athanasou, N., Ansorge, O., Whitwell, D., Pratap, S., Hassan, A.B., Middleton, M.R., Macaulay, V.M., 2016. Durable Response of Spinal Chordoma to Combined Inhibition of IGF-1R and EGFR. Front Oncol 6, 98–98. https://doi.org/10.3389/fonc.2016.00098

Aleksic, T., Chitnis, M.M., Perestenko, O.V., Gao, S., Thomas, P.H., Turner, G.D., Protheroe, A.S., Howarth, M., Macaulay, V.M., 2010. Type 1 insulin-like growth factor receptor translocates to the nucleus of human tumor cells. Cancer Res 70, 6412–6419. https://doi.org/10.1158/0008-5472.CAN-10-0052

Aleksic, T., Gray, N., Wu, X., Rieunier, G., Osher, E., Mills, J., Verrill, C., Bryant, R.J., Han, C., Hutchinson, K., Lambert, A.G., Kumar, R., Hamdy, F.C., Weyer-Czernilofsky, U., Sanderson, M.P., Bogenrieder, T., Taylor, S., Macaulay, V.M., 2018. Nuclear IGF1R Interacts with Regulatory Regions of Chromatin to Promote RNA

Polymerase II Recruitment and Gene Expression Associated with Advanced Tumor Stage. Cancer Res 78, 3497. https://doi.org/10.1158/0008-5472.CAN-17-3498

Aleksic, T., Verrill, C., Bryant, R.J., Han, C., Worrall, A.R., Brureau, L., Larré, S., Higgins, G.S., Fazal, F., Sabbagh, A., Haider, S., Buffa, F.M., Cole, D., Macaulay, V.M., 2017. IGF-1R associates with adverse outcomes after radical radiotherapy for prostate cancer. Br J Cancer 117, 1600–1606. https://doi.org/10.1038/bjc.2017.337

Alessi, D.R., James, S.R., Downes, C.P., Holmes, A.B., Gaffney, P.R.J., Reese, C.B., Cohen, P., 1997. Characterization of a 3-phosphoinositide-dependent protein kinase which phosphorylates and activates protein kinase Bα. Current Biology 7, 261–269. https://doi.org/10.1016/S0960-9822(06)00122-9

Alhazzazi, T., Kamarajan, P., Verdin, E., Kapila, Y., 2011. SIRT3 and Cancer: Tumor Promoter or Suppressor? Biochimica et biophysica acta 1816, 80–8. https://doi.org/10.1016/j.bbcan.2011.04.004

Allen, F., Crepaldi, L., Alsinet, C., Strong, A.J., Kleshchevnikov, V., De Angeli, P., Páleníková, P., Khodak, A., Kiselev, V., Kosicki, M., Bassett, A.R., Harding, H., Galanty, Y., Muñoz-Martínez, F., Metzakopian, E., Jackson, S.P., Parts, L., 2019. Predicting the mutations generated by repair of Cas9-induced double-strand breaks. Nature Biotechnology 37, 64–72. https://doi.org/10.1038/nbt.4317

Almeida, L.O., Goto, R.N., Pestana, C.R., Uyemura, S.A., Gutkind, S., Curti, C., Leopoldino, A.M., 2012. SET overexpression decreases cell detoxification efficiency: ALDH2 and GSTP1 are downregulated, DDR is impaired and DNA damage accumulates. The FEBS Journal 279, 4615–4628. https://doi.org/10.1111/febs.12047

Almeida, L.O., Neto, M.P.C., Sousa, L.O., Tannous, M.A., Curti, C., Leopoldino, A.M., 2017. SET oncoprotein accumulation regulates transcription through DNA demethylation and histone hypoacetylation. Oncotarget 8, 26802–26818. https://doi.org/10.18632/oncotarget.15818

Amin, H.M., Morani, A.C., Daw, N.C., Lamhamedi-Cherradi, S.-E., Subbiah, V., Menegaz, B.A., Vishwamitra, D., Eskandari, G., George, B., Benjamin, R.S., Patel, S., Song, J., Lazar, A.J., Wang, W.-L., Kurzrock, R., Pappo, A., Anderson, P.M., Schwartz, G.K., Araujo, D., Cuglievan, B., Ratan, R., McCall, D., Mohiuddin, S., Livingston, J.A., Molina, E.R., Naing, A., Ludwig, J.A., 2020. IGF-1R/mTOR Targeted Therapy for Ewing Sarcoma: A Meta-Analysis of Five IGF-1R-Related Trials Matched to Proteomic and Radiologic Predictive Biomarkers. Cancers (Basel) 12, 1768. https://doi.org/10.3390/cancers12071768

An, H., Ordureau, A., Paulo, J.A., Shoemaker, C.J., Denic, V., Harper, J.W., 2019. TEX264 Is an Endoplasmic Reticulum-Resident ATG8-Interacting Protein Critical for ER Remodeling during Nutrient Stress. Molecular Cell 74, 891-908.e10. https://doi.org/10.1016/j.molcel.2019.03.034

Anastasiou, D., 2017. Tumour microenvironment factors shaping the cancer metabolism landscape. British Journal of Cancer 116, 277–286. https://doi.org/10.1038/bjc.2016.412

Anderson, L., Henderson, C., Adachi, Y., 2001. Phosphorylation and rapid relocalization of 53BP1 to nuclear foci upon DNA damage. Mol Cell Biol 21, 1719–1729. https://doi.org/10.1128/MCB.21.5.1719-1729.2001

Anderson, P.M., Bielack, S.S., Gorlick, R.G., Skubitz, K., Daw, N.C., Herzog, C.E., Monge, O.R., Lassaletta, A., Boldrini, E., Pápai, Z., Rubino, J., Pathiraja, K., Hille, D.A., Ayers, M., Yao, S.-L., Nebozhyn, M., Lu, B., Mauro, D., 2016. A phase II study of clinical activity of SCH 717454 (robatumumab) in patients with relapsed osteosarcoma and Ewing sarcoma. Pediatr Blood Cancer 63, 1761–1770. https://doi.org/10.1002/pbc.26087

Anzalone, A.V., Koblan, L.W., Liu, D.R., 2020. Genome editing with CRISPR–Cas nucleases, base editors, transposases and prime editors. Nature Biotechnology 38, 824–844. https://doi.org/10.1038/s41587-020-0561-9

Anzalone, A.V., Randolph, P.B., Davis, J.R., Sousa, A.A., Koblan, L.W., Levy, J.M., Chen, P.J., Wilson, C., Newby, G.A., Raguram, A., Liu, D.R., 2019. Search-and-replace genome editing without double-strand breaks or donor DNA. Nature 576, 149–157. https://doi.org/10.1038/s41586-019-1711-4

Arnold, A.P., Gorski, R.A., 1984. Gonadal Steroid Induction of Structural Sex Differences in the Central Nervous System. Annu. Rev. Neurosci. 7, 413–442. https://doi.org/10.1146/annurev.ne.07.030184.002213

Arnoult, N., Correia, A., Ma, J., Merlo, A., Garcia-Gomez, S., Maric, M., Tognetti, M., Benner, C.W., Boulton, S.J., Saghatelian, A., Karlseder, J., 2017. Regulation of DNA repair pathway choice in S and G2 phases by the NHEJ inhibitor CYREN. Nature 549, 548–552. https://doi.org/10.1038/nature24023

Asati, V., Mahapatra, D.K., Bharti, S.K., 2016. PI3K/Akt/mTOR and Ras/Raf/MEK/ERK signaling pathways inhibitors as anticancer agents: Structural and pharmacological perspectives. European Journal of Medicinal Chemistry 109, 314–341. https://doi.org/10.1016/j.ejmech.2016.01.012

Ashburner, M., Ball, C.A., Blake, J.A., Botstein, D., Butler, H., Cherry, J.M., Davis, A.P., Dolinski, K., Dwight, S.S., Eppig, J.T., Harris, M.A., Hill, D.P., Issel-Tarver, L., Kasarskis, A., Lewis, S., Matese, J.C., Richardson, J.E., Ringwald, M., Rubin, G.M., Sherlock, G., 2000. Gene ontology: tool for the unification of biology. The Gene Ontology Consortium. Nat Genet 25, 25–29. https://doi.org/10.1038/75556

Ashley, A.K., Shrivastav, M., Nie, J., Amerin, C., Troksa, K., Glanzer, J.G., Liu, S., Opiyo, S.O., Dimitrova, D.D., Le, P., Sishc, B., Bailey, S.M., Oakley, G.G., Nickoloff, J.A., 2014. DNA-PK phosphorylation of RPA32 Ser4/Ser8 regulates replication stress checkpoint activation, fork restart, homologous recombination and mitotic catastrophe. DNA Repair (Amst) 21, 131–139. https://doi.org/10.1016/j.dnarep.2014.04.008

Ashworth, A., Lord, C.J., 2018. Synthetic lethal therapies for cancer: what's next after PARP inhibitors? Nature Reviews Clinical Oncology 15, 564–576. https://doi.org/10.1038/s41571-018-0055-6

Assou, S., Cerecedo, D., Tondeur, S., Pantesco, V., Hovatta, O., Klein, B., Hamamah, S., De Vos, J., 2009. A gene expression signature shared by human mature oocytes and embryonic stem cells. BMC Genomics 10, 10. https://doi.org/10.1186/1471-2164-10-10

Astuti, P., Pike, T., Widberg, C., Payne, E., Harding, A., Hancock, J., Gabrielli, B., 2009. MAPK Pathway Activation Delays G2/M Progression by Destabilizing Cdc25B. Journal of Biological Chemistry 284, 33781–33788. https://doi.org/10.1074/jbc.M109.027516

Augello, M.A., Liu, D., Deonarine, L.D., Robinson, B.D., Huang, D., Stelloo, S., Blattner, M., Doane, A.S., Wong, E.W.P., Chen, Y., Rubin, M.A., Beltran, H., Elemento, O., Bergman, A.M., Zwart, W., Sboner, A., Dephoure, N., Barbieri, C.E., 2019. CHD1 Loss Alters AR Binding at Lineage-Specific Enhancers and Modulates Distinct Transcriptional Programs to Drive Prostate Tumorigenesis. Cancer Cell 35, 603-617.e8. https://doi.org/10.1016/j.ccell.2019.03.001

Ayars, M., Eshleman, J., Goggins, M., 2017. Susceptibility of ATM-deficient pancreatic cancer cells to radiation. Cell Cycle 16, 991–998. https://doi.org/10.1080/15384101.2017.1312236

Ayoub, N., Jeyasekharan, A.D., Bernal, J.A., Venkitaraman, A.R., 2008. HP1-β mobilization promotes chromatin changes that initiate the DNA damage response. Nature 453, 682–686. https://doi.org/10.1038/nature06875

Badzio, A., Wynes, M.W., Dziadziuszko, R., Merrick, D.T., Pardo, M., Rzyman, W., Kowalczyk, A., Singh, S., Ranger-Moore, J., Manriquez, G., Gaire, F., Jassem, J., Hirsch, F.R., 2010. Increased insulin-like growth factor 1 receptor protein expression and gene copy number in small cell lung cancer. J Thorac Oncol 5, 1905–1911. https://doi.org/10.1097/JTO.0b013e3181f38f57

Baig, S., Seevasant, I., Mohamad, J., Mukheem, A., Huri, H.Z., Kamarul, T., 2016. Potential of apoptotic pathway-targeted cancer therapeutic research: Where do we stand? Cell Death & Disease 7, e2058–e2058. https://doi.org/10.1038/cddis.2015.275

Bailey, M.H., Tokheim, C., Porta-Pardo, E., Sengupta, S., Bertrand, D., Weerasinghe, A., Colaprico, A., Wendl, M.C., Kim, J., Reardon, B., Ng, P.K.-S., Jeong, K.J., Cao, S., Wang, Z., Gao, J., Gao, Q., Wang, F., Liu, E.M., Mularoni, L., Rubio-Perez, C., Nagarajan, N., Cortés-Ciriano, I., Zhou, D.C., Liang, W.-W., Hess, J.M., Yellapantula, V.D., Tamborero, D., Gonzalez-Perez, A., Suphavilai, C., Ko, J.Y., Khurana, E., Park, P.J., Van Allen, E.M., Liang, H., MC3 Working Group, Cancer Genome Atlas Research Network, Lawrence, M.S., Godzik, A., Lopez-Bigas, N., Stuart, J., Wheeler, D., Getz, G., Chen, K., Lazar, A.J., Mills, G.B., Karchin, R., Ding, L., 2018. Comprehensive Characterization of Cancer Driver Genes and Mutations. Cell 173, 371-385.e18. https://doi.org/10.1016/j.cell.2018.02.060

Bailyes, E., Nave, B., SOOS, M., Orr, S., Hayward, A., SIDDLE, K., 1997. Insulin receptor/IGF-I receptor hybrids are widely distributed in mammalian tissues: Quantification of individual receptor species by selective immunoprecipitation and immunoblotting. The Biochemical journal 327 (Pt 1), 209–15. https://doi.org/10.1042/bj3270209

Baker, J., Liu, J.-P., Robertson, E.J., Efstratiadis, A., 1993. Role of insulin-like growth factors in embryonic and postnatal growth. Cell 75, 73–82. https://doi.org/10.1016/S0092-8674(05)80085-6

Bakin, R.E., Carr, T., Dimtchev, A., Valena, A., Jung, M., 2004. Inhibition of histone deacetylase (HDAC) activity: Enhancement of prostate cancer radiosensitivity. Cancer Res 64, 295.

Bakkenist, C.J., Kastan, M.B., 2003. DNA damage activates ATM through intermolecular autophosphorylation and dimer dissociation. Nature 421, 499–506. https://doi.org/10.1038/nature01368

Bancroft, J., 1980. Endocrinology of Sexual Function. Clinics in Obstetrics and Gynaecology 7, 253–281. https://doi.org/10.1016/S0306-3356(21)00235-1

Bansal, P., Lazo, J.S., 2007. Induction of Cdc25B Regulates Cell Cycle Resumption after Genotoxic Stress. Cancer Res 67, 3356. https://doi.org/10.1158/0008-5472.CAN-06-3685

Bao, B., Wang, Z., Ali, S., Ahmad, A., Azmi, A.S., Sarkar, S.H., Banerjee, S., Kong, D., Li, Y., Thakur, S., Sarkar, F.H., 2012. Metformin inhibits cell proliferation, migration and invasion by attenuating CSC function mediated by deregulating miRNAs in pancreatic cancer cells. Cancer Prev Res (Phila) 5, 355–364. https://doi.org/10.1158/1940-6207.CAPR-11-0299

Barbieri, S., Babini, G., Morini, J., Friedland, W., Buonanno, M., Grilj, V., Brenner, D.J., Ottolenghi, A., Baiocco, G., 2019. Predicting DNA damage foci and their experimental readout with 2D microscopy: a unified approach applied to photon and neutron exposures. Scientific Reports 9, 14019. https://doi.org/10.1038/s41598-019-50408-5

Barclay, R.D., Burd, N.A., Tyler, C., Tillin, N.A., Mackenzie, R.W., 2019. The Role of the IGF-1 Signaling Cascade in Muscle Protein Synthesis and Anabolic Resistance in Aging Skeletal Muscle. Front Nutr 6, 146–146. https://doi.org/10.3389/fnut.2019.00146

Barr, A.R., Cooper, S., Heldt, F.S., Butera, F., Stoy, H., Mansfeld, J., Novák, B., Bakal, C., 2017. DNA damage during S-phase mediates the proliferation-quiescence decision in the subsequent G1 via p21 expression. Nature Communications 8, 14728. https://doi.org/10.1038/ncomms14728

Bartkowiak, D., Högner, S., Nothdurft, W., Röttinger, E.M., 2001. Cell cycle and growth response of CHO cells to X-irradiation: Threshold-free repair at low doses. International Journal of Radiation Oncology*Biology*Physics 50, 221–227. https://doi.org/10.1016/S0360-3016(01)01455-9

Baserga, R., 1999. The IGF-I Receptor in Cancer Research. Experimental Cell Research 253, 1–6. https://doi.org/10.1006/excr.1999.4667

Baserga, R., Hongo, A., Rubini, M., Prisco, M., Valentinis, B., 1997. The IGF-I receptor in cell growth, transformation and apoptosis. Biochimica et Biophysica Acta (BBA) - Reviews on Cancer 1332, F105–F126. https://doi.org/10.1016/S0304-419X(97)00007-3

Bassing, C.H., Alt, F.W., 2004. The cellular response to general and programmed DNA double strand breaks. DNA Repair 3, 781–796. https://doi.org/10.1016/j.dnarep.2004.06.001

Bayarkhangai, B., Noureldin, S., Yu, L., Zhao, N., Gu, Y., Xu, H., Guo, C., 2018. A comprehensive and perspective view of oncoprotein SET in cancer. Cancer Med 7, 3084–3094. https://doi.org/10.1002/cam4.1526

Beaumont, K.A., Mohana-Kumaran, N., Haass, N.K., 2013. Modeling Melanoma In Vitro and In Vivo. Healthcare (Basel) 2, 27–46. https://doi.org/10.3390/healthcare2010027

Bedford, L., Paine, S., Sheppard, P.W., Mayer, R.J., Roelofs, J., 2010. Assembly, structure, and function of the 26S proteasome. Trends in Cell Biology 20, 391–401. https://doi.org/10.1016/j.tcb.2010.03.007

Beere, H.M., Green, D.R., 2017. Chapter 28 - Immunologic Repercussions of Cell Death, in: Firestein, G.S., Budd, R.C., Gabriel, S.E., McInnes, I.B., O'Dell, J.R. (Eds.), Kelley and Firestein's Textbook of Rheumatology (Tenth Edition). Elsevier, pp. 418-448.e6. https://doi.org/10.1016/B978-0-323-31696-5.00028-0

Bekker-Jensen, S., Lukas, C., Kitagawa, R., Melander, F., Kastan, M.B., Bartek, J., Lukas, J., 2006. Spatial organization of the mammalian genome surveillance machinery in response to DNA strand breaks. Journal of Cell Biology 173, 195–206. https://doi.org/10.1083/jcb.200510130

Belfiore, A., Frasca, F., Pandini, G., Sciacca, L., Vigneri, R., 2009. Insulin Receptor Isoforms and Insulin Receptor/Insulin-Like Growth Factor Receptor Hybrids in Physiology and Disease. Endocrine Reviews 30, 586–623. https://doi.org/10.1210/er.2008-0047

Bendjennat, M., Boulaire, J., Jascur, T., Brickner, H., Barbier, V., Sarasin, A., Fotedar, A., Fotedar, R., 2003. UV Irradiation Triggers Ubiquitin-Dependent Degradation of p21WAF1 to Promote DNA Repair. Cell 114, 599–610. https://doi.org/10.1016/j.cell.2003.08.001

Benito-Jardón, L., Díaz-Martínez, M., Arellano-Sánchez, N., Vaquero-Morales, P., Esparís-Ogando, A., Teixidó, J., 2019. Resistance to MAPK Inhibitors in Melanoma Involves Activation of the IGF1R–MEK5–Erk5 Pathway. Cancer Res 79, 2244. https://doi.org/10.1158/0008-5472.CAN-18-2762

Benyoucef, S., Surinya, K.H., Hadaschik, D., Siddle, K., 2007. Characterization of insulin/IGF hybrid receptors: contributions of the insulin receptor L2 and Fn1 domains and the alternatively spliced exon 11 sequence to ligand binding and receptor activation. Biochemical Journal 403, 603–613. https://doi.org/10.1042/BJ20061709

Bergers, G., Benjamin, L.E., 2003. Tumorigenesis and the angiogenic switch. Nature Reviews Cancer 3, 401–410. https://doi.org/10.1038/nrc1093

Bernhard, E.J., Maity, A., Muschel, R.J., McKenna, W.G., 1995. Effects of ionizing radiation on cell cycle progression. Radiation and Environmental Biophysics 34, 79–83. https://doi.org/10.1007/BF01275210

Bertoli, C., Skotheim, J.M., de Bruin, R.A.M., 2013. Control of cell cycle transcription during G1 and S phases. Nat Rev Mol Cell Biol 14, 518–528. https://doi.org/10.1038/nrm3629

Bethune, G., Bethune, D., Ridgway, N., Xu, Z., 2010. Epidermal growth factor receptor (EGFR) in lung cancer: an overview and update. J Thorac Dis 2, 48–51.

Bhargava, R., Sandhu, M., Muk, S., Lee, G., Vaidehi, N., Stark, J.M., 2018. C-NHEJ without indels is robust and requires synergistic function of distinct XLF domains. Nature Communications 9, 2484. https://doi.org/10.1038/s41467-018-04867-5

Bian, Y., Li, L., Dong, M., Liu, X., Kaneko, T., Cheng, K., Liu, H., Voss, C., Cao, X., Wang, Y., Litchfield, D., Ye, M., Li, S.S.-C., Zou, H., 2016. Ultra-deep tyrosine phosphoproteomics enabled by a phosphotyrosine superbinder. Nature Chemical Biology 12, 959–966. https://doi.org/10.1038/nchembio.2178

Bibikova, M., Carroll, D., Segal, D.J., Trautman, J.K., Smith, J., Kim, Y.-G., Chandrasegaran, S., 2001. Stimulation of Homologous Recombination through Targeted Cleavage by Chimeric Nucleases. Mol. Cell. Biol. 21, 289. https://doi.org/10.1128/MCB.21.1.289-297.2001

Bid, H.K., Zhan, J., Phelps, D.A., Kurmasheva, R.T., Houghton, P.J., 2012. Potent Inhibition of Angiogenesis by the IGF-1 Receptor-Targeting Antibody SCH717454 Is Reversed by IGF-2. Mol Cancer Ther 11, 649. https://doi.org/10.1158/1535-7163.MCT-11-0575

Biehs, R., Steinlage, M., Barton, O., Juhász, S., Künzel, J., Spies, J., Shibata, A., Jeggo, P.A., Löbrich, M., 2017. DNA Double-Strand Break Resection Occurs during Non-homologous End Joining in G1 but Is Distinct from Resection during Homologous Recombination. Mol Cell 65, 671-684.e5. https://doi.org/10.1016/j.molcel.2016.12.016

Bindra, R.S., Gibson, S.L., Meng, A., Westermark, U., Jasin, M., Pierce, A.J., Bristow, R.G., Classon, M.K., Glazer, P.M., 2005. Hypoxia-Induced Down-regulation of BRCA1 Expression by E2Fs. Cancer Res 65, 11597. https://doi.org/10.1158/0008-5472.CAN-05-2119

Bindra, R.S., Glazer, P.M., 2007. Repression of RAD51 gene expression by E2F4/p130 complexes in hypoxia. Oncogene 26, 2048–2057. https://doi.org/10.1038/sj.onc.1210001

Bindra, R.S., Schaffer, P.J., Meng, A., Woo, J., Måseide, K., Roth, M.E., Lizardi, P., Hedley, D.W., Bristow, R.G., Glazer, P.M., 2004. Down-regulation of Rad51 and decreased homologous recombination in hypoxic cancer cells. Mol Cell Biol 24, 8504–8518. https://doi.org/10.1128/MCB.24.19.8504-8518.2004

Binz, S.K., Sheehan, A.M., Wold, M.S., 2004. Replication Protein A phosphorylation and the cellular response to DNA damage. DNA Repair 3, 1015–1024. https://doi.org/10.1016/j.dnarep.2004.03.028

Bird, A.W., Yu, D.Y., Pray-Grant, M.G., Qiu, Q., Harmon, K.E., Megee, P.C., Grant, P.A., Smith, M.M., Christman, M.F., 2002. Acetylation of histone H4 by Esa1 is required for DNA double-strand break repair. Nature 419, 411–415. https://doi.org/10.1038/nature01035

Blackford, A.N., Jackson, S.P., 2017. ATM, ATR, and DNA-PK: The Trinity at the Heart of the DNA Damage Response. Molecular Cell 66, 801–817. https://doi.org/10.1016/j.molcel.2017.05.015

Blasco, M.A., Lee, H.-W., Hande, M.P., Samper, E., Lansdorp, P.M., DePinho, R.A., Greider, C.W., 1997. Telomere Shortening and Tumor Formation by Mouse Cells Lacking Telomerase RNA. Cell 91, 25–34. https://doi.org/10.1016/S0092-8674(01)80006-4

Blier, P., Griffith, A., Craft, J., Hardin, J., 1993. Binding of Ku protein to DNA. Measurement of affinity for ends and demonstration of binding to nicks. The Journal of biological chemistry 268, 7594–601.

Bloch, K., Smith, H., van Hamel Parsons, V., Gavaghan, D., Kelly, C., Fletcher, A., Maini, P., Callaghan, R., 2014. Metabolic Alterations During the Growth of Tumour Spheroids. Cell Biochemistry and Biophysics 68, 615–628. https://doi.org/10.1007/s12013-013-9757-7

Block, Yu, Y., Merkle, D., Gifford, J.L., Ding, Q., Meek, K., Lees-Miller, S.P., 2004. Autophosphorylation-dependent remodeling of the DNA-dependent protein kinase catalytic subunit regulates ligation of DNA ends. Nucleic Acids Res 32, 4351–4357. https://doi.org/10.1093/nar/gkh761

Boch, J., Scholze, H., Schornack, S., Landgraf, A., Hahn, S., Kay, S., Lahaye, T., Nickstadt, A., Bonas, U., 2009. Breaking the Code of DNA Binding Specificity of TAL-Type III Effectors. Science 326, 1509. https://doi.org/10.1126/science.1178811

Boehme, K.A., Kulikov, R., Blattner, C., 2008. p53 stabilization in response to DNA damage requires Akt/PKB and DNA-PK. Proc Natl Acad Sci U S A 105, 7785–7790. https://doi.org/10.1073/pnas.0703423105

Boettcher, M., McManus, M.T., 2015. Choosing the Right Tool for the Job: RNAi, TALEN, or CRISPR. Molecular Cell 58, 575–585. https://doi.org/10.1016/j.molcel.2015.04.028

Bolotin, A., Quinquis, B., Sorokine, A., Ehrlich, S., 2005. Clustered regularly interspaced short palindrome repeats (CRISPRs) have spacers of extrachromosomal origin. Microbiology (Reading, England) 151, 2551–61. https://doi.org/10.1099/mic.0.28048-0

Bonapace, G., Concolino, D., Formicola, S., Strisciuglio, P., 2003. A novel mutation in a patient with insulin-like growth factor 1 (IGF1) deficiency. J Med Genet 40, 913. https://doi.org/10.1136/jmg.40.12.913

Bonner, J.A., Harari, P.M., Giralt, J., Azarnia, N., Shin, D.M., Cohen, R.B., Jones, C.U., Sur, R., Raben, D., Jassem, J., Ove, R., Kies, M.S., Baselga, J., Youssoufian, H., Amellal, N., Rowinsky, E.K., Ang, K.K., 2006. Radiotherapy plus Cetuximab for Squamous-Cell Carcinoma of the Head and Neck. N Engl J Med 354, 567–578. https://doi.org/10.1056/NEJMoa053422

Boone, D.N., Lee, A.V., 2012. Targeting the insulin-like growth factor receptor: developing biomarkers from gene expression profiling. Crit Rev Oncog 17, 161–173. https://doi.org/10.1615/critrevoncog.v17.i2.30

Bose, A., Guilherme, A., Robida, S.I., Nicoloro, S.M.C., Zhou, Q.L., Jiang, Z.Y., Pomerleau, D.P., Czech, M.P., 2002. Glucose transporter recycling in response to insulin is facilitated by myosin Myo1c. Nature 420, 821–824. https://doi.org/10.1038/nature01246

Boswell-Casteel, R.C., Fukuda, Y., Schuetz, J.D., 2017. ABCB6, an ABC Transporter Impacting Drug Response and Disease. AAPS J 20, 8–8. https://doi.org/10.1208/s12248-017-0165-6

Bothmer, A., Robbiani, D.F., Feldhahn, N., Gazumyan, A., Nussenzweig, A., Nussenzweig, M.C., 2010. 53BP1 regulates DNA resection and the choice between classical and alternative end joining during class switch recombination. J Exp Med 207, 855–865. https://doi.org/10.1084/jem.20100244

Boucher, J., Charalambous, M., Zarse, K., Mori, M.A., Kleinridders, A., Ristow, M., Ferguson-Smith, A.C., Kahn, C.R., 2014. Insulin and insulin-like growth factor 1 receptors are required for normal expression of imprinted genes. Proc Natl Acad Sci U S A 111, 14512–14517. https://doi.org/10.1073/pnas.1415475111

Boucher, J., Macotela, Y., Bezy, O., Mori, M.A., Kriauciunas, K., Kahn, C.R., 2010a. A kinase-independent role for unoccupied insulin and IGF-1 receptors in the control of apoptosis. Sci Signal 3, ra87–ra87. https://doi.org/10.1126/scisignal.2001173

Boucher, J., Tseng, Y.-H., Kahn, C., 2010b. Insulin and Insulin-like Growth Factor-1 Receptors Act as Ligand-specific Amplitude Modulators of a Common Pathway Regulating Gene Transcription. The Journal of biological chemistry 285, 17235–45. https://doi.org/10.1074/jbc.M110.118620

Bouwman, P., Aly, A., Escandell, J.M., Pieterse, M., Bartkova, J., van der Gulden, H., Hiddingh, S., Thanasoula, M., Kulkarni, A., Yang, Q., Haffty, B.G., Tommiska, J., Blomqvist, C., Drapkin, R., Adams, D.J., Nevanlinna, H.,

Bartek, J., Tarsounas, M., Ganesan, S., Jonkers, J., 2010. 53BP1 loss rescues BRCA1 deficiency and is associated with triple-negative and BRCA-mutated breast cancers. Nat Struct Mol Biol 17, 688–695. https://doi.org/10.1038/nsmb.1831

Bozulic, L., Surucu, B., Hynx, D., Hemmings, B.A., 2008. PKBα/Akt1 Acts Downstream of DNA-PK in the DNA Double-Strand Break Response and Promotes Survival. Molecular Cell 30, 203–213. https://doi.org/10.1016/j.molcel.2008.02.024

Brennan, P., Babbage, J.W., Burgering, B.M.T., Groner, B., Reif, K., Cantrell, D.A., 1997. Phosphatidylinositol 3-Kinase Couples the Interleukin-2 Receptor to the Cell Cycle Regulator E2F. Immunity 7, 679–689. https://doi.org/10.1016/S1074-7613(00)80388-X

Brentnall, M., Rodriguez-Menocal, L., De Guevara, R.L., Cepero, E., Boise, L.H., 2013. Caspase-9, caspase-3 and caspase-7 have distinct roles during intrinsic apoptosis. BMC Cell Biol 14, 32–32. https://doi.org/10.1186/1471-2121-14-32

Breuleux, M., Klopfenstein, M., Stephan, C., Doughty, C.A., Barys, L., Maira, S.-M., Kwiatkowski, D., Lane, H.A., 2009. Increased AKT S473 phosphorylation after mTORC1 inhibition is rictor dependent and does not predict tumor cell response to PI3K/mTOR inhibition. Mol Cancer Ther 8, 742. https://doi.org/10.1158/1535-7163.MCT-08-0668

Bristow, R.G., Hill, R.P., 2008. Hypoxia, DNA repair and genetic instability. Nature Reviews Cancer 8, 180–192. https://doi.org/10.1038/nrc2344

Britton, S., Coates, J., Jackson, S.P., 2013. A new method for high-resolution imaging of Ku foci to decipher mechanisms of DNA double-strand break repair. Journal of Cell Biology 202, 579–595. https://doi.org/10.1083/jcb.201303073

Brognard, J., Clark, A.S., Ni, Y., Dennis, P.A., 2001. Akt/Protein Kinase B Is Constitutively Active in Non-Small Cell Lung Cancer Cells and Promotes Cellular Survival and Resistance to Chemotherapy and Radiation. Cancer Res 61, 3986.

Brooks, C.L., Gu, W., 2004. Dynamics in the p53-Mdm2 Ubiquitination Pathway. Cell Cycle 3, 893–897. https://doi.org/10.4161/cc.3.7.997

Brouns, S.J.J., Jore, M.M., Lundgren, M., Westra, E.R., Slijkhuis, R.J.H., Snijders, A.P.L., Dickman, M.J., Makarova, K.S., Koonin, E.V., van der Oost, J., 2008. Small CRISPR RNAs Guide Antiviral Defense in Prokaryotes. Science 321, 960. https://doi.org/10.1126/science.1159689

Brown, J.S., Jackson, S.P., 2015. Ubiquitylation, neddylation and the DNA damage response. Open Biol 5, 150018–150018. https://doi.org/10.1098/rsob.150018

Brown, J.S., Lukashchuk, N., Sczaniecka-Clift, M., Britton, S., le Sage, C., Calsou, P., Beli, P., Galanty, Y., Jackson, S.P., 2015. Neddylation promotes ubiquitylation and release of Ku from DNA-damage sites. Cell Rep 11, 704–714. https://doi.org/10.1016/j.celrep.2015.03.058

Brunet, A., Bonni, A., Zigmond, M.J., Lin, M.Z., Juo, P., Hu, L.S., Anderson, M.J., Arden, K.C., Blenis, J., Greenberg, M.E., 1999. Akt Promotes Cell Survival by Phosphorylating and Inhibiting a Forkhead Transcription Factor. Cell 96, 857–868. https://doi.org/10.1016/S0092-8674(00)80595-4

Buckley, S.M., Aranda-Orgilles, B., Strikoudis, A., Apostolou, E., Loizou, E., Moran-Crusio, K., Farnsworth, C.L., Koller, A.A., Dasgupta, R., Silva, J.C., Stadtfeld, M., Hochedlinger, K., Chen, E.I., Aifantis, I., 2012. Regulation of Pluripotency and Cellular Reprogramming by the Ubiquitin-Proteasome System. Cell Stem Cell 11, 783–798. https://doi.org/10.1016/j.stem.2012.09.011

Budman, J., Kim, S.A., Chu, G., 2007. Processing of DNA for Nonhomologous End-joining Is Controlled by Kinase Activity and XRCC4/Ligase IV. Journal of Biological Chemistry 282, 11950–11959. https://doi.org/10.1074/jbc.M610058200

Buisson, R., Boisvert, J.L., Benes, C.H., Zou, L., 2015. Distinct but Concerted Roles of ATR, DNA-PK, and Chk1 in Countering Replication Stress during S Phase. Molecular Cell 59, 1011–1024. https://doi.org/10.1016/j.molcel.2015.07.029

Bulteau, A.-L., Moreau, M., Nizard, C., Friguet, B., 2002. Impairment of proteasome function upon UVA- and UVB-irradiation of human keratinocytes. Free Radical Biology and Medicine 32, 1157–1170. https://doi.org/10.1016/S0891-5849(02)00816-X

Bunting, S.F., Callén, E., Wong, N., Chen, H.-T., Polato, F., Gunn, A., Bothmer, A., Feldhahn, N., Fernandez-Capetillo, O., Cao, L., Xu, X., Deng, C.-X., Finkel, T., Nussenzweig, M., Stark, J.M., Nussenzweig, A., 2010. 53BP1 inhibits homologous recombination in Brca1-deficient cells by blocking resection of DNA breaks. Cell 141, 243–254. https://doi.org/10.1016/j.cell.2010.03.012

Burke, J.R., Deshong, A.J., Pelton, J.G., Rubin, S.M., 2010. Phosphorylation-induced Conformational Changes in the Retinoblastoma Protein Inhibit E2F Transactivation Domain Binding. Journal of Biological Chemistry 285, 16286–16293. https://doi.org/10.1074/jbc.M110.108167

Burrell, R.A., McGranahan, N., Bartek, J., Swanton, C., 2013. The causes and consequences of genetic heterogeneity in cancer evolution. Nature 501, 338–345. https://doi.org/10.1038/nature12625

Bussink, J., van der Kogel, A.J., Kaanders, J.H., 2008. Activation of the PI3-K/AKT pathway and implications for radioresistance mechanisms in head and neck cancer. The Lancet Oncology 9, 288–296. https://doi.org/10.1016/S1470-2045(08)70073-1

Cabail, M.Z., Li, S., Lemmon, E., Bowen, M.E., Hubbard, S.R., Miller, W.T., 2015. The insulin and IGF1 receptor kinase domains are functional dimers in the activated state. Nature Communications 6, 6406. https://doi.org/10.1038/ncomms7406

Cadet, J., Douki, T., Ravanat, J.-L., 2008. Oxidatively Generated Damage to the Guanine Moiety of DNA: Mechanistic Aspects and Formation in Cells. Acc. Chem. Res. 41, 1075–1083. https://doi.org/10.1021/ar700245e

Cai, B., Chang, S., Becker, E., Bonni, A., Xia, Z., 2006. p38 MAP Kinase Mediates Apoptosis through Phosphorylation of BimEL at Ser-65. The Journal of biological chemistry 281, 25215–22. https://doi.org/10.1074/jbc.M512627200

Cai, S.-L., Tee, A.R., Short, J.D., Bergeron, J.M., Kim, J., Shen, J., Guo, R., Johnson, C.L., Kiguchi, K., Walker, C.L., 2006. Activity of TSC2 is inhibited by AKT-mediated phosphorylation and membrane partitioning. Journal of Cell Biology 173, 279–289. https://doi.org/10.1083/jcb.200507119

Cai, W., Sakaguchi, M., Kleinridders, A., Gonzalez-Del Pino, G., Dreyfuss, J.M., O'Neill, B.T., Ramirez, A.K., Pan, H., Winnay, J.N., Boucher, J., Eck, M.J., Kahn, C.R., 2017. Domain-dependent effects of insulin and IGF-1 receptors on signalling and gene expression. Nature Communications 8, 14892. https://doi.org/10.1038/ncomms14892

Cairns, R.A., Harris, I.S., Mak, T.W., 2011. Regulation of cancer cell metabolism. Nature Reviews Cancer 11, 85–95. https://doi.org/10.1038/nrc2981

Calsou, P., Frit, P., Humbert, O., Muller, C., Chen, D.J., Salles, B., 1999. The DNA-dependent protein kinase catalytic activity regulates DNA end processing by means of Ku entry into DNA. J Biol Chem 274, 7848–56.

Camphausen, K., Scott, T., Sproull, M., Tofilon, P.J., 2004. Enhancement of Xenograft Tumor Radiosensitivity by the Histone Deacetylase Inhibitor MS-275 and Correlation with Histone Hyperacetylation. Clin Cancer Res 10, 6066. https://doi.org/10.1158/1078-0432.CCR-04-0537

Campisi, J., d'Adda di Fagagna, F., 2007. Cellular senescence: when bad things happen to good cells. Nature Reviews Molecular Cell Biology 8, 729–740. https://doi.org/10.1038/nrm2233

Cao, H., Dong, W., Qu, X., Shen, H., Xu, J., Zhu, L., Liu, Q., Du, J., 2016. Metformin Enhances the Therapy Effects of Anti-IGF-1R mAb Figitumumab to NSCLC. Sci Rep 6, 31072–31072. https://doi.org/10.1038/srep31072

Cao, H., Dong, W., Shen, H., Xu, J., Zhu, L., Liu, Q., Du, J., 2015. Combinational Therapy Enhances the Effects of Anti-IGF-1R mAb Figitumumab to Target Small Cell Lung Cancer. PLoS One 10, e0135844–e0135844. https://doi.org/10.1371/journal.pone.0135844

Cao, L., Xu, X., Bunting, S.F., Liu, J., Wang, R.-H., Cao, L.L., Wu, J.J., Peng, T.-N., Chen, J., Nussenzweig, A., Deng, C.-X., Finkel, T., 2009. A selective requirement for 53BP1 in the biological response to genomic instability induced by Brca1 deficiency. Mol Cell 35, 534–541. https://doi.org/10.1016/j.molcel.2009.06.037

Caporali, S., Levati, L., Starace, G., Ragone, G., Bonmassar, E., Alvino, E., D'Atri, S., 2008. AKT Is Activated in an Ataxia-Telangiectasia and Rad3-Related-Dependent Manner in Response to Temozolomide and Confers Protection against Drug-Induced Cell Growth Inhibition. Mol Pharmacol 74, 173. https://doi.org/10.1124/mol.107.044743

Cardone, M.H., Roy, N., Stennicke, H.R., Salvesen, G.S., Franke, T.F., Stanbridge, E., Frisch, S., Reed, J.C., 1998. Regulation of Cell Death Protease Caspase-9 by Phosphorylation. Science 282, 1318. https://doi.org/10.1126/science.282.5392.1318

Carmeliet, P., Jain, R.K., 2000. Angiogenesis in cancer and other diseases. Nature 407, 249–257. https://doi.org/10.1038/35025220

Carrasco-Garcia, E., Martinez-Lacaci, I., Mayor-López, L., Tristante, E., Carballo-Santana, M., García-Morales, P., Ventero Martin, M.P., Fuentes-Baile, M., Rodriguez-Lescure, Á., Saceda, M., 2018. PDGFR and IGF-1R Inhibitors Induce a G2/M Arrest and Subsequent Cell Death in Human Glioblastoma Cell Lines. Cells 7, 131. https://doi.org/10.3390/cells7090131

Carthew, R.W., Sontheimer, E.J., 2009. Origins and Mechanisms of miRNAs and siRNAs. Cell 136, 642–655. https://doi.org/10.1016/j.cell.2009.01.035

Cary, R.B., Peterson, S.R., Wang, J., Bear, D.G., Bradbury, E.M., Chen, D.J., 1997. DNA looping by Ku and the DNA-dependent protein kinase. Proc Natl Acad Sci U S A 94, 4267–4272. https://doi.org/10.1073/pnas.94.9.4267

Ceccaldi, R., Rondinelli, B., D'Andrea, A.D., 2016. Repair Pathway Choices and Consequences at the Double-Strand Break. Trends in Cell Biology 26, 52–64. https://doi.org/10.1016/j.tcb.2015.07.009

Cha, H., Lowe, J.M., Li, H., Lee, J.-S., Belova, G.I., Bulavin, D.V., Fornace, A.J., Jr, 2010. Wip1 directly dephosphorylates gamma-H2AX and attenuates the DNA damage response. Cancer Res 70, 4112–4122. https://doi.org/10.1158/0008-5472.CAN-09-4244

Cha, H., Wang, X., Li, H., Fornace, A.J., 2007. A Functional Role for p38 MAPK in Modulating Mitotic Transit in the Absence of Stress. Journal of Biological Chemistry 282, 22984–22992. https://doi.org/10.1074/jbc.M700735200

Chae, Y.K., Anker, J.F., Carneiro, B.A., Chandra, S., Kaplan, J., Kalyan, A., Santa-Maria, C.A., Platanias, L.C., Giles, F.J., 2016. Genomic landscape of DNA repair genes in cancer. Oncotarget; Vol 7, No 17.

Chailleux, C., Tyteca, S., Papin, C., Boudsocq, F., Puget, N., Courilleau, C., Grigoriev, M., Canitrot, Y., Trouche, D., 2010. Physical interaction between the histone acetyl transferase Tip60 and the DNA double-strand breaks sensor MRN complex. Biochemical Journal 426, 365–371. https://doi.org/10.1042/BJ20091329

Chalhoub, N., Baker, S.J., 2009. PTEN and the PI3-kinase pathway in cancer. Annu Rev Pathol 4, 127–150. https://doi.org/10.1146/annurev.pathol.4.110807.092311

Chambard, J.-C., Lefloch, R., Pouysségur, J., Lenormand, P., 2007. ERK implication in cell cycle regulation. Biochimica et Biophysica Acta (BBA) - Molecular Cell Research 1773, 1299–1310. https://doi.org/10.1016/j.bbamcr.2006.11.010

Chan, D.W., Chen, B.P.-C., Prithivirajsingh, S., Kurimasa, A., Story, M.D., Qin, J., Chen, D.J., 2002. Autophosphorylation of the DNA-dependent protein kinase catalytic subunit is required for rejoining of DNA double-strand breaks. Genes Dev 16, 2333–2338. https://doi.org/10.1101/gad.1015202

Chan, D.W., Ting, N.S.Y., Lees-Miller, S.P., Mody, C.H., 1996. Purification and characterization of the double-stranded DNA-activated protein kinase, DNA-PK, from human placenta. Biochem. Cell Biol. 74, 67–73. https://doi.org/10.1139/o96-007

Chan, J.M., Stampfer, M.J., Giovannucci, E., Gann, P.H., Ma, J., Wilkinson, P., Hennekens, C.H., Pollak, M., 1998. Plasma Insulin-Like Growth Factor-I and Prostate Cancer Risk: A Prospective Study. Science 279, 563. https://doi.org/10.1126/science.279.5350.563

Chang, H.-C., Guarente, L., 2014. SIRT1 and other sirtuins in metabolism. Trends in Endocrinology & Metabolism 25, 138–145. https://doi.org/10.1016/j.tem.2013.12.001

Chang, H.H.Y., Pannunzio, N.R., Adachi, N., Lieber, M.R., 2017. Non-homologous DNA end joining and alternative pathways to double-strand break repair. Nature Reviews Molecular Cell Biology 18, 495–506. https://doi.org/10.1038/nrm.2017.48

Chang, L., Graham, P.H., Hao, J., Ni, J., Bucci, J., Cozzi, P.J., Kearsley, J.H., Li, Y., 2014. PI3K/Akt/mTOR pathway inhibitors enhance radiosensitivity in radioresistant prostate cancer cells through inducing apoptosis, reducing autophagy, suppressing NHEJ and HR repair pathways. Cell Death Dis 5, e1437–e1437. https://doi.org/10.1038/cddis.2014.415

Chang, Y., Lee, Y., Tejima, T., Tanaka, K., Omura, S., Heintz, N., Mitsui, Y., Magae, J., 1998. mdm2 and bax, downstream mediators of the p53 response, are degraded by the ubiquitin-proteasome pathway. Cell Growth Differ 9, 79–84.

Chapman, J.R., Barral, P., Vannier, J.-B., Borel, V., Steger, M., Tomas-Loba, A., Sartori, A.A., Adams, I.R., Batista, F.D., Boulton, S.J., 2013. RIF1 is essential for 53BP1-dependent nonhomologous end joining and suppression of DNA double-strand break resection. Mol Cell 49, 858–871. https://doi.org/10.1016/j.molcel.2013.01.002

Chappell, W.H., Lehmann, B.D., Terrian, D.M., Abrams, S.L., Steelman, L.S., McCubrey, J.A., 2012. p53 expression controls prostate cancer sensitivity to chemotherapy and the MDM2 inhibitor Nutlin-3. Cell Cycle 11, 4579–4588. https://doi.org/10.4161/cc.22852

Charvet, C., Wissler, M., Brauns-Schubert, P., Wang, S.-J., Tang, Y., Sigloch, F.C., Mellert, H., Brandenburg, M., Lindner, S.E., Breit, B., Green, D.R., McMahon, S.B., Borner, C., Gu, W., Maurer, U., 2011. Phosphorylation of Tip60 by GSK-3 Determines the Induction of PUMA and Apoptosis by p53. Molecular Cell 42, 584–596. https://doi.org/10.1016/j.molcel.2011.03.033

Chen, B.P.C., Chan, D.W., Kobayashi, J., Burma, S., Asaithamby, A., Morotomi-Yano, K., Botvinick, E., Qin, J., Chen, D.J., 2005. Cell Cycle Dependence of DNA-dependent Protein Kinase Phosphorylation in Response to DNA Double Strand Breaks*. Journal of Biological Chemistry 280, 14709–14715. https://doi.org/10.1074/jbc.M408827200

Chen, B.P.C., Uematsu, N., Kobayashi, J., Lerenthal, Y., Krempler, A., Yajima, H., Löbrich, M., Shiloh, Y., Chen, D.J., 2007. Ataxia Telangiectasia Mutated (ATM) Is Essential for DNA-PKcs Phosphorylations at the Thr-2609 Cluster upon DNA Double Strand Break. Journal of Biological Chemistry 282, 6582–6587. https://doi.org/10.1074/jbc.M611605200

Chen, J., Alberts, I., Li, X., 2014. Dysregulation of the IGF-I/PI3K/AKT/mTOR signaling pathway in autism spectrum disorders. International Journal of Developmental Neuroscience 35, 35–41. https://doi.org/10.1016/j.ijdevneu.2014.03.006

Chen, J., Nagle, A., Wang, Y.-F., Boone, D., Lee, A., 2018. Controlled dimerization of insulin-like growth factor-1 and insulin receptors reveal shared and distinct activities of holo and hybrid receptors. Journal of Biological Chemistry 293, jbc.M117.789503. https://doi.org/10.1074/jbc.M117.789503

Chen, M., Nowak, D.G., Trotman, L.C., 2014. Molecular Pathways: PI3K Pathway Phosphatases as Biomarkers for Cancer Prognosis and Therapy. Clin Cancer Res 20, 3057. https://doi.org/10.1158/1078-0432.CCR-12-3680

Chen, W.-J., Ho, C.-C., Chang, Y.-L., Chen, H.-Y., Lin, C.-A., Ling, T.-Y., Yu, S.-L., Yuan, S.-S., Louisa Chen, Y.-J., Lin, C.-Y., Pan, S.-H., Elizabeth Chou, H.-Y., Chen, Y.-J., Chang, G.-C., Chu, W.-C., Lee, Y.-M., Lee, J.-Y., Lee, P.-J., Li, K.-C., Chen, H.-W., Yang, P.-C., 2014. Cancer-associated fibroblasts regulate the plasticity of lung cancer stemness via paracrine signalling. Nature Communications 5, 3472. https://doi.org/10.1038/ncomms4472

Chen, X., Barton, L.F., Chi, Y., Clurman, B.E., Roberts, J.M., 2007. Ubiquitin-Independent Degradation of Cell-Cycle Inhibitors by the REGγ Proteasome. Molecular Cell 26, 843–852. https://doi.org/10.1016/j.molcel.2007.05.022

Cheng, J.Y., 2013. The Prostate Cancer Intervention Versus Observation Trial (PIVOT) in Perspective. J Clin Med Res 5, 266–268. https://doi.org/10.4021/jocmr1395w

Chitnis, M.M., Lodhia, K.A., Aleksic, T., Gao, S., Protheroe, A.S., Macaulay, V.M., 2014. IGF-1R inhibition enhances radiosensitivity and delays double-strand break repair by both non-homologous end-joining and homologous recombination. Oncogene 33, 5262–5273. https://doi.org/10.1038/onc.2013.460

Chitnis, M.M., Yuen, J.S.P., Protheroe, A.S., Pollak, M., Macaulay, V.M., 2008. The Type 1 Insulin-Like Growth Factor Receptor Pathway. Clin Cancer Res 14, 6364. https://doi.org/10.1158/1078-0432.CCR-07-4879

Cho, S.W., Kim, S., Kim, J.M., Kim, J.-S., 2013. Targeted genome engineering in human cells with the Cas9 RNA-guided endonuclease. Nature Biotechnology 31, 230–232. https://doi.org/10.1038/nbt.2507

Cho, W.-H., Lee, Y.-J., Kong, S.-I., Hurwitz, J., Lee, J.-K., 2006. CDC7 kinase phosphorylates serine residues adjacent to acidic amino acids in the minichromosome maintenance 2 protein. Proc Natl Acad Sci USA 103, 11521. https://doi.org/10.1073/pnas.0604990103

Choi, E.J., Ryu, Y.K., Kim, S.Y., Wu, H.G., Kim, J.S., Kim, I.H., Kim, I.A., 2010. Targeting Epidermal Growth Factor Receptor–Associated Signaling Pathways in Non–Small Cell Lung Cancer Cells: Implication in Radiation Response. Mol Cancer Res 8, 1027. https://doi.org/10.1158/1541-7786.MCR-09-0507

Choi, J., Yoon, Y.N., Kim, N., Park, C.S., Seol, H., Park, I.-C., Kim, H.-A., Noh, W.C., Kim, J.-S., Seong, M.-K., 2020. Predicting Radiation Resistance in Breast Cancer with Expression Status of Phosphorylated S6K1. Scientific Reports 10, 641. https://doi.org/10.1038/s41598-020-57496-8

Choi, S.E., Kwon, S., Seok, S., Xiao, Z., Lee, K.-W., Kang, Y., Li, X., Shinoda, K., Kajimura, S., Kemper, B., Kemper, J.K., 2017. Obesity-Linked Phosphorylation of SIRT1 by Casein Kinase 2 Inhibits Its Nuclear Localization and Promotes Fatty Liver. Mol. Cell. Biol. 37, e00006-17. https://doi.org/10.1128/MCB.00006-17

Choudhry, H., Harris, A.L., 2018. Advances in Hypoxia-Inducible Factor Biology. Cell Metabolism 27, 281–298. https://doi.org/10.1016/j.cmet.2017.10.005

Chowdhury, D., Keogh, M.-C., Ishii, H., Peterson, C.L., Buratowski, S., Lieberman, J., 2005. γ-H2AX Dephosphorylation by Protein Phosphatase 2A Facilitates DNA Double-Strand Break Repair. Molecular Cell 20, 801–809. https://doi.org/10.1016/j.molcel.2005.10.003

Christian, M., Cermak, T., Doyle, E.L., Schmidt, C., Zhang, F., Hummel, A., Bogdanove, A.J., Voytas, D.F., 2010. Targeting DNA Double-Strand Breaks with TAL Effector Nucleases. Genetics 186, 757. https://doi.org/10.1534/genetics.110.120717

Chung, J.H., 2018. The role of DNA-PK in aging and energy metabolism. FEBS J 285, 1959–1972. https://doi.org/10.1111/febs.14410

Ciccarelli, C., Di Rocco, A., Gravina, G.L., Mauro, A., Festuccia, C., Del Fattore, A., Berardinelli, P., De Felice, F., Musio, D., Bouché, M., Tombolini, V., Zani, B.M., Marampon, F., 2018. Disruption of MEK/ERK/c-Myc signaling radiosensitizes prostate cancer cells in vitro and in vivo. Journal of Cancer Research and Clinical Oncology 144, 1685–1699. https://doi.org/10.1007/s00432-018-2696-3

Ciccia, A., Elledge, S.J., 2010. The DNA Damage Response: Making It Safe to Play with Knives. Molecular Cell 40, 179–204. https://doi.org/10.1016/j.molcel.2010.09.019

Ciechanover, A., 1994. The ubiquitin-proteasome proteolytic pathway. Cell 79, 13–21. https://doi.org/10.1016/0092-8674(94)90396-4

Cimprich, K.A., Cortez, D., 2008. ATR: an essential regulator of genome integrity. Nature Reviews Molecular Cell Biology 9, 616–627. https://doi.org/10.1038/nrm2450

Clark, D.P., Pazdernik, N.J., McGehee, M.R., 2019. Chapter 7 - Cloning Genes for Synthetic Biology, in: Clark, D.P., Pazdernik, N.J., McGehee, M.R. (Eds.), Molecular Biology (Third Edition). Academic Cell, pp. 199–239. https://doi.org/10.1016/B978-0-12-813288-3.00007-0

Clarke, N.W., Ali, A., Ingleby, F.C., Hoyle, A., Amos, C.L., Attard, G., Brawley, C.D., Calvert, J., Chowdhury, S., Cook, A., Cross, W., Dearnaley, D.P., Douis, H., Gilbert, D., Gillessen, S., Jones, R.J., Langley, R.E., MacNair, A., Malik, Z., Mason, M.D., Matheson, D., Millman, R., Parker, C.C., Ritchie, A.W.S., Rush, H., Russell, J.M., Brown, J., Beesley, S., Birtle, A., Capaldi, L., Gale, J., Gibbs, S., Lydon, A., Nikapota, A., Omlin, A., O'Sullivan, J.M., Parikh, O., Protheroe, A., Rudman, S., Srihari, N.N., Simms, M., Tanguay, J.S., Tolan, S., Wagstaff, J., Wallace, J., Wylie, J., Zarkar, A., Sydes, M.R., Parmar, M.K.B., James, N.D., 2019. Addition of docetaxel to hormonal therapy in low- and high-burden metastatic hormone sensitive prostate cancer: long-term survival results from the STAMPEDE trial. Ann Oncol 30, 1992–2003. https://doi.org/10.1093/annonc/mdz396

Codony-Servat, J., Cuatrecasas, M., Asensio, E., Montironi, C., Martínez-Cardús, A., Marín-Aguilera, M., Horndler, C., Martínez-Balibrea, E., Rubini, M., Jares, P., Reig, O., Victoria, I., Gaba, L., Martín-Richard, M., Alonso, V.,

Escudero, P., Fernández-Martos, C., Feliu, J., Méndez, J.C., Méndez, M., Gallego, J., Salud, A., Rojo, F., Castells, A., Prat, A., Rosell, R., García-Albéniz, X., Camps, J., Maurel, J., 2017. Nuclear IGF-1R predicts chemotherapy and targeted therapy resistance in metastatic colorectal cancer. British Journal of Cancer 117, 1777–1786. https://doi.org/10.1038/bjc.2017.279

Codony-Servat, J., Viteri, S., Codony-Servat, C., Ito, M., Bracht, J., Berenguer, J., Chaib, I., Molina-Vila, M., Karachaliou, N., Rosell, R., 2019. Hsp90 inhibitors enhance the antitumoral effect of osimertinib in parental and osimertinib-resistant non-small cell lung cancer cell lines. Translational Lung Cancer Research 8, 340–351. https://doi.org/10.21037/tlcr.2019.08.22

Coffey, K., Rogerson, L., Ryan-Munden, C., Alkharaif, D., Stockley, J., Heer, R., Sahadevan, K., O'Neill, D., Jones, D., Darby, S., Staller, P., Mantilla, A., Gaughan, L., Robson, C.N., 2013. The lysine demethylase, KDM4B, is a key molecule in androgen receptor signalling and turnover. Nucleic Acids Res 41, 4433–4446. https://doi.org/10.1093/nar/gkt106

Cohen, H.Y., Miller, C., Bitterman, K.J., Wall, N.R., Hekking, B., Kessler, B., Howitz, K.T., Gorospe, M., de Cabo, R., Sinclair, D.A., 2004. Calorie Restriction Promotes Mammalian Cell Survival by Inducing the SIRT1 Deacetylase. Science 305, 390. https://doi.org/10.1126/science.1099196

Cohen, P., Graves, H.C., Peehl, D.M., Kamarei, M., Giudice, L.C., Rosenfeld, R.G., 1992. Prostate-specific antigen (PSA) is an insulin-like growth factor binding protein-3 protease found in seminal plasma. The Journal of Clinical Endocrinology & Metabolism 75, 1046–1053. https://doi.org/10.1210/jcem.75.4.1383255

Cohen, P., Peehl, D.M., Graves, H.C.B., Rosenfeld, R.G., 1994. Biological effects of prostate specific antigen as an insulin-like growth factor binding protein-3 protease. Journal of Endocrinology 142.

Cohn, M.A., D'Andrea, A.D., 2008. Chromatin recruitment of DNA repair proteins: lessons from the fanconi anemia and double-strand break repair pathways. Mol Cell 32, 306–312. https://doi.org/10.1016/j.molcel.2008.10.009

Collins, S.L., Hervé, R., Keevil, C.W., Blaydes, J.P., Webb, J.S., 2011. Down-regulation of DNA mismatch repair enhances initiation and growth of neuroblastoma and brain tumour multicellular spheroids. PLoS One 6, e28123–e28123. https://doi.org/10.1371/journal.pone.0028123

Cong, L., Ran, F.A., Cox, D., Lin, S., Barretto, R., Habib, N., Hsu, P.D., Wu, X., Jiang, W., Marraffini, L.A., Zhang, F., 2013. Multiplex Genome Engineering Using CRISPR/Cas Systems. Science 339, 819. https://doi.org/10.1126/science.1231143

Cook, M.B., Rosenberg, P.S., McCarty, F.A., Wu, M., King, J., Eheman, C., Anderson, W.F., 2015. Racial disparities in prostate cancer incidence rates by census division in the United States, 1999-2008. Prostate 75, 758–763. https://doi.org/10.1002/pros.22958

Copps, K.D., White, M.F., 2012. Regulation of insulin sensitivity by serine/threonine phosphorylation of insulin receptor substrate proteins IRS1 and IRS2. Diabetologia 55, 2565–2582. https://doi.org/10.1007/s00125-012-2644-8

Cortez, D., Guntuku, S., Qin, J., Elledge, S.J., 2001. ATR and ATRIP: Partners in Checkpoint Signaling. Science 294, 1713. https://doi.org/10.1126/science.1065521

Cosentino, C., Grieco, D., Costanzo, V., 2011. ATM activates the pentose phosphate pathway promoting anti-oxidant defence and DNA repair. EMBO J 30, 546–555. https://doi.org/10.1038/emboj.2010.330

Costantini, S., Woodbine, L., Andreoli, L., Jeggo, P.A., Vindigni, A., 2007. Interaction of the Ku heterodimer with the DNA ligase IV/Xrcc4 complex and its regulation by DNA-PK. DNA Repair 6, 712–722. https://doi.org/10.1016/j.dnarep.2006.12.007

Cousineau, I., Abaji, C., Belmaaza, A., 2005. BRCA1 Regulates RAD51 Function in Response to DNA Damage and Suppresses Spontaneous Sister Chromatid Replication Slippage: Implications for Sister Chromatid Cohesion, Genome Stability, and Carcinogenesis. Cancer Res 65, 11384. https://doi.org/10.1158/0008-5472.CAN-05-2156

Cox, D.B.T., Platt, R.J., Zhang, F., 2015. Therapeutic genome editing: prospects and challenges. Nat Med 21, 121–131. https://doi.org/10.1038/nm.3793

Croce, C.M., 2008. Oncogenes and Cancer. N Engl J Med 358, 502–511. https://doi.org/10.1056/NEJMra072367

Cron, K.R., Zhu, K., Kushwaha, D.S., Hsieh, G., Merzon, D., Rameseder, J., Chen, C.C., D'Andrea, A.D., Kozono, D., 2013. Proteasome Inhibitors Block DNA Repair and Radiosensitize Non-Small Cell Lung Cancer. PLOS ONE 8, e73710. https://doi.org/10.1371/journal.pone.0073710

Cross, D.A.E., Alessi, D.R., Cohen, P., Andjelkovich, M., Hemmings, B.A., 1995. Inhibition of glycogen synthase kinase-3 by insulin mediated by protein kinase B. Nature 378, 785–789. https://doi.org/10.1038/378785a0

Crowe, E., Sell, C., Thomas, J.D., Johannes, G.J., Torres, C., 2009. Activation of proteasome by insulin-like growth factor-I may enhance clearance of oxidized proteins in the brain. Mechanisms of Ageing and Development 130, 793–800. https://doi.org/10.1016/j.mad.2009.10.005

Crowe, J.L., Wang, X.S., Shao, Z., Lee, B.J., Estes, V.M., Zha, S., 2020. DNA-PKcs phosphorylation at the T2609 cluster alters the repair pathway choice during immunoglobulin class switch recombination. Proc Natl Acad Sci U S A 117, 22953–22961. https://doi.org/10.1073/pnas.2007455117

Crudden, C., Song, D., Cismas, S., Trocmé, E., Pasca, S., Calin, G.A., Girnita, A., Girnita, L., 2019. Below the Surface: IGF-1R Therapeutic Targeting and Its Endocytic Journey. Cells 8. https://doi.org/10.3390/cells8101223

Cruz-García, A., López-Saavedra, A., Huertas, P., 2014. BRCA1 Accelerates CtIP-Mediated DNA-End Resection. Cell Reports 9, 451–459. https://doi.org/10.1016/j.celrep.2014.08.076

Cui, H., Cruz-Correa, M., Giardiello, F.M., Hutcheon, D.F., Kafonek, D.R., Brandenburg, S., Wu, Y., He, X., Powe, N.R., Feinberg, A.P., 2003. Loss of IGF2 Imprinting: A Potential Marker of Colorectal Cancer Risk. Science 299, 1753. https://doi.org/10.1126/science.1080902

Cui, X., Yu, Y., Gupta, S., Cho, Y.-M., Lees-Miller, S.P., Meek, K., 2005. Autophosphorylation of DNA-Dependent Protein Kinase Regulates DNA End Processing and May Also Alter Double-Strand Break Repair Pathway Choice. Mol. Cell. Biol. 25, 10842. https://doi.org/10.1128/MCB.25.24.10842-10852.2005

Cunha, G.R., Vezina, C.M., Isaacson, D., Ricke, W.A., Timms, B.G., Cao, M., Franco, O., Baskin, L.S., 2018. Development of the human prostate. Differentiation 103, 24–45. https://doi.org/10.1016/j.diff.2018.08.005

Czernilofsky, A.P., Levinson, A.D., Varmus, H.E., Bishop, J.M., Tischer, E., Goodman, H.M., 1980. Nucleotide sequence of an avian sarcoma virus oncogene (src) and proposed amino acid sequence for gene product. Nature 287, 198–203. https://doi.org/10.1038/287198a0

Dai, Z.-J., Gao, J., Kang, H.-F., Ma, Y.-G., Ma, X.-B., Lu, W.-F., Lin, S., Ma, H.-B., Wang, X.-J., Wu, W.-Y., 2013. Targeted inhibition of mammalian target of rapamycin (mTOR) enhances radiosensitivity in pancreatic carcinoma cells. Drug Des Devel Ther 7, 149–159. https://doi.org/10.2147/DDDT.S42390

Daley, J.M., Sung, P., 2014. 53BP1, BRCA1, and the choice between recombination and end joining at DNA double-strand breaks. Mol Cell Biol 34, 1380–1388. https://doi.org/10.1128/MCB.01639-13

Daniel, J.A., Pellegrini, M., Lee, J.-H., Paull, T.T., Feigenbaum, L., Nussenzweig, A., 2008. Multiple autophosphorylation sites are dispensable for murine ATM activation in vivo. J Cell Biol 183, 777–783. https://doi.org/10.1083/jcb.200805154

Datta, S.R., Dudek, H., Tao, X., Masters, S., Fu, H., Gotoh, Y., Greenberg, M.E., 1997. Akt Phosphorylation of BAD Couples Survival Signals to the Cell-Intrinsic Death Machinery. Cell 91, 231–241. https://doi.org/10.1016/S0092-8674(00)80405-5

Datta, S.R., Katsov, A., Hu, L., Petros, A., Fesik, S.W., Yaffe, M.B., Greenberg, M.E., 2000. 14-3-3 Proteins and Survival Kinases Cooperate to Inactivate BAD by BH3 Domain Phosphorylation. Molecular Cell 6, 41–51. https://doi.org/10.1016/S1097-2765(05)00012-2

Daughaday, W.H., Rotwein, P., 1989. Insulin-Like Growth Factors I and II. Peptide, Messenger Ribonucleic Acid and Gene Structures, Serum, and Tissue Concentrations*. Endocrine Reviews 10, 68–91. https://doi.org/10.1210/edrv-10-1-68

Davies, M.A., Samuels, Y., 2010. Analysis of the genome to personalize therapy for melanoma. Oncogene 29, 5545–5555. https://doi.org/10.1038/onc.2010.323

Dayal, S., Sparks, A., Jacob, J., Allende-Vega, N., Lane, D.P., Saville, M.K., 2009. Suppression of the Deubiquitinating Enzyme USP5 Causes the Accumulation of Unanchored Polyubiquitin and the Activation of p53. Journal of Biological Chemistry 284, 5030–5041. https://doi.org/10.1074/jbc.M805871200

de Bono, J.S., Logothetis, C.J., Molina, A., Fizazi, K., North, S., Chu, L., Chi, K.N., Jones, R.J., Goodman, O.B., Saad, F., Staffurth, J.N., Mainwaring, P., Harland, S., Flaig, T.W., Hutson, T.E., Cheng, T., Patterson, H., Hainsworth, J.D., Ryan, C.J., Sternberg, C.N., Ellard, S.L., Fléchon, A., Saleh, M., Scholz, M., Efstathiou, E., Zivi, A., Bianchini, D., Loriot, Y., Chieffo, N., Kheoh, T., Haqq, C.M., Scher, H.I., 2011. Abiraterone and Increased Survival in Metastatic Prostate Cancer. N Engl J Med 364, 1995–2005. https://doi.org/10.1056/NEJMoa1014618

de Bono, J.S., Piulats, J.M., Pandha, H.S., Petrylak, D.P., Saad, F., Aparicio, L.M.A., Sandhu, S.K., Fong, P., Gillessen, S., Hudes, G.R., Wang, T., Scranton, J., Pollak, M.N., 2014. Phase II Randomized Study of Figitumumab plus Docetaxel and Docetaxel Alone with Crossover for Metastatic Castration-Resistant Prostate Cancer. Clin Cancer Res 20, 1925. https://doi.org/10.1158/1078-0432.CCR-13-1869

De Meyts, P., URSø, B., CHRISTOFFERSEN, C.T., SHYMKO, R.M., 1995. Mechanism of Insulin and IGF-I. Annals of the New York Academy of Sciences 766, 388–401. https://doi.org/10.1111/j.1749-6632.1995.tb26688.x

De Meyts, P., Wallach, B., Christoffersen, C.T., Ursø, B., Grønskov, K., Latus, L.-J., Yakushiji, F., Ilondo, M.M., Shymko, R.M., 1994. The Insulin-Like Growth Factor-I Receptor. Hormone Research in Paediatrics 42, 152–169. https://doi.org/10.1159/000184188

De Meyts, P., Whittaker, J., 2002. Structural biology of insulin and IGF1 receptors: implications for drug design. Nature Reviews Drug Discovery 1, 769–783. https://doi.org/10.1038/nrd917

De Schutter, Nuyts, 2009. Radiosensitizing Potential of Epigenetic Anticancer Drugs. Anti-Cancer Agents in Medicinal Chemistry 9, 99–108. https://doi.org/10.2174/187152009787047707

DeBerardinis, R.J., Chandel, N.S., 2016. Fundamentals of cancer metabolism. Sci Adv 2, e1600200–e1600200. https://doi.org/10.1126/sciadv.1600200

Deckbar, D., Birraux, J., Krempler, A., Tchouandong, L., Beucher, A., Walker, S., Stiff, T., Jeggo, P., Löbrich, M., 2007. Chromosome breakage after G2 checkpoint release. J Cell Biol 176, 749–755. https://doi.org/10.1083/jcb.200612047

Deckbar, D., Stiff, T., Koch, B., Reis, C., Löbrich, M., Jeggo, P.A., 2010. The Limitations of the G1-S Checkpoint. Cancer Res 70, 4412. https://doi.org/10.1158/0008-5472.CAN-09-3198

DeHaven, J.E., Robinson, K.A., Nelson, B.A., Buse, M.G., 2001. A novel variant of glutamine: fructose-6-phosphate amidotransferase-1 (GFAT1) mRNA is selectively expressed in striated muscle. Diabetes 50, 2419. https://doi.org/10.2337/diabetes.50.11.2419

Delacôte, F., Lopez, B.S., 2008. Importance of the cell cycle phase for the choice of the appropriate DSB repair pathway, for genome stability mintenance: the trans-S double-strand break repair model. null 7, 33–38. https://doi.org/10.4161/cc.7.1.5149

DeMichele, A., Yee, D., Berry, D.A., Albain, K.S., Benz, C.C., Boughey, J., Buxton, M., Chia, S.K., Chien, A.J., Chui, S.Y., Clark, A., Edmiston, K., Elias, A.D., Forero-Torres, A., Haddad, T.C., Haley, B., Haluska, P., Hylton, N.M., Isaacs, C., Kaplan, H., Korde, L., Leyland-Jones, B., Liu, M.C., Melisko, M., Minton, S.E., Moulder, S.L., Nanda, R., Olopade, O.I., Paoloni, M., Park, J.W., Parker, B.A., Perlmutter, J., Petricoin, E.F., Rugo, H., Symmans, F., Tripathy, D., van't Veer, L.J., Viscusi, R.K., Wallace, A., Wolf, D., Yau, C., Esserman, L.J., 2015. The Neoadjuvant Model Is Still the Future for Drug Development in Breast Cancer. Clin Cancer Res 21, 2911–2915. https://doi.org/10.1158/1078-0432.CCR-14-1760

Denley, A., Wallace, J.C., Cosgrove, L.J., Forbes, B.E., 2004. The Insulin Receptor Isoform Exon 11- (IR-A) in Cancer and Other Diseases: A Review. Horm Metab Res 35, 778–785. https://doi.org/10.1055/s-2004-814157

Dergham, S., Dugan, M., Kucway, R., Du, W., Kamarauskiene, D., Vaitkevicius, V., Crissman, J., Sarkar, F., 1997. Prevalence and clinical significance of combined K-ras mutation and p53 aberration in pancreatic adenocarcinoma. Int J Pancreatol 21, 127–143. https://doi.org/10.1007/bf02822384

Deshpande, R.A., Myler, L.R., Soniat, M.M., Makharashvili, N., Lee, L., Lees-Miller, S.P., Finkelstein, I.J., Paull, T.T., 2020. DNA-dependent protein kinase promotes DNA end processing by MRN and CtIP. Sci Adv 6, eaay0922–eaay0922. https://doi.org/10.1126/sciadv.aay0922

Deveau, H., Barrangou, R., Garneau, J.E., Labonté, J., Fremaux, C., Boyaval, P., Romero, D.A., Horvath, P., Moineau, S., 2008. Phage Response to CRISPR-Encoded Resistance in Streptococcus thermophilus. J. Bacteriol. 190, 1390. https://doi.org/10.1128/JB.01412-07

Dhanasekaran, D.N., Reddy, E.P., 2008. JNK signaling in apoptosis. Oncogene 27, 6245–6251. https://doi.org/10.1038/onc.2008.301

Dhillon, A.S., Hagan, S., Rath, O., Kolch, W., 2007. MAP kinase signalling pathways in cancer. Oncogene 26, 3279–3290. https://doi.org/10.1038/sj.onc.1210421

Di Cosimo, S., Sathyanarayanan, S., Bendell, J.C., Cervantes, A., Stein, M.N., Braña, I., Roda, D., Haines, B.B., Zhang, T., Winter, C.G., Jha, S., Xu, Y., Frazier, J., Klinghoffer, R.A., Leighton-Swayze, A., Song, Y., Ebbinghaus, S., Baselga, J., 2015. Combination of the mTOR inhibitor ridaforolimus and the anti-IGF1R monoclonal antibody dalotuzumab: preclinical characterization and phase I clinical trial. Clin Cancer Res 21, 49–59. https://doi.org/10.1158/1078-0432.CCR-14-0940

Di Virgilio, M., Ying, C.Y., Gautier, J., 2009. PIKK-dependent phosphorylation of Mre11 induces MRN complex inactivation by disassembly from chromatin. DNA Repair (Amst) 8, 1311–1320. https://doi.org/10.1016/j.dnarep.2009.07.006

Diehl, J.A., Cheng, M., Roussel, M.F., Sherr, C.J., 1998. Glycogen synthase kinase-3beta regulates cyclin D1 proteolysis and subcellular localization. Genes Dev 12, 3499–3511. https://doi.org/10.1101/gad.12.22.3499

Difilippantonio, S., Celeste, A., Kruhlak, M.J., Lee, Y., Difilippantonio, M.J., Feigenbaum, L., Jackson, S.P., McKinnon, P.J., Nussenzweig, A., 2007. Distinct domains in Nbs1 regulate irradiation-induced checkpoints and apoptosis. J Exp Med 204, 1003–1011. https://doi.org/10.1084/jem.20070319

Dijkers, P.F., Birkenkamp, K.U., Lam, E.W.-F., Thomas, N.S.B., Lammers, J.-W.J., Koenderman, L., Coffer, P.J., 2002. FKHR-L1 can act as a critical effector of cell death induced by cytokine withdrawal: protein kinase B-enhanced cell survival through maintenance of mitochondrial integrity. J Cell Biol 156, 531–542. https://doi.org/10.1083/jcb.200108084

Dimmeler, S., Breitschopf, K., Haendeler, J., Zeiher, A.M., 1999. Dephosphorylation Targets Bcl-2 for Ubiquitin-dependent Degradation: A Link between the Apoptosome and the Proteasome Pathway. Journal of Experimental Medicine 189, 1815–1822. https://doi.org/10.1084/jem.189.11.1815

Ding, H., Wu, T., 2018. Insulin-Like Growth Factor Binding Proteins in Autoimmune Diseases. Frontiers in Endocrinology 9, 499. https://doi.org/10.3389/fendo.2018.00499

Ding, Q., Reddy, Y.V.R., Wang, W., Woods, T., Douglas, P., Ramsden, D.A., Lees-Miller, S.P., Meek, K., 2003. Autophosphorylation of the catalytic subunit of the DNA-dependent protein kinase is required for efficient end processing during DNA double-strand break repair. Mol Cell Biol 23, 5836–5848. https://doi.org/10.1128/MCB.23.16.5836-5848.2003

Djavan, B., Moul, J.W., Zlotta, A., Remzi, M., Ravery, V., 2003. PSA Progression Following Radical Prostatectomy and Radiation Therapy: New Standards in the New Millenium. European Urology 43, 12–27. https://doi.org/10.1016/S0302-2838(02)00505-5

Dobbs, T.A., Tainer, J.A., Lees-Miller, S.P., 2010. A structural model for regulation of NHEJ by DNA-PKcs autophosphorylation. DNA Repair (Amst) 9, 1307–1314. https://doi.org/10.1016/j.dnarep.2010.09.019

Donohoe, C.L., Doyle, S.L., McGarrigle, S., Cathcart, M.C., Daly, E., O'Grady, A., Lysaght, J., Pidgeon, G.P., Reynolds, J.V., 2012. Role of the insulin-like growth factor 1 axis and visceral adiposity in oesophageal adenocarcinoma. BJS (British Journal of Surgery) 99, 387–396. https://doi.org/10.1002/bjs.8658

Donzelli, M., Draetta, G.F., 2003. Regulating mammalian checkpoints through Cdc25 inactivation. EMBO reports 4, 671–677. https://doi.org/10.1038/sj.embor.embor887

Dougan, M., Dranoff, G., Dougan, S.K., 2019. Cancer Immunotherapy: Beyond Checkpoint Blockade. Annu. Rev. Cancer Biol. 3, 55–75. https://doi.org/10.1146/annurev-cancerbio-030518-055552

Douglas, P., Cui, X., Block, W.D., Yu, Y., Gupta, S., Ding, Q., Ye, R., Morrice, N., Lees-Miller, S.P., Meek, K., 2007. The DNA-dependent protein kinase catalytic subunit is phosphorylated in vivo on threonine 3950, a highly conserved amino acid in the protein kinase domain. Mol Cell Biol 27, 1581–1591. https://doi.org/10.1128/MCB.01962-06

Douglas, P., Moorhead, G.B.G., Ye, R., Lees-Miller, S.P., 2001. Protein Phosphatases Regulate DNA-dependent Protein Kinase Activity*. Journal of Biological Chemistry 276, 18992–18998. https://doi.org/10.1074/jbc.M011703200

Douglas, P., Sapkota, G.P., Morrice, N., Yu, Y., Goodarzi, A.A., Merkle, D., Meek, K., Alessi, D.R., Lees-Miller, S.P., 2002. Identification of in vitro and in vivo phosphorylation sites in the catalytic subunit of the DNA-dependent protein kinase. Biochem J 368, 243–251. https://doi.org/10.1042/BJ20020973

Douglas, P., Ye, R., Trinkle-Mulcahy, L., Neal, J.A., De Wever, V., Morrice, N.A., Meek, K., Lees-Miller, S.P., 2014. Polo-like kinase 1 (PLK1) and protein phosphatase 6 (PP6) regulate DNA-dependent protein kinase catalytic subunit (DNA-PKcs) phosphorylation in mitosis. Biosci Rep 34, e00113. https://doi.org/10.1042/BSR20140051

Duan, L., Maki, C.G., 2016. The IGF-1R/AKT pathway determines cell fate in response to p53. Translational Cancer Research; Vol 5, No 6 (December 2016): Translational Cancer Research (Focused Issue: p53 Biology and Cancer).

Dubrez, L., Causse, S., Borges Bonan, N., Dumétier, B., Garrido, C., 2020. Heat-shock proteins: chaperoning DNA repair. Oncogene 39, 516–529. https://doi.org/10.1038/s41388-019-1016-y

Duckworth-Rysiecki, G., Taylor, A.M.R., 1985. Effects of Ionizing Radiation on Cells from Fanconi's Anemia Patients. Cancer Res 45, 416.

Dudáš, A., Chovanec, M., 2004. DNA double-strand break repair by homologous recombination. Mutation Research/Reviews in Mutation Research 566, 131–167. https://doi.org/10.1016/j.mrrev.2003.07.001

Dufourny, B., Alblas, J., van Teeffelen, H.A.A.M., van Schaik, F.M.A., van der Burg, B., Steenbergh, P.H., Sussenbach, J.S., 1997. Mitogenic Signaling of Insulin-like Growth Factor I in MCF-7 Human Breast Cancer Cells Requires Phosphatidylinositol 3-Kinase and Is Independent of Mitogen-activated Protein Kinase. Journal of Biological Chemistry 272, 31163–31171. https://doi.org/10.1074/jbc.272.49.31163

Dunlop, M.G., Farrington, S.M., Carothers, A.D., Wyllie, A.H., Sharp, L., Burn, J., Liu, B., Kinzler, K.W., Vogelstein, B., 1997. Cancer Risk Associated with Germline DNA Mismatch Repair Gene Mutations. Human Molecular Genetics 6, 105–110. https://doi.org/10.1093/hmg/6.1.105

Dupont, J., Fernandez, A.M., Glackin, C.A., Helman, L., LeRoith, D., 2001. Insulin-like Growth Factor 1 (IGF-1)-induced Twist Expression Is Involved in the Anti-apoptotic Effects of the IGF-1 Receptor. Journal of Biological Chemistry 276, 26699–26707. https://doi.org/10.1074/jbc.M102664200

Dupont, J., Karas, M., LeRoith, D., 2000. The Potentiation of Estrogen on Insulin-like Growth Factor I Action in MCF-7 Human Breast Cancer Cells Includes Cell Cycle Components. Journal of Biological Chemistry 275, 35893–35901. https://doi.org/10.1074/jbc.M006741200

Dupont, J., Le Roith, D., 2001. Insulin-like growth factor 1 and oestradiol promote cell proliferation of MCF-7 breast cancer cells: new insights into their synergistic effects. Mol Pathol 54, 149–154. https://doi.org/10.1136/mp.54.3.149

Durand, R.E., Raleigh, J.A., 1998. Identification of Nonproliferating but Viable Hypoxic Tumor Cells in Vivo. Cancer Res 58, 3547.

Durocher, D., Jackson, S.P., 2001. DNA-PK, ATM and ATR as sensors of DNA damage: variations on a theme? Current Opinion in Cell Biology 13, 225–231. https://doi.org/10.1016/S0955-0674(00)00201-5

Dvir, A., Peterson, S.R., Knuth, M.W., Lu, H., Dynan, W.S., 1992. Ku autoantigen is the regulatory component of a template-associated protein kinase that phosphorylates RNA polymerase II. Proc Natl Acad Sci U S A 89, 11920–11924. https://doi.org/10.1073/pnas.89.24.11920

Dvir, A., Stein, L., Calore, B., Dynan, W., 1993. Purification and characterization of a template-associated protein kinase that phosphorylates RNA polymerase II. The Journal of biological chemistry 268, 10440–7.

Dynan, W.S., Yoo, S., 1998. Interaction of Ku protein and DNA-dependent protein kinase catalytic subunit with nucleic acids. Nucleic Acids Res 26, 1551–1559. https://doi.org/10.1093/nar/26.7.1551

Ebner, M., Lučić, I., Leonard, T.A., Yudushkin, I., 2017. PI(3,4,5)P3 Engagement Restricts Akt Activity to Cellular Membranes. Molecular Cell 65, 416-431.e6. https://doi.org/10.1016/j.molcel.2016.12.028

Eccles, L.J., O'Neill, P., Lomax, M.E., 2011. Delayed repair of radiation induced clustered DNA damage: friend or foe? Mutat Res 711, 134–141. https://doi.org/10.1016/j.mrfmmm.2010.11.003

Edraki, A., Mir, A., Ibraheim, R., Gainetdinov, I., Yoon, Y., Song, C.-Q., Cao, Y., Gallant, J., Xue, W., Rivera-Pérez, J.A., Sontheimer, E.J., 2019. A Compact, High-Accuracy Cas9 with a Dinucleotide PAM for In Vivo Genome Editing. Molecular Cell 73, 714-726.e4. https://doi.org/10.1016/j.molcel.2018.12.003

Edwards, H.V., Scott, J.D., Baillie, G.S., 2012. The A-kinase-anchoring protein AKAP-Lbc facilitates cardioprotective PKA phosphorylation of Hsp20 on Ser(16). Biochem J 446, 437–443. https://doi.org/10.1042/BJ20120570

Ehlinger, A., Walters, K.J., 2013. Structural insights into proteasome activation by the 19S regulatory particle. Biochemistry 52, 3618–3628. https://doi.org/10.1021/bi400417a

Ehrich, M., Nelson, M.R., Stanssens, P., Zabeau, M., Liloglou, T., Xinarianos, G., Cantor, C.R., Field, J.K., van den Boom, D., 2005. Quantitative high-throughput analysis of DNA methylation patterns by base-specific cleavage and mass spectrometry. Proc Natl Acad Sci U S A 102, 15785. https://doi.org/10.1073/pnas.0507816102

Ejkova, E., Tansey, W.P., 2002. Old dogs and new tricks: meeting on mechanisms of eukaryotic transcription. EMBO Rep 3, 219–223. https://doi.org/10.1093/embo-reports/kvf054

El Dika, I., Lim, H.Y., Yong, W.P., Lin, C.-C., Yoon, J.-H., Modiano, M., Freilich, B., Choi, H.J., Chao, T.-Y., Kelley, R.K., Brown, J., Knox, J., Ryoo, B.-Y., Yau, T., Abou-Alfa, G.K., 2019. An Open-Label, Multicenter, Phase I, Dose Escalation Study with Phase II Expansion Cohort to Determine the Safety, Pharmacokinetics, and Preliminary Antitumor Activity of Intravenous TKM-080301 in Subjects with Advanced Hepatocellular Carcinoma. Oncologist 24, 747-e218. https://doi.org/10.1634/theoncologist.2018-0838

Eliasz, S., Liang, S., Chen, Y., De Marco, M.A., Machek, O., Skucha, S., Miele, L., Bocchetta, M., 2010. Notch-1 stimulates survival of lung adenocarcinoma cells during hypoxia by activating the IGF-1R pathway. Oncogene 29, 2488–2498. https://doi.org/10.1038/onc.2010.7

Elliott, B., Richardson, C., Winderbaum, J., Nickoloff, J.A., Jasin, M., 1998. Gene Conversion Tracts from Double-Strand Break Repair in Mammalian Cells. Mol. Cell. Biol. 18, 93. https://doi.org/10.1128/MCB.18.1.93

Elong Edimo, W., Vanderwinden, J.-M., Erneux, C., 2013. SHIP2 signalling at the plasma membrane, in the nucleus and at focal contacts. Advances in Biological Regulation 53, 28–37. https://doi.org/10.1016/j.jbior.2012.09.003

Estrada-Bernal, A., Chatterjee, M., Haque, S.J., Yang, L., Morgan, M.A., Kotian, S., Morrell, D., Chakravarti, A., Williams, T.M., 2015. MEK inhibitor GSK1120212-mediated radiosensitization of pancreatic cancer cells involves inhibition of DNA double-strand break repair pathways. Cell Cycle 14, 3713–3724. https://doi.org/10.1080/15384101.2015.1104437

Falk, M., Lukášová, E., Kozubek, S., 2008. Chromatin structure influences the sensitivity of DNA to γ-radiation. Biochimica et Biophysica Acta (BBA) - Molecular Cell Research 1783, 2398–2414. https://doi.org/10.1016/j.bbamcr.2008.07.010

Fang, X., Yu, S., Eder, A., Mao, M., Bast, R.C., Boyd, D., Mills, G.B., 1999. Regulation of BAD phosphorylation at serine 112 by the Ras-mitogen-activated protein kinase pathway. Oncogene 18, 6635–6640. https://doi.org/10.1038/sj.onc.1203076

Fantini, D., Huang, S., Asara, J.M., Bagchi, S., Raychaudhuri, P., 2017. Chromatin association of XRCC5/6 in the absence of DNA damage depends on the XPE gene product DDB2. MBoC 28, 192–200. https://doi.org/10.1091/mbc.e16-08-0573

Favaro, E., Bensaad, K., Chong, M.G., Tennant, D.A., Ferguson, D.J.P., Snell, C., Steers, G., Turley, H., Li, J.-L., Günther, U.L., Buffa, F.M., McIntyre, A., Harris, A.L., 2012. Glucose Utilization via Glycogen Phosphorylase Sustains Proliferation and Prevents Premature Senescence in Cancer Cells. Cell Metabolism 16, 751–764. https://doi.org/10.1016/j.cmet.2012.10.017

Favelyukis, S., Till, J.H., Hubbard, S.R., Miller, W.T., 2001. Structure and autoregulation of the insulin-like growth factor 1 receptor kinase. Nature Structural Biology 8, 1058–1063. https://doi.org/10.1038/nsb721

Featherstone, C., Jackson, S.P., 1999. DNA double-strand break repair. Current Biology 9, R759–R761. https://doi.org/10.1016/S0960-9822(00)80005-6

Feiersinger, G.E., Trattnig, K., Leitner, P.D., Guggenberger, F., Oberhuber, A., Peer, S., Hermann, M., Skvortsova, I., Vrbkova, J., Bouchal, J., Culig, Z., Santer, F.R., 2018. Olaparib is effective in combination with, and as maintenance therapy after, first-line endocrine therapy in prostate cancer cells. Mol Oncol 12, 561–576. https://doi.org/10.1002/1878-0261.12185

Feitelson, M.A., Arzumanyan, A., Kulathinal, R.J., Blain, S.W., Holcombe, R.F., Mahajna, J., Marino, M., Martinez-Chantar, M.L., Nawroth, R., Sanchez-Garcia, I., Sharma, D., Saxena, N.K., Singh, N., Vlachostergios, P.J., Guo, S., Honoki, K., Fujii, H., Georgakilas, A.G., Bilsland, A., Amedei, A., Niccolai, E., Amin, A., Ashraf, S.S., Boosani, C.S., Guha, G., Ciriolo, M.R., Aquilano, K., Chen, S., Mohammed, S.I., Azmi, A.S., Bhakta, D., Halicka, D., Keith, W.N., Nowsheen, S., 2015. Sustained proliferation in cancer: Mechanisms and novel therapeutic targets. Seminars in Cancer Biology 35, S25–S54. https://doi.org/10.1016/j.semcancer.2015.02.006

Feldser, D., Agani, F., Iyer, N.V., Pak, B., Ferreira, G., Semenza, G.L., 1999. Reciprocal Positive Regulation of Hypoxia-inducible Factor 1α and Insulin-like Growth Factor 2. Cancer Res 59, 3915.

Feng, B., Jiao, P., Helou, Y., Li, Y., He, Q., Walters, M.S., Salomon, A., Xu, H., 2014. Mitogen-activated protein kinase phosphatase 3 (MKP-3)-deficient mice are resistant to diet-induced obesity. Diabetes 63, 2924–2934. https://doi.org/10.2337/db14-0066

Feng, L., Li, N., Li, Y., Wang, J., Gao, M., Wang, W., Chen, J., 2015. Cell cycle-dependent inhibition of 53BP1 signaling by BRCA1. Cell Discov 1, 15019–15019. https://doi.org/10.1038/celldisc.2015.19

Fielder, P., Gargosky, S., Vaccarello, M., Wilson, K., Cohen, P., Diamond, F., Guevara-Aguirre, J., Rosenbloom, A., Rosenfeld, R., 1993. Serum profiles of insulin-like growth factors and their binding proteins in adults with growth hormone receptor deficiency treated with insulin like growth factor I. Acta Paediatrica 82, 40–43. https://doi.org/10.1111/j.1651-2227.1993.tb12838.x

Flanigan, S.A., Pitts, T.M., Eckhardt, S.G., Tentler, J.J., Tan, A.C., Thorburn, A., Leong, S., 2010. The insulin-like growth factor I receptor/insulin receptor tyrosine kinase inhibitor PQIP exhibits enhanced antitumor effects in combination with chemotherapy against colorectal cancer models. Clin Cancer Res 16, 5436–5446. https://doi.org/10.1158/1078-0432.CCR-10-2054

Fonfara, I., Richter, H., Bratovič, M., Le Rhun, A., Charpentier, E., 2016. The CRISPR-associated DNA-cleaving enzyme Cpf1 also processes precursor CRISPR RNA. Nature 532, 517–521. https://doi.org/10.1038/nature17945

Forbes, K., Westwood, M., 2010. Maternal growth factor regulation of human placental development and fetal growth. The Journal of endocrinology 207, 1–16. https://doi.org/10.1677/JOE-10-0174

Forest, A., Amatulli, M., Ludwig, D.L., Damoci, C.B., Wang, Y., Burns, C.A., Donoho, G.P., Zanella, N., Fiebig, H.H., Prewett, M.C., Surguladze, D., DeLigio, J.T., Houghton, P.J., Smith, M.A., Novosiadly, R., 2015. Intrinsic Resistance to Cixutumumab Is Conferred by Distinct Isoforms of the Insulin Receptor. Mol Cancer Res 13, 1615–1626. https://doi.org/10.1158/1541-7786.MCR-15-0279

Foulstone, E., Prince, S., Zaccheo, O., Burns, J., Harper, J., Jacobs, C., Church, D., Hassan, A., 2005. Insulin-like growth factor ligands, receptors, and binding proteins in cancer. The Journal of Pathology 205, 145–153. https://doi.org/10.1002/path.1712

Franke, T.F., 2008. PI3K/Akt: getting it right matters. Oncogene 27, 6473–6488. https://doi.org/10.1038/onc.2008.313

Franke, T.F., Kaplan, D.R., Cantley, L.C., Toker, A., 1997. Direct Regulation of the Akt Proto-Oncogene Product by Phosphatidylinositol-3,4-bisphosphate. Science 275, 665. https://doi.org/10.1126/science.275.5300.665

Frasca F., Pandini G., Scalia P., Sciacca L., Mineo R., Costantino A., Goldfine I. D., Belfiore A., Vigneri R., 1999. Insulin Receptor Isoform A, a Newly Recognized, High-Affinity Insulin-Like Growth Factor II Receptor in Fetal and Cancer Cells. Molecular and Cellular Biology 19, 3278–3288. https://doi.org/10.1128/MCB.19.5.3278

Frasca, F., Pandini, G., Scalia, P., Sciacca, L., Mineo, R., Costantino, A., Goldfine, I.D., Belfiore, A., Vigneri, R., 1999. Insulin receptor isoform A, a newly recognized, high-affinity insulin-like growth factor II receptor in fetal and cancer cells. Mol Cell Biol 19, 3278–3288. https://doi.org/10.1128/MCB.19.5.3278

Fraser, M., Harding, S.M., Zhao, H., Coackley, C., Durocher, D., Bristow, R.G., 2011. MRE11 promotes AKT phosphorylation in direct response to DNA double-strand breaks. Cell Cycle 10, 2218–2232. https://doi.org/10.4161/cc.10.13.16305

Fraser, M., Zhao, H., Luoto, K.R., Lundin, C., Coackley, C., Chan, N., Joshua, A.M., Bismar, T.A., Evans, A., Helleday, T., Bristow, R.G., 2012. PTEN Deletion in Prostate Cancer Cells Does Not Associate with Loss of RAD51 Function: Implications for Radiotherapy and Chemotherapy. Clin Cancer Res 18, 1015. https://doi.org/10.1158/1078-0432.CCR-11-2189

Frederick, T.J., Wood, T.L., 2004. IGF-I and FGF-2 coordinately enhance cyclin D1 and cyclin E–cdk2 association and activity to promote G1 progression in oligodendrocyte progenitor cells. Molecular and Cellular Neuroscience 25, 480–492. https://doi.org/10.1016/j.mcn.2003.11.015

Frederiksen, J.H., Jensen, S.B., Tümer, Z., Hansen, T.V.O., 2021. Classification of MSH6 Variants of Uncertain Significance Using Functional Assays. Int J Mol Sci 22, 8627. https://doi.org/10.3390/ijms22168627

Friedbichler, K., Hofmann, M.H., Kroez, M., Ostermann, E., Lamche, H.R., Koessl, C., Borges, E., Pollak, M.N., Adolf, G., Adam, P.J., 2013. Pharmacodynamic and antineoplastic activity of BI 836845, a fully human IGF ligand neutralizing antibody, and mechanistic rationale for combination with rapamycin. Mol Cancer Ther molcanther.0598.2013. https://doi.org/10.1158/1535-7163.MCT-13-0598

Fu, Y., Foden, J.A., Khayter, C., Maeder, M.L., Reyon, D., Joung, J.K., Sander, J.D., 2013. High-frequency off-target mutagenesis induced by CRISPR-Cas nucleases in human cells. Nature Biotechnology 31, 822–826. https://doi.org/10.1038/nbt.2623

Fukuda, R., Hirota, K., Fan, F., Jung, Y.D., Ellis, L.M., Semenza, G.L., 2002. Insulin-like Growth Factor 1 Induces Hypoxia-inducible Factor 1-mediated Vascular Endothelial Growth Factor Expression, Which is Dependent on MAP Kinase and Phosphatidylinositol 3-Kinase Signaling in Colon Cancer Cells*. Journal of Biological Chemistry 277, 38205–38211. https://doi.org/10.1074/jbc.M203781200

Furukawa, J., Wraight, C.J., Freier, S.M., Peralta, E., Atley, L.M., Monia, B.P., Gleave, M.E., Cox, M.E., 2010. Antisense oligonucleotide targeting of insulin-like growth factor-1 receptor (IGF-1R) in prostate cancer. The Prostate 70, 206–218. https://doi.org/10.1002/pros.21054

Gaj, T., Gersbach, C.A., Barbas, C.F., III, 2013. ZFN, TALEN, and CRISPR/Cas-based methods for genome engineering. Trends in Biotechnology 31, 397–405. https://doi.org/10.1016/j.tibtech.2013.04.004

Gallagher, D.N., Haber, J.E., 2018. Repair of a Site-Specific DNA Cleavage: Old-School Lessons for Cas9-Mediated Gene Editing. ACS Chem Biol 13, 397–405. https://doi.org/10.1021/acschembio.7b00760

Gallini, S., Carminati, M., De Mattia, F., Pirovano, L., Martini, E., Oldani, A., Asteriti, I.A., Guarguaglini, G., Mapelli, M., 2016. NuMA Phosphorylation by Aurora-A Orchestrates Spindle Orientation. Current Biology 26, 458–469. https://doi.org/10.1016/j.cub.2015.12.051

Gao, N., Flynn, D.C., Zhang, Z., Zhong, X.-S., Walker, V., Liu, K.J., Shi, X., Jiang, B.-H., 2004. G1 cell cycle progression and the expression of G1 cyclins are regulated by PI3K/AKT/mTOR/p70S6K1 signaling in human ovarian cancer cells. American Journal of Physiology-Cell Physiology 287, C281–C291. https://doi.org/10.1152/ajpcell.00422.2003

Gao, S., Gao, Y., He, H.H., Han, D., Han, W., Avery, A., Macoska, J.A., Liu, X., Chen, Sen, Ma, F., Chen, Shaoyong, Balk, S.P., Cai, C., 2016. Androgen Receptor Tumor Suppressor Function Is Mediated by Recruitment of Retinoblastoma Protein. Cell Rep 17, 966–976. https://doi.org/10.1016/j.celrep.2016.09.064

Garcia-Jove Navarro, M., Basset, C., Arcondéguy, T., Touriol, C., Perez, G., Prats, H., Lacazette, E., 2013. Api5 contributes to E2F1 control of the G1/S cell cycle phase transition. PLoS One 8, e71443–e71443. https://doi.org/10.1371/journal.pone.0071443

Garneau, J.E., Dupuis, M.-È., Villion, M., Romero, D.A., Barrangou, R., Boyaval, P., Fremaux, C., Horvath, P., Magadán, A.H., Moineau, S., 2010. The CRISPR/Cas bacterial immune system cleaves bacteriophage and plasmid DNA. Nature 468, 67–71. https://doi.org/10.1038/nature09523

Gaspar-Maia, A., Alajem, A., Polesso, F., Sridharan, R., Mason, M.J., Heidersbach, A., Ramalho-Santos, J., McManus, M.T., Plath, K., Meshorer, E., Ramalho-Santos, M., 2009. Chd1 regulates open chromatin and pluripotency of embryonic stem cells. Nature 460, 863–868. https://doi.org/10.1038/nature08212

Gatei, M., Jakob, B., Chen, P., Kijas, A.W., Becherel, O.J., Gueven, N., Birrell, G., Lee, J.-H., Paull, T.T., Lerenthal, Y., Fazry, S., Taucher-Scholz, G., Kalb, R., Schindler, D., Waltes, R., Dörk, T., Lavin, M.F., 2011. ATM protein-dependent phosphorylation of Rad50 protein regulates DNA repair and cell cycle control. J Biol Chem 286, 31542–31556. https://doi.org/10.1074/jbc.M111.258152

Gaudelli, N.M., Komor, A.C., Rees, H.A., Packer, M.S., Badran, A.H., Bryson, D.I., Liu, D.R., 2017. Programmable base editing of A•T to G•C in genomic DNA without DNA cleavage. Nature 551, 464–471. https://doi.org/10.1038/nature24644

Gaudelli, N.M., Lam, D.K., Rees, H.A., Solá-Esteves, N.M., Barrera, L.A., Born, D.A., Edwards, A., Gehrke, J.M., Lee, S.-J., Liquori, A.J., Murray, R., Packer, M.S., Rinaldi, C., Slaymaker, I.M., Yen, J., Young, L.E., Ciaramella, G., 2020. Directed evolution of adenine base editors with increased activity and therapeutic application. Nature Biotechnology 38, 892–900. https://doi.org/10.1038/s41587-020-0491-6

Geldof, A.A., Plaizier, M.A.B.D., Duivenvoorden, I., Ringelberg, M., Versteegh, R.T., Newling, D.W.W., Teule, G.J.J., 2003. Cell cycle perturbations and radiosensitization effects in a human prostate cancer cell line. Journal of Cancer Research and Clinical Oncology 129, 175–182. https://doi.org/10.1007/s00432-002-0412-8

Gell, D., Jackson, S.P., 1999. Mapping of protein-protein interactions within the DNA-dependent protein kinase complex. Nucleic Acids Res 27, 3494–3502. https://doi.org/10.1093/nar/27.17.3494

The Gene Ontology Consortium, 2018. The Gene Ontology Resource: 20 years and still GOing strong. Nucleic Acids Research 47, D330–D338. https://doi.org/10.1093/nar/gky1055

Gilbreath, C., Ma, S., Yu, L., Sonavane, R., Roggero, C.M., Devineni, A., Mauck, R., Desai, N.B., Bagrodia, A., Kittler, R., Raj, G.V., Yin, Y., 2021. Dynamic differences between DNA damage repair responses in primary tumors and cell lines. Translational Oncology 14, 100898. https://doi.org/10.1016/j.tranon.2020.100898

Girnita, L., Shenoy, S.K., Sehat, B., Vasilcanu, R., Vasilcanu, D., Girnita, A., Lefkowitz, R.J., Larsson, O., 2007. β-Arrestin and Mdm2 Mediate IGF-1 Receptor-stimulated ERK Activation and Cell Cycle Progression. Journal of Biological Chemistry 282, 11329–11338. https://doi.org/10.1074/jbc.M611526200

Glozak, M.A., Sengupta, N., Zhang, X., Seto, E., 2005. Acetylation and deacetylation of non-histone proteins. Gene 363, 15–23. https://doi.org/10.1016/j.gene.2005.09.010

Goi, K., Takagi, M., Iwata, S., Delia, D., Asada, M., Donghi, R., Tsunematsu, Y., Nakazawa, S., Yamamoto, H., Yokota, J., Tamura, K., Saeki, Y., Utsunomiya, J., Takahashi, T., Ueda, R., Ishioka, C., Eguchi, M., Kamata, N., Mizutani, S., 1997. DNA Damage-associated Dysregulation of the Cell Cycle and Apoptosis Control in Cells with Germ-line p53 Mutation. Cancer Res 57, 1895.

Golding, S.E., Morgan, R.N., Adams, B.R., Hawkins, A.J., Povirk, L.F., Valerie, K., 2009. Pro-survival AKT and ERK signaling from EGFR and mutant EGFRvIII enhances DNA double-strand break repair in human glioma cells. Cancer Biol Ther 8, 730–738. https://doi.org/10.4161/cbt.8.8.7927

Golding, S.E., Rosenberg, E., Neill, S., Dent, P., Povirk, L.F., Valerie, K., 2007. Extracellular Signal-Related Kinase Positively Regulates Ataxia Telangiectasia Mutated, Homologous Recombination Repair, and the DNA Damage Response. Cancer Res 67, 1046. https://doi.org/10.1158/0008-5472.CAN-06-2371

Goodarzi, A.A., Noon, A.T., Deckbar, D., Ziv, Y., Shiloh, Y., Löbrich, M., Jeggo, P.A., 2008. ATM Signaling Facilitates Repair of DNA Double-Strand Breaks Associated with Heterochromatin. Molecular Cell 31, 167–177. https://doi.org/10.1016/j.molcel.2008.05.017

Goodarzi, A.A., Noon, A.T., Jeggo, P.A., 2009. The impact of heterochromatin on DSB repair. Biochemical Society Transactions 37, 569–576. https://doi.org/10.1042/BST0370569

Goodarzi, A.A., Yu, Y., Riballo, E., Douglas, P., Walker, S.A., Ye, R., Härer, C., Marchetti, C., Morrice, N., Jeggo, P.A., Lees-Miller, S.P., 2006. DNA-PK autophosphorylation facilitates Artemis endonuclease activity. EMBO J 25, 3880–3889. https://doi.org/10.1038/sj.emboj.7601255

Göttlich, B., Reichenberger, S., Feldmann, E., Pfeiffer, P., 1998. Rejoining of DNA double-strand breaks in vitro by single-strand annealing. European Journal of Biochemistry 258, 387–395. https://doi.org/10.1046/j.1432-1327.1998.2580387.x

Gottlieb, T.M., Jackson, S.P., 1993. The DNA-dependent protein kinase: Requirement for DNA ends and association with Ku antigen. Cell 72, 131–142. https://doi.org/10.1016/0092-8674(93)90057-W

Gottschalk, A.R., Doan, A., Nakamura, J.L., Stokoe, D., Haas-Kogan, D.A., 2005. Inhibition of phosphatidylinositol-3-kinase causes increased sensitivity to radiation through a PKB-dependent mechanism. International Journal of Radiation Oncology • Biology • Physics 63, 1221–1227. https://doi.org/10.1016/j.ijrobp.2005.08.014

Gottschalk, W.K., 1991. The pathway mediating insulin's effects on pyruvate dehydrogenase bypasses the insulin receptor tyrosine kinase. Journal of Biological Chemistry 266, 8814–8819.

Goytisolo, F.A., Samper, E., Edmonson, S., Taccioli, G.E., Blasco, M.A., 2001. The absence of the dna-dependent protein kinase catalytic subunit in mice results in anaphase bridges and in increased telomeric fusions with normal telomere length and G-strand overhang. Mol Cell Biol 21, 3642–3651. https://doi.org/10.1128/MCB.21.11.3642-3651.2001

Graham, T.R., Zhau, H.E., Odero-Marah, V.A., Osunkoya, A.O., Kimbro, K.S., Tighiouart, M., Liu, T., Simons, J.W., O'Regan, R.M., 2008. Insulin-like Growth Factor-I–Dependent Up-regulation of ZEB1 Drives Epithelial-to-Mesenchymal Transition in Human Prostate Cancer Cells. Cancer Res 68, 2479. https://doi.org/10.1158/0008-5472.CAN-07-2559

Gray, L.H., Conger, A.D., Ebert, M., Hornsey, S., Scott, O.C.A., 1953. The Concentration of Oxygen Dissolved in Tissues at the Time of Irradiation as a Factor in Radiotherapy. BJR 26, 638–648. https://doi.org/10.1259/0007-1285-26-312-638

Green, S.M., Mostaghel, E.A., Nelson, P.S., 2012. Androgen action and metabolism in prostate cancer. Mol Cell Endocrinol 360, 3–13. https://doi.org/10.1016/j.mce.2011.09.046

Greenwood, H., Crafter, C., Davies, B., Cosulich, S., 2011. Abstract 1052: In vitro mechanism of action of AZD5363, a novel AKT inhibitor, in breast and prostate cancer cell lines. Cancer Res 71, 1052. https://doi.org/10.1158/1538-7445.AM2011-1052

Groffen, J., Stephenson, J.R., Heisterkamp, N., de Klein, A., Bartram, C.R., Grosveld, G., 1984. Philadelphia chromosomal breakpoints are clustered within a limited region, bcr, on chromosome 22. Cell 36, 93–99. https://doi.org/10.1016/0092-8674(84)90077-1

Guenther, L.M., Dharia, N.V., Ross, L., Conway, A., Robichaud, A.L., Catlett, J.L., 2nd, Wechsler, C.S., Frank, E.S., Goodale, A., Church, A.J., Tseng, Y.-Y., Guha, R., McKnight, C.G., Janeway, K.A., Boehm, J.S., Mora, J., Davis, M.I., Alexe, G., Piccioni, F., Stegmaier, K., 2019. A Combination CDK4/6 and IGF1R Inhibitor Strategy for Ewing Sarcoma. Clin Cancer Res 25, 1343–1357. https://doi.org/10.1158/1078-0432.CCR-18-0372

Guertin, D.A., Sabatini, D.M., 2007. Defining the Role of mTOR in Cancer. Cancer Cell 12, 9–22. https://doi.org/10.1016/j.ccr.2007.05.008

Guevara-Aguirre, J., Balasubramanian, P., Guevara-Aguirre, M., Wei, M., Madia, F., Cheng, C.-W., Hwang, D., Martin-Montalvo, A., Saavedra, J., Ingles, S., de Cabo, R., Cohen, P., Longo, V.D., 2011. Growth Hormone Receptor Deficiency Is Associated with a Major Reduction in Pro-Aging Signaling, Cancer, and Diabetes in Humans. Science Translational Medicine 3, 70ra13. https://doi.org/10.1126/scitranslmed.3001845

Guirouilh-Barbat, J., Rass, E., Plo, I., Bertrand, P., Lopez, B.S., 2007. Defects in XRCC4 and KU80 differentially affect the joining of distal nonhomologous ends. Proc Natl Acad Sci U S A 104, 20902–20907. https://doi.org/10.1073/pnas.0708541104

Gunn, A., Stark, J.M., 2012. I-SceI-Based Assays to Examine Distinct Repair Outcomes of Mammalian Chromosomal Double Strand Breaks, in: Bjergbæk, L. (Ed.), DNA Repair Protocols. Humana Press, Totowa, NJ, pp. 379–391. https://doi.org/10.1007/978-1-61779-998-3_27

Gupta, A.K., McKenna, W.G., Weber, C.N., Feldman, M.D., Goldsmith, J.D., Mick, R., Machtay, M., Rosenthal, D.I., Bakanauskas, V.J., Cerniglia, G.J., Bernhard, E.J., Weber, R.S., Muschel, R.J., 2002. Local Recurrence in Head and Neck Cancer. Clin Cancer Res 8, 885.

Gupta, A.K., Soto, D.E., Feldman, M.D., Goldsmith, J.D., Mick, R., Hahn, S.M., Machtay, M., Muschel, R.J., McKenna, W.G., 2004. Signaling Pathways in NSCLC as a Predictor of Outcome and Response to Therapy. Lung 182, 151–162. https://doi.org/10.1007/s00408-004-0310-8

Gusscott, S., Jenkins, C.E., Lam, S.H., Giambra, V., Pollak, M., Weng, A.P., 2016a. IGF1R Derived PI3K/AKT Signaling Maintains Growth in a Subset of Human T-Cell Acute Lymphoblastic Leukemias. PLOS ONE 11, e0161158. https://doi.org/10.1371/journal.pone.0161158

Gusscott, S., Jenkins, C.E., Lam, S.H., Giambra, V., Pollak, M., Weng, A.P., 2016b. IGF1R Derived PI3K/AKT Signaling Maintains Growth in a Subset of Human T-Cell Acute Lymphoblastic Leukemias. PLOS ONE 11, e0161158. https://doi.org/10.1371/journal.pone.0161158

Haar, E.V., Lee, S., Bandhakavi, S., Griffin, T.J., Kim, D.-H., 2007. Insulin signalling to mTOR mediated by the Akt/PKB substrate PRAS40. Nature Cell Biology 9, 316–323. https://doi.org/10.1038/ncb1547

Hahn, A.T., Jones, J.T., Meyer, T., 2009. Quantitative analysis of cell cycle phase durations and PC12 differentiation using fluorescent biosensors. Cell Cycle 8, 1044–1052. https://doi.org/10.4161/cc.8.7.8042

Hakuno, F., Takahashi, S.-I., 2018. 40 YEARS OF IGF1: IGF1 receptor signaling pathways. Journal of Molecular Endocrinology 61, T69–T86. https://doi.org/10.1530/JME-17-0311

Halazonetis, T.D., Gorgoulis, V.G., Bartek, J., 2008. An Oncogene-Induced DNA Damage Model for Cancer Development. Science 319, 1352. https://doi.org/10.1126/science.1140735

Haluska, P., Menefee, M., Plimack, E.R., Rosenberg, J., Northfelt, D., LaVallee, T., Shi, L., Yu, X.-Q., Burke, P., Huang, J., Viner, J., McDevitt, J., LoRusso, P., 2014. Phase I dose-escalation study of MEDI-573, a bispecific, antiligand monoclonal antibody against IGFI and IGFII, in patients with advanced solid tumors. Clin Cancer Res 20, 4747–4757. https://doi.org/10.1158/1078-0432.CCR-14-0114

Hamdy, F.C., Donovan, J.L., Lane, J.A., Mason, M., Metcalfe, C., Holding, P., Davis, M., Peters, T.J., Turner, E.L., Martin, R.M., Oxley, J., Robinson, M., Staffurth, J., Walsh, E., Bollina, P., Catto, J., Doble, A., Doherty, A., Gillatt, D., Kockelbergh, R., Kynaston, H., Paul, A., Powell, P., Prescott, S., Rosario, D.J., Rowe, E., Neal, D.E., 2016. 10-Year Outcomes after Monitoring, Surgery, or Radiotherapy for Localized Prostate Cancer. N Engl J Med 375, 1415–1424. https://doi.org/10.1056/NEJMoa1606220

Hammel, M., Yu, Y., Mahaney, B.L., Cai, B., Ye, R., Phipps, B.M., Rambo, R.P., Hura, G.L., Pelikan, M., So, S., Abolfath, R.M., Chen, D.J., Lees-Miller, S.P., Tainer, J.A., 2010. Ku and DNA-dependent protein kinase dynamic conformations and assembly regulate DNA binding and the initial non-homologous end joining complex. J Biol Chem 285, 1414–1423. https://doi.org/10.1074/jbc.M109.065615

Hamoen, E.H., Reukers, D.F., Numans, M.E., Barentsz, J.O., Witjes, J.A., Rovers, M.M., 2013. Discrepancies between guidelines and clinical practice regarding prostate-specific antigen testing. Family Practice 30, 648–654. https://doi.org/10.1093/fampra/cmt045

Han, K., Pierce, S.E., Li, A., Spees, K., Anderson, G.R., Seoane, J.A., Lo, Y.-H., Dubreuil, M., Olivas, M., Kamber, R.A., Wainberg, M., Kostyrko, K., Kelly, M.R., Yousefi, M., Simpkins, S.W., Yao, D., Lee, K., Kuo, C.J., Jackson, P.K., Sweet-Cordero, A., Kundaje, A., Gentles, A.J., Curtis, C., Winslow, M.M., Bassik, M.C., 2020. CRISPR screens in cancer spheroids identify 3D growth-specific vulnerabilities. Nature 580, 136–141. https://doi.org/10.1038/s41586-020-2099-x

Hanahan, D., Weinberg, R.A., 2011. Hallmarks of Cancer: The Next Generation. Cell 144, 646–674. https://doi.org/10.1016/j.cell.2011.02.013

Hankinson, S.E., Willett, W.C., Colditz, G.A., Hunter, D.J., Michaud, D.S., Deroo, B., Rosner, B., Speizer, F.E., Pollak, M., 1998. Circulating concentrations of insulin-like growth factor I and risk of breast cancer. The Lancet 351, 1393–1396. https://doi.org/10.1016/S0140-6736(97)10384-1

Hao, P., Yu, J., Ward, R., Liu, Y., Hao, Q., An, S., Xu, T., 2020. Eukaryotic translation initiation factors as promising targets in cancer therapy. Cell Communication and Signaling 18, 175. https://doi.org/10.1186/s12964-020-00607-9

Happo, L., Strasser, A., Cory, S., 2012. BH3-only proteins in apoptosis at a glance. J. Cell Sci. 125, 1081. https://doi.org/10.1242/jcs.090514

Harbour, J.W., Dean, D.C., 2000. The Rb/E2F pathway: expanding roles and emerging paradigms. Genes & Development 14, 2393–2409. https://doi.org/10.1101/gad.813200

Harley, C.B., 2008. Telomerase and cancer therapeutics. Nature Reviews Cancer 8, 167–179. https://doi.org/10.1038/nrc2275

Harrington, K.J., Billingham, L.J., Brunner, T.B., Burnet, N.G., Chan, C.S., Hoskin, P., Mackay, R.I., Maughan, T.S., Macdougall, J., McKenna, W.G., Nutting, C.M., Oliver, A., Plummer, R., Stratford, I.J., Illidge, T., 2011. Guidelines for preclinical and early phase clinical assessment of novel radiosensitisers. Br J Cancer 105, 628–639. https://doi.org/10.1038/bjc.2011.240

Hart, J.R., Vogt, P.K., 2011. Phosphorylation of AKT: a mutational analysis. Oncotarget 2, 467–476. https://doi.org/10.18632/oncotarget.293

Hartmann, L.C., Sellers, T.A., Frost, M.H., Lingle, W.L., Degnim, A.C., Ghosh, K., Vierkant, R.A., Maloney, S.D., Pankratz, V.S., Hillman, D.W., Suman, V.J., Johnson, J., Blake, C., Tlsty, T., Vachon, C.M., Melton, L.J., Visscher, D.W., 2005. Benign Breast Disease and the Risk of Breast Cancer. N Engl J Med 353, 229–237. https://doi.org/10.1056/NEJMoa044383

Haruta, T., Uno, T., Kawahara, J., Takano, A., Egawa, K., Sharma, P.M., Olefsky, J.M., Kobayashi, M., 2000. A Rapamycin-Sensitive Pathway Down-Regulates Insulin Signaling via Phosphorylation and Proteasomal Degradation of Insulin Receptor Substrate-1. Molecular Endocrinology 14, 783–794. https://doi.org/10.1210/mend.14.6.0446

Harvey, A., Mielke, N., Grimstead, J.W., Jones, R.E., Nguyen, T., Mueller, M., Baird, D.M., Hendrickson, E.A., 2018. PARP1 is required for preserving telomeric integrity but is dispensable for A-NHEJ. Oncotarget; Vol 9, No 78.

Hatfield, S.M., Kjaergaard, J., Lukashev, D., Schreiber, T.H., Belikoff, B., Abbott, R., Sethumadhavan, S., Philbrook, P., Ko, K., Cannici, R., Thayer, M., Rodig, S., Kutok, J.L., Jackson, E.K., Karger, B., Podack, E.R., Ohta, A., Sitkovsky, M.V., 2015. Immunological mechanisms of the antitumor effects of supplemental oxygenation. Sci Transl Med 7, 277ra30-277ra30. https://doi.org/10.1126/scitranslmed.aaa1260

Hattab, D., Gazzali, A.M., Bakhtiar, A., 2021. Clinical Advances of siRNA-Based Nanotherapeutics for Cancer Treatment. Pharmaceutics 13, 1009. https://doi.org/10.3390/pharmaceutics13071009

Heemers, H.V., Tindall, D.J., 2007. Androgen Receptor (AR) Coregulators: A Diversity of Functions Converging on and Regulating the AR Transcriptional Complex. Endocrine Reviews 28, 778–808. https://doi.org/10.1210/er.2007-0019

Heibeck, T.H., Ding, S.-J., Opresko, L.K., Zhao, R., Schepmoes, A.A., Yang, F., Tolmachev, A.V., Monroe, M.E., Camp, D.G., 2nd, Smith, R.D., Wiley, H.S., Qian, W.-J., 2009. An extensive survey of tyrosine phosphorylation revealing new sites in human mammary epithelial cells. J Proteome Res 8, 3852–3861. https://doi.org/10.1021/pr900044c

Heldin, C.-H., 2013. Targeting the PDGF signaling pathway in tumor treatment. Cell Communication and Signaling 11, 97. https://doi.org/10.1186/1478-811X-11-97

Hellawell, G.O., Turner, G.D.H., Davies, D.R., Poulsom, R., Brewster, S.F., Macaulay, V.M., 2002. Expression of the Type 1 Insulin-like Growth Factor Receptor Is Up-Regulated in Primary Prostate Cancer and Commonly Persists in Metastatic Disease. Cancer Res 62, 2942.

Helleday, T., 2011. The underlying mechanism for the PARP and BRCA synthetic lethality: clearing up the misunderstandings. Mol Oncol 5, 387–393. https://doi.org/10.1016/j.molonc.2011.07.001

Hennessy, B.T., Smith, D.L., Ram, P.T., Lu, Y., Mills, G.B., 2005. Exploiting the PI3K/AKT Pathway for Cancer Drug Discovery. Nature Reviews Drug Discovery 4, 988–1004. https://doi.org/10.1038/nrd1902

Henry, M.K., Lynch, J.T., Eapen, A.K., Quelle, F.W., 2001. DNA damage–induced cell-cycle arrest of hematopoietic cells is overridden by activation of the PI-3 kinase/Akt signaling pathway. Blood 98, 834–841. https://doi.org/10.1182/blood.V98.3.834

Herold, M.J., Rohrbeck, L., Lang, M.J., Grumont, R., Gerondakis, S., Tai, L., Bouillet, P., Kaufmann, T., Strasser, A., 2013. Foxo-mediated Bim transcription is dispensable for the apoptosis of hematopoietic cells that is mediated by this BH3-only protein. EMBO Rep 14, 992–998. https://doi.org/10.1038/embor.2013.152

Héron-Milhavet, L., Karas, M., Goldsmith, C., Baum, B., LeRoith, D., 2001. Insulin-like growth factor-I (IGF-I) receptor activation rescues UV-damaged cells through a p38 signaling pathway. Potential role of the IGF-I receptor in DNA repair. The Journal of biological chemistry 276, 18185–18192. https://doi.org/10.1074/jbc.m011490200

Heskamp, S., Boerman, O.C., Molkenboer-Kuenen, J.D.M., Wauters, C.A., Strobbe, L.J.A., Mandigers, C.M.P.W., Bult, P., Oyen, W.J.G., van der Graaf, W.T.A., van Laarhoven, H.W.M., 2015. Upregulation of IGF-1R expression during neoadjuvant therapy predicts poor outcome in breast cancer patients. PLoS One 10, e0117745–e0117745. https://doi.org/10.1371/journal.pone.0117745

Hideshima, T., Anderson, K.C., 2002. Molecular mechanisms of novel therapeutic approaches for multiple myeloma. Nature Reviews Cancer 2, 927–937. https://doi.org/10.1038/nrc952

Hirose, Y., Katayama, M., Mirzoeva, O.K., Berger, M.S., Pieper, R.O., 2005. Akt Activation Suppresses Chk2-Mediated, Methylating Agent–Induced G_2 Arrest and Protects from Temozolomide-Induced Mitotic Catastrophe and Cellular Senescence. Cancer Res 65, 4861. https://doi.org/10.1158/0008-5472.CAN-04-2633

Hockemeyer, D., Wang, H., Kiani, S., Lai, C.S., Gao, Q., Cassady, J.P., Cost, G.J., Zhang, L., Santiago, Y., Miller, J.C., Zeitler, B., Cherone, J.M., Meng, X., Hinkley, S.J., Rebar, E.J., Gregory, P.D., Urnov, F.D., Jaenisch, R., 2011. Genetic engineering of human pluripotent cells using TALE nucleases. Nature Biotechnology 29, 731–734. https://doi.org/10.1038/nbt.1927

Horakova, O., Kroupova, P., Bardova, K., Buresova, J., Janovska, P., Kopecky, J., Rossmeisl, M., 2019. Metformin acutely lowers blood glucose levels by inhibition of intestinal glucose transport. Sci Rep 9, 6156–6156. https://doi.org/10.1038/s41598-019-42531-0

Hsiau, T., Conant, D., Rossi, N., Maures, T., Waite, K., Yang, J., Joshi, S., Kelso, R., Holden, K., Enzmann, B., Stoner, R., 2018. Inference of CRISPR Edits from Sanger Trace Data. https://doi.org/10.1101/251082

Hsu, P.D., Lander, E.S., Zhang, F., 2014. Development and applications of CRISPR-Cas9 for genome engineering. Cell 157, 1262–1278. https://doi.org/10.1016/j.cell.2014.05.010

Hu, Z.-Z., Huang, H., Cheema, A., Jung, M., Dritschilo, A., Wu, C.H., 2008. Integrated Bioinformatics for Radiation-Induced Pathway Analysis from Proteomics and Microarray Data. J Proteomics Bioinform 1, 47–60. https://doi.org/10.4172/jpb.1000009

Hua, H., Kong, Q., Yin, J., Zhang, J., Jiang, Y., 2020. Insulin-like growth factor receptor signaling in tumorigenesis and drug resistance: a challenge for cancer therapy. J Hematol Oncol 13, 64–64. https://doi.org/10.1186/s13045-020-00904-3

Huang, L.C., Clarkin, K.C., Wahl, G.M., 1996. Sensitivity and selectivity of the DNA damage sensor responsible for activating p53-dependent G1 arrest. Proc Natl Acad Sci U S A 93, 4827–4832. https://doi.org/10.1073/pnas.93.10.4827

Huang, R.-X., Zhou, P.-K., 2020. DNA damage response signaling pathways and targets for radiotherapy sensitization in cancer. Signal Transduction and Targeted Therapy 5, 60. https://doi.org/10.1038/s41392-020-0150-x

Huang, T.P., Zhao, K.T., Miller, S.M., Gaudelli, N.M., Oakes, B.L., Fellmann, C., Savage, D.F., Liu, D.R., 2019. Circularly permuted and PAM-modified Cas9 variants broaden the targeting scope of base editors. Nature Biotechnology 37, 626–631. https://doi.org/10.1038/s41587-019-0134-y

Huang, X., Luan, B., Wu, J., Shi, Y., 2016. An atomic structure of the human 26S proteasome. Nature Structural & Molecular Biology 23, 778–785. https://doi.org/10.1038/nsmb.3273

Huggins, C., Hodges, C.V., 1941. Studies on Prostatic Cancer. I. The Effect of Castration, of Estrogen and of Androgen Injection on Serum Phosphatases in Metastatic Carcinoma of the Prostate. Cancer Res 1, 293.

Huggins, C., Stevens, R.E., Jr., Hodges, C.V., 1941. Studies on Prostatic Cancer: II. The Effects of Castration on Advanced Carcinoma of the Prostate Gland. Archives of Surgery 43, 209–223. https://doi.org/10.1001/archsurg.1941.01210140043004

Huggins, C.F., Chafin, D.R., Aoyagi, S., Henricksen, L.A., Bambara, R.A., Hayes, J.J., 2002. Flap Endonuclease 1 Efficiently Cleaves Base Excision Repair and DNA Replication Intermediates Assembled into Nucleosomes. Molecular Cell 10, 1201–1211. https://doi.org/10.1016/S1097-2765(02)00736-0

Hunt, S.E., McLaren, W., Gil, L., Thormann, A., Schuilenburg, H., Sheppard, D., Parton, A., Armean, I.M., Trevanion, S.J., Flicek, P., Cunningham, F., 2018. Ensembl variation resources. Database 2018. https://doi.org/10.1093/database/bay119

Hussain, M.A., Schmitz, O., Mengel, A., Keller, A., Christiansen, J.S., Zapf, J., Froesch, E.R., 1993. Insulin-like growth factor I stimulates lipid oxidation, reduces protein oxidation, and enhances insulin sensitivity in humans. J Clin Invest 92, 2249–2256. https://doi.org/10.1172/JCI116828

Hussain, S.A., Maroto, P., Climent, M.Á., Bianchini, D., Jones, R.H., Lin, C.-C., Wang, S.-S., Dean, E., Crossley, K., Schlieker, L., Bogenrieder, T., De Bono, J.S., 2019. Targeting IGF-1/2 with xentuzumab (Xe) plus enzalutamide (En) in metastatic castration-resistant prostate cancer (mCRPC) after progression on docetaxel chemotherapy (DCt) and abiraterone (Abi): Randomized phase II trial results. JCO 37, 5030–5030. https://doi.org/10.1200/JCO.2019.37.15_suppl.5030

Hyun, K., Jeon, J., Park, K., Kim, J., 2017. Writing, erasing and reading histone lysine methylations. Experimental & Molecular Medicine 49, e324–e324. https://doi.org/10.1038/emm.2017.11

Igney, F.H., Krammer, P.H., 2002. Death and anti-death: tumour resistance to apoptosis. Nature Reviews Cancer 2, 277–288. https://doi.org/10.1038/nrc776

Iliakis, G., Murmann, T., Soni, A., 2015. Alternative end-joining repair pathways are the ultimate backup for abrogated classical non-homologous end-joining and homologous recombination repair: Implications for the formation of chromosome translocations. Mutation Research/Genetic Toxicology and Environmental Mutagenesis 793, 166–175. https://doi.org/10.1016/j.mrgentox.2015.07.001

Imseng, S., Aylett, C.H., Maier, T., 2018. Architecture and activation of phosphatidylinositol 3-kinase related kinases. Current Opinion in Structural Biology 49, 177–189. https://doi.org/10.1016/j.sbi.2018.03.010

Ishino, Y., Shinagawa, H., Makino, K., Amemura, M., Nakata, A., 1987. Nucleotide sequence of the iap gene, responsible for alkaline phosphatase isozyme conversion in Escherichia coli, and identification of the gene product. J Bacteriol 169, 5429–5433. https://doi.org/10.1128/jb.169.12.5429-5433.1987

Isobe, S.-Y., Nagao, K., Nozaki, N., Kimura, H., Obuse, C., 2017. Inhibition of RIF1 by SCAI Allows BRCA1-Mediated Repair. Cell Reports 20, 297–307. https://doi.org/10.1016/j.celrep.2017.06.056

Isono, M., Niimi, A., Oike, T., Hagiwara, Y., Sato, H., Sekine, R., Yoshida, Y., Isobe, S.-Y., Obuse, C., Nishi, R., Petricci, E., Nakada, S., Nakano, T., Shibata, A., 2017. BRCA1 Directs the Repair Pathway to Homologous Recombination by Promoting 53BP1 Dephosphorylation. Cell Reports 18, 520–532. https://doi.org/10.1016/j.celrep.2016.12.042

Isozaki, H., Ichihara, E., Takigawa, N., Ohashi, K., Ochi, N., Yasugi, M., Ninomiya, T., Yamane, H., Hotta, K., Sakai, K., Matsumoto, K., Hosokawa, S., Bessho, A., Sendo, T., Tanimoto, M., Kiura, K., 2016. Non–Small Cell Lung Cancer Cells Acquire Resistance to the ALK Inhibitor Alectinib by Activating Alternative Receptor Tyrosine Kinases. Cancer Res 76, 1506. https://doi.org/10.1158/0008-5472.CAN-15-1010

Iwasa, T., Okamoto, I., Suzuki, M., Hatashita, E., Yamada, Y., Fukuoka, M., Ono, K., Nakagawa, K., 2009. Inhibition of Insulin-Like Growth Factor 1 Receptor by CP-751,871 Radiosensitizes Non–Small Cell Lung Cancer Cells. Clin Cancer Res 15, 5117. https://doi.org/10.1158/1078-0432.CCR-09-0478

Jaaks, P., Meier, G., Alijaj, N., Brack, E., Bode, P., Koscielniak, E., Wachtel, M., Schäfer, B.W., Bernasconi, M., 2016. The proprotein convertase furin is required to maintain viability of alveolar rhabdomyosarcoma cells. Oncotarget; Vol 7, No 47.

Jackson, S.P., 2002. Sensing and repairing DNA double-strand breaks. Carcinogenesis 23, 687–696. https://doi.org/10.1093/carcin/23.5.687

Jackson, S.P., Bartek, J., 2009. The DNA-damage response in human biology and disease. Nature 461, 1071–1078. https://doi.org/10.1038/nature08467

Jacq, X., Kemp, M., Martin, N.M.B., Jackson, S.P., 2013. Deubiquitylating enzymes and DNA damage response pathways. Cell Biochem Biophys 67, 25–43. https://doi.org/10.1007/s12013-013-9635-3

Janecka, A., KOŁODZIEJ-RZEPA, M., BIESAGA, B., 2016. Clinical and Molecular Features of Laron Syndrome, A Genetic Disorder Protecting from Cancer. In Vivo 30, 375–381.

Jang, S.M., Kauzlaric, A., Quivy, J.-P., Pontis, J., Rauwel, B., Coluccio, A., Offner, S., Duc, J., Turelli, P., Almouzni, G., Trono, D., 2018. KAP1 facilitates reinstatement of heterochromatin after DNA replication. Nucleic Acids Research 46, 8788–8802. https://doi.org/10.1093/nar/gky580

Janssen, A., Medema, R.H., 2013. Genetic instability: tipping the balance. Oncogene 32, 4459–4470. https://doi.org/10.1038/onc.2012.576

Jaques, G., Noll, K., Wegmann, B., Witten, S., Kogan, E., Radulescu, R.T., Havemann, K., 1997. Nuclear Localization of Insulin-Like Growth Factor Binding Protein 3 in a Lung Cancer Cell Line. Endocrinology 138, 1767–1770. https://doi.org/10.1210/endo.138.4.5177

Jasin, M., Haber, J.E., 2016. The democratization of gene editing: Insights from site-specific cleavage and double-strand break repair. DNA Repair 44, 6–16. https://doi.org/10.1016/j.dnarep.2016.05.001

Jassal, B., Matthews, L., Viteri, G., Gong, C., Lorente, P., Fabregat, A., Sidiropoulos, K., Cook, J., Gillespie, M., Haw, R., Loney, F., May, B., Milacic, M., Rothfels, K., Sevilla, C., Shamovsky, V., Shorser, S., Varusai, T., Weiser, J., Wu, G., Stein, L., Hermjakob, H., D'Eustachio, P., 2019. The reactome pathway knowledgebase. Nucleic Acids Research 48, D498–D503. https://doi.org/10.1093/nar/gkz1031

Javle, M., Curtin, N.J., 2011. The role of PARP in DNA repair and its therapeutic exploitation. Br J Cancer 105, 1114–1122. https://doi.org/10.1038/bjc.2011.382

Jeggo, P.A., 1998. 5 DNA Breakage and Repair, in: Hall, J.C., Dunlap, J.C., Friedmann, T., Giannelli, F. (Eds.), Advances in Genetics. Academic Press, pp. 185–218. https://doi.org/10.1016/S0065-2660(08)60144-3

Jenner, T.J., deLara, C.M., O'Neill, P., Stevens, D.L., 1993. Induction and Rejoining of DNA Double-strand Breaks in V79-4 Mammalian Cells Following γ- and α-irradiation. null 64, 265–273. https://doi.org/10.1080/09553009314551421

Jeong, S.M., Xiao, C., Finley, L.W.S., Lahusen, T., Souza, A.L., Pierce, K., Li, Y.-H., Wang, X., Laurent, G., German, N.J., Xu, X., Li, C., Wang, R.-H., Lee, J., Csibi, A., Cerione, R., Blenis, J., Clish, C.B., Kimmelman, A., Deng, C.-X., Haigis, M.C., 2013. SIRT4 has tumor-suppressive activity and regulates the cellular metabolic response to DNA damage by inhibiting mitochondrial glutamine metabolism. Cancer Cell 23, 450–463. https://doi.org/10.1016/j.ccr.2013.02.024

Jernberg, E., Bergh, A., Wikström, P., 2017. Clinical relevance of androgen receptor alterations in prostate cancer. Endocr Connect 6, R146–R161. https://doi.org/10.1530/EC-17-0118

Jette, N., Lees-Miller, S.P., 2015. The DNA-dependent protein kinase: A multifunctional protein kinase with roles in DNA double strand break repair and mitosis. Prog Biophys Mol Biol 117, 194–205. https://doi.org/10.1016/j.pbiomolbio.2014.12.003

Jiang, F., Taylor, D.W., Chen, J.S., Kornfeld, J.E., Zhou, K., Thompson, A.J., Nogales, E., Doudna, J.A., 2016. Structures of a CRISPR-Cas9 R-loop complex primed for DNA cleavage. Science 351, 867. https://doi.org/10.1126/science.aad8282

Jiang, T., Henderson, J.M., Coote, K., Cheng, Y., Valley, H.C., Zhang, X.-O., Wang, Q., Rhym, L.H., Cao, Y., Newby, G.A., Bihler, H., Mense, M., Weng, Z., Anderson, D.G., McCaffrey, A.P., Liu, D.R., Xue, W., 2020. Chemical modifications of adenine base editor mRNA and guide RNA expand its application scope. Nat Commun 11, 1979–1979. https://doi.org/10.1038/s41467-020-15892-8

Jiang, W., Crowe, J.L., Liu, X., Nakajima, S., Wang, Y., Li, C., Lee, B.J., Dubois, R.L., Liu, C., Yu, X., Lan, L., Zha, S., 2015. Differential Phosphorylation of DNA-PKcs Regulates the Interplay between End-Processing and End-Ligation during Nonhomologous End-Joining. Molecular Cell 58, 172–185. https://doi.org/10.1016/j.molcel.2015.02.024

Jiang, X., Sun, Y., Chen, S., Roy, K., Price, B.D., 2006. The FATC Domains of PIKK Proteins Are Functionally Equivalent and Participate in the Tip60-dependent Activation of DNA-PKcs and ATM. Journal of Biological Chemistry 281, 15741–15746. https://doi.org/10.1074/jbc.M513172200

Jiang, Y., Chan, J.L.-K., Zong, C.S., Wang, L.-H., 1996. Effect of Tyrosine Mutations on the Kinase Activity and Transforming Potential of an Oncogenic Human Insulin-like Growth Factor I Receptor. Journal of Biological Chemistry 271, 160–167. https://doi.org/10.1074/jbc.271.1.160

Jiang, Y., Cheng, D.W., Levi, E., Singh, L.P., 2006. IGF-1 increases laminin, cyclin D1, and P21Cip1 expression in glomerular mesangial cells: An investigation of the intracellular signaling pathway and cell-cycle progression. Journal of Cellular Biochemistry 98, 208–220. https://doi.org/10.1002/jcb.20771

Jiang, Y., Steinle, J.J., 2010. Regulation of IRS-2 signaling by IGF-1 receptor in the diabetic rat heart. Can. J. Physiol. Pharmacol. 88, 553–561. https://doi.org/10.1139/Y10-006

Jinek, M., Chylinski, K., Fonfara, I., Hauer, M., Doudna, J.A., Charpentier, E., 2012. A Programmable Dual-RNA–Guided DNA Endonuclease in Adaptive Bacterial Immunity. Science 337, 816. https://doi.org/10.1126/science.1225829

Jinek, M., East, A., Cheng, A., Lin, S., Ma, E., Doudna, J., 2013. RNA-programmed genome editing in human cells. eLife 2, e00471. https://doi.org/10.7554/eLife.00471

Jinek, M., Jiang, F., Taylor, D.W., Sternberg, S.H., Kaya, E., Ma, E., Anders, C., Hauer, M., Zhou, K., Lin, S., Kaplan, M., Iavarone, A.T., Charpentier, E., Nogales, E., Doudna, J.A., 2014. Structures of Cas9 endonucleases reveal RNA-mediated conformational activation. Science 343, 1247997–1247997. https://doi.org/10.1126/science.1247997

Johnson, G.L., Nakamura, K., 2007. The c-jun kinase/stress-activated pathway: regulation, function and role in human disease. Biochim Biophys Acta 1773, 1341–1348. https://doi.org/10.1016/j.bbamcr.2006.12.009

Johnson, R.D., Jasin, M., 2001. Double-strand-break-induced homologous recombination in mammalian cells. Biochemical Society Transactions 29, 196–201. https://doi.org/10.1042/bst0290196

Jones, R.L., Kim, E.S., Nava-Parada, P., Alam, S., Johnson, F.M., Stephens, A.W., Simantov, R., Poondru, S., Gedrich, R., Lippman, S.M., Kaye, S.B., Carden, C.P., 2015. Phase I Study of Intermittent Oral Dosing of the Insulin-like Growth Factor-1 and Insulin Receptors Inhibitor OSI-906 in Patients With Advanced Solid Tumors. Clin Cancer Res 21, 693. https://doi.org/10.1158/1078-0432.CCR-14-0265

Jowsey, P., Morrice, N.A., Hastie, C.J., McLauchlan, H., Toth, R., Rouse, J., 2007. Characterisation of the sites of DNA damage-induced 53BP1 phosphorylation catalysed by ATM and ATR. DNA Repair 6, 1536–1544. https://doi.org/10.1016/j.dnarep.2007.04.011

Jungmichel, S., Rosenthal, F., Altmeyer, M., Lukas, J., Hottiger, M.O., Nielsen, M.L., 2013. Proteome-wide Identification of Poly(ADP-Ribosyl)ation Targets in Different Genotoxic Stress Responses. Molecular Cell 52, 272–285. https://doi.org/10.1016/j.molcel.2013.08.026

Junnila, R.K., List, E.O., Berryman, D.E., Murrey, J.W., Kopchick, J.J., 2013. The GH/IGF-1 axis in ageing and longevity. Nat Rev Endocrinol 9, 366–376. https://doi.org/10.1038/nrendo.2013.67

Kabacik, S., Mackay, A., Tamber, N., Manning, G., Finnon, P., Paillier, F., Ashworth, A., Bouffler, S., Badie, C., 2011. Gene expression following ionising radiation: Identification of biomarkers for dose estimation and prediction of individual response. null 87, 115–129. https://doi.org/10.3109/09553002.2010.519424

Kaleko, M., Rutter, W.J., Miller, A.D., 1990. Overexpression of the human insulinlike growth factor I receptor promotes ligand-dependent neoplastic transformation. Mol. Cell. Biol. 10, 464. https://doi.org/10.1128/MCB.10.2.464

Kallio, P.J., Pongratz, I., Gradin, K., McGuire, J., Poellinger, L., 1997. Activation of hypoxia-inducible factor 1alpha: posttranscriptional regulation and conformational change by recruitment of the Arnt transcription factor. Proc Natl Acad Sci U S A 94, 5667–5672. https://doi.org/10.1073/pnas.94.11.5667

Kalluri, R., Weinberg, R.A., 2009. The basics of epithelial-mesenchymal transition. J Clin Invest 119, 1420–1428. https://doi.org/10.1172/JCI39104

Kandel, E.S., Skeen, J., Majewski, N., Di Cristofano, A., Pandolfi, P.P., Feliciano, C.S., Gartel, A., Hay, N., 2002. Activation of Akt/protein kinase B overcomes a G(2)/m cell cycle checkpoint induced by DNA damage. Mol Cell Biol 22, 7831–7841. https://doi.org/10.1128/mcb.22.22.7831-7841.2002

Kang, H.J., Kim, I.H., Sung, C.O., Shim, J.H., Yu, E., 2015. Expression of carbonic anhydrase 9 is a novel prognostic marker in resectable hepatocellular carcinoma. Virchows Archiv 466, 403–413. https://doi.org/10.1007/s00428-014-1709-0

Kang, Z., Pirskanen, A., Jänne, O.A., Palvimo, J.J., 2002. Involvement of Proteasome in the Dynamic Assembly of the Androgen Receptor Transcription Complex. Journal of Biological Chemistry 277, 48366–48371. https://doi.org/10.1074/jbc.M209074200

Kao, G.D., Jiang, Z., Fernandes, A.M., Gupta, A.K., Maity, A., 2007. Inhibition of Phosphatidylinositol-3-OH Kinase/Akt Signaling Impairs DNA Repair in Glioblastoma Cells following Ionizing Radiation. Journal of Biological Chemistry 282, 21206–21212. https://doi.org/10.1074/jbc.M703042200

Karagiannis, T.C., El-Osta, A., 2006. Modulation of cellular radiation responses by histone deacetylase inhibitors. Oncogene 25, 3885–3893. https://doi.org/10.1038/sj.onc.1209417

Karbowniczek, M., Robertson, G.P., Henske, E.P., 2006. Rheb Inhibits C-Raf Activity and B-Raf/C-Raf Heterodimerization*. Journal of Biological Chemistry 281, 25447–25456. https://doi.org/10.1074/jbc.M605273200

Kari, V., Mansour, W.Y., Raul, S.K., Baumgart, S.J., Mund, A., Grade, M., Sirma, H., Simon, R., Will, H., Dobbelstein, M., Dikomey, E., Johnsen, S.A., 2016. Loss of CHD1 causes DNA repair defects and enhances prostate cancer therapeutic responsiveness. EMBO reports 17, 1609–1623. https://doi.org/10.15252/embr.201642352

Kasprzak, A., Adamek, A., 2019. Insulin-Like Growth Factor 2 (IGF2) Signaling in Colorectal Cancer-From Basic Research to Potential Clinical Applications. Int J Mol Sci 20, 4915. https://doi.org/10.3390/ijms20194915

Kastan, M.B., Bartek, J., 2004. Cell-cycle checkpoints and cancer. Nature 432, 316–323. https://doi.org/10.1038/nature03097

Katayama, K., Fujita, N., Tsuruo, T., 2005. Akt/protein kinase B-dependent phosphorylation and inactivation of WEE1Hu promote cell cycle progression at G2/M transition. Mol Cell Biol 25, 5725–5737. https://doi.org/10.1128/MCB.25.13.5725-5737.2005

Kato, H., Faria, T.N., Stannard, B., Roberts, C.T., Jr, LeRoith, D., 1994. Essential role of tyrosine residues 1131, 1135, and 1136 of the insulin-like growth factor-I (IGF-I) receptor in IGF-I action. Molecular Endocrinology 8, 40–50. https://doi.org/10.1210/mend.8.1.7512194

Kato, H., Faria, T.N., Stannard, B., Roberts, C.T., LeRoith, D., 1993. Role of tyrosine kinase activity in signal transduction by the insulin-like growth factor-I (IGF-I) receptor. Characterization of kinase-deficient IGF-I receptors and the action of an IGF-I-mimetic antibody (alpha IR-3). Journal of Biological Chemistry 268, 2655–2661.

Kaufmann, W.K., Paules, R.S., 1996. DNA damage and cell cycle checkpoints. The FASEB Journal 10, 238–247. https://doi.org/10.1096/fasebj.10.2.8641557

Kawano, H., Sato, T., Yamada, T., Matsumoto, T., Sekine, K., Watanabe, T., Nakamura, T., Fukuda, T., Yoshimura, K., Yoshizawa, T., Aihara, K., Yamamoto, Y., Nakamichi, Y., Metzger, D., Chambon, P., Nakamura, K., Kawaguchi, H., Kato, S., 2003. Suppressive function of androgen receptor in bone resorption. Proc Natl Acad Sci USA 100, 9416. https://doi.org/10.1073/pnas.1533500100

Kee, Y., Huang, T.T., 2016. Role of Deubiquitinating Enzymes in DNA Repair. Mol. Cell. Biol. 36, 524. https://doi.org/10.1128/MCB.00847-15

Kelland, L., 2007. Targeting the Limitless Replicative Potential of Cancer: The Telomerase/Telomere Pathway. Clin Cancer Res 13, 4960. https://doi.org/10.1158/1078-0432.CCR-07-0422

Kent, W.J., Sugnet, C.W., Furey, T.S., Roskin, K.M., Pringle, T.H., Zahler, A.M., Haussler, and D., 2002. The Human Genome Browser at UCSC. Genome Research 12, 996–1006. https://doi.org/10.1101/gr.229102

Keshet, Y., Seger, R., 2010. The MAP Kinase Signaling Cascades: A System of Hundreds of Components Regulates a Diverse Array of Physiological Functions. Methods in molecular biology (Clifton, N.J.) 661, 3–38. https://doi.org/10.1007/978-1-60761-795-2_1

Khan, M.A., Han, M., Partin, A.W., Epstein, J.I., Walsh, P.C., 2003. Long-term cancer control of radical prostatectomy in men younger than 50 years of age: update 2003. Urology 62, 86–91. https://doi.org/10.1016/S0090-4295(03)00404-7

Khan, S.H., 2019. Genome-Editing Technologies: Concept, Pros, and Cons of Various Genome-Editing Techniques and Bioethical Concerns for Clinical Application. Molecular Therapy - Nucleic Acids 16, 326–334. https://doi.org/10.1016/j.omtn.2019.02.027

Khanna, K.K., Jackson, S.P., 2001. DNA double-strand breaks: signaling, repair and the cancer connection. Nature Genetics 27, 247–254. https://doi.org/10.1038/85798

Khatib, A.-M., Siegfried, G., Prat, A., Luis, J., Chrétien, M., Metrakos, P., Seidah, N.G., 2001. Inhibition of Proprotein Convertases Is Associated with Loss of Growth and Tumorigenicity of HT-29 Human Colon Carcinoma Cells: IMPORTANCE OF INSULIN-LIKE GROWTH FACTOR-1 (IGF-1) RECEPTOR PROCESSING IN IGF-1-MEDIATED FUNCTIONS. Journal of Biological Chemistry 276, 30686–30693. https://doi.org/10.1074/jbc.M101725200

Ki, Y.-W., Park, J.H., Lee, J.E., Shin, I.C., Koh, H.C., 2013. JNK and p38 MAPK regulate oxidative stress and the inflammatory response in chlorpyrifos-induced apoptosis. Toxicology Letters 218, 235–245. https://doi.org/10.1016/j.toxlet.2013.02.003

Kido, Y., Nakae, J., Accili, D., 2001. The Insulin Receptor and Its Cellular Targets1. The Journal of Clinical Endocrinology & Metabolism 86, 972–979. https://doi.org/10.1210/jcem.86.3.7306

Kiely, P.A., Sant, A., O'Connor, R., 2002. RACK1 Is an Insulin-like Growth Factor 1 (IGF-1) Receptor-interacting Protein That Can Regulate IGF-1-mediated Akt Activation and Protection from Cell Death. Journal of Biological Chemistry 277, 22581–22589. https://doi.org/10.1074/jbc.M201758200

Kim, Daesik, Kim, Da-eun, Lee, G., Cho, S.-I., Kim, J.-S., 2019. Genome-wide target specificity of CRISPR RNA-guided adenine base editors. Nature Biotechnology 37, 430–435. https://doi.org/10.1038/s41587-019-0050-1

Kim, H.-J., Litzenburger, B.C., Cui, X., Delgado, D.A., Grabiner, B.C., Lin, X., Lewis, M.T., Gottardis, M.M., Wong, T.W., Attar, R.M., Carboni, J.M., Lee, A.V., 2007. Constitutively active type I insulin-like growth factor receptor causes transformation and xenograft growth of immortalized mammary epithelial cells and is accompanied by an epithelial-to-mesenchymal transition mediated by NF-kappaB and snail. Mol Cell Biol 27, 3165–3175. https://doi.org/10.1128/MCB.01315-06

Kim, H.-S., Rosenfeld, R.G., Oh, Y., 1997. Biological roles of insulin-like growth factor binding proteins (IGFBPs). Experimental & Molecular Medicine 29, 85–96. https://doi.org/10.1038/emm.1997.13

Kim, I.-A., Bae, S.-S., Fernandes, A., Wu, J., Muschel, R.J., McKenna, W.G., Birnbaum, M.J., Bernhard, E.J., 2005. Selective Inhibition of Ras, Phosphoinositide 3 Kinase, and Akt Isoforms Increases the Radiosensitivity of Human Carcinoma Cell Lines. Cancer Res 65, 7902. https://doi.org/10.1158/0008-5472.CAN-05-0513

Kim, J.J., Gonzalez-Roibon, N., Chaux, A., Munari, E., Faraj, S.F., Ellis, C., Sharma, R., Bivalacqua, T., Schoenberg, M., Carducci, M.A., Netto, G.J., 2013. Overexpression of IGF1R to predict outcome in invasive urothelial carcinoma of urinary bladder. JCO 31, 280–280. https://doi.org/10.1200/jco.2013.31.6_suppl.280

Kim, J.-Y., Lee, K.-S., Seol, J.-E., Yu, K., Chakravarti, D., Seo, S.-B., 2011. Inhibition of p53 acetylation by INHAT subunit SET/TAF-Iβ represses p53 activity. Nucleic Acids Research 40, 75–87. https://doi.org/10.1093/nar/gkr614

Kim, K., Brush, J.M., Watson, P.A., Cacalano, N.A., Iwamoto, K.S., McBride, W.H., 2008. Epidermal Growth Factor Receptor vIII Expression in U87 Glioblastoma Cells Alters Their Proteasome Composition, Function, and Response to Irradiation. Mol Cancer Res 6, 426. https://doi.org/10.1158/1541-7786.MCR-07-0313

Kim, M.-K., Kim, T.-J., Sung, C.O., Choi, C.H., Lee, J.-W., Kim, B.-G., Bae, D.-S., 2010. High expression of mTOR is associated with radiation resistance in cervical cancer. J Gynecol Oncol 21, 181–185. https://doi.org/10.3802/jgo.2010.21.3.181

Kim, Y.G., Cha, J., Chandrasegaran, S., 1996. Hybrid restriction enzymes: zinc finger fusions to Fok I cleavage domain. Proc Natl Acad Sci USA 93, 1156. https://doi.org/10.1073/pnas.93.3.1156

Kinner, A., Wu, W., Staudt, C., Iliakis, G., 2008. γ-H2AX in recognition and signaling of DNA double-strand breaks in the context of chromatin. Nucleic Acids Res 36, 5678–5694. https://doi.org/10.1093/nar/gkn550

Kitazawa, H., Iida, J., Uchida, A., Haino-Fukushima, K., J. Itoh, T., Hotani, H., Ookata, K., Murofushi, H., Chloe Bulinski, J., Kishimoto, T., Hisanaga, S., 2000. Ser787 in the Proline-Rich Region of Human MAP4 is a Critical

Phosphorylation Site that Reduces its Activity to Promote Tubulin Polymerization. Cell Structure and Function 25, 33–39. https://doi.org/10.1247/csf.25.33

Kleinstiver, B.P., Prew, M.S., Topkar, V.V., Tsai, S.Q., Joung, J.K., 2015. 58. Engineered Cas9 Variants with Novel PAM Specificities Expand the Targeting Range of CRISPR/Cas Nucleases. Molecular Therapy 23, S26. https://doi.org/10.1016/S1525-0016(16)33663-2

Kluesner, M.G., Nedveck, D.A., Lahr, W.S., Garbe, J.R., Abrahante, J.E., Webber, B.R., Moriarity, B.S., 2018. EditR: A Method to Quantify Base Editing from Sanger Sequencing. CRISPR J 1, 239–250. https://doi.org/10.1089/crispr.2018.0014

Klug, A., Rhodes, D., 1987. Zinc Fingers: A Novel Protein Fold for Nucleic Acid Recognition. Cold Spring Harbor Symposia on Quantitative Biology 52, 473–482. https://doi.org/10.1101/SQB.1987.052.01.054

Knudsen, E.S., Wang, J.Y., 1997. Dual mechanisms for the inhibition of E2F binding to RB by cyclin-dependent kinase-mediated RB phosphorylation. Mol. Cell. Biol. 17, 5771. https://doi.org/10.1128/MCB.17.10.5771

Ko, Y.G., Kang, Y.S., Kim, E.K., Park, S.G., Kim, S., 2000. Nucleolar localization of human methionyl-tRNA synthetase and its role in ribosomal RNA synthesis. J Cell Biol 149, 567–574. https://doi.org/10.1083/jcb.149.3.567

Kobayashi, J., 2004. Molecular Mechanism of the Recruitment of NBS1/hMRE11/hRAD50 Complex to DNA Double-strand Breaks: NBS1 Binds to γ-H2AX through FHA/BRCT Domain. Journal of Radiation Research 45, 473–478. https://doi.org/10.1269/jrr.45.473

Kobayashi, J., Tauchi, H., Sakamoto, S., Nakamura, A., Morishima, K., Matsuura, S., Kobayashi, T., Tamai, K., Tanimoto, K., Komatsu, K., 2002. NBS1 Localizes to γ-H2AX Foci through Interaction with the FHA/BRCT Domain. Current Biology 12, 1846–1851. https://doi.org/10.1016/S0960-9822(02)01259-9

Kommaddi, R.P., Jean-Charles, P.-Y., Shenoy, S.K., 2015. Phosphorylation of the Deubiquitinase USP20 by Protein Kinase A Regulates Post-endocytic Trafficking of β2 Adrenergic Receptors to Autophagosomes during Physiological Stress. Journal of Biological Chemistry 290, 8888–8903. https://doi.org/10.1074/jbc.M114.630541

Komor, A.C., Kim, Y.B., Packer, M.S., Zuris, J.A., Liu, D.R., 2016. Programmable editing of a target base in genomic DNA without double-stranded DNA cleavage. Nature 533, 420–424. https://doi.org/10.1038/nature17946

Kong, X., Shen, Y., Jiang, N., Fei, X., Mi, J., 2011. Emerging roles of DNA-PK besides DNA repair. Cellular Signalling 23, 1273–1280. https://doi.org/10.1016/j.cellsig.2011.04.005

Kori, Y., Sidoli, S., Yuan, Z.-F., Lund, P.J., Zhao, X., Garcia, B.A., 2017. Proteome-wide acetylation dynamics in human cells. Scientific Reports 7, 10296. https://doi.org/10.1038/s41598-017-09918-3

Kosicki, M., Tomberg, K., Bradley, A., 2018. Repair of double-strand breaks induced by CRISPR–Cas9 leads to large deletions and complex rearrangements. Nature Biotechnology 36, 765–771. https://doi.org/10.1038/nbt.4192

Kovacina, K.S., Park, G.Y., Bae, S.S., Guzzetta, A.W., Schaefer, E., Birnbaum, M.J., Roth, R.A., 2003. Identification of a Proline-rich Akt Substrate as a 14-3-3 Binding Partner. Journal of Biological Chemistry 278, 10189–10194. https://doi.org/10.1074/jbc.M210837200

Krüger, M., Kratchmarova, I., Blagoev, B., Tseng, Y.-H., Kahn, C.R., Mann, M., 2008. Dissection of the insulin signaling pathway via quantitative phosphoproteomics. Proc Natl Acad Sci USA 105, 2451. https://doi.org/10.1073/pnas.0711713105

Kruis, T., Klammt, J., Galli-Tsinopoulou, A., Wallborn, T., Schlicke, M., Müller, E., Kratzsch, J., Körner, A., Odeh, R., Kiess, W., Pfäffle, R., 2010. Heterozygous Mutation within a Kinase-Conserved Motif of the Insulin-Like Growth Factor I Receptor Causes Intrauterine and Postnatal Growth Retardation. The Journal of Clinical Endocrinology & Metabolism 95, 1137–1142. https://doi.org/10.1210/jc.2009-1433

Kucab, J.E., Dunn, S.E., 2003. Role of IGF-1R in Mediating Breast Cancer Invasion and Metastasis. Breast Disease 17, 41–47. https://doi.org/10.3233/BD-2003-17105

Kühne, M., Riballo, E., Rief, N., Rothkamm, K., Jeggo, P.A., Löbrich, M., 2004. A Double-Strand Break Repair Defect in ATM-Deficient Cells Contributes to Radiosensitivity. Cancer Res 64, 500. https://doi.org/10.1158/0008-5472.CAN-03-2384

Kumagai, A., Lee, J., Yoo, H.Y., Dunphy, W.G., 2006. TopBP1 Activates the ATR-ATRIP Complex. Cell 124, 943–955. https://doi.org/10.1016/j.cell.2005.12.041

Kumar Deshmukh, F., Yaffe, D., Olshina, M.A., Ben-Nissan, G., Sharon, M., 2019. The Contribution of the 20S Proteasome to Proteostasis. Biomolecules 9, 190. https://doi.org/10.3390/biom9050190

Kumthekar, P., Ko, C.H., Paunesku, T., Dixit, K., Sonabend, A.M., Bloch, O., Tate, M., Schwartz, M., Zuckerman, L., Lezon, R., Lukas, R.V., Jovanovic, B., McCortney, K., Colman, H., Chen, S., Lai, B., Antipova, O., Deng, J., Li, L., Tommasini-Ghelfi, S., Hurley, L.A., Unruh, D., Sharma, N.V., Kandpal, M., Kouri, F.M., Davuluri, R.V., Brat, D.J., Muzzio, M., Glass, M., Vijayakumar, V., Heidel, J., Giles, F.J., Adams, A.K., James, C.D., Woloschak, G.E., Horbinski, C., Stegh, A.H., 2021. A first-in-human phase 0 clinical study of RNA interference-based spherical nucleic acids in patients with recurrent glioblastoma. Sci Transl Med 13, eabb3945. https://doi.org/10.1126/scitranslmed.abb3945

Kunz-Schughart, L.A., Groebe, K., Mueller-Klieser, W., 1996. Three-dimensional cell culture induces novel proliferative and metabolic alterations associated with oncogenic transformation. International Journal of Cancer 66, 578–586. https://doi.org/10.1002/(SICI)1097-0215(19960516)66:4<578::AID-IJC25>3.0.CO;2-2

Kuo, L.J., Yang, L.-X., 2008. γ-H2AX - A Novel Biomarker for DNA Double-strand Breaks. In Vivo 22, 305–309.

Kurimasa, A., Kumano, S., Boubnov, N.V., Story, M.D., Tung, C.S., Peterson, S.R., Chen, D.J., 1999. Requirement for the kinase activity of human DNA-dependent protein kinase catalytic subunit in DNA strand break rejoining. Mol Cell Biol 19, 3877–3884. https://doi.org/10.1128/MCB.19.5.3877

Kurosawa, A., 2021. Autophosphorylation and Self-Activation of DNA-Dependent Protein Kinase. Genes (Basel) 12, 1091. https://doi.org/10.3390/genes12071091

Kusch, T., Florens, L., MacDonald, W.H., Swanson, S.K., Glaser, R.L., Yates, J.R., Abmayr, S.M., Washburn, M.P., Workman, J.L., 2004. Acetylation by Tip60 Is Required for Selective Histone Variant Exchange at DNA Lesions. Science 306, 2084–2087. https://doi.org/10.1126/science.1103455

Kwon, N.H., Kang, T., Lee, J.Y., Kim, H.H., Kim, H.R., Hong, J., Oh, Y.S., Han, J.M., Ku, M.J., Lee, S.Y., Kim, S., 2011. Dual role of methionyl-tRNA synthetase in the regulation of translation and tumor suppressor activity of aminoacyl-tRNA synthetase-interacting multifunctional protein-3. Proc Natl Acad Sci U S A 108, 19635–19640. https://doi.org/10.1073/pnas.1103922108

Kyrylenko, S., Kyrylenko, O., Suuronen, T., Salminen, A., 2003. Differential regulation of the Sir2 histone deacetylase gene family by inhibitors of class I and II histone deacetylases. Cellular and Molecular Life Sciences CMLS 60, 1990–1997. https://doi.org/10.1007/s00018-003-3090-z

La Vignera, S., Condorelli, R.A., Russo, G.I., Morgia, G., Calogero, A.E., 2016. Endocrine control of benign prostatic hyperplasia. Andrology 4, 404–411. https://doi.org/10.1111/andr.12186

Labhart, P., 1999. Nonhomologous DNA end joining in cell-free systems. European Journal of Biochemistry 265, 849–861. https://doi.org/10.1046/j.1432-1327.1999.00805.x

Lamouille, S., Xu, J., Derynck, R., 2014. Molecular mechanisms of epithelial-mesenchymal transition. Nat Rev Mol Cell Biol 15, 178–196. https://doi.org/10.1038/nrm3758

Landrum, M.J., Lee, J.M., Benson, M., Brown, G., Chao, C., Chitipiralla, S., Gu, B., Hart, J., Hoffman, D., Hoover, J., Jang, W., Katz, K., Ovetsky, M., Riley, G., Sethi, A., Tully, R., Villamarin-Salomon, R., Rubinstein, W., Maglott, D.R., 2015. ClinVar: public archive of interpretations of clinically relevant variants. Nucleic Acids Research 44, D862–D868. https://doi.org/10.1093/nar/gkv1222

Langan, L.M., Dodd, N.J.F., Owen, S.F., Purcell, W.M., Jackson, S.K., Jha, A.N., 2016. Direct Measurements of Oxygen Gradients in Spheroid Culture System Using Electron Parametric Resonance Oximetry. PLoS One 11, e0149492–e0149492. https://doi.org/10.1371/journal.pone.0149492

Laplante, M., Sabatini, D.M., 2013. Regulation of mTORC1 and its impact on gene expression at a glance. J Cell Sci 126, 1713–1719. https://doi.org/10.1242/jcs.125773

Larsen, M.R., Trelle, M.B., Thingholm, T.E., Jensen, O.N., 2006. Analysis of posttranslational modifications of proteins by tandem mass spectrometry. BioTechniques 40, 790–798. https://doi.org/10.2144/000112201

Larsson, O., Girnita, A., Girnita, L., 2005. Role of insulin-like growth factor 1 receptor signalling in cancer. Br J Cancer 92, 2097–2101. https://doi.org/10.1038/sj.bjc.6602627

LaRue, K.E.A., Khalil, M., Freyer, J.P., 2004. Microenvironmental Regulation of Proliferation in Multicellular Spheroids Is Mediated through Differential Expression of Cyclin-Dependent Kinase Inhibitors. Cancer Res 64, 1621. https://doi.org/10.1158/0008-5472.CAN-2902-2

Lau, A., Liu, P., Inuzuka, H., Gao, D., 2014. SIRT1 phosphorylation by AMP-activated protein kinase regulates p53 acetylation. American journal of cancer research 4, 245–55.

Leavy, O., 2008. BIM and FAS: the ultimate death squad. Nature Reviews Immunology 8, 245–245. https://doi.org/10.1038/nri2300

Lee, C.-P., Huang, Y.-H., Lin, S.-F., Chang, Y., Chang, Y.-H., Takada, K., Chen, M.-R., 2008. Epstein-Barr virus BGLF4 kinase induces disassembly of the nuclear lamina to facilitate virion production. J Virol 82, 11913–11926. https://doi.org/10.1128/JVI.01100-08

Lee, C.-W., Wong, L.L.-Y., Tse, E.Y.-T., Liu, H.-F., Leong, V.Y.-L., Lee, J.M.-F., Hardie, D.G., Ng, I.O.-L., Ching, Y.-P., 2012. AMPK Promotes p53 Acetylation via Phosphorylation and Inactivation of SIRT1 in Liver Cancer Cells. Cancer Res 72, 4394. https://doi.org/10.1158/0008-5472.CAN-12-0429

Lee, D.-H., Acharya, S.S., Kwon, M., Drane, P., Guan, Y., Adelmant, G., Kalev, P., Shah, J., Pellman, D., Marto, J.A., Chowdhury, D., 2014. Dephosphorylation Enables the Recruitment of 53BP1 to Double-Strand DNA Breaks. Molecular Cell 54, 512–525. https://doi.org/10.1016/j.molcel.2014.03.020

Lee, D.H., Goldberg, A.L., 1996. Selective Inhibitors of the Proteasome-dependent and Vacuolar Pathways of Protein Degradation in Saccharomyces cerevisiae. Journal of Biological Chemistry 271, 27280–27284. https://doi.org/10.1074/jbc.271.44.27280

Lee, K.-J., Saha, J., Sun, J., Fattah, K.R., Wang, S.-C., Jakob, B., Chi, L., Wang, S.-Y., Taucher-Scholz, G., Davis, A.J., Chen, D.J., 2016. Phosphorylation of Ku dictates DNA double-strand break (DSB) repair pathway choice in S phase. Nucleic Acids Res 44, 1732–1745. https://doi.org/10.1093/nar/gkv1499

Lee, Y.-R., Chen, M., Pandolfi, P.P., 2018. The functions and regulation of the PTEN tumour suppressor: new modes and prospects. Nature Reviews Molecular Cell Biology 19, 547–562. https://doi.org/10.1038/s41580-018-0015-0

Leek, R., Grimes, D.R., Harris, A.L., McIntyre, A., 2016. Methods: Using Three-Dimensional Culture (Spheroids) as an In Vitro Model of Tumour Hypoxia, in: Koumenis, C., Coussens, L.M., Giaccia, A., Hammond, E. (Eds.), Tumor Microenvironment. Springer International Publishing, Cham, pp. 167–196.

Leek, R.D., Stratford, I., Harris, A.L., 2005. The Role of Hypoxia-Inducible Factor-1 in Three-dimensional Tumor Growth, Apoptosis, and Regulation by the Insulin-Signaling Pathway. Cancer Res 65, 4147. https://doi.org/10.1158/0008-5472.CAN-04-2184

Lees-Miller, S., Godbout, R., Chan, D., Weinfeld, M., Day, R., Barron, G., Allalunis-Turner, J., 1995. Absence of p350 subunit of DNA-activated protein kinase from a radiosensitive human cell line. Science 267, 1183. https://doi.org/10.1126/science.7855602

Lehmann, B.D., McCubrey, J.A., Jefferson, H.S., Paine, M.S., Chappell, W.H., Terrian, D.M., 2007. A Dominant Role for p53-Dependent Cellular Senescence in Radiosensitization of Human Prostate Cancer Cells. Cell Cycle 6, 595–605. https://doi.org/10.4161/cc.6.5.3901

Leick, M.B., Shoff, C.J., Wang, E.C., Congress, J.L., Gallicano, G.I., 2011. Loss of imprinting of IGF2 and the epigenetic progenitor model of cancer. Am J Stem Cells 1, 59–74.

Leimbacher, P.-A., Jones, S.E., Shorrocks, A.-M.K., de Marco Zompit, M., Day, M., Blaauwendraad, J., Bundschuh, D., Bonham, S., Fischer, R., Fink, D., Kessler, B.M., Oliver, A.W., Pearl, L.H., Blackford, A.N., Stucki, M., 2019. MDC1 Interacts with TOPBP1 to Maintain Chromosomal Stability during Mitosis. Mol Cell 74, 571-583.e8. https://doi.org/10.1016/j.molcel.2019.02.014

Lemaire, M., Froment, C., Boutros, R., Mondesert, O., Nebreda, A.R., Monsarrat, B., Ducommun, B., 2006. CDC25B Phosphorylation by p38 and MK-2. Cell Cycle 5, 1649–1653. https://doi.org/10.4161/cc.5.15.3006

Lemercier, C., Legube, G., Caron, C., Louwagie, M., Garin, J., Trouche, D., Khochbin, S., 2003. Tip60 Acetyltransferase Activity Is Controlled by Phosphorylation. Journal of Biological Chemistry 278, 4713–4718. https://doi.org/10.1074/jbc.M211811200

Lemercier, C., To, R.Q., Carrasco, R.A., Konieczny, S.F., 1998. The basic helix-loop-helix transcription factor Mist1 functions as a transcriptional repressor of myoD. EMBO J 17, 1412–1422. https://doi.org/10.1093/emboj/17.5.1412

Lengauer, C., Kinzler, K.W., Vogelstein, B., 1998. Genetic instabilities in human cancers. Nature 396, 643–649. https://doi.org/10.1038/25292

Leszczynska, K.B., Foskolou, I.P., Abraham, A.G., Anbalagan, S., Tellier, C., Haider, S., Span, P.N., O'Neill, E.E., Buffa, F.M., Hammond, E.M., 2015. Hypoxia-induced p53 modulates both apoptosis and radiosensitivity via AKT. J Clin Invest 125, 2385–2398. https://doi.org/10.1172/JCI80402

Lewitt, M.S., Saunders, H., Phuyal, J.L., Baxter, R.C., 1994. Complex formation by human insulin-like growth factor-binding protein-3 and human acid-labile subunit in growth hormone-deficient rats. Endocrinology 134, 2404–2409. https://doi.org/10.1210/endo.134.6.7514998

Li, B., Lu, W., Chen, Z., 2014. Regulation of Androgen Receptor by E3 Ubiquitin Ligases: for More or Less. Receptors Clin Investig 1, 10.14800%2Frci.122. https://doi.org/10.14800/rci.122

Li, H., Xu, L., Li, C., Zhao, L., Ma, Y., Zheng, H., Li, Z., Zhang, Y., Wang, R., Liu, Y., Qu, X., 2014. Ubiquitin ligase Cbl-b represses IGF-I-induced epithelial mesenchymal transition via ZEB2 and microRNA-200c regulation in gastric cancer cells. Mol Cancer 13, 136–136. https://doi.org/10.1186/1476-4598-13-136

Li, H., Xu, L., Zhao, L., Ma, Y., Zhu, Z., Liu, Y., Qu, X., 2015. Insulin-like growth factor-I induces epithelial to mesenchymal transition via GSK-3β and ZEB2 in the BGC-823 gastric cancer cell line. Oncol Lett 9, 143–148. https://doi.org/10.3892/ol.2014.2687

Li, H.-F., Kim, J.-S., Waldman, T., 2009. Radiation-induced Akt activation modulates radioresistance in human glioblastoma cells. Radiat Oncol 4, 43–43. https://doi.org/10.1186/1748-717X-4-43

Li, J., Choi, E., Yu, H., Bai, X., 2019. Structural basis of the activation of type 1 insulin-like growth factor receptor. Nature Communications 10, 4567. https://doi.org/10.1038/s41467-019-12564-0

Li, L., Hu, J., He, T., Zhang, Q., Yang, X., Lan, X., Zhang, D., Mei, H., Chen, B., Huang, Y., 2015. P38/MAPK contributes to endothelial barrier dysfunction via MAP4 phosphorylation-dependent microtubule disassembly in inflammation-induced acute lung injury. Sci Rep 5, 8895–8895. https://doi.org/10.1038/srep08895

Li, P., Ge, J., Li, H., 2020. Lysine acetyltransferases and lysine deacetylases as targets for cardiovascular disease. Nature Reviews Cardiology 17, 96–115. https://doi.org/10.1038/s41569-019-0235-9

Li, T., Huang, S., Zhao, X., Wright, D.A., Carpenter, S., Spalding, M.H., Weeks, D.P., Yang, B., 2011. Modularly assembled designer TAL effector nucleases for targeted gene knockout and gene replacement in eukaryotes. Nucleic Acids Res 39, 6315–6325. https://doi.org/10.1093/nar/gkr188

Li, W., Bai, X., Li, J., Zhao, Y., Liu, J., Zhao, H., Liu, L., Ding, M., Wang, Q., Shi, F.-Y., Hou, M., Ji, J., Gao, G., Guo, R., Sun, Y., Liu, Y., Xu, D., 2019. The nucleoskeleton protein IFFO1 immobilizes broken DNA and suppresses chromosome translocation during tumorigenesis. Nature Cell Biology 21, 1273–1285. https://doi.org/10.1038/s41556-019-0388-0

Li, Xiaotao, Amazit, L., Long, W., Lonard, D.M., Monaco, J.J., O'Malley, B.W., 2007. Ubiquitin- and ATP-Independent Proteolytic Turnover of p21 by the REGγ-Proteasome Pathway. Molecular Cell 26, 831–842. https://doi.org/10.1016/j.molcel.2007.05.028

Li, Xiaoling, Zhang, S., Blander, G., Tse, J.G., Krieger, M., Guarente, L., 2007. SIRT1 Deacetylates and Positively Regulates the Nuclear Receptor LXR. Molecular Cell 28, 91–106. https://doi.org/10.1016/j.molcel.2007.07.032

Liang, J., Zubovitz, J., Petrocelli, T., Kotchetkov, R., Connor, M.K., Han, K., Lee, J.-H., Ciarallo, S., Catzavelos, C., Beniston, R., Franssen, E., Slingerland, J.M., 2002. PKB/Akt phosphorylates p27, impairs nuclear import of p27 and opposes p27-mediated G1 arrest. Nature Medicine 8, 1153–1160. https://doi.org/10.1038/nm761

Liaw, H., Lee, D., Myung, K., 2011. DNA-PK-dependent RPA2 hyperphosphorylation facilitates DNA repair and suppresses sister chromatid exchange. PLoS One 6, e21424–e21424. https://doi.org/10.1371/journal.pone.0021424

Lieber, M.R., 2010. The mechanism of double-strand DNA break repair by the nonhomologous DNA end-joining pathway. Annu Rev Biochem 79, 181–211. https://doi.org/10.1146/annurev.biochem.052308.093131

Lieberman, H.B., Bernstock, J.D., Broustas, C.G., Hopkins, K.M., Leloup, C., Zhu, A., 2011. The role of RAD9 in tumorigenesis. J Mol Cell Biol 3, 39–43. https://doi.org/10.1093/jmcb/mjq039

Lim, D.-S., Kim, S.-T., Xu, B., Maser, R.S., Lin, J., Petrini, J.H.J., Kastan, M.B., 2000. ATM phosphorylates p95/nbs1 in an S-phase checkpoint pathway. Nature 404, 613–617. https://doi.org/10.1038/35007091

Lin, H.-K., Yeh, S., Kang, H.-Y., Chang, C., 2001. Akt suppresses androgen-induced apoptosis by phosphorylating and inhibiting androgen receptor. Proc Natl Acad Sci USA 98, 7200. https://doi.org/10.1073/pnas.121173298

Lin, S., Staahl, B.T., Alla, R.K., Doudna, J.A., 2014. Enhanced homology-directed human genome engineering by controlled timing of CRISPR/Cas9 delivery. Elife 3, e04766–e04766. https://doi.org/10.7554/eLife.04766

Lin, S., Zhang, Q., Shao, X., Zhang, T., Xue, C., Shi, S., Zhao, D., Lin, Y., 2017. IGF-1 promotes angiogenesis in endothelial cells/adipose-derived stem cells co-culture system with activation of PI3K/Akt signal pathway. Cell Proliferation 50, e12390. https://doi.org/10.1111/cpr.12390

Lin, Y.-F., Shih, H.-Y., Shang, Z., Matsunaga, S., Chen, B.P., 2014. DNA-PKcs is required to maintain stability of Chk1 and Claspin for optimal replication stress response. Nucleic Acids Res 42, 4463–4473. https://doi.org/10.1093/nar/gku116

Lin, Y.-F., Shih, H.-Y., Shang, Z.-F., Kuo, C.-T., Guo, J., Du, C., Lee, H., Chen, B.P.C., 2018. PIDD mediates the association of DNA-PKcs and ATR at stalled replication forks to facilitate the ATR signaling pathway. Nucleic Acids Res 46, 1847–1859. https://doi.org/10.1093/nar/gkx1298

Lingohr, M.K., Dickson, L.M., McCuaig, J.F., Hugl, S.R., Twardzik, D.R., Rhodes, C.J., 2002. Activation of IRS-2—Mediated Signal Transduction by IGF-1, but not TGF-α or EGF, Augments Pancreatic β-Cell Proliferation. Diabetes 51, 966. https://doi.org/10.2337/diabetes.51.4.966

Linke, S.P., Clarkin, K.C., Wahl, G.M., 1997. p53 Mediates Permanent Arrest over Multiple Cell Cycles in Response to γ-Irradiation. Cancer Res 57, 1171.

Liu, J., Kruswick, A., Dang, H., Tran, A.D., Kwon, S.M., Wang, X.W., Oberdoerffer, P., 2017. Ubiquitin-specific protease 21 stabilizes BRCA2 to control DNA repair and tumor growth. Nature Communications 8, 137. https://doi.org/10.1038/s41467-017-00206-2

Liu, P., Cheng, H., Roberts, T.M., Zhao, J.J., 2009. Targeting the phosphoinositide 3-kinase pathway in cancer. Nature Reviews Drug Discovery 8, 627–644. https://doi.org/10.1038/nrd2926

Liu, P., Gan, W., Guo, C., Xie, A., Gao, D., Guo, J., Zhang, J., Willis, N., Su, A., Asara, J.M., Scully, R., Wei, W., 2015. Akt-mediated phosphorylation of XLF impairs non-homologous end-joining DNA repair. Mol Cell 57, 648–661. https://doi.org/10.1016/j.molcel.2015.01.005

Liu, S., Opiyo, S.O., Manthey, K., Glanzer, J.G., Ashley, A.K., Amerin, C., Troksa, K., Shrivastav, M., Nickoloff, J.A., Oakley, G.G., 2012. Distinct roles for DNA-PK, ATM and ATR in RPA phosphorylation and checkpoint activation in response to replication stress. Nucleic Acids Res 40, 10780–10794. https://doi.org/10.1093/nar/gks849

Liu, Y., Kao, H.-I., Bambara, R.A., 2004. Flap Endonuclease 1: A Central Component of DNA Metabolism. Annu. Rev. Biochem. 73, 589–615. https://doi.org/10.1146/annurev.biochem.73.012803.092453

Livneh, I., Cohen-Kaplan, V., Cohen-Rosenzweig, C., Avni, N., Ciechanover, A., 2016. The life cycle of the 26S proteasome: from birth, through regulation and function, and onto its death. Cell Research 26, 869–885. https://doi.org/10.1038/cr.2016.86

Löbrich, M., Jeggo, P.A., 2007. The impact of a negligent G2/M checkpoint on genomic instability and cancer induction. Nature Reviews Cancer 7, 861–869. https://doi.org/10.1038/nrc2248

Löbrich, M., Shibata, A., Beucher, A., Fisher, A., Ensminger, M., Goodarzi, A.A., Barton, O., Jeggo, P.A., 2010. γH2AX foci analysis for monitoring DNA double-strand break repair: Strengths, limitations and optimization. null 9, 662–669. https://doi.org/10.4161/cc.9.4.10764

Lomax, M., K. Gulston, M., O'Neill (INVITED), P., 2002. Chemical Aspects of Clustered DNA Damage Induction by Ionising Radiation. Radiation Protection Dosimetry 99, 63–68. https://doi.org/10.1093/oxfordjournals.rpd.a006840

Lomax, M.E., Folkes, L.K., O'Neill, P., 2013. Biological Consequences of Radiation-induced DNA Damage: Relevance to Radiotherapy. Clinical Oncology 25, 578–585. https://doi.org/10.1016/j.clon.2013.06.007

Lord, C.J., Ashworth, A., 2017. PARP inhibitors: Synthetic lethality in the clinic. Science 355, 1152–1158. https://doi.org/10.1126/science.aam7344

Lovly, C.M., Yan, L., Ryan, C.E., Takada, S., Piwnica-Worms, H., 2008. Regulation of Chk2 Ubiquitination and Signaling through Autophosphorylation of Serine 379. Mol. Cell. Biol. 28, 5874. https://doi.org/10.1128/MCB.00821-08

Löw, P., Bussell, K., Dawson, S.P., Billett, M.A., Mayer, R.J., Reynolds, S.E., 1997. Expression of a 26S proteasome ATPase subunit, MS73, in muscles that undergo developmentally programmed cell death, and its control by ecdysteroid hormones in the insect Manduca sexta. FEBS Letters 400, 345–349. https://doi.org/10.1016/S0014-5793(96)01413-5

Lowe, S.W., Lin, A.W., 2000. Apoptosis in cancer. Carcinogenesis 21, 485–495. https://doi.org/10.1093/carcin/21.3.485

Lowndes, N.F., Toh, G.W.-L., 2005. DNA Repair: The Importance of Phosphorylating Histone H2AX. Current Biology 15, R99–R102. https://doi.org/10.1016/j.cub.2005.01.029

Lu, G., Punj, V., Chaudhary, P.M., 2008. Proteasome inhibitor Bortezomib induces cell-cycle arrest and apoptosis in cell lines derived from Ewing's sarcoma family of tumors and synergizes with TRAIL. Cancer Biology & Therapy 7, 603–608. https://doi.org/10.4161/cbt.7.4.5564

Lubahn, D., Joseph, D., Sullivan, P., Willard, H., French, F., Wilson, E., 1988. Cloning of human androgen receptor complementary DNA and localization to the X chromosome. Science 240, 327. https://doi.org/10.1126/science.3353727

Lukacsovich, T., Yang, D., Waldman, A.S., 1994. Repair of a specific double-strand break generated within a mammalian chromosome by yeast endonuclease I-Scel. Nucleic Acids Research 22, 5649–5657. https://doi.org/10.1093/nar/22.25.5649

Lupien, M., Eeckhoute, J., Meyer, C.A., Wang, Q., Zhang, Y., Li, W., Carroll, J.S., Liu, X.S., Brown, M., 2008. FoxA1 Translates Epigenetic Signatures into Enhancer-Driven Lineage-Specific Transcription. Cell 132, 958–970. https://doi.org/10.1016/j.cell.2008.01.018

Lyko, F., 2018. The DNA methyltransferase family: a versatile toolkit for epigenetic regulation. Nature Reviews Genetics 19, 81–92. https://doi.org/10.1038/nrg.2017.80

Ma, Y., Vassetzky, Y., Dokudovskaya, S., 2018. mTORC1 pathway in DNA damage response. Biochimica et Biophysica Acta (BBA) - Molecular Cell Research 1865, 1293–1311. https://doi.org/10.1016/j.bbamcr.2018.06.011

Macaulay, V.M., Middleton, M.R., Eckhardt, S.G., Rudin, C.M., Juergens, R.A., Gedrich, R., Gogov, S., McCarthy, S., Poondru, S., Stephens, A.W., Gadgeel, S.M., 2016. Phase I Dose-Escalation Study of Linsitinib (OSI-906) and Erlotinib in Patients with Advanced Solid Tumors. Clin Cancer Res 22, 2897–2907. https://doi.org/10.1158/1078-0432.CCR-15-2218

Macaulay, V.M., Salisbury, A.J., Bohula, E.A., Playford, M.P., Smorodinsky, N.I., Shiloh, Y., 2001. Downregulation of the type 1 insulin-like growth factor receptor in mouse melanoma cells is associated with enhanced radiosensitivity and impaired activation of Atm kinase. Oncogene 20, 4029–4040. https://doi.org/10.1038/sj.onc.1204565

Macdonald, J.I., Dick, F.A., 2012. Posttranslational modifications of the retinoblastoma tumor suppressor protein as determinants of function. Genes Cancer 3, 619–633. https://doi.org/10.1177/1947601912473305

Machiels, B., Henfling, M., Gerards, W., Broers, J., Bloemendal, H., Ramaekers, F., Schutte, B., 1997. Detailed analysis of cell cycle kinetics upon proteasome inhibition. Cytometry 28, 243–252. https://doi.org/10.1002/(sici)1097-0320(19970701)28:3<243::aid-cyto9>3.0.co;2-e

Maddika, S., Ande, S.R., Wiechec, E., Hansen, L.L., Wesselborg, S., Los, M., 2008. Akt-mediated phosphorylation of CDK2 regulates its dual role in cell cycle progression and apoptosis. J Cell Sci 121, 979–988. https://doi.org/10.1242/jcs.009530

Maeda, A., Tamura, K., Wakui, H., Dejima, T., Ohsawa, M., Azushima, K., Kanaoka, T., Uneda, K., Matsuda, M., Yamashita, A., Miyazaki, N., Yatsu, K., Hirawa, N., Toya, Y., Umemura, S., 2013. Angiotensin receptor-binding protein ATRAP/Agtrap inhibits metabolic dysfunction with visceral obesity. J Am Heart Assoc 2, e000312–e000312. https://doi.org/10.1161/JAHA.113.000312

Maeda, H., Yonou, H., Yano, K., Ishii, G., Saito, S., Ochiai, A., 2009. Prostate-specific antigen enhances bioavailability of insulin-like growth factor by degrading insulin-like growth factor binding protein 5. Biochemical and Biophysical Research Communications 381, 311–316. https://doi.org/10.1016/j.bbrc.2009.01.096

Maehama, T., Dixon, J.E., 1998. The Tumor Suppressor, PTEN/MMAC1, Dephosphorylates the Lipid Second Messenger, Phosphatidylinositol 3,4,5-Trisphosphate. Journal of Biological Chemistry 273, 13375–13378. https://doi.org/10.1074/jbc.273.22.13375

Mah, L.-J., El-Osta, A., Karagiannis, T.C., 2010. γH2AX: a sensitive molecular marker of DNA damage and repair. Leukemia 24, 679–686. https://doi.org/10.1038/leu.2010.6

Maier, P., Hartmann, L., Wenz, F., Herskind, C., 2016. Cellular Pathways in Response to Ionizing Radiation and Their Targetability for Tumor Radiosensitization. Int J Mol Sci 17, 102. https://doi.org/10.3390/ijms17010102

Mailand, N., Podtelejnikov, A.V., Groth, A., Mann, M., Bartek, J., Lukas, J., 2002. Regulation of G2/M events by Cdc25A through phosphorylation-dependent modulation of its stability. The EMBO Journal 21, 5911–5920. https://doi.org/10.1093/emboj/cdf567

Mairet-Coello, G., Tury, A., DiCicco-Bloom, E., 2009. Insulin-like growth factor-1 promotes G1/S cell cycle progression through bidirectional regulation of cyclins and cyclin-dependent kinase inhibitors via the phosphatidylinositol 3-kinase/Akt pathway in developing rat cerebral cortex. J Neurosci 29, 775–788. https://doi.org/10.1523/JNEUROSCI.1700-08.2009

Makarova, K.S., Wolf, Y.I., Iranzo, J., Shmakov, S.A., Alkhnbashi, O.S., Brouns, S.J.J., Charpentier, E., Cheng, D., Haft, D.H., Horvath, P., Moineau, S., Mojica, F.J.M., Scott, D., Shah, S.A., Siksnys, V., Terns, M.P., Venclovas, Č., White, M.F., Yakunin, A.F., Yan, W., Zhang, F., Garrett, R.A., Backofen, R., van der Oost, J., Barrangou, R., Koonin, E.V., 2020. Evolutionary classification of CRISPR–Cas systems: a burst of class 2 and derived variants. Nature Reviews Microbiology 18, 67–83. https://doi.org/10.1038/s41579-019-0299-x

Maki, C.G., Huibregtse, J.M., Howley, P.M., 1996. In Vivo Ubiquitination and Proteasome-mediated Degradation of p53. Cancer Res 56, 2649.

Malec, V., Coulson, J.M., Urbé, S., Clague, M.J., 2015. Combined Analyses of the VHL and Hypoxia Signaling Axes in an Isogenic Pairing of Renal Clear Cell Carcinoma Cells. J. Proteome Res. 14, 5263–5272. https://doi.org/10.1021/acs.jproteome.5b00692

Mali, P., Yang, L., Esvelt, K.M., Aach, J., Guell, M., DiCarlo, J.E., Norville, J.E., Church, G.M., 2013. RNA-Guided Human Genome Engineering via Cas9. Science 339, 823. https://doi.org/10.1126/science.1232033

Manning, B.D., Tee, A.R., Logsdon, M.N., Blenis, J., Cantley, L.C., 2002. Identification of the Tuberous Sclerosis Complex-2 Tumor Suppressor Gene Product Tuberin as a Target of the Phosphoinositide 3-Kinase/Akt Pathway. Molecular Cell 10, 151–162. https://doi.org/10.1016/S1097-2765(02)00568-3

Mantovani, F., Collavin, L., Del Sal, G., 2019. Mutant p53 as a guardian of the cancer cell. Cell Death & Differentiation 26, 199–212. https://doi.org/10.1038/s41418-018-0246-9

Mao, Z., Bozzella, M., Seluanov, A., Gorbunova, V., 2008. Comparison of nonhomologous end joining and homologous recombination in human cells. DNA Repair 7, 1765–1771. https://doi.org/10.1016/j.dnarep.2008.06.018

Maor, S.B., Abramovitch, S., Erdos, M.R., Brody, L.C., Werner, H., 2000. BRCA1 Suppresses Insulin-like Growth Factor-I Receptor Promoter Activity: Potential Interaction between BRCA1 and Sp1. Molecular Genetics and Metabolism 69, 130–136. https://doi.org/10.1006/mgme.1999.2958

Marampon, F., Gravina, G.L., Di Rocco, A., Bonfili, P., Di Staso, M., Fardella, C., Polidoro, L., Ciccarelli, C., Festuccia, C., Popov, V.M., Pestell, R.G., Tombolini, V., Zani, B.M., 2011. MEK/ERK Inhibitor U0126 Increases the Radiosensitivity of Rhabdomyosarcoma Cells In vitro and In vivo by Downregulating Growth and DNA Repair Signals. Mol Cancer Ther 10, 159. https://doi.org/10.1158/1535-7163.MCT-10-0631

Maréchal, A., Zou, L., 2015. RPA-coated single-stranded DNA as a platform for post-translational modifications in the DNA damage response. Cell Research 25, 9–23. https://doi.org/10.1038/cr.2014.147

Maréchal, A., Zou, L., 2013. DNA damage sensing by the ATM and ATR kinases. Cold Spring Harb Perspect Biol 5, a012716. https://doi.org/10.1101/cshperspect.a012716

Mari, P.-O., Florea, B.I., Persengiev, S.P., Verkaik, N.S., Brüggenwirth, H.T., Modesti, M., Giglia-Mari, G., Bezstarosti, K., Demmers, J.A.A., Luider, T.M., Houtsmuller, A.B., van Gent, D.C., 2006. Dynamic assembly of end-joining complexes requires interaction between Ku70/80 and XRCC4. Proc Natl Acad Sci U S A 103, 18597–18602. https://doi.org/10.1073/pnas.0609061103

Mariotti, L.G., Pirovano, G., Savage, K.I., Ghita, M., Ottolenghi, A., Prise, K.M., Schettino, G., 2013. Use of the γ-H2AX assay to investigate DNA repair dynamics following multiple radiation exposures. PLoS One 8, e79541–e79541. https://doi.org/10.1371/journal.pone.0079541

Marková, E., Schultz, N., Belyaev, I.Y., 2007. Kinetics and dose-response of residual 53BP1/γ-H2AX foci: Co-localization, relationship with DSB repair and clonogenic survival. null 83, 319–329. https://doi.org/10.1080/09553000601170469

Martin, G.S., 2001. The hunting of the Src. Nature Reviews Molecular Cell Biology 2, 467–475. https://doi.org/10.1038/35073094

Martinez-Quetglas, I., Pinyol, R., Dauch, D., Torrecilla, S., Tovar, V., Moeini, A., Alsinet, C., Portela, A., Rodriguez-Carunchio, L., Solé, M., Lujambio, A., Villanueva, A., Thung, S., Esteller, M., Zender, L., Llovet, J.M., 2016. IGF2 Is Up-regulated by Epigenetic Mechanisms in Hepatocellular Carcinomas and Is an Actionable Oncogene Product in Experimental Models. Gastroenterology 151, 1192–1205. https://doi.org/10.1053/j.gastro.2016.09.001

Matheson, E.C., Hall, A.G., 2003. Assessment of mismatch repair function in leukaemic cell lines and blasts from children with acute lymphoblastic leukaemia. Carcinogenesis 24, 31–38. https://doi.org/10.1093/carcin/24.1.31

Matsubara, J., Yamada, Y., Nakajima, T.E., Kato, K., Hamaguchi, T., Shirao, K., Shimada, Y., Shimoda, T., 2008. Clinical Significance of Insulin-Like Growth Factor Type 1 Receptor and Epidermal Growth Factor Receptor in Patients with Advanced Gastric Cancer. Oncology 74, 76–83. https://doi.org/10.1159/000139127

Matsumoto, T., Sakari, M., Okada, M., Yokoyama, A., Takahashi, S., Kouzmenko, A., Kato, S., 2013. The Androgen Receptor in Health and Disease. Annu. Rev. Physiol. 75, 201–224. https://doi.org/10.1146/annurev-physiol-030212-183656

Matsuoka Shuhei, Ballif Bryan A., Smogorzewska Agata, McDonald E. Robert, Hurov Kristen E., Luo Ji, Bakalarski Corey E., Zhao Zhenming, Solimini Nicole, Lerenthal Yaniv, Shiloh Yosef, Gygi Steven P., Elledge Stephen J., 2007. ATM and ATR Substrate Analysis Reveals Extensive Protein Networks Responsive to DNA Damage. Science 316, 1160–1166. https://doi.org/10.1126/science.1140321

Matsushima-Nishiwaki, R., Toyoda, H., Nagasawa, T., Yasuda, E., Chiba, N., Okuda, S., Maeda, A., Kaneoka, Y., Kumada, T., Kozawa, O., 2016. Phosphorylated Heat Shock Protein 20 (HSPB6) Regulates Transforming Growth Factor-α-Induced Migration and Invasion of Hepatocellular Carcinoma Cells. PLoS One 11, e0151907–e0151907. https://doi.org/10.1371/journal.pone.0151907

Mattarocci, S., Reinert, J.K., Bunker, R.D., Fontana, G.A., Shi, T., Klein, D., Cavadini, S., Faty, M., Shyian, M., Hafner, L., Shore, D., Thomä, N.H., Rass, U., 2017. Rif1 maintains telomeres and mediates DNA repair by encasing DNA ends. Nature Structural & Molecular Biology 24, 588–595. https://doi.org/10.1038/nsmb.3420

Maurel, J., López-Pousa, A., Calabuig, S., Bagué, S., del Muro, X.G., Sanjuan, X., Rubió-Casadevall, J., Cuatrecasas, M., Martinez-Trufero, J., Horndler, C., Fra, J., Valverde, C., Redondo, A., Poveda, A., Sevilla, I., Lainez, N.,

Rubini, M., García-Albéniz, X., Martín-Broto, J., de Alava, E., 2016. Phosphorylated-insulin growth factor I receptor (p-IGF1R) and metalloproteinase-3 (MMP3) expression in advanced gastrointestinal stromal tumors (GIST). A GEIS 19 study. Clinical Sarcoma Research 6, 10. https://doi.org/10.1186/s13569-016-0050-6

Maurer, U., Charvet, C., Wagman, A.S., Dejardin, E., Green, D.R., 2006. Glycogen Synthase Kinase-3 Regulates Mitochondrial Outer Membrane Permeabilization and Apoptosis by Destabilization of MCL-1. Molecular Cell 21, 749–760. https://doi.org/10.1016/j.molcel.2006.02.009

Mawson, A., Lai, A., Carroll, J., Sergio, C.M., Mitchell, C., Sarcevic, B., 2005. Estrogen and insulin/IGF-1 cooperatively stimulate cell cycle progression in MCF-7 breast cancer cells through differential regulation of c-Myc and cyclin D1. Molecular and cellular endocrinology 229, 161–73. https://doi.org/10.1016/j.mce.2004.08.002

Mayo, L.D., Donner, D.B., 2001. A phosphatidylinositol 3-kinase/Akt pathway promotes translocation of Mdm2 from the cytoplasm to the nucleus. Proc Natl Acad Sci U S A 98, 11598–11603. https://doi.org/10.1073/pnas.181181198

McBride, W.H., Iwamoto, K.S., Syljuasen, R., Pervan, M., Pajonk, F., 2003. The role of the ubiquitin/proteasome system in cellular responses to radiation. Oncogene 22, 5755–5773. https://doi.org/10.1038/sj.onc.1206676

McCall, P., Gemmell, L.K., Mukherjee, R., Bartlett, J.M.S., Edwards, J., 2008. Phosphorylation of the androgen receptor is associated with reduced survival in hormone-refractory prostate cancer patients. British Journal of Cancer 98, 1094–1101. https://doi.org/10.1038/sj.bjc.6604152

McGowan, D.R., Skwarski, M., Bradley, K.M., Campo, L., Fenwick, J.D., Gleeson, F.V., Green, M., Horne, A., Maughan, T.S., McCole, M.G., Mohammed, S., Muschel, R.J., Ng, S.M., Panakis, N., Prevo, R., Strauss, V.Y., Stuart, R., Tacconi, E.M.C., Vallis, K.A., McKenna, W.G., Macpherson, R.E., Higgins, G.S., 2019. Buparlisib with thoracic radiotherapy and its effect on tumour hypoxia: A phase I study in patients with advanced non-small cell lung carcinoma. Eur J Cancer 113, 87–95. https://doi.org/10.1016/j.ejca.2019.03.015

McKenna, Gillies.W., Muschel, R.J., Gupta, A.K., Hahn, S.M., Bernhard, E.J., 2003. The RAS signal transduction pathway and its role in radiation sensitivity. Oncogene 22, 5866–5875. https://doi.org/10.1038/sj.onc.1206699

McKinnon, P.J., 2012. ATM and the Molecular Pathogenesis of Ataxia Telangiectasia. Annu. Rev. Pathol. Mech. Dis. 7, 303–321. https://doi.org/10.1146/annurev-pathol-011811-132509

Mebratu, Y., Tesfaigzi, Y., 2009. How ERK1/2 activation controls cell proliferation and cell death: Is subcellular localization the answer? Cell Cycle 8, 1168–1175. https://doi.org/10.4161/cc.8.8.8147

Medyouf, H., Gusscott, S., Wang, H., Tseng, J.-C., Wai, C., Nemirovsky, O., Trumpp, A., Pflumio, F., Carboni, J., Gottardis, M., Pollak, M., Kung, A.L., Aster, J.C., Holzenberger, M., Weng, A.P., 2011a. High-level IGF1R expression is required for leukemia-initiating cell activity in T-ALL and is supported by Notch signaling. Journal of Experimental Medicine 208, 1809–1822. https://doi.org/10.1084/jem.20110121

Medyouf, H., Gusscott, S., Wang, H., Tseng, J.-C., Wai, C., Nemirovsky, O., Trumpp, A., Pflumio, F., Carboni, J., Gottardis, M., Pollak, M., Kung, A.L., Aster, J.C., Holzenberger, M., Weng, A.P., 2011b. High-level IGF1R expression is required for leukemia-initiating cell activity in T-ALL and is supported by Notch signaling. J Exp Med 208, 1809–1822. https://doi.org/10.1084/jem.20110121

Meek, K., 2020. Activation of DNA-PK by hairpinned DNA ends reveals a stepwise mechanism of kinase activation. Nucleic Acids Res 48, 9098–9108. https://doi.org/10.1093/nar/gkaa614

Mehta, A., Haber, J.E., 2014. Sources of DNA double-strand breaks and models of recombinational DNA repair. Cold Spring Harb Perspect Biol 6, a016428–a016428. https://doi.org/10.1101/cshperspect.a016428

Mehta, G., Hsiao, A.Y., Ingram, M., Luker, G.D., Takayama, S., 2012. Opportunities and challenges for use of tumor spheroids as models to test drug delivery and efficacy. J Control Release 164, 192–204. https://doi.org/10.1016/j.jconrel.2012.04.045

Menoyo, A., Alazzouzi, H., Espín, E., Armengol, M., Yamamoto, H., Schwartz, S., 2001. Somatic Mutations in the DNA Damage-Response Genes ATR and CHK1 in Sporadic Stomach Tumors with Microsatellite Instability. Cancer Res 61, 7727.

Merkle, D., Douglas, P., Moorhead, G.B.G., Leonenko, Z., Yu, Y., Cramb, D., Bazett-Jones, D.P., Lees-Miller, S.P., 2002. The DNA-Dependent Protein Kinase Interacts with DNA To Form a Protein−DNA Complex That Is Disrupted by Phosphorylation. Biochemistry 41, 12706–12714. https://doi.org/10.1021/bi0263558

Meyer, N., Penn, L.Z., 2008. Reflecting on 25 years with MYC. Nature Reviews Cancer 8, 976–990. https://doi.org/10.1038/nrc2231

Meyers, M., Hwang, A., Wagner, M.W., Bruening, A.J., Veigl, M.L., Sedwick, W.D., Boothman, D.A., 2003. A role for DNA mismatch repair in sensing and responding to fluoropyrimidine damage. Oncogene 22, 7376–7388. https://doi.org/10.1038/sj.onc.1206941

Mialon, A., Thastrup, J., Kallunki, T., Mannermaa, L., Westermarck, J., Holmström, T.H., 2008. Identification of nucleolar effects in JNK-deficient cells. FEBS Letters 582, 3145–3151. https://doi.org/10.1016/j.febslet.2008.08.004

Milatz, S., Krug, S.M., Rosenthal, R., Günzel, D., Müller, D., Schulzke, J.-D., Amasheh, S., Fromm, M., 2010. Claudin-3 acts as a sealing component of the tight junction for ions of either charge and uncharged solutes. Biochimica et Biophysica Acta (BBA) - Biomembranes 1798, 2048–2057. https://doi.org/10.1016/j.bbamem.2010.07.014

Miller, J.C., Tan, S., Qiao, G., Barlow, K.A., Wang, J., Xia, D.F., Meng, X., Paschon, D.E., Leung, E., Hinkley, S.J., Dulay, G.P., Hua, K.L., Ankoudinova, I., Cost, G.J., Urnov, F.D., Zhang, H.S., Holmes, M.C., Zhang, L., Gregory, P.D., Rebar, E.J., 2011. A TALE nuclease architecture for efficient genome editing. Nature Biotechnology 29, 143–148. https://doi.org/10.1038/nbt.1755

Mimae, T., Tsuta, K., Kondo, T., Nitta, H., Grogan, T.M., Okada, M., Asamura, H., Tsuda, H., 2012. Protein expression and gene copy number changes of receptor tyrosine kinase in thymomas and thymic carcinomas. Annals of Oncology 23, 3129–3137. https://doi.org/10.1093/annonc/mds147

Mimori, T., Hardin, J.A., 1986. Mechanism of interaction between Ku protein and DNA. Journal of Biological Chemistry 261, 10375–10379.

Mimori, T., Ohosone, Y., Hama, N., Suwa, A., Akizuki, M., Homma, M., Griffith, A.J., Hardin, J.A., 1990. Isolation and characterization of cDNA encoding the 80-kDa subunit protein of the human autoantigen Ku (p70/p80) recognized by autoantibodies from patients with scleroderma-polymyositis overlap syndrome. Proc Natl Acad Sci U S A 87, 1777–1781. https://doi.org/10.1073/pnas.87.5.1777

Min, J., Singh, S., Fitzgerald-Bocarsly, P., Wood, T.L., 2012. Insulin-like growth factor I regulates G2/M progression through mammalian target of rapamycin signaling in oligodendrocyte progenitors. Glia 60, 1684–1695. https://doi.org/10.1002/glia.22387

Mireuta, M., Birman, E., Barmash, M., Pollak, M., 2014. Quantification of Binding of IGF-1 to BI 836845, a Candidate Therapeutic Antibody Against IGF-1 and IGF-2, and Effects of This Antibody on IGF-1:IGFBP-3 Complexes In Vitro and in Male C57BL/6 Mice. Endocrinology 155, 703–715. https://doi.org/10.1210/en.2013-1791

Mo, W., Liu, Q., Lin, C.C.-J., Dai, H., Peng, Y., Liang, Y., Peng, G., Meric-Bernstam, F., Mills, G.B., Li, K., Lin, S.-Y., 2016. mTOR Inhibitors Suppress Homologous Recombination Repair and Synergize with PARP Inhibitors via Regulating SUV39H1 in BRCA-Proficient Triple-Negative Breast Cancer. Clin Cancer Res 22, 1699–1712. https://doi.org/10.1158/1078-0432.CCR-15-1772

Modi, P.K., Komaravelli, N., Singh, N., Sharma, P., 2012. Interplay between MEK-ERK signaling, cyclin D1, and cyclin-dependent kinase 5 regulates cell cycle reentry and apoptosis of neurons. Mol Biol Cell 23, 3722–3730. https://doi.org/10.1091/mbc.E12-02-0125

Mohammadian Gol, T., Rodemann, H.P., Dittmann, K., 2019. Depletion of Akt1 and Akt2 Impairs the Repair of Radiation-Induced DNA Double Strand Breaks via Homologous Recombination. Int J Mol Sci 20, 6316. https://doi.org/10.3390/ijms20246316

Mohiuddin, I.S., Kang, M.H., 2019. DNA-PK as an Emerging Therapeutic Target in Cancer. Frontiers in Oncology 9, 635. https://doi.org/10.3389/fonc.2019.00635

Mojica, F.J.M., Díez-Villaseñor, C., García-Martínez, J., Soria, E., 2005. Intervening Sequences of Regularly Spaced Prokaryotic Repeats Derive from Foreign Genetic Elements. Journal of Molecular Evolution 60, 174–182. https://doi.org/10.1007/s00239-004-0046-3

Montagnoli, A., Valsasina, B., Brotherton, D., Troiani, S., Rainoldi, S., Tenca, P., Molinari, A., Santocanale, C., 2006. Identification of Mcm2 Phosphorylation Sites by S-phase-regulating Kinases. Journal of Biological Chemistry 281, 10281–10290. https://doi.org/10.1074/jbc.M512921200

Moromisato, D.Y., Moromisato, M.Y., Zanconato, S., Roberts, J., Brasel, J.A., Cooper, D.M., 1996. Effect of hypoxia on lung, heart, and liver insulin-like growth factor-I gene and receptor expression in the newborn rat. Critical Care Medicine 24.

Moschos, S.J., Mantzoros, C.S., 2002. The Role of the IGF System in Cancer: From Basic to Clinical Studies and Clinical Applications. Oncology 63, 317–332. https://doi.org/10.1159/000066230

Moscou, M.J., Bogdanove, A.J., 2009. A Simple Cipher Governs DNA Recognition by TAL Effectors. Science 326, 1501. https://doi.org/10.1126/science.1178817

Mueck, K., Rebholz, S., Harati, M.D., Rodemann, H.P., Toulany, M., 2017. Akt1 Stimulates Homologous Recombination Repair of DNA Double-Strand Breaks in a Rad51-Dependent Manner. Int J Mol Sci 18, 2473. https://doi.org/10.3390/ijms18112473

Mulholland, D.J., Kobayashi, N., Ruscetti, M., Zhi, A., Tran, L.M., Huang, J., Gleave, M., Wu, H., 2012. Pten loss and RAS/MAPK activation cooperate to promote EMT and metastasis initiated from prostate cancer stem/progenitor cells. Cancer Res 72, 1878–1889. https://doi.org/10.1158/0008-5472.CAN-11-3132

Müller, H., Bracken, A.P., Vernell, R., Moroni, M.C., Christians, F., Grassilli, E., Prosperini, E., Vigo, E., Oliner, J.D., Helin, K., 2001. E2Fs regulate the expression of genes involved in differentiation, development, proliferation, and apoptosis. Genes & Development 15, 267–285. https://doi.org/10.1101/gad.864201

Müller, H., Lukas, J., Schneider, A., Warthoe, P., Bartek, J., Eilers, M., Strauss, M., 1994. Cyclin D1 expression is regulated by the retinoblastoma protein. Proc Natl Acad Sci USA 91, 2945. https://doi.org/10.1073/pnas.91.8.2945

Muñoz, I.M., Rouse, J., 2009. Control of histone methylation and genome stability by PTIP. EMBO Rep 10, 239–245. https://doi.org/10.1038/embor.2009.21

Murphy, S.K., Huang, Z., Wen, Y., Spillman, M.A., Whitaker, R.S., Simel, L.R., Nichols, T.D., Marks, J.R., Berchuck, A., 2006. Frequent IGF2/H19 Domain Epigenetic Alterations and Elevated IGF2 Expression in Epithelial Ovarian Cancer. Mol Cancer Res 4, 283. https://doi.org/10.1158/1541-7786.MCR-05-0138

Murr, R., Loizou, J.I., Yang, Y.-G., Cuenin, C., Li, H., Wang, Z.-Q., Herceg, Z., 2006. Histone acetylation by Trrap–Tip60 modulates loading of repair proteins and repair of DNA double-strand breaks. Nature Cell Biology 8, 91–99. https://doi.org/10.1038/ncb1343

Mustachio, L.M., Kawakami, M., Lu, Y., Rodriguez-Canales, J., Mino, B., Behrens, C., Wistuba, I., Bota-Rabassedas, N., Yu, J., Lee, J.J., Roszik, J., Zheng, L., Liu, X., Freemantle, S.J., Dmitrovsky, E., 2017. The ISG15-specific protease USP18 regulates stability of PTEN. Oncotarget 8, 3–14. https://doi.org/10.18632/oncotarget.13914

Myers, J.S., Zhao, R., Xu, X., Ham, A.-J.L., Cortez, D., 2007. Cyclin-Dependent Kinase 2–Dependent Phosphorylation of ATRIP Regulates the G_2-M Checkpoint Response to DNA Damage. Cancer Res 67, 6685. https://doi.org/10.1158/0008-5472.CAN-07-0495

Nagasawa, H., Lin, Y.-F., Kato, T.A., Brogan, J.R., Shih, H.-Y., Kurimasa, A., Bedford, J.S., Chen, B.P.C., Little, J.B., 2017. Coordination of the Ser2056 and Thr2609 Clusters of DNA-PKcs in Regulating Gamma Rays and Extremely Low Fluencies of Alpha-Particle Irradiation to G(0)/G(1) Phase Cells. Radiat Res 187, 259–267. https://doi.org/10.1667/RR14679.1

Nagasawa, H., Little, J.B., Lin, Y.-F., So, S., Kurimasa, A., Peng, Y., Brogan, J.R., Chen, D.J., Bedford, J.S., Chen, B.P.C., 2011. Differential role of DNA-PKcs phosphorylations and kinase activity in radiosensitivity and chromosomal instability. Radiat Res 175, 83–89. https://doi.org/10.1667/RR2092.1

Nakade, S., Tsubota, T., Sakane, Y., Kume, S., Sakamoto, N., Obara, M., Daimon, T., Sezutsu, H., Yamamoto, T., Sakuma, T., Suzuki, K.T., 2014. Microhomology-mediated end-joining-dependent integration of donor DNA in cells and animals using TALENs and CRISPR/Cas9. Nature Communications 5, 5560. https://doi.org/10.1038/ncomms6560

Nakayama, J., Rice, J.C., Strahl, B.D., Allis, C.D., Grewal, S.I.S., 2001. Role of Histone H3 Lysine 9 Methylation in Epigenetic Control of Heterochromatin Assembly. Science 292, 110. https://doi.org/10.1126/science.1060118

Nambiar, T.S., Billon, P., Diedenhofen, G., Hayward, S.B., Taglialatela, A., Cai, K., Huang, J.-W., Leuzzi, G., Cuella-Martin, R., Palacios, A., Gupta, A., Egli, D., Ciccia, A., 2019. Stimulation of CRISPR-mediated homology-directed repair by an engineered RAD18 variant. Nature Communications 10, 3395. https://doi.org/10.1038/s41467-019-11105-z

Narayanan, R., Jiang, J., Gusev, Y., Jones, A., Kearbey, J.D., Miller, D.D., Schmittgen, T.D., Dalton, J.T., 2010. MicroRNAs Are Mediators of Androgen Action in Prostate and Muscle. PLOS ONE 5, e13637. https://doi.org/10.1371/journal.pone.0013637

Nasa, Cressey Lauren E., Kruse Thomas, Hertz Emil P. T., Gui Jiang, Graves Lee M., Nilsson Jakob, Kettenbach Arminja N., 2020. Quantitative kinase and phosphatase profiling reveal that CDK1 phosphorylates PP2Ac to promote mitotic entry. Science Signaling 13, eaba7823. https://doi.org/10.1126/scisignal.aba7823

Neal, J.A., Dang, V., Douglas, P., Wold, M.S., Lees-Miller, S.P., Meek, K., 2011. Inhibition of homologous recombination by DNA-dependent protein kinase requires kinase activity, is titratable, and is modulated by autophosphorylation. Mol Cell Biol 31, 1719–1733. https://doi.org/10.1128/MCB.01298-10

Neal, J.A., Dunger, K., Geith, K., Meek, K., 2020. Deciphering the role of distinct DNA-PK phosphorylations at collapsed replication forks. DNA Repair (Amst) 94, 102925–102925. https://doi.org/10.1016/j.dnarep.2020.102925

Negrini, S., Gorgoulis, V.G., Halazonetis, T.D., 2010. Genomic instability — an evolving hallmark of cancer. Nature Reviews Molecular Cell Biology 11, 220–228. https://doi.org/10.1038/nrm2858

Ng, F., Tang, B., 2013. When is Sirt1 activity bad for dying neurons? Frontiers in cellular neuroscience 7, 186. https://doi.org/10.3389/fncel.2013.00186

Ng, N., Purshouse, K., Foskolou, I.P., Olcina, M.M., Hammond, E.M., 2018. Challenges to DNA replication in hypoxic conditions. The FEBS Journal 285, 1563–1571. https://doi.org/10.1111/febs.14377

Nguyen, H.L., Gruber, D., Bulinski, J.C., 1999. Microtubule-associated protein 4 (MAP4) regulates assembly, protomer-polymer partitioning and synthesis of tubulin in cultured cells. Journal of Cell Science 112, 1813–1824. https://doi.org/10.1242/jcs.112.12.1813

Nick McElhinny, S.A., Snowden, C.M., McCarville, J., Ramsden, D.A., 2000. Ku Recruits the XRCC4-Ligase IV Complex to DNA Ends. Mol. Cell. Biol. 20, 2996. https://doi.org/10.1128/MCB.20.9.2996-3003.2000

Nicolaou, P., Knöll, R., Haghighi, K., Fan, G.-C., Dorn, G.W., 2nd, Hasenfub, G., Kranias, E.G., 2008. Human mutation in the anti-apoptotic heat shock protein 20 abrogates its cardioprotective effects. J Biol Chem 283, 33465–33471. https://doi.org/10.1074/jbc.M802307200

Nicosia, R.F., Nicosia, S.V., Smith, M., 1994. Vascular endothelial growth factor, platelet-derived growth factor, and insulin-like growth factor-1 promote rat aortic angiogenesis in vitro. Am J Pathol 145, 1023–1029.

Nieder, C., Pawinski, A., Dalhaug, A., Andratschke, N., 2012. A review of clinical trials of cetuximab combined with radiotherapy for non-small cell lung cancer. Radiat Oncol 7, 3–3. https://doi.org/10.1186/1748-717X-7-3

Niederst, M.J., Sequist, L.V., Poirier, J.T., Mermel, C.H., Lockerman, E.L., Garcia, A.R., Katayama, R., Costa, C., Ross, K.N., Moran, T., Howe, E., Fulton, L.E., Mulvey, H.E., Bernardo, L.A., Mohamoud, F., Miyoshi, N., VanderLaan, P.A., Costa, D.B., Jänne, P.A., Borger, D.R., Ramaswamy, S., Shioda, T., Iafrate, A.J., Getz, G., Rudin, C.M., Mino-Kenudson, M., Engelman, J.A., 2015. RB loss in resistant EGFR mutant lung adenocarcinomas that transform to small-cell lung cancer. Nature Communications 6, 6377. https://doi.org/10.1038/ncomms7377

Nijman, S.M.B., Luna-Vargas, M.P.A., Velds, A., Brummelkamp, T.R., Dirac, A.M.G., Sixma, T.K., Bernards, R., 2005. A Genomic and Functional Inventory of Deubiquitinating Enzymes. Cell 123, 773–786. https://doi.org/10.1016/j.cell.2005.11.007

Nishida, K., Arazoe, T., Yachie, N., Banno, S., Kakimoto, M., Tabata, M., Mochizuki, M., Miyabe, A., Araki, M., Hara, K.Y., Shimatani, Z., Kondo, A., 2016. Targeted nucleotide editing using hybrid prokaryotic and vertebrate adaptive immune systems. Science 353, aaf8729. https://doi.org/10.1126/science.aaf8729

Nishimasu, H., Ran, F.A., Hsu, P.D., Konermann, S., Shehata, S.I., Dohmae, N., Ishitani, R., Zhang, F., Nureki, O., 2014. Crystal Structure of Cas9 in Complex with Guide RNA and Target DNA. Cell 156, 935–949. https://doi.org/10.1016/j.cell.2014.02.001

Noh, S.-E., Juhnn, Y.-S., 2020. Inhibition of non-homologous end joining of gamma ray-induced DNA double-strand breaks by cAMP signaling in lung cancer cells. Scientific Reports 10, 14455. https://doi.org/10.1038/s41598-020-71522-9

Noon, A.T., Shibata, A., Rief, N., Löbrich, M., Stewart, G.S., Jeggo, P.A., Goodarzi, A.A., 2010. 53BP1-dependent robust localized KAP-1 phosphorylation is essential for heterochromatic DNA double-strand break repair. Nature Cell Biology 12, 177–184. https://doi.org/10.1038/ncb2017

O'Brien, A.R., Wilson, L.O.W., Burgio, G., Bauer, D.C., 2019. Unlocking HDR-mediated nucleotide editing by identifying high-efficiency target sites using machine learning. Scientific Reports 9, 2788. https://doi.org/10.1038/s41598-019-39142-0

Ochi, T., Blackford, A.N., Coates, J., Jhujh, S., Mehmood, S., Tamura, N., Travers, J., Wu, Q., Draviam, V.M., Robinson, C.V., Blundell, T.L., Jackson, S.P., 2015. DNA repair. PAXX, a paralog of XRCC4 and XLF, interacts with Ku to promote DNA double-strand break repair. Science 347, 185–188. https://doi.org/10.1126/science.1261971

Ochs, F., Somyajit, K., Altmeyer, M., Rask, M.-B., Lukas, J., Lukas, C., 2016. 53BP1 fosters fidelity of homology-directed DNA repair. Nature Structural & Molecular Biology 23, 714–721. https://doi.org/10.1038/nsmb.3251

O'Driscoll, M., Jeggo, P.A., 2008. The role of the DNA damage response pathways in brain development and microcephaly: Insight from human disorders. DNA Repair 7, 1039–1050. https://doi.org/10.1016/j.dnarep.2008.03.018

O'Driscoll, M., Ruiz-Perez, V.L., Woods, C.G., Jeggo, P.A., Goodship, J.A., 2003. A splicing mutation affecting expression of ataxia–telangiectasia and Rad3–related protein (ATR) results in Seckel syndrome. Nature Genetics 33, 497–501. https://doi.org/10.1038/ng1129

Ogawara, Y., Kishishita, S., Obata, T., Isazawa, Y., Suzuki, T., Tanaka, K., Masuyama, N., Gotoh, Y., 2002. Akt Enhances Mdm2-mediated Ubiquitination and Degradation of p53. Journal of Biological Chemistry 277, 21843–21850. https://doi.org/10.1074/jbc.M109745200

Oh, S., Harvey, A., Zimbric, J., Wang, Y., Nguyen, T., Jackson, P.J., Hendrickson, E.A., 2014. DNA ligase III and DNA ligase IV carry out genetically distinct forms of end joining in human somatic cells. DNA Repair (Amst) 21, 97–110. https://doi.org/10.1016/j.dnarep.2014.04.015

Ohlsson, C., Mohan, S., Sjögren, K., Tivesten, Å., Isgaard, J., Isaksson, O., Jansson, J.-O., Svensson, J., 2009. The Role of Liver-Derived Insulin-Like Growth Factor-I. Endocrine Reviews 30, 494–535. https://doi.org/10.1210/er.2009-0010

Okamoto, S., Amaishi, Y., Maki, I., Enoki, T., Mineno, J., 2019. Highly efficient genome editing for single-base substitutions using optimized ssODNs with Cas9-RNPs. Scientific Reports 9, 4811. https://doi.org/10.1038/s41598-019-41121-4

Olmos, D., Postel-Vinay, S., Molife, L.R., Okuno, S.H., Schuetze, S.M., Paccagnella, M.L., Batzel, G.N., Yin, D., Pritchard-Jones, K., Judson, I., Worden, F.P., Gualberto, A., Scurr, M., de Bono, J.S., Haluska, P., 2010. Safety, pharmacokinetics, and preliminary activity of the anti-IGF-1R antibody figitumumab (CP-751,871) in patients with sarcoma and Ewing's sarcoma: a phase 1 expansion cohort study. Lancet Oncol 11, 129–135. https://doi.org/10.1016/S1470-2045(09)70354-7

Olsen, J.V., Vermeulen, M., Santamaria, A., Kumar, C., Miller, M.L., Jensen, L.J., Gnad, F., Cox, J., Jensen, T.S., Nigg, E.A., Brunak, S., Mann, M., 2010. Quantitative Phosphoproteomics Reveals Widespread Full Phosphorylation Site Occupancy During Mitosis. Sci. Signal. 3, ra3. https://doi.org/10.1126/scisignal.2000475

Oni, T.E., Biffi, G., Baker, L.A., Hao, Y., Tonelli, C., Somerville, T.D.D., Deschênes, A., Belleau, P., Hwang, C.-I., Sánchez-Rivera, F.J., Cox, H., Brosnan, E., Doshi, A., Lumia, R.P., Khaledi, K., Park, Y., Trotman, L.C., Lowe, S.W., Krasnitz, A., Vakoc, C.R., Tuveson, D.A., 2020. SOAT1 promotes mevalonate pathway dependency in pancreatic cancer. J Exp Med 217, e20192389. https://doi.org/10.1084/jem.20192389

Ookata, K., Hisanaga, S., Sugita, M., Okuyama, A., Murofushi, H., Kitazawa, H., Chari, S., Bulinski, J.C., Kishimoto, T., 1997. MAP4 Is the in Vivo Substrate for CDC2 Kinase in HeLa Cells: Identification of an M-Phase Specific

and a Cell Cycle-Independent Phosphorylation Site in MAP4. Biochemistry 36, 15873–15883. https://doi.org/10.1021/bi971251w

Ormaza, G., Rodríguez, J.A., Ibáñez de Opakua, A., Merino, N., Villate, M., Gorroño, I., Rábano, M., Palmero, I., Vilaseca, M., Kypta, R., Vivanco, M. d.M., Rojas, A.L., Blanco, F.J., 2019. The Tumor Suppressor ING5 Is a Dimeric, Bivalent Recognition Molecule of the Histone H3K4me3 Mark. Journal of Molecular Biology 431, 2298–2319. https://doi.org/10.1016/j.jmb.2019.04.018

Ornitz, D.M., Itoh, N., 2015. The Fibroblast Growth Factor signaling pathway. WIREs Developmental Biology 4, 215–266. https://doi.org/10.1002/wdev.176

Osher, E., Macaulay, V.M., 2019. Therapeutic Targeting of the IGF Axis. Cells 8, 895. https://doi.org/10.3390/cells8080895

Pacheco-Marín, R., Melendez-Zajgla, J., Castillo-Rojas, G., Mandujano-Tinoco, E., Garcia-Venzor, A., Uribe-Carvajal, S., Cabrera-Orefice, A., Gonzalez-Torres, C., Gaytan-Cervantes, J., Mitre-Aguilar, I.B., Maldonado, V., 2016. Transcriptome profile of the early stages of breast cancer tumoral spheroids. Sci Rep 6, 23373–23373. https://doi.org/10.1038/srep23373

Padgett, K.A., Sorge, J.A., 1996. Creating seamless junctions independent of restriction sites in PCR cloning. Gene 168, 31–35. https://doi.org/10.1016/0378-1119(95)00731-8

Pagano, M., Tam, S., Theodoras, A., Beer-Romero, P., Del Sal, G., Chau, V., Yew, P., Draetta, G., Rolfe, M., 1995. Role of the ubiquitin-proteasome pathway in regulating abundance of the cyclin-dependent kinase inhibitor p27. Science 269, 682. https://doi.org/10.1126/science.7624798

Painter, R.B., 1982. Structural changes in chromatin as the basis for radiosensitivity in ataxia telangiectasia. Cytogenetic and Genome Research 33, 139–144. https://doi.org/10.1159/000131738

Pajonk, F., McBride, W.H., 2001. Ionizing radiation affects 26s proteasome function and associated molecular responses, even at low doses. Radiotherapy and Oncology 59, 203–212. https://doi.org/10.1016/S0167-8140(01)00311-5

Pandini, G., Frasca, F., Mineo, R., Sciacca, L., Vigneri, R., Belfiore, A., 2002. Insulin/Insulin-like Growth Factor I Hybrid Receptors Have Different Biological Characteristics Depending on the Insulin Receptor Isoform Involved. Journal of Biological Chemistry 277, 39684–39695. https://doi.org/10.1074/jbc.M202766200

Pandini, G., Wurch, T., Akla, B., Corvaia, N., Belfiore, A., Goetsch, L., 2007. Functional responses and in vivo anti-tumour activity of h7C10: A humanised monoclonal antibody with neutralising activity against the insulin-like growth factor-1 (IGF-1) receptor and insulin/IGF-1 hybrid receptors. European Journal of Cancer 43, 1318–1327. https://doi.org/10.1016/j.ejca.2007.03.009

Panier, S., Boulton, S.J., 2014. Double-strand break repair: 53BP1 comes into focus. Nature Reviews Molecular Cell Biology 15, 7–18. https://doi.org/10.1038/nrm3719

Papa, S., Choy, P.M., Bubici, C., 2019. The ERK and JNK pathways in the regulation of metabolic reprogramming. Oncogene 38, 2223–2240. https://doi.org/10.1038/s41388-018-0582-8

Park, S.-J., Gavrilova, O., Brown, A.L., Soto, J.E., Bremner, S., Kim, J., Xu, X., Yang, S., Um, J.-H., Koch, L.G., Britton, S.L., Lieber, R.L., Philp, A., Baar, K., Kohama, S.G., Abel, E.D., Kim, M.K., Chung, J.H., 2017. DNA-PK Promotes the Mitochondrial, Metabolic, and Physical Decline that Occurs During Aging. Cell Metab 25, 1135-1146.e7. https://doi.org/10.1016/j.cmet.2017.04.008

Parker, A.S., Cheville, J.C., Janney, C.A., Cerhan, J.R., 2002. High expression levels of insulin-like growth factor–I receptor predict poor survival among women with clear-cell renal cell carcinomas. Human Pathology 33, 801–805. https://doi.org/10.1053/hupa.2002.126186

Parker, C.C., James, N.D., Brawley, C.D., Clarke, N.W., Hoyle, A.P., Ali, A., Ritchie, A.W.S., Attard, G., Chowdhury, S., Cross, W., Dearnaley, D.P., Gillessen, S., Gilson, C., Jones, R.J., Langley, R.E., Malik, Z.I., Mason, M.D., Matheson, D., Millman, R., Russell, J.M., Thalmann, G.N., Amos, C.L., Alonzi, R., Bahl, A., Birtle, A., Din, O., Douis, H., Eswar, C., Gale, J., Gannon, M.R., Jonnada, S., Khaksar, S., Lester, J.F., O'Sullivan, J.M., Parikh, O.A., Pedley, I.D., Pudney, D.M., Sheehan, D.J., Srihari, N.N., Tran, A.T.H., Parmar, M.K.B., Sydes, M.R., 2018. Radiotherapy to the primary tumour for newly diagnosed, metastatic prostate cancer (STAMPEDE): a randomised controlled phase 3 trial. The Lancet 392, 2353–2366. https://doi.org/10.1016/S0140-6736(18)32486-3

Parmar, H., Edwards, L., Phillips, R.H., Allen, L., Lightman, S.L., 1987. Orchiectomy versus Long-acting D-Trp-6-LHRH in Advanced Prostatic Cancer. British Journal of Urology 59, 248–254. https://doi.org/10.1111/j.1464-410X.1987.tb04616.x

Patel, A.R., Klein, E.A., 2009. Risk factors for prostate cancer. Nature Clinical Practice Urology 6, 87–95. https://doi.org/10.1038/ncpuro1290

Patiar, S., Harris, A.L., 2006. Role of hypoxia-inducible factor-1α as a cancer therapy target. Endocrine-Related Cancer Endocr Relat Cancer 13, S61–S75. https://doi.org/10.1677/erc.1.01290

Paull, T.T., 2015. Mechanisms of ATM Activation. Annu. Rev. Biochem. 84, 711–738. https://doi.org/10.1146/annurev-biochem-060614-034335

Pautsch, A., Zoephel, A., Ahorn, H., Spevak, W., Hauptmann, R., Nar, H., 2001. Crystal Structure of Bisphosphorylated IGF-1 Receptor Kinase: Insight into Domain Movements upon Kinase Activation. Structure 9, 955–965. https://doi.org/10.1016/S0969-2126(01)00655-4

Pavlova, N.N., Thompson, C.B., 2016. The Emerging Hallmarks of Cancer Metabolism. Cell Metab 23, 27–47. https://doi.org/10.1016/j.cmet.2015.12.006

Pawlik, T.M., Keyomarsi, K., 2004. Role of cell cycle in mediating sensitivity to radiotherapy. International Journal of Radiation Oncology, Biology, Physics 59, 928–942. https://doi.org/10.1016/j.ijrobp.2004.03.005

Pedram, A., Razandi, M., Evinger, A.J., Lee, E., Levin, E.R., 2009. Estrogen inhibits ATR signaling to cell cycle checkpoints and DNA repair. Mol Biol Cell 20, 3374–3389. https://doi.org/10.1091/mbc.e09-01-0085

Pennisi, R., Ascenzi, P., di Masi, A., 2015. Hsp90: A New Player in DNA Repair? Biomolecules 5, 2589–2618. https://doi.org/10.3390/biom5042589

Peponi, E., Drakos, E., Reyes, G., Leventaki, V., Rassidakis, G.Z., Medeiros, L.J., 2006. Activation of mammalian target of rapamycin signaling promotes cell cycle progression and protects cells from apoptosis in mantle cell lymphoma. Am J Pathol 169, 2171–2180. https://doi.org/10.2353/ajpath.2006.051078

Persson, J., Ekwall, K., 2010. Chd1 remodelers maintain open chromatin and regulate the epigenetics of differentiation. Experimental Cell Research 316, 1316–1323. https://doi.org/10.1016/j.yexcr.2010.02.029

Pervan, M., Iwamoto, K.S., McBride, W.H., 2005. Proteasome Structures Affected by Ionizing Radiation. Mol Cancer Res 3, 381. https://doi.org/10.1158/1541-7786.MCR-05-0032

Peso, L. del, González-García, M., Page, C., Herrera, R., Nuñez, G., 1997. Interleukin-3-Induced Phosphorylation of BAD Through the Protein Kinase Akt. Science 278, 687. https://doi.org/10.1126/science.278.5338.687

Pfaeffle, R., Kies, W., Klammt, J., 2011. From GHRH to IGF-1 and downstream: Clinical phenotypes and biological mechanisms. Pediatric endocrinology reviews : PER 9 Suppl 1, 529–34.

Pitts, T.M., Tan, A.C., Kulikowski, G.N., Tentler, J.J., Brown, A.M., Flanigan, S.A., Leong, S., Coldren, C.D., Hirsch, F.R., Varella-Garcia, M., Korch, C., Eckhardt, S.G., 2010. Development of an integrated genomic classifier for a novel agent in colorectal cancer: approach to individualized therapy in early development. Clin Cancer Res 16, 3193–3204. https://doi.org/10.1158/1078-0432.CCR-09-3191

Plas, D.R., Thompson, C.B., 2005. Akt-dependent transformation: there is more to growth than just surviving. Oncogene 24, 7435–7442. https://doi.org/10.1038/sj.onc.1209097

Plo, I., Laulier, C., Gauthier, L., Lebrun, F., Calvo, F., Lopez, B.S., 2008. AKT1 Inhibits Homologous Recombination by Inducing Cytoplasmic Retention of BRCA1 and RAD51. Cancer Res 68, 9404. https://doi.org/10.1158/0008-5472.CAN-08-0861

Plotnikov, A., Zehorai, E., Procaccia, S., Seger, R., 2011. The MAPK cascades: Signaling components, nuclear roles and mechanisms of nuclear translocation. Biochimica et Biophysica Acta (BBA) - Molecular Cell Research 1813, 1619–1633. https://doi.org/10.1016/j.bbamcr.2010.12.012

Png, K.J., Halberg, N., Yoshida, M., Tavazoie, S.F., 2012. A microRNA regulon that mediates endothelial recruitment and metastasis by cancer cells. Nature 481, 190–194. https://doi.org/10.1038/nature10661

Podhorecka, M., Skladanowski, A., Bozko, P., 2010. H2AX Phosphorylation: Its Role in DNA Damage Response and Cancer Therapy. Journal of nucleic acids 2010. https://doi.org/10.4061/2010/920161

Pollak, M., 2012. The insulin and insulin-like growth factor receptor family in neoplasia: an update. Nature Reviews Cancer 12, 159–169. https://doi.org/10.1038/nrc3215

Pollak, M., 2008. Targeting insulin and insulin-like growth factor signalling in oncology. Current Opinion in Pharmacology 8, 384–392. https://doi.org/10.1016/j.coph.2008.07.004

Pollak, M.N., Schernhammer, E.S., Hankinson, S.E., 2004. Insulin-like growth factors and neoplasia. Nature Reviews Cancer 4, 505–518. https://doi.org/10.1038/nrc1387

Polo, S.E., Jackson, S.P., 2011. Dynamics of DNA damage response proteins at DNA breaks: a focus on protein modifications. Genes Dev 25, 409–433. https://doi.org/10.1101/gad.2021311

Popp, H.D., Brendel, S., Hofmann, W.-K., Fabarius, A., 2017. Immunofluorescence Microscopy of γH2AX and 53BP1 for Analyzing the Formation and Repair of DNA Double-strand Breaks. J Vis Exp 56617. https://doi.org/10.3791/56617

Pópulo, H., Lopes, J.M., Soares, P., 2012. The mTOR signalling pathway in human cancer. Int J Mol Sci 13, 1886–1918. https://doi.org/10.3390/ijms13021886

Poreba, E., Durzynska, J., 2020. Nuclear localization and actions of the insulin-like growth factor 1 (IGF-1) system components: Transcriptional regulation and DNA damage response. Mutation Research/Reviews in Mutation Research 784, 108307. https://doi.org/10.1016/j.mrrev.2020.108307

Porter, A.G., Jänicke, R.U., 1999. Emerging roles of caspase-3 in apoptosis. Cell Death & Differentiation 6, 99–104. https://doi.org/10.1038/sj.cdd.4400476

Porteus, M.H., Baltimore, D., 2003. Chimeric Nucleases Stimulate Gene Targeting in Human Cells. Science 300, 763. https://doi.org/10.1126/science.1078395

Pourcel, C., Salvignol, G., Vergnaud, G., 2005. CRISPR elements in Yersinia pestis acquire new repeats by preferential uptake of bacteriophage DNA, and provide additional tools for evolutionary studies. Microbiology (Reading, England) 151, 653–63. https://doi.org/10.1099/mic.0.27437-0

Prabhu, A.V., Luu, W., Sharpe, L.J., Brown, A.J., 2017. Phosphorylation regulates activity of 7-dehydrocholesterol reductase (DHCR7), a terminal enzyme of cholesterol synthesis. The Journal of Steroid Biochemistry and Molecular Biology 165, 363–368. https://doi.org/10.1016/j.jsbmb.2016.08.003

Pray-Grant, M.G., Daniel, J.A., Schieltz, D., Yates, J.R., Grant, P.A., 2005. Chd1 chromodomain links histone H3 methylation with SAGA- and SLIK-dependent acetylation. Nature 433, 434–438. https://doi.org/10.1038/nature03242

Prostate cancer statistics | Cancer Research UK [WWW Document], n.d. URL https://www.cancerresearchuk.org/health-professional/cancer-statistics/statistics-by-cancer-type/prostate-cancer (accessed 4.2.20).

Prostate cancer statistics | World Cancer Research Fund [WWW Document], n.d. URL https://www.wcrf.org/dietandcancer/cancer-trends/prostate-cancer-statistics (accessed 4.2.20).

Pylayeva-Gupta, Y., Grabocka, E., Bar-Sagi, D., 2011. RAS oncogenes: weaving a tumorigenic web. Nature Reviews Cancer 11, 761–774. https://doi.org/10.1038/nrc3106

Qi, L.S., Larson, M.H., Gilbert, L.A., Doudna, J.A., Weissman, J.S., Arkin, A.P., Lim, W.A., 2013. Repurposing CRISPR as an RNA-Guided Platform for Sequence-Specific Control of Gene Expression. Cell 152, 1173–1183. https://doi.org/10.1016/j.cell.2013.02.022

Qureishi, A., Rieunier, G., Shah, K.A., Aleksic, T., Winter, S.C., Møller, H., Macaulay, V.M., 2019. Radioresistant laryngeal cancers upregulate type 1 IGF receptor and exhibit increased cellular dependence on IGF and EGF signalling. Clinical Otolaryngology 44, 1026–1036. https://doi.org/10.1111/coa.13434

Raile, K., Klammt, J., Schneider, A., Keller, A., Laue, S., Smith, R., Pfäffle, R., Kratzsch, J., Keller, E., Kiess, W., 2006. Clinical and Functional Characteristics of the Human Arg59Ter Insulin-Like Growth Factor I Receptor (IGF1R) Mutation: Implications for a Gene Dosage Effect of the Human IGF1R. The Journal of Clinical Endocrinology & Metabolism 91, 2264–2271. https://doi.org/10.1210/jc.2005-2146

Rainey, M., Harhen, B., Wang, G.-N., Murphy, P., Santocanale, C., 2013. Cdc7-dependent and -independent phosphorylation of Claspin in the induction of the DNA replication checkpoint. Cell Cycle 12, 1560–1568. https://doi.org/10.4161/cc.24675

Rakatzi, I., Stosik, M., Gromke, T., Siddle, K., Eckel, J., 2006. Differential phosphorylation of IRS-1 and IRS-2 by insulin and IGF-I receptors. null 112, 37–47. https://doi.org/10.1080/13813450500500332

Ramcharan, R., Aleksic, T., Kamdoum, W.P., Gao, S., Pfister, S.X., Tanner, J., Bridges, E., Asher, R., Watson, A.J., Margison, G.P., Woodcock, M., Repapi, E., Li, J.-L., Middleton, M.R., Macaulay, V.M., 2015. IGF-1R inhibition induces schedule-dependent sensitization of human melanoma to temozolomide. Oncotarget 6, 39877–39890. https://doi.org/10.18632/oncotarget.5631

Ran, F.A., Hsu, P.D., Wright, J., Agarwala, V., Scott, D.A., Zhang, F., 2013. Genome engineering using the CRISPR-Cas9 system. Nature Protocols 8, 2281–2308. https://doi.org/10.1038/nprot.2013.143

Rastogi, N., Mishra, D.P., 2012. Therapeutic targeting of cancer cell cycle using proteasome inhibitors. Cell Div 7, 26–26. https://doi.org/10.1186/1747-1028-7-26

Ratcliffe, P.J., 2013. Oxygen sensing and hypoxia signalling pathways in animals: the implications of physiology for cancer. The Journal of Physiology 591, 2027–2042. https://doi.org/10.1113/jphysiol.2013.251470

Rea, S., Eisenhaber, F., O'Carroll, D., Strahl, B.D., Sun, Z.-W., Schmid, M., Opravil, S., Mechtler, K., Ponting, C.P., Allis, C.D., Jenuwein, T., 2000. Regulation of chromatin structure by site-specific histone H3 methyltransferases. Nature 406, 593–599. https://doi.org/10.1038/35020506

Reddy, E.P., Reynolds, R.K., Santos, E., Barbacid, M., 1982. A point mutation is responsible for the acquisition of transforming properties by the T24 human bladder carcinoma oncogene. Nature 300, 149–152. https://doi.org/10.1038/300149a0

Reddy, Y.V.R., Ding, Q., Lees-Miller, S.P., Meek, K., Ramsden, D.A., 2004. Non-homologous End Joining Requires That the DNA-PK Complex Undergo an Autophosphorylation-dependent Rearrangement at DNA Ends. Journal of Biological Chemistry 279, 39408–39413. https://doi.org/10.1074/jbc.M406432200

Rees, H.A., Liu, D.R., 2018. Base editing: precision chemistry on the genome and transcriptome of living cells. Nature Reviews Genetics 19, 770–788. https://doi.org/10.1038/s41576-018-0059-1

Reinheckel, T., SITTE, N., ULLRICH, O., KUCKELKORN, U., DAVIES, K.J.A., GRUNE, T., 1998. Comparative resistance of the 20S and 26S proteasome to oxidative stress. Biochemical Journal 335, 637–642. https://doi.org/10.1042/bj3350637

Reinheckel, T., Ullrich, O., Sitte, N., Grune, T., 2000. Differential Impairment of 20S and 26S Proteasome Activities in Human Hematopoietic K562 Cells during Oxidative Stress. Archives of Biochemistry and Biophysics 377, 65–68. https://doi.org/10.1006/abbi.2000.1717

Reitsema, T.J., Banáth, J.P., MacPhail, S.H., Olive, P.L., 2004. Hypertonic Saline Enhances Expression of Phosphorylated Histone H2AX after Irradiation. Radiation Research 161, 402–408. https://doi.org/10.1667/RR3153

Ren, M., Zhong, X., Ma, C., Sun, Y., Guan, Q., Cui, B., Guo, J., Wang, H., Gao, L., Zhao, J., 2009. Insulin-like growth factor-1 promotes cell cycle progression via upregulation of cyclin D1 expression through the phosphatidylinositol 3-kinase/nuclear factor-κB signaling pathway in FRTL thyroid cells. Acta Pharmacologica Sinica 30, 113–119. https://doi.org/10.1038/aps.2008.8

Renehan, A.G., Zwahlen, M., Minder, C., O'Dwyer, S.T., Shalet, S.M., Egger, M., 2004. Insulin-like growth factor (IGF)-I, IGF binding protein-3, and cancer risk: systematic review and meta-regression analysis. The Lancet 363, 1346–1353. https://doi.org/10.1016/S0140-6736(04)16044-3

Resnicoff, M., Coppola, D., Sell, C., Rubin, R., Ferrone, S., Baserga, R., 1994. Growth Inhibition of Human Melanoma Cells in Nude Mice by Antisense Strategies to the Type 1 Insulin-like Growth Factor Receptor. Cancer Res 54, 4848.

Riballo, E., Kühne, M., Rief, N., Doherty, A., Smith, G.C.M., Recio, M.-J., Reis, C., Dahm, K., Fricke, A., Krempler, A., Parker, A.R., Jackson, S.P., Gennery, A., Jeggo, P.A., Löbrich, M., 2004. A Pathway of Double-Strand Break Rejoining Dependent upon ATM, Artemis, and Proteins Locating to γ-H2AX Foci. Molecular Cell 16, 715–724. https://doi.org/10.1016/j.molcel.2004.10.029

Ribeiro, T.C., Jorge, A.A., Almeida, M.Q., Mariani, B.M. de P., Nishi, M.Y., Mendonca, B.B., Fragoso, M.C.B.V., Latronico, A.C., 2014. Amplification of the insulin-like growth factor 1 receptor gene is a rare event in adrenocortical adenocarcinomas: searching for potential mechanisms of overexpression. Biomed Res Int 2014, 936031–936031. https://doi.org/10.1155/2014/936031

Richardson, C., Jasin, M., 2000. Frequent chromosomal translocations induced by DNA double-strand breaks. Nature 405, 697–700. https://doi.org/10.1038/35015097

Richardson, C.D., Ray, G.J., DeWitt, M.A., Curie, G.L., Corn, J.E., 2016. Enhancing homology-directed genome editing by catalytically active and inactive CRISPR-Cas9 using asymmetric donor DNA. Nature Biotechnology 34, 339–344. https://doi.org/10.1038/nbt.3481

Riedemann, J., Macaulay, V.M., 2006. IGF1R signalling and its inhibition. Endocrine-Related Cancer Endocr Relat Cancer 13, S33–S43. https://doi.org/10.1677/erc.1.01280

Riedl, A., Schlederer, M., Pudelko, K., Stadler, M., Walter, S., Unterleuthner, D., Unger, C., Kramer, N., Hengstschläger, M., Kenner, L., Pfeiffer, D., Krupitza, G., Dolznig, H., 2017. Comparison of cancer cells in 2D vs 3D culture reveals differences in AKT–mTOR–S6K signaling and drug responses. Journal of Cell Science 130, 203–218. https://doi.org/10.1242/jcs.188102

Rieger, L., O'Connor, R., 2021. Controlled Signaling-Insulin-Like Growth Factor Receptor Endocytosis and Presence at Intracellular Compartments. Front Endocrinol (Lausanne) 11, 620013–620013. https://doi.org/10.3389/fendo.2020.620013

Rieger, L., O'Shea Sandra, Godsmark Grant, Stanicka Joanna, Kelly Geraldine, O'Connor Rosemary, 2020. IGF-1 receptor activity in the Golgi of migratory cancer cells depends on adhesion-dependent phosphorylation of Tyr1250 and Tyr1251. Science Signaling 13, eaba3176. https://doi.org/10.1126/scisignal.aba3176

Rieunier, G., Wu, X., Harris, L.E., Mills, J.V., Nandakumar, A., Colling, L., Seraia, E., Hatch, S.B., Ebner, D.V., Folkes, L.K., Weyer-Czernilofsky, U., Bogenrieder, T., Ryan, A.J., Macaulay, V.M., 2021. Targeting IGF Perturbs Global Replication through Ribonucleotide Reductase Dysfunction. Cancer Res 81, 2128. https://doi.org/10.1158/0008-5472.CAN-20-2860

Riffle, S., Pandey, R.N., Albert, M., Hegde, R.S., 2017. Linking hypoxia, DNA damage and proliferation in multicellular tumor spheroids. BMC Cancer 17, 338–338. https://doi.org/10.1186/s12885-017-3319-0

Rochester, M.A., Riedemann, J., Hellawell, G.O., Brewster, S.F., Macaulay, V.M., 2005. Silencing of the IGF1R gene enhances sensitivity to DNA-damaging agents in both PTEN wild-type and mutant human prostate cancer. Cancer Gene Therapy 12, 90–100. https://doi.org/10.1038/sj.cgt.7700775

Rodgers, J.T., Lerin, C., Haas, W., Gygi, S.P., Spiegelman, B.M., Puigserver, P., 2005. Nutrient control of glucose homeostasis through a complex of PGC-1α and SIRT1. Nature 434, 113–118. https://doi.org/10.1038/nature03354

Rose, J.C., Popp, N.A., Richardson, C.D., Stephany, J.J., Mathieu, J., Wei, C.T., Corn, J.E., Maly, D.J., Fowler, D.M., 2020. Suppression of unwanted CRISPR-Cas9 editing by co-administration of catalytically inactivating truncated guide RNAs. Nature Communications 11, 2697. https://doi.org/10.1038/s41467-020-16542-9

Rosenfeld, R.G., 2005. The molecular basis of idiopathic short stature. Growth Hormone & IGF Research 15, 3–5. https://doi.org/10.1016/j.ghir.2005.06.014

Rosenthal, S.M., Cheng, Z.Q., 1995. Opposing early and late effects of insulin-like growth factor I on differentiation and the cell cycle regulatory retinoblastoma protein in skeletal myoblasts. Proc Natl Acad Sci U S A 92, 10307–10311. https://doi.org/10.1073/pnas.92.22.10307

Rota, L.M., Wood, T.L., 2015. Crosstalk of the Insulin-Like Growth Factor Receptor with the Wnt Signaling Pathway in Breast Cancer. Front Endocrinol (Lausanne) 6, 92–92. https://doi.org/10.3389/fendo.2015.00092

Rothkamm, K., Löbrich, M., 2003. Evidence for a lack of DNA double-strand break repair in human cells exposed to very low x-ray doses. PNAS 100, 5057–5062. https://doi.org/10.1073/pnas.0830918100

Rouet, P., Smih, F., Jasin, M., 1994a. Expression of a site-specific endonuclease stimulates homologous recombination in mammalian cells. Proc Natl Acad Sci USA 91, 6064. https://doi.org/10.1073/pnas.91.13.6064

Rouet, P., Smih, F., Jasin, M., 1994b. Introduction of double-strand breaks into the genome of mouse cells by expression of a rare-cutting endonuclease. Mol Cell Biol 14, 8096–8106. https://doi.org/10.1128/mcb.14.12.8096

Rubini, M., D'Ambrosio, C., Carturan, S., Yumet, G., Catalano, E., Shan, S., Huang, Z., Criscuolo, M., Pifferi, M., Baserga, R., 1999. Characterization of an Antibody That Can Detect an Activated IGF-I Receptor in Human Cancers. Experimental Cell Research 251, 22–32. https://doi.org/10.1006/excr.1999.4562

Ruderman, N.B., Julia Xu, X., Nelson, L., Cacicedo, J.M., Saha, A.K., Lan, F., Ido, Y., 2010. AMPK and SIRT1: a long-standing partnership? American Journal of Physiology-Endocrinology and Metabolism 298, E751–E760. https://doi.org/10.1152/ajpendo.00745.2009

Rudin, N., Sugarman, E., Haber, J.E., 1989. Genetic and physical analysis of double-strand break repair and recombination in Saccharomyces cerevisiae. Genetics 122, 519–534.

Ryan, C.J., Smith, M.R., Fizazi, K., Saad, F., Mulders, P.F.A., Sternberg, C.N., Miller, K., Logothetis, C.J., Shore, N.D., Small, E.J., Carles, J., Flaig, T.W., Taplin, M.-E., Higano, C.S., de Souza, P., de Bono, J.S., Griffin, T.W., De Porre, P., Yu, M.K., Park, Y.C., Li, J., Kheoh, T., Naini, V., Molina, A., Rathkopf, D.E., 2015. Abiraterone acetate plus prednisone versus placebo plus prednisone in chemotherapy-naive men with metastatic castration-resistant prostate cancer (COU-AA-302): final overall survival analysis of a randomised, double-blind, placebo-controlled phase 3 study. The Lancet Oncology 16, 152–160. https://doi.org/10.1016/S1470-2045(14)71205-7

Ryu, J.M., Lee, M.Y., Yun, S.P., Han, H.J., 2010. High glucose regulates cyclin D1/E of human mesenchymal stem cells through TGF-β1 expression via Ca2+/PKC/MAPKs and PI3K/Akt/mTOR signal pathways. Journal of Cellular Physiology 224, 59–70. https://doi.org/10.1002/jcp.22091

Sabio, G., Davis, R.J., 2014. TNF and MAP kinase signalling pathways. Semin Immunol 26, 237–245. https://doi.org/10.1016/j.smim.2014.02.009

Sachdev, D., Singh, R., Fujita-Yamaguchi, Y., Yee, D., 2006. Down-regulation of Insulin Receptor by Antibodies against the Type I Insulin-Like Growth Factor Receptor: Implications for Anti–Insulin-Like Growth Factor Therapy in Breast Cancer. Cancer Res 66, 2391. https://doi.org/10.1158/0008-5472.CAN-05-3126

Sak, M.S., R. Wurm, V. Budach, A., 2000. Protection of DNA from radiation-induced double-strand breaks: influence of replication and nuclear proteins. International Journal of Radiation Biology 76, 749–756. https://doi.org/10.1080/09553000050028896

Salani, B., Passalacqua, M., Maffioli, S., Briatore, L., Hamoudane, M., Contini, P., Cordera, R., Maggi, D., 2010. IGF-IR Internalizes with Caveolin-1 and PTRF/Cavin in Hacat Cells. PLOS ONE 5, e14157. https://doi.org/10.1371/journal.pone.0014157

Salesse, S., Verfaillie, C.M., 2002. BCR/ABL: from molecular mechanisms of leukemia induction to treatment of chronic myelogenous leukemia. Oncogene 21, 8547–8559. https://doi.org/10.1038/sj.onc.1206082

Sallmyr, A., Tomkinson, A.E., 2018. Repair of DNA double-strand breaks by mammalian alternative end-joining pathways. J Biol Chem 293, 10536–10546. https://doi.org/10.1074/jbc.TM117.000375

Salvador Moreno, N., Liu, J., Haas, K.M., Parker, L.L., Chakraborty, C., Kron, S.J., Hodges, K., Miller, L.D., Langefeld, C., Robinson, P.J., Lelièvre, S.A., Vidi, P.-A., 2019. The nuclear structural protein NuMA is a negative regulator of 53BP1 in DNA double-strand break repair. Nucleic Acids Research 47, 2703–2715. https://doi.org/10.1093/nar/gkz138

Sancak, Y., Thoreen, C.C., Peterson, T.R., Lindquist, R.A., Kang, S.A., Spooner, E., Carr, S.A., Sabatini, D.M., 2007. PRAS40 Is an Insulin-Regulated Inhibitor of the mTORC1 Protein Kinase. Molecular Cell 25, 903–915. https://doi.org/10.1016/j.molcel.2007.03.003

Sansone, L., Reali, V., Pellegrini, L., Villanova, L., Aventaggiato, M., Marfe, G., Rosa, R., Nebbioso, M., Tafani, M., Fini, M., Russo, M.A., Pucci, B., 2013. SIRT1 silencing confers neuroprotection through IGF-1 pathway activation. Journal of Cellular Physiology 228, 1754–1761. https://doi.org/10.1002/jcp.24334

Santosh, V., Arivazhagan, A., Sreekanthreddy, P., Srinivasan, H., Thota, B., Srividya, M.R., Vrinda, M., Sridevi, S., Shailaja, B.C., Samuel, C., Prasanna, K.V., Thennarasu, K., Balasubramaniam, A., Chandramouli, B.A., Hegde, A.S., Somasundaram, K., Kondaiah, P., Rao, M.R.S., 2010. Grade-Specific Expression of Insulin-like Growth Factor–Binding Proteins-2, -3, and -5 in Astrocytomas: IGFBP-3 Emerges as a Strong Predictor of Survival in

Patients with Newly Diagnosed Glioblastoma. Cancer Epidemiol Biomarkers Prev 19, 1399. https://doi.org/10.1158/1055-9965.EPI-09-1213

Sapranauskas, R., Gasiunas, G., Fremaux, C., Barrangou, R., Horvath, P., Siksnys, V., 2011. The Streptococcus thermophilus CRISPR/Cas system provides immunity in Escherichia coli. Nucleic Acids Research 39, 9275–9282. https://doi.org/10.1093/nar/gkr606

Sarbassov, D.D., Guertin, D.A., Ali, S.M., Sabatini, D.M., 2005. Phosphorylation and Regulation of Akt/PKB by the Rictor-mTOR Complex. Science 307, 1098. https://doi.org/10.1126/science.1106148

Sarfstein, R., Friedman, Y., Attias-Geva, Z., Fishman, A., Bruchim, I., Werner, H., 2013. Metformin downregulates the insulin/IGF-I signaling pathway and inhibits different uterine serous carcinoma (USC) cells proliferation and migration in p53-dependent or -independent manners. PLoS One 8, e61537–e61537. https://doi.org/10.1371/journal.pone.0061537

Sarkar, P.L., Lee, W., Williams, E.D., Lubik, A.A., Stylianou, N., Shokoohmand, A., Lehman, M.L., Hollier, B.G., Gunter, J.H., Nelson, C.C., 2019. Insulin Enhances Migration and Invasion in Prostate Cancer Cells by Up-Regulation of FOXC2. Frontiers in Endocrinology 10.

Sasaki, T., Maier, B., Koclega, K.D., Chruszcz, M., Gluba, W., Stukenberg, P.T., Minor, W., Scrable, H., 2008. Phosphorylation regulates SIRT1 function. PLoS One 3, e4020–e4020. https://doi.org/10.1371/journal.pone.0004020

Sassone-Corsi, P., Mizzen Craig A., Cheung Peter, Crosio Claudia, Monaco Lucia, Jacquot Sylvie, Hanauer André, Allis C. David, 1999. Requirement of Rsk-2 for Epidermal Growth Factor-Activated Phosphorylation of Histone H3. Science 285, 886–891. https://doi.org/10.1126/science.285.5429.886

Savitsky, K., Bar-Shira, A., Gilad, S., Rotman, G., Ziv, Y., Vanagaite, L., Tagle, D., Smith, S., Uziel, T., Sfez, S., al., et, 1995. A single ataxia telangiectasia gene with a product similar to PI-3 kinase. Science 268, 1749. https://doi.org/10.1126/science.7792600

Savkur, R.S., Philips, A.V., Cooper, T.A., Dalton, J.C., Moseley, M.L., Ranum, L.P.W., Day, J.W., 2004. Insulin Receptor Splicing Alteration in Myotonic Dystrophy Type 2. The American Journal of Human Genetics 74, 1309–1313. https://doi.org/10.1086/421528

Saxton, R.A., Sabatini, D.M., 2017. mTOR Signaling in Growth, Metabolism, and Disease. Cell 168, 960–976. https://doi.org/10.1016/j.cell.2017.02.004

Scarth, J.P., 2006. Modulation of the growth hormone–insulin-like growth factor (GH–IGF) axis by pharmaceutical, nutraceutical and environmental xenobiotics: An emerging role for xenobiotic-metabolizing enzymes and the transcription factors regulating their expression. A review. Xenobiotica 36, 119–218. https://doi.org/10.1080/00498250600621627

Schaeffer, E.M., Marchionni, L., Huang, Z., Simons, B., Blackman, A., Yu, W., Parmigiani, G., Berman, D.M., 2008. Androgen-induced programs for prostate epithelial growth and invasion arise in embryogenesis and are reactivated in cancer. Oncogene 27, 7180–7191. https://doi.org/10.1038/onc.2008.327

Schedlich, L.J., Young, T.F., Firth, S.M., Baxter, R.C., 1998. Insulin-like Growth Factor-binding Protein (IGFBP)-3 and IGFBP-5 Share a Common Nuclear Transport Pathway in T47D Human Breast Carcinoma Cells. Journal of Biological Chemistry 273, 18347–18352. https://doi.org/10.1074/jbc.273.29.18347

Schmid, J.A., Berti, M., Walser, F., Raso, M.C., Schmid, F., Krietsch, J., Stoy, H., Zwicky, K., Ursich, S., Freire, R., Lopes, M., Penengo, L., 2018. Histone Ubiquitination by the DNA Damage Response Is Required for Efficient DNA Replication in Unperturbed S Phase. Molecular Cell 71, 897-910.e8. https://doi.org/10.1016/j.molcel.2018.07.011

Schmid, P., Sablin, M.-P., Bergh, J., Im, S.-A., Lu, Y.-S., Martínez, N., Neven, P., Lee, K.S., Morales, S., Pérez-Fidalgo, J.A., Adamson, D., Gonçalves, A., Prat, A., Jerusalem, G., Schlieker, L., Espadero, R.-M., Bogenrieder, T., Huang, D.C.-L., Crown, J., Cortés, J., 2021. A phase Ib/II study of xentuzumab, an IGF-neutralising antibody, combined with exemestane and everolimus in hormone receptor-positive, HER2-negative locally advanced/metastatic breast cancer. Breast Cancer Res 23, 8–8. https://doi.org/10.1186/s13058-020-01382-8

Schoenfeld, A.R., Apgar, S., Dolios, G., Wang, R., Aaronson, S.A., 2004. BRCA2 is ubiquitinated in vivo and interacts with USP11, a deubiquitinating enzyme that exhibits prosurvival function in the cellular response to DNA damage. Mol Cell Biol 24, 7444–7455. https://doi.org/10.1128/MCB.24.17.7444-7455.2004

Sciacca, L., Costantino, A., Pandini, G., Mineo, R., Frasca, F., Scalia, P., Sbraccia, P., Goldfine, I.D., Vigneri, R., Belfiore, A., 1999. Insulin receptor activation by IGF-II in breast cancers: evidence for a new autocrine/paracrine mechanism. Oncogene 18, 2471–2479. https://doi.org/10.1038/sj.onc.1202600

Sciacca, L., Prisco, M., Wu, A., Belfiore, A., Vigneri, R., Baserga, R., 2003. Signaling Differences from the A and B Isoforms of the Insulin Receptor (IR) in 32D Cells in the Presence or Absence of IR Substrate-1. Endocrinology 144, 2650–2658. https://doi.org/10.1210/en.2002-0136

Sebastiano, V., Maeder, M.L., Angstman, J.F., Haddad, B., Khayter, C., Yeo, D.T., Goodwin, M.J., Hawkins, J.S., Ramirez, C.L., Batista, L.F.Z., Artandi, S.E., Wernig, M., Joung, J.K., 2011. In Situ Genetic Correction of the Sickle Cell Anemia Mutation in Human Induced Pluripotent Stem Cells Using Engineered Zinc Finger Nucleases. STEM CELLS 29, 1717–1726. https://doi.org/10.1002/stem.718

Sedelnikova, O.A., Rogakou, E.P., Panyutin, I.G., Bonner, W.M., 2002. Quantitative Detection of 125IdU-Induced DNA Double-Strand Breaks with γ-H2AX Antibody. Radiation Research 158, 486–492. https://doi.org/10.1667/0033-7587(2002)158[0486:QDOIID]2.0.CO;2

Segal, M., Niazi, S., Simons, M.P., Galati, S.A., Zangrilli, J.G., 2007. Bid activation during induction of extrinsic and intrinsic apoptosis in eosinophils. Immunology & Cell Biology 85, 518–524. https://doi.org/10.1038/sj.icb.7100075

Sehat, B., Andersson, S., Vasilcanu, R., Girnita, L., Larsson, O., 2007. Role of ubiquitination in IGF-1 receptor signaling and degradation. PLoS One 2, e340–e340. https://doi.org/10.1371/journal.pone.0000340

Sehat, B., Tofigh, A., Lin, Y., Trocmé, E., Liljedahl, U., Lagergren, J., Larsson, O., 2010. SUMOylation Mediates the Nuclear Translocation and Signaling of the IGF-1 Receptor. Sci. Signal. 3, ra10. https://doi.org/10.1126/scisignal.2000628

Sell, C., Dumenil, G., Deveaud, C., Miura, M., Coppola, D., DeAngelis, T., Rubin, R., Efstratiadis, A., Baserga, R., 1994. Effect of a null mutation of the insulin-like growth factor I receptor gene on growth and transformation of mouse embryo fibroblasts. Mol Cell Biol 14, 3604–3612. https://doi.org/10.1128/mcb.14.6.3604

Seto, E., Yoshida, M., 2014. Erasers of histone acetylation: the histone deacetylase enzymes. Cold Spring Harb Perspect Biol 6, a018713–a018713. https://doi.org/10.1101/cshperspect.a018713

Seyfried, T.N., Flores, R.E., Poff, A.M., D'Agostino, D.P., 2013. Cancer as a metabolic disease: implications for novel therapeutics. Carcinogenesis 35, 515–527. https://doi.org/10.1093/carcin/bgt480

Sfeir, A., Symington, L.S., 2015. Microhomology-Mediated End Joining: A Back-up Survival Mechanism or Dedicated Pathway? Trends Biochem Sci 40, 701–714. https://doi.org/10.1016/j.tibs.2015.08.006

Shah, P., Zhao, B., Qiang, L., He, Y.-Y., 2018. Phosphorylation of xeroderma pigmentosum group C regulates ultraviolet-induced DNA damage repair. Nucleic Acids Research 46, 5050–5060. https://doi.org/10.1093/nar/gky239

Shang, Y., Myers, M., Brown, M., 2002. Formation of the Androgen Receptor Transcription Complex. Molecular Cell 9, 601–610. https://doi.org/10.1016/S1097-2765(02)00471-9

Shanware, N.P., Bray, K., Eng, C.H., Wang, F., Follettie, M., Myers, J., Fantin, V.R., Abraham, R.T., 2014. Glutamine deprivation stimulates mTOR-JNK-dependent chemokine secretion. Nature Communications 5, 4900. https://doi.org/10.1038/ncomms5900

Sharda, N., Yang, C.-R., Kinsella, T., Boothman, D., 2002. Radiation Resistance, in: Bertino, J.R. (Ed.), Encyclopedia of Cancer (Second Edition). Academic Press, New York, pp. 1–11. https://doi.org/10.1016/B0-12-227555-1/00519-0

Sharma, R.A., Plummer, R., Stock, J.K., Greenhalgh, T.A., Ataman, O., Kelly, S., Clay, R., Adams, R.A., Baird, R.D., Billingham, L., Brown, S.R., Buckland, S., Bulbeck, H., Chalmers, A.J., Clack, G., Cranston, A.N., Damstrup, L., Ferraldeschi, R., Forster, M.D., Golec, J., Hagan, R.M., Hall, E., Hanauske, A.-R., Harrington, K.J., Haswell, T., Hawkins, M.A., Illidge, T., Jones, H., Kennedy, A.S., McDonald, F., Melcher, T., O'Connor, J.P.B., Pollard, J.R., Saunders, M.P., Sebag-Montefiore, D., Smitt, M., Staffurth, J., Stratford, I.J., Wedge, S.R.,

on behalf of the NCRI CTRad Academia-Pharma Joint Working Group, 2016. Clinical development of new drug–radiotherapy combinations. Nature Reviews Clinical Oncology 13, 627–642. https://doi.org/10.1038/nrclinonc.2016.79

Sharma, S., Javadekar, S.M., Pandey, M., Srivastava, M., Kumari, R., Raghavan, S.C., 2015. Homology and enzymatic requirements of microhomology-dependent alternative end joining. Cell Death Dis 6, e1697–e1697. https://doi.org/10.1038/cddis.2015.58

Shay, J.W., 2016. Role of Telomeres and Telomerase in Aging and Cancer. Cancer Discov 6, 584. https://doi.org/10.1158/2159-8290.CD-16-0062

Shechner, D.M., Hacisuleyman, E., Younger, S.T., Rinn, J.L., 2015. Multiplexable, locus-specific targeting of long RNAs with CRISPR-Display. Nature Methods 12, 664–670. https://doi.org/10.1038/nmeth.3433

Shenoy, T.R., Boysen, G., Wang, M.Y., Xu, Q.Z., Guo, W., Koh, F.M., Wang, C., Zhang, L.Z., Wang, Y., Gil, V., Aziz, S., Christova, R., Rodrigues, D.N., Crespo, M., Rescigno, P., Tunariu, N., Riisnaes, R., Zafeiriou, Z., Flohr, P., Yuan, W., Knight, E., Swain, A., Ramalho-Santos, M., Xu, D.Y., de Bono, J., Wu, H., 2017. CHD1 loss sensitizes prostate cancer to DNA damaging therapy by promoting error-prone double-strand break repair. Ann Oncol 28, 1495–1507. https://doi.org/10.1093/annonc/mdx165

Sherr, C.J., 2004. Principles of Tumor Suppression. Cell 116, 235–246. https://doi.org/10.1016/S0092-8674(03)01075-4

Sherr, C.J., McCormick, F., 2002. The RB and p53 pathways in cancer. Cancer Cell 2, 103–112. https://doi.org/10.1016/S1535-6108(02)00102-2

Sherr, C.J., Roberts, J.M., 1999. CDK inhibitors: positive and negative regulators of G1-phase progression. Genes & Development 13, 1501–1512.

Shigematsu, H., Imasaki, T., Doki, C., Sumi, T., Aoki, M., Uchikubo-Kamo, T., Sakamoto, A., Tokuraku, K., Shirouzu, M., Nitta, R., 2018. Structural insight into microtubule stabilization and kinesin inhibition by Tau family MAPs. J Cell Biol 217, 4155–4163. https://doi.org/10.1083/jcb.201711182

Shimasaki, S., Ling, N., 1991. Identification and molecular characterization of insulin-like growth factor binding proteins (IGFBP-1, -2, -3, -4, -5 and -6). Progress in growth factor research 3, 243–266. https://doi.org/10.1016/0955-2235(91)90003-m

Shiotani, B., Zou, L., 2009. Single-stranded DNA orchestrates an ATM-to-ATR switch at DNA breaks. Mol Cell 33, 547–558. https://doi.org/10.1016/j.molcel.2009.01.024

Showkat, M., Beigh, M.A., Andrabi, K.I., 2014. mTOR Signaling in Protein Translation Regulation: Implications in Cancer Genesis and Therapeutic Interventions. Molecular Biology International 2014, 686984. https://doi.org/10.1155/2014/686984

Shtivelman, E., Lifshitz, B., Gale, R.P., Canaani, E., 1985. Fused transcript of abl and bcr genes in chronic myelogenous leukaemia. Nature 315, 550–554. https://doi.org/10.1038/315550a0

Siemeister, G., Al-Hasani, H., Klein, H.W., Kellner, S., Streicher, R., Krone, W., Müller-Wieland, D., 1995. Recombinant Human Insulin Receptor Substrate-1 Protein: TYROSINE PHOSPHORYLATION AND IN VITRO BINDING OF INSULIN RECEPTOR KINASE. Journal of Biological Chemistry 270, 4870–4874. https://doi.org/10.1074/jbc.270.9.4870

Sigoillot, F.D., King, R.W., 2011. Vigilance and validation: Keys to success in RNAi screening. ACS Chem Biol 6, 47–60. https://doi.org/10.1021/cb100358f

Simpson, A., Petnga, W., Macaulay, V.M., Weyer-Czernilofsky, U., Bogenrieder, T., 2017. Insulin-Like Growth Factor (IGF) Pathway Targeting in Cancer: Role of the IGF Axis and Opportunities for Future Combination Studies. Target Oncol 12, 571–597. https://doi.org/10.1007/s11523-017-0514-5

Simpson, A.D., Soo, Y.W.J., Rieunier, G., Aleksic, T., Ansorge, O., Jones, C., Macaulay, V.M., 2020. Type 1 IGF receptor associates with adverse outcome and cellular radioresistance in paediatric high-grade glioma. British Journal of Cancer 122, 624–629. https://doi.org/10.1038/s41416-019-0677-1

Simsek, D., Jasin, M., 2010. Alternative end-joining is suppressed by the canonical NHEJ component Xrcc4-ligase IV during chromosomal translocation formation. Nat Struct Mol Biol 17, 410–416. https://doi.org/10.1038/nsmb.1773

Singh, S., Khar, A., 2006. Activation of NFκB and Ub-proteasome pathway during apoptosis induced by a serum factor is mediated through the upregulation of the 26S proteasome subunits. Apoptosis 11, 845–859. https://doi.org/10.1007/s10495-006-5878-4

Singleton, B.K., Torres-Arzayus, M.I., Rottinghaus, S.T., Taccioli, G.E., Jeggo, P.A., 1999. The C terminus of Ku80 activates the DNA-dependent protein kinase catalytic subunit. Mol Cell Biol 19, 3267–3277. https://doi.org/10.1128/MCB.19.5.3267

Sivakumar, R., Koga, H., Selvendiran, K., Maeyama, M., Ueno, T., Sata, M., 2009. Autocrine loop for IGF-I receptor signaling in SLUG-mediated epithelial-mesenchymal transition. Int J Oncol 34, 329–338. https://doi.org/10.3892/ijo_00000155

Sizemore, S.T., Zhang, M., Cho, J.H., Sizemore, G.M., Hurwitz, B., Kaur, B., Lehman, N.L., Ostrowski, M.C., Robe, P.A., Miao, W., Wang, Y., Chakravarti, A., Xia, F., 2018. Pyruvate kinase M2 regulates homologous recombination-mediated DNA double-strand break repair. Cell Res 28, 1090–1102. https://doi.org/10.1038/s41422-018-0086-7

Skwarski, M., McGowan, D.R., Belcher, E., Di Chiara, F., Stavroulias, D., McCole, M., Derham, J.L., Chu, K.-Y., Teoh, E., Chauhan, J., O'Reilly, D., Harris, B.H.L., Macklin, P.S., Bull, J.A., Green, M., Rodriguez-Berriguete, G., Prevo, R., Folkes, L.K., Campo, L., Ferencz, P., Croal, P.L., Flight, H., Qi, C., Holmes, J., O'Connor, J.P.B., Gleeson, F.V., McKenna, W.G., Harris, A.L., Bulte, D., Buffa, F.M., Macpherson, R.E., Higgins, G.S., 2021. Mitochondrial Inhibitor Atovaquone Increases Tumor Oxygenation and Inhibits Hypoxic Gene Expression in Patients with Non–Small Cell Lung Cancer. Clin Cancer Res 27, 2459. https://doi.org/10.1158/1078-0432.CCR-20-4128

Slaaby, R., Schäffer, L., Lautrup-Larsen, I., Andersen, A.S., Shaw, A.C., Mathiasen, I.S., Brandt, J., 2006. Hybrid Receptors Formed by Insulin Receptor (IR) and Insulin-like Growth Factor I Receptor (IGF-IR) Have Low Insulin and High IGF-1 Affinity Irrespective of the IR Splice Variant. Journal of Biological Chemistry 281, 25869–25874. https://doi.org/10.1074/jbc.M605189200

Slijepcevic, P., Natarajan, A., 1994. Distribution of radiation-induced G1 exchange and terminal deletion breakpoints in Chinese hamster chromosomes as detected by G banding. International journal of radiation biology 66, 747–755.

Smith, M.L., Seo, Y.R., 2002. p53 regulation of DNA excision repair pathways. Mutagenesis 17, 149–156. https://doi.org/10.1093/mutage/17.2.149

Smithies, O., Gregg, R.G., Boggs, S.S., Koralewski, M.A., Kucherlapati, R.S., 1985. Insertion of DNA sequences into the human chromosomal β-globin locus by homologous recombination. Nature 317, 230–234. https://doi.org/10.1038/317230a0

Snell, C.E., Turley, H., McIntyre, A., Li, D., Masiero, M., Schofield, C.J., Gatter, K.C., Harris, A.L., Pezzella, F., 2014. Proline-hydroxylated hypoxia-inducible factor 1α (HIF-1α) upregulation in human tumours. PLoS One 9, e88955–e88955. https://doi.org/10.1371/journal.pone.0088955

Snyder, A.R., Morgan, W.F., 2004. Gene expression profiling after irradiation: Clues to understanding acute and persistent responses? Cancer and Metastasis Reviews 23, 259–268. https://doi.org/10.1023/B:CANC.0000031765.17886.fa

Sobhani, N., Roviello, G., Corona, S.P., Scaltriti, M., Ianza, A., Bortul, M., Zanconati, F., Generali, D., 2018. The prognostic value of PI3K mutational status in breast cancer: A meta-analysis. J Cell Biochem 119, 4287–4292. https://doi.org/10.1002/jcb.26687

Solomon-Zemler, R., Sarfstein, R., Werner, H., 2017. Nuclear insulin-like growth factor-1 receptor (IGF1R) displays proliferative and regulatory activities in non-malignant cells. PLoS One 12, e0185164–e0185164. https://doi.org/10.1371/journal.pone.0185164

Song, G., Ouyang, G., Bao, S., 2005. The activation of Akt/PKB signaling pathway and cell survival. J Cell Mol Med 9, 59–71. https://doi.org/10.1111/j.1582-4934.2005.tb00337.x

Song, G., Zhang, S., Tian, M., Zhang, L., Guo, R., Zhuo, W., Yang, M., 2021. Molecular insights into the human ABCB6 transporter. Cell Discov 7, 55–55. https://doi.org/10.1038/s41421-021-00284-z

Soos, M.A., Field, C.E., Siddle, K., 1993. Purified hybrid insulin/insulin-like growth factor-I receptors bind insulin-like growth factor-I, but not insulin, with high affinity. Biochemical Journal 290, 419–426. https://doi.org/10.1042/bj2900419

Sottile, M.L., Nadin, S.B., 2018. Heat shock proteins and DNA repair mechanisms: an updated overview. Cell Stress Chaperones 23, 303–315. https://doi.org/10.1007/s12192-017-0843-4

Spears, M., Cunningham, C., Thomas, J., Kerr, G., Jack, W., Campbell, F., McKay, L., Kunkler, I., Cameron, D., Chetty, U., Bartlett, J., 2009. The Expression of Insulin-Like Growth Factor-1 Receptor (IGF-1R) in Early Breast Cancer. Cancer Res 69, 2128. https://doi.org/10.1158/0008-5472.SABCS-09-2128

Spentzos, D., Cannistra, S.A., Grall, F., Levine, D.A., Pillay, K., Libermann, T.A., Mantzoros, C.S., 2007. IGF axis gene expression patterns are prognostic of survival in epithelial ovarian cancer. Endocrine-Related Cancer Endocr Relat Cancer 14.

Spichal, M., Fabre, E., 2017. The Emerging Role of the Cytoskeleton in Chromosome Dynamics. Front Genet 8, 60–60. https://doi.org/10.3389/fgene.2017.00060

Sramkoski, R.M., Pretlow, T.G., Giaconia, J.M., Pretlow, T.P., Schwartz, S., Sy, M.-S., Marengo, S.R., Rhim, J.S., Zhang, D., Jacobberger, J.W., 1999. A new human prostate carcinoma cell line, 22Rv1. In Vitro Cellular & Developmental Biology - Animal 35, 403–409. https://doi.org/10.1007/s11626-999-0115-4

Stambolic, V., Suzuki, A., de la Pompa, J.L., Brothers, G.M., Mirtsos, C., Sasaki, T., Ruland, J., Penninger, J.M., Siderovski, D.P., Mak, T.W., 1998. Negative Regulation of PKB/Akt-Dependent Cell Survival by the Tumor Suppressor PTEN. Cell 95, 29–39. https://doi.org/10.1016/S0092-8674(00)81780-8

Stamey, T.A., Yang, N., Hay, A.R., McNeal, J.E., Freiha, F.S., Redwine, E., 1987. Prostate-Specific Antigen as a Serum Marker for Adenocarcinoma of the Prostate. N Engl J Med 317, 909–916. https://doi.org/10.1056/NEJM198710083171501

Steigen, S.E., Schaeffer, D.F., West, R.B., Nielsen, T.O., 2009. Expression of insulin-like growth factor 2 in mesenchymal neoplasms. Modern Pathology 22, 914–921. https://doi.org/10.1038/modpathol.2009.48

Sterneck, E., Poria, D.K., Balamurugan, K., 2020. Slug and E-Cadherin: Stealth Accomplices? Frontiers in Molecular Biosciences 7, 138. https://doi.org/10.3389/fmolb.2020.00138

Sterner, D.E., Berger, S.L., 2000. Acetylation of Histones and Transcription-Related Factors. Microbiol. Mol. Biol. Rev. 64, 435. https://doi.org/10.1128/MMBR.64.2.435-459.2000

Steuerman, R., Shevah, O., Laron, Z., 2011. Congenital IGF1 deficiency tends to confer protection against post-natal development of malignancies. European Journal of Endocrinology 164.

Stevenson, L.F., Sparks, A., Allende-Vega, N., Xirodimas, D.P., Lane, D.P., Saville, M.K., 2007. The deubiquitinating enzyme USP2a regulates the p53 pathway by targeting Mdm2. The EMBO Journal 26, 976–986. https://doi.org/10.1038/sj.emboj.7601567

Stewart, G.S., Wang, B., Bignell, C.R., Taylor, A.M.R., Elledge, S.J., 2003. MDC1 is a mediator of the mammalian DNA damage checkpoint. Nature 421, 961–966. https://doi.org/10.1038/nature01446

Stiles, B., Groszer, M., Wang, S., Jiao, J., Wu, H., 2004. PTENless means more. Developmental Biology 273, 175–184. https://doi.org/10.1016/j.ydbio.2004.06.008

Stokoe, D., Stephens, L.R., Copeland, T., Gaffney, P.R.J., Reese, C.B., Painter, G.F., Holmes, A.B., McCormick, F., Hawkins, P.T., 1997. Dual Role of Phosphatidylinositol-3,4,5-trisphosphate in the Activation of Protein Kinase B. Science 277, 567. https://doi.org/10.1126/science.277.5325.567

Stolz, A., Ertych, N., Bastians, H., 2011. Tumor Suppressor CHK2: Regulator of DNA Damage Response and Mediator of Chromosomal Stability. Clin Cancer Res 17, 401. https://doi.org/10.1158/1078-0432.CCR-10-1215

Stone, K.R., Mickey, D.D., Wunderli, H., Mickey, G.H., Paulson, D.F., 1978. Isolation of a human prostate carcinoma cell line (DU 145). Int. J. Cancer 21, 274–81.

Storch, K., Eke, I., Borgmann, K., Krause, M., Richter, C., Becker, K., Schröck, E., Cordes, N., 2010. Three-Dimensional Cell Growth Confers Radioresistance by Chromatin Density Modification. Cancer Res 70, 3925. https://doi.org/10.1158/0008-5472.CAN-09-3848

Strasser-Wozak, E.M., Hartmann, B.L., Geley, S., Sgonc, R., Böck, G., Oliveira Dos Santos, A.J., Hattmannstorfer, R., Wolf, H., Pavelka, M., Kofler, R., 1998. Irradiation induces G2/M cell cycle arrest and apoptosis in p53-deficient lymphoblastic leukemia cells without affecting Bcl-2 and Bax expression. Cell Death & Differentiation 5, 687–693. https://doi.org/10.1038/sj.cdd.4400402

Ström, C.E., Johansson, F., Uhlén, M., Szigyarto, C.A.-K., Erixon, K., Helleday, T., 2011. Poly (ADP-ribose) polymerase (PARP) is not involved in base excision repair but PARP inhibition traps a single-strand intermediate. Nucleic Acids Res 39, 3166–3175. https://doi.org/10.1093/nar/gkq1241

Stronach, E.A., Chen, M., Maginn, E.N., Agarwal, R., Mills, G.B., Wasan, H., Gabra, H., 2011. DNA-PK mediates AKT activation and apoptosis inhibition in clinically acquired platinum resistance. Neoplasia 13, 1069–1080. https://doi.org/10.1593/neo.111032

Strub, T., Ghiraldini, F.G., Carcamo, S., Li, M., Wroblewska, A., Singh, R., Goldberg, M.S., Hasson, D., Wang, Z., Gallagher, S.J., Hersey, P., Ma'ayan, A., Long, G.V., Scolyer, R.A., Brown, B., Zheng, B., Bernstein, E., 2018. SIRT6 haploinsufficiency induces BRAF(V600E) melanoma cell resistance to MAPK inhibitors via IGF signalling. Nat Commun 9, 3440–3440. https://doi.org/10.1038/s41467-018-05966-z

Strumberg, D., Pilon, A.A., Smith, M., Hickey, R., Malkas, L., Pommier, Y., 2000. Conversion of topoisomerase I cleavage complexes on the leading strand of ribosomal DNA into 5'-phosphorylated DNA double-strand breaks by replication runoff. Mol Cell Biol 20, 3977–3987. https://doi.org/10.1128/MCB.20.11.3977-3987.2000

Sudarsanam, S., Johnson, D., 2010. Functional consequences of mTOR inhibition. Current opinion in drug discovery & development 13, 31–40.

Sui, J., Lin, Y.-F., Xu, K., Lee, K.-J., Wang, D., Chen, B.P.C., 2015. DNA-PKcs phosphorylates hnRNP-A1 to facilitate the RPA-to-POT1 switch and telomere capping after replication. Nucleic Acids Res 43, 5971–5983. https://doi.org/10.1093/nar/gkv539

Sui, J., Zhang, S., Chen, B.P.C., 2020. DNA–dependent protein kinase in telomere maintenance and protection. Cellular & Molecular Biology Letters 25, 2. https://doi.org/10.1186/s11658-020-0199-0

Sulkowski, P.L., Sundaram, R.K., Oeck, S., Corso, C.D., Liu, Y., Noorbakhsh, S., Niger, M., Boeke, M., Ueno, D., Kalathil, A.N., Bao, X., Li, J., Shuch, B., Bindra, R.S., Glazer, P.M., 2018. Krebs-cycle-deficient hereditary cancer syndromes are defined by defects in homologous-recombination DNA repair. Nat Genet 50, 1086–1092. https://doi.org/10.1038/s41588-018-0170-4

Sullivan, L.B., Gui, D.Y., Heiden, M.G.V., 2016. Altered metabolite levels in cancer: implications for tumour biology and cancer therapy. Nature Reviews Cancer 16, 680–693. https://doi.org/10.1038/nrc.2016.85

Sullivan, M.R., Bernstein, K.A., 2018. RAD-ical New Insights into RAD51 Regulation. Genes (Basel) 9, 629. https://doi.org/10.3390/genes9120629

Sun, L.Y., D'Ercole, A.J., 2006. Insulin-Like Growth Factor-I Stimulates Histone H3 and H4 Acetylation in the Brain in Vivo. Endocrinology 147, 5480–5490. https://doi.org/10.1210/en.2006-0586

Sun, X.-X., Sears, R.C., Dai, M.-S., 2015. Deubiquitinating c-Myc: USP36 steps up in the nucleolus. Cell Cycle 14, 3786–3793. https://doi.org/10.1080/15384101.2015.1093713

Sun, Y., Jiang, X., Chen, S., Fernandes, N., Price, B.D., 2005. A role for the Tip60 histone acetyltransferase in the acetylation and activation of ATM. Proc Natl Acad Sci U S A 102, 13182. https://doi.org/10.1073/pnas.0504211102

Sun, Y., Jiang, X., Price, B.D., 2010. Tip60: Connecting chromatin to DNA damage signaling. Cell Cycle 9, 930–936. https://doi.org/10.4161/cc.9.5.10931

Sun, Y., Jiang, X., Xu, Y., Ayrapetov, M.K., Moreau, L.A., Whetstine, J.R., Price, B.D., 2009. Histone H3 methylation links DNA damage detection to activation of the tumour suppressor Tip60. Nature Cell Biology 11, 1376–1382. https://doi.org/10.1038/ncb1982

Sun, Y., Xu, Y., Roy, K., Price, B.D., 2007. DNA Damage-Induced Acetylation of Lysine 3016 of ATM Activates ATM Kinase Activity. Mol. Cell. Biol. 27, 8502. https://doi.org/10.1128/MCB.01382-07

Sundaresan, N.R., Vasudevan, P., Zhong, L., Kim, G., Samant, S., Parekh, V., Pillai, V.B., Ravindra, P.V., Gupta, M., Jeevanandam, V., Cunningham, J.M., Deng, C.-X., Lombard, D.B., Mostoslavsky, R., Gupta, M.P., 2012. The sirtuin SIRT6 blocks IGF-Akt signaling and development of cardiac hypertrophy by targeting c-Jun. Nature Medicine 18, 1643–1650. https://doi.org/10.1038/nm.2961

Swietach, P., Patiar, S., Supuran, C.T., Harris, A.L., Vaughan-Jones, R.D., 2009. The role of carbonic anhydrase 9 in regulating extracellular and intracellular ph in three-dimensional tumor cell growths. J Biol Chem 284, 20299–20310. https://doi.org/10.1074/jbc.M109.006478

Symington, L.S., Gautier, J., 2011. Double-Strand Break End Resection and Repair Pathway Choice. Annu. Rev. Genet. 45, 247–271. https://doi.org/10.1146/annurev-genet-110410-132435

Synthego Performance Analysis, ICE Analysis. 2019. v2.0. Synthego, n.d. , Synthego Performance Analysis.

Szklarczyk, D., Gable, A.L., Lyon, D., Junge, A., Wyder, S., Huerta-Cepas, J., Simonovic, M., Doncheva, N.T., Morris, J.H., Bork, P., Jensen, L.J., Mering, C. von, 2018. STRING v11: protein–protein association networks with increased coverage, supporting functional discovery in genome-wide experimental datasets. Nucleic Acids Research 47, D607–D613. https://doi.org/10.1093/nar/gky1131

Taccioli, G., Gottlieb, T., Blunt, T., Priestley, A., Demengeot, J., Mizuta, R., Lehmann, A., Alt, F., Jackson, S., Jeggo, P., 1994. Ku80: product of the XRCC5 gene and its role in DNA repair and V(D)J recombination. Science 265, 1442. https://doi.org/10.1126/science.8073286

Tailor, T.D., Hanna, G., Yarmolenko, P.S., Dreher, M.R., Betof, A.S., Nixon, A.B., Spasojevic, I., Dewhirst, M.W., 2010. Effect of pazopanib on tumor microenvironment and liposome delivery. Mol Cancer Ther 9, 1798–1808. https://doi.org/10.1158/1535-7163.MCT-09-0856

Takahari, D., Yamada, Y., Okita, N.T., Honda, T., Hirashima, Y., Matsubara, J., Takashima, A., Kato, K., Hamaguchi, T., Shirao, K., Shimada, Y., Shimoda, T., 2009. Relationships of Insulin-Like Growth Factor-1 Receptor and Epidermal Growth Factor Receptor Expression to Clinical Outcomes in Patients with Colorectal Cancer. Oncology 76, 42–48. https://doi.org/10.1159/000178164

Takahashi, Y., Tobe, K., Kadowaki, H., Katsumata, D., Fukushima, Y., Yazaki, Y., Akanuma, Y., Kadowaki, T., 1997. Roles of Insulin Receptor Substrate-1 and Shc on Insulin-Like Growth Factor I Receptor Signaling in Early Passages of Cultured Human Fibroblasts. Endocrinology 138, 741–750. https://doi.org/10.1210/endo.138.2.4910

Takano, A., Usui, I., Haruta, T., Kawahara, J., Uno, T., Iwata, M., Kobayashi, M., 2001. Mammalian Target of Rapamycin Pathway Regulates Insulin Signaling via Subcellular Redistribution of Insulin Receptor Substrate 1 and Integrates Nutritional Signals and Metabolic Signals of Insulin. Mol. Cell. Biol. 21, 5050. https://doi.org/10.1128/MCB.21.15.5050-5062.2001

Takata, H., Hanafusa, T., Mori, T., Shimura, M., Iida, Y., Ishikawa, K., Yoshikawa, K., Yoshikawa, Y., Maeshima, K., 2013. Chromatin Compaction Protects Genomic DNA from Radiation Damage. PLOS ONE 8, e75622. https://doi.org/10.1371/journal.pone.0075622

Takayama and Estrada, 2018. The Biological Role of Androgen Receptor in Prostate Cancer Progression, in: Advances in Testosterone Action. IntechOpen, Rijeka, p. Ch. 3. https://doi.org/10.5772/intechopen.76360

Taliaferro-Smith, L., Oberlick, E., Liu, T., McGlothen, T., Alcaide, T., Tobin, R., Donnelly, S., Commander, R., Kline, E., Nagaraju, G.P., Havel, L., Marcus, A., Nahta, R., O'Regan, R., 2015. FAK activation is required for IGF1R-mediated regulation of EMT, migration, and invasion in mesenchymal triple negative breast cancer cells. Oncotarget 6, 4757–4772. https://doi.org/10.18632/oncotarget.3023

Talks, K.L., Turley, H., Gatter, K.C., Maxwell, P.H., Pugh, C.W., Ratcliffe, P.J., Harris, A.L., 2000. The expression and distribution of the hypoxia-inducible factors HIF-1alpha and HIF-2alpha in normal human tissues, cancers, and tumor-associated macrophages. Am J Pathol 157, 411–421. https://doi.org/10.1016/s0002-9440(10)64554-3

Tanaka, T., Huang, X., Halicka, H.D., Zhao, H., Traganos, F., Albino, A.P., Dai, W., Darzynkiewicz, Z., 2007. Cytometry of ATM activation and histone H2AX phosphorylation to estimate extent of DNA damage induced by exogenous agents. Cytometry A 71, 648–661. https://doi.org/10.1002/cyto.a.20426

Tang, B.L., 2006. SIRT1, neuronal cell survival and the insulin/IGF-1 aging paradox. Neurobiology of Aging 27, 501–505. https://doi.org/10.1016/j.neurobiolaging.2005.02.001

Tang, L., Yang, J., Chen, J., Yu, J., Zhou, Q., Lu, X., Wang, Y., 2017. IGF-1R promotes the expression of cyclin D1 protein and accelerates the G1/S transition by activating Ras/Raf/MEK/ERK signaling pathway. Int J Clin Exp Pathol 10, 11652–11658.

Tang, W., Hu, J.H., Liu, D.R., 2017. Aptazyme-embedded guide RNAs enable ligand-responsive genome editing and transcriptional activation. Nature Communications 8, 15939. https://doi.org/10.1038/ncomms15939

Tapon, N., Ito, N., Dickson, B.J., Treisman, J.E., Hariharan, I.K., 2001. The Drosophila Tuberous Sclerosis Complex Gene Homologs Restrict Cell Growth and Cell Proliferation. Cell 105, 345–355. https://doi.org/10.1016/S0092-8674(01)00332-4

Tarry-Adkins, J.L., Aiken, C.E., Ashmore, T.J., Fernandez-Twinn, D.S., Chen, J.-H., Ozanne, S.E., 2019. A suboptimal maternal diet combined with accelerated postnatal growth results in an altered aging profile in the thymus of male rats. The FASEB Journal 33, 239–253. https://doi.org/10.1096/fj.201701350RR

Taylor, A.M.R., Harnden, D.G., Arlett, C.F., Harcourt, S.A., Lehmann, A.R., Stevens, S., Bridges, B.A., 1975. Ataxia telangiectasia: a human mutation with abnormal radiation sensitivity. Nature 258, 427–429. https://doi.org/10.1038/258427a0

Tennagels, N., Werner, U., 2013. The metabolic and mitogenic properties of basal insulin analogues. Arch Physiol Biochem 119, 1–14. https://doi.org/10.3109/13813455.2012.754474

Terada, Y., Inoshita, S., Nakashima, O., Kuwahara, M., Sasaki, S., Marumo, F., 1999. Regulation of cyclin D1 expression and cell cycle progression by mitogen-activated protein kinase cascade. Kidney International 56, 1258–1261. https://doi.org/10.1046/j.1523-1755.1999.00704.x

Tezuka, M., Watanabe, H., Nakamura, S., Yu, D., Aung, W., Sasaki, T., Shibuya, H., Miura, M., 2001a. Antiapoptotic Activity Is Dispensable for Insulin-like Growth Factor I Receptor-mediated Clonogenic Radioresistance after γ-Irradiation. Clin Cancer Res 7, 3206.

Tezuka, M., Watanabe, H., Nakamura, S., Yu, D., Aung, W., Sasaki, T., Shibuya, H., Miura, M., 2001b. Antiapoptotic Activity Is Dispensable for Insulin-like Growth Factor I Receptor-mediated Clonogenic Radioresistance after γ-Irradiation. Clin Cancer Res 7, 3206.

Thomas, K.R., Folger, K.R., Capecchi, M.R., 1986. High frequency targeting of genes to specific sites in the mammalian genome. Cell 44, 419–428. https://doi.org/10.1016/0092-8674(86)90463-0

Thomson, E., Rappsilber, J., Tollervey, D., 2007. Nop9 is an RNA binding protein present in pre-40S ribosomes and required for 18S rRNA synthesis in yeast. RNA 13, 2165–2174. https://doi.org/10.1261/rna.747607

Tichý, A., Muthna, D., Zölzer, F., Vávrová, J., Sinkorova, Z., Pejchal, J., Osterreicher, J., Rezácová, M., 2009. Gamma-Radiation-Induced Phosphorylation of p53 on Serine 15 Is Dose-Dependent in MOLT-4 Leukaemia Cells. Folia biologica 55, 41–4.

Tolcher, A.W., Sarantopoulos, J., Patnaik, A., Papadopoulos, K., Lin, C.-C., Rodon, J., Murphy, B., Roth, B., McCaffery, I., Gorski, K.S., Kaiser, B., Zhu, M., Deng, H., Friberg, G., Puzanov, I., 2009. Phase I, Pharmacokinetic, and Pharmacodynamic Study of AMG 479, a Fully Human Monoclonal Antibody to Insulin-Like Growth Factor Receptor 1. JCO 27, 5800–5807. https://doi.org/10.1200/JCO.2009.23.6745

Tolnay, M., Juang, Y.-T., Tsokos, G.C., 2002. Protein kinase A enhances, whereas glycogen synthase kinase-3 beta inhibits, the activity of the exon 2-encoded transactivator domain of heterogeneous nuclear ribonucleoprotein D in a hierarchical fashion. Biochem J 363, 127–136. https://doi.org/10.1042/0264-6021:3630127

Tonic, I., Yu, W.-N., Park, Y., Chen, C.-C., Hay, N., 2010. Akt activation emulates Chk1 inhibition and Bcl2 overexpression and abrogates G2 cell cycle checkpoint by inhibiting BRCA1 foci. J Biol Chem 285, 23790–23798. https://doi.org/10.1074/jbc.M110.104372

Tonini, T., Rossi, F., Claudio, P.P., 2003. Molecular basis of angiogenesis and cancer. Oncogene 22, 6549–6556. https://doi.org/10.1038/sj.onc.1206816

Topacio, B.R., Zatulovskiy, E., Cristea, S., Xie, S., Tambo, C.S., Rubin, S.M., Sage, J., Kõivomägi, M., Skotheim, J.M., 2019. Cyclin D-Cdk4,6 Drives Cell-Cycle Progression via the Retinoblastoma Protein's C-Terminal Helix. Mol Cell 74, 758-770.e4. https://doi.org/10.1016/j.molcel.2019.03.020

Toulany, M., Iida, M., Keinath, S., Iyi, F.F., Mueck, K., Fehrenbacher, B., Mansour, W.Y., Schaller, M., Wheeler, D.L., Rodemann, H.P., 2016. Dual targeting of PI3K and MEK enhances the radiation response of K-RAS mutated non-small cell lung cancer. Oncotarget 7, 43746–43761. https://doi.org/10.18632/oncotarget.9670

Toulany, M., Kasten-Pisula, U., Brammer, I., Wang, S., Chen, J., Dittmann, K., Baumann, M., Dikomey, E., Rodemann, H.P., 2006. Blockage of Epidermal Growth Factor Receptor-Phosphatidylinositol 3-Kinase-AKT Signaling Increases Radiosensitivity of K-RAS Mutated Human Tumor Cells In vitro by Affecting DNA Repair. Clin Cancer Res 12, 4119. https://doi.org/10.1158/1078-0432.CCR-05-2454

Toulany, M., Kehlbach, R., Florczak, U., Sak, A., Wang, S., Chen, J., Lobrich, M., Rodemann, H.P., 2008. Targeting of AKT1 enhances radiation toxicity of human tumor cells by inhibiting DNA-PKcs-dependent DNA double-strand break repair. Mol Cancer Ther 7, 1772. https://doi.org/10.1158/1535-7163.MCT-07-2200

Toulany, M., Kehlbach, R., Rodemann, H.P., Mozdarani, H., 2010. Radiocontrast media affect radiation-induced DNA damage repair in vitro and in vivo by affecting Akt signalling. Radiotherapy and Oncology 94, 110–116. https://doi.org/10.1016/j.radonc.2009.11.006

Toulany, M., Lee, K.-J., Fattah, K.R., Lin, Y.-F., Fehrenbacher, B., Schaller, M., Chen, B.P., Chen, D.J., Rodemann, H.P., 2012. Akt Promotes Post-Irradiation Survival of Human Tumor Cells through Initiation, Progression, and Termination of DNA-PKcs–Dependent DNA Double-Strand Break Repair. Mol Cancer Res 10, 945. https://doi.org/10.1158/1541-7786.MCR-11-0592

Toulany, M., Maier, J., Iida, M., Rebholz, S., Holler, M., Grottke, A., Jüker, M., Wheeler, D.L., Rothbauer, U., Rodemann, H.P., 2017. Akt1 and Akt3 but not Akt2 through interaction with DNA-PKcs stimulate proliferation and post-irradiation cell survival of K-RAS-mutated cancer cells. Cell Death Discovery 3, 17072. https://doi.org/10.1038/cddiscovery.2017.72

Toulany, M., Schickfluß, T.-A., Fattah, K.R., Lee, K.-J., Chen, B.P.C., Fehrenbacher, B., Schaller, M., Chen, D.J., Rodemann, H.P., 2011. Function of erbB receptors and DNA-PKcs on phosphorylation of cytoplasmic and nuclear Akt at S473 induced by erbB1 ligand and ionizing radiation. Radiotherapy and Oncology 101, 140–146. https://doi.org/10.1016/j.radonc.2011.06.004

Tounekti, O., Kenani, A., Foray, N., Orlowski, S., Mir, L.M., 2001. The ratio of single- to double-strand DNA breaks and their absolute values determine cell death pathway. Br J Cancer 84, 1272–1279. https://doi.org/10.1054/bjoc.2001.1786

Toyoshima, H., Hunter, T., 1994. p27, a novel inhibitor of G1 cyclin-Cdk protein kinase activity, is related to p21. Cell 78, 67–74. https://doi.org/10.1016/0092-8674(94)90573-8

Tran, D., Bergholz, J., Zhang, H., He, H., Wang, Y., Zhang, Y., Li, Q., Kirkland, J.L., Xiao, Z.-X., 2014. Insulin-like growth factor-1 regulates the SIRT1-p53 pathway in cellular senescence. Aging Cell 13, 669–678. https://doi.org/10.1111/acel.12219

Tran, H., Brunet, A., Grenier, J.M., Datta, S.R., Fornace, A.J., DiStefano, P.S., Chiang, L.W., Greenberg, M.E., 2002. DNA Repair Pathway Stimulated by the Forkhead Transcription Factor FOXO3a Through the Gadd45 Protein. Science 296, 530. https://doi.org/10.1126/science.1068712

Tran, H., Brunet, A., Griffith, E.C., Greenberg, M.E., 2003. The Many Forks in FOXO's Road. Sci. STKE 2003, re5. https://doi.org/10.1126/stke.2003.172.re5

Tran, N.H., Wu, X., Frost, J.A., 2005. B-Raf and Raf-1 Are Regulated by Distinct Autoregulatory Mechanisms*. Journal of Biological Chemistry 280, 16244–16253. https://doi.org/10.1074/jbc.M501185200

Treins, C., Giorgetti-Peraldi, S., Murdaca, J., Monthouël-Kartmann, M.-N., Van Obberghen, E., 2005. Regulation of Hypoxia-Inducible Factor (HIF)-1 Activity and Expression of HIF Hydroxylases in Response to Insulin-Like Growth Factor I. Molecular Endocrinology 19, 1304–1317. https://doi.org/10.1210/me.2004-0239

Trojanek, J., Ho, T., Del Valle, L., Nowicki, M., Wang, J.Y., Lassak, A., Peruzzi, F., Khalili, K., Skorski, T., Reiss, K., 2003. Role of the Insulin-Like Growth Factor I/Insulin Receptor Substrate 1 Axis in Rad51 Trafficking and DNA Repair by Homologous Recombination. Mol. Cell. Biol. 23, 7510. https://doi.org/10.1128/MCB.23.21.7510-7524.2003

Tsai, S.Q., Zheng, Z., Nguyen, N.T., Liebers, M., Topkar, V.V., Thapar, V., Wyvekens, N., Khayter, C., Iafrate, A.J., Le, L.P., Aryee, M.J., Joung, J.K., 2015. GUIDE-seq enables genome-wide profiling of off-target cleavage by CRISPR-Cas nucleases. Nature Biotechnology 33, 187–197. https://doi.org/10.1038/nbt.3117

Tsvetkov, P., Mendillo, M.L., Zhao, J., Carette, J.E., Merrill, P.H., Cikes, D., Varadarajan, M., van Diemen, F.R., Penninger, J.M., Goldberg, A.L., Brummelkamp, T.R., Santagata, S., Lindquist, S., 2015. Compromising the 19S proteasome complex protects cells from reduced flux through the proteasome. eLife 4, e08467. https://doi.org/10.7554/eLife.08467

Turgeon, M.-O., Perry, N.J.S., Poulogiannis, G., 2018. DNA Damage, Repair, and Cancer Metabolism. Frontiers in Oncology 8, 15. https://doi.org/10.3389/fonc.2018.00015

Turner, B.C., Haffty, B.G., Narayanan, L., Yuan, J., Havre, P.A., Gumbs, A.A., Kaplan, L., Burgaud, J.-L., Carter, D., Baserga, R., Glazer, P.M., 1997. Insulin-like Growth Factor-I Receptor Overexpression Mediates Cellular Radioresistance and Local Breast Cancer Recurrence after Lumpectomy and Radiation. Cancer Res 57, 3079.

Turney, B.W., Kerr, M., Chitnis, M.M., Lodhia, K., Wang, Y., Riedemann, J., Rochester, M., Protheroe, A.S., Brewster, S.F., Macaulay, V.M., 2012. Depletion of the type 1 IGF receptor delays repair of radiation-induced DNA double strand breaks. Radiotherapy and Oncology 103, 402–409. https://doi.org/10.1016/j.radonc.2012.03.009

Turney, B.W., Turner, G.D.H., Brewster, S.F., Macaulay, V.M., 2011. Serial analysis of resected prostate cancer suggests up-regulation of type 1 IGF receptor with disease progression. BJU International 107, 1488–1499. https://doi.org/10.1111/j.1464-410X.2010.09556.x

Ubersax, J.A., Ferrell Jr, J.E., 2007. Mechanisms of specificity in protein phosphorylation. Nature Reviews Molecular Cell Biology 8, 530–541. https://doi.org/10.1038/nrm2203

Uematsu, N., Weterings, E., Yano, K., Morotomi-Yano, K., Jakob, B., Taucher-Scholz, G., Mari, P.-O., van Gent, D.C., Chen, B.P.C., Chen, D.J., 2007. Autophosphorylation of DNA-PKCS regulates its dynamics at DNA double-strand breaks. Journal of Cell Biology 177, 219–229. https://doi.org/10.1083/jcb.200608077

Ullrich, A., Gray, A., Tam, A.W., Yang-Feng, T., Tsubokawa, M., Collins, C., Henzel, W., Le Bon, T., Kathuria, S., Chen, E., et al., 1986. Insulin-like growth factor I receptor primary structure: comparison with insulin receptor suggests structural determinants that define functional specificity. EMBO J 5, 2503–2512.

Urnov, F.D., Miller, J.C., Lee, Y.-L., Beausejour, C.M., Rock, J.M., Augustus, S., Jamieson, A.C., Porteus, M.H., Gregory, P.D., Holmes, M.C., 2005. Highly efficient endogenous human gene correction using designed zinc-finger nucleases. Nature 435, 646–651. https://doi.org/10.1038/nature03556

Ushijima, H., Suzuki, Y., Oike, T., Komachi, M., Yoshimoto, Y., Ando, K., Okonogi, N., Sato, H., Noda, S.-E., Saito, J.-I., Nakano, T., 2015. Radio-sensitization effect of an mTOR inhibitor, temsirolimus, on lung adenocarcinoma A549 cells under normoxic and hypoxic conditions. J Radiat Res 56, 663–668. https://doi.org/10.1093/jrr/rrv021

Vadlakonda, L., Dash, A., Pasupuleti, M., Kotha, A.K., Reddanna, P., 2013. The Paradox of Akt-mTOR Interactions. Frontiers in Oncology 3, 165. https://doi.org/10.3389/fonc.2013.00165

Valsecchi, M.E., McDonald, M., Brody, J.R., Hyslop, T., Freydin, B., Yeo, C.J., Solomides, C., Peiper, S.C., Witkiewicz, A.K., 2012. Epidermal growth factor receptor and insulinlike growth factor 1 receptor expression predict poor survival in pancreatic ductal adenocarcinoma. Cancer 118, 3484–3493. https://doi.org/10.1002/cncr.26661

Vasilcanu, R., Vasilcanu, D., Sehat, B., Yin, S., Girnita, A., Axelson, M., Girnita, L., 2008. Insulin-Like Growth Factor Type-I Receptor-Dependent Phosphorylation of Extracellular Signal-Regulated Kinase 1/2 but not Akt (Protein Kinase B) Can Be Induced by Picropodophyllin. Mol Pharmacol 73, 930. https://doi.org/10.1124/mol.107.040014

Verdin, E., Ott, M., 2015. 50 years of protein acetylation: from gene regulation to epigenetics, metabolism and beyond. Nature Reviews Molecular Cell Biology 16, 258–264. https://doi.org/10.1038/nrm3931

Verkaik, N.S., Esveldt-van Lange, R.E.E., Heemst, D. van, Brüggenwirth, H.T., Hoeijmakers, J.H.J., Zdzienicka, M.Z., Gent, D.C. van, 2002. Different types of V(D)J recombination and end-joining defects in DNA double-strand break repair mutant mammalian cells. European Journal of Immunology 32, 701–709. https://doi.org/10.1002/1521-4141(200203)32:3<701::AID-IMMU701>3.0.CO;2-T

Vermeulen, K., Van Bockstaele, D.R., Berneman, Z.N., 2003. The cell cycle: a review of regulation, deregulation and therapeutic targets in cancer. Cell Proliferation 36, 131–149. https://doi.org/10.1046/j.1365-2184.2003.00266.x

Vilchez, D., Boyer, L., Morantte, I., Lutz, M., Merkwirth, C., Joyce, D., Spencer, B., Page, L., Masliah, E., Berggren, W.T., Gage, F.H., Dillin, A., 2012. Increased proteasome activity in human embryonic stem cells is regulated by PSMD11. Nature 489, 304–308. https://doi.org/10.1038/nature11468

Vinay, D.S., Ryan, E.P., Pawelec, G., Talib, W.H., Stagg, J., Elkord, E., Lichtor, T., Decker, W.K., Whelan, R.L., Kumara, H.M.C.S., Signori, E., Honoki, K., Georgakilas, A.G., Amin, A., Helferich, W.G., Boosani, C.S., Guha, G., Ciriolo, M.R., Chen, S., Mohammed, S.I., Azmi, A.S., Keith, W.N., Bilsland, A., Bhakta, D., Halicka, D., Fujii, H., Aquilano, K., Ashraf, S.S., Nowsheen, S., Yang, X., Choi, B.K., Kwon, B.S., 2015. Immune evasion in cancer: Mechanistic basis and therapeutic strategies. Seminars in Cancer Biology 35, S185–S198. https://doi.org/10.1016/j.semcancer.2015.03.004

Vincent, E.E., Sergushichev, A., Griss, T., Gingras, M.-C., Samborska, B., Ntimbane, T., Coelho, P.P., Blagih, J., Raissi, T.C., Choinière, L., Bridon, G., Loginicheva, E., Flynn, B.R., Thomas, E.C., Tavaré, J.M., Avizonis, D., Pause, A., Elder, D.J.E., Artyomov, M.N., Jones, R.G., 2015. Mitochondrial Phosphoenolpyruvate Carboxykinase Regulates Metabolic Adaptation and Enables Glucose-Independent Tumor Growth. Molecular Cell 60, 195–207. https://doi.org/10.1016/j.molcel.2015.08.013

Vinciguerra, M., Santini, M.P., Claycomb, W.C., Ladurner, A.G., Rosenthal, N., 2010. Local IGF-1 isoform protects cardiomyocytes from hypertrophic and oxidative stresses via SirT1 activity. Aging (Albany NY) 2, 43–62. https://doi.org/10.18632/aging.100107

Viniegra, J.G., Martínez, N., Modirassari, P., Losa, J.H., Cobo, C.P., Lobo, V.J.S.-A., Luquero, C.I.A., Álvarez-Vallina, L., Ramón y Cajal, S., Rojas, J.M., Sánchez-Prieto, R., 2005. Full Activation of PKB/Akt in Response to Insulin or Ionizing Radiation Is Mediated through ATM. Journal of Biological Chemistry 280, 4029–4036. https://doi.org/10.1074/jbc.M410344200

Vitale, G., Pellegrino, G., Vollery, M., Hofland, L.J., 2019. ROLE of IGF-1 System in the Modulation of Longevity: Controversies and New Insights From a Centenarians' Perspective. Front Endocrinol (Lausanne) 10, 27–27. https://doi.org/10.3389/fendo.2019.00027

Vlachostergios, P.J., Patrikidou, A., Daliani, D.D., Papandreou, C.N., 2009. The ubiquitin-proteasome system in cancer, a major player in DNA repair. Part 1: post-translational regulation. J Cell Mol Med 13, 3006–3018. https://doi.org/10.1111/j.1582-4934.2009.00824.x

von Wichert, G., Haeussler, U., Greten, F.R., Kliche, S., Dralle, H., Böhm, B.O., Adler, G., Seufferlein, T., 2005. Regulation of cyclin D1 expression by autocrine IGF-I in human BON neuroendocrine tumour cells. Oncogene 24, 1284–1289. https://doi.org/10.1038/sj.onc.1208264

Waldman, A.D., Fritz, J.M., Lenardo, M.J., 2020. A guide to cancer immunotherapy: from T cell basic science to clinical practice. Nature Reviews Immunology. https://doi.org/10.1038/s41577-020-0306-5

Wang, F., Zhang, C., Xu, W., Yuan, S., Song, J., Li, L., Zhao, J., Yang, J., 2020. Developing high-efficiency base editors by combining optimized synergistic core components with new types of nuclear localization signal peptide. The Crop Journal. https://doi.org/10.1016/j.cj.2020.01.003

Wang, Huamin, Rosen, D.G., Wang, Hua, Fuller, G.N., Zhang, W., Liu, J., 2006. Insulin-like growth factor-binding protein 2 and 5 are differentially regulated in ovarian cancer of different histologic types. Modern Pathology 19, 1149–1156. https://doi.org/10.1038/modpathol.3800637

Wang, J., Kobayashi, T., Floc'h, N., Kinkade, C.W., Aytes, A., Dankort, D., Lefebvre, C., Mitrofanova, A., Cardiff, R.D., McMahon, M., Califano, A., Shen, M.M., Abate-Shen, C., 2012. B-Raf activation cooperates with PTEN loss to drive c-Myc expression in advanced prostate cancer. Cancer Res 72, 4765–4776. https://doi.org/10.1158/0008-5472.CAN-12-0820

Wang, M., Valenzuela, L., Murphy, G., Chu, T., 2002. Purification of a human prostate specific antigen. 1979 [classical article]. The Journal of urology 167, 1226–30. https://doi.org/10.1016/S0022-5347(05)65270-6

Wang, R., Yamada, T., Kita, K., Taniguchi, H., Arai, S., Fukuda, K., Terashima, M., Ishimura, A., Nishiyama, A., Tanimoto, A., Takeuchi, S., Ohtsubo, K., Yamashita, K., Yamano, T., Yoshimura, A., Takayama, K., Kaira, K., Taniguchi, Y., Atagi, S., Uehara, H., Hanayama, R., Matsumoto, I., Han, X., Matsumoto, K., Wang, W., Suzuki,

T., Yano, S., 2020. Transient IGF-1R inhibition combined with osimertinib eradicates AXL-low expressing EGFR mutated lung cancer. Nat Commun 11, 4607–4607. https://doi.org/10.1038/s41467-020-18442-4

Wang, S.-A., Wang, Y.-C., Chuang, Y.-P., Huang, Y.-H., Su, W.-C., Chang, W.-C., Hung, J.-J., 2017. EGF-mediated inhibition of ubiquitin-specific peptidase 24 expression has a crucial role in tumorigenesis. Oncogene 36, 2930–2945. https://doi.org/10.1038/onc.2016.445

Wang, Z., Liu, G., Mao, J., Xie, M., Zhao, M., Guo, X., Liang, S., Li, H., Li, X., Wang, R., 2019. IGF-1R Inhibition Suppresses Cell Proliferation and Increases Radiosensitivity in Nasopharyngeal Carcinoma Cells. Mediators of Inflammation 2019, 5497467. https://doi.org/10.1155/2019/5497467

Wanigasooriya, K., Tyler, R., Barros-Silva, J.D., Sinha, Y., Ismail, T., Beggs, A.D., 2020. Radiosensitising Cancer Using Phosphatidylinositol-3-Kinase (PI3K), Protein Kinase B (AKT) or Mammalian Target of Rapamycin (mTOR) Inhibitors. Cancers (Basel) 12, 1278. https://doi.org/10.3390/cancers12051278

Waraky, A., Akopyan, K., Parrow, V., Strömberg, T., Axelson, M., Abrahmsén, L., Lindqvist, A., Larsson, O., Aleem, E., 2014. Picropodophyllin causes mitotic arrest and catastrophe by depolymerizing microtubules via insulin-like growth factor-1 receptor-independent mechanism. Oncotarget 5, 8379–8392. https://doi.org/10.18632/oncotarget.2292

Waraky, A., Lin, Y., Warsito, D., Haglund, F., Aleem, E., Larsson, O., 2017. Nuclear insulin-like growth factor 1 receptor phosphorylates proliferating cell nuclear antigen and rescues stalled replication forks after DNA damage. Journal of Biological Chemistry 292, 18227–18239. https://doi.org/10.1074/jbc.M117.781492

Ward, E., Stewart, B., 1987. Persistent and heritable structural damage induced in heterochromatic DNA from rat liver by N-nitrosodimethylamine. Biochemistry 26, 1709–1717. https://doi.org/10.1021/bi00380a033

Ward, I.M., Minn, K., Jorda, K.G., Chen, J., 2003. Accumulation of Checkpoint Protein 53BP1 at DNA Breaks Involves Its Binding to Phosphorylated Histone H2AX *. Journal of Biological Chemistry 278, 19579–19582. https://doi.org/10.1074/jbc.C300117200

Warsito, D., Lin, Y., Gnirck, A.-C., Sehat, B., Larsson, O., 2016. Nuclearly translocated insulin-like growth factor 1 receptor phosphorylates histone H3 at tyrosine 41 and induces SNAI2 expression via Brg1 chromatin remodeling protein. Oncotarget 7, 42288–42302. https://doi.org/10.18632/oncotarget.9785

Warsito, D., Sjöström, S., Andersson, S., Larsson, O., Sehat, B., 2012. Nuclear IGF1R is a transcriptional co-activator of LEF1/TCF. EMBO reports 13, 244–250. https://doi.org/10.1038/embor.2011.251

Wawrzynow, B., Zylicz, A., Zylicz, M., 2018. Chaperoning the guardian of the genome. The two-faced role of molecular chaperones in p53 tumor suppressor action. Biochimica et Biophysica Acta (BBA) - Reviews on Cancer 1869, 161–174. https://doi.org/10.1016/j.bbcan.2017.12.004

Weber, A.M., Drobnitzky, N., Devery, A.M., Bokobza, S.M., Adams, R.A., Maughan, T.S., Ryan, A.J., 2016. Phenotypic consequences of somatic mutations in the ataxia-telangiectasia mutated gene in non-small cell lung cancer. Oncotarget 7, 60807–60822. https://doi.org/10.18632/oncotarget.11845

Wee, P., Wang, Z., 2017. Epidermal Growth Factor Receptor Cell Proliferation Signaling Pathways. Cancers 9, 52. https://doi.org/10.3390/cancers9050052

Wei, F., Xie, Y., Tao, L., Tang, D., 2010. Both ERK1 and ERK2 kinases promote G2/M arrest in etoposide-treated MCF7 cells by facilitating ATM activation. Cellular Signalling 22, 1783–1789. https://doi.org/10.1016/j.cellsig.2010.07.007

Wei, F., Yan, J., Tang, D., 2011. Extracellular signal-regulated kinases modulate DNA damage response - a contributing factor to using MEK inhibitors in cancer therapy. Curr Med Chem 18, 5476–5482. https://doi.org/10.2174/092986711798194388

Weinfeld, M., Rasouli-Nia, A., Chaudhry, M.A., Britten, R.A., 2001. Response of Base Excision Repair Enzymes to Complex DNA Lesions. Radiation Research 156, 584–589. https://doi.org/10.1667/0033-7587(2001)156[0584:ROBERE]2.0.CO;2

Welcker, M., Singer, J., Loeb, K.R., Grim, J., Bloecher, A., Gurien-West, M., Clurman, B.E., Roberts, J.M., 2003. Multisite Phosphorylation by Cdk2 and GSK3 Controls Cyclin E Degradation. Molecular Cell 12, 381–392. https://doi.org/10.1016/S1097-2765(03)00287-9

Werner, H., Karnieli, E., Rauscher, F.J., LeRoith, D., 1996. Wild-type and mutant p53 differentially regulate transcription of the insulin-like growth factor I receptor gene. Proc Natl Acad Sci U S A 93, 8318–8323. https://doi.org/10.1073/pnas.93.16.8318

Werner, H., Re, G.G., Drummond, I.A., Sukhatme, V.P., Rauscher, F.J., Sens, D.A., Garvin, A.J., LeRoith, D., Roberts, C.T., 1993. Increased expression of the insulin-like growth factor I receptor gene, IGF1R, in Wilms tumor is correlated with modulation of IGF1R promoter activity by the WT1 Wilms tumor gene product. Proc Natl Acad Sci USA 90, 5828. https://doi.org/10.1073/pnas.90.12.5828

Werner, H., Sarfstein, R., 2014. Transcriptional and epigenetic control of IGF1R gene expression: Implications in metabolism and cancer. Growth Hormone & IGF Research 24, 112–118. https://doi.org/10.1016/j.ghir.2014.03.006

Werner, S., Engler, C., Weber, E., Gruetzner, R., Marillonnet, S., 2012. Fast track assembly of multigene constructs using Golden Gate cloning and the MoClo system. Bioengineered 3, 38–43. https://doi.org/10.4161/bbug.3.1.18223

Weroha, S.J., Haluska, P., 2008. IGF-1 receptor inhibitors in clinical trials--early lessons. J Mammary Gland Biol Neoplasia 13, 471–483. https://doi.org/10.1007/s10911-008-9104-6

Westphal, D., Kluck, R.M., Dewson, G., 2014. Building blocks of the apoptotic pore: how Bax and Bak are activated and oligomerize during apoptosis. Cell Death & Differentiation 21, 196–205. https://doi.org/10.1038/cdd.2013.139

Weterings, E., Chen, D.J., 2008. The endless tale of non-homologous end-joining. Cell Research 18, 114–124. https://doi.org/10.1038/cr.2008.3

Weterings, E., van Gent, D.C., 2004. The mechanism of non-homologous end-joining: a synopsis of synapsis. DNA Repair 3, 1425–1435. https://doi.org/10.1016/j.dnarep.2004.06.003

Weterings, E., Verkaik, N.S., Brüggenwirth, H.T., Hoeijmakers, J.H.J., van Gent, D.C., 2003. The role of DNA dependent protein kinase in synapsis of DNA ends. Nucleic Acids Res 31, 7238–7246. https://doi.org/10.1093/nar/gkg889

Weyer-Czernilofsky, U., Hofmann, M.H., Friedbichler, K., Baumgartinger, R., Adam, P.J., Solca, F., Kraut, N., Nguyen, H.M., Corey, E., Liu, G., Sprenger, C.C., Plymate, S.R., Bogenrieder, T., 2020. Antitumor Activity of the IGF-1/IGF-2–Neutralizing Antibody Xentuzumab (BI 836845) in Combination with Enzalutamide in Prostate Cancer Models. Mol Cancer Ther 19, 1059. https://doi.org/10.1158/1535-7163.MCT-19-0378

White, D.E., Negorev, D., Peng, H., Ivanov, A.V., Maul, G.G., Rauscher, F.J., 2006. KAP1, a Novel Substrate for PIKK Family Members, Colocalizes with Numerous Damage Response Factors at DNA Lesions. Cancer Res 66, 11594. https://doi.org/10.1158/0008-5472.CAN-06-4138

White, M.F., 2002. IRS proteins and the common path to diabetes. American Journal of Physiology-Endocrinology and Metabolism 283, E413–E422. https://doi.org/10.1152/ajpendo.00514.2001

White, M.F., Livingston, J.N., Backer, J.M., Lauris, V., Dull, T.J., Ullrich, A., Kahn, C.R., 1988. Mutation of the insulin receptor at tyrosine 960 inhibits signal transmission but does not affect its tyrosine kinase activity. Cell 54, 641–649. https://doi.org/10.1016/S0092-8674(88)80008-4

Willoughby, C.E., Jiang, Y., Thomas, H.D., Willmore, E., Kyle, S., Wittner, A., Phillips, N., Zhao, Y., Tudhope, S.J., Prendergast, L., Junge, G., Lourenco, L.M., Finlay, M.R.V., Turner, P., Munck, J.M., Griffin, R.J., Rennison, T., Pickles, J., Cano, C., Newell, D.R., Reeves, H.L., Ryan, A.J., Wedge, S.R., 2020. Selective DNA-PKcs inhibition extends the therapeutic index of localized radiotherapy and chemotherapy. J Clin Invest 130, 258–271. https://doi.org/10.1172/JCI127483

Wilson, G.M., Lu, J., Sutphen, K., Suarez, Y., Sinha, S., Brewer, B., Villanueva-Feliciano, E.C., Ysla, R.M., Charles, S., Brewer, G., 2003. Phosphorylation of p40AUF1 Regulates Binding to A + U-rich mRNA-destabilizing Elements and Protein-induced Changes in Ribonucleoprotein Structure. Journal of Biological Chemistry 278, 33039–33048. https://doi.org/10.1074/jbc.M305775200

Wong, W., 2013. Surviving Glutamine Deprivation. Sci. Signal. 6, ec100. https://doi.org/10.1126/scisignal.2004286

Wonkyoung, Jin Xiongjie, Pang Junfeng, Wang Yan, Mivechi Nahid F., Moskophidis Demetrius, 2019. The Molecular Chaperone Heat Shock Protein 70 Controls Liver Cancer Initiation and Progression by Regulating

Adaptive DNA Damage and Mitogen-Activated Protein Kinase/Extracellular Signal-Regulated Kinase Signaling Pathways. Molecular and Cellular Biology 39, e00391-18. https://doi.org/10.1128/MCB.00391-18

Wu, W., Ma, J., Shao, N., Shi, Y., Liu, R., Li, W., Lin, Y., Wang, S., 2017. Co-Targeting IGF-1R and Autophagy Enhances the Effects of Cell Growth Suppression and Apoptosis Induced by the IGF-1R Inhibitor NVP-AEW541 in Triple-Negative Breast Cancer Cells. PLOS ONE 12, e0169229. https://doi.org/10.1371/journal.pone.0169229

Wu, X, Seraia, E., Hatch, S., Wan, X., Ebner, D., Aroldi, F., Jiang, Y., Ryan, A.J., Bogenrieder, T., Weyer-Czernilofsky, U., Rieunier, G., Macaulay, V.M., 2021. CHK1 inhibition exacerbates replication stress induced by IGF blockade. Oncogene In press.

Wu, Xiaoning, Seraia, E., Hatch, S.B., Wan, X., Ebner, D.V., Aroldi, F., Jiang, Y., Ryan, A.J., Bogenrieder, T., Weyer-Czernilofsky, U., Rieunier, G., Macaulay, V.M., 2021. CHK1 inhibition exacerbates replication stress induced by IGF blockade. Oncogene. https://doi.org/10.1038/s41388-021-02080-1

Wu, Z.-Q., Liu, X., 2008. Role for Plk1 phosphorylation of Hbo1 in regulation of replication licensing. Proc Natl Acad Sci USA 105, 1919. https://doi.org/10.1073/pnas.0712063105

Xia, Z., Dickens, M., Raingeaud, J., Davis, R.J., Greenberg, M.E., 1995. Opposing Effects of ERK and JNK-p38 MAP Kinases on Apoptosis. Science 270, 1326. https://doi.org/10.1126/science.270.5240.1326

Xie, Xiaoduo, Hu, H., Tong, X., Li, L., Liu, X., Chen, M., Yuan, H., Xie, Xia, Li, Q., Zhang, Y., Ouyang, H., Wei, M., Huang, J., Liu, P., Gan, W., Liu, Y., Xie, A., Kuai, X., Chirn, G.-W., Zhou, H., Zeng, R., Hu, R., Qin, J., Meng, F.-L., Wei, W., Ji, H., Gao, D., 2018. The mTOR-S6K pathway links growth signalling to DNA damage response by targeting RNF168. Nat Cell Biol 20, 320–331. https://doi.org/10.1038/s41556-017-0033-8

Xie, Y., Liu, Y.-K., Guo, Z.-P., Guan, H., Liu, X.-D., Xie, D.-F., Jiang, Y.-G., Ma, T., Zhou, P.-K., 2020. RBX1 prompts degradation of EXO1 to limit the homologous recombination pathway of DNA double-strand break repair in G1 phase. Cell Death & Differentiation 27, 1383–1397. https://doi.org/10.1038/s41418-019-0424-4

Xie, Y., Wang, J.-L., Ji, M., Yuan, Z.-F., Peng, Z., Zhang, Y., Wen, J.-G., Shi, H.-R., 2014. Regulation of insulin-like growth factor signaling by metformin in endometrial cancer cells. Oncol Lett 8, 1993–1999. https://doi.org/10.3892/ol.2014.2466

Xiong, H., Veedu, R.N., Diermeier, S.D., 2021. Recent Advances in Oligonucleotide Therapeutics in Oncology. Int J Mol Sci 22, 3295. https://doi.org/10.3390/ijms22073295

Xu, N., Hegarat, N., Black, E.J., Scott, M.T., Hochegger, H., Gillespie, D.A., 2010. Akt/PKB suppresses DNA damage processing and checkpoint activation in late G2. J Cell Biol 190, 297–305. https://doi.org/10.1083/jcb.201003004

Xu, N., Lao, Y., Zhang, Y., Gillespie, D.A., 2012. Akt: A Double-Edged Sword in Cell Proliferation and Genome Stability. Journal of Oncology 2012, 951724. https://doi.org/10.1155/2012/951724

Xue, L., Chen, F., Yue, F., Camacho, L., Kothapalli, S., Wei, G., Huang, S., Mo, Q., Ma, F., Li, Y., Jiralerspong, S., 2021. Metformin and an insulin/IGF-1 receptor inhibitor are synergistic in blocking growth of triple-negative breast cancer. Breast Cancer Research and Treatment 185, 73–84. https://doi.org/10.1007/s10549-020-05927-5

Yacoub, A., McKinstry, R., Hinman, D., Chung, T., Dent, P., Hagan, M.P., 2003. Epidermal Growth Factor and Ionizing Radiation Up-regulate the DNA Repair Genes XRCC1 and ERCC1 in DU145 and LNCaP Prostate Carcinoma through MAPK Signaling. Radiation Research 159, 439–452. https://doi.org/10.1667/0033-7587(2003)159[0439:EGFAIR]2.0.CO;2

Yamaguchi, R., Dutta, A., 2000. Proteasome inhibitors alter the orderly progression of DNA synthesis during S-phase in HeLa cells and lead to rereplication of DNA. Experimental cell research 261, 271–283. https://doi.org/10.1006/excr.2000.5053

Yamaguchi, Y., Flier, J.S., Benecke, H., Ransil, B.J., Moller, D.E., 1993. Ligand-binding properties of the two isoforms of the human insulin receptor. Endocrinology 132, 1132–1138. https://doi.org/10.1210/en.132.3.1132

Yamamoto, T., Oshima, T., Yoshihara, K., Nishi, T., Arai, H., Inui, K., Kaneko, T., Nozawa, A., Adachi, H., Rino, Y., Masuda, M., Imada, T., 2012. Clinical significance of immunohistochemical expression of insulin-like growth factor-1 receptor and matrix metalloproteinase-7 in resected non-small cell lung cancer. Exp Ther Med 3, 797–802. https://doi.org/10.3892/etm.2012.493

Yan, J., Cirincione, A., Adamson, B., 2020. Prime Editing: Precision Genome Editing by Reverse Transcription. Molecular Cell 77, 210–212. https://doi.org/10.1016/j.molcel.2019.12.016

Yan, L.-B., Shi, K., Bing, Z.-T., Sun, Y.-L., Shen, Y., 2013. Proteomic analysis of energy metabolism and signal transduction in irradiated melanoma cells. Int J Ophthalmol 6, 286–294. https://doi.org/10.3980/j.issn.2222-3959.2013.03.06

Yan, Y., Black, C.P., Cowan, K.H., 2007. Irradiation-induced G2/M checkpoint response requires ERK1/2 activation. Oncogene 26, 4689–4698. https://doi.org/10.1038/sj.onc.1210268

Yang, C., Zhang, Y., Segar, N., Huang, C., Zeng, P., Tan, X., Mao, L., Chen, Zhikang, Haglund, F., Larsson, O., Chen, Zihua, Lin, Y., 2021. Nuclear IGF1R interacts with NuMA and regulates 53BP1-dependent DNA double-strand break repair in colorectal cancer. Oncol Rep 46, 168. https://doi.org/10.3892/or.2021.8119

Yang, J., Nie, J., Ma, X., Wei, Y., Peng, Y., Wei, X., 2019. Targeting PI3K in cancer: mechanisms and advances in clinical trials. Molecular Cancer 18, 26. https://doi.org/10.1186/s12943-019-0954-x

Ye, J., Coulouris, G., Zaretskaya, I., Cutcutache, I., Rozen, S., Madden, T.L., 2012. Primer-BLAST: a tool to design target-specific primers for polymerase chain reaction. BMC Bioinformatics 13, 134–134. https://doi.org/10.1186/1471-2105-13-134

Yee, D., 2015. A Tale of Two Receptors: Insulin and Insulin-Like Growth Factor Signaling in Cancer. Clin Cancer Res 21, 667. https://doi.org/10.1158/1078-0432.CCR-14-2056

Yeh, C.D., Richardson, C.D., Corn, J.E., 2019. Advances in genome editing through control of DNA repair pathways. Nature Cell Biology 21, 1468–1478. https://doi.org/10.1038/s41556-019-0425-z

Yeh, E., Cunningham, M., Arnold, H., Chasse, D., Monteith, T., Ivaldi, G., Hahn, W.C., Stukenberg, P.T., Shenolikar, S., Uchida, T., Counter, C.M., Nevins, J.R., Means, A.R., Sears, R., 2004. A signalling pathway controlling c-Myc degradation that impacts oncogenic transformation of human cells. Nature Cell Biology 6, 308–318. https://doi.org/10.1038/ncb1110

Yeh, W.-H., Chiang, H., Rees, H.A., Edge, A.S.B., Liu, D.R., 2018. In vivo base editing of post-mitotic sensory cells. Nature Communications 9, 2184. https://doi.org/10.1038/s41467-018-04580-3

Yen, C.-L.E., Monetti, M., Burri, B.J., Farese, R.V., 2005. The triacylglycerol synthesis enzyme DGAT1 also catalyzes the synthesis of diacylglycerols, waxes, and retinyl esters. Journal of Lipid Research 46, 1502–1511. https://doi.org/10.1194/jlr.M500036-JLR200

Yew, P.R., 2001. Ubiquitin-mediated proteolysis of vertebrate G1- and S-phase regulators. Journal of Cellular Physiology 187, 1–10. https://doi.org/10.1002/1097-4652(2001)9999:9999<1::AID-JCP1049>3.0.CO;2-O

Yi, H.K., Hwang, P.H., Yang, D.-H., Kang, C.-W., Lee, D.-Y., 2001. Expression of the insulin-like growth factors (IGFs) and the IGF-binding proteins (IGFBPs) in human gastric cancer cells. European Journal of Cancer 37, 2257–2263. https://doi.org/10.1016/S0959-8049(01)00269-6

Yin, X., Liu, M., Tian, Y., Wang, J., Xu, Y., 2017. Cryo-EM structure of human DNA-PK holoenzyme. Cell Research 27, 1341–1350. https://doi.org/10.1038/cr.2017.110

Yoneyama, Y., Lanzerstorfer, P., Niwa, H., Umehara, T., Shibano, T., Yokoyama, S., Chida, K., Weghuber, J., Hakuno, F., Takahashi, S.-I., 2018. IRS-1 acts as an endocytic regulator of IGF-I receptor to facilitate sustained IGF signaling. eLife 7. https://doi.org/10.7554/eLife.32893

Yoo, S., Dynan, W.S., 1999. Geometry of a complex formed by double strand break repair proteins at a single DNA end: recruitment of DNA-PKcs induces inward translocation of Ku protein. Nucleic Acids Res 27, 4679–4686. https://doi.org/10.1093/nar/27.24.4679

Yoshida, K., Yoshida, S.-H., Shimoda, C., Morita, T., 2003. Expression and Radiation-induced Phosphorylation of Histone H2AX in Mammalian Cells. Journal of Radiation Research 44, 47–51. https://doi.org/10.1269/jrr.44.47

Youn, C.-K., Cho, H.-J., Kim, S.-H., Kim, H.-B., Kim, M.-H., Chang, I.-Y., Lee, J.-S., Chung, M.-H., Hahm, K.-S., You, H.J., 2005. Bcl-2 expression suppresses mismatch repair activity through inhibition of E2F transcriptional activity. Nature Cell Biology 7, 137–147. https://doi.org/10.1038/ncb1215

Young, A.P., Nagarajan, R., Longmore, G.D., 2003. Mechanisms of transcriptional regulation by Rb-E2F segregate by biological pathway. Oncogene 22, 7209–7217. https://doi.org/10.1038/sj.onc.1206804

Young, M.-J., Hsu, K.-C., Lin, T.E., Chang, W.-C., Hung, J.-J., 2019. The role of ubiquitin-specific peptidases in cancer progression. Journal of Biomedical Science 26, 42. https://doi.org/10.1186/s12929-019-0522-0

Youngren, J.F., Gable, K., Penaranda, C., Maddux, B.A., Zavodovskaya, M., Lobo, M., Campbell, M., Kerner, J., Goldfine, I.D., 2005. Nordihydroguaiaretic acid (NDGA) inhibits the IGF-1 and c-erbB2/HER2/neu receptors and suppresses growth in breast cancer cells. Breast Cancer Res Treat 94, 37–46. https://doi.org/10.1007/s10549-005-6939-z

Yu, H., Rohan, T., 2000. Role of the Insulin-Like Growth Factor Family in Cancer Development and Progression. JNCI: Journal of the National Cancer Institute 92, 1472–1489. https://doi.org/10.1093/jnci/92.18.1472

Yu, J., Lu, R., Nedrow, J.R., Sgouros, G., 2020. Response of breast cancer carcinoma spheroids to combination therapy with radiation and DNA-PK inhibitor: growth arrest without a change in α/β ratio. null 96, 1534–1540. https://doi.org/10.1080/09553002.2020.1838659

Yu, W., Gu, K., Yu, Z., Yuan, D., He, M., Ma, N., Lai, S., Zhao, J., Ren, Z., Zhang, X., Shao, C., Jiang, G.-L., 2013. Sorafenib potentiates irradiation effect in hepatocellular carcinoma in vitro and in vivo. Cancer Letters 329, 109–117. https://doi.org/10.1016/j.canlet.2012.10.024

Yuan, T.L., Cantley, L.C., 2008. PI3K pathway alterations in cancer: variations on a theme. Oncogene 27, 5497–5510. https://doi.org/10.1038/onc.2008.245

Yuan, Y., Britton, S., Delteil, C., Coates, J., Jackson, S.P., Barboule, N., Frit, P., Calsou, P., 2015. Single-stranded DNA oligomers stimulate error-prone alternative repair of DNA double-strand breaks through hijacking Ku protein. Nucleic Acids Res 43, 10264–10276. https://doi.org/10.1093/nar/gkv894

Yuen, J.S.P., Akkaya, E., Wang, Y., Takiguchi, M., Peak, S., Sullivan, M., Protheroe, A.S., Macaulay, V.M., 2009. Validation of the type 1 insulin-like growth factor receptor as a therapeutic target in renal cancer. Mol Cancer Ther 8, 1448. https://doi.org/10.1158/1535-7163.MCT-09-0101

Yuen, J.S.P., Cockman, M.E., Sullivan, M., Protheroe, A., Turner, G.D.H., Roberts, I.S., Pugh, C.W., Werner, H., Macaulay, V.M., 2007. The VHL tumor suppressor inhibits expression of the IGF1R and its loss induces IGF1R upregulation in human clear cell renal carcinoma. Oncogene 26, 6499–6508. https://doi.org/10.1038/sj.onc.1210474

Zadora, P.K., Chumduri, C., Imami, K., Berger, H., Mi, Y., Selbach, M., Meyer, T.F., Gurumurthy, R.K., 2019. Integrated Phosphoproteome and Transcriptome Analysis Reveals Chlamydia-Induced Epithelial-to-Mesenchymal Transition in Host Cells. Cell Reports 26, 1286-1302.e8. https://doi.org/10.1016/j.celrep.2019.01.006

Zakikhani, M., Dowling, R., Fantus, I.G., Sonenberg, N., Pollak, M., 2006. Metformin Is an AMP Kinase–Dependent Growth Inhibitor for Breast Cancer Cells. Cancer Res 66, 10269. https://doi.org/10.1158/0008-5472.CAN-06-1500

Zannini, L., Delia, D., Buscemi, G., 2014. CHK2 kinase in the DNA damage response and beyond. J Mol Cell Biol 6, 442–457. https://doi.org/10.1093/jmcb/mju045

Zech, T., Calaminus, S.D.J., Caswell, P., Spence, H.J., Carnell, M., Insall, R.H., Norman, J., Machesky, L.M., 2011. The Arp2/3 activator WASH regulates α5β1-integrin-mediated invasive migration. Journal of Cell Science 124, 3753–3759. https://doi.org/10.1242/jcs.080986

Zeke, A., Misheva, M., Reményi, A., Bogoyevitch, M.A., 2016. JNK Signaling: Regulation and Functions Based on Complex Protein-Protein Partnerships. Microbiol. Mol. Biol. Rev. 80, 793. https://doi.org/10.1128/MMBR.00043-14

Zeng, X., Sachdev, D., Zhang, H., Gaillard-Kelly, M., Yee, D., 2009. Sequencing of type I insulin-like growth factor receptor inhibition affects chemotherapy response in vitro and in vivo. Clin Cancer Res 15, 2840–2849. https://doi.org/10.1158/1078-0432.CCR-08-1401

Zha, S., Boboila, C., Alt, F.W., 2009. Mre11: roles in DNA repair beyond homologous recombination. Nature Structural & Molecular Biology 16, 798–800. https://doi.org/10.1038/nsmb0809-798

Zhang, F., Cong, L., Lodato, S., Kosuri, S., Church, G.M., Arlotta, P., 2011. Efficient construction of sequence-specific TAL effectors for modulating mammalian transcription. Nature Biotechnology 29, 149–153. https://doi.org/10.1038/nbt.1775

Zhang, Jianwei, Li, Q., Zhang, S., Xu, Q., Wang, T., 2016. Lgr4 promotes prostate tumorigenesis through the Jmjd2a/AR signaling pathway. Experimental Cell Research 349, 77–84. https://doi.org/10.1016/j.yexcr.2016.09.023

Zhang, Jun, McCann, K.L., Qiu, C., Gonzalez, L.E., Baserga, S.J., Hall, T.M.T., 2016. Nop9 is a PUF-like protein that prevents premature cleavage to correctly process pre-18S rRNA. Nat Commun 7, 13085–13085. https://doi.org/10.1038/ncomms13085

Zhang, L.-N., Li, J.-Y., Xu, W., 2013. A review of the role of Puma, Noxa and Bim in the tumorigenesis, therapy and drug resistance of chronic lymphocytic leukemia. Cancer Gene Therapy 20, 1–7. https://doi.org/10.1038/cgt.2012.84

Zhang, S., Matsunaga, S., Lin, Y.-F., Sishc, B., Shang, Z., Sui, J., Shih, H.-Y., Zhao, Y., Foreman, O., Story, M.D., Chen, D.J., Chen, B.P.C., 2016. Spontaneous tumor development in bone marrow-rescued DNA-PKcs(3A/3A) mice due to dysfunction of telomere leading strand deprotection. Oncogene 35, 3909–3918. https://doi.org/10.1038/onc.2015.459

Zhang, S., Yajima, H., Huynh, H., Zheng, J., Callen, E., Chen, H.-T., Wong, N., Bunting, S., Lin, Y.-F., Li, M., Lee, K.-J., Story, M., Gapud, E., Sleckman, B.P., Nussenzweig, A., Zhang, C.C., Chen, D.J., Chen, B.P.C., 2011. Congenital bone marrow failure in DNA-PKcs mutant mice associated with deficiencies in DNA repair. J Cell Biol 193, 295–305. https://doi.org/10.1083/jcb.201009074

Zhang, W., Liu, H.T., 2002. MAPK signal pathways in the regulation of cell proliferation in mammalian cells. Cell Research 12, 9–18. https://doi.org/10.1038/sj.cr.7290105

Zhang, X., Berger, F.G., Yang, J., Lu, X., 2011. USP4 inhibits p53 through deubiquitinating and stabilizing ARF-BP1. EMBO J 30, 2177–2189. https://doi.org/10.1038/emboj.2011.125

Zhang, X.-H., Tee, L.Y., Wang, X.-G., Huang, Q.-S., Yang, S.-H., 2015. Off-target Effects in CRISPR/Cas9-mediated Genome Engineering. Molecular Therapy - Nucleic Acids 4, e264. https://doi.org/10.1038/mtna.2015.37

Zhang, Y., Rohde, L.H., Wu, H., 2009. Involvement of nucleotide excision and mismatch repair mechanisms in double strand break repair. Curr Genomics 10, 250–258. https://doi.org/10.2174/138920209788488544

Zhang, Y., Wester, L., He, J., Geiger, T., Moerkens, M., Siddappa, R., Helmijr, J.A., Timmermans, M.M., Look, M.P., van Deurzen, C.H.M., Martens, J.W.M., Pont, C., de Graauw, M., Danen, E.H.J., Berns, E.M.J.J., Meerman, J.H.N., Jansen, M.P.H.M., van de Water, B., 2018. IGF1R signaling drives antiestrogen resistance through PAK2/PIX activation in luminal breast cancer. Oncogene 37, 1869–1884. https://doi.org/10.1038/s41388-017-0027-9

Zhang, Z., Zhou, C., Li, X., Barnes, S.D., Deng, S., Hoover, E., Chen, C.-C., Lee, Y.S., Zhang, Y., Wang, C., Metang, L.A., Wu, C., Tirado, C.R., Johnson, N.A., Wongvipat, J., Navrazhina, K., Cao, Z., Choi, D., Huang, C.-H., Linton, E., Chen, X., Liang, Y., Mason, C.E., de Stanchina, E., Abida, W., Lujambio, A., Li, S., Lowe, S.W., Mendell, J.T., Malladi, V.S., Sawyers, C.L., Mu, P., 2020. Loss of CHD1 Promotes Heterogeneous Mechanisms of Resistance to AR-Targeted Therapy via Chromatin Dysregulation. Cancer Cell 37, 584-598.e11. https://doi.org/10.1016/j.ccell.2020.03.001

Zhao, D., Lu, X., Wang, G., Lan, Z., Liao, W., Li, J., Liang, X., Chen, J.R., Shah, S., Shang, X., Tang, M., Deng, P., Dey, P., Chakravarti, D., Chen, P., Spring, D.J., Navone, N.M., Troncoso, P., Zhang, J., Wang, Y.A., DePinho, R.A., 2017. Synthetic essentiality of chromatin remodelling factor CHD1 in PTEN-deficient cancer. Nature 542, 484–488. https://doi.org/10.1038/nature21357

Zhao, H., Dupont, J., Yakar, S., Karas, M., LeRoith, D., 2004. PTEN inhibits cell proliferation and induces apoptosis by downregulating cell surface IGF-IR expression in prostate cancer cells. Oncogene 23, 786–794. https://doi.org/10.1038/sj.onc.1207162

Zhao, H., Gu, X., 2014. Silencing of insulin-like growth factor-1 receptor enhances the radiation sensitivity of human esophageal squamous cell carcinoma in vitro and in vivo. World J Surg Oncol 12, 325–325. https://doi.org/10.1186/1477-7819-12-325

Zhao, R., DeCoteau, J.F., Geyer, C.R., Gao, M., Cui, H., Casson, A.G., 2009. Loss of imprinting of the insulin-like growth factor II (IGF2) gene in esophageal normal and adenocarcinoma tissues. Carcinogenesis 30, 2117–2122. https://doi.org/10.1093/carcin/bgp254

Zhao, Y., Thomas, H.D., Batey, M.A., Cowell, I.G., Richardson, C.J., Griffin, R.J., Calvert, A.H., Newell, D.R., Smith, G.C.M., Curtin, N.J., 2006. Preclinical Evaluation of a Potent Novel DNA-Dependent Protein Kinase Inhibitor NU7441. Cancer Res 66, 5354. https://doi.org/10.1158/0008-5472.CAN-05-4275

Zheng, H., Hu, P., Quinn, D.F., Wang, Y.K., 2005. Phosphotyrosine Proteomic Study of Interferon α Signaling Pathway Using a Combination of Immunoprecipitation and Immobilized Metal Affinity Chromatography*. Molecular & Cellular Proteomics 4, 721–730. https://doi.org/10.1074/mcp.M400077-MCP200

Zhou, B.-B.S., Chaturvedi, P., Spring, K., Scott, S.P., Johanson, R.A., Mishra, R., Mattern, M.R., Winkler, J.D., Khanna, K.K., 2000. Caffeine Abolishes the Mammalian G2/M DNA Damage Checkpoint by Inhibiting Ataxia-Telangiectasia-mutated Kinase Activity *. Journal of Biological Chemistry 275, 10342–10348. https://doi.org/10.1074/jbc.275.14.10342

Zhou, B.P., Deng, J., Xia, W., Xu, J., Li, Y.M., Gunduz, M., Hung, M.-C., 2004. Dual regulation of Snail by GSK-3β-mediated phosphorylation in control of epithelial–mesenchymal transition. Nature Cell Biology 6, 931–940. https://doi.org/10.1038/ncb1173

Zhou, B.P., Liao, Y., Xia, W., Spohn, B., Lee, M.-H., Hung, M.-C., 2001a. Cytoplasmic localization of p21Cip1/WAF1 by Akt-induced phosphorylation in HER-2/neu-overexpressing cells. Nature Cell Biology 3, 245–252. https://doi.org/10.1038/35060032

Zhou, B.P., Liao, Y., Xia, W., Zou, Y., Spohn, B., Hung, M.-C., 2001b. HER-2/neu induces p53 ubiquitination via Akt-mediated MDM2 phosphorylation. Nature Cell Biology 3, 973–982. https://doi.org/10.1038/ncb1101-973

Zhou, J., Li, J., Serafim, R., Ketchum, S., Ferreira, C., Liu, J., Coe, K., Price, B., Yusufzai, T., 2018. Human CHD1 is required for early DNA-damage signaling and is uniquely regulated by its N terminus. Nucleic acids research 46. https://doi.org/10.1093/nar/gky128

Zhou, Y., Lee, J.-H., Jiang, W., Crowe, J.L., Zha, S., Paull, T.T., 2017. Regulation of the DNA Damage Response by DNA-PKcs Inhibitory Phosphorylation of ATM. Molecular Cell 65, 91–104. https://doi.org/10.1016/j.molcel.2016.11.004

Zhou, Y., Liu, Y., Hussmann, D., Brøgger, P., Al-Saaidi, R.A., Tan, S., Lin, L., Petersen, T.S., Zhou, G.Q., Bross, P., Aagaard, L., Klein, T., Rønn, S.G., Pedersen, H.D., Bolund, L., Nielsen, A.L., Sørensen, C.B., Luo, Y., 2016. Enhanced genome editing in mammalian cells with a modified dual-fluorescent surrogate system. Cellular and Molecular Life Sciences 73, 2543–2563. https://doi.org/10.1007/s00018-015-2128-3

Zimmermann, M., de Lange, T., 2014. 53BP1: pro choice in DNA repair. Trends Cell Biol 24, 108–117. https://doi.org/10.1016/j.tcb.2013.09.003

Zimmermann, M., Lottersberger, F., Buonomo, S.B., Sfeir, A., de Lange, T., 2013. 53BP1 regulates DSB repair using Rif1 to control 5' end resection. Science 339, 700–704. https://doi.org/10.1126/science.1231573

Ziv, Y., Bielopolski, D., Galanty, Y., Lukas, C., Taya, Y., Schultz, D.C., Lukas, J., Bekker-Jensen, S., Bartek, J., Shiloh, Y., 2006. Chromatin relaxation in response to DNA double-strand breaks is modulated by a novel ATM- and KAP-1 dependent pathway. Nature Cell Biology 8, 870–876. https://doi.org/10.1038/ncb1446

Zou, J., Mali, P., Huang, X., Dowey, S.N., Cheng, L., 2011. Site-specific gene correction of a point mutation in human iPS cells derived from an adult patient with sickle cell disease. Blood 118, 4599–4608. https://doi.org/10.1182/blood-2011-02-335554

Zou, L., Elledge, S.J., 2003. Sensing DNA Damage Through ATRIP Recognition of RPA-ssDNA Complexes. Science 300, 1542. https://doi.org/10.1126/science.1083430